Detrital U-Pb geochronology provenance analyses: case studies in the Greater Green River Basin, Wyoming, and the Book Cliffs, Utah

By

Peter Gregory Lippert

Submitted to the graduate degree program in Geology and the Graduate Faculty of the University of Kansas in partial fulfillment of the requirements for the degree of Master of Arts.

____

Chairperson Andreas Möller

____

Diane Kamola

____

J. Douglas Walker

Date Defended: 1/29/14

The Thesis Committee for Peter Gregory Lippert
certifies that this is the approved version of the following thesis:

Detrital U-Pb geochronology provenance analyses: case studies in the Greater Green River Basin, Wyoming, and the Book Cliffs, Utah

Chairperson Andreas Möller

Date approved: 1/29/14

Abstract

Heavy mineral modal abundances and U-Pb geochronology are used to determine sediment provenance, provenance changes through time, and timing of crustal exhumation. Optimal preparation of datable detrital minerals (zircon, rutile, monazite, etc.) for provenance research using U-Pb geochronology has been a subject of debate and concern. Potential biases that are a concern consist of preferentially including or excluding datable detrital grains during mineral separation and data processing techniques. Exclusion of grains can lead to under-representation of source areas for a given sedimentary unit and alter the U-Pb age signature. The purpose of this study is to provide insight into this potential biasing by performing Laser Ablation-Inductively Coupled Plasma-Mass Spectrometer (LA-ICP-MS) U-Pb analyses of rutile and zircon with an optimized mineral separation and grain selection procedure. The **Q**uantitative **E**valuation of **M**inerals by **SCAN**ning electron microscopy (QEMSCAN®) was thus used to provide insight into potential biasing by automated quantification of modal abundances of minerals. A reliable technique for sample preparation was developed based on the LA-ICP-MS U-Pb analyses and QEMSCAN® mineralogical data. This technique includes minimal separation steps without preferential loss of mineral grains, representative sample splitting, and random and representative selection of grains to be dated. The result is a more comprehensive dataset for provenance analysis.

The Late Cretaceous sedimentary rocks of the Pine Ridge Sandstone and Almond Formation of the Mesaverde Group, Lewis Shale and Fox Hills Sandstone in the Greater Green River Basin, Rawlins, Wyoming, were investigated to test and develop mineral separation techniques. The methods developed here were also used to test whether there are variations in U-Pb provenance signal and modal mineralogy due to changes in depositional facies using samples from the Upper Cretaceous Blackhawk Formation and Castlegate Sandstone from the Book Cliffs, Utah. These stratal units were selected because while the age of the potential source areas are well known and the sequence stratigraphy, and sedimentology of the strata is well characterized, provenance has not been determined.

The results from LA-ICP-MS and QEMCAN analyses of Greater Green River Basin sedimentary rocks show that standard mineral separation procedures are not ideal for detrital provenance investigations. The standard mineral separation procedures introduce bias, resulting in a

misrepresentation of the modal mineralogy and provenance age signal. LA-ICP-MS and QEMSCAN analyses of sedimentary samples from the Book Cliffs, Utah show that there are variations in the U-Pb provenance signal and modal mineralogy between samples from different depositional facies.

Table of Contents

List of Figures and Tables

List of Figures

List of Tables

Chapter 1. Introduction

Long established and common techniques used to determine the provenance of material in sedimentary units include manual point counting of detrital minerals to estimate modal percentages (e.g. Morton, 1991), and measuring paleoflow directions (e.g. Soyinka and Slatt, 2008). Advances in higher precision thermochronology, geochronology, and trace element determinations of detrital minerals have placed new emphasis on provenance investigations (Vermeesch, 2004). Determining U-Pb ages in heavy minerals is a well-established technique in detrital provenance analysis, which helps constrain sediment source areas, temporal variations of sediment source, and the timing of tectonic activity or exhumation of source materials (e.g. Kosler et al., 2002; Sircombe and Stern, 2002; Fedo et al., 2003). Trace element thermometry of detrital minerals (e.g. Zr-in-rutile) can provide insight into the thermal history of the sediment source and help further differentiate the provenance of sediment (e.g. Zack et al., 2004; Watson et al., 2006). Other trace element characteristics may be used to link detrital minerals to particular source rock types. This is being attempted using the Cr-Nb ratio in rutile to discriminate between metamafic and metapelitic protoliths (e.g Zack et al. 2002; 2004; Triebold et al. 2007, 2012). There is some discussion about the validity of this in ultrahigh-temperature (UHT) granulites, but this appears to have been largely resolved by an adjustment in the discrimination calculation by Triebold et al. (2012).

There are three main purposes of this case study in mineral separation procedures for detrital provenance research using heavy minerals:

(1) to establish and test mineral separation and sample preparation techniques for detrital heavy mineral analyses, with specific focus on the U-Pb dating of zircon and rutile.

(2) the application of the mineral separation procedure to the late Cretaceous Pine Ridge Sandstone and Almond Formation of the Mesaverde Group, the Dad Member of the Lewis Shale, and the Fox Hills Sandstone of the Greater Green River Basin in Wyoming. The sedimentary units were used to test the hypothesis of a sediment source shift during the late Cretaceous potentially associated with regional tectonic events (Pyles and Slatt, 2000).

(3) the mineral separation procedure developed in this study was then used to determine the variations in the U-Pb provenance signal and modal mineralogy between samples from different depositional facies using the Star Point Sandstone, members of the Blackhawk Formation, and Castlegate Sandstone of the Book Cliffs, Utah. The following paragraphs will outline these topics, their relevance and some background aspects in more detail.

The introduction of bias, with the potential to alter the provenance age signature, is actively debated (e.g. Sircombe and Stern, 2002; Vermeesch, 2004; Andersen, 2005). Potential biases involve preferentially including or excluding datable detrital grains. Excluding or including certain detrital minerals can result in a non-representative sample fraction to be analyzed and ultimately in an incomplete or inaccurate dataset for provenance interpretations. Another potential source of bias is the exclusive use of zircon U-Pb ages for provenance analyses, because it underrepresents rock types with no zircon or low amounts of zircon (e.g. Sircombe and Stern, 2002). Due to its overall durability and abundance in source rocks, zircon is the most widely used mineral for U-Pb geochronology, but interest in other heavy minerals datable by U-Pb such as rutile (e.g. Zack et al., 2004, Meinhold, 2008) and monazite (e.g. Machado and Gauthier, 1996) is increasing.

Another source of bias is introduced when certain grains are removed during the mineral separation procedures. To minimize potential bias during mineral separation procedures, a simplified mineral separation method was developed in this study. This procedure resulted in a more representative mineral fraction to be analyzed and minimizes the amount of bias. U-Pb geochronology of detrital zircon and rutile from Late Cretaceous sedimentary rock units of the Greater Green River Basin (GGRB), Wyoming (Figure 1) were investigated to test the developed mineral separation method. The sedimentary units sampled in the GGRB include the Pine Ridge Sandstone and the Almond Formation of the Mesaverde Group, the Lewis Shale and the Fox Hills Sandstone. These sedimentary units were targeted because the ages of the possible source areas are relatively well known (Dickinson and Gehrels, 2009), and the sequence stratigraphy, sedimentology, and tectonic activity of the area are well characterized (e.g. Martinsen, et al, 1993). Between 2 and 3 samples from each of the target units were sampled from outcrops in the easternmost part of the Great Divide Basin and the western flank of the Rawlins Uplift (Figure 2).

To provide insight into the potential bias introduced during mineral separation procedures, the Excimer Laser Ablation-Inductively Coupled Plasma-Mass Spectrometer (LA-ICP-MS) at the Department of Geology of the University of Kansas was used to measure U-Pb isotopes and trace element concentrations. The LA-ICP-MS analyses were used to detect differences between the resulting U-Pb age population signatures of sample aliquots produced by different mineral separation techniques and also differences between the zircon and rutile datasets. The high throughput of the LA-ICP-MS makes it possible to measure >117 U-Pb dates needed for representative statistics on detrital age populations (Vermeesch, 2004) within 6-8 hours. The **Q**uantitative **E**valuation of **M**inerals by **SCAN**ning electron microscopy (QEMSCAN®) was used to help quantify potential bias introduced during mineral separation methods. QEMSCAN® rapidly determines modal abundances of a large number of heavy minerals (see method section below) and can eliminate errors associated with misidentification by optical point counting; therefore, it is a powerful tool for detrital mineral provenance analysis.

To determine whether there are variations in the detrital U-Pb age signature due to the depositional environment sampled, the method outlined above was employed to Late Cretaceous strata of the Book Cliffs, Utah. The sedimentary units of the Book Cliffs, Utah include the Panther Tongue of the Star Point Formation, the Spring Canyon, Aberdeen, and Desert members of the Blackhawk Formation and the Castlegate Member of the Price River Formation (Figure 3). Based on lithostratigraphic correlations, regional seismic and structural data, during the deposition of these strata the sediment supply was dominated by Precambrian basement rocks in the hinterland (DeCelles, et al., 1995; Lawton, 1985). Thus, the age populations of the deposited sediment should remain relatively consistent in the absence of syndepositional biases such as erosion of the sedimentary units and hydrologic sorting. However, changes in the depositional environment, especially those associated with relative sea level change or changes in regional base level could result in an altered provenance signature. This was tested by sampling strata from different systems tracts within a stratigraphic section with a well-defined sequence stratigraphic framework. The hypothesis to be tested is whether there are changes in the detrital source age in samples collected in highstand, lowstand, and transgressive system tracts of the same formation. An underlying assumption is that changes in sea level could result in changes in drainage systems and sedimentation patterns.

Sequence stratigraphy is defined by Mitchum and Van Wagoner (1991) as "the study of rock relationships within in a chronostratigraphic framework of repetitive, genetically related strata bounded by surfaces of erosion or non-deposition, or their correlative conformities." The fundamental unit of sequence stratigraphy is a sequence. In the rock record a sequence is bounded by unconformities and their correlative conformities (Mitchum and Van Wagoner, 1991). Sequences can be subdivided into system tracts. System tracts (lowstand, highstand, and transgressive system tracts) are defined by their position within a sequence and by the stacking patterns of parasequences (Mitchum and Van Wagoner, 1991). Parasequences are a conformable succession of genetically related beds and bedsets that are bounded by marine flooding surface that generally represent a relative rise in sea level (Mitchum and Van Wagoner, 1991). Lowstand system tracts (LST) are commonly represented by rocks that lie above sequence boundaries and represent a period of relative sea level fall (Mitchum and Van Wagoner, 1991). Transgressive system tracts (TST) are characterized by retrogradational parasequence sets and commonly marked by a transgressive surface at the base (Van Wagoner et al., 1988). TST are deposited during periods of rapid rise in relative sea level (Van Wagoner et al., 1988). Highstand System Tracts (HST) are generally widespread on the shelf and included one or more aggradational parasequence sets that are followed by one or more progradational parasequence sets. HST are deposited during a late part of relative sea level rise, stillstand, and early part of the relative sea level fall and commonly form on top of LST or TST (Van Wagoner et al., 1988).

Using a sequence stratigraphic approach, Van Wagoner (1988, 1995) has characterized and interpreted possible sea level variations during deposition of the Star Point Sandstone, members of the Blackhawk Formation, and the Castlegate Sandstone of the Book Cliffs, Utah. During deposition of these units, significant sea level changes had the potential to result in variations in drainage patterns, resulting in the addition of new sedimentary source areas. These changes could alter the U-Pb provenance signatures and the detrital mineral modes in the sedimentary deposits. Various HST and LST were sampled from the sedimentary units in the Book Cliffs of Utah. Samples were collected from the HST of the Spring Canyon Member, the

LST in the Aberdeen member, the HST and LST of the Desert member of the Blackhawk Formation and the LST of the Castlegate sandstone. TST are not well represented in nearshore marine strata, and therefore were not sampled. The goal of this part of the study is to effectively determine the effect relative changes in sea level have on the modal abundances of heavy minerals and the detrital U-Pb age signature in these strata.

The Panther Tongue and the Spring Canyon member of the Blackhawk Formation were used to determine the effect that grain size has on the modal abundances of heavy minerals and the detrital U-Pb age signature detected in these strata. A transgressive lag deposit, with medium-to-coarse grain size sandstone, was collected directly above the LST of the Panther Tongue and within the HST of the Spring Canyon Member of the Blackhawk Formation. Finer grain sandstones were collected from the LST in the Panther Tongue and the HST in Spring Canyon Member. Transgressive lag deposits are formed by wave reworking during a transgression in a near shore environment that is characterized by shoreline erosion and winnowing resulting in a relatively course lag deposit (Swift, 1968; Van Wagoner et al., 1988). Based on the sampling scheme outlined in this paragraph, this part of the study draws comparisons between coarse and fine grained samples to determine if and how grain size affects the modal abundances of heavy minerals and the detrital U-Pb age signature.

Chapter 2. Geologic History

The geologic history summarized below is intended to outline geologic events of North America that are relevant to this study. Section 2.1 intends to summarize the evolution of terranes that are potential sources of sediment for the stratal units in the Greater Green River Basin, Wyoming and Book Cliffs, Utah. Section 2.2 summarizes the necessary geologic background for this study and includes the evolution of the North American Cordillera and the development of the Cretaceous Western Interior Seaway. Section 2.3 summarizes the depositional history of the sedimentary units of the Greater Green River Basin, Wyoming. Section 2.4 summarizes the depositional history of the sedimentary units of the Book Cliffs, Utah.

Chapter 2.1 The Evolution of the North American Craton

The North American continent is composed of numerous terranes recording a complex geologic history of accretion, rifting, and uplift (Figure 4)(Hoffman, 1988). The evolution of the North American Craton or Laurentia initiated in the Paleoproterozoic with the collision of numerous continental Archean terranes (e.g. Hoffman, 1988; Whitmeyer and Karlstrom, 2007). Notable collisional events in the Paleoproterozoic included the collision of the Slave Province with the Rae Province around 1.96-1.92 Ga. The collision of the Slave and Rae Provinces created numerous volcanic arcs and orogenic belts along the margins of Laurentia (Whitmeyer and Karlstrom, 2007). Continued northwest-southeast shortening resulted in the collision of the Archean Superior Province with the Archean Rae-Hearne Province creating the Trans-Hudson Orogen at ~1.84-1.82 Ga. This was immediately followed by the collision of the Medicine Hat Block and Wyoming Province along the southwest corner of the Laurentia at ~1.82 Ga (Whitmeyer and Karlstrom, 2007). From ~1.8-1.2 Ga collisional events were isolated to the southeastern-eastern edge of the continent and include the accretion of the Yavapai Province, Mazatzal Province, Granite-Rhyolite Province, and Grenville Province. The Yavapai Province (1.8-1.7 Ga) is interpreted to include several volcanic arc terranes that coalesced outboard of Laurentia prior to the collisional event known as the Yavapai Orogeny at ~1.71-1.68 Ga (e.g. Van Schmus et al., 2007, Whitmeyer and Karlstrom, 2007). The Yavapai orogenic deformation was followed by granitic magmatism that intruded the Yavapai Province and surrounding terranes (Whitmeyer and Karlstrom, 2007). Following the same geographic trend, the Mazatzal Province accreted along the southeast side of the Yavapai Province around 1.69-1.65 Ma and was followed by the Granite-Rhyolite Province at ~1.55-1.35 Ga. Coeval with the collision of the Granite-Rhyolite Province with the Yavapai and Mazatzal, large volumes of granites intruded the Yavapai, Mazatzal, and Granite-Rhyolite Provinces.

The accretion of the Grenville Province along the northeast side of Laurentia marked the beginning of large-scale continent-continent collision between North American, Africa and South America at ~1.2-1.1 Ga (Whitmeyer and Karlstrom, 2007). This is better known as the formation of the supercontinent Rodinia (Figure 5). The breakup of Rodinia occurred in a two-stage process that began along the western margin with the opening the paleo-Pacific ocean around ~0.78-0.68 Ga. The second stage of disassembly occurred along the eastern margin at ~0.62-0.55 Ga and created the Iapetus ocean (Bogdanova et al., 2007; Whitmeyer and Karlstrom, 2007). In the Cambrian, the eastern margin of Laurentia transitioned to an active margin and resulted in the accretion of numerous outboard terranes. During the Paleozoic, further subduction along the eastern margin resulted in the docking of Gondwana and finally the formation of the supercontinent Pangaea (Figure 6; Blakey, 2008; Bogdanova et al., 2007). In the earliest Paleozoic, collision of Laurentia with Gondwana drove numerous orogenic events along the margins of the colliding continents and resulted in the Appalachian mountain chain along the eastern margin of Laurentia (Hatcher, 1989). Separation of Pangaea initiated in the Triassic with rifting along the margins of Laurentia and North Africa and resulted in the opening of the Atlantic Ocean and the Gulf of Mexico. The breakup of Pangaea marks the end of major continent building events in the eastern half of Laurentia, however this was not the case for the western portion of Laurentia. Development of an active margin along the western coast of Laurentia docked several outboard terranes and resulted in the development of the North American Cordillera, described in more detail in the next chapter.

Chapter 2.2 Evolution of the North American Cordillera and Development of the Cretaceous Western Interior Seaway

The North American Cordillera (NAC) linearly extends from Alaska to the southern regions of Mexico and has a maximum width of 1,600km (Figure 7) (Blakey, 2008; Burchfiel et al., 1992). The complex evolution of the NAC initiated in the late Proterozoic with the development of a passive margin along the western continental margin of North America (Poole et al., 1992). In the Early Mississippian and Permian-Triassic, a westward propagating subduction complex transitioned to outer continental margin sedimentation. Further eastward migration of the once offshore subduction zone created an active margin immediately adjacent to North American continent. Subduction of the proto-Pacific plate was associated with continental arc magmatism in the Triassic and Jurassic (Saleeby et al., 1992). Late Jurassic-Cretaceous subduction along the active margin was dominated by thin-skinned tectonism (Sevier Orogeny) and resulted in an eastern retroarc foreland basin in the interior of western North America, which is known as the Sevier foreland basin (SFLB)(Cowan and Bruhn, 1992). Due to a large global sea level rise in the Aptian, marine water inundated the SFLB and areas to the east, forming the intercontinental seaway known as the Cretaceous Western Interior Seaway (KWIS)(Kauffman, 1984). The KWIS was an epeiric sea located east of the Sevier Orogenic belt that extended from the Arctic Ocean to the proto-Gulf of Mexico (Figure 7)(Kauffman, 1977; Snoke, 1993). Sedimentary units deposited in the KWIS consist of intertonguing nonmarine and marine units that record a history of sea-level transgression and regression (Kauffman, 1977; Steidtmann, 1993). Sediment deposited in the SFLB, along the western margin of the KWIS, contains evidence for major variations in sediment supply due its large geographical extent, axial parallel transport of sediment and the many deformational events in the North American Craton (e.g. Martinsen et al., 1993). Both study areas of this work are situated along the western margin of the KWIS, within the SFLB, immediately east of the Sevier Thrust Belt (Figure 7) and Cordilleran Fold and Thrust Belt (Figure 8).

The Laramide orogeny followed the Sevier Orogeny and is characterized by thick-skinned deformation events (Miller et al., 1992). Laramide orogenic deformation segmented the broad Sevier foreland basin resulting in numerous localized sedimentary basins (Figure 8; Miller et al., 1992), including the Green River Basin in Wyoming. The Laramide Orogeny initiated at ~75 Ma and continued until ~35 Ma (Hamilton, 1981; Miller et al., 1992; Cowan and Bruhn 1992; Bird, 1998).

Chapter 2.3 Geologic History of the Greater Green River Basin, Wyoming

This section is a generalized explanation of the geologic history of the Pine Ridge Sandstone and Almond Formation of the Mesaverde Group, the Dad Member of the Lewis Shale, and the Fox Hills Sandstone in the Greater Green River Basin, Wyoming. A summary of significant tectonic events and subsequent environment of deposition during the deposition of the sedimentary units of the Greater Green River Basin is provided. The Sevier Fold and Thrust belt was located west of the late Cretaceous Pine Ridge Sandstone and the Almond Formation of the

Mesaverde Group, the Dad Member of the Lewis Shale, and the Fox Hills Sandstone. Following deposition of these late Cretaceous units, the Laramide orogeny began to segment the Sevier foreland basin (Figure 7; Miller et al., 1992). Laramide deformation formed Precambrian basement-cored uplifts that include the Uinta Mountains, Wind River Range, Granite Mountains, Teton Range, Idaho-Wyoming Thrust Belt, and Sierra Madre Mountains (Figure 9; Baars et al., 1988). These tectonic highs segmented the Sevier foreland basin into smaller localized basins and formed the current embayment form of the Greater Green River Basin, Wyoming (GGRB) (Figure 8 and 9). Localized sedimentary basins resulted in localized sedimentation patterns. The Laramide uplifts resulted new sources of sediment in the GGRB. (Miller et al., 1992; Pyles and Slatt, 2000, 2002, and 2007; Soy and Slatt, 2008). According to Pyles and Slatt (2007), paleocurrent measurements and facies changes suggest a provenance shift in the Maastrichtian Dad Member of the Lewis shale, which marks the transition to Laramide deformation in Wyoming.

Within the GGRB, the following stratigraphic units were deposited in the late Cretaceous(from oldest to youngest): the Pine Ridge Sandstone and Almond Formation of the Mesaverde Group, the Dad Member of the Lewis Shale, and the Fox Hills Sandstone (Figure 1; Pyles and Slatt, 2000, 2002, and 2007; Soy and Slatt, 2008). The lower part of the Upper Campanian Pine Ridge Sandstone of the Mesaverde Group is a very heterogeneous unit and has been interpreted as a tidally influenced fluvial system; this unit transitions to a wave-influenced deltaic setting up-section (Martinsen et al., 1993). The youngest member of the Mesaverde Group in this locality is the Campanian Almond Formation, interpreted as consisting of tidal and coastal plain mudstones and sandstones (Pyles and Slatt, 2000). The Maastrichtian Lewis Shale lies conformably above the Almond Formation and is divided into three members: the Lower, Dad, and Upper members (Pyles and Slatt, 2000). The Lower Member is interpreted as being deposited in a deep-water setting or below storm wave base and consists of black shale (Pyles and Slatt, 2000). The Dad Member sits stratigraphically between the Upper and Lower members of the Lewis Shale and is composed of sandstones and mudstones from turbidite-dominated, submarine fan strata (Pyles and Slatt, 2000). The Upper Member is composed of dark gray and olive muddy shelf and basinal mudstones. The Lewis Shale interfingers with the overlying Fox Hills Sandstone, which is composed of interbedded sandstone and mudstone. The Fox Hills Sandstone is interpreted as deposited in deltaic, shoreface, and backshore settings (Figure 10 and 11; Pyles and Slatt, 2000).

Chapter 2.4 Geologic History of the Book Cliffs, Utah

The late Cretaceous sedimentary units of the Book Cliffs were deposited in the Sevier foreland basin during the Sevier Orogeny and prior to the Laramide Orogeny. In the late Cretaceous, there was a relatively constant supply of sediment sourced from the Sevier Orogenic belt and deposited into the Sevier Foreland Basin (Burchfiel and Davis, 1975; Lawton, 1985). However, the deposition of these sedimentary units in the Book Cliffs was interrupted by periods of relative sea level fall (Van Wagoner, 1995). Previous studies have interpreted that the stratigraphic section throughout the Book Cliffs to record changes in the relative position of sea level which affects sedimentation and drainage patterns (Van Wagoner, et al., 1988; Van Wagoner, 1991, 1995; Kamola and Huntoon, 1992; Kamola and Van Wagoner, 1995; Yoshida, et al., 1996, 1998; Posamentier and Morris, 2000; Miall and Arush, 2001; Hwang and Heller, 2002).

The stratal units studied in the Book Cliffs include the Star Point Formation, the Blackhawk Formation, and the Castlegate Sandstone of the Price River Formation (Figure 3).

These strata are Santonian to Campanian in age and were deposited in the Sevier foreland basin as a late Cretaceous, eastward prograding clastic wedge that intertongues with the Mancos Shale to the east (Figure 3; Young, 1955). The sedimentary units make up the lower and upper portions of the Campanian Mesaverde Group and consist of non-marine, marginal marine, and shallow marine deposits that intertongue with the deeper water Mancos shale (Young, 1955). The Star Point Sandstone, members of the Blackhawk Formation, and the Castlegate Sandstone contain numerous sequence boundaries. These strata are divided into numerous depositional sequences and depositional systems tracts (Van Wagoner, et al., 1988; Van Wagoner, 1991, 1995; Kamola and Huntoon, 1992; Kamola and Van Wagoner, 1995; Yoshida, et al., 1996, 1998; Posamentier and Morris, 2000; Miall and Arush, 2001; Hwang and Heller, 2002).

The Panther Tongue of the Star Point Formation is interpreted as a deltaic LST that is capped by a transgressive lag deposit (Posamentier and Morris, 2000; Hwang and Heller, 2002). The depositional facies in the Panther Tongue is predominantly deltaic (Hwang and Heller, 2002). The transgressive lag deposit in the Panther Tongue consists of a thin (~ 10 cm thick) coarse grained sandstone that was deposited during a relative sea level rise (Posamentier and Morris, 2000; Hwang and Heller, 2002).

The Blackhawk Formation includes six members that consist of progradationally to aggradationally stacked shoreface sandstones that interfinger with the Mancos Shale to the east (Young, 1955). In stratigraphic order, from oldest to youngest, the six members of the Blackhawk Formation are the Spring Canyon, Aberdeen, Kenilworth, Sunnyside, Grassy, and Desert members. The members of the Blackhawk Formation that are important to this study include the Spring Canyon, Aberdeen, and the Desert members and will be descried below. The Spring Canyon Member is comprised of numerous progradational tongues of coastal plain, shoreface sandstones, and siltstones that were deposited within a HST (Kamola and Van Wagoner, 1995). The Spring Canyon Member is overlain by a marine flooding surface and does not contain any sequence boundaries (Kamola and Van Wagoner, 1995). The Spring Canyon Member is overlain by the Aberdeen Member, which consists of similar facies as the Spring Canyon Member. The Aberdeen Member, however, contains two sequence boundaries, one near the base of the member and one at the top of the member (Kamola and Huntoon, 1992). The Aberdeen member contains strata of the LST and HST (Kamola and Huntoon, 1992). The Desert Member of the Blackhawk Formation contains HST, LST, and TST. The HST is composed of shoreface and shelf facies sandstones and occurs at the base of the member. It is erosionally overlain by a sequence boundary, which is the overlain by incised valley fill with strata of the LST and TST (Van Wagoner, 1995). A shoreface sandstone, interpreted as the TST, overlies the incised valley fill (Van Wagoner, 1995).

The Castlegate Sandstone lies unconformably above the Blackhawk Formation, and includes fluvial sandstones that grade into marine sandstone down depositional dip (Van Wagoner, 1995). This formation varies regionally and is mainly fluvial in the northern part of the Book Cliffs and fluvial to marine in the southern exposures of the Book Cliffs. In the Green River, Utah area, the base of the Castlegate Sandstone is a sequence boundary which unconformable overlies the Desert Member of the Blackhawk Formation (Van Wagoner, 1995). Stacked fluvial strata of an incised valley fill occur above the sequence boundary (Van Wagoner, 1995).

Chapter 3. Methodology

3.1 Field Sampling

Samples were collected from the Pine Ridge Sandstone and Almond Formation of the Mesaverde Group, the Dad Member of the Lewis Shale, and the Fox Hills Sandstone in the GGRB, Wyoming, and the Star Point Formation, the Blackhawk Formation, and the Castlegate Sandstone of the Price River Formation from the Book Cliffs, Utah. In the GGRB, samples were collected from steeply dipping Upper Cretaceous units in the Stratton Ranch located on the flanks of the Rawlins Uplift, located on the eastern edge of the Great Divide sub-basin north of I-80 (Figure 2 and 12; Table 2). Samples were collected from the Dad Member of the Lewis Shale as well as from sedimentary rock units above and below this statal unit (Figure 1 and 2; Table 2).

Samples collected from the Star Point Formation, Blackhawk Formation, and the Castlegate Sandstone were taken from various canyons in the northern and southern Book Cliffs, Utah. These canyons include Gentile Wash, Hardscrabble Canyon, Tusher Canyon, Kenilworth Canyon, and 9-mile Canyon. Gentile Wash and Hardscrabble Canyon are located on the northwestern end of the Book Cliffs, along HWY-6, north of Helper, Utah (Figure 13). Samples collected within Gentile Wash include the deltaic sample from the LST in the Panther Tongue Member of the Star Point Formation (11-PTH-09). The shoreface sandstone from the HST in the Spring Canyon Member of the Blackhawk Formation (11-SPC-05) was also collected in Gentile Wash. The transgressive lag deposit from the Panther Tongue (10-PTH-01) was collected in Hardscrabble Canyon located just south of Gentile Wash on HWY-6 (Figure 3 and 13; Table 3). The transgressive lag deposit of the Spring Canyon Member (10-SPC-01) was collected from the locally named Tramway section in Kenilworth Canyon which is located west of Gentile Wash near the town of Kenilworth, Utah (Figure 3 and 13; Table 3). Tusher Canyon is located in the southern portion of the Book Cliffs, north of Green River, Utah (Figure 3 and 13; Table 3). Samples collected from Tusher Canyon include the LST of the Desert Member of the Blackhawk Formation (11-TUS3C-2-17) and the LSTs of the Castlegate Sandstone (11-CSTG-07; 11-TUS3C-22.3-23.4)(Figure 3 and 13; Table 3). The HST within the Desert Member of the Blackhawk Formation (11-BH-06) was also collected in Tusher Canyon (Figure 3 and 13; Table 3). The LST of the Aberdeen Member of the Blackhawk Formation (11-AB-LST) was collected in 9-Mile Canyon located west of Helper, Utah on 9-mile road (Figure 3 and 13; Table 3).

3.2 Mineral Separation Techniques

Established mineral separation procedures for U-Pb geochronology investigations of heavy minerals include water table separation (e.g. Shaker table, Gemini® Table, and Wilfley® Table), heavy liquid separation, magnetic separation (Frantz® Isodynamic magnetic separator), splitting of sample, and grain selection or hand picking (Sircombe and Stern, 2002). This separation method fractionates heavy minerals and light minerals based on mineral characteristics and properties.

During transport and deposition, detrital grains are subject to various sorting and fractionation processes (Sircombe and Stern, 2002). They may be sorted based on grain size and become significantly weathered during sediment transportation in to the basin (Sircombe and Stern, 2002). Also, sandstones may contain framework grains that are sourced from igneous and metamorphic terranes, as well as from material recycled from pre-existing sedimentary units. These complex sources commonly contain minerals with a variety of cooling and crystallization histories. As a result, framework grains sampled from sedimentary units contains mineral grains that have a wide range of grain sizes, grain shapes, density, and magnetic susceptibility (Rittenhouse, 1943; Lawrence et al., 2011) As an example, a single sedimentary sample commonly contains zircons that are euhedral, subhedral, anhedral, metamict, range in grain size from 30-200 μm; and that contain inclusions. Established mineral separation methods preferentially remove the zircons that are <50 μm, are metamict, and contain inclusions (Sircombe and Stern, 2002). The zircon grains left to be analyzed are then commonly 50-200 μm, euhedral to subhedral, non-metamict, and relatively free of impurities. Removing mineral grains that are metamict or smaller than 50 μm can lead to a sample fraction to be analyzed that underrepresents a source that has metamict zircon or that is distal from the site of deposition. Therefore, using these established mineral separation procedures for provenance research potentially results in incomplete (biased) datasets.

The following paragraphs review the standard mineral separation techniques and provide a recommended mineral separation procedure for detrital provenance investigations based on the findings of this study. It is not the intention of this study to suggest that previous work using standard mineral separation techniques for detrital provenance investigations are faulty. The mineral separation procedures outlined in this thesis are seen as best practice and should result in more comprehensive datasets for detrital provenance investigations.

Crushing

After a sample is collected, the first procedure in the majority of mineral separation methods is to set aside a representative hand sample of the original material and crush the remaining whole rock. Sedimentary rock samples should be broken at the grain boundaries while leaving the individual mineral grains intact, thereby ensuring to preserve the minerals original size, and shape. In this study, samples were crushed very coarsely and sieved at 500 μm before further grain size reduction. This ensures that material that was already sufficiently crushed was removed and not over-crushed. Over-crushing of mineral grains can effectively destroy the grains original shape, and can drastically reduce the grains size. Significantly reducing a grains size can render it unusable for common investigative tools. After a sample is crushed the next step involves using a water table to remove the very fine mineral grains and concentrate heavy minerals.

Water table

Water table separation techniques, by design, segregate minerals based on specific gravity, shape and size of grains. Specifically, the water table tested in this study (Gemini® table) is tuned to concentrate minerals with a specific gravity (s.g.) higher than 2.8 g/cm^3 and a grain size larger than 40 μm from the bulk material. Removing mineral grains that are <40 μm could potentially remove certain mineral populations that are highly metamict, distal from the site of deposition, or from a source that is aphanitic. The preferential removal of grains <40 μm from the sampled material to be analyzed is called grain size biasing (Sircombe and Stern, 2002).

The Gemini® water table set-up at the KU geology department was used to test the separation efficiency of concentrating minerals with a s.g. higher than 2.8 g/cm^3 and >40 μm by water table separation techniques. The tested sample was composed of ~1 g of 30-200 μm silicon carbide mixed with pure quartz sand. The synthetic silicon carbide (SiC) material used consists of hexagonal crystals with a well-characterized specific gravity of 3.1-3.2 g/cm^3 and is used as an analog for apatite in this investigation. By qualitatively examining the material after water separation, it was noticed that the majority of SiC smaller than ~50 μm remained mixed with the quartz sand. Also, ~40% of the silicon carbide grains remained in the quartz sand or light fraction. Removing grains smaller than ~50 μm could effectively remove mineral grains that are from aphanitic source rocks (<62.5 μm grain size) and mineral grains that are distal from the site of deposition. Since the LA-ICP-MS technique used can reliably measure isotopes from mineral grains as small as 35 μm, the water table separation was not used in the separation procedure for samples in this study.

Water table separation is commonly used to concentrate heavy minerals while decreasing the sample size to a manageable volume of <500 ml for mineral separation using heavy liquids. Since no water table separation was used in the mineral separation procedure for this study it was necessary to split the bulk material. Sample splitting was performed after the sample was crushed and sieved to <500 μm. The material smaller than 500 μm was then split. One approach to representatively split a sample is to pour the sample exactly centered over a narrow divider which allows grains of varying grain size to be split in equal amounts (Otto, 1933). Representative splitting of the sample minimizes grain size bias and is considered best practice and was used here.

Heavy liquids

Heavy liquids commonly used in mineral separation are Bromoform (max. s.g. 2.85 g/cm^3), Lithium Metatungstate (LMT) (max. s.g. ~2.85 g/cm^3), and Methylene Iodide (MEI) (max. 3.3 g/cm^3). This technique separates minerals in two fractions by density or specific gravity: minerals with a specific gravity higher than the heavy liquid (heavy mineral fraction) and minerals with a specific gravity lower than the heavy liquid (light mineral fraction). To test the effectiveness of the mineral separation procedure using Bromoform and MEI, either 1 or 5 g of SiC where mixed with ca. 5 to 50 g of pure quartz sand (Table 1). Different ratios of SiC to pure quartz sand were used to determine the effect rafting had on the separation efficiency of heavy liquid separation methods. Rafting occurs during heavy liquid separation when heavy minerals are held in suspension in the buoyant light minerals and are inhibited from separating from the light minerals. The heavy liquids separation procedure, relative to water table separation, yielded more heavy minerals from the bulk material and no contamination of light minerals in the heavy mineral fraction, with minimal to no rafting of heavy minerals (Table 1).

After representatively splitting a sample to ~500 ml sample material, two 1 l separatory funnels containing Bromoform were used as the first separation step. Two separation vessels were used in the Bromoform step in order to minimize crowding of material within the vessels, which could result in rafting of heavy minerals within the buoyant light minerals. After Bromoform separation, a Methylene Iodide step with constriction test tubes followed. The heavy mineral fraction extracted with Bromoform was ~2-8 ml, an adequate volume for MEI heavy liquid separation in large restriction tubes. These two heavy liquid separation steps generally resulted in a ~0.05 ml heavy mineral fraction with a s.g. 3.3 g/cm^3 or higher and yielded >117 grains for LA-ICP-MS analyses. If this separation technique did not result in >117 datable mineral grains, the procedure was repeated on more unprocessed sample material. After the heavy liquid mineral separation the Frantz Isodynamic magnetic separator was used to further concentrate the desired minerals.

Magnetic separation

The Frantz Isodynamic magnetic separator is a device that separates minerals based on their magnetic susceptibility or paramagnetism (e.g. Sircombe and Stern, 2002). Magnetic susceptibility is the effectiveness an applied magnetic field has on a material, in this case a mineral grain (Sircombe and Stern, 2002). The Frantz electromagnet can be set to a specific current ranging from 0.1 A to 1.8 A. The slide or ramp that contains the barrier separating magnetic from non-magnetic grains can be tilted at an angle perpendicular to the slide of ±30°. The slide is commonly used to separate material or minerals that have similar magnetic susceptibilities (Sircombe and Stern, 2002). Standard mineral separation procedures commonly concentrate zircon with a final step of 1.8 A at 5° (Sircombe and Stern, 2002).

Magnetic susceptibly of zircon and rutile grains is directly dependent on the degree of impurities, overgrowths, and inclusions in these mineral grains. Magnetic susceptibility of zircon also increases with degree of metamictization, which is a function of uranium (U) and thorium (Th) concentration, time, and annealing history (Sircombe and Stern, 2002). Metamictization allows Fe and other foreign contaminates to be more readily incorporated into the crystal structure of the mineral (Lewis and Senftle, 1966; Geisler et al., 2002). Rutile may contain inclusions of Fe-rich oxides and hydroxides formed during breakdown of the mineral grains associated with diagenetic processes and alteration (Zack et al., 2004). Rutile and zircon, if free of these secondary features, would not be magnetically susceptible and would only be present in the non-magnetic fraction after Frantz magnetic barrier separation. After sampled material was run through the Frantz magnetic barrier separator set at 1.0 A at 10° tilt it was observed that the magnetic mineral fraction contained large amounts of zircon. Therefore, the Frantz magnetic separation technique was not used for zircon and a mineral fraction was split from the MEI heavy mineral fraction to be set aside for grain mounting.

Rutile is a ubiquitous mineral in medium- to high-grade metamorphic rocks and highly resistant to mechanical and chemical alteration associated with transport, weathering and diagenesis (Triebold et al., 2012; Zack et al., 2012). Therefore, rutile is a relatively common detrital mineral in sedimentary units. Other TiO_2 detrital minerals that are found in sedimentary units include brookite and anatase (Triebold et al., 2011), which are indistinguishable from rutile by optical microscopy and Raman spectroscopy (Triebold et al., 2011). Anatase and brookite are polymorphs of rutile, which renders them chemically identical and indistinguishable using

Energy Dispersive Analysis X-Ray (EDAX) on a Scanning Electron Microscope (SEM). It was observed in this study that anatase and brookite typically are more magnetic than rutile (see also Triebold et al., 2011). Therefore, to ensure that rutile was the mineral being used for U-Pb and trace element measurements, the mineral fractions acquired after MEI heavy liquid separation were run through the Frantz magnetic separator at 1.8 A and 5^{o}. The magnetic minerals from this step were discarded, ensuring that the minerals with higher amounts of Fe where removed from the mineral fraction to be dated. The non-magnetic fraction was then hand picked for minerals that were closest to the optical mineralogical characteristics of rutile (stubby to needle shaped and reddish brown to black). For this study this was the concluding mineral separation step prior to mounting detrital rutile in epoxy.

Grain mount preparation

Mounting relevant mineral grains in epoxy is a necessary step prior to imaging minerals grains using SEM and QEMSCAN® (Appendix A: CL Images; Appendix B: QEMSCAN® Images). Mineral grains mounted in epoxy were polished cutting approximately halfway into the grains. This ensured that the largest possible area of the mineral grain was exposed at the grain mount surface revealing internal complexities such as sector zoning, oscillatory zoning, and inherited cores, or mineral intergrowths. Polishing the grain mount also ensured a flat surface for more precise focusing of the laser beam for U-Pb and trace elements determinations using LA-ICP-MS.

The initial step to embed the heavy mineral fraction in epoxy is to representatively split the heavy mineral fraction. As uniformly as possible, these minerals were then spread onto doubled-sided adhesive tape fixed on a glass plate in order to minimize crowding and overlapping of minerals. Under a binocular microscope, grains where laid flat to ensure that after the grain mount is polished the mineral grains have the largest exposure at the grain mount surface. Once mounted on double-sided adhesive tape, a 25mm ring mold was placed around the grains and ~3-5 g of epoxy was poured into the mold. The grain mount cured and hardened for a minimum of two days and was then polished to cut approximately halfway into the grains.

*3.3 **Q**uantitative **E**valuation of **M**inerals by **SCAN**ning electron microscopy (QEMSCAN®)*

Whole rock billets and polished grain mounts where sent to the Advanced Mineralogy Research Center at the Colorado School of Mines (CSM) in Golden, CO, for **Q**uantitative **E**valuation of **M**inerals by **SCAN**ning electron microscopy (QEMSCAN®). The QEMSCAN® instrument is an automated scanning electron microscope (SEM) coupled with four Bruker X275HR silicon drift energy dispersive x-ray spectrometers (EDS) and a four-quadrant semiconductor diode backscatter electron (BSE) detector. This setup allows rapid acquisition of X-ray spectra and backscattered electron images. Measuring the X-ray spectra and using the backscattered electron images, the QEMSCAN® software identifies mineral phases in rock billets or polished grain mounts (Pirrie et al., 2004).

Common to the majority of SEM imaging techniques, the first step before imaging the sample is to coat the surface with a metal or carbon, with a thickness of approximately 50 angstroms ($1x10^{-10}$ m), to dissipate charges the electron beam builds up on the sample surface. Gold or silver metal coating commonly contains other metals such as Pb that could contaminate the mineral grains resulting in a high Pb background during LA-ICP-MS analyses. This could result in less precise and/or erroneously old U-Pb ages. A carbon coat does not contain metals or other elements that could possibly contaminate the sample surface and was therefore used in this study.

For QEMSCAN® analyses, minerals on a sample surface are rapidly located by measuring the high contrast of BSE signal between the minerals and the carbon coated epoxy (Pirrie et al., 2004). Once the minerals are located, the electron beam does not analyze the carbon coated epoxy between grains, but only the mineral surfaces are rastered by the electron beam at a previously set resolution. During rastering of the electron beam, the resulting x-ray spectra are simultaneously collected by the four Bruker X275HR silicon drift energy dispersive x-ray spectrometers. The EDS spectra are then compared to a database of known mineral EDS signatures to positively identify the minerals in a given sample. Identification of mineral phases at each pixel requires ~10 ms data collection time. Therefore, the amount of time needed to identify all mineral grains in a given sample is dependent on the pixel resolution set, the number of grains to be identified, and the size of the grains (Pirrie et al., 2004). In this study, a 15 μm resolution false-color map of the mineral phases was produced in ~1-2 hours for a grain mount, and in ~2-4 hours for a thin section billet. A 4 μm resolution grayscale BSE image was collected in ~15 minutes per grain mount. After data acquisition and data processing, a false-color map of the mineral phases in the grain mount or thin section is produced, as well as an Excel© spreadsheet detailing the modal abundance of each mineral phase in mass and volume percent (Appendix B).

A key advantage of the QEMSCAN® is that it allows minerals to be positively identified that could be misidentified during manual optical identification and point counting. Due to the destructive nature of sediment transport from the source to the site of deposition, the detrital particles can have a large variety of grain shape, texture, size, and color. This can make some grains difficult to identify during manual point counting or selection of mineral grains under a binocular microscope, depending on the experience of the operator. Misidentification of mineral grains during manual selection of mineral grains or manual point counting could potentially underrepresent relevant mineral populations or an age population in the provenance signal and thus introduce a source of bias. However, polymorphs such as rutile, anatase, and brookite are not discernible from each other by QEMSCAN® EDS analyses, because chemically identical polymorphs produce non-unique EDS signatures and get identified as the same phase by the software. A manual check after QEMSCAN® analyses is therefore necessary for minerals with polymorphs.

3.4 Laser Ablation- Inductively Couple Plasma-Mass Spectrometry (LA-ICP-MS)

Laser Ablation-Inductively Coupled Plasma-Mass Spectrometry (LA-ICP-MS) was originally developed as an *in situ* approach for trace element determinations and quickly became a common tool used for *in situ* U-Pb geochronological investigations of accessory minerals (e.g. Jackson, et al., 1992). LA-ICP-MS *in situ* techniques result in zircon age data with an accuracy conservatively estimated to be within 2-4% (2σ) of the a Isotope Dilution Thermal Ionization Mass Spectrometry (ID-TIMS) age (Horn et al., 2000; Kosler and Sylvester, 2003). Secondary Ion Mass Spectrometry (SIMS) provides U-Pb zircon ages within 0.5-2% (2σ) of the ID-TIMS age and allows ablation spots as small as ~15 μm in diameter and is relatively non-destructive compared to LA-ICP-MS analyses (Ireland and Williams, 2003), because of the shallow, maximal 3 μm deep pits produced. Concentrations of U, Th, and Pb contained in a targeted sample, the sensitivity of the mass spectrometer, and the precision required for the analysis largely determine the allowable spot size for LA-ICP-MS U-Th-Pb investigations. Therefore, minimum spot sizes of LA-ICP-MS analyses necessary for 2% accuracy do not allow the high spatial resolution of a SIMS (Davis et al., 2003; Kosler and Sylvester, 2003). Spot sizes of LA-ICP-MS U-Pb analyses can theoretically range from ~5-200 μm depending on the laser hardware, but spots of 20-30 μm are most routinely used to achieve single spot precision of better than 2%. Depending on the LA-ICP-MS equipment used and the type of analyses performed, data acquisition time on a single spot can range between 30-120 s (Kosler and Sylvester, 2003; Ireland and Williams, 2003). Short data acquisition times allow a large number of LA-ICP-MS (>117 grains) analyses to be performed in a short period of time (6-8 hours). Therefore, LA-ICP-MS is a powerful tool for provenance investigations using U-Pb geochronology and trace element determinations on heavy detrital minerals (Kosler and Sylvester, 2003).

The LA-ICP-MS system at the Department of Geology, University of Kansas was used for this provenance investigation by measuring U-Pb isotopes in rutile and zircon and trace element determinations of rutile. This system couples a Photon Machines 193 nm wavelength Ar-F Excimer laser to a Thermo Element2 inductively coupled plasma mass spectrometer. For LA-ICP-MS analyses, we used a 29 μm laser spot at a laser fluency of 2.66 J/cm^2 at 10 Hz for U-Pb analyses of zircon and rutile and a 22 μm spot size at a laser fluency of 2.66 J/cm^2 at 10 Hz to determine rutile trace element concentrations. These laser spot parameters allow enough ablated sample material to enter the Element2 to get a stable signal and minimize the effects of down-hole fractionation or mass fractionation (Eggins et al. 1998; Mank and Mason 1999).

Mass fractionation is defined as a change in measured isotopic ratios throughout the analysis time. Down-hole fractionation is mass fractionation that occurs due to complex interactions between the laser beam, sample surface, and the laser pit created during the ablation of material and the laser excavating progressively deeper into a material. This results in a discrepancy between the measured isotopic content and the "true" isotopic content (Kosler and Sylvester, 2003). Empirical evidence suggests that to minimize down-hole mass fractionation, the ablated spot depth should not exceed the diameter, the argument being that limited laser drill depth limits the defocusing of the laser beam and thereby minimizes the effect of down-hole fractionation (Kosler and Sylvester, 2003). Limiting the laser drill depth also ensures that the ablated material or plasma plume is efficiently carried out of the sample chamber (Hirata and Nesbitt, 1995). The ablated material is transferred, via Festo® polyurethane tubing, from the sample chamber into the Element2 mass spectrometer using helium (He) as the carrier gas at a flow rate of ~0.4.-0.46 l/min. Just prior to sample introduction into the Element2 plasma torch, the sample material carried in He is mixed with Ar gas in a Y tubing connector or glass mixing chamber at a Ar gas flow rate of 1.15-1.30 l/min.

As an external calibration material the GJ-1 zircon reference standard (Jackson et al., 2004) was used to correct for U-Pb age fractionation of unknown zircons, and the accuracy was checked using Plesovice (PL) zircon as a secondary reference standard. GJ-1 and PL are widely used zircon reference standards and have ID-TIMS $^{207}Pb/^{206}Pb$ age of 608.5±0.4 Ma (GJ-1; Frei and Gerdes, 2009) and 337.13±0.37 Ma (PL; Slama et al., 2008), respectively. For U-Pb dating and trace element determinations of rutile, R10 was used as the primary rutile reference standards and T-139 was used as the secondary rutile reference standard. R10 has a $^{207}Pb/^{206}Pb$ TIMS age of 1090±5 Ma (Luvizotto et al., 2009) and T139 has an $^{206}Pb/^{238}U$ TIMS age of 519±2 Ma (Möller et al., 2000). For individual analyses of U-Pb isotope measurements of zircon, this system has a precision of ~0.5-1% 2 sigma standard deviation (SD), and an accuracy of ~1-2% 2 sigma SD for a population of zircon analyses. For U-Pb analyses of rutile, a precision of 2-3% 2 sigma SD is achieved for individual analyses and 2-4% 2 sigma SD is achieved for a population of analyses.

3.5 Detrital U-Pb Geochronology by LA-ICP-MS

Making grain mounts for LA-ICP-MS analyses involves pouring minerals on to double-sided adhesive tape. As mentioned in the section "Mineral Separation techniques" above, the first grains to be poured will be the coarsest material followed by finer material. Pouring the grains onto the adhesive tape therefore created a heterogeneous grain size distribution across the epoxy grain mount. To ensure that a representative amount of fine and coarse grained material was selected during LA-ICP-MS analyses, analysis spots were placed on grains in every quadrant across the grain mount. During laser spot placement, more than 130 laser spots were placed on any grains that appeared to be a relevant datable grain (zircon, rutile). Grains were selected for analysis from all grain shapes and sizes.

Vermeesch (2004) concluded that in order to be 95% certain that no age population >5% is excluded in provenance investigations at least 117 grains must be dated per sample. The number of grains (n) analyzed per sample in this study was commonly >117 and therefore data that were >15% discordant could be filtered out while still having enough age data to fit the criterion of Vermeesch (2004) and for meaningful probability density plots to be constructed (Vermeesch, 2004). Relative to standard mineral separation procedures, the mineral separation and data acquisition procedures outlined above are interpreted to be following best practice procedures in minimizing potential bias.

3.6 Data Reduction Scheme for LA-ICP-MS U-Pb and Trace Element Analyses

U-Pb LA-ICP-MS data from analyses of sediments from the Greater Green River Basin were processed using the PepiAGE program, and the Iolite® software for trace elements. Among other aspects, the PepiAGE program corrects for down-hole mass fractionation, corrects for drift throughout the measurement, and allows both manual and automatic outlier filtering (Dunkl et al., 2009). The processed masterfile was exported from PepiAGE (Dunkl et al., 2009) and imported into Isoplot/Ex® (Ludwig, 2003). Isoplot/Ex® was used to construct U-Pb probability density/histogram plots and U-Pb concordia diagrams, and to calculate the weighted average of U-Pb age populations. U-Pb LA-ICP-MS data from analyses of sediments from the Book Cliffs were processed using VisualAge DRS in Iolite® (Paton et al., 2010, 2011). This program corrects for down-hole mass fractionation and has the option to correct for common Pb and Pb-loss using the Andersen (2002) model. The data was exported including propagated and internal errors in the exported masterfile. Data was further processed in Isoplot/Ex® producing probability density/histogram plots and calculating weighted mean averages for age populations (Ludwig, 2003). Age data >15% discordant were not used in the construction of probability density plots, but where retained for the concordia diagram plots.

The Iolite® software was also employed for data reduction of rutile LA-ICP-MS trace element determinations (Paton et al., 2010, 2011). Collected data were exported from Iolite and imported into Excel, where niobium and zirconium contents were plotted versus the age of the rutile grains. The zirconium content was also used to calculate the crystallization temperature of rutile grains using the calibration equation of Watson et al. (2006).

3.7 Variations of Zircon and Rutile U-Pb Age Signatures Using Standard Mineral Separation Procedures and the Developed Mineral Separation Method

A sandstone sample from the Dad Member of the Lewis shale (GR-09-19) was divided into three aliquots (GR-09-19A; GR-09-19B; GR-09-19C) and each aliquot was separated using a different mineral separation procedure. Each aliquot was analyzed using LA-ICP-MS to detect variations in the resulting zircon U-Pb age signatures. The whole rock sample was crushed and sieved to <500 μm and representatively split into three aliquots. One sample aliquot was processed with standard mineral separation procedures with water-table separation, heavy liquid separation, and Frantz Isodynamic magnetic separation at a setting of 1.8 A at 5^{o} (GR-09-19C).

During Frantz magnetic separation, it was common for zircon to be present in the magnetic fraction above a current setting of 0.7 A. Therefore, a second aliquot was processed through water table separation, heavy liquids separation, but Frantz Isodynamic magnetic separation only to a maximum current of 0.7 A at 10^{o} (GR-09-19B). The third aliquot was only processed by heavy liquid separation (GR-09-19A). The mineral grains from these different separation procedures were mounted in epoxy and LA-ICP-MS U-Pb dating of the zircon content was performed. U-Pb LA-ICP-MS results of zircon from samples GR-09-19A, GR-09-19B, and GR-09-19C are described in chapter 4 section 1 and are represented in figure 14.

For rutile, samples GR-09-14 and GR-09-19 from the Greater Green River Basin were separated using two different mineral separation procedures. The two samples are from the Dad Member of the Lewis shale (GR-09-19) and from the Almond formation (GR-09-14). Each sample was representatively split in half in preparation for two different mineral separation procedures (GR-09-14A and GR-09-14B; GR-09-19A and GR-09-19B). One aliquot from the Dad member (GR-09-19B) and one aliquot from the Almond Formation (GR-09-14B) were separated using exclusively Bromoform heavy liquid separation. One aliquot from the Dad member (GR-09-19B) and one aliquot from the Almond Formation (GR-09-14B) were separated using standard mineral separation procedures that includes Frantz magnetic separation to 1.8 A at 5^{o}. The mineral grains from these different separation procedures were mounted in epoxy and LA-ICP-MS U-Pb dating of the rutile was performed. U-Pb LA-ICP-MS results of rutile from samples GR-09-14A, GR-09-14B, GR-09-19A, and GR-09-19B are described in chapter 4 section 2 and represented in figure 15.1-4.

Chapter 4. Results for Testing Various Mineral Separation Procedures

LA-ICP-MS U-Pb analyses are used in this study to test the effect various mineral separation methods have on the resulting U-Pb age data. The results of analyses of Greater Green River Basin, Wyoming sedimentary rocks are described in the following section.

4.1 LA-ICP-MS U-Pb Age Data of Zircon Using Different Mineral Separation Procedures

Figure 14 shows three zircon U-Pb probability density plots for zircon fractions from a sample of the Dad Member of the Lewis Shale (GR-09-19). Zircon from one fraction of Dad Member was obtained using exclusively Bromoform heavy liquid separation methods (GR-09-19A; Figure 14). Zircon from another fraction of Dad Member was separated at a Frantz setting of 0.7 A at 10^{o} (GR-09-19B; Figure 14). Zircon from a third fraction from GR-09-19 was separated at a Frantz setting of 1.8 A at 5^{o} (GR-09-19C; Figure 14), which is the setting used in standard mineral separation methods for zircon.

All samples show significant U-Pb age populations at 70-80 Ma, 92-98 Ma, 400-500 Ma, 1000-1100 Ma, 1400-1550 Ma, and ~1700 Ma. However, sample GR-09-19A that was separated using only Bromoform also contained U-Pb age peaks at 600-700 Ma and 2200-2400 Ma, which were not detected in samples that were magnetically separated using the Frantz (GR-09-19B and GR-09-19C). A U-Pb age peak at ~2715-2775 Ma was detected in GR-09-19A and GR-09-19B, but not in sample GR-09-19C (Figure 14).

4.2 LA-ICP-MS U-Pb Age Data of Rutile Using Different Mineral Separation Procedures

Samples from the Almond Formation (GR-09-14) and the Dad Member of the Lewis shale (GR-09-19) from the Greater Green River Basin, Wyoming were used to detect potential variations in U-Pb age spectra of rutile due to the use of the Frantz Isodynamic magnetic separator. Each sample was representatively split in half in preparation for two different mineral separation procedures (GR-09-14A and GR-09-14B; GR-09-19A and GR-09-19B). One aliquot from the Dad Member (GR-09-19A) and one aliquot from the Almond Formation (GR-09-14A) were separated using only Bromoform heavy liquid. One aliquot from the Dad Member (GR-09-19B) and one aliquot from the Almond Formation (GR-09-14B) were separated using standard mineral separation procedures including Frantz magnetic separation to 1.8 A at 5^{o}. The resulting sample fractions from these different separation procedures were mounted in epoxy and LA-ICP-MS U-Pb dating of the containing rutile was performed.

All four sample aliquots described above contain significant age populations at ~400-600 Ma and ~1600-2000 Ma (Figure 15.1-15.4). The most significant difference between the aliquots treated with the different separation methods is the amount of discordant analyses in the U-Pb age data. LA-ICP-MS U-Pb analyses of rutile that was non-magnetic at a Frantz setting of 1.8A and 5° contained a higher percentage of concordant U-Pb age data (GR-09-14B, Figure 15.2; GR-09-19B, Figure 15.4) than the rutile from the aliquots not magnetically separated (GR-09-14A, Figure 15.1; GR-09-19A, Figure 15.3).

Chapter 5. Results for Sedimentary Rocks from the Greater Green River Basin, Wyoming

5.1 QEMSCAN® Data

The mineralogical data collected using the QEMSCAN® are assessed in volume percent (vol. %) diagrams (Figure 16). All minerals with a vol. % <1 in all samples were not plotted because they were judged to be not quantitatively significant. Since heavy minerals are used in this study to mark relevant changes in mineralogy between samples, quartz was also removed from the original dataset. After the data were thus filtered for low vol. % minerals and quartz, the mineralogical data was normalized to 100%, plotted with Excel© (Figure 16.1-4) and listed in stratigraphic order from youngest to oldest.

Samples from the Greater Green River Basin have notable variations in the vol. % of pyrite, barite, and TiO_2 minerals (Figure 16.1-4). The Fox Hills Sandstone (GR-09-05) is the highest stratigraphic unit sampled and contains the largest amount of pyrite with 2.9 vol. % (Figure 16.1). Underlying the Fox Hills Sandstone are the Dad Member (GR-09-19; Figure 16.2) and the Almond Formation (GR-09-14; Figure 16.3). Pyrite was not detected in either of these samples. The Pine Ridge Sandstone (GR-09-09) is the lowest stratigraphic unit sampled and contains just 0.5 vol. % of pyrite (Figure 16.4).

There is a large variation in the vol. % of TiO_2 minerals measured across all analyzed samples. The Fox Hills Sandstone (GR-09-05) contains 8 vol. % of TiO_2 minerals (Figure 16.1). The underlying Dad Member (GR-09-19) contains ~1 vol. %, which is the lowest vol. % of TiO_2 minerals measured between all samples (Figure 16.2). Stratigraphically below the Dad Member, the Almond Formation sample (GR-09-14; Figure 16.3) and the Pine Ridge Sandstone sample (GR-09-09; Figure 16.4) have the highest vol. % of TiO_2 minerals, with ~9 vol. % for the former and ~29 vol.% for the latter.

5.2 LA-ICP-MS U-Pb Age Data of Zircon

Age probability diagrams and U-Pb concordia diagrams of LA-ICP-MS analyses of zircon from samples collected in the GGRB can be found in Figure 17. Samples are listed in stratigraphic order with the youngest samples at the top and oldest at the bottom. When constructing age probability diagrams, Pb^{206}/U^{238} dates were used for LA-ICP-MS analyses that are <800 Ma and Pb^{207}/Pb^{206} dates for LA-ICP-MS analyses that are >800 Ma. U-Pb LA-ICP-MS analyses that are >15% discordant were not used for the age probability diagrams. However, all U-Pb LA-ICP-MS analyses were included in the U-Pb concordia diagrams.

U-Pb LA-ICP-MS analyses of zircon from samples collected in the GGRB show three significant concordant age populations in all samples (Figure 17). The oldest major concordant U-Pb age population includes a Paleoproterozoic group with a concordant age range of ~1600-1800 Ma. The second oldest major population has a concordant age range of ~400-700 Ma. The youngest population has a concordant age range of 70-120 Ma and constitutes the largest population in the age-probability diagrams. U-Pb age data of zircon from these sedimentary rocks show minor or less abundant populations with age ranges of ~1000-1200 Ma and ~1400-1450 Ma. A population at 340-370 Ma is present in the Fox Hills sandstone (GR-09-05), Almond Formation (GR-09-14), and the Pine Ridge Sandstone (GR-09-09) samples. A significant age population at 2650-2700 Ma is present in the Pine Ridge sandstone sample (GR-09-09) and the Dad Member of the Lewis Shale (GR-09-19). The LA-ICP-MS U-Pb age data of zircon from the Greater Green River Basin, Wyoming are listed in appendix C (Table A-1-4).

5.3 LA-ICP-MS U-Pb Age Data of Rutile

LA-ICP-MS U-Pb data for rutile from the GGRB sediments produced a large amount of discordant data (Figure 18.1-4). However, there are two significant U-Pb age populations that are

>85% concordant. All samples showed significant concordant U-Pb age populations at ~100 Ma, and 400-600 Ma. Rutile from the Fox Hills Sandstone (GR-09-05; Figure 18.1), Dad Member (GR-09-19; Figure 18.2), and the Almond Formation (GR-09-14) have U-Pb age populations at 1600-1800 Ma (Figure 18.3). Rutile from the Dad Member (GR-09-19) contains a significant age population at 1800-2200 Ma (Figure 18.4). The LA-ICP-MS U-Pb age data of rutile from the GGRB are listed in appendix D (Table B-1-4).

Chapter 6. Results for Sedimentary Rocks from the Book Cliffs, Utah

6.1 QEMSCAN® Data

The mineralogical data collected using the QEMSCAN® are plotted in vol. % diagrams. Minerals with <1 vol. % abundance in all samples were not plotted. Since heavy minerals are used in this study to assess relevant mineralogical changes between samples, quartz was also removed from the original dataset. After these filters were applied, the data were renormalized to 100% and plotted with Excel© (Figure 19.1-10). QEMSCAN® analyses of samples from the Book Cliffs, Utah, are described below in stratigraphic order from oldest to youngest (Figure 19.1-10).

Samples from the Book Cliffs have notable variations in the vol. % of pyrite, barite, apatite, ilmenite, and TiO_2 minerals (Figure 19.1-10). The deltaic sample of the LST from the Panther Tongue of the Star Point Formation (11-PTH-09; Figure 19.1) contains 3.4 vol. % of barite, whereas a sample from a transgressive lag deposit of the Panther Tongue LST (10-PTH-01; Figure 19.2) contains 0.1 vol. % of barite. Both samples (11-PTH-09; Figure 19.1)(10-PTH-01; Figure 19.2) from the Panther Tongue show remarkably similar vol. % of zircon and TiO_2 polymorphs. The deltaic sample (11-PTH-09; Figure 19.1) has 16.9 vol. % of TiO_2 polymorphs and the transgressive lag deposit (10-PTH-01; Figure 19.2) has 17.5 vol. % of TiO_2 polymorphs. The deltaic sample (11-PTH-09; Figure 19.1) has 32.5% vol. of zircon and the transgressive lag deposit (10-PTH-01; Figure 19.2) has 39.3% vol. of zircon.

The two HST samples from the Spring Canyon Member show heavy mineral differences, with a higher amount barite and a lower amount of TiO_2 polymorphs in the transgressive lag deposit of the Spring Canyon Member (11-SPC-01; Figure 19.3) relative to the shoreface sandstone of the Spring Canyon Member (11-SPC-05; Figure 19.4). The transgressive lag deposit of the Spring Canyon Member (11-SPC-01; Figure 19.3) has a high amount of barite at 13.7 vol. %, whereas the shoreface sandstone of the Spring Canyon (11-SPC-05; Figure 19.4) has only 3.5 vol. %. The shoreface sandstone of the Spring Canyon (11-SPC-05; Figure 19.4) has a higher amount of TiO_2 polymorphs at 37.1 vol. % compared to the transgressive lag deposit (11-SPC-01; Figure 19.3) with 19.5 vol. %. Both samples have a similar abundance of ilmenite with 3.4 vol. % for the transgressive lag deposit (Figure 19.3) and 2.5 vol. % for the shoreface sandstone (Figure 19.4).

Comparing the LST of the Aberdeen Member (11-AB-LST; Figure 19.5) to the shoreface sandstone HST of the Spring Canyon Member (11-SPC-05; Figure 19.6) shows notable variations in the vol. % of barite, pyrite, ilmenite, and TiO_2 polymorphs. The LST of the Aberdeen Member (11-AB-LST; Figure 19.5) has 7.3 vol. % of pyrite, whereas the HST of the Spring Canyon Member has only 0.2 vol. % (11-SPC-05; Figure 19.6). The HST of the Spring Canyon Member (11-SPC-05; Figure 19.6) contains 2.5 vol. % of ilmenite, 3.5 vol. % of barite and 37.1 vol. % of TiO_2 minerals whereas the LST of the Aberdeen Member contains 0.4 vol. % ilmenite, no barite and 22.3 vol. % TiO_2 minerals (Figure 19.6).

LST (11-BH-06) and HST (11-TUS3C-2-17) of the Desert Member of the Blackhawk Formation contain similar abundances of TiO_2 polymorphs, ilmenite, and apatite, (Figure 19.7), but the LST (11-BH-06) has a relatively high pyrite signal of 4.7 vol. %. (Figure 19.7), whereas the HST (11-TUS3C-2-17) has only 0.1 vol. % pyrite (Figure 19.8). The incised valley fill sample (11-TUS3C-22.3-22.4) of the Castlegate Sandstone contains high amounts of TiO_2 polymorphs (18.9 vol. %) and barite (18.7 vol. %; Figure 19.10) relative to the other incised valley fill sample (11-CSTG-07; Figure 19.9) with no barite and 11 vol. % TiO_2 minerals. Illite, kaolinite, chlorite, calcite, and dolomite are not mentioned above because these minerals do not show significant variation between samples or the vol. % measured is too low to be significant or reliable.

6.2 LA-ICP-MS U-Pb Age Data of Zircon

Age probability diagrams and U-Pb concordia diagrams of LA-ICP-MS analyses of zircon from samples collected in the Book Cliffs, Utah are shown in Figures 20.1-5. Samples are listed in stratigraphic order from oldest to youngest. When constructing the age probability diagrams, Pb^{206}/U^{238} dates were used for LA-ICP-MS analyses <800 Ma and Pb^{207}/Pb^{206} dates were used for LA-ICP-MS analyses >800 Ma. U-Pb LA-ICP-MS analyses that were >15% discordant were not used for the age probability diagrams, but all U-Pb LA-ICP-MS analyses are included in the U-Pb concordia diagrams.

The oldest stratigraphic unit analyzed in this region is the LST of the Panther Tongue within the Star Point Formation. The samples (11-PTH-09 and 10-PTH-01) share significant age populations at approximately 95 Ma, 430 Ma, 1000 Ma, 1200 Ma, 1450 Ma and 1600 Ma (Figure 20.1). The deltaic sample of the Panther Tongue (11-PTH-09) has additional age populations at ~300 Ma, and 600 Ma, which are not present in sample from the transgressive lag deposit (10-PTH-01). The deltaic sample shows a higher number of grains at ~1750 Ma (n=~8) compared to the sample from the transgressive lag deposit (n=2), whereas the transgressive lag deposit sample has a more significant Late Archean age peak at ~2550 Ma (n=7) compared to the deltaic sample (n=1)(Figure 20.1).

Zircons from samples collected in the HST of the Spring Canyon Member show only minor differences in U-Pb age signature. Both the shoreface sandstone (11-SPC-05) and the transgressive lag deposit (11-SPC-01) have significant age populations at ~95- Ma, 370-420 Ma, 590-615 Ma, 1000-1050 Ma, 1150 Ma, and 1700-1760 Ma (Figure 20.2). However, the transgressive lag deposit (11-SPC-01) of the Spring Canyon has an additional minor age peak at ~2100 Ma (n=~2) not present in the shoreface sandstone (11-SPC-05). The shoreface sandstone sample (11-SPC-05) has 2 grains with an age ~165 Ma not present in the transgressive lag deposit sample (11-SPC-01) (Figure 20.2).

Up-section, the shoreface sandstone HST sample of the Spring Canyon Member (11-SPC-05) and the LST of the Aberdeen Member (11-AB-LST) share all age peaks, but diverge in the number of grains at each age peak (Figure 20.3). Both HST (11-SPC-05) and the LST (11-AB-LST) samples contain U-Pb age populations U-Pb at ~90-95 Ma, 165 Ma, 400 Ma, 590-615 Ma 1000-1060 Ma, 1100-1150 Ma, 1350 Ma, 1500 Ma, 1700-1750 Ma, and 2600 Ma. However, the proportion of grains analyzed at U-Pb age peaks of 400 Ma, 590-615 Ma, 1350 Ma, and 2600 Ma differed. Compared to the HST sample, the LST sample contains more grains at 400 Ma (n=5 vs. n=2), ~590-615 Ma (n=5 vs. n=1), ~1350 Ma (n=6 vs. n=1), and ~2600 Ma (n=3 vs. n=1) (Figure 20.3).

The HST (11-BH-06) and LST samples (11-TUS3C-2-17) of the Desert Member both have significant age populations at ~95-110 Ma, ~400-425 Ma, ~950 Ma, 1450 Ma, and 1700-1750 Ma (Figure 20.4). Compared to the HST sample, the LST sample contains more grains at ~270 Ma (n=4 vs. n=1) and 2550 Ma (n=5 vs. n=1). HST sample (11-BH-06) of the Desert Member has a significant age peak at ~660 Ma, which is not detected in the LST sample (11-TUS3C-2-17; Figure 20.4).

The LST samples from the Castlegate Sandstone have significant age populations at ~80-95 Ma, 1100 Ma, 1350 Ma, 1700 Ma, 2100 Ma and 2700 Ma (Figure 20.5). Age peaks at ~450 Ma, 600 Ma, 750-800 Ma, 1200 Ma, and 1500 Ma are also present in both the LST (11-CSTG-07, Incised valley fill; 11-TUS3C-22.3-22.4, Incised valley fill) samples. However, the proportion of grains at these ages varies significantly despite similar total grain numbers (n=86 vs. n=92). Sample 11-CSTG-07 contains n=3 at 450 Ma, n=4 at 600 Ma, n=2 at 750-800 Ma, n=7 at 1200 Ma, and n=11 at 1500 Ma. Sample 11-TUS3C-22.3-22.4 overall has a lower n at these age peaks with n=1 at 450 Ma, n=~1 at 600 Ma, n=~5 at 750-800 Ma, n=1 at 1200 Ma, and n=1 at 1500 Ma (Figure 20.5). Sample 11-CSTG-07 of the Castlegate sandstone contains a higher proportion of older zircons. The LA-ICP-MS U-Pb age data of zircon from the Book Cliffs, Utah can be reviewed in the tables found in appendix E.

6.3 LA-ICP-MS U-Pb Age Data of Rutile

Samples that contain >117 rutile grains for U-Pb dating included the HST of the Spring Canyon Member, HST and LST of the Desert Member, and the LST of the Castlegate (Figure 21.1-3). The HST of the Spring Canyon Member has concordant U-Pb age populations at ~300-600 Ma, 1400 Ma, 1600-1800 Ma and 2600-2800 Ma (Figure 21.1). The HST and LST of the Desert Member share concordant U-Pb age populations at ~200 Ma, 400-600 Ma, 1600-1800, and 2000-2200 Ma (Figure 21.2). The LST samples of the Castlegate Sandstone has concordant U-Pb age populations at ~300-600 Ma, 1000-1200 Ma, 1400-1800, and 1800-2000 Ma (Figure 21.3). All samples have a large amount of U-Pb analyses that are more than 15% discordant. The LA-ICP-MS U-Pb age data of rutile from the Book Cliffs, UT can be reviewed in the tables found in appendix F.

6.4 LA-ICP-MS Trace Element Determinations of Rutile

Concentrations of zirconium (Zr) and niobium (Nb) were analyzed in four samples from the Book Cliffs sample set: from the LST samples of the Castlegate Member (11-CSTG-07; 11-TUS3C-22.3-22.4), the HST of the Desert Member (11-BH-06) and the LST of the Desert Member (11-TUS3C-2-17). All four samples analyzed showed similar relationships when plotting Nb versus age, and Zr versus $^{206}Pb/^{238}U$ age (Figure 22.1-4). Rutiles with dates of ~400-600 Ma have Zr concentrations ranging from 0 to 2000 ppm, with the majority of rutile of this age clustering at ~500 ppm. Rutile that are >600 Ma old consistently show Zr concentrations ranging between 100-750 ppm and do not show any significant clustering around a mean value.

Niobium versus age graphs show similar relationships to the Zr versus age graphs. Rutile with dates of 400-600 Ma show the most significant clustering of Nb concentrations. Most analyses in all samples have Nb concentrations ranging of ~1000-9000 ppm for rutile of the 400-600 Ma age group. Rutile from the HST sample from the Desert Member had lower Nb concentrations at the age of ~500 Ma that ranged from 0-4000 ppm. Rutile older than 600 Ma has Nb concentrations ranging between 0-6000 ppm without significant clustering. The LA-ICP-MS trace element data of rutile from the Book Cliffs, Utah are listed in tables E1-E4 in appendix G.

Discussion

Chapter 7. Interpretation of Results from Greater Green River Basin, Wyoming Samples

7.1 The Potential Influence of Mineral Separation Procedures on Provenance Analyses

The results that highlight the effect standard mineral separation procedures have on provenance analyses using zircon and rutile is discussed in the following section. LA-ICP-MS U-Pb analyses are used in this study to test the effect various mineral separation methods has on the resulting U-Pb age data.

According to Sircombe and Stern (2002), there is a correlation between magnetic susceptibility of zircon grains and discordance of U-Pb analyses. They concluded that the degree of discordance increases with the degree of magnetic susceptibility (Sircombe and Stern, 2002). However, in this study and shown in the test described above (Ch. 4.1, Figure 14), 4% of U-Pb analyses were >10% discordant for zircon minerals that were separated using only heavy liquids (GR-09-19A; Figure 14) whereas approximately 7% of U-Pb analyses were >10% discordant for zircon grains that were separated using a Frantz setting of 0.7 A and 5° (GR-09-19B; Figure 14) and approximately 2% of U-Pb analyses were >10% discordant for zircon grains separated using a Frantz setting of 1.8 A and 5° (GR-09-19C; Figure 14). Therefore, this study suggests that the Frantz magnetic separator has a negligible effect on the degree of discordance for U-Pb analyses of zircon.

Results from this study indicate that separating zircon grains using the Frantz magnetic separator can alter the resulting U-Pb age spectrum, but not discordance. U-Pb analyses of the aliquot of sample GR-09-19A (Figure 14), separated using only heavy liquids (GR-09-19A) contained a significant age populations at ~2715-2775 Ma (n=4), which was not detected in the aliquots separated using the Frantz magnetic separator (GR-09-19B; GR-09-19C; Figure 14).

Aliquot GR-09-19A also contains a higher amount of grains at 600-700 Ma (n=3)(Figure 14) relative to the aliquot GR-09-19B (n=1) and GR-09-19C (n=1) (Figure 14). Due to this change in the proportion of zircon grains at these U-Pb age groups, it is interpreted that using the Frantz magnetic separator influences the age proportions of zircon grains analyzed. Since the Frantz magnetic separator has only a small effect on the degree of discordance and can alter the resulting U-Pb age signature, separating zircon based on magnetic susceptibility is interpreted as a superfluous mineral separation step for LA-ICP-MS analyses of zircon. However, it was found in this study that using the Frantz magnetic separator was necessary prior to U-Pb and trace element analyses of rutile.

Rutile from sample aliquots that were magnetically separated contained a higher number of concordant U-Pb analyses. Samples collected from the Almond Formation (GR-09-14) and the Dad Member of the Lewis shale (GR-09-19) from the GGRB were used to determine how the Frantz magnetic separator alters the resulting U-Pb age signature of rutile. Both GR-09-14 and GR-09-19 were split into two sample aliquots (GR-09-14A, GR-09-14B; GR-09-19A, GR-09-19B). One aliquot from each sample was magnetically separated at a setting of 1.8 A and 5° (GR-09-14B and GR-09-19B) and one aliquot from each sample was not magnetically separated (GR-09-14A and GR-09-19A). Between 25 and 33% of U-Pb analyses were >15% discordant in the aliquots separated using only heavy liquids (GR-09-14A, Figure 15.1; GR-09-19A; Figure 15.3). Only 14-17% of U-Pb analyses were >15% discordant in aliquots separated using a Frantz setting of 1.8 A and 5° (GR-09-14B, Figure 15.2; GR-09-19B, Figure 15.4).

There are several possible reasons for rutile U-Pb analyses to be discordant. As mentioned above in the section 3.2 that reviews the mineral separation techniques, anatase, brookite, and rutile are TiO2 polymorphs that are chemically identically and cannot be distinguished from one another by SEM or EDAX (Triebold et al., 2011). According to Triebold (2012), anatase and brookite have systematically different trace element compositions to that of rutile. Anatase and brookite contain very low concentrations of U and proportionally high concentrations of Pb, which makes them difficult to date using U-Pb geochronology (Zack, 2004; Triebold et al., 2011). Therefore, it is possible that the mineral grains that resulted in U-Pb analyses that were >15% discordant and/or have nominal dates >4.5 Ga are actually anatase or brookite.

Partial Pb-loss during a low-grade metamorphic event can result in discordant U-Pb analyses of rutile (Mezger et al., 1989; Möller et al., 1995; Kooijman et al., 2010). Mezger (1989) states that partial homogenization of isotopes during a heating event of isotopes can occur if temperatures do not exceed 430°C, which would result in discordant U-Pb analyses. Also, during slow cooling Pb diffusion can occur resulting in discordant U-Pb analyses (Blackburn et al., 2011) Lastly, rutile grains can become contaminated by Pb during breakdown reactions associated with diagenetic processes and alteration (Zack et al., 2004). During these processes Pb may contaminate rutile grains and therefore result in highly discordant U-Pb analyses. It is common for Fe-oxides and/or hydroxides to contaminate rutile grains during diagenesis and alteration (Zack et al., 2004). Therefore, only the least magnetic rutile fractions were used for analyses in this study. U-Pb analyses in this study show that rutile that was magnetically separated using the Frantz Magnetic separator resulted in ~9-15% more U-Pb analyses that were <15% discordant (Figure 15.1-4).

7.2 Interpretation of QEMSCAN® Data of Sedimentary Rocks from the Greater Green River Basin, Wyoming

As stated by Morton and Hallsworth (1994) the abundances of heavy minerals can provide a valuable insight in to the characteristics of a source rock. The abundance of heavy minerals in sedimentary units is heavily influenced by processes associated with sediment transport, deposition, and diagenesis (Morton and Hallsworth, 1994). However, certain mechanically and chemically stable heavy minerals survive these geologic processes without significant modification and are particularly suited for provenance investigations (Morton and Hallsworth, 1994). Minerals such as the TiO_2 polymorphs, pyrite, zircon, and apatite are relatively unaffected by destructive processes associated with the sedimentary cycle (Morton and Hallsworth, 1994). However, pyrite should be used with caution because it is possible that it can be authigenic, it may crystallize during or after deposition of these sedimentary units (Love et al., 1983; Qing, 1981). The heavy minerals used in this study include pyrite and TiO_2 polymorphs such as rutile, brookite and anatase. The presence of pyrite in the Fox Hills Sandstone potentially marks the input of pyrite into the basin from a source area that did not contribute to the deposition of the underlying Dad Member (Figure 1 and Figure 16.1-2). Pyrite extracted from the Fox Hills sandstone was examined using QEMSCAN® and optical microscopy and based on the mineral euhedral shape of the pyrite grains it is interpreted not to be authigenic.

Variations in the modal percentage of TiO_2 polymorphs potentially represent fluctuations in the source of sediment during the deposition of the sedimentary units of the GGRB. The TiO_2 polymorphs rutile, anatase, and brookite are common accessory minerals in metamorphic and igneous rocks (Force, 1980; Tropper & Manning 2008). The Dad member of the Lewis shale contains the lowest volume percent of TiO_2 minerals with 2.2 vol % (Figure 16.2). The sample from the Pine Ridge Sandstone, deposited earlier at ca. 72 Ma (Pyles and Slatt, 2000; Figure 1) on the other hand contains the highest abundance of rutile at 32.0 vol %, which represents the strongest influence of rutile-bearing source rocks in the sampled sequences (Figure 16.4). Therefore, I conclude that there was a transition to source rocks with relatively low abundances of rutile during the deposition of the Dad Member at 69.9-70.4 Ma, which is accordance with the interpretation of Pyles and Slatt (2000).

7.3 Interpretation of LA-ICP-MS U-Pb Results for Zircon from the Greater Green River Basin, Wyoming

The LA-ICP-MS U-Pb data of zircon from the Greater Green River Basin samples shows three significant age populations that potentially represent three different sediment source areas. A ~1600-1800 Ma Paleoproterozoic group is interpreted to represent sediment sourced from the Yavapai-Mazatzal terrane, which has extensive exposures in the western Sevier Orogenic belt in the late Cretaceous (Figure 4 and 7; Dickinson and Gehrels, 2009; Whitmeyer and Karlstrom, 2007; Blakey, 2008). The second significant age population has an age range of ~400-700 Ma, which can be interpreted as a detrital component from the Appalachian orogen in the southeast (Figure 4, Dickinson and Gehrels, 2009). The most abundant U-Pb age population in all analyzed samples is at ~70-120 Ma and is interpreted as first cycle detrital input from the Sevier Orogenic belt. Though it cannot be ruled out, it is assumed that there is not enough lag time for zircon of the youngest age to be significantly recycled and re-deposited into the basin. It is possible and likely that the older zircon where recycled from previously deposited sediment and redeposited in the KWIS.

U-Pb data of zircon in the samples from the GGRB also shows a less significant U-Pb age population at 1000-1200 Ma, interpreted to represent sediment from either the Grenville orogenic belt or the Llano Province (Figure 4; Dickinson and Gehrels, 2009; Whitmeyer and Karlstrom, 2007). Due the large geographical distance between the KWIS and the Grenville Orogenic belt, there would need to be a very large drainage system that transported sediment directly into the basin from the northeast. Another possibility would be that the sediment derived from this terrane could have been repeatedly recycled until finally deposited in the KWIS.

However, paleocurrent measurements conducted in the sedimentary units of the GGRB do not show any significant trend of sediment transport from the northeast (Pyles and Slatt, 2007). Also, CL images of the zircon grains of this age do not exhibit a more rounded grain shape or size difference relative to other imaged zircons (CL images, Appendix. A). The other potential source regions would be closer, may easier explain the lack of additional rounding, and require drainage and transport from the south or southwest. Pyles and Slaat paleocurrent measurements support a south to south-south west drainage pattern and transport direction (Pyles and Slatt, 2007).

The oldest U-Pb population at ~2700 Ma first appears in the Dad member of the Lewis Shale and is interpreted to represent sediment sourced from the Superior Province or the Wyoming-Hearne-Rae terrane in the north, or the immediately adjacent Wind River Uplift, Granite Mts. or Sierra Madre. This U-Pb population at ~2700 Ma was not detected in the underlying Almond formation or the overlying Fox Hills sandstone. Therefore, this U-Pb population represents a shift in the source of sediment or sediment transport during the deposition of the Dad member of the Lewis shale at 69.9-70.4 Ma (Pyles and Slatt 2007; Figure 1). This interpretation is supported by paleocurrent measurements that show a north to south trend of sediment transport (Figure 10; Pyles and Slatt, 2007) with an area of high elevation in modern-day Wind River Range.

7.4 Interpretation of LA-ICP-MS U-Pb Analyses of Rutile from Greater Green River Basin, Wyoming

Rutile is a mechanically robust mineral that can be used a geochronometer, which provides insight in to the cooling history of metamorphic terranes (e.g. Kooijman et al., 2010; Mezger et al., 1989; Möller et al., 1995; Möller et al., 2000; Zack et al., 2004). Since rutile is not stable at greenschist facies conditions and its closure temperature for Pb (T_c) has been determined empirically at 430-550° C, U-Pb analyses provide valuable information about the cooling through greenschist facies conditions after the last higher grade metamorphic cycle (e.g. Kooijman et al., 2010; Mezger et al., 1989; Möller et al., 1995; Möller et al., 2000; Zack et al., 2004). U-Pb analyses of rutile from the samples collected in the Greater Green River Basin contain three significant T_c age populations that are consistent with the zircon U-Pb analyses. However, a detailed interpretation is hampered by the large analytical errors and the high amount of discordant data. Within the admittedly unsatisfactory precision of the U-Pb data obtained on rutile age populations from this study it can be assumed that there are only small differences between the rutile U-Pb T_c age and zircon U-Pb crystallization age. The rutile T_c age populations are used here to support interpretations made using zircon U-Pb ages and further characterize the sources of sediment.

Significant rutile T_c age populations at ~1600-1800 Ma, ~400-600 Ma, and ~100 Ma were detected in all samples collected from the GGRB. The oldest age population consists of an ~1600-1800 Ma Paleoproterozoic group interpreted as sediment sourced from the Yavapai-Mazatzal terrane (Figure 4). The second group has an age range of ~400-600 Ma interpreted as sediment sourced from the Appalachian orogen (Figure 4; Dickinson and Gehrels, 2009; Whitmeyer and Karlstrom, 2007) or potentially from the Amarill-Wichita block or Yucatan-Campeche and Suwanee terranes, in the south and southeast (Figure 4). The third U-Pb age population at ~100 Ma is interpreted as a first cycle input of sediment sourced from the Sevier Orogenic belt (Figure 4; Dickinson and Gehrels, 2009). The Dad member of the Lewis Shale contains an age population at ~1800-2200 Ma not detected in other analyzed samples from the GGRB. This age population chronologically overlaps with the Trans-Hudson terrane, which occupied the northern extent of the North American craton in the late Cretaceous (Figure 4; Dickinson and Gehrels, 2009; Whitmeyer and Karlstrom, 2007). The detection of this age population at ~1800-2200 Ma further supports a change in the source of sediment or in sediment transport during the deposition of the Dad member of the Lewis.

Chapter 8. Interpretation of Results from the Book Cliffs, Utah

8.1 Interpretation of QEMSCAN® Data of Sedimentary Rocks from the Book Cliffs, Utah

The results of QEMSCAN® analyses of heavy mineral separates from the Book Cliff can are described in chapter 5.1 and shown in figures 19.1-10. The results of QEMSCAN® heavy mineral analyses of samples from the Book Cliffs, Utah are discussed below starting with the oldest stratigraphic units (Figure 19.1-10). These QEMSCAN® analyses were acquired to detect the control sequence stratigraphic system tracts and the environment of deposition has on the percentage of heavy minerals in the studied samples.

There are notable differences in the vol. % of pyrite and TiO_2 polymorphs when comparing QEMSCAN® analyses from different sequence stratigraphic system tracts within the units sampled at the Book Cliffs, Utah. The shoreface sandstone from the HST of the Spring Canyon Member (11-SPC-05; Figure 19.4) of the Blackhawk Formation has 37.1 vol. % of TiO_2 minerals compared to 19.5 vol. % measured in the transgressive lag deposit of the Spring Canyon Member (11-SPC-01; Figure 19.3). This study proposes that there are two geological reasons for the variation in vol. % of TiO_2 polymorphs between these samples (11-SPC-05 and 11-SPC-01). During the deposition of the transgressive lag deposit, fine-grained material can be preferentially winnowed away from the deposited sediment (Hwang and Heller, 2002), resulting in a deposited sedimentary unit that consists of a greater percentage of coarse-grained material (Hwang and Heller, 2002). Erosion of fine-grained material from the deposited sediment could include TiO_2 minerals if they are mostly fine-grained. The other possibility is that there could have been a change in drainage patterns in the KWIS during the deposition of the shoreface sandstone of the Spring Canyon Member. In this case, the change in drainage patterns during the deposition of the shoreface sandstone of the Spring Canyon Member (11-SPC-05) would have resulted in a switch to a sediment source that contained a relatively higher amount of TiO_2 minerals. A change in sediment source area may be accompanied by a change in the age of the detrital minerals (zircon as well as rutile), which could be detected in the U-Pb age spectra discussed below (Ch. 8.2 and 8.3).

The LST of the Desert Member (11-TUS3C-2-17) and the LST of the Aberdeen Member (11-AB-LST) contain higher amounts of pyrite relative to the respective HST samples (11-BH-06; 11-SPC-05). The LST sample from the Desert Member (11-TUS3C-2-17; Figure 19.8) contains 4.7 vol. % of pyrite compared to 0.1 vol. % in the HST sample (11-BH-06; Figure 19.7). The LST of the Aberdeen Member (11-AB-LST; Figure 19.5) contains 7.3 vol. % of pyrite compared to 0.2 vol. % in the HST of the Spring Canyon Member (11-SPC-05; Figure 19.6). As stated in the previous paragraph, a change in drainage patterns in the KWIS during the deposition of the LST of these units could alter the location of the sediment source. It is also possible that during the LST, drainage patterns could have been different in such a way that they would facilitate better preservation of the sourced sediment resulting in higher vol. % of these indicator minerals to be deposited.

8.2 Interpretation of LA-ICP-MS U-Pb Results for Zircon from the Book Cliffs, Utah.

All sedimentary rock samples from the Book Cliffs, Utah have significant U-Pb age populations of zircon at 90-100 Ma, 400-600 Ma, 1000-1200 Ma, 1400 Ma, and 1600-1800 Ma (Figure 20.1-5). The U-Pb age population at 90-100 Ma is interpreted as a first cycle sediment input sourced from the Sevier Orogenic belt in the west (Figure 20.1-5). The 400-600 Ma population is interpreted as sediment sourced from the Appalachian orogen or further outboard terranes in the south or southeast (Figure 4 and 20.1-5; Dickinson and Gehrels, 2009; Whitmeyer and Karlstrom, 2007). The population with an U-Pb age range of 1000-1200 Ma is the most significant age population and represents sediment sourced either from the Grenville terrane in the east or the Llano Province (Figure 20.1-5; Dickinson and Gehrels, 2009). As stated above for the Greater Green River Basin samples, the large geographical distance between the KWIS and the Grenville Orogenic belt would make a very large drainage system necessary to transport sediment directly into the basin from the northeast. Another possibility would be that the sediment derived from this terrane could have been repeatedly recycled until finally deposited in the KWIS. The age population at ~1400 Ma potentially represents the mid-continent terrane from the landmass to the east of the KWIS (Figure 4, 7, and 20.1-5; Dickinson and Gehrels, 2009; Blakey 2008). Lastly, there is a significant ~1600-1800 Ma Paleoproterozoic group, which represents sediment sourced from the Yavapai-Mazatzal terrane (Figure 4 and 20.1-5; Dickinson and Gehrels, 2009).

The deltaic sandstone sample (11-PTH-09; Figure 20.1) of the Panther Tongue contains a significant U-Pb population at ~250-300 Ma not detected in the transgressive lag deposit (11-PTH-01; Figure 20.2). The shoreface sandstone (11-SPC-05) of the Spring Canyon Member also contains additional minor age peaks not detected in the transgressive lag deposit (10-PTH-01; Figure 20.2). The shoreface sandstone sample (11-SPC-05) has 2 grains with an age ~165 Ma not present in transgressive lag deposit sample (11-SPC-01) (Figure 20.2).

The transgressive lag deposits from the Panther Tongue (11-PTH-01) and the Spring Canyon Member (10-SPC-01) contain a higher amount of coarse sediment and heavy minerals relative to the deltaic sandstone and shoreface sandstone samples (11-PTH-09; 11-SPC-05). It is expected that the transgressive lag deposit would be coarser than the deltaic sandstone because during the deposition of the transgressive lag deposit the fine grained material commonly erodes away leaving only the coarse grained material (Hwang and Heller, 2002). If the deposited zircons with a U-Pb age of ~250-300 Ma (Panther Tongue) and ~165 Ma (Spring Canyon) were fine grained they could have been winnowed away during post-depositional processes associated with the transgressive lag deposit and thus removed from detrital minerals. This would lead to a different representation of the U-Pb age signature relative to the originally deposited sediment.

There are significant variations in U-Pb age signatures when comparing different system tracts. The LST of the Aberdeen Member (11-AB-LST) and the LST of the Desert Member (11-TUS3C-2-17) contain a high proportion of grains at each significant U-Pb populations relative to the HST of these units. The LST sample from Aberdeen Member (11-AB-LST) contains more grains at 400 Ma (n=5 vs. n=2), ~590-615 Ma (n=5 vs. n=1), ~1350 Ma (n=6 vs. n=1), and ~2600 Ma (n=3 vs. n=1) (Figure 20.3). The LST sample from the Desert Member contains more grains at ~270 Ma (n=4 vs. n=1) and 2550 Ma (n=5 vs. n=1). During lowstand conditions, drainage patterns could have been different in such a way that they would better preserve sediment of these ages. It is also possible that sources of sediment that were once inundated during periods of highstand conditions could potentially become areas of high geographical relief during lowstand condition, thus being eroded and becoming a new source of sediment.

Both incised valley fill samples (11-CSTG-07; 11-TUS3C-22.3-22.4) of the Castlegate Sandstone contain significant age populations at ~80-95 Ma, 1100 Ma, 1350 Ma, 1700 Ma, 2100 Ma and 2700 Ma (Figure 20.5). Age peaks at ~450 Ma, 600 Ma, 750-800 Ma, 1200 Ma, and 1500 Ma are also present in both LST samples. However, the proportion of grains at these ages varies significantly despite similar total grain numbers (n=86 vs. n=92). Therefore, there is significant variation in the U-Pb age signatures when samples from the same depositional facies.

8.3 Interpretation of LA-ICP-MS U-Pb Results of Rutile from Book Cliffs, Utah

Only five out of the nine sedimentary samples collected from the Book Cliffs, Utah contained more than 117 non-magnetic rutile grains for U-Pb LA-ICP-MS analyses. These sedimentary units may contain only low amounts of non-magnetic rutile but more rutile with a higher magnetic susceptibility, which would have been removed during Frantz magnetic separation. As discussed above, rutile can become altered during breakdown reactions associated with diagenetic processes and alteration (Zack et al., 2004). During diagenesis and alteration it is common for Fe-oxides and/or hydroxides to be included in rutile grains (Zack et al., 2004). Therefore, these samples could contain rutile that experienced breakdown associated with diagenetic processes and alteration and would be excluded from the sample fraction to be analyzed by using the Frantz magnetic separator (Zack et al., 2004). It was observed in this study that a large amount of rutile in these samples is magnetic at a Frantz setting of 0.7 A and 5°. It is therefore proposed that the low rutile contents in the samples is due to ilmenite exsolution or diagenetic and alteration processes that made the rutile grains magnetic.

Samples that contained more than 117 grains of rutile and made them suitable for LA-ICP-MS U-Pb analyses include the samples from the LST of the (11-CSTG-07; 11-TUS3C-22.3-22.4) of the Castlegate Sandstone (Figure 21.1), the HST (11-BH-06) and LST (11-TUS3C-2-17) of the Desert Member (Fig, 21.2), and the transgressive lag deposit (11-SPC-01) of the Spring Canyon Member (Figure 21.3). When comparing different system tracts from the same unit, the rutile U-Pb age signatures are indistinguishable. Both samples from the LST of the Castlegate Sandstone (11-CSTG-07; 11-TUS3C-22.3-22.4) contain U-Pb populations with age ranges from 300-600 Ma, 1000-1200 Ma, 1400-1800 Ma, and 1800-2000 Ma (Figure 21.1). The U-Pb age group from 300-600 Ma is interpreted as sediment sourced from the Appalachian Orogen in the east (Figure 4; Dickinson and Gehrels, 2009). The 1000-1200 Ma age group is interpreted as sediment being source from the Grenville terrane or Llano Uplift in east (Figure 4; Dickinson and Gehrels, 2009). Rutile with an age range of 1400-1800 Ma is interpreted as derived from the Yavapai-Mazatzal terrane and the Mid-Continent terrane and the 1800-2000 Ma age group represent sediment sourced from the Trans-Hudson terrane in the north (Figure 4; Dickinson and Gehrels, 2009). The HST (11-BH-06) and the LST (11-TUS3C-2-17) samples of the Desert Member also have these significant U-Pb age groups that represent the Appalachian orogen (300-600 Ma), the Yavapai-Mazatzal terrane (1600-1800 Ma), and the Trans-Hudson terrane (2000 Ma) (Figure 21.2). The transgressive lag deposit (11-SPC-01) of the Spring Canyon Member has age populations interpreted to be of Appalachian Orogen (300-600 Ma), and of Yavapai-Mazatzal terrane (1600-1800 Ma) origin (Figure 21.3). The transgressive lag deposit of Spring Canyon Member (11-SPC-01) has a significant U-Pb age population at 2600-2800 Ma, interpreted as sediment sourced from the Superior province or the Wyoming-Hearne-Rae province in the north (Figure 4 and 21.3) or the immediately adjacent Archean uplifts (Figure 10).

8.4 Interpretation of LA-ICP-MS Trace Element Determinations of Rutile from the Book Cliffs, Utah

Using the calibration equation of Watson (2006), the Zr concentration in rutile can be used to calculate the crystallization temperature or peak metamorphic temperature. The underlying rationale is that the incorporation of Zr into Rutile is a function of temperature in metamorphic assemblages that contain zircon, rutile and quartz in equilibrium (Zack et al., 2004). In the absence of fluid influx during retrograde metamorphism, reequilibration of Zr content in rutile is negligible and thus the rutile crystallization temperature conditions are preserved (Zack et al., 2004; Kooijman et al., 2010). Rutile also readily incorporates U, and incorporates minimal common Pb, which allows U-Pb dating.

Results of this study show that rutile with U-Pb cooling ages of 400-600 Ma had the most significant clustering of crystallization temperatures (Figure 23.1-4). The crystallization temperatures of this age population are 600-800^{o}C for the detrital rutile sourced from the Appalachian Orogen. Rutile with U-Pb cooling ages >600 Ma showed little clustering of crystallization temperature and ranged between 400-900^{o}C, which covers most of the temperature range in which rutile crystallizes in crustal rocks (Kooijman et al., 2010).

The range of Zr concentration in rutile measured here is consistent with results from other studies that used rutile as a geothermometer. Koojiman et al. (2012) showed that whereas Zr concentrations within a single grain are relatively homogeneous, the Zr concentration between different grains from a single granulite facies rock sample may range between 200-4500 ppm (2012). Triebold et al. (2012) provides two explanations for the large range of Zr concentrations measured in rutile. It may either be caused by analyzing inherited rutile versus rutile that are newly grown, or it may be caused by analyzing rutile that grow at peak metamorphic conditions versus rutile that re-equilibrate during retrograde metamorphism (Triebold et al., 2012). Unfortunately, it is not possible to assess these different processes in detrital rutile. Therefore, it is not surprising that detrital rutile from a specific age populations show a significant range in Zr concentration and calculated crystallization temperatures. However, given that rutile is most commonly a metamorphic mineral derived from metamafic or metasedimentary rocks (Zack et al. 2004) above greenschist grade, an abundance of rutile within certain U-Pb age groups points towards a provenance from a terrane with abundant relative high-grade metamorphic rocks, whereas absence of rutile from a U-Pb age group may be interpreted as a lack of such rocks in the source area and a predominance of igneous rocks.

Conclusions

Chapter 9. Conclusions for Sedimentary Rocks from the Greater Green River Basin, Wyoming

9.1 U-Pb LA-ICP-MS Results and the Implications for Mineral Separation Procedures for Provenance Investigations Using Zircon

This study concludes that the mineral separation method developed in this study results in a representative sample fraction to be analyzed and thus a more complete dataset of LA-ICP-MS U-Pb analyses (Figure 14). The mineral separation procedure developed in this study reduces bias in provenance analyses of zircon by only using crushing, milling, washing to remove dust and heavy liquids, without any water table separation, magnetic separation, or selection of grains under a binocular microscope.

Removing relevant detrital minerals from a sample fraction to be analyzed for provenance investigations is also known as introducing bias (Sircombe and Stern, 2002). Using SiC and pure quartz sand it was shown that the water table separation technique removes a significant portion of fine grained material and is thus not a recommended means to concentrate heavy minerals when compared to the heavy liquids separation methods (Table 1). By using only heavy liquids and not using the Frantz Magnetic separator for the mineral separation procedure, relevant age populations were detected in U-Pb analyses of zircon that were not detected in U-Pb analyses of zircon that were magnetically separated (Figure 14). A QEMSCAN® was used to identify all minerals of concern, which eliminates potential bias introduced during hand selecting of zircon to be analyzed. Commonly, hand selecting mineral grains under an optical microscope relies on the user experience to positively identify relevant mineral grains and select a representative sample fraction to be analyzed. Detrital minerals can have a wide range of mineral characteristics and are sometimes difficult to identify optically, making it very difficult to hand select a representative aliquot.

Therefore, this study concludes that some mineral separation techniques introduce bias by fractionating zircon from the bulk material with regard to small grain sizes, grain shapes, density, and magnetic susceptibility. The standard mineral separation procedure has tendencies to bias towards zircon that have a size of are 100-200 μm, are relatively euhedral, and free of inclusions. Clastic sedimentary units commonly contain zircon that have all possible grain shapes, may be metamict, range in size between 30-200 μm and beyond, and may contain inclusions. Therefore, using standard mineral separation procedures has the potential to remove zircon that do not exhibit very specific mineralogical parameters. The removed zircons potentially represent significant populations within the U-Pb age signature.

9.2 U-Pb LA-ICP-MS Results and the Implications for Mineral Separation Procedures for Provenance Investigations Using Rutile

This study found that non-magnetic rutile separated using the Frantz magnetic separator produced significantly less discordant LA-ICP-MS U-Pb analyses than slightly magnetic rutile (GR-09-14; GR-09-19; Figure 15.1-4). Rutile grains separated using only heavy liquids contained 25-33% of U-Pb analyses that are >15% discordant (GR-09-14M; Figure 15.1)(GR-09-19M; Figure 15.3), whereas 14-17% of U-Pb analyses are >15% discordant for rutile grains that are separated using a Frantz setting of 1.8 A and 5° (GR-09-14N; Figure 15.2)(GR-09-19N; Figure 15.4). The specific processes that result in a greater percentage of discordant analyses cannot be specifically discerned in this study. However, it can be assumed that it is related to partial Pb-loss within rutile, altered grains or analyzing TiO_2 polymorphs other than rutile (Kooijman et al., 2010, 2012; Triebold et al., 2011, 2012; Zack et al., 2004). It is determined that using the Frantz magnetic separator results in a greater percentage of concordant U-Pb analyses.

Therefore, it is advantageous to use the Frantz magnetic separator for the separation of rutile from the sample fraction to be analyzed by the LA-ICP-MS. It is important to note that using this technique resulted in similar U-Pb age ranges of concordant results to be detected in the magnetic and non-magnetic fraction of the same sample which was not the case for zircon U-Pb analyses. The mineral separation procedures developed here should result in more comprehensive datasets for detrital provenance investigations and are recommended as best practice to minimize potential bias towards particular mineral fractions and thereby possibly age populations.

9.3 Provenance of the Sedimentary Rocks from the Greater Green River Basin, Wyoming

This study improves our understanding of the provenance of the Late Cretaceous sediments from the Greater Green River Basin, Wyoming using QEMSCAN® and LA-ICP-MS analyses. Detailed sequence stratigraphy and paleocurrent directions from previous studies suggest that there is a significant shift in the provenance of sediment recorded in the Dad Member of the Lewis shale (Miller et al., 1992; Pyles and Slatt, 2000, 2002, and 2007; Soy and Slatt, 2008). Pyles and Slatt (2000, 2002, and 2007) propose that this shift in sediment provenance is related to the first appearance of Laramide deformation in Wyoming during deposition of the Dad Member of the Lewis shale. These interpretations helped to target which units in the GGRG to sample and helped set the initial framework of hypotheses for this study The QEMSCAN® and U-Pb analyses results of this study support the hypothesis of such a change by detecting notable changes in the U-Pb age patterns of zircon and rutile as well as changes in the modal mineral percentages of the TiO_2 polymorphs and pyrite in the Dad Member of the Lewis shale (GR-09-19, Figure 16.1-4; Figure 18). LA-ICP-MS U-Pb analyses of zircon show that there was a shift to a northern detrital source with an input of ~2700 Ma zircon during the deposition of the Dad Member that is interpreted as being sourced from the Superior Province, Wyoming-Hearne-Rae terrane or Archean age outcrops in the immediate vicinity (GR-09-19; Figure 17; Figure 4, Dickinson and Gehrels, 2009; Karlstrom & Whitmeyer, 2007; Figure 10, Pyles & Slatt, 2000). LA-ICP-MS U-Pb analyses of rutile showed similar age populations as the zircon U-Pb age populations and further confirmed a northern derived source of sediment from the Superior Province or Wyoming-Hearne-Rae terrane (Figure 16.1-4; Figure 4, Dickinson and Gehrels, 2009)

Provenance determination of sediment from the GGRB, Wyoming, is difficult due to the large geographical extent of the KWIS, axial parallel transport of sediment in the basin, multiple deformational events on the North American Craton, and non-unique U-Pb age ranges of zircon and rutile (Martinsen et al., 1993). While QEMSCAN® and U-Pb analyses support Pyles and Slatt (2000, 2002, 2007) proposal of a provenance shift in the Dad member, this study cannot confirm nor rule out whether this is related to Laramide orogenic deformation in Wyoming.

Chapter 10. Conclusions for the Sedimentary Rocks from the Book Cliffs, Utah

10.1 Potential Controls of Sequence Stratigraphic System Tracts and the Resulting Environment of Deposition on Provenance Signals

Late Cretaceous sedimentary units of the Star Point Formation, Blackhawk Formation, and Castlegate Sandstone from the Book Cliffs, Utah contain U-Pb age populations that are interpreted as sediment sourced from the Sevier Orogenic belt in the west, the Appalachian orogen, the Grenville terrane or the Llano Province, the Mid-continent terrane, and the Yavapai-Mazatzal terrane (Figure 4) (Whitmeyer and Karlstrom 2007; Dickinson and Gehrels, 2009). The Grenville terrane or the Llano Province material is the most significant age population represented in the Book Cliffs samples (Figure 20.1-5). Due the large geographical distance between the KWIS and the Grenville Orogenic belt, there would need to be a very large drainage system that transported sediment directly into the basin from the northeast. Another possibility would be that the sediment derived from this terrane could have been repeatedly recycled until finally deposited in the KWIS.

There are notable differences in the vol. % of pyrite and TiO_2 polymorphs when comparing QEMSCAN® analyses from different sequence stratigraphic system tracts within the units sampled at the Book Cliffs, Utah (Figure 19.1-10). QEMSCAN® analyses of samples from HST contained on average 17.3 vol. % more pyrite and TiO_2 polymorphs than the transgressive lag deposits (Figure 19.1-4). QEMSCAN® analyses of samples from LST contained on average 5.2 vol. % more pyrite and TiO_2 polymorphs than the HST (Figure 19.5-10).

LA-ICP-MS U-Pb analyses of zircon and rutile from these sedimentary rock units of the Book Cliffs, Utah, reveal quite large variations between differing sequence stratigraphic system tracts and depositional facies (Figure 20.1-5; Figure 21.1-3; Figure 22.1-4; 23.1-4). The deltaic sandstone sample (11-PTH-09) of the Panther Tongue contains significant U-Pb age populations at 290 Ma, 600 Ma, and 1750 Ma, which were not detected in the transgressive lag deposit samples (10-PTH-01; Figure 20.1). LA-ICP-MS U-Pb analyses of detrital samples from shoreface sandstone of the Spring Canyon Member (11-SPC-05) contains significant U-Pb age populations at 170 Ma, and 1150 Ma not detected in the transgressive lag deposit (11-SPC-01; Figure 20.2). The LST of the Aberdeen Member (11-AB-LST) contains significant U-Pb age populations at 1350 Ma and 2580 Ma, which were not detected in the HST of the Spring Canyon member (11-SPC-05; Figure 20.3). U-Pb analyses of zircon from the LST of the Desert member (11-TUS3C-2-17) shows a similar trend and has significant U-Pb age populations at 275 Ma, 1050 Ma, and 2550 Ma, which we not detected in the HST (11-BH-06), whereas the HST sample has an age population at ca. 670 Ma not found in the LST sample, and minor population peaks at ca. 960 and 1140 Ma (Figure 20.4). In the LST of Castlegate sandstone, there was significant variation in the U-Pb age spectrum when comparing the two different incised valley fill samples (11-CSTG-07; 11-TUS3C-22.3-22.4).

This study shows that more different age groups and thus potentially more different detrital sources of sediment are detected in U-Pb analyses of samples from LST relative to the HST and transgressive lag deposits. This study proposes that there are potentially two geological reasons for this result. During the transgressive lag deposit, fine grained sediment can be eroded away resulting in a sedimentary unit that is grain size biased. This grain size bias could result in the removal of fine-grained sediment from a distal source area relative to the site of deposition or a source area that contains rocks that are aphanitic. Alternatively, drainage patterns during lowstand conditions could have been different in such a way that they would better preserve sediment of this age. It is also possible that sources of sediment that were once inundated during periods of highstand conditions could potentially become areas of high geographical relief during lowstand condition, thus being eroded and becoming a new source of sediment.

Overall, the data from the Book Cliffs samples show a large variation in mineral abundances and U-Pb age signatures when comparing depositional facies. The environment of deposition or the sequence stratigraphic system tract of a given sedimentary unit has the potential to yield different detrital provenance signatures. The data from the Book Cliffs samples also shows a large variation in mineral abundances and U-Pb age signatures when comparing samples from the same depositional facies. Therefore, choosing one sample to represent an entire formation potentially results in an incomplete dataset for provenance analyses. This study proposes that it is necessary to collect 2-3 samples throughout a formation for provenance investigations. Such a sampling scheme may result in more complete and representative datasets for detrital provenance analyses, but was beyond the scope of the study.

References Cited

Andersen, T., 2002, Correction of common lead in U-Pb analyses that do not report ^{204}Pb. Chemical Geology, v. 192, p. 59-79.

Andersen, T., 2005, Detrital zircons as tracers of sedimentary provenance: limiting conditions from statistics and numerical simulation. Chemical Geology, v. 216, p. 249–270.

Baars, D.L., 1966, Pre-Pennsylvania paleotectonics; Key to basin evolution and petroleum occurrences in Paradox Basin, Utah and Colorado. American Association of Petroleum Geologists Bulletin, v. 50, no. 10, p. 2082-2111.

Baars, D.L., Bartleson, B.L., Chapin, C.E., Curtis, B.F., De Voto, R.H., Everett, J.R., Johnson, R.C., Molenaar, C.M., Peterson, F., Schenk, C.J., Love, J.D., Merin, I.S., Rose, P.R., Ryder, R.T., Waechter, N.B., Woodward, L.A., 1988, Basins of the Rocky Mountain region; in, Sedimentary Cover-North American Craton, L.L. Sloss, eds.: The Geology of North America, Geological Society of America, v. D-2, p. 109-220.

Bird, P., 1998, Kinematic history of the Laramide orogeny in latitudes 35–49 N, western United States. Tectonics, v. 17, no. 5, p. 780-801.

Blackburn, T., Bowring, S. A., Schoene, B., Mahan, K., Dudas, F., 2011, U-Pb thermochronology: creating a temporal record of lithosphere thermal evolution. Contributions to Mineralogy and Petrology, v. 162, no. 3, p. 479-500.

Blakey, R.C., 2008, Gondwana paleogeogrpahy from assembly to breakup - A 500 m.y. odyssey, in Fielding, C.R., Frank, T.D., and Isbell, J.L., eds., Resolving the Late Paleozoic Ice Age in Time and Space. Geological Society of America Special Paper 441, p. 1-28.

Bogdanova, S. V., Pisarevsky, S. A., Li, Z. X., 2009, Assembly and Breakup of Rodinia (Some results of IGCP project 440). Stratigraphy and Geological Correlation, v. 17, no. 3, p. 259-274.

Burchfiel, B.C., Davis, G.A., 1975, Nature and controls of Cordilleran orogenesis, western United States: extensions of an earlier synthesis. American Journal of Science, v. 275A, p. 363-396.

Burchfiel, B.C., Lipman, P.W., Zoback, M.L., 1992, Introduction, in Burchfiel, B.C., Lipman, P.W., Zoback, M.L., eds., The Cordilleran Orogen: Conterminous U.S.: Geological Society of America. The Geology of North America, v. G-3, p. 1-7.

Christiansen, R.L., Yeats, R.S., 1992, Post-Laramide geology of the U.S. Cordillera region, in Burchfiel, B.C., Lipman, P.W., Zoback, M.L., eds., The Cordilleran Orogen: Conterminous U.S.. Geological Society of America, The Geology of North America, v. G-3, p. 261-405.

Cowan, D.S., Bruhn, R.L., 1992, Late Jurassic to early Late Cretaceous geology of the U.S. Cordillera, in Burchfiel, B.C., Lipman, P.W., Zoback, M.L., eds., The Cordilleran Orogen: Conterminous U.S.. Geological Society of America, The Geology of North America, v. G-3, p. 169-203.

Davis, D.W., Williams, I.S., Krogh, T.E., 2003, Historical development of zircon geochronology, Mineralogical Society of America. Reviews in Mineralogy and Geochemistry, v. 53, p. 146-181.

DeCelles, P.G., and Giles, K.A., 1996, Foreland basin systems. Basin Research, v. 8, p. 105–123.

Dickinson, W.R., Gehrels, G.E., 2009, U-Pb ages of detrital zircons in Jurassic eolian and associated sandstones of the Colorado Plateau: Evidence for transcontinental dispersal and intraregional recycling of sediment. Geological Society of America Bulletin, v. 121, p. 408–433.

Dunkl, I., Mikes, D., Frei, A., von Eynatten, H., 2009, PepiAGE: data reduction program for time-resolved U/Pb analyses-Introduction and call for tests and discussion. Short Introduction to PepiAGE, p. 1-15.

Eggins, S.M., Kinsley, L.P.J., Shelley, J.M.M., 1998, Deposition and element fractionation processes during atmospheric pressure laser sampling for analysis by ICPMS. Applied Surface Science, v. 129, p. 278-286.

Evans, K.V., 1984, Ordovician plutonism in east-central Idaho; Variation on a Canadian theme. Geological Society of America Abstracts with Programs, v. 16, p. 504.

Fedo, C.M., Sircombe, K.N., Rainbird, R.H., 2003, Detrital zircon analysis of the sedimentary record. Reviews in Mineralogy and Geochemistry, Zircon, v. 53, p. 277–303.

Frei, D., Gerdes, A., 2009, Precise and accurate in situ U-Pb dating of zircon with high sample throughput by automated LA-SF-ICP-MS. Chemical Geology, v. 261, is. 3-4, p. 261-270.

Force, E.R., 1980, The provenance of rutile. Journal of Sedimentary Petrology, v. 50, p. 485–488.

Fouch, T.D., Lawton, T.F., Nichols, D.J., Cashion, W.B., and Cobban, W.A., 1983, Patterns and timing of synorogenic sedimentation in Upper Cretaceous rocks of central and northeast Utah, *in* Reynolds, M., Dolly, E., and Spearing, D.R., eds., Mesozoic Paleogeography of west-central United States. Society of Economic Paleontologists and Mineralogists, Rocky Mountain Section, Symposium 2, p. 305-336.

Geisler, T., Pidgeon, R.T., van Bronswijk, W., Kurtz, R., 2002, Transport of uranium, thorium, and lead in metamict zircon under low-temperature hydrothermal conditions. Chemical Geology, v. 191 is. 1-3, p. 141-154.

Gill, J.R., and W.J. Hail, Jr., 1975, Stratigraphic sections across Upper Cretaceous Mancos Shale-Mesa Verde Group boundary, eastern Utah and western Colorado. USGS Oil and Gas Investigations Chart OC-68.

Hamilton, W., 1981, Plate-tectonic mechanism of Laramide deformation. Rock Mountain Geology, v. 19, no. 2, p. 87-92.

Hatcher, R.D., Jr., 1989, Tectonic synthesis of the U.S. Appalachians, in Hatcher, R.D., Jr., Thomas, W.A., and Viele, G.W., eds., The Appalachian-Ouachita orogen in the United States. Geological Society of America, Geology of North America, v. F-2, p. 511-535.

Hintze, L.F., 1988, Geologic history of Utah: Provo, Utah. Brigham Young University Geology Studies, Special Publication 7, p. 202.

Hirata, T., Nesbitt, R.W., 1995, U-Pb isotope geochronology of zircon: Evaluation of the laser probe-inductively coupled plasma mass spectrometry technique. Geochimica et Cosmochimica Acta, v. 59, p. 2491-2500.

Hoffman, P.F., 1988, United plates of America, the birth of a craton; early Proterozoic assembly and growth of Laurentia. Annual Review of Earth and Planetary Sciences, v. 16, p. 543-603.

Horn, I., Rudnick, R.L., McDonough, W.F., 2000, Precise elemental and isotope ratio measurement by simultaneous solution nebulisation and laser ablation-ICP-MS: Application to U-Pb Geochronology. Chemical Geology, v. 164, p. 281-301.

Hwang, I. G. and P. L. Heller, 2002, Anatomy of a transgressive lag: Panther Tongue Sandstone, Star Point Formation, central Utah: Sedimentology, v. 49, p. 977-1000.

Ireland, T.R., Williams, I.S., 2003, Considerations in zircon geochronology by SIMS. Mineralogical Society of America, Reviews in Mineralogy and Geochemistry, v. 53, p. 215-241.

Jackson, S.E., Longerich, H.P., Dunning, R., Fryer, B.J., 1992, The application of laser-ablation microprobe –inductively coupled plasma mass spectrometry LAM-ICP-MS to in situ trace element determinations in minerals. Mineralogical Society of Canada, v. 30, p. 1049-1064.

Johnson, P.L., Anderson D.W., 2009, Concurrent growth with dissimilar orientations in the southern Green River Basin, Wyoming: Implications for Paleocene-Eocene patterns of foreland shortening. Rocky Mountain Geology, v. 44, p. 1-16.

Jordan, T.E., 1981, Thrust Loads and Foreland basin Evolution, Cretaceous, Western United States. American Association of Petroleum Geologists, Bulletin, v. 65, no. 12, p. 2506-2520.

Kamola, D.L., Huntoon, J.E., 1992, Sequence boundary variations within the Aberdeen Member, Cretaceous Blackhawk Formation, Utah. Abs,: American Association of Petroleum Geologists Annual Convention Official Program, p. 61-62.

Kamola, D.L., Van Wagoner, J.C., 1995, Parasequence stratigraphy and facies architecture of the Spring Canyon Member, Upper Cretaceous Blackhawk Formation, in: J.C. Van Wagoner, G.T. Bertram., eds., Sequence Stratigraphy of Foreland Basin Deposits, Am. Assoc. Petrol. Geol. Memoir, v. 64 p. 27–54.

Kauffman, E.G., 1977, Geologic and Biological overview, Western Interior Cretaceous basin, in Kauffman, E.G., eds., Cretaceous facies, faunas, and paleoenvironments across the Western Interior basin. The Mountain Geologist, v. 14, p. 75-99.

Kauffman, E.G., 1984, Paleobiogeography and evolutionary response dynamic in the Cretaceous Western Interior Seaway of North America: in G.E.G. Westermann, ed., Jurassic-Cretaceous Biochronology and Paleogeography of North America. Geological Association of Canada Special Paper 27.

Kauffman, E.G., Sageman, B.B., Kirkland, W.P., Harries, P.J., Villamil, T., 1993, Molluscan biostratigraphy of the Cretaceous Western Interior Seaway, North America, Kauffman, E.G., eds., Evolution of the Western Interior Basin. Geological Association of Canada Special Paper 39, p. 397-434.

Kooijman, E., Mezger, K., Berndt, J., 2010, Constraints on the U-Pb systematics of metamorphic rutile from in situ LA-ICP-MS analysis. Earth and Planetary Letter, v. 293, p. 321-330.

Kooijman, E., Smit, M.A., Mezger, K., Berndt, J., 2012, Trace element systematics in granulite facies rutile: implications for Zr geothermometry and provenance studies. Metamorphic Geology, v. 30, p. 397-412.

Košler, J., Fonneland, H., Sylvester, P., Tubrett, M., Pedersen, R.B., 2002, U–Pb dating of detrital zircons for sediment provenance studies a comparison of laser ablation ICPMS and SIMS techniques. Chemical Geology, v. 1823, p. 605–618.

Košler, J., Sylvester, P., 2003, Present trends and the future of zircon in Geochronology: Laser Ablation ICPMS. Mineralogical Society of America, Reviews in Mineralogy and Geochemistry, v. 53, p. 243-274.

Loutit, T.S., Hardenbol, J., Vail, P.R., Baum, G.R., 1988, Condensed sections: the key to age-dating and correlation of continental margin sequences. In: Wilgus, C.K., Hastings, B.S., Kendall, C.G.St.C., Posamentier, H.W., Ross, C.A., Van Wagoner, J.C. (Eds.), Sea Level Changes—An Integrated Approach, SEPM Special Publication, v. 42. p. 183–213.

Lawton, T.F., 1985, Style and timing of frontal structure, thrust belt, central Utah. AAPG Bulletin, v. 69, p. 1145-1159.

Lawrence, R.L., Cox, R., Mapes, R.W., Coleman, D.S., 2011, Hydrodynamic fractionation of zircon age populations. Geological Society of America Bullentin, v. 123, n.1-2, p. 295-305.

Lewis, R., Senftle, F., 1966, The source of ferromagnatism in zircon. American Minerals, v. 51, p. 1467-1475.

Loring, A.K., Armstrong, D.G., 1980, Cambrian-Ordovician syenites of New Mexico, part of a regional alkalic intrusive episode. Geology, v. 8, p. 344-348.

Love, J.D., Christiansen A.C., 1985, Geological map of Wyoming. US Geological Survey, scale, 1:500,000.

Love, L. G., Coleman, M. L., Curtis, C. D., 1983, Diagenetic pyrite formation and sulphur isotope fractionation associated with a Westphalian marine incursion, northern England. Transactions of the Royal Society of Edinburgh: Earth Sciences, v. 74, p. 165-182.

Ludwig, K. R., 2003, Isoplot 3.00 – A geochronological toolkit for Microsoft Excel. Berkeley Geochronology Center Special Publication 4, p. 1–70.

Luvizotto, G.L., Zack, T., Meyer, H.P., Ludwig, T., Triebold, S., Kronz, A., Münker, C., Stockli, C.F., Prowatke, S., Klemme, S., Jacob, D.E., von Eynatten, H., 2009, Rutile crystals as potential trace element and isotope mineral standards for microanalysis. Chemical Geology, v. 261, is. 3-4, p. 346-369.

Machado, N., Gauthier, G., 1996, Determination of $^{207}Pb/^{206}Pb$ ages on zircon and monazite by laser ablation ICPMS and application to a study of sedimentary provenance and metamorphism in southeastern Brazil. Geochimica et Cosmochimica Acta, v. 60, p. 5063–5073.

Mank, A.J.G., Mason, P.S.D., 1999, A critical assessment of laser ablation ICP-MS as an analytical tool for depth analysis in silica-based samples. Journal of Analytical Atomic Spectrometry, v. 14 p. 1142-1153.

Martinsen, O.J., Martinsen, R.S., Steidmann, J.R., 1993, Mesaverde Group (Upper Cretaceous), Southeastern Wyoming: Allostratigraphy versus sequence stratigraphy in a tectonically active area. The American Association of Petroleum Geologist Bulletin, v. 77, p. 1351-1373.

Mezger, K., Hanson, G.N., Bohlem, S.R., 1989, High-precision U-Pb ages of metamorphic rutile: Application to the cooling history of high-grade terranes. Earth and Planetary Science Letters, v. 96, p. 106-118.

Miall, A.D., Arush, M., 2001, The Castlegate Sandstone of the Book Cliffs, Utah: sequence stratigraphy, paleogeography, and tectonic controls. Journal of Sedimentary Research, v. 71, p. 536-547.

Miller, D.M., Nilsen T.H., Bilodeau, B.L., 1992, Late Cretaceous to early Eocene geologic evolution of the U.S. Cordillera, in Burchfiel, B.C., Lipman, P.W., Zoback, M.L., eds., The Cordilleran Orogen: Conterminous U.S.. Geological Society of America, The Geology of North America, v. G-3, p. 205-260.

Miller, M.L., Miller, M.M., Stevens, C.H., Wright, J.E., Madrid, R., 1992, Late Paleozoic paleographic and tectonic evolution of the western U.S. Cordillera, in Burchfiel, B.C., Lipman, P.W., Zoback, M.L., eds., The Cordilleran Orogen: Conterminous U.S.. Geological Society of America, The Geology of North America, v. G-3, p. 57-106.

Mitchell, R.H., 1973, Magnesian ilmenite and its role in kimberlite petrogenesis. Geology, v. 81, no. 3, p. 301-311.

Möller, A., Appel, P., Mezger, K., Schenk, V., 1995, Evidence for a 2 Ga subduction zone: Eclogites in the Usagaran belt of Tanzania. Geology, v. 23, no. 12, p. 1067-1070.

Möller, A., Mezger K., Schenk, V., 2000, U–Pb dating of metamorphic minerals: Pan-African metamorphism and prolonged slow cooling of high pressure granulites in Tanzania, East Africa. Precambrian Research v. 104, p. 123-146.

Morton, A.C., 1987, Influences of provenance and diagenesis on detrital garnet suites in the Forties sandstone, Paleocene, central North Sea. Sedimentary Petrology, v. 57, p. 1027–1032.

Morton, A.C., 1991, Geochemical studies of detrital heavy minerals and their application to provenance studies. In: Morton A.C., Todd, S.P., Haughton, P.D.W. (Eds.), Developments in Sedimentary Provenance Studies. Geologic Society of London, Special Publication 57, p. 31–45.

Morton, A. C., Hallsworth, C., 1994, Identifying provenance-specific features of detrital heavy mineral assemblages in sandstones. Sedimentary Geology, v. 90, p. 241-256.

North, C.P., Hole, M.J., Jones, D.G., 2005, Geochemical correlation in deltaic successions: a reality check. Geologic Society of America Bulletin, v. 117, p. 620–632.

Obradovich, J.D., 1993, A Cretaceous time scale, in Caldwell, G.E., Kauffman, E.G., eds., Evolution of the Western Interior Basin. Geological Association of Canada, special paper 39, p. 379-396.

Olson, J.C., Marvin, R.F., Parker, R.L., Mehnert, H.H., 1977, Age and tectonic setting of lower Paleozoic alkalic and mafic rocks, carbonatites, and thorium veins in south-central Colorado. U.S. Geological Survey Journal of Research, v. 5, no. 6, p. 673-687.

Olsen, T., Steel. R.J., Hogseth, K., Skar, T., and Roe, S.L., 1995, Sequential architecture in a fluvial succession: sequence stratigraphy in the Upper Cretaceous Mesaverde Group, Price Canyon, Utah: Journal of Sedimentary Research, v. B65, p. 265-280.

Otto, G.H., 1933, Comparative tests of several methods of sampling heavy mineral concentrates. Sedimentary Research, v. 3, n. 1, p. 30-39.

Paton, C., Woodhead, J., Hellstrom, J., Hergt, J., Greig, A., Roland, Maas., 2010, Improved laser ablation U-Pb zircon geochronology through robust downhole fractionation correction. Geochemistry, Geophysics, Geosystems, v. 11, is. 3.

Paton, C., Hellstrom, J., Paul. B., Woodhead, J., Hergt, J., 2011, Iolite: freeware for the visualization and processing of mass spectrometer data. Analytical Atomic Spectrometry v. 26, p. 2508-2518.

Perman, R.C., 1990, Depositional history of the Maastrichtian Lewis Shale in south-central Wyoming: deltaic and interdeltaic, marginal marine through deep-water marine, environments. AAPG Bulletin, v. 74, p. 1695-1717.

Pirrie, D., Butcher, A.R., Power, M.R., Gottlieb, p., Miller, G.L., 1004, Rapid quanitative mineral and phase analysis using automated scanning electron microscopy (QEMSCAN®); potential applications in forensic geoscience. Geological Society, London, Special Publication, v. 232, p. 123-136.

Poole, F.G., Stewart, J.H., Palmer, A.R., Sandberg, C.A., Madrid, R.J., Ross, R.J., Jr., Hintze, L.F., Miller, M.M., Wrucke, C.T., 1992, Latest Precambrian to latest Devonian time; Development of a continental margin, in Burchfiel, B.C., Lipman, P.W., Zoback, M.L., eds., The Cordilleran Orogen: Conterminous U.S.. Geological Society of America, The Geology of North America, v. G-3, p. 9-56.

Posamentier, H.W., and Morris, W.R., 2000, Aspects of the stratal architecture of forced regressive deposits, *in* Hunt, D., and Gawthorpe, R.L., eds., Sedimentary Responses to Forced Regressions. Geological Society of London, Special Publication v. 172, p. 19–46.

Pyles, D., 2007, Cretaceous through Lower Tertiary Geology of the Rawlins Uplift. Compilation/Guidebook, Colorado School of Mines.

Pyles, D.R., Slatt R.M., 2000, A high-frequency sequence stratigraphic framework for shallow through deep-water deposits of the Lewis Shale and Fox Hills Sandstone, Great Divide and Washakie basins, Wyoming. Deep-water Reservoirs of the World, Gulf Coast Section SEPM, p. 836–861.

Pyles, D.R., Slatt R.M., 2002, Lewis Shale and Fox Hills Sandstone, eastern margin of the Greater Green River basin. Rocky Mountain Section AAPG/SEPM Field Trip no. 1, p. 49–94.

Pyles, D.R., Slatt, R.M., 2007, Stratigraphic evolution of the upper cretaceous Lewis Shale, Southern Wyoming: applications to understanding shelf to base-of-slope changes in stratigraphic architecture of mud-dominated, progradational depositional systems. AAPG Studies in Geology, Atlas of Deepwater Outcrops CD-ROM, v. 56, p. 19.

Pyles, D.R., Weimer P., Bouroullec, R., 2001, Stratigraphic and tectonic framework of the Desoto canyon and Lloyd ridge protraction areas, Northeastern Deep Gulf of Mexico: implications for the petroleum system and potential play types, Gulf Coast Section SEPM. Special Publication, Petroleum Systems of Deep-water Basins: Global and Gulf of Mexico Experience, v. 21, p. 285–314.

Qing, C., 1981, Study on authigenic pyrites in sediments of the South Huanghai Sea. Acta Geological Sinica, v. *3*, p. 6.

Rittenhouse, G., 1943, Transportation and deposition of heavy minerals. Geological Society of America Bulletin, v. 54, p. 1725-1780.

Ross, R.J., Jr., 1977, Ordovician paleogeography of the western United States, in Stewart, J.H., Stevens, C.H., Fritsche, A.E., eds., Paleozoic paleogeography of the western United States. Pacific Coast Symposium 1: Society of Economic Paleontologists and Mineralogists, p. 19-38.

Ruppel, E.T., 1985, Lemhi Arch, a late Proterozoic and early Paleozoic landmass, central Idaho. American Association of Petroleum Geologists Section Meeting Abstracts; American Association of Petroleum Geologist Bulletin, v. 69, no. 5, p. 864.

Saleeby, J.B., Busby-Spera, C., 1992, Early Mesozoic tectonic evolution of the western U.S. Cordillera, in Burchfiel, B.C., Lipman, P.W., Zoback, M.L., eds., The Cordilleran Orogen: Conterminous U.S.: Geological Society of America, The Geology of North America, v. G-3, p. 107-168.

Sandberg, C.A., Mapel, W.J., 1967, Devonian of the Northern Rocky Mountians and Plains. Oswald, D.H., eds., International Symposium on the Devonian System: Calgary, Alberta Society of Petroleum Geologists, v. 1, p. 843-877.

Sircombe, K.N., Stern, R.A., 2002, An investigation of artificial biasing in detrital zircon U-Pb geochronology due to magnetic separation in sample preparation. Geochimica et Cosmochimica Acta, v. 66, p. 2379 –2397.

Slama, J., Košler, J., Condon, D.J., Crowley, J.L., Gerdes, A., Hanchar, J.M., Hortswood, M.S.A., Morris, G.A., Nasdala, L., Norberg, N., Schaltegger, U., Schoene, B., Turbett, M.N., Whitehouse, M.J., 2008, Plesovice zircon-A new natural reference material for U-Pb and Hf isotopic microanalysis. Chemical Geology, v. 249, is. 1-2, p. 1-35.

Snoke, A.W., 1993, Geologic history of Wyoming within the tectonic framework of the North American Cordillera, in Snoke, A.W., Steidtmann, J.R., Roberts, S.M., eds., Geology of Wyoming: Geological Survey of Wyoming Memoir no. 5, p. 1-56.

Soyinka, O.A., Slatt, R.M., 2008, Identification and micro-stratigraphy of hyperpycnites and turbidites in Cretaceous Lewis Shale, Wyoming. Sedimentology v. 55, p. 1117–1133.

Steidtmann, J.R., 1993, The Cretaceous foreland basin and its sedimentary record, in Snoke, A.W., Steidtmann, J.R., Roberts, S.M., eds., Geology of Wyoming: Geological Survey of Wyoming Memoir no. 5, p. 250-271.

Sterner, R.J., 1995, Digital elevation map of Wyoming, John Hopkins University Applied Physics Laboratory.

Stewart, J.H., Suczek, C.A., 1977, Cambrian and latest Precambrian paleogeography and tectonics in the western United States, in Stewart, J.H., Stevens, C.H., Fritsche, A.E., eds., Paleozoic paleogeography of the western United States, Pacific Coast Symposium 1: Society of Economic Paleontologists and Mineralogists, p. 1-17.

Thomas, W.A., Astini, R.A., 1996, The Argentine Precordillera: A traveler from the Ouachita embayment of North America Laurentia. Science, v. 273, p. 752-757.

Triebold, S., Luvizotto, G.L., Tolosana-Delgado, R., Zack, T., von Eynatten, H., 2011, Discrimination of TiO2 polymorphs in sedimentary and metamorphic rocks. Contrib Mineral Petrol, v. 161, p. 581-596.

Triebold, S., von Eynatten, H., Zack, T., 2012, A recipe for the use of rutile in sedimentary provenance analysis. Sedimentary Geology, v. 283, p. 268-275.

Vail, P.R., Hardenbol, J., Todd, R.G., 1984, Jurassic unconformities, ChronoStratigraphy and sea-level changes from seismic stratigraphy and BioStratigraphy. In: Schlee, J.S. Ed., Interregional Unconformities and Hydrocarbon accumulation, American Association of Petroleum Geologists Memoir, v. 36 p. 129–144.

Vail, P. R., Mitchum, R. M. Jr., 1979, Global cycles of relative changes of sea level from seismic stratigraphy, in Geological and geophysical investigations of continental margins. American Association of Petroleum Geologists, Memoir 29, p. 469-472.

Vermeesch P., 2004, How many grains are needed for a provenance study? Earth Planet Sci Lett v. 224, p. 441-451.

Van Schmus, W.R., Schneider, D.A., Holm, D.K., Dodson, S., Nelson, B.K., 2007, New insights into the southern margin of the Archean-Proterozoic boundary in the north-central United States based on U-Pb, Sm-Nd, and Ar-Ar geochronology. Precambrian Research, v. 157, p. 80-105.

Van Wagoner, J. C., 1991, Sequence stratigraphy and facies architecture of the Desert Member of the Blackhawk Formation and the Castlegate Formation in the Book Cliffs of eastern Utah and western Colorado, in J. C. Van Wagoner, D. Nummedal, C. R. Jones, D. R. Taylor, D. C. Jennette, and G. W. Riley, eds., Sequence stratigraphy applications to shelf sandstone reservoirs; outcrop to subsurface examples: AAPG Field Conference Guidebook.

Van Wagoner, J.C., 1995, Sequence stratigraphy and marine to nonmarine facies architecture of foreland basin strata, Book Cliffs, Utah, U.S.A. Sequence Stratigraphy of Foreland Basin Deposits. American Association of Petroleum Geologists Bulletin, v. 81, p. 1607-1618.

Van Wagoner, J. C., Posamentier, H.W., Mitchum, R.M., Vail, P.R., Sarg, J.F., Loutit, T.S., Hardenbol, J., 1988, An overview of the fundamentals of sequence stratigraphy and key definitions. Sea-level changes: An integrated approach: SEPM, special publication, v. 42, p. 39-45.

Watson, E.B., Wark, D.A., Thomas, J.B., 2006, Crystallization thermometers for zircon and rutile. Contributions to Mineralogy and Petrology, v. 151, p. 413-433.

Weimer, R.J., 1988, Record of relative sea-level changes, Cretaceous of Western Interior, USA. In: Sea-Level Changes: an Intergrated Approach. Eds C.K. Wilgus et al., SEPM Special Publication, v. 42, p. 285-288.

Whitmeyer, S.J., Karlstrom, K.E., 2007, Tectonic model for the Proterozoic growth of North America. Geosphere, v. 3, no. 4, p. 220-249.

Winn, R.D., Jr., Bishop, M.G., Gardner, P.S., 1987, Shallow-water and sub-storm-base deposition of Lewis Shale in Cretaceous Western Interior Seaway, south-central Wyoming. American Association of Petroleum Geologists Bulletin, v. 71, p. 859-881.

Young, R.G., 1955, Sedimentary facies and intertonguing in the Upper Cretaceous of the Book Cliffs, Utah-Colorado. Bulletin of the Geological Society of America, v. 66, p. 177-202.

Yoshida, S., Miall, A.D., and Willis, A., 1998, Sequence stratigraphy and marine to nonmarine facies architecture of foreland basin strata, Book Cliffs, Utah, U.S.A. Discussion: American Association of Petroleum Geologists, Bulletin, v. 82, p. 1596-1606.

Yoshida, S., Willis, A., and Miall, A.D., 1996, Tectonic control of nested sequence architecture in the Castlegate Sandstone (Upper Cretaceous), Book Cliffs, Utah. Sedimentary Research, v. 66, p. 737-748.

Zack T., von Eynatten, H., Kronz A., 2004, Rutile geochemistry and its potential use in quantitative provenance studies. Sedimentary Geology, v. 171, p. 37-58.

Figures

Figure 1.) Simplified stratigraphic cross section and sample numbers of Upper Cretaceous sedimentary units from the Greater Green River Basin, Wyoming. Modified from Obradovich (1993), Kauffman et al. (1993), and Pyles and Slatt (2000).

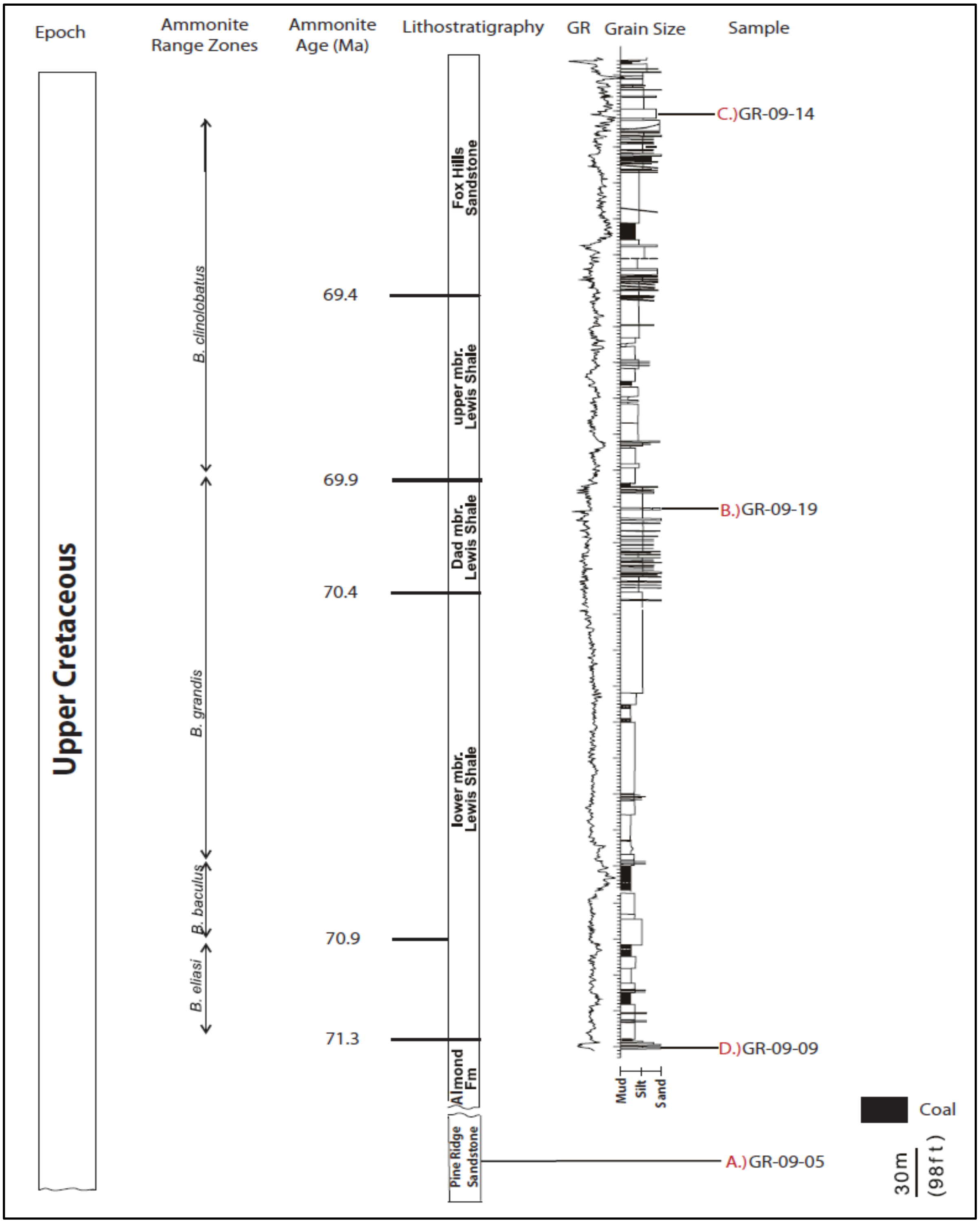
Epoch
Ammonite Range Zones
Ammonite Age (Ma)
Lithostratigraphy
GR
Grain Size
Sample
Upper Cretaceous
B. clinolobatus
B. grandis
B. baculus
B. eliasi
69.4
69.9
70.4
70.9
71.3
Fox Hills Sandstone
upper mbr. Lewis Shale
Dad mbr. Lewis Shale
lower mbr. Lewis Shale
Almond Fm
Pine Ridge Sandstone
C.)GR-09-14
B.)GR-09-19
D.)GR-09-09
A.)GR-09-05
Mud
Silt
Sand
Coal
30m
(98ft)

Figure 2.) Greater Green River Basin, Wyoming sample location map. Samples from the Fox Hills Sandstone, Almond Formation, and Pine Ridge Sandstone where collected from road cuts along I-80. The Dad Member of the Lewis shale was sampled from outcrops in the Stratton Ranch located northwest of Rawlins, Wyoming. Map modified from Pyles and Slatt, (2007).

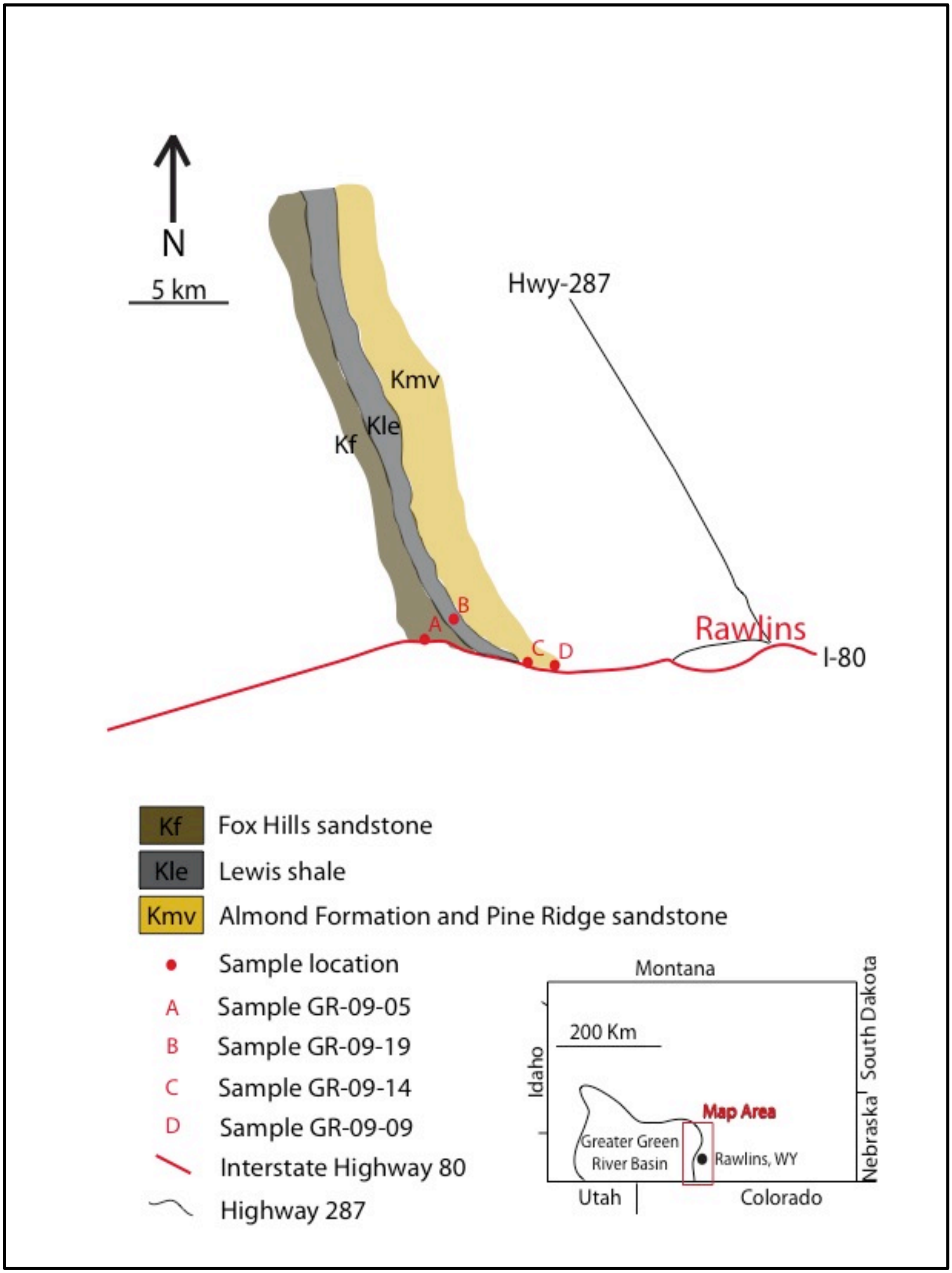
N
5 km
Hwy-287
Kmv
Kle
Kf
B
A
C
D
Rawlins
I-80
Kf
Fox Hills sandstone
Kle
Lewis shale
Kmv
Almond Formation and Pine Ridge sandstone
Sample location
A
Sample GR-09-05
B
Sample GR-09-19
C
Sample GR-09-14
D
Sample GR-09-09
Interstate Highway 80
Highway 287
Montana
200 Km
Idaho
South Dakota
Nebraska
Map Area
Greater Green
River Basin
Rawlins, WY
Utah
Colorado

Figure 3.) Simplified stratigraphic cross section of Late Cretaceous Star Point Formation, Blackhawk Formation, and Castlegate Sandstone of the Book Cliffs, Utah. Cross section shows the sampled units and the sequence stratigraphic framework. There are numerous sequences in of Late Cretaceous Star Point Formation, Blackhawk Formation, and Castlegate Sandstone of the Book Cliffs, Utah. The sequences relevant to this study are represented in the stratigraphic cross section. HST-High Stand System Tract, LST-Lowstand System Tract, and TST-Transgressive System Tract. Figure modified from North et. al, (2005). Sequence stratigraphic framework was gathered from Kamola and Huntoon, (1992), Kamola and Van Wagoner, (1995), Posamentier and Morris, (2000), and Van Wagoner, (1995).

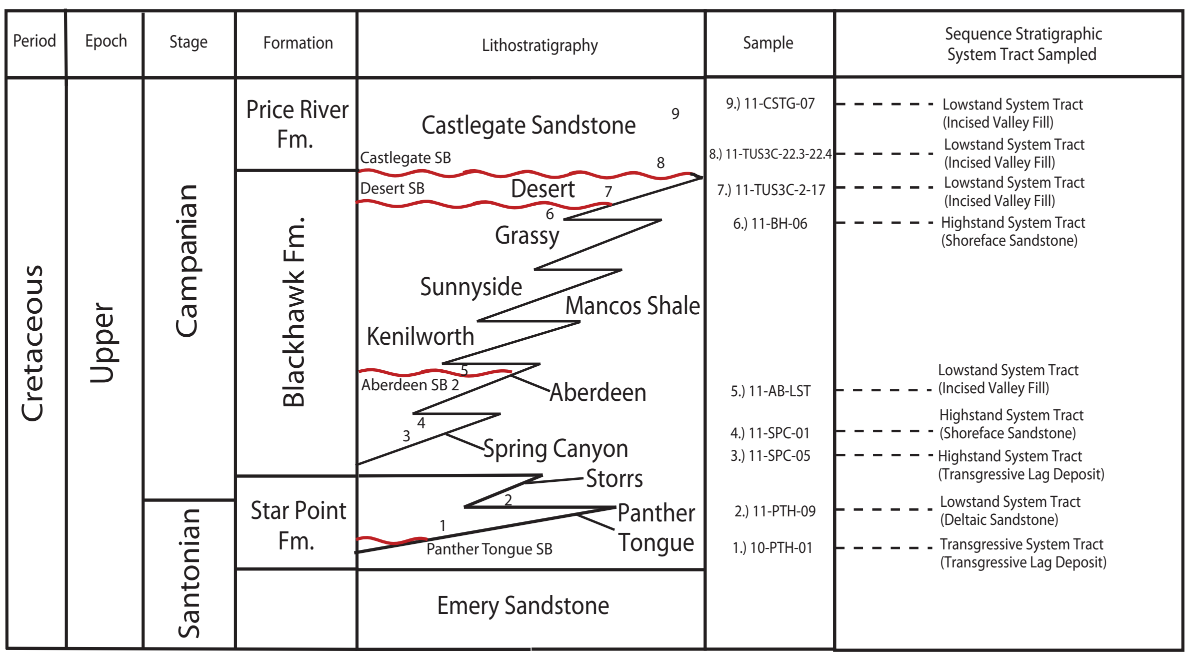
Period
Epoch
Stage
Formation
Lithostratigraphy
Sample
Sequence Stratigraphic System Tract Sampled
Cretaceous
Upper
Campanian
Santonian
Price River Fm.
Blackhawk Fm.
Star Point Fm.
Castlegate Sandstone
Castlegate SB
Desert SB
Desert
Grassy
Sunnyside
Mancos Shale
Kenilworth
Aberdeen SB 2
Aberdeen
Spring Canyon
Storrs
Panther Tongue
Panther Tongue SB
Emery Sandstone
9.) 11-CSTG-07
8.) 11-TUS3C-22.3-22.4
7.) 11-TUS3C-2-17
6.) 11-BH-06
5.) 11-AB-LST
4.) 11-SPC-01
3.) 11-SPC-05
2.) 11-PTH-09
1.) 10-PTH-01
Lowstand System Tract (Incised Valley Fill)
Lowstand System Tract (Incised Valley Fill)
Lowstand System Tract (Incised Valley Fill)
Highstand System Tract (Shoreface Sandstone)
Lowstand System Tract (Incised Valley Fill)
Highstand System Tract (Shoreface Sandstone)
Highstand System Tract (Transgressive Lag Deposit)
Lowstand System Tract (Deltaic Sandstone)
Transgressive System Tract (Transgressive Lag Deposit)

Figure 4.) Simplified map of significant Precambrian terranes of North American. The terranes highlighted are potential source of sediment for the Pine Ridge Sandstone and Almond Formation of the Mesaverde Group, the Dad Member of the Lewis Shale, and the Fox Hills Sandstone in the Greater Green River Basin, Wyoming of the Greater Green River Basin, Wyoming and the Star Point Formation, Blackhawk Formation, and the Castlegate Sandstone of the Book Cliffs, Utah. Modified from Dickinson and Gehrels (2009).

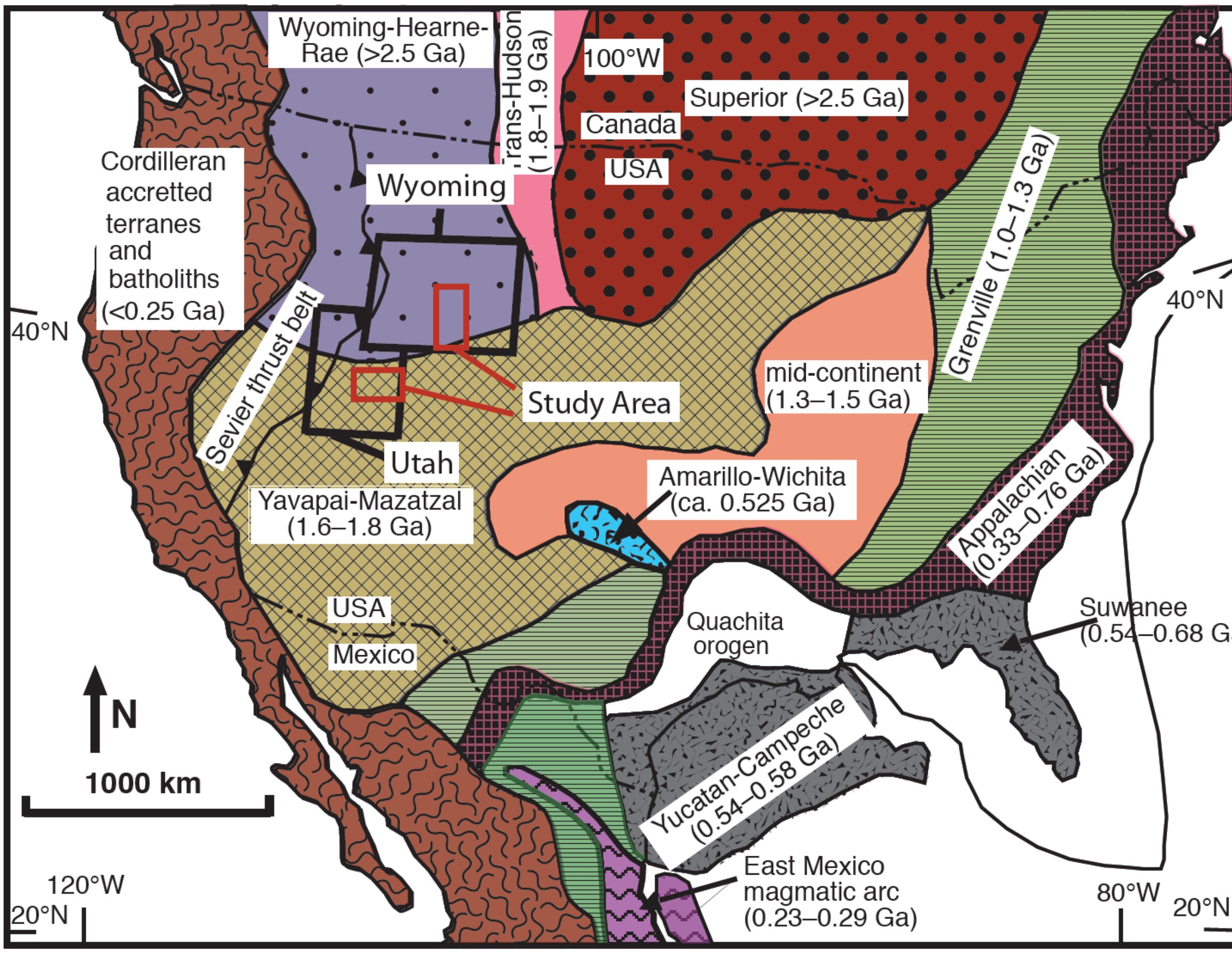

Wyoming-Hearne-Rae (>2.5 Ga)
Trans-Hudson (1.8–1.9 Ga)
100°W
Superior (>2.5 Ga)
Canada
USA
Cordilleran accretted terranes and batholiths (<0.25 Ga)
Wyoming
40°N
Sevier thrust belt
Study Area
mid-continent (1.3–1.5 Ga)
Grenville (1.0–1.3 Ga)
40°N
Utah
Yavapai-Mazatzal (1.6–1.8 Ga)
Amarillo-Wichita (ca. 0.525 Ga)
Appalachian (0.33–0.76 Ga)
USA
Mexico
Quachita orogen
Suwanee (0.54–0.68 Ga
N
1000 km
Yucatan-Campeche (0.54–0.58 Ga)
East Mexico magmatic arc (0.23–0.29 Ga)
120°W
20°N
80°W
20°N

Figure 5.) Simplified paleogeographic map of the supercontinent Rodinia. The assembly of Rodinia and subsequent continent-continent collision between Laurentia, Africa and South America created large-scale deformation along the margins of Laurentia and intrusions of mafic dikes in the north. The final stage in the assembly of Rodinia was marked by the accretion of the Grenville terrane along the eastern margin of Laurentia. The break up Rodinia at ~.78-.54 Ga, initiated with rifting along the western margin of Laurentia opening the paleo-Pacific Ocean (Whitmeyer and Karlstrom, 2007). Modified from Bogdanova et al., 2007.

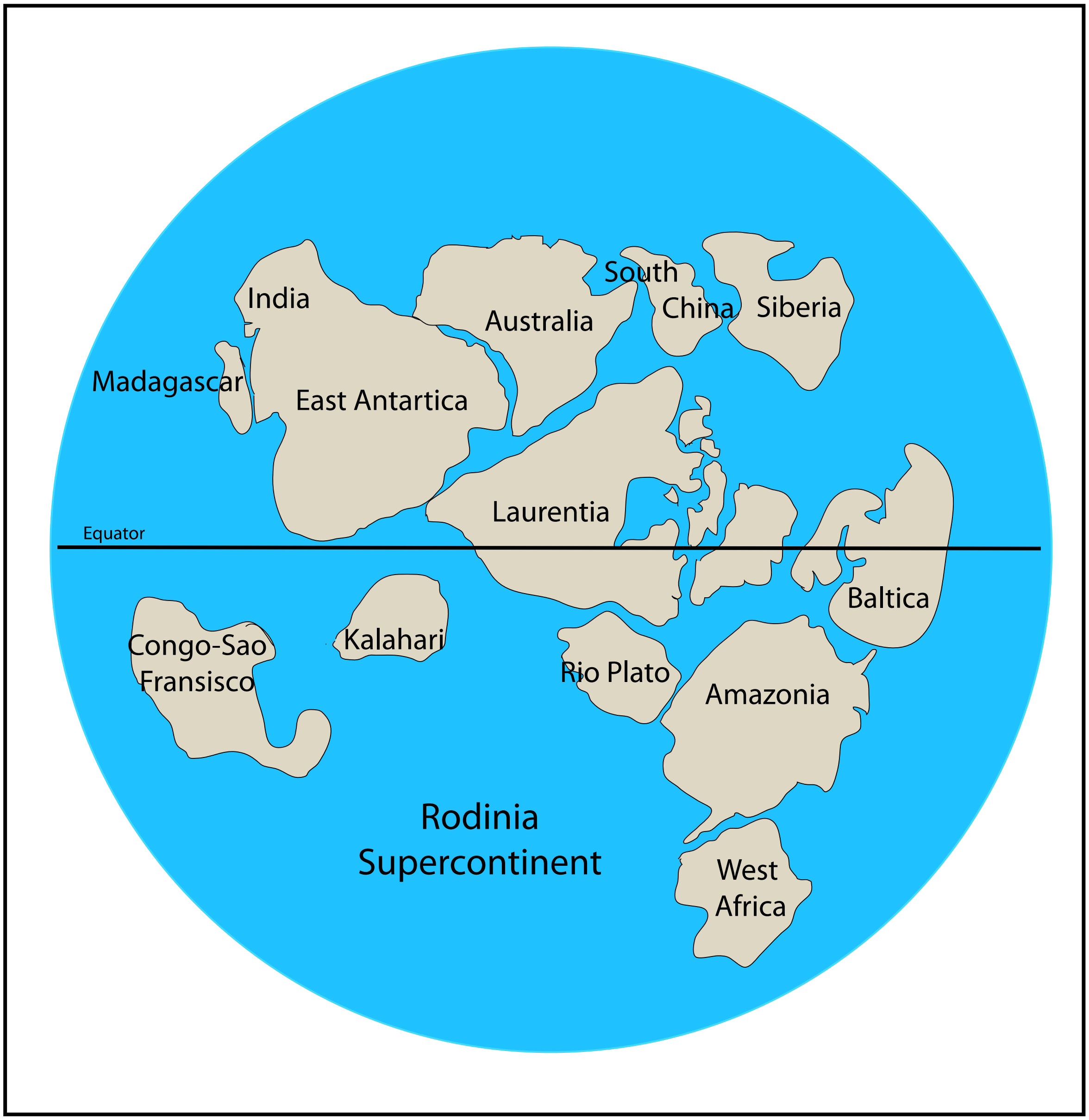
India
Australia
South
China
Siberia
Madagascar
East Antartica
Laurentia
Equator
Baltica
Congo-Sao
Fransisco
Kalahari
Rio Plato
Amazonia
Rodinia
Supercontinent
West
Africa

Figure 6.) Simplified paleogeographic map of the supercontinent Pangaea. Assembly of Pangaea began in the Late Paleozoic with the docking of Gondwanaland with Laurasia. Disassembly of Pangaea initiated in the Late Jurassic with rifting between Africa and Laurentia. Map modified from Bogdanova and others (2007).

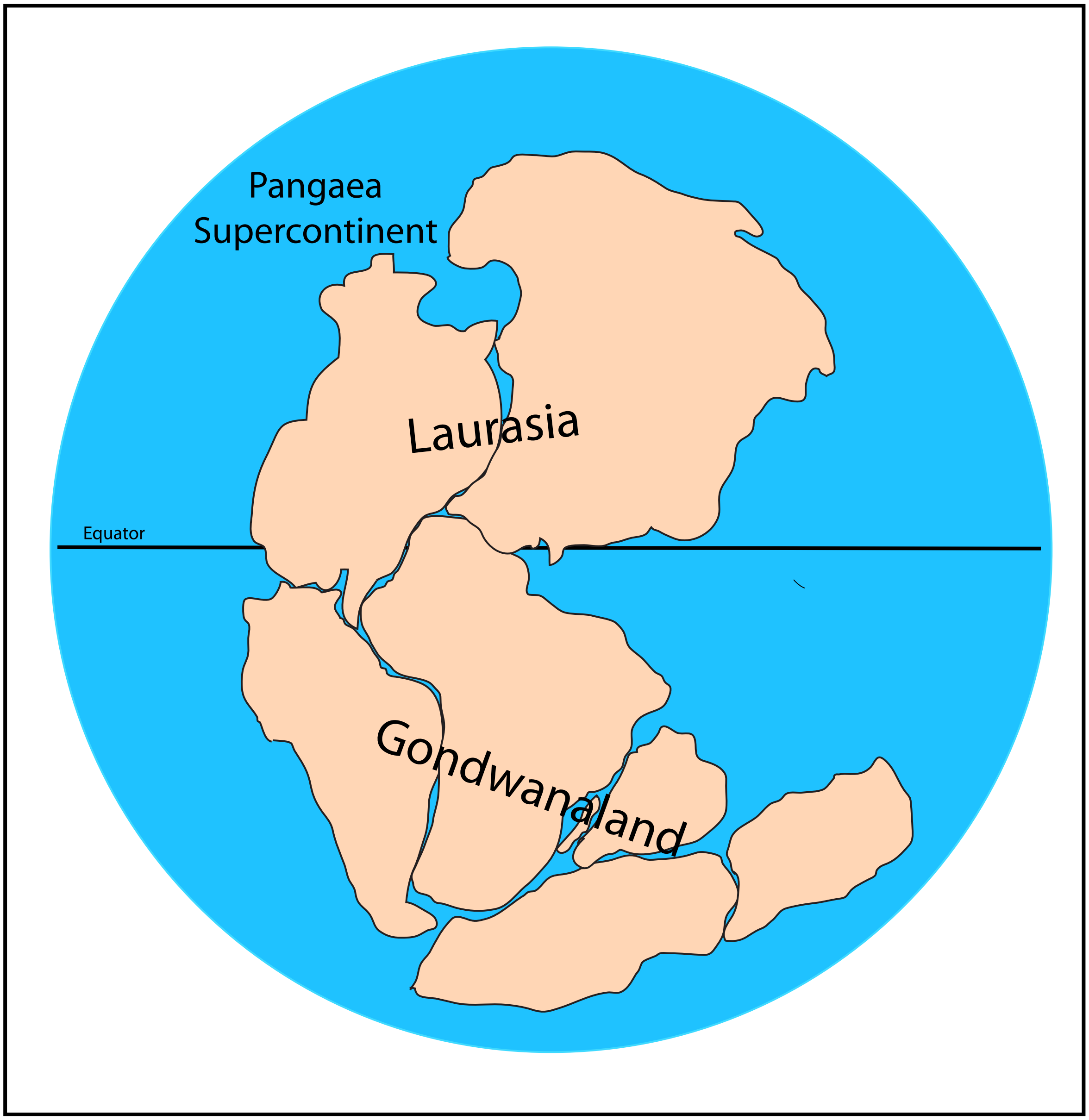
Pangaea
Supercontinent
Laurasia
Equator
Gondwanaland

Figure 7.) Paleogeographic map of North America in the Late Cretaceous (75 Ma). The map shows the generalized locations of the Sevier Orogenic belt, the North American Cordillera, and Cretaceous Western Interior Seaway. Modified from Blakey (2008).

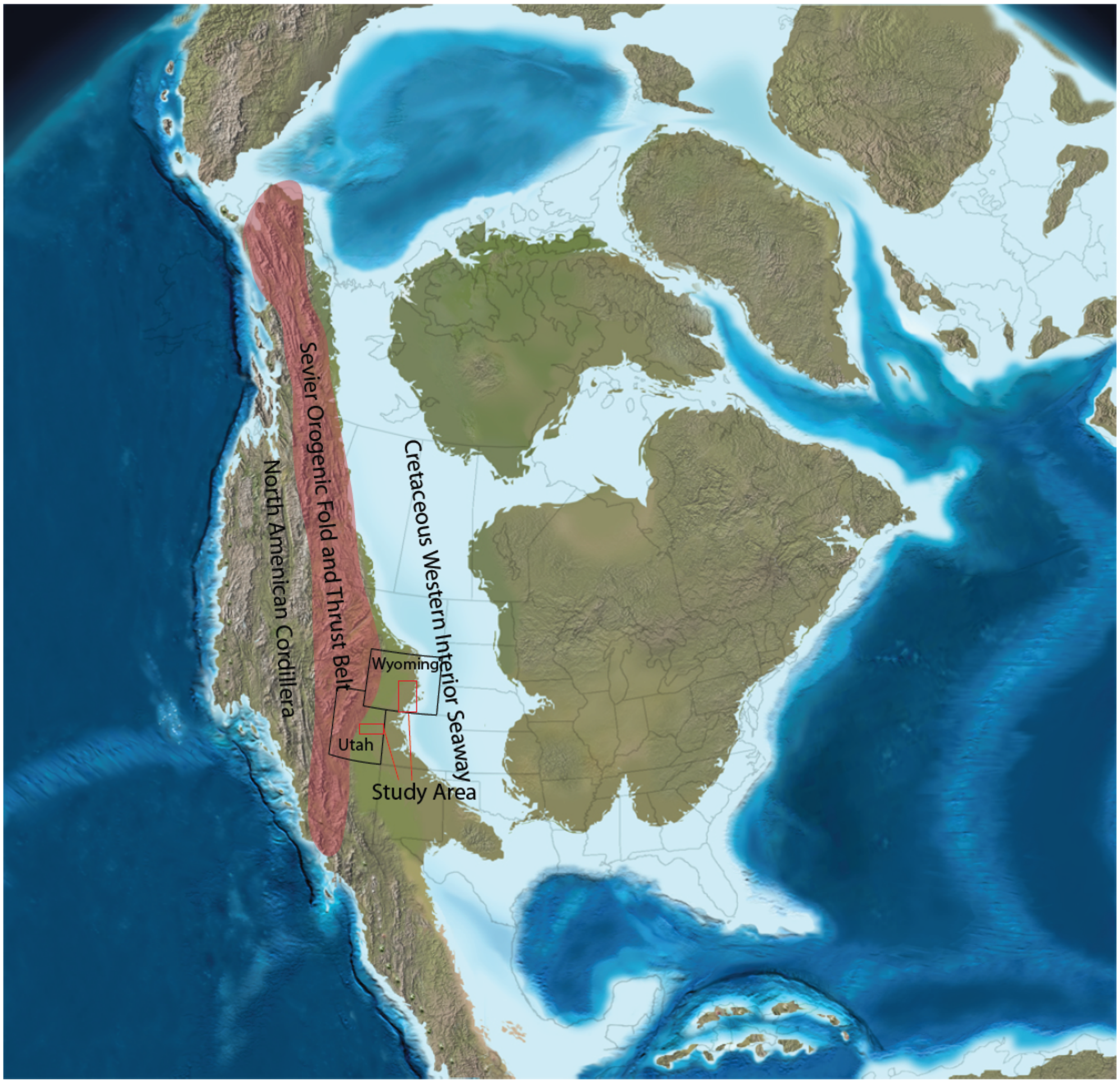
Sevier Orogenic Fold and Thrust Belt
North American Cordillera
Cretaceous Western Interior Seaway
Wyoming
Utah
Study Area

Figure 8.) Simplified map showing Laramide sedimentary basins and major Laramide thrust-block uplifts. During the latest Cretaceous, thick-skinned Laramide deformation segmented the broad Sevier foreland basin forming localized sedimentary basins. The red rectangles highlight the areas of interest for this study. Map modified from Miller et al. (1992).

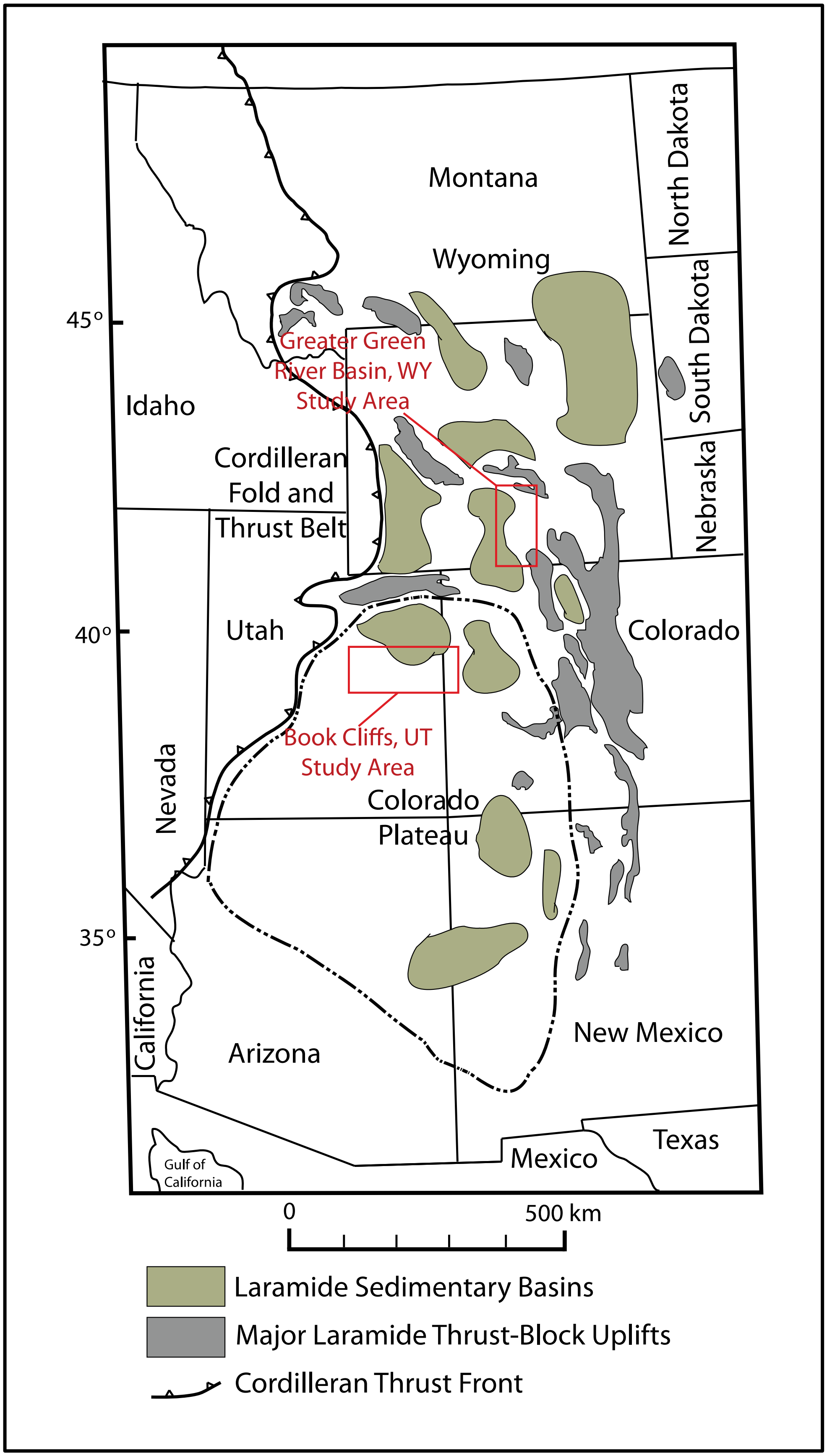

Montana
Wyoming
North Dakota
South Dakota
Nebraska
45°
40°
35°
Idaho
Greater Green River Basin, WY Study Area
Cordilleran Fold and Thrust Belt
Utah
Colorado
Book Cliffs, UT Study Area
Nevada
Colorado Plateau
California
Arizona
New Mexico
Texas
Mexico
Gulf of California
0
500 km
Laramide Sedimentary Basins
Major Laramide Thrust-Block Uplifts
Cordilleran Thrust Front

Figure 9.) Simplified regional tectonic map showing Laramide Orogenic uplifts in the southwest corner of Wyoming and adjacent states. The red rectangle represents the focus area for this study and the general area where samples were collected. Modified from Baars et al. (1988).

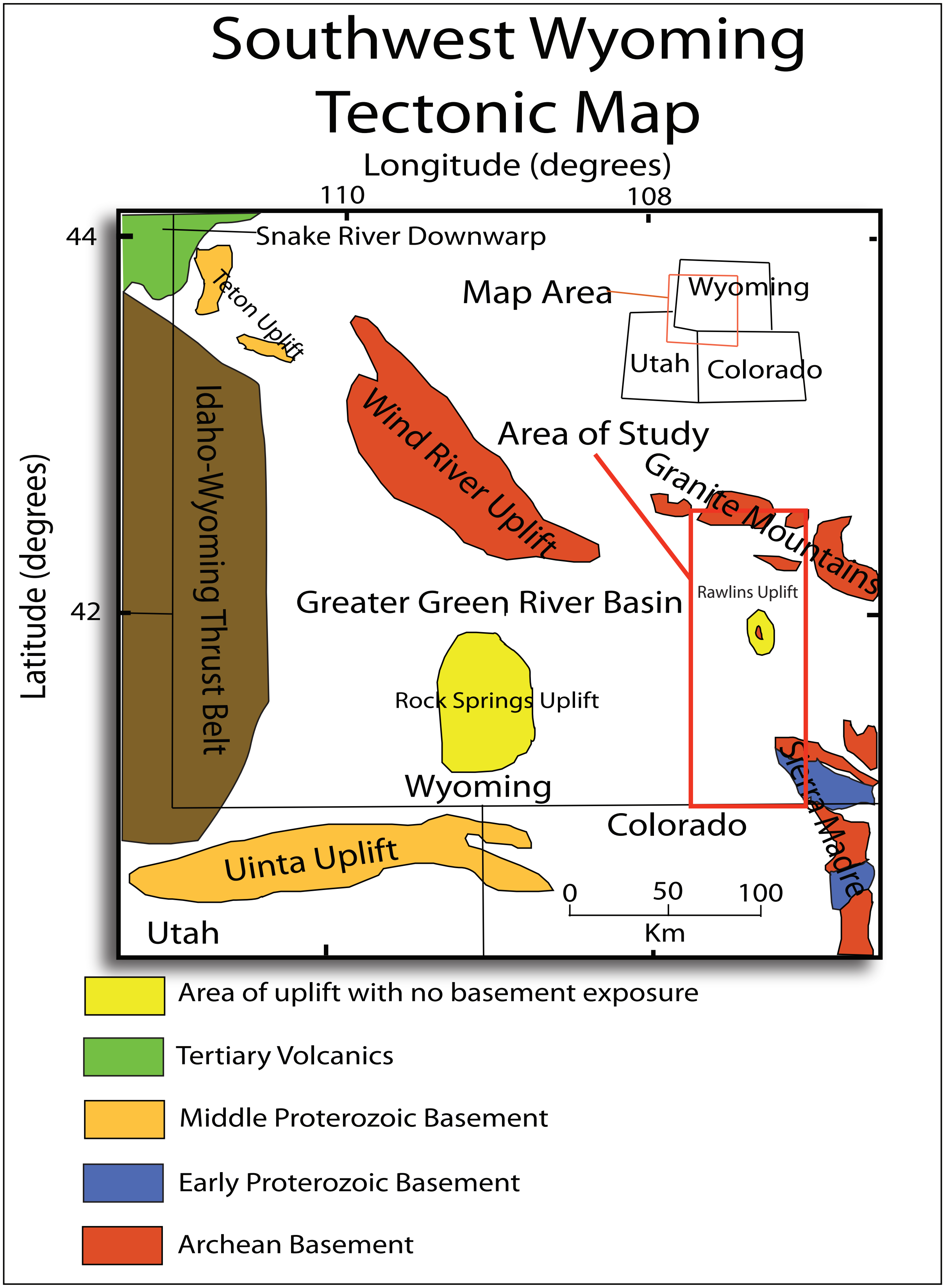

Southwest Wyoming
Tectonic Map
Longitude (degrees)
110
108
44
42
Latitude (degrees)
Snake River Downwarp
Teton Uplift
Map Area
Wyoming
Utah
Colorado
Wind River Uplift
Area of Study
Granite Mountains
Rawlins Uplift
Greater Green River Basin
Idaho-Wyoming Thrust Belt
Rock Springs Uplift
Wyoming
Sierra Madre
Colorado
Uinta Uplift
0
50
100
Km
Utah
Area of uplift with no basement exposure
Tertiary Volcanics
Middle Proterozoic Basement
Early Proterozoic Basement
Archean Basement

Figure 10.) Map of the Cretaceous Western Interior Seaway in Wyoming. The initiation of the Laramide Orogeny in Wyoming created an area of high elevation (in red) segmenting the once broad foreland basin. This created localized sedimentation patterns in the Greater Green River Basin, Wyoming. Modified from Pyles and Slatt (2007).

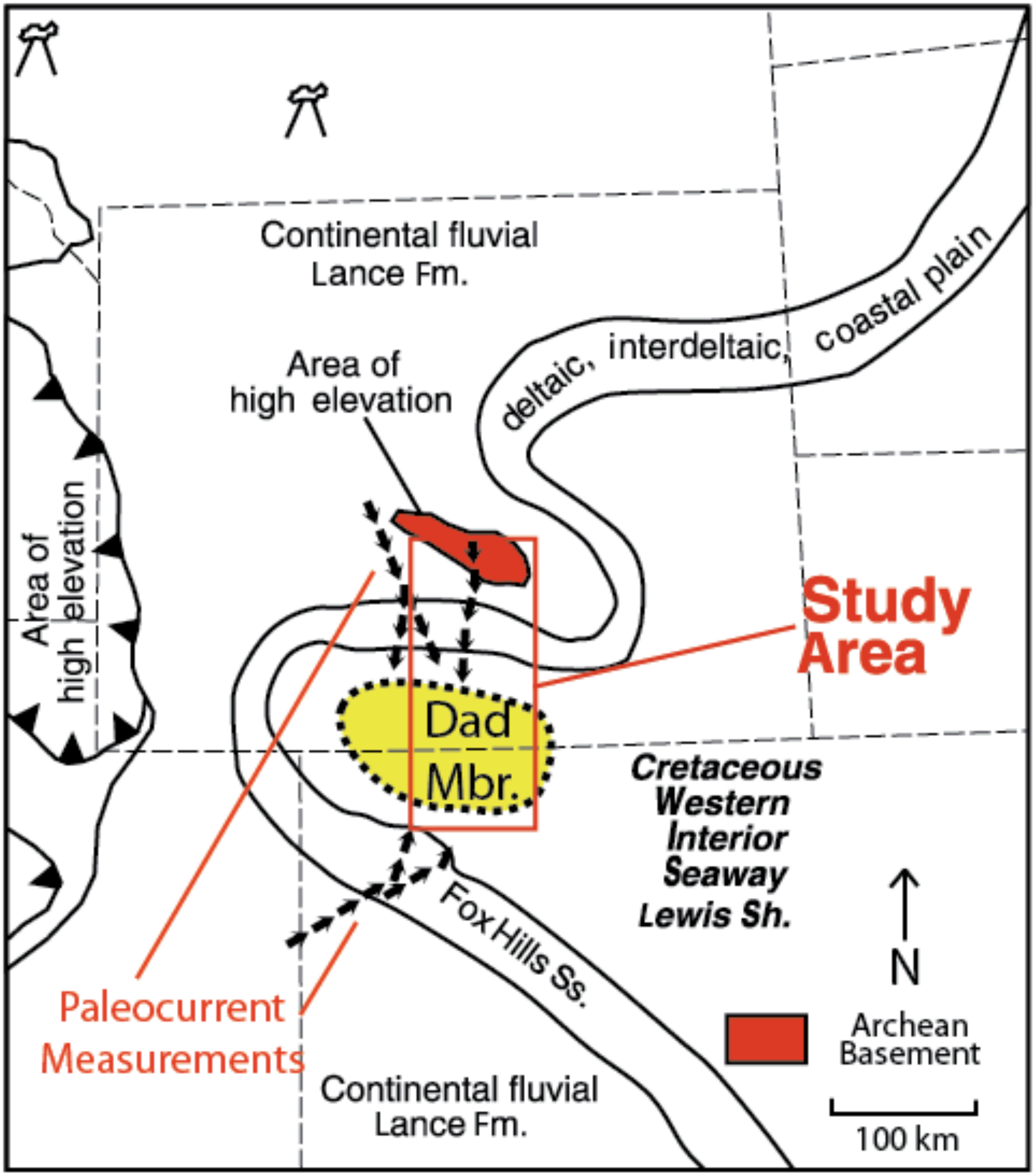
Continental fluvial
Lance Fm.
Area of
high elevation
deltaic, interdeltaic, coastal plain
Area of
high elevation
Study
Area
Dad
Mbr.
Cretaceous
Western
Interior
Seaway
Lewis Sh.
Fox Hills Ss.
N
Paleocurrent
Measurements
Archean
Basement
Continental fluvial
Lance Fm.
100 km

Figure 11.) Stratigraphic cross section of the Fox Hills Sandstone, Lewis Shale, Dad Member of the Lewis Shale, and Almond Formation. These Late cretaceous sedimentary units were deposited as a southward prorating clastic wedge in the Greater Green River Basin, Wyoming. Modified from Pyles and Slatt (2007).

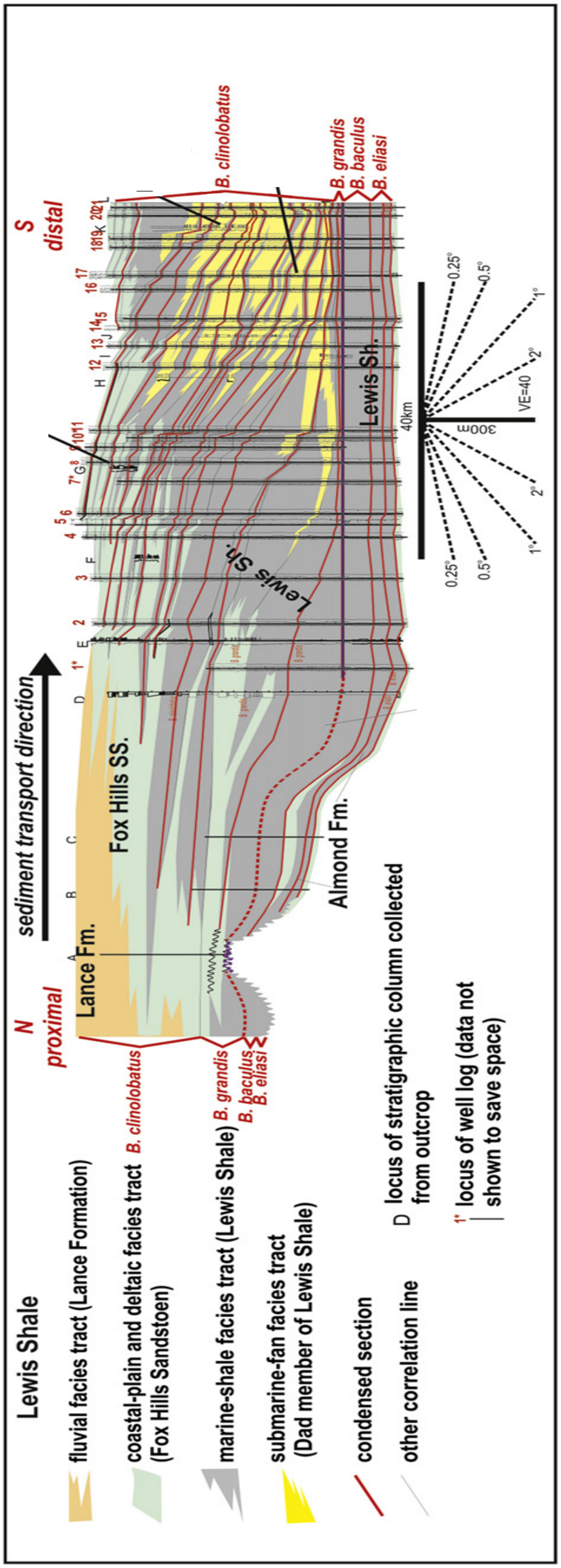
Lewis Shale
fluvial facies tract (Lance Formation)
coastal-plain and deltaic facies tract (Fox Hills Sandstoen)
marine-shale facies tract (Lewis Shale)
submarine-fan facies tract (Dad member of Lewis Shale)
condensed section
other correlation line
D locus of stratigraphic column collected from outcrop
1* locus of well log (data not shown to save space)
N proximal
S distal
sediment transport direction
Lance Fm.
Fox Hills SS.
Almond Fm.
Lewis Sh.
Lewis Sh.
B. clinolobatus
B. grandis
B. baculus
B. eliasi
40km
300m
VE=40

Figure 12.) Digital elevation map of Wyoming, showing the Greater Green River Basin and the three associated sub-basins. The field area for this study is located east of Rawlins, Wyoming in the Great Divide and Washakie sub-basins of the Greater Green River Basin. Modified from Sterner (1995).

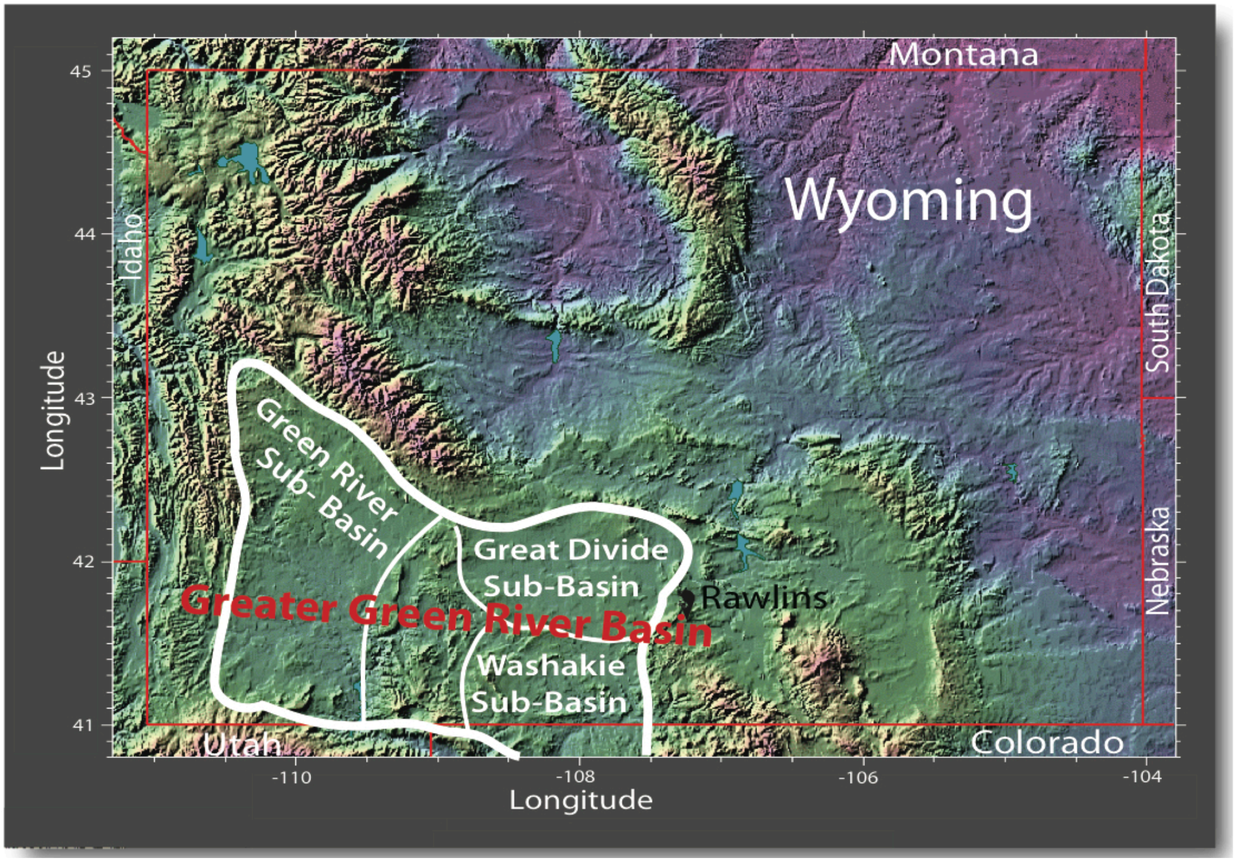
Montana
Wyoming
Idaho
South Dakota
Nebraska
Utah
Colorado
Green River
Sub- Basin
Great Divide
Sub-Basin
Washakie
Sub-Basin
Greater Green River Basin
Rawlins
Longitude
Longitude
45
44
43
42
41
-110
-108
-106
-104

Figure 13.) Simplified map of the study area in the Book Cliffs, Utah. Solid red boxes show the canyons where samples were acquired for this study. Modified from Van Wagoner (1995).

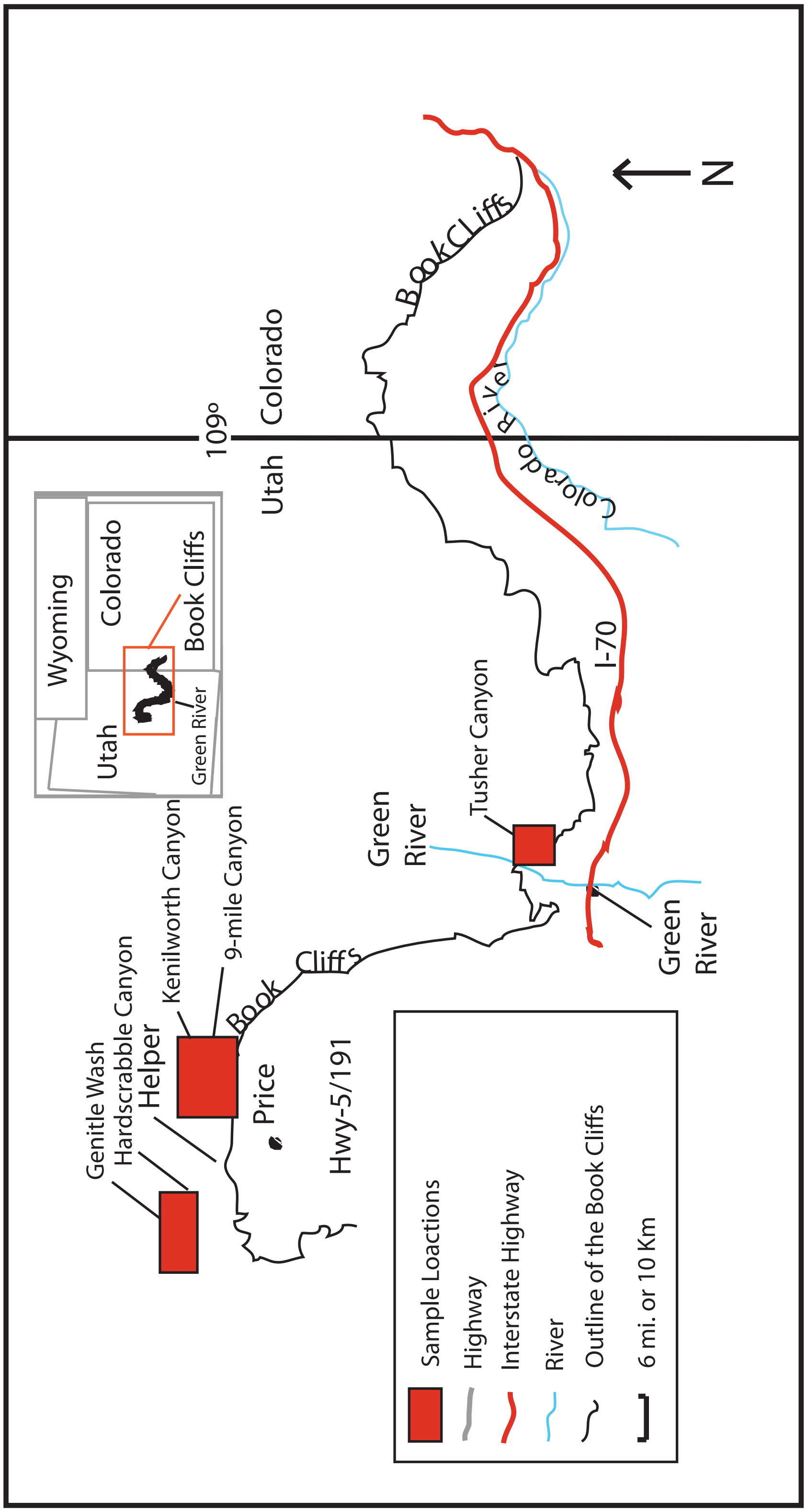

N
Book Cliffs
Colorado
109°
Utah
Colorado River
I-70
Tusher Canyon
Green River
Green River
Wyoming
Colorado
Book Cliffs
Utah
Green River
Genitle Wash
Hardscrabble Canyon
Helper
Kenilworth Canyon
9-mile Canyon
Book Cliffs
Price
Hwy-5/191
Sample Loactions
Highway
Interstate Highway
River
Outline of the Book Cliffs
6 mi. or 10 Km

Figure 14.) LA-ICP-MS U-Pb concordia diagrams and probability density/histogram plots of zircon from the Dad Member of the Lewis Shale. Plots show the resulting U-Pb age signature using mineral different separation procedures. Probability density plots and U-Pb concordia diagrams were constructed in Isoplot®/Ex. The Concordia diagrams include all U-Pb analyses and the probability density plots show all analyses that are <15% discordant. The number of grains (n) represents the number of analyses. LA-ICP-MS U-Pb isotope data of zircon can be found in Appendix C.

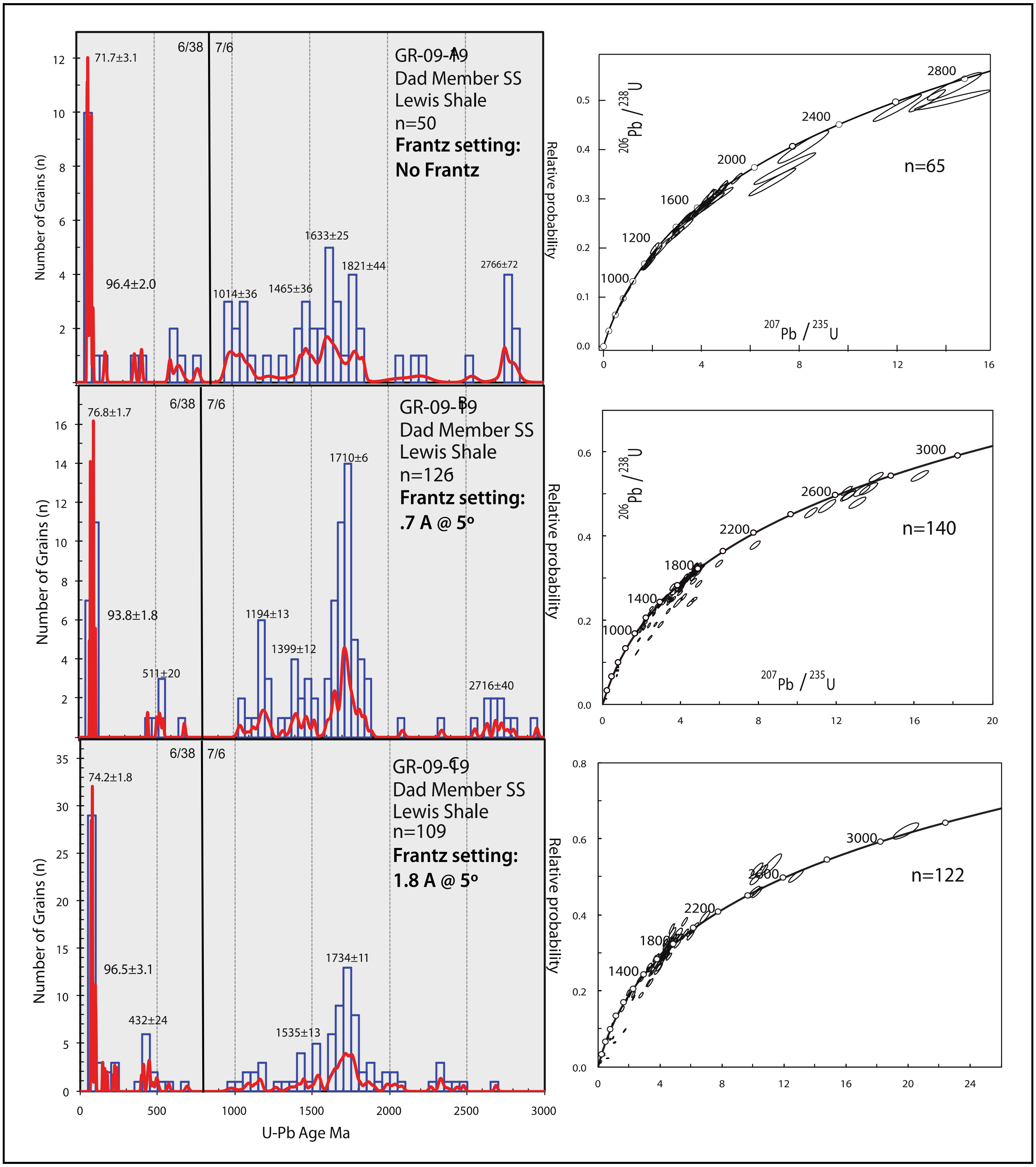
GR-09-19 A
Dad Member SS
Lewis Shale
n=50
Frantz setting:
No Frantz
71.7±3.1
96.4±2.0
1014±36
1465±36
1633±25
1821±44
2766±72
6/38
7/6
n=65
GR-09-19 B
Dad Member SS
Lewis Shale
n=126
Frantz setting:
.7 A @ 5°
76.8±1.7
93.8±1.8
511±20
1194±13
1399±12
1710±6
2716±40
n=140
GR-09-19 C
Dad Member SS
Lewis Shale
n=109
Frantz setting:
1.8 A @ 5°
74.2±1.8
96.5±3.1
432±24
1535±13
1734±11
n=122
Number of Grains (n)
Relative probability
U-Pb Age Ma
$^{206}Pb/^{238}U$
$^{207}Pb/^{235}U$

Figure 15.1-4) U-Pb concordia diagrams for LA-ICP-MS analyses of detrital rutile from samples collected in the Greater Green River Basin, Wyoming. Figure 16.1 contains U-Pb age data of rutile that was not separated using the Frantz Isodynamic separator. Figure 16.2 contains U-Pb age data of rutile from the non-magnetic fraction at a Frantz setting of 1.8A at 5°. Figure 16.3 contains U-Pb age data of rutile that was not separated based on magnetic susceptibility. Figure 16.4 contains U-Pb age data of rutile from the non-magnetic fraction at a Frantz setting of 1.8A at 5°. U-Pb concordia diagrams were constructed in Iolite®. The number of grains (n) represents the number of analyses. LA-ICP-MS U-Pb isotope data of rutile can be found in Appendix D.

15.1)

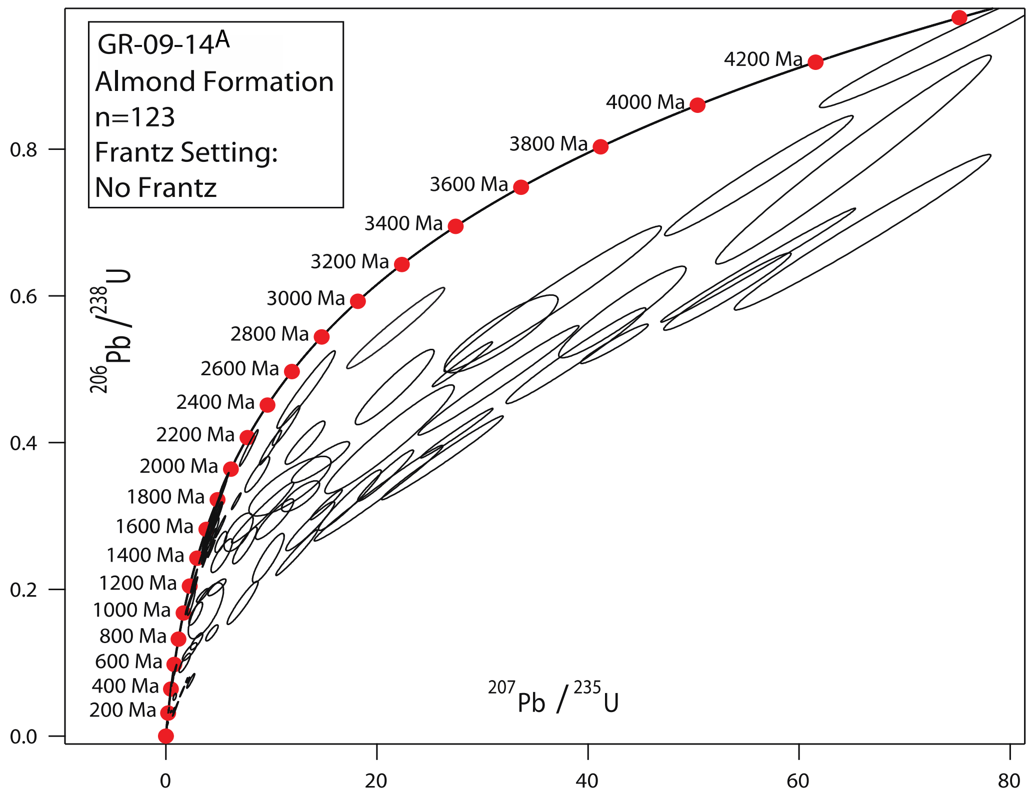
GR-09-14A
Almond Formation
n=123
Frantz Setting:
No Frantz
4200 Ma
4000 Ma
3800 Ma
3600 Ma
3400 Ma
3200 Ma
3000 Ma
2800 Ma
2600 Ma
2400 Ma
2200 Ma
2000 Ma
1800 Ma
1600 Ma
1400 Ma
1200 Ma
1000 Ma
800 Ma
600 Ma
400 Ma
200 Ma
$^{206}Pb/^{238}U$
$^{207}Pb/^{235}U$
0.0
0.2
0.4
0.6
0.8
0
20
40
60
80

15.2)

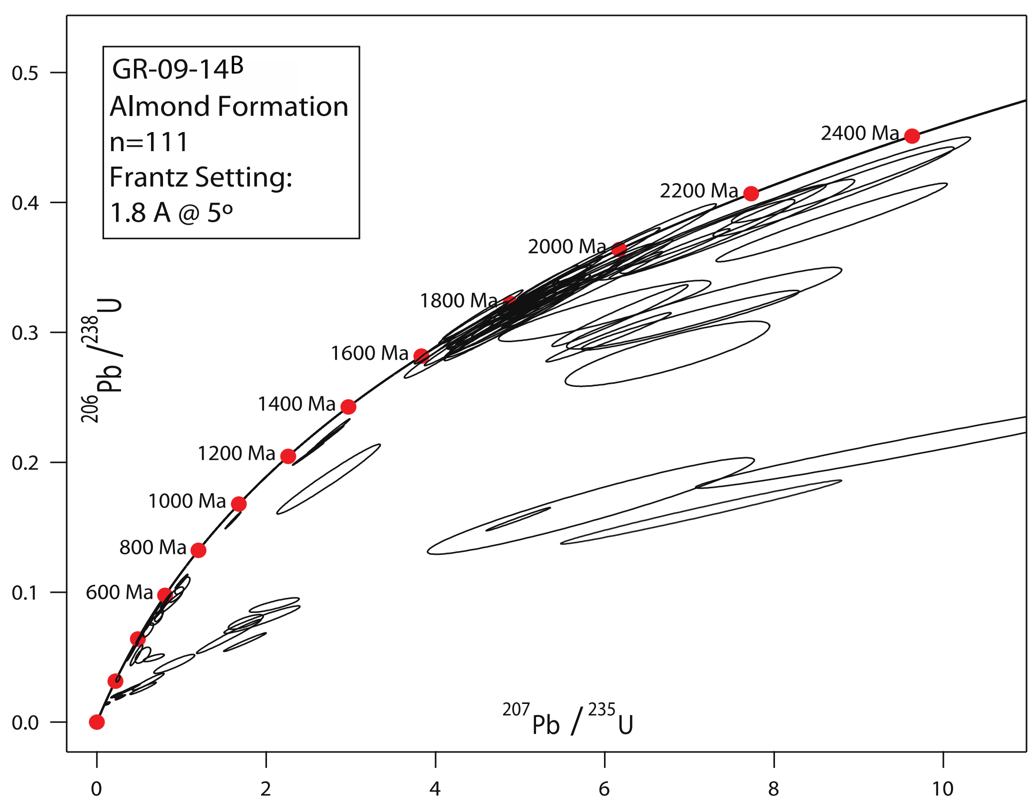
GR-09-14B
Almond Formation
n=111
Frantz Setting:
1.8 A @ 5°
2400 Ma
2200 Ma
2000 Ma
1800 Ma
1600 Ma
1400 Ma
1200 Ma
1000 Ma
800 Ma
600 Ma
$^{206}Pb/^{238}U$
$^{207}Pb/^{235}U$
0.0
0.1
0.2
0.3
0.4
0.5
0
2
4
6
8
10

15.3)

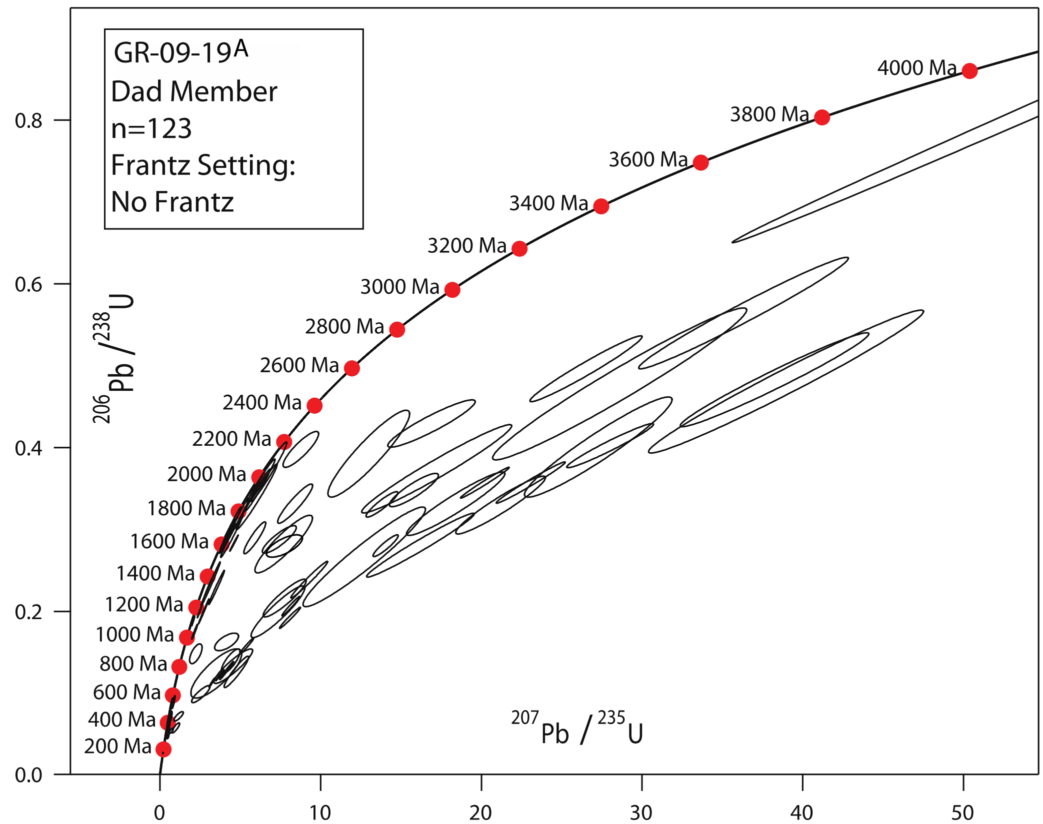
GR-09-19A
Dad Member
n=123
Frantz Setting:
No Frantz
4000 Ma
3800 Ma
3600 Ma
3400 Ma
3200 Ma
3000 Ma
2800 Ma
2600 Ma
2400 Ma
2200 Ma
2000 Ma
1800 Ma
1600 Ma
1400 Ma
1200 Ma
1000 Ma
800 Ma
600 Ma
400 Ma
200 Ma
$^{206}Pb/^{238}U$
$^{207}Pb/^{235}U$
0.0
0.2
0.4
0.6
0.8
0
10
20
30
40
50

15.4)

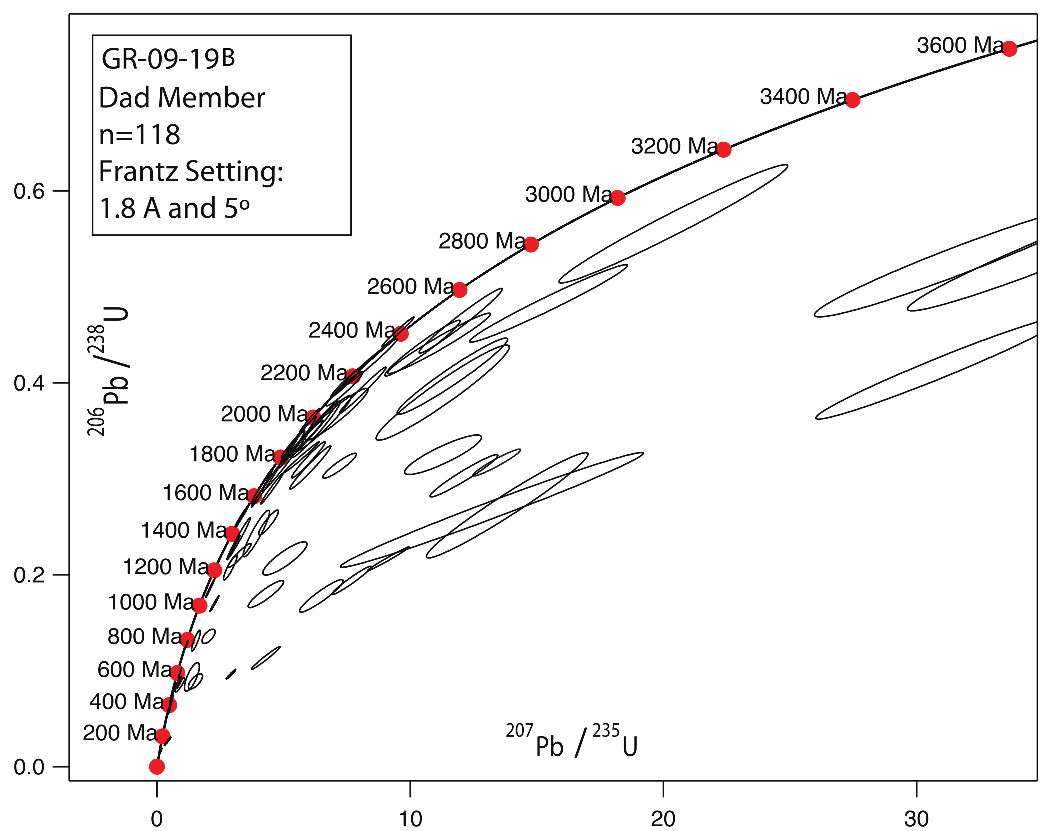
GR-09-19B
Dad Member
n=118
Frantz Setting:
1.8 A and 5°
3600 Ma
3400 Ma
3200 Ma
3000 Ma
2800 Ma
2600 Ma
2400 Ma
2200 Ma
2000 Ma
1800 Ma
1600 Ma
1400 Ma
1200 Ma
1000 Ma
800 Ma
600 Ma
400 Ma
200 Ma
$^{206}Pb/^{238}U$
$^{207}Pb/^{235}U$
0.0
0.2
0.4
0.6
0
10
20
30

Figure 16.1-4: QEMSCAN analyses of Bromoform heavy minerals (>2.85 g/cm^3) for sedimentary samples collected from the Greater Green River Basin, Wyoming. Graphs are listed in stratigraphic order from youngest to oldest.

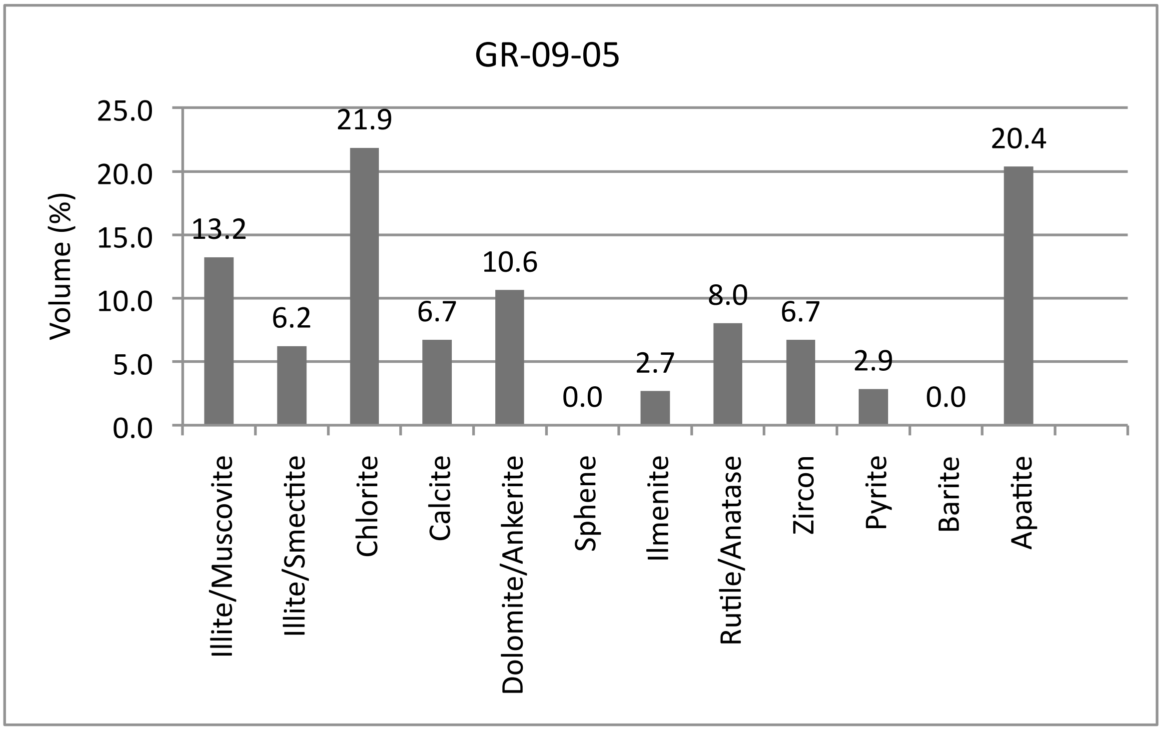

Figure 16.1: Fox Hill Sandstone.

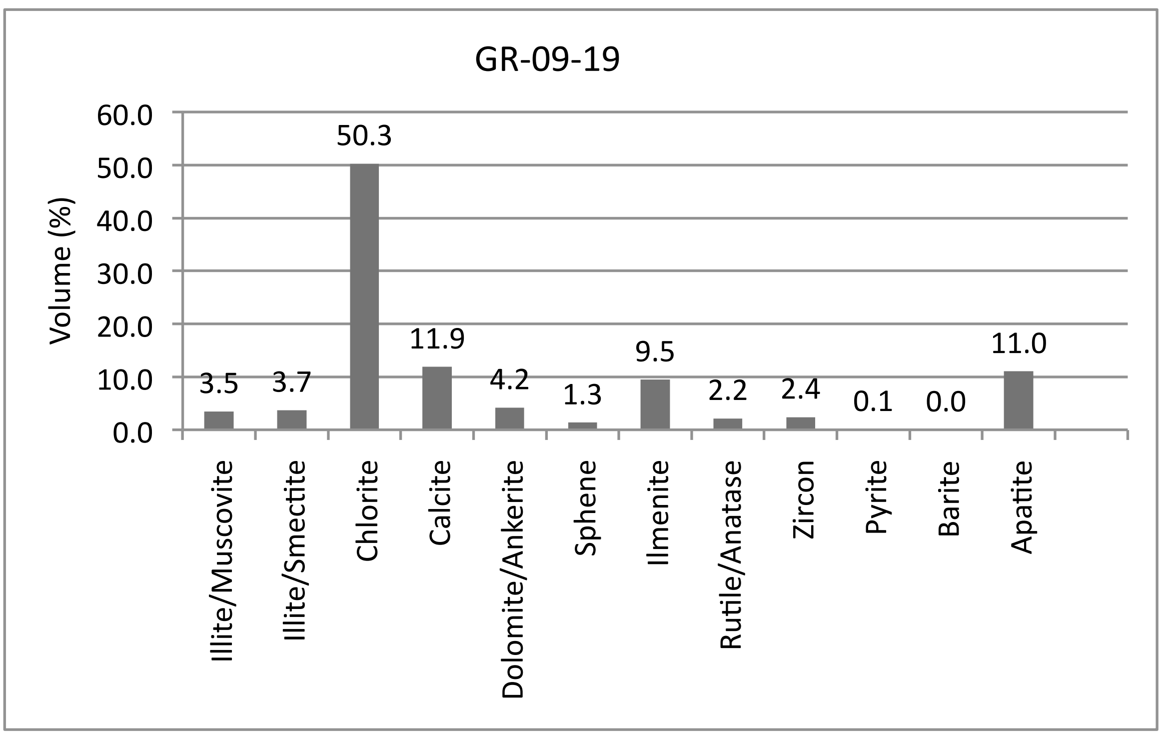

Figure 16.2: Dad Member of the Lewis Shale.

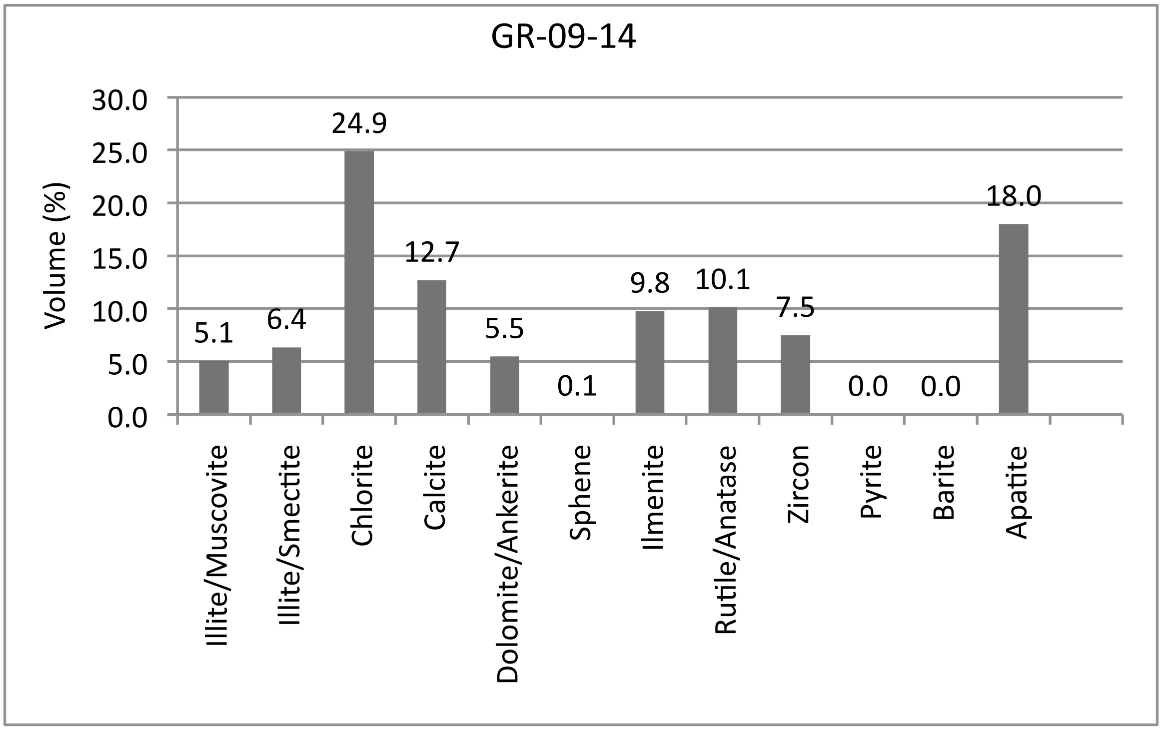

Figure 16.3: Almond Formation Sandstone.

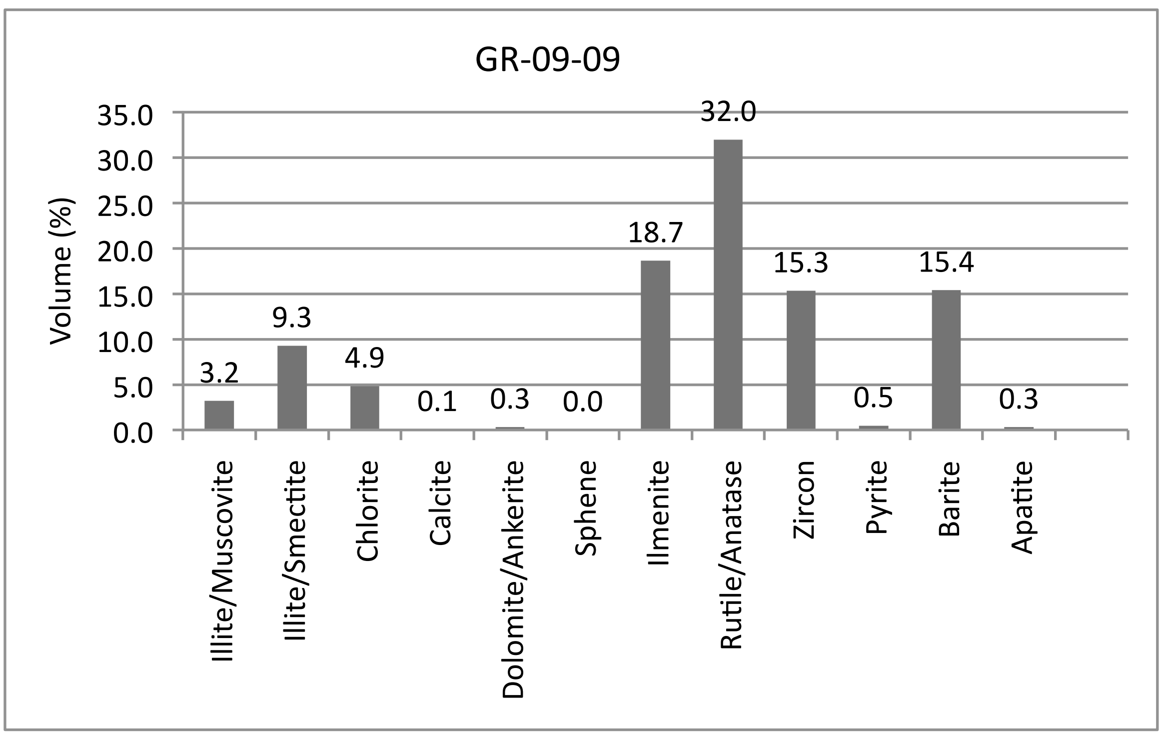

Figure 16.4: Pine Ridge Sandstone of the Mesaverde Group.

Figure 17.) Probability density plots and U-Pb concordia diagrams for LA-ICP-MS analyses of zircon from samples collected in the Greater Green River Basin, Wyoming. Probability density plots and U-Pb concordia diagrams were constructed in Isoplot®/Ex. The Concordia diagrams include all U-Pb analyses and the probability density plots show all analyses that are <15% discordant. The number of grains (n) represents the number of analyses. LA-ICP-MS U-Pb isotopic data of rutile can be found in Appendix C.

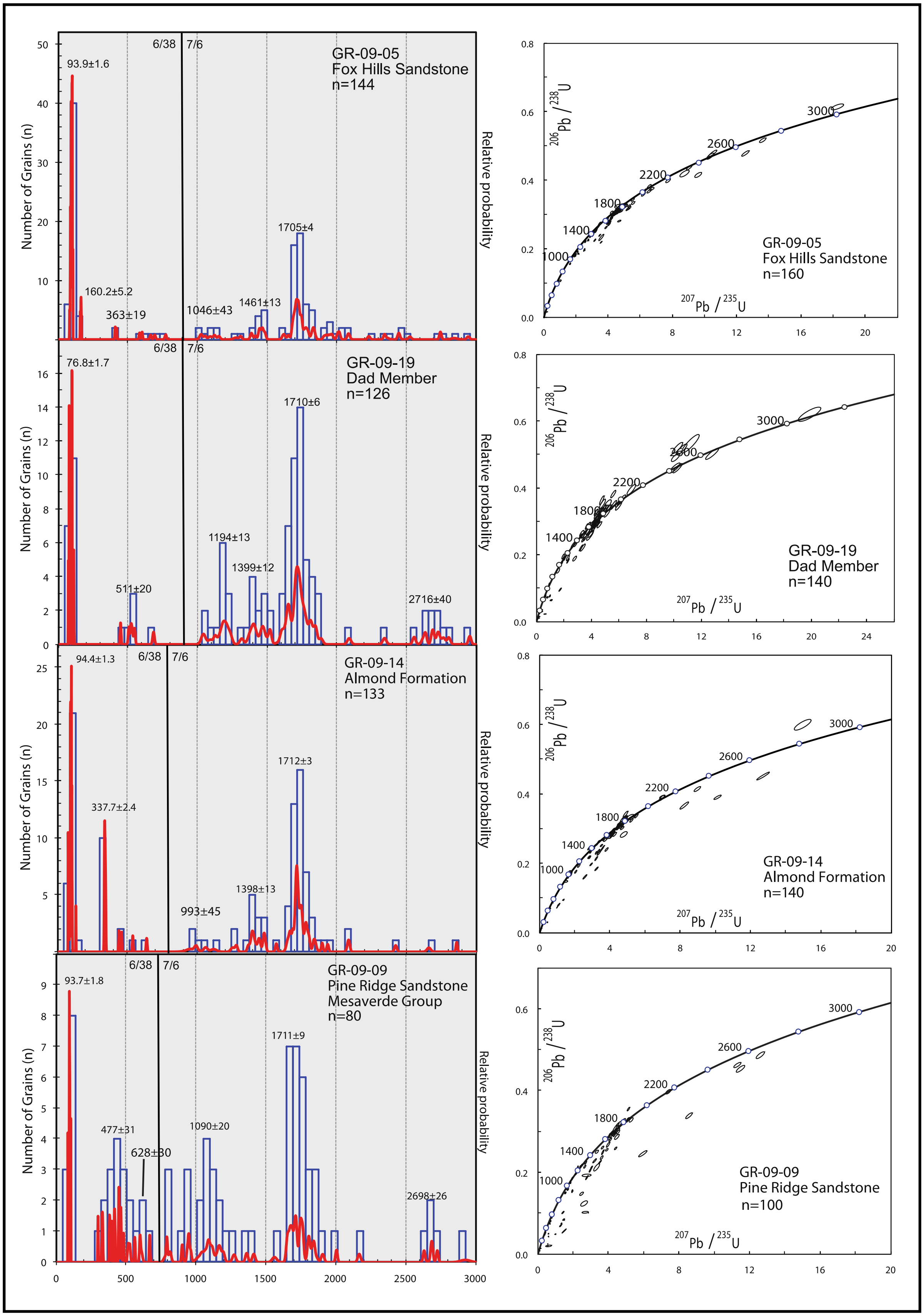
GR-09-05
Fox Hills Sandstone
n=144
93.9±1.6
160.2±5.2
363±19
1046±43
1461±13
1705±4
6/38
7/6
GR-09-19
Dad Member
n=126
76.8±1.7
511±20
1194±13
1399±12
1710±6
2716±40
GR-09-14
Almond Formation
n=133
94.4±1.3
337.7±2.4
993±45
1398±13
1712±3
GR-09-09
Pine Ridge Sandstone
Mesaverde Group
n=80
93.7±1.8
477±31
628±30
1090±20
1711±9
2698±26
Number of Grains (n)
Relative probability
GR-09-05
Fox Hills Sandstone
n=160
GR-09-19
Dad Member
n=140
GR-09-14
Almond Formation
n=140
GR-09-09
Pine Ridge Sandstone
n=100
206Pb / 238U
207Pb / 235U

Figure 18.1-4) U-Pb concordia diagrams for LA-ICP-MS analyses of detrital rutile from samples collected in the Greater Green River Basin, Wyoming. U-Pb concordia diagrams were constructed in Iolite®. The number of grains (n) represents the number of analyses. Supplemental data of LA-ICP-MS U-Pb age data of rutile can be found in Appendix D.

18.1)

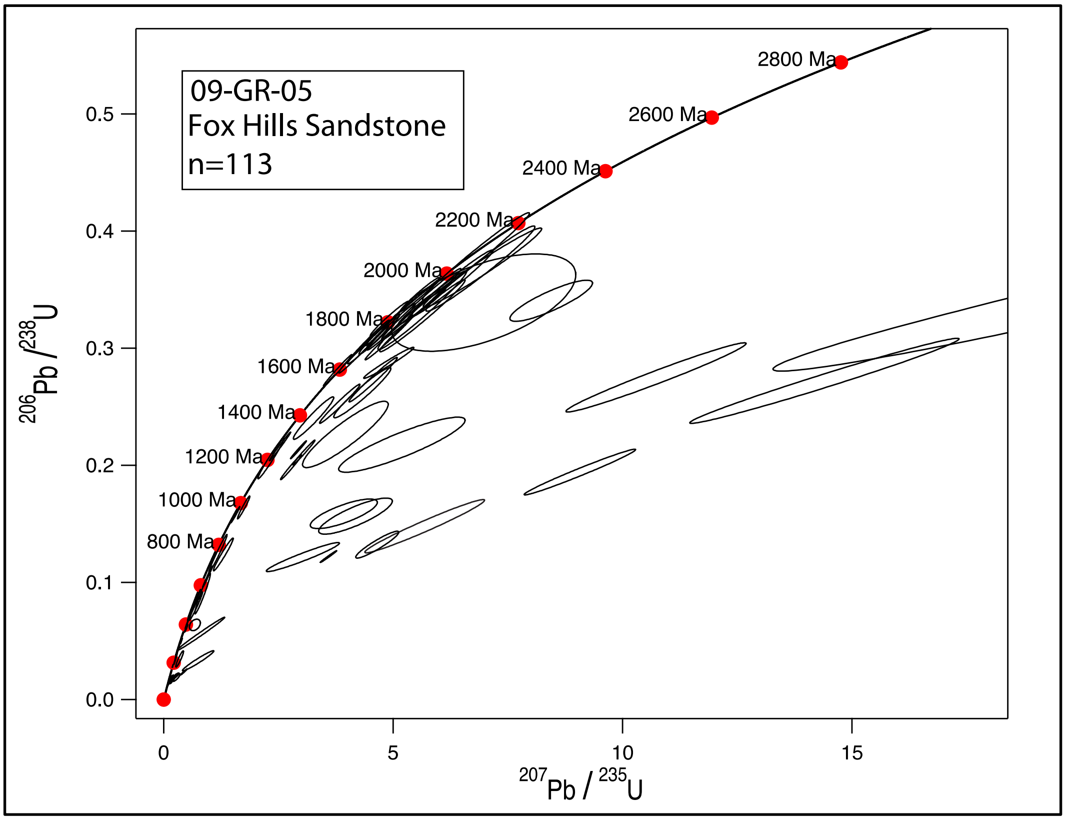
09-GR-05
Fox Hills Sandstone
n=113
2800 Ma
2600 Ma
2400 Ma
2200 Ma
2000 Ma
1800 Ma
1600 Ma
1400 Ma
1200 Ma
1000 Ma
800 Ma
0.5
0.4
0.3
0.2
0.1
0.0
0
5
10
15
206Pb / 238U
207Pb / 235U

18.2)

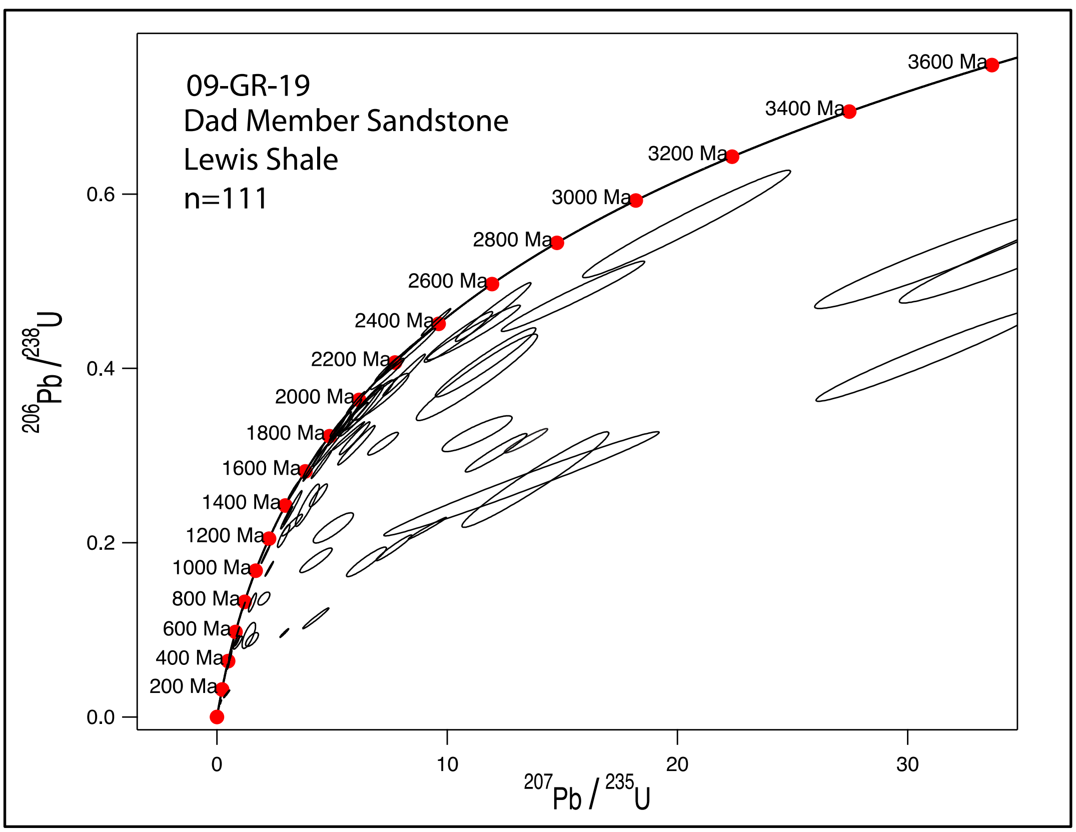
09-GR-19
Dad Member Sandstone
Lewis Shale
n=111
3600 Ma
3400 Ma
3200 Ma
3000 Ma
2800 Ma
2600 Ma
2400 Ma
2200 Ma
2000 Ma
1800 Ma
1600 Ma
1400 Ma
1200 Ma
1000 Ma
800 Ma
600 Ma
400 Ma
200 Ma
0.6
0.4
0.2
0.0
0
10
20
30
206Pb / 238U
207Pb / 235U

18.3)

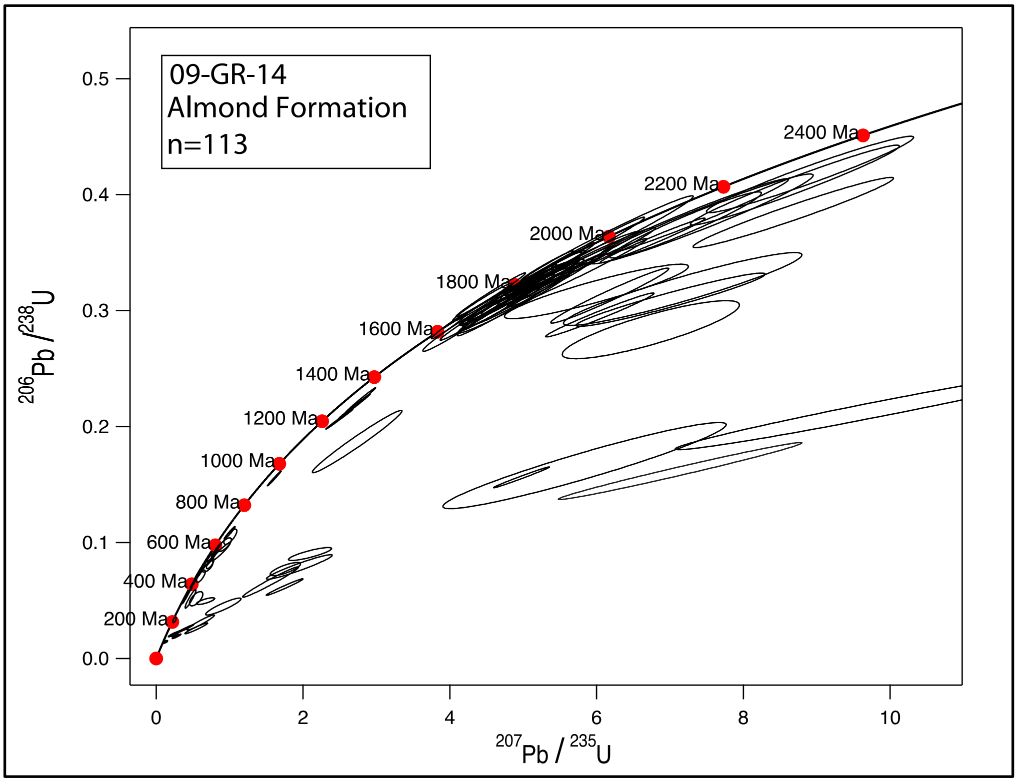
09-GR-14
Almond Formation
n=113
2400 Ma
2200 Ma
2000 Ma
1800 Ma
1600 Ma
1400 Ma
1200 Ma
1000 Ma
800 Ma
600 Ma
400 Ma
200 Ma
0.5
0.4
0.3
0.2
0.1
0.0
0
2
4
6
8
10
$^{206}Pb/^{238}U$
$^{207}Pb/^{235}U$

18.4)

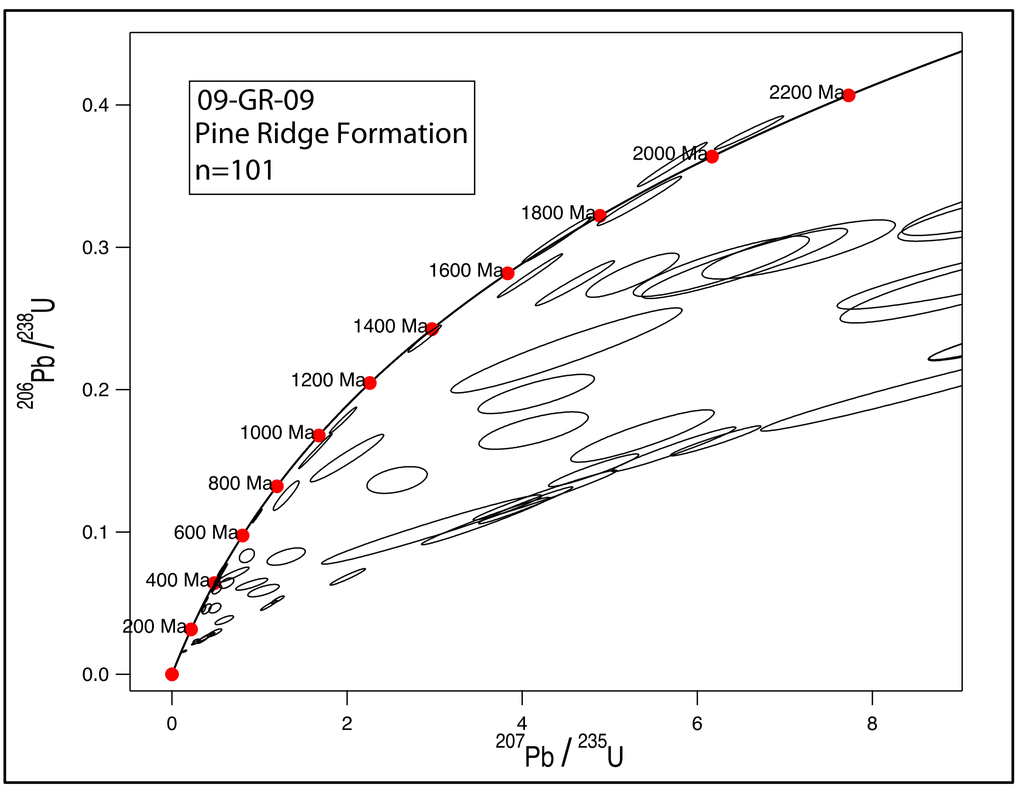
09-GR-09
Pine Ridge Formation
n=101
2200 Ma
2000 Ma
1800 Ma
1600 Ma
1400 Ma
1200 Ma
1000 Ma
800 Ma
600 Ma
400 Ma
200 Ma
0.4
0.3
0.2
0.1
0.0
0
2
4
6
8
$^{206}Pb/^{238}U$
$^{207}Pb/^{235}U$

Figure 19.1-10: QEMSCAN analytical results for sedimentary samples collected from the Book Cliffs, Utah. Graphs are ordered in pairs showing QEMSCAN analyses of samples collected from contrasting sequence stratigraphic system tracts in the Blackhawk Formation and the Star Point Formation.

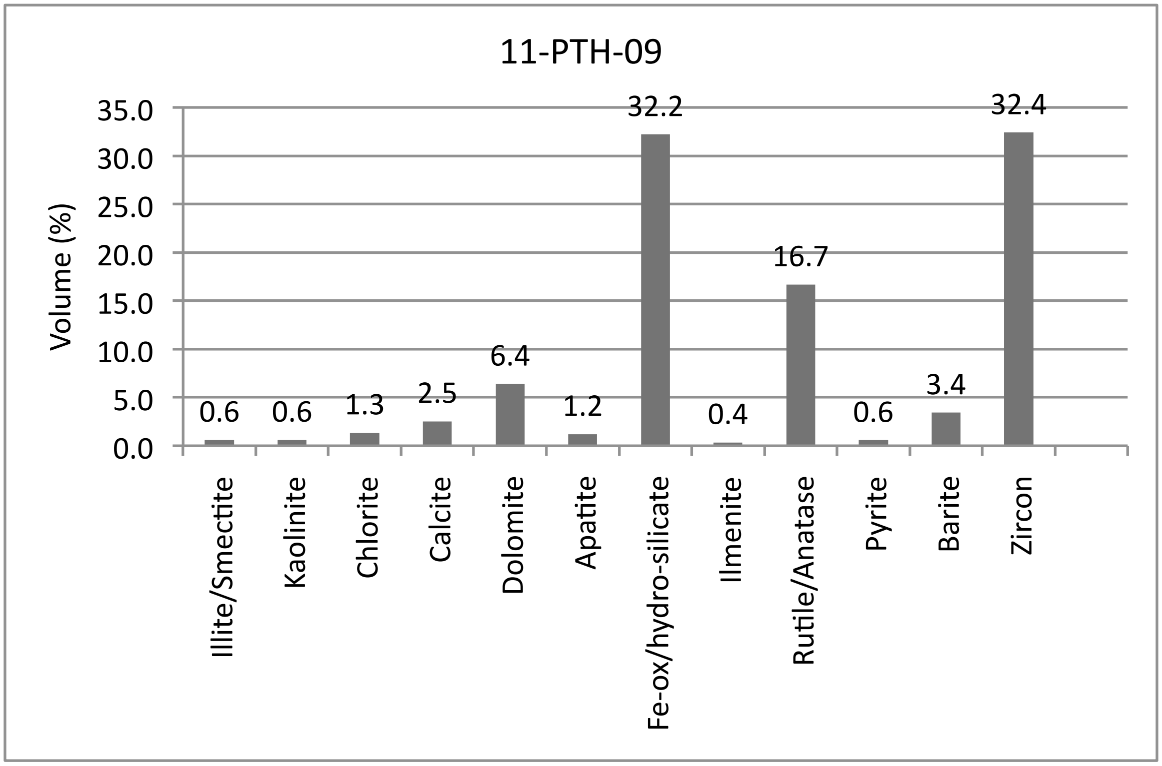

Figure 19.1: Deltaic sandstone of the Panther Tongue, Star Point Formation. Lowstand system tract.

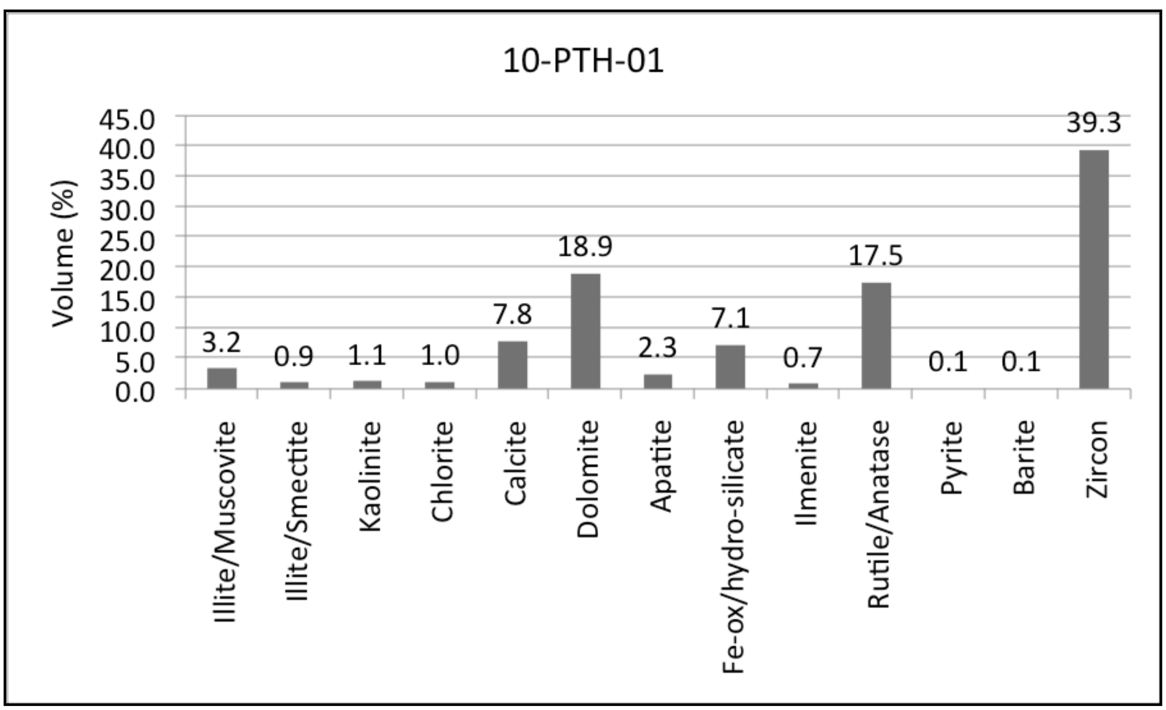

Figure 19.2: Coarse grained transgressive lag deposit of the Panther Tongue, Star Point Formation. Transgressive system tract.

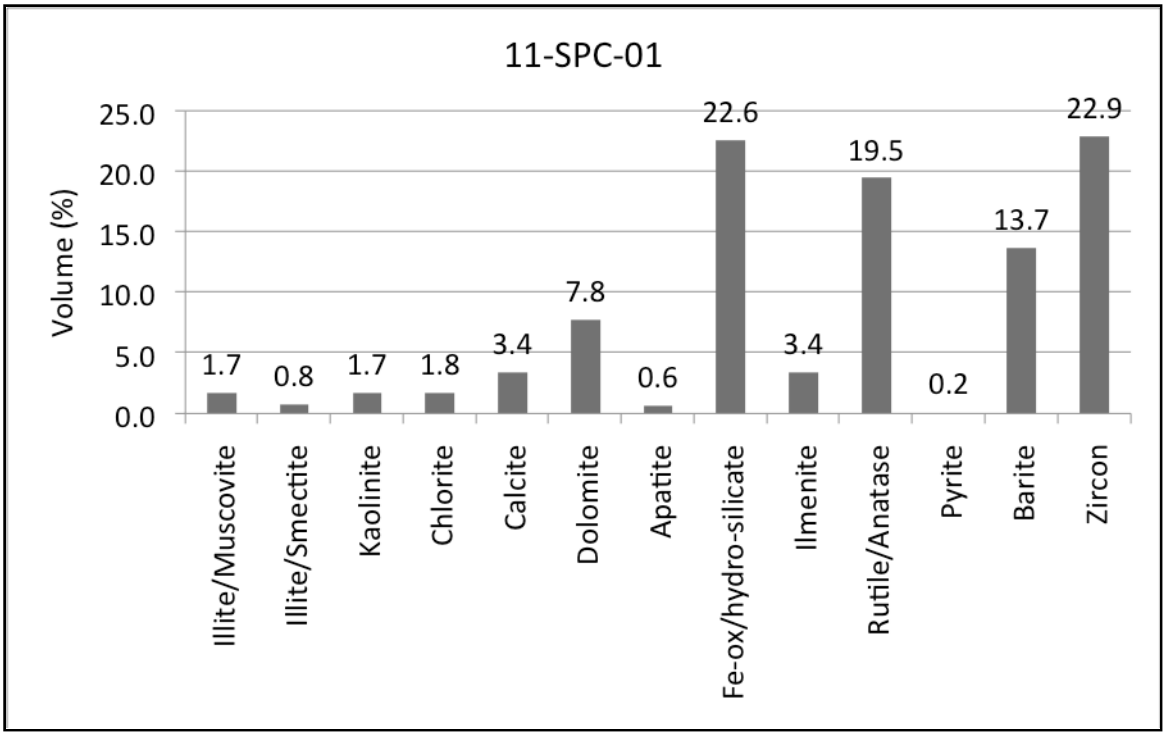

Figure 19.3: Transgressive lag deposit of the Spring Canyon Member, Blackhawk Formation. Highstand system tract.

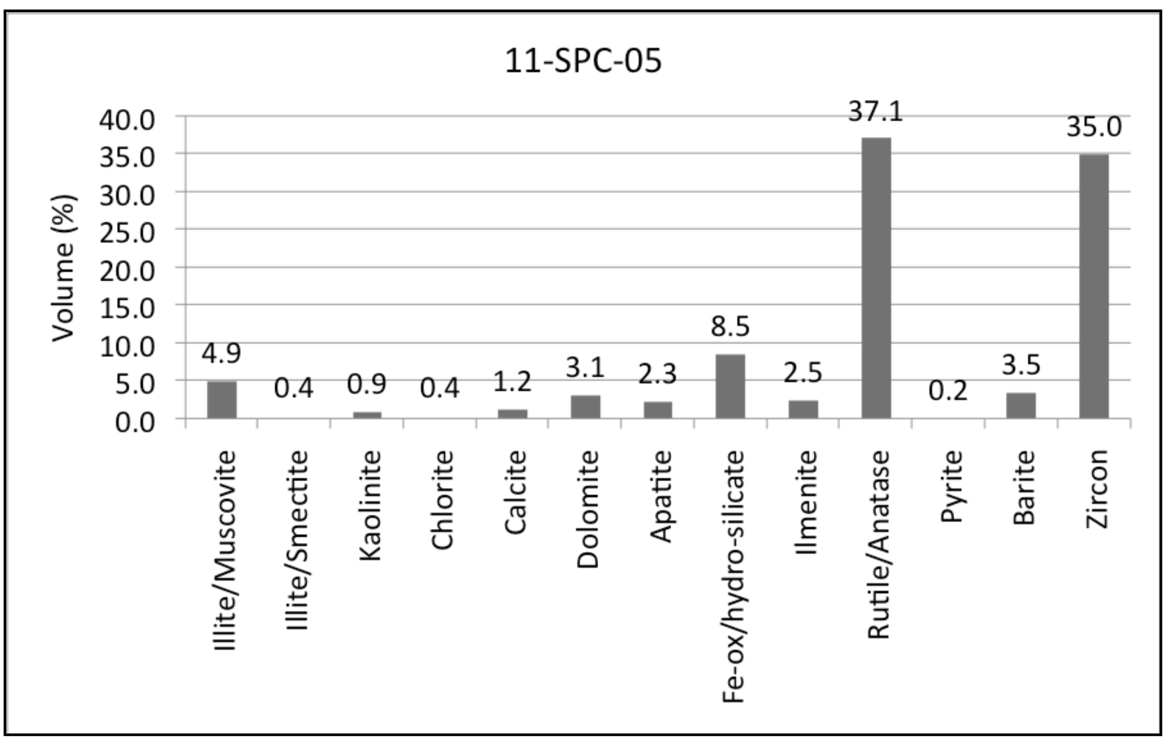

Figure 19.4: Shoreface sandstone of the Spring Canyon Member, Blackhawk Formation. Highstand system tract.

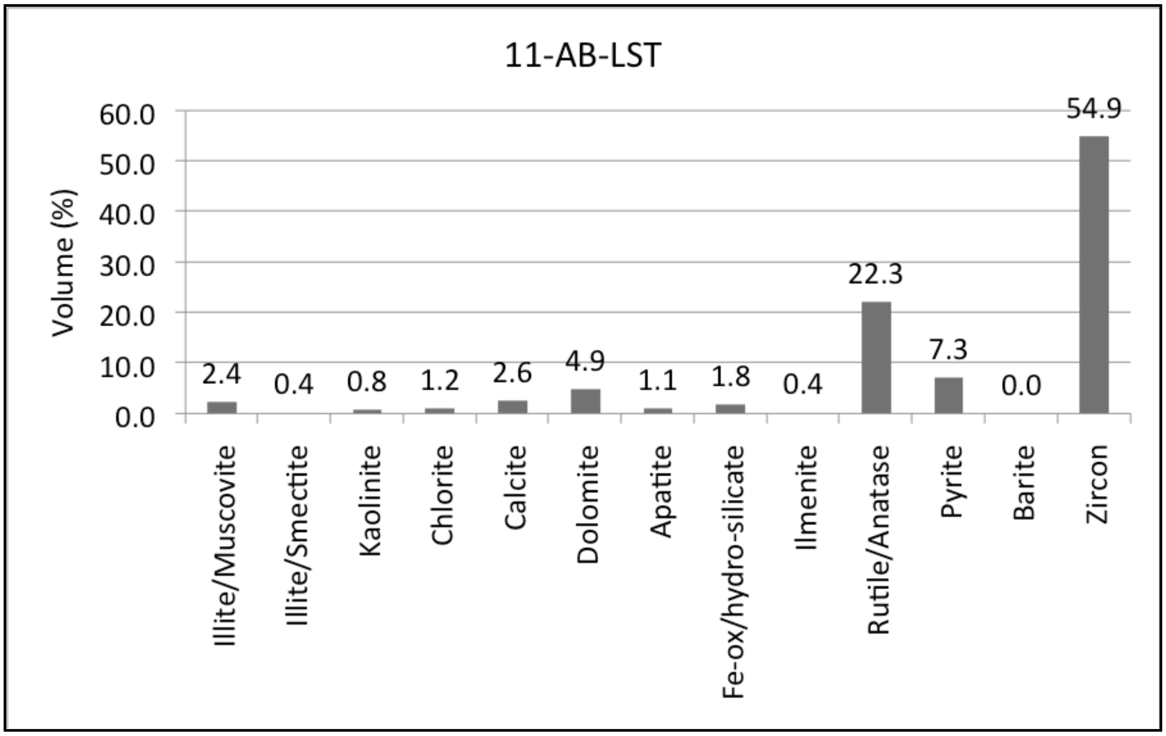

Figure 19.5: Incised valley fill setting of the Aberdeen Member, Blackhawk Formation. Lowstand system tract.

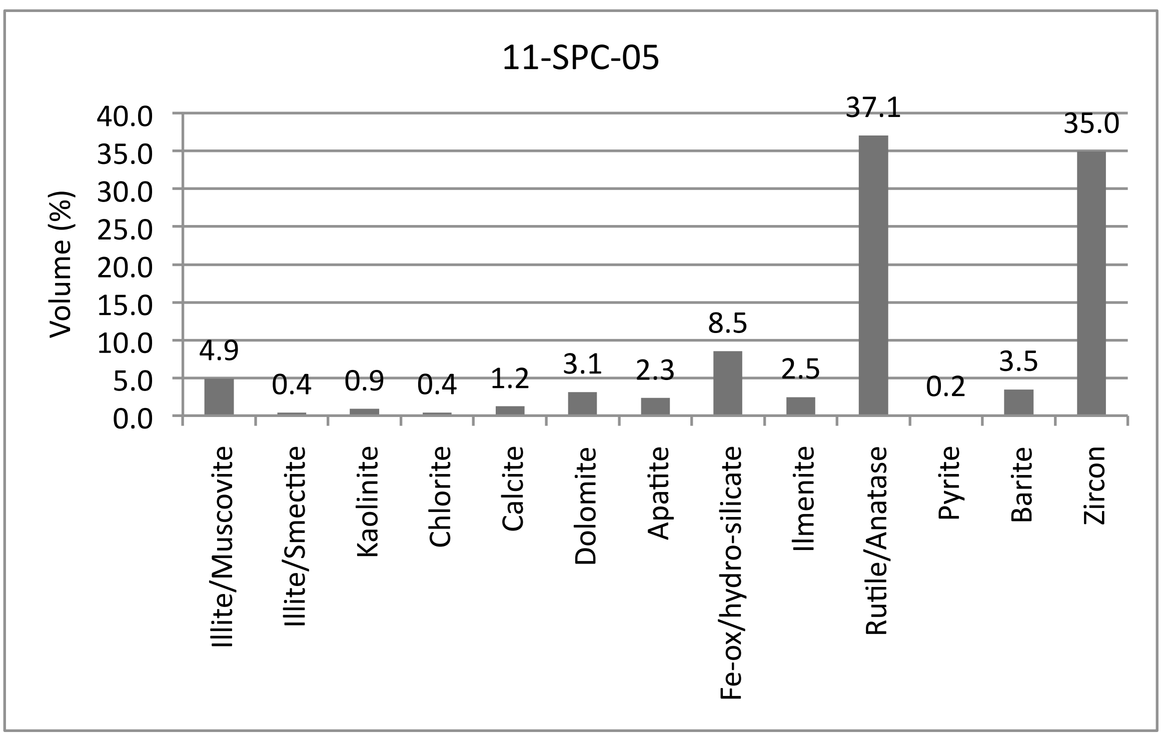

Figure 19.6: Shoreface sandstone of the Spring Canyon Member, Blackhawk Formation. Highstand system tract.

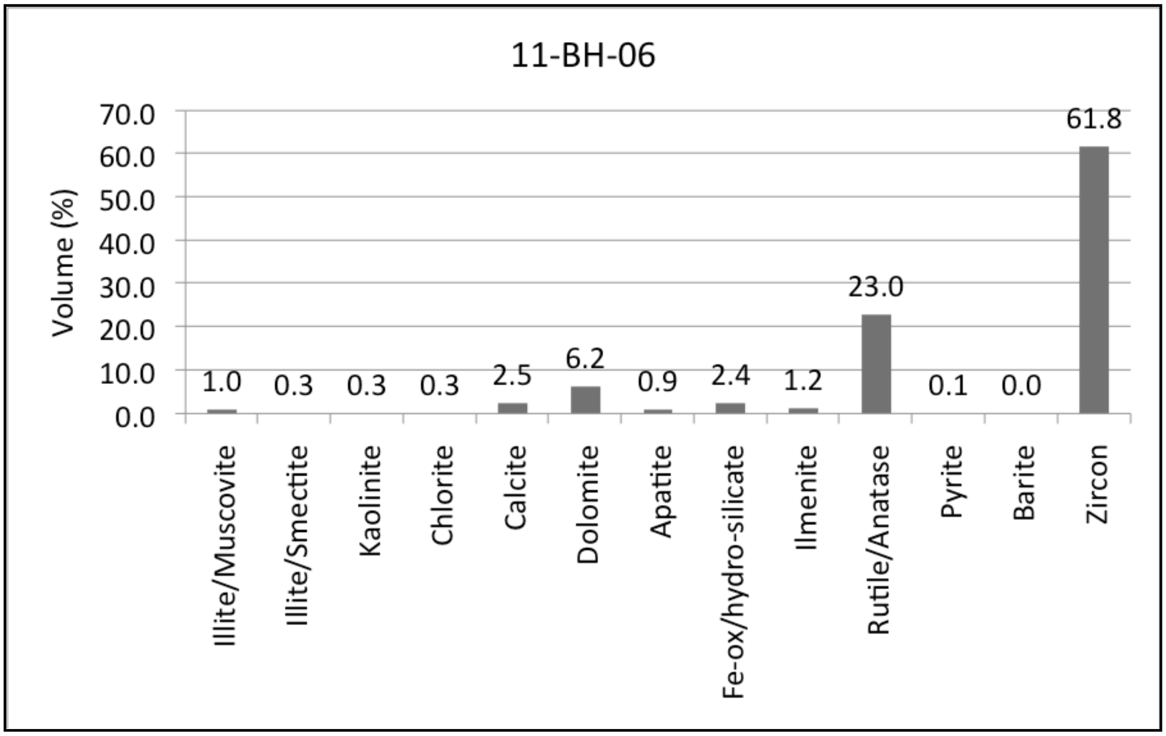

Figure 19.7: Shoreface sandstone of the Desert Member, Blackhawk Formation. Highstand se system tract.

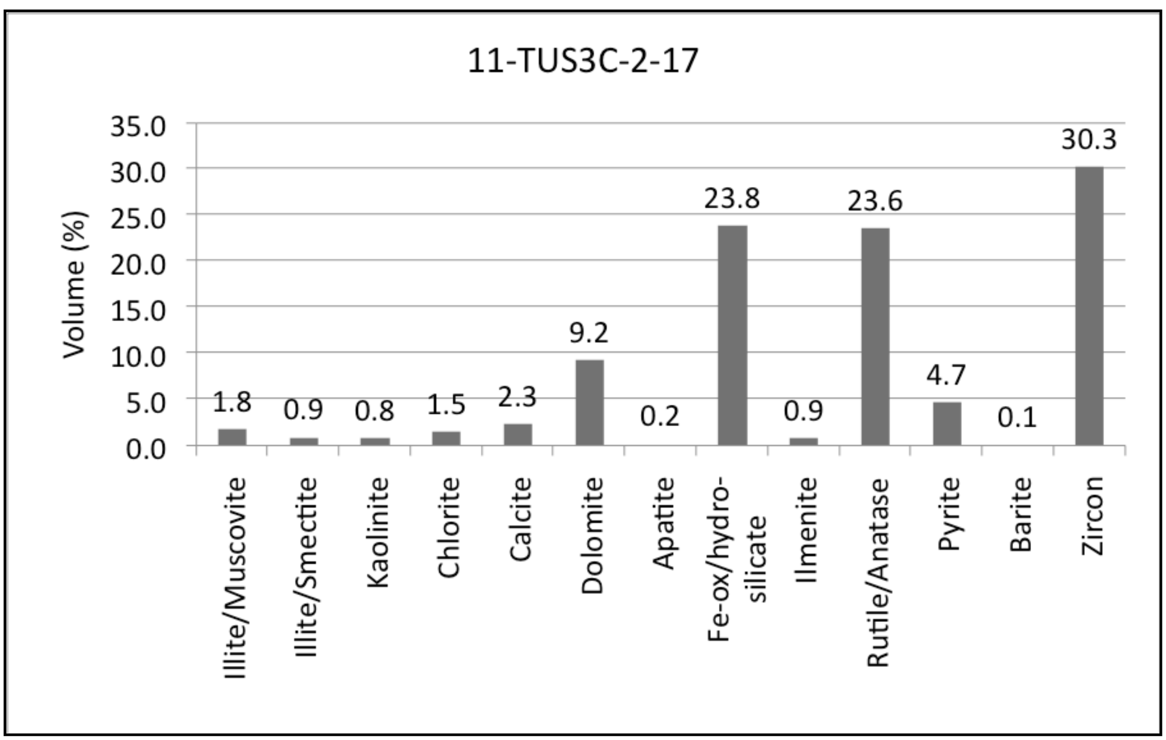

Figure 19.8: Incised valley fill of the Desert Member, Blackhawk Formation. Lowstand system tract.

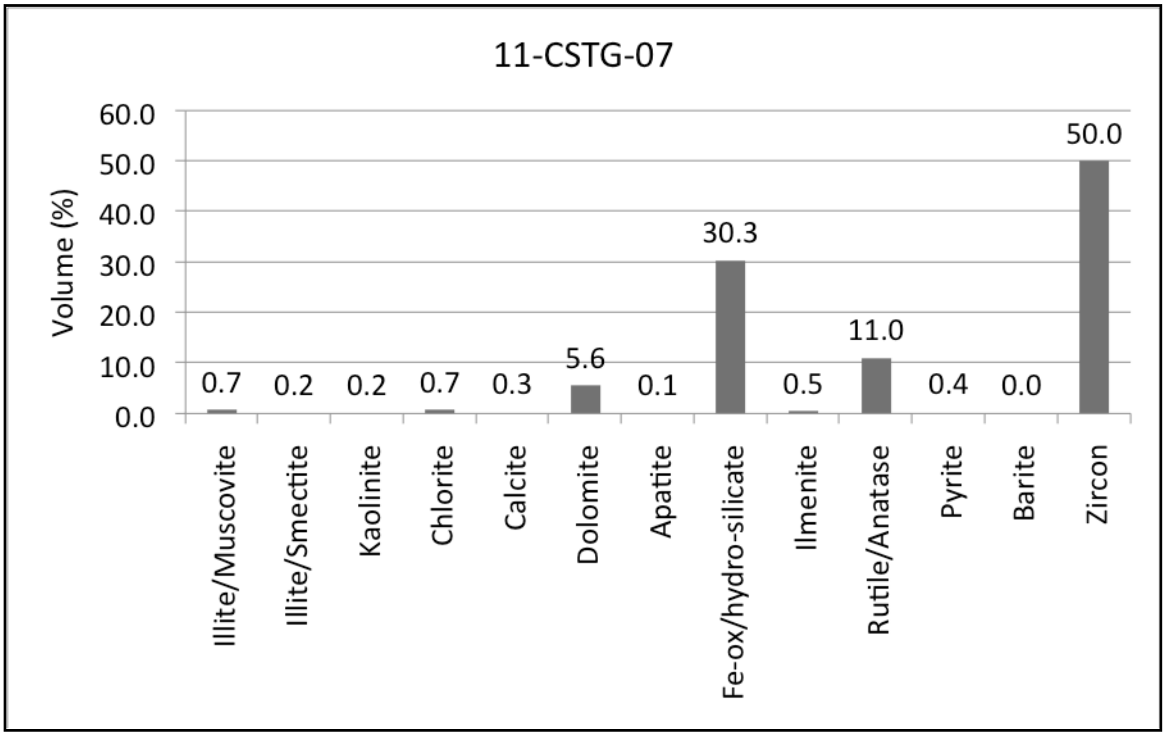

Figure 19.9: Incised valley fill of the Castlegate Sandstone Member, Blackhawk Formation. Lowstand system tract.

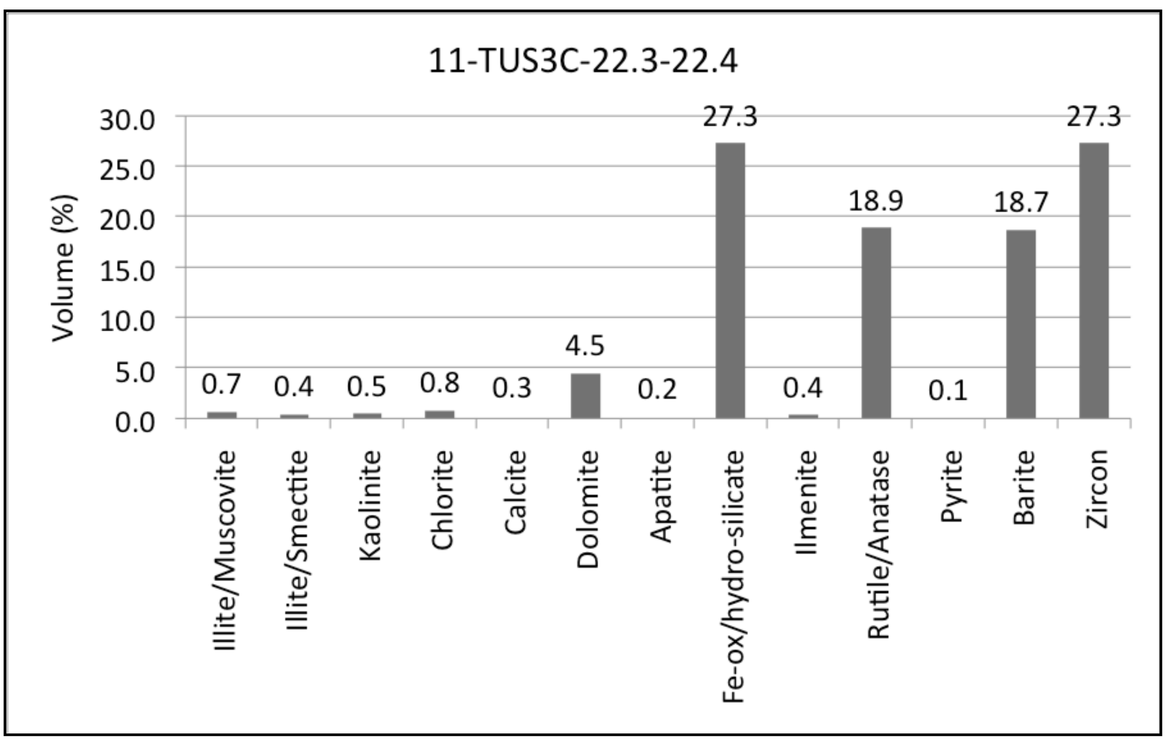

Figure 19.10: Incised valley fill of the Castlegate Sandstone Member, Blackhawk Formation. Lowstand system tract.

Figure. 20.1-5) Probability density plots and U-Pb concordia diagrams for LA-ICP-MS analyses of zircon from samples collected in the Book Cliffs, Utah. Probability density plots were constructed in Isoplot®/Ex and U-Pb concordia diagrams were constructed in Iolite®. The Concordia diagrams include all U-Pb analyses whereas the probability density plots show only analyses that are <15% discordant. The number of grains (n) represents the number of analyses. LA-ICP-MS U-Pb isotopic data of zircon can be found in Appendix E.

20.1)

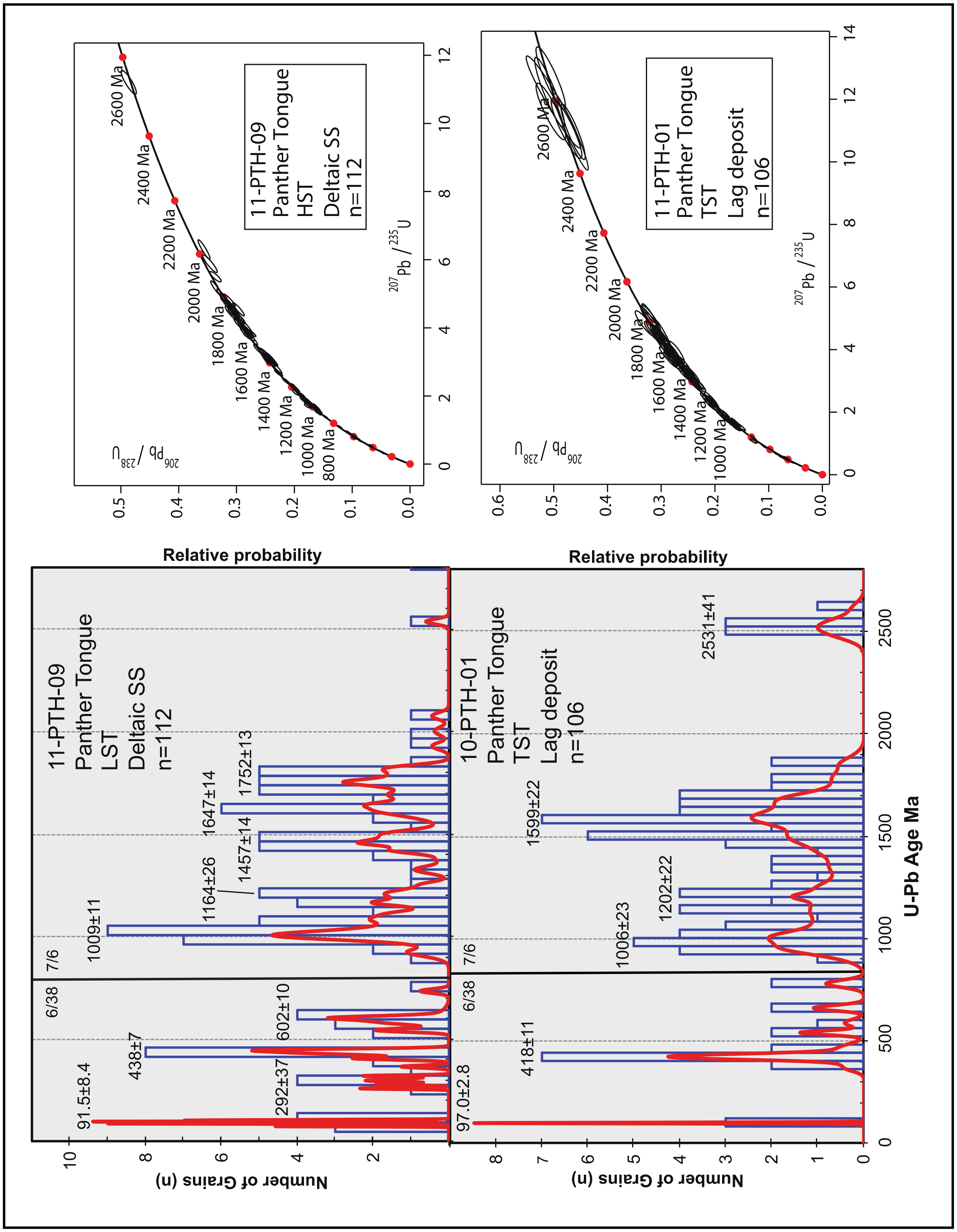
11-PTH-09
Panther Tongue
LST
Deltaic SS
n=112
10-PTH-01
Panther Tongue
TST
Lag deposit
n=106
11-PTH-09
Panther Tongue
HST
Deltaic SS
n=112
11-PTH-01
Panther Tongue
TST
Lag deposit
n=106
Relative probability
Number of Grains (n)
U-Pb Age Ma
91.5±8.4
438±7
292±37
602±10
1009±11
1164±26
1457±14
1647±14
1752±13
97.0±2.8
418±11
1006±23
1202±22
1599±22
2531±41
6/38
7/6
$^{207}Pb/^{235}U$
$^{206}Pb/^{238}U$
800 Ma
1000 Ma
1200 Ma
1400 Ma
1600 Ma
1800 Ma
2000 Ma
2200 Ma
2400 Ma
2600 Ma

20.2)

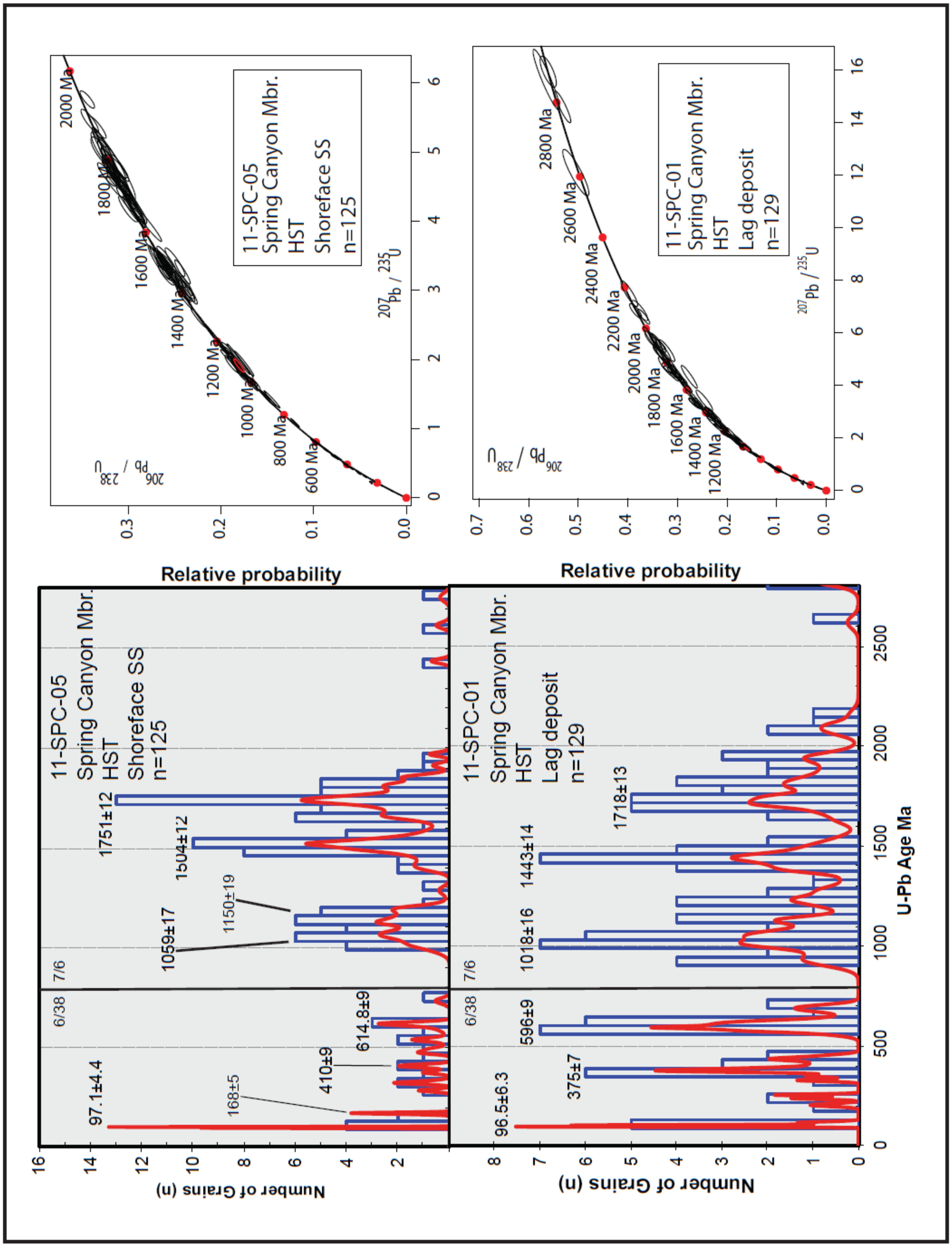

11-SPC-05
Spring Canyon Mbr.
HST
Shoreface SS
n=125
11-SPC-01
Spring Canyon Mbr.
HST
Lag deposit
n=129
Relative probability
Number of Grains (n)
U-Pb Age Ma
6/38
7/6
97.1±4.4
168±5
410±9
614.8±9
1059±17
1150±19
1504±12
1751±12
96.5±6.3
375±7
596±9
1018±16
1443±14
1718±13
206Pb / 238U
207Pb / 235U
600 Ma
800 Ma
1000 Ma
1200 Ma
1400 Ma
1600 Ma
1800 Ma
2000 Ma
2200 Ma
2400 Ma
2600 Ma
2800 Ma

20.3)

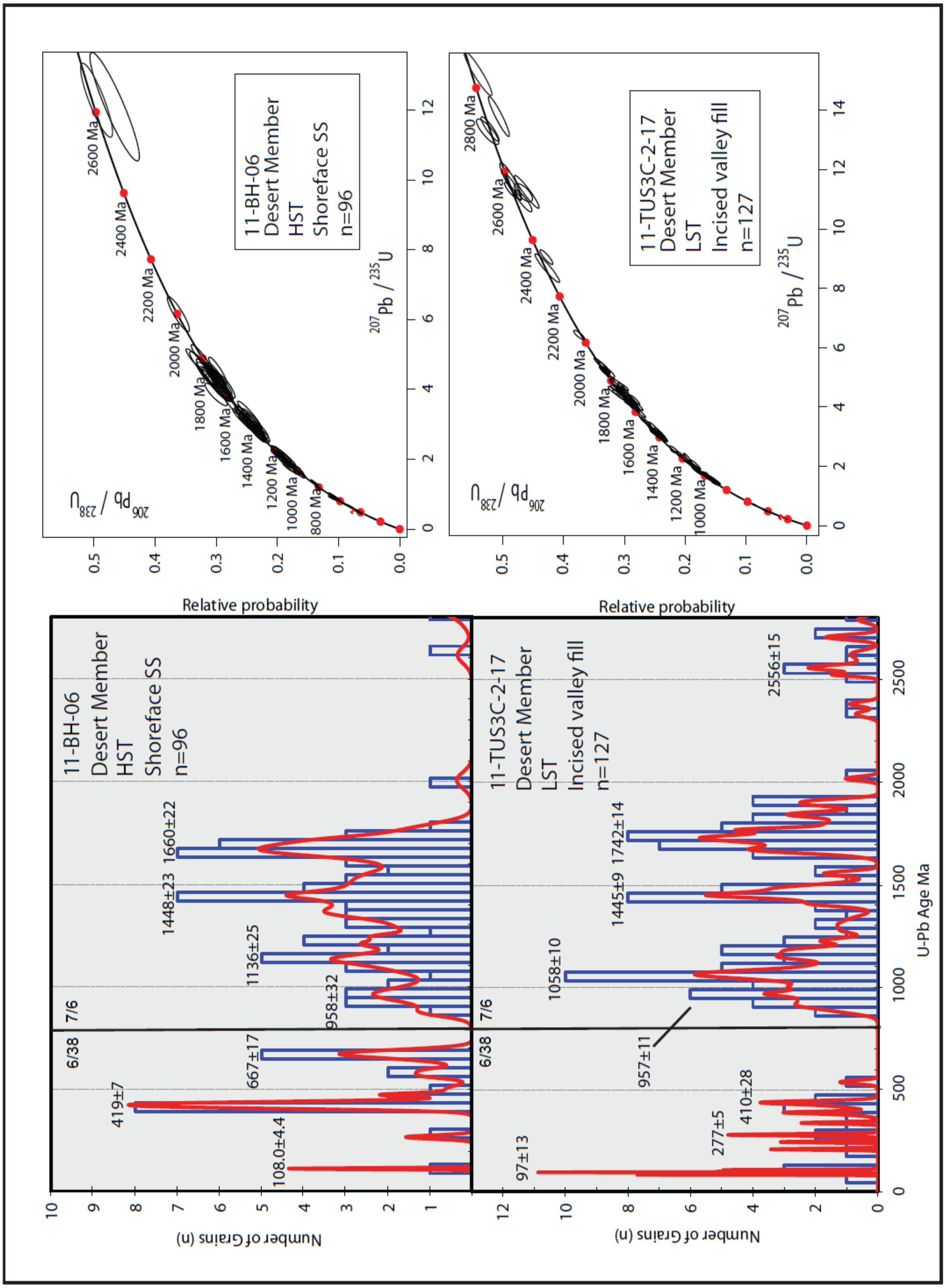
11-BH-06
Desert Member
HST
Shoreface SS
n=96
11-TUS3C-2-17
Desert Member
LST
Incised valley fill
n=127
Relative probability
Number of Grains (n)
U-Pb Age Ma
6/38
7/6
108.0±4.4
419±7
667±17
958±32
1136±25
1448±23
1660±22
97±13
277±5
410±28
957±11
1058±10
1445±9
1742±14
2556±15
^{206}Pb / ^{238}U
^{207}Pb / ^{235}U
800 Ma
1000 Ma
1200 Ma
1400 Ma
1600 Ma
1800 Ma
2000 Ma
2200 Ma
2400 Ma
2600 Ma
2800 Ma

20.4)

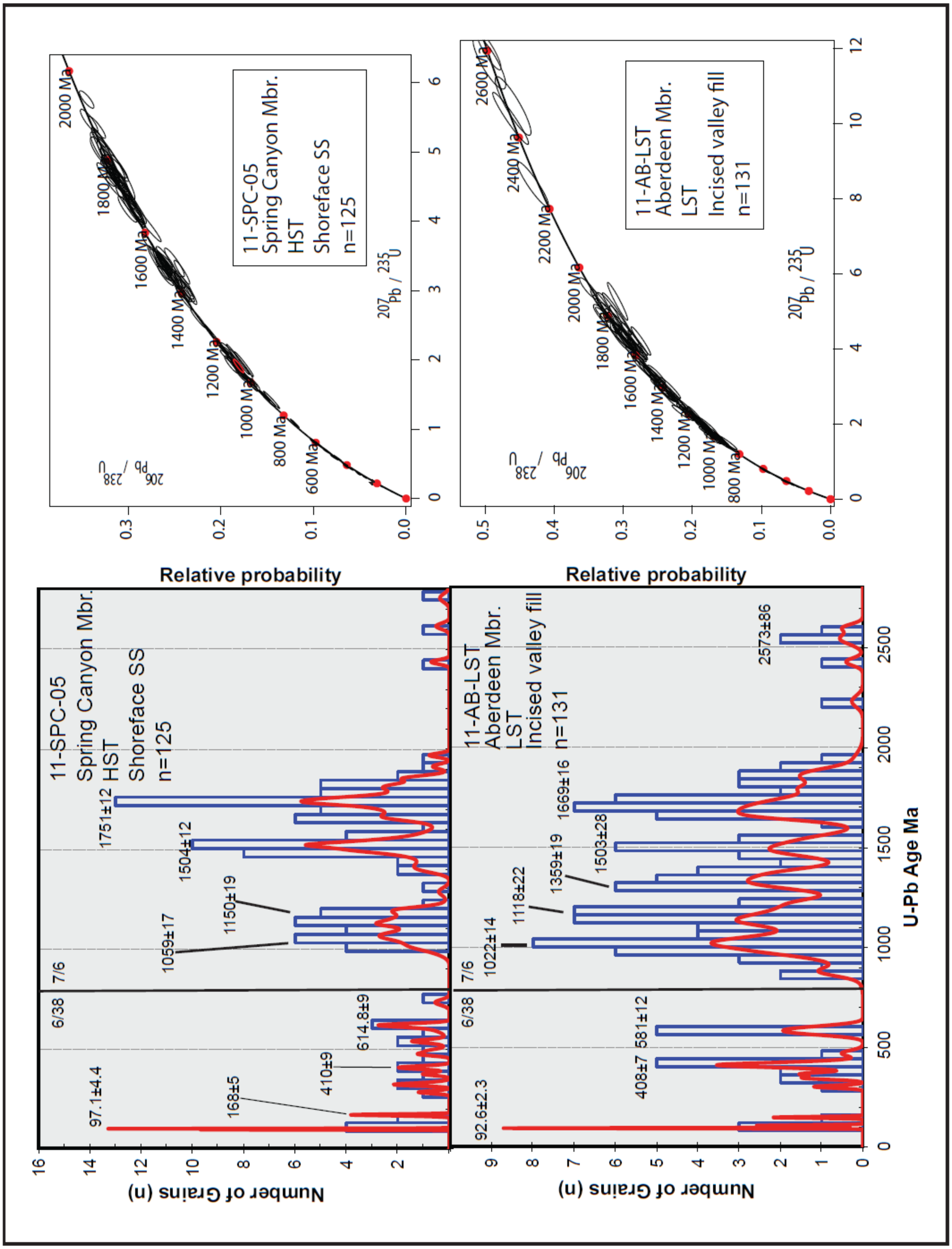

11-SPC-05
Spring Canyon Mbr.
HST
Shoreface SS
n=125
11-AB-LST
Aberdeen Mbr.
LST
Incised valley fill
n=131
Relative probability
Number of Grains (n)
U-Pb Age Ma
6/38
7/6
97.1±4.4
168±5
410±9
614.8±9
1059±17
1150±19
1504±12
1751±12
92.6±2.3
408±7
581±12
1022±14
1118±22
1359±19
1503±28
1669±16
2573±86
$^{206}Pb/^{238}U$
$^{207}Pb/^{235}U$

20.5)

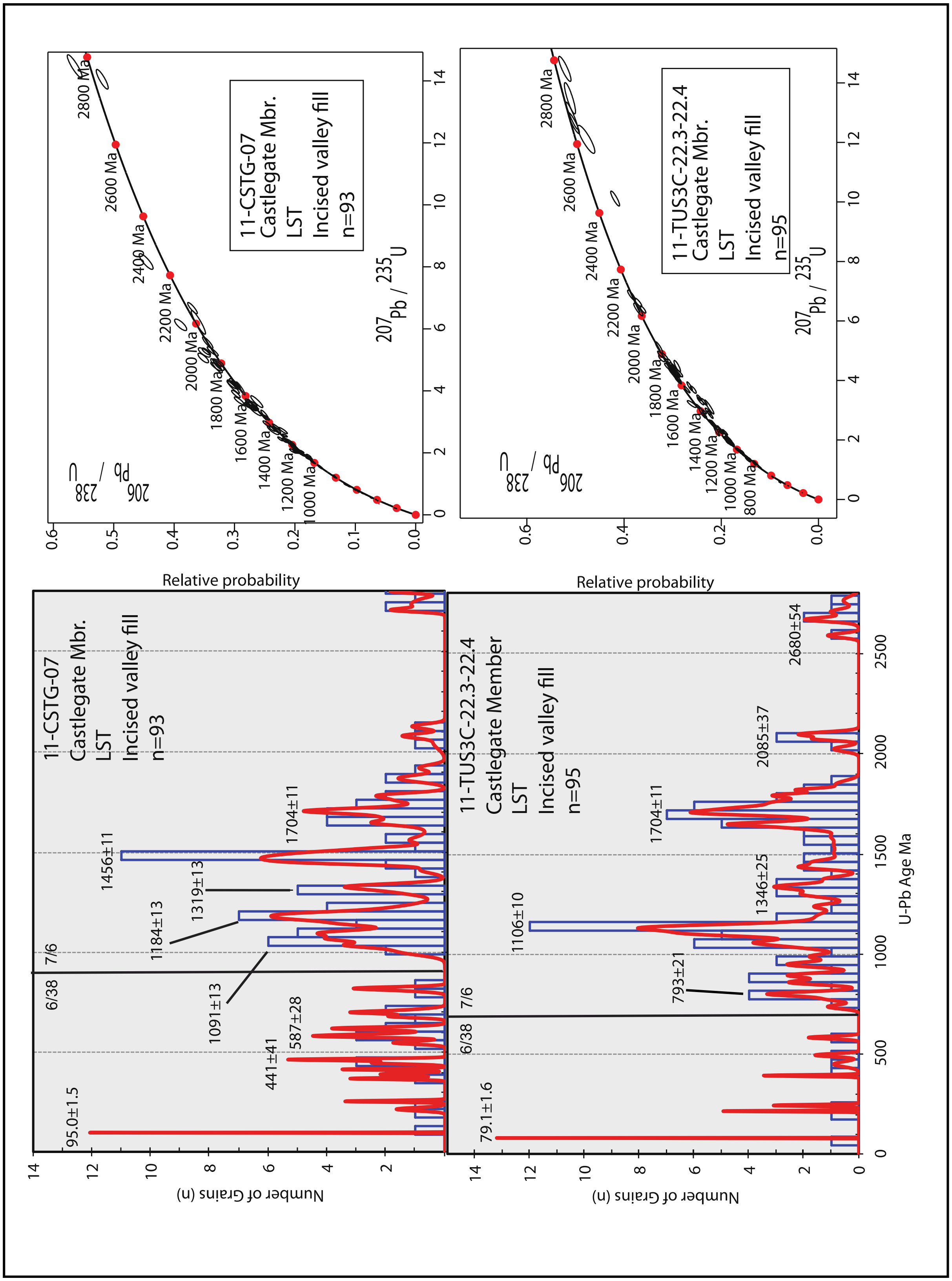

11-CSTG-07
Castlegate Mbr.
LST
Incised valley fill
n=93
11-TUS3C-22.3-22.4
Castlegate Member
LST
Incised valley fill
n=95
11-TUS3C-22.3-22.4
Castlegate Mbr.
LST
Incised valley fill
n=95
Relative probability
Number of Grains (n)
U-Pb Age Ma
95.0±1.5
441±41
587±28
1091±13
1184±13
1319±13
1456±11
1704±11
6/38
7/6
79.1±1.6
793±21
1106±10
1346±25
1704±11
2085±37
2680±54
$^{206}Pb / ^{238}U$
$^{207}Pb / ^{235}U$
1000 Ma
1200 Ma
1400 Ma
1600 Ma
1800 Ma
2000 Ma
2200 Ma
2400 Ma
2600 Ma
2800 Ma
800 Ma

Figure 21.1-3) U-Pb concordia diagrams for LA-ICP-MS analyses of detrital rutile from samples collected in the Book Cliffs, Utah. U-Pb concordia diagrams were constructed in Iolite®. The number of grains (n) represents the number of analyses. LA-ICP-MS U-Pb isotopic data of rutile can be found in Appendix F.

21.1)

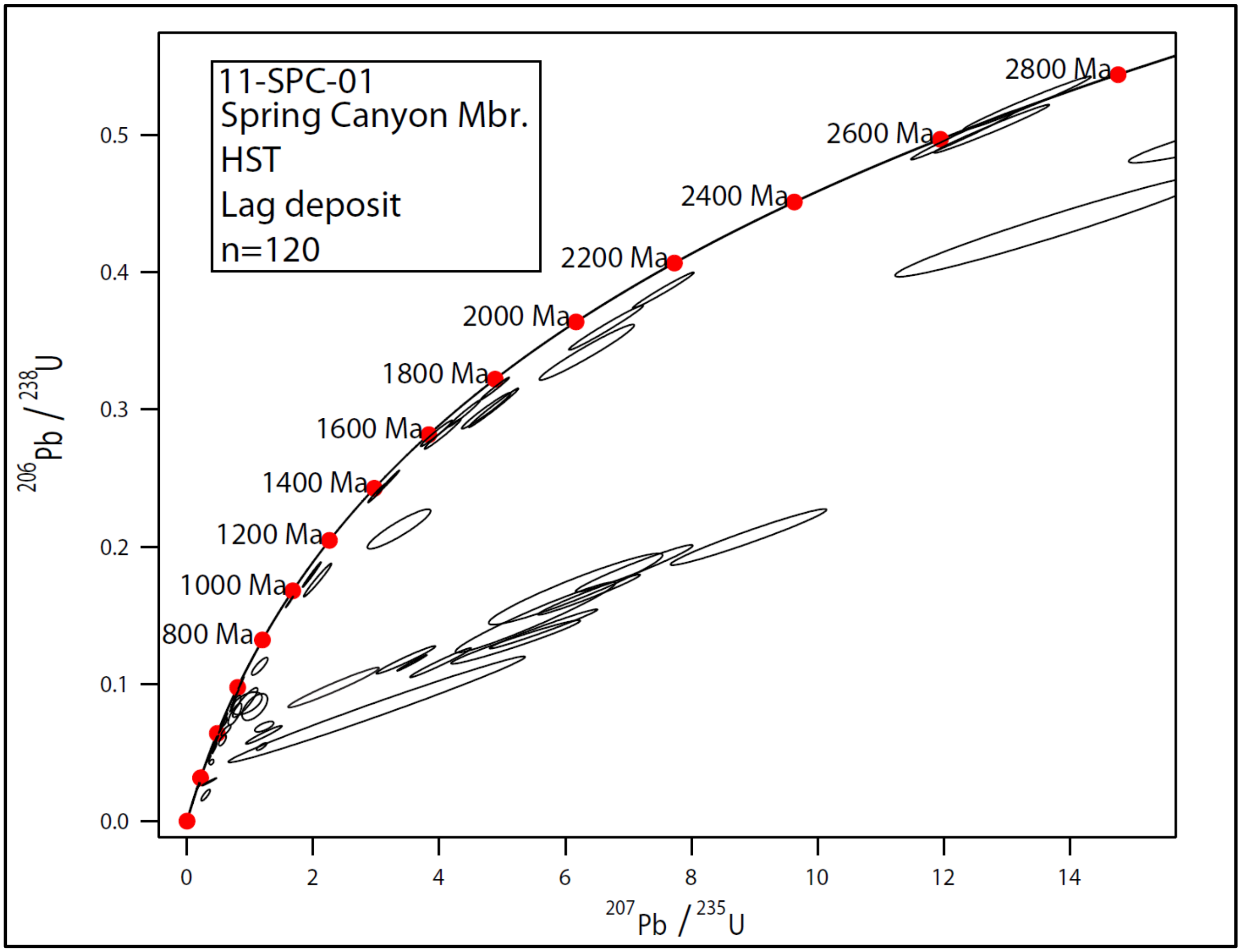

11-SPC-01
Spring Canyon Mbr.
HST
Lag deposit
n=120
2800 Ma
2600 Ma
2400 Ma
2200 Ma
2000 Ma
1800 Ma
1600 Ma
1400 Ma
1200 Ma
1000 Ma
800 Ma
0.0
0.1
0.2
0.3
0.4
0.5
0
2
4
6
8
10
12
14
206Pb / 238U
207Pb / 235U

21.2)

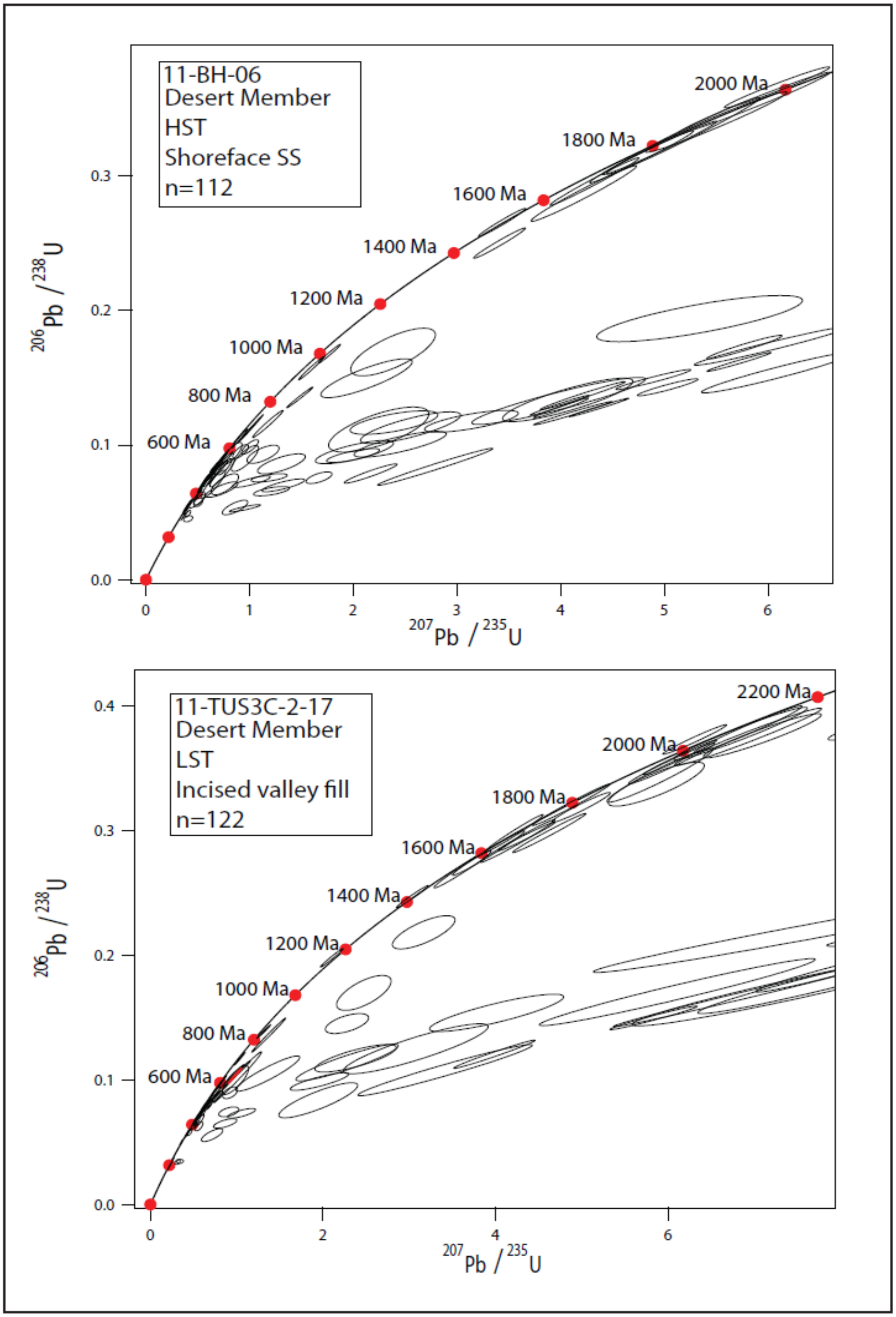

11-BH-06
Desert Member
HST
Shoreface SS
n=112
2000 Ma
1800 Ma
1600 Ma
1400 Ma
1200 Ma
1000 Ma
800 Ma
600 Ma
0.3
0.2
0.1
0.0
0
1
2
3
4
5
6
^{206}Pb / ^{238}U
^{207}Pb / ^{235}U
11-TUS3C-2-17
Desert Member
LST
Incised valley fill
n=122
2200 Ma
2000 Ma
1800 Ma
1600 Ma
1400 Ma
1200 Ma
1000 Ma
800 Ma
600 Ma
0.4
0.3
0.2
0.1
0.0
0
2
4
6
^{206}Pb / ^{238}U
^{207}Pb / ^{235}U

21.3)

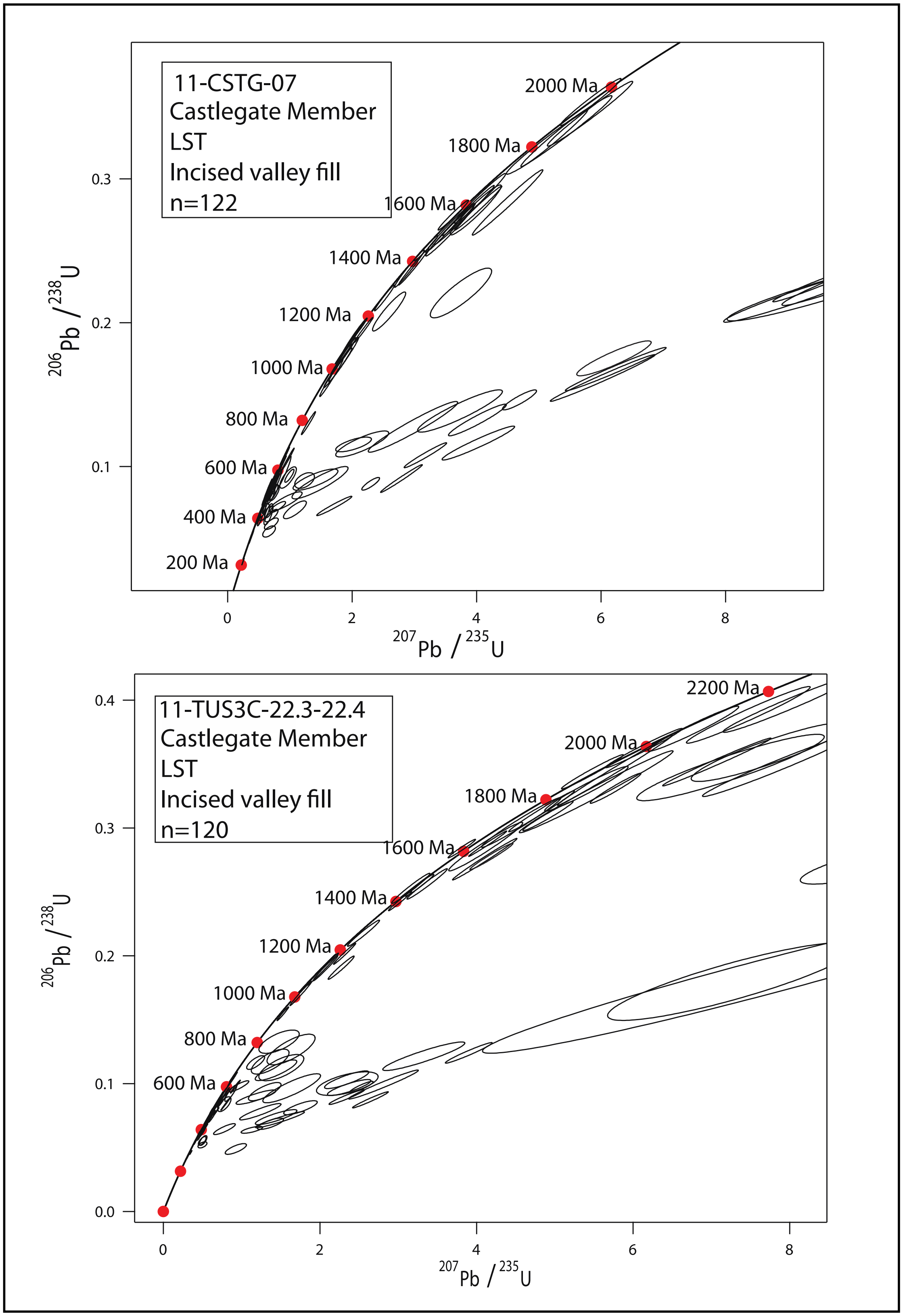
11-CSTG-07
Castlegate Member
LST
Incised valley fill
n=122
2000 Ma
1800 Ma
1600 Ma
1400 Ma
1200 Ma
1000 Ma
800 Ma
600 Ma
400 Ma
200 Ma
0.3
0.2
0.1
0
2
4
6
8
$^{206}Pb/^{238}U$
$^{207}Pb/^{235}U$
11-TUS3C-22.3-22.4
Castlegate Member
LST
Incised valley fill
n=120
2200 Ma
2000 Ma
1800 Ma
1600 Ma
1400 Ma
1200 Ma
1000 Ma
800 Ma
600 Ma
0.4
0.3
0.2
0.1
0.0
0
2
4
6
8
$^{206}Pb/^{238}U$
$^{207}Pb/^{235}U$

Figure 22.1-4) Plots showing concentrations of Nb and Zr versus U-Pb age of the analyzed rutile grains. LA-ICP-MS trace element data can be found in Appendix G.

22.1)

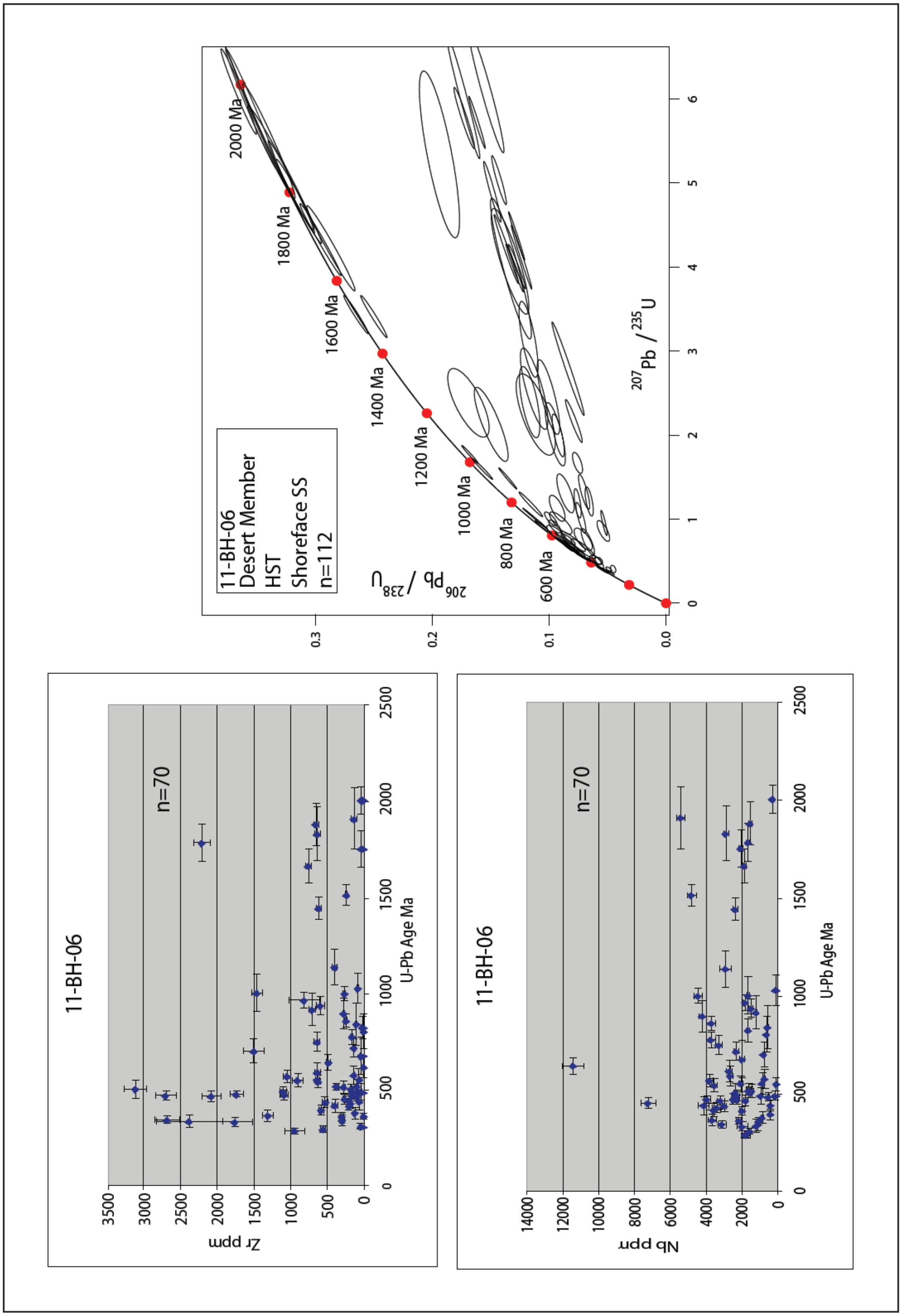

11-BH-06
Desert Member
HST
Shoreface SS
n=112
600 Ma
800 Ma
1000 Ma
1200 Ma
1400 Ma
1600 Ma
1800 Ma
2000 Ma
^{206}Pb / ^{238}U
^{207}Pb / ^{235}U
11-BH-06
n=70
Zr ppm
U-Pb Age Ma
11-BH-06
n=70
Nb ppm
U-Pb Age Ma

22.2)

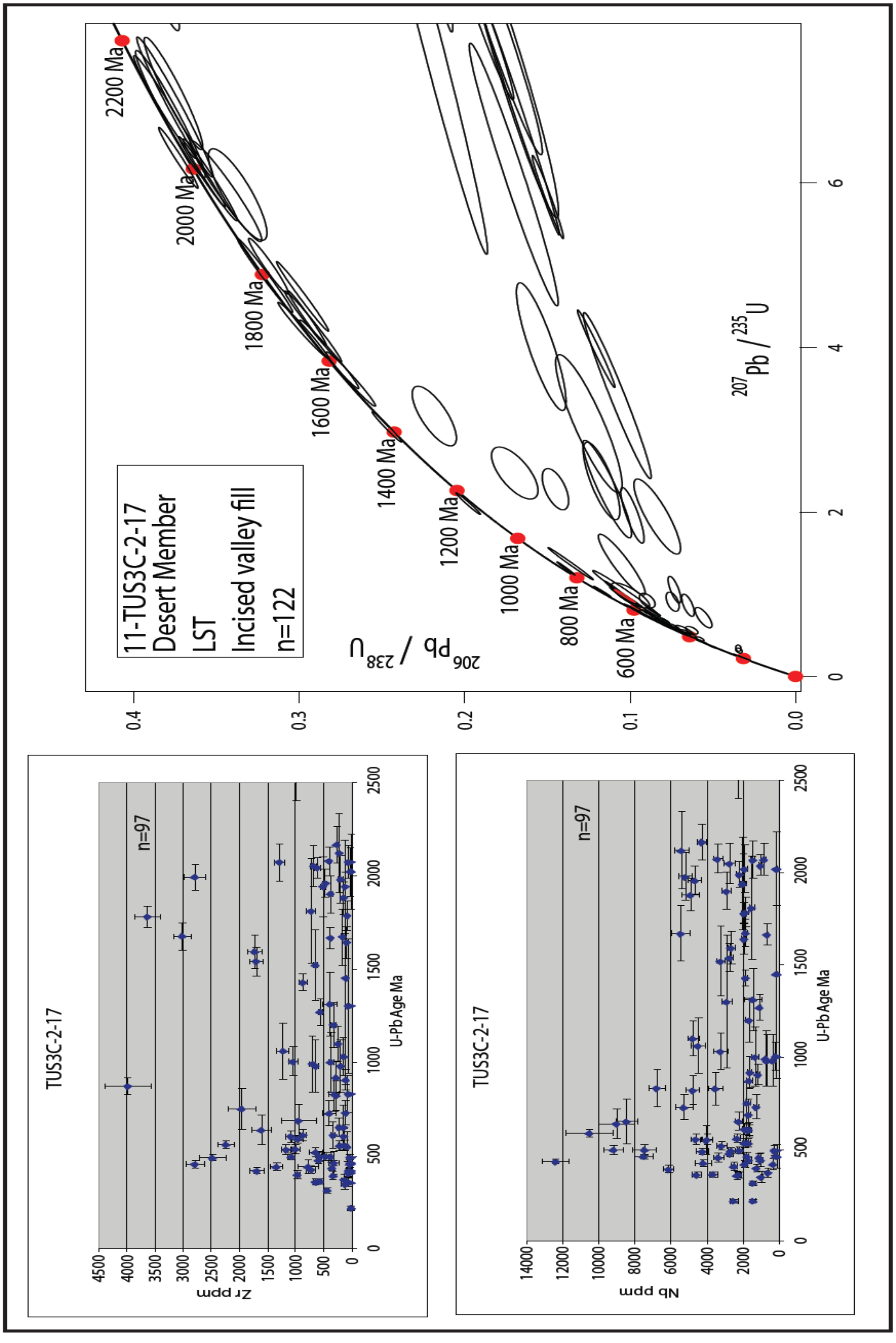
11-TUS3C-2-17
Desert Member
LST
Incised valley fill
n=122
600 Ma
800 Ma
1000 Ma
1200 Ma
1400 Ma
1600 Ma
1800 Ma
2000 Ma
2200 Ma
$^{206}Pb / ^{238}U$
$^{207}Pb / ^{235}U$
TUS3C-2-17
n=97
Zr ppm
U-Pb Age Ma
TUS3C-2-17
n=97
Nb ppm
U-Pb Age Ma

22.3)

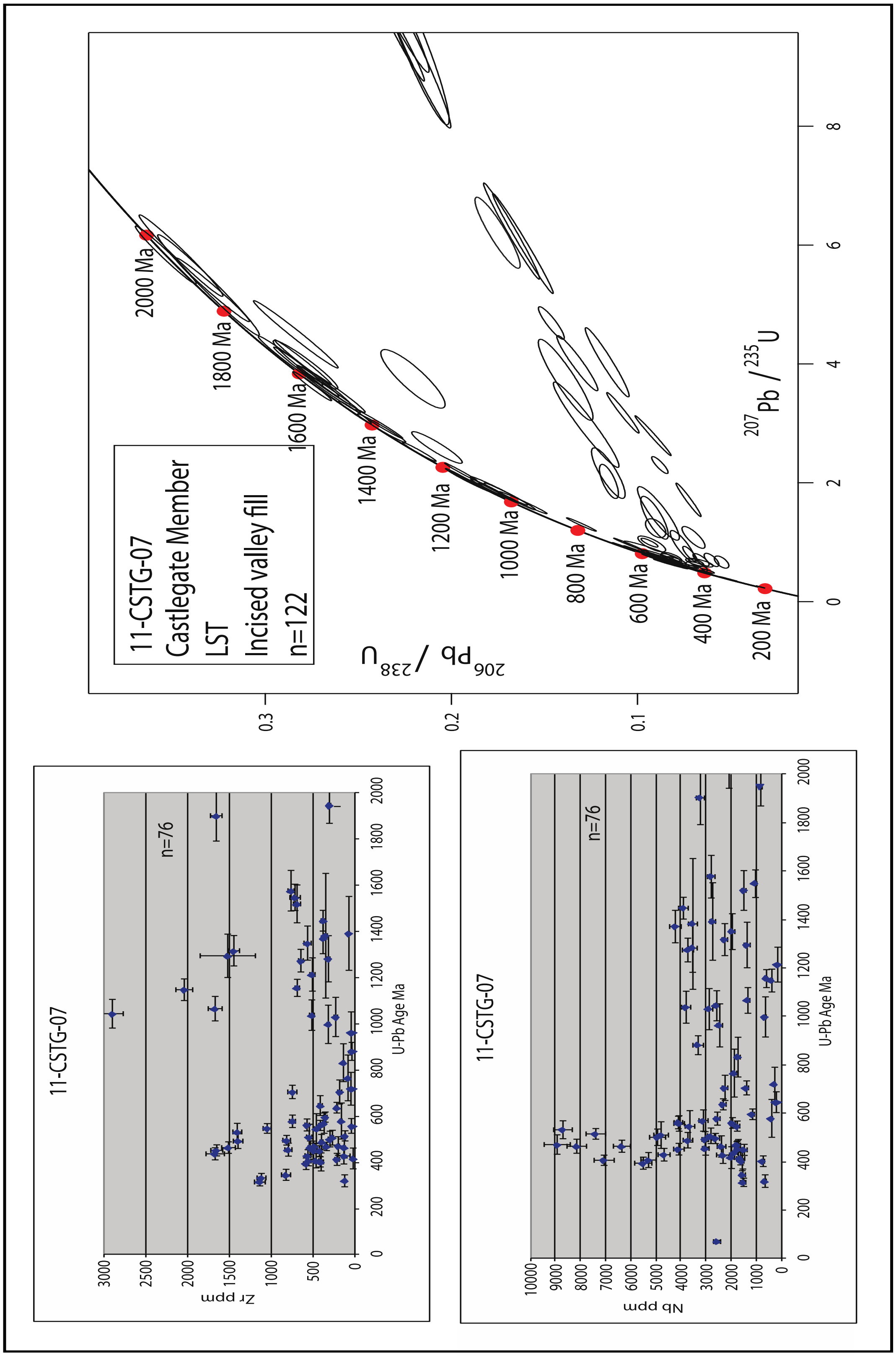

11-CSTG-07
Castlegate Member
LST
Incised valley fill
n=122
2000 Ma
1800 Ma
1600 Ma
1400 Ma
1200 Ma
1000 Ma
800 Ma
600 Ma
400 Ma
200 Ma
$^{206}Pb\,/\,^{238}U$
$^{207}Pb\,/\,^{235}U$
11-CSTG-07
n=76
Zr ppm
U-Pb Age Ma
11-CSTG-07
n=76
Nb ppm
U-Pb Age Ma

22.4)

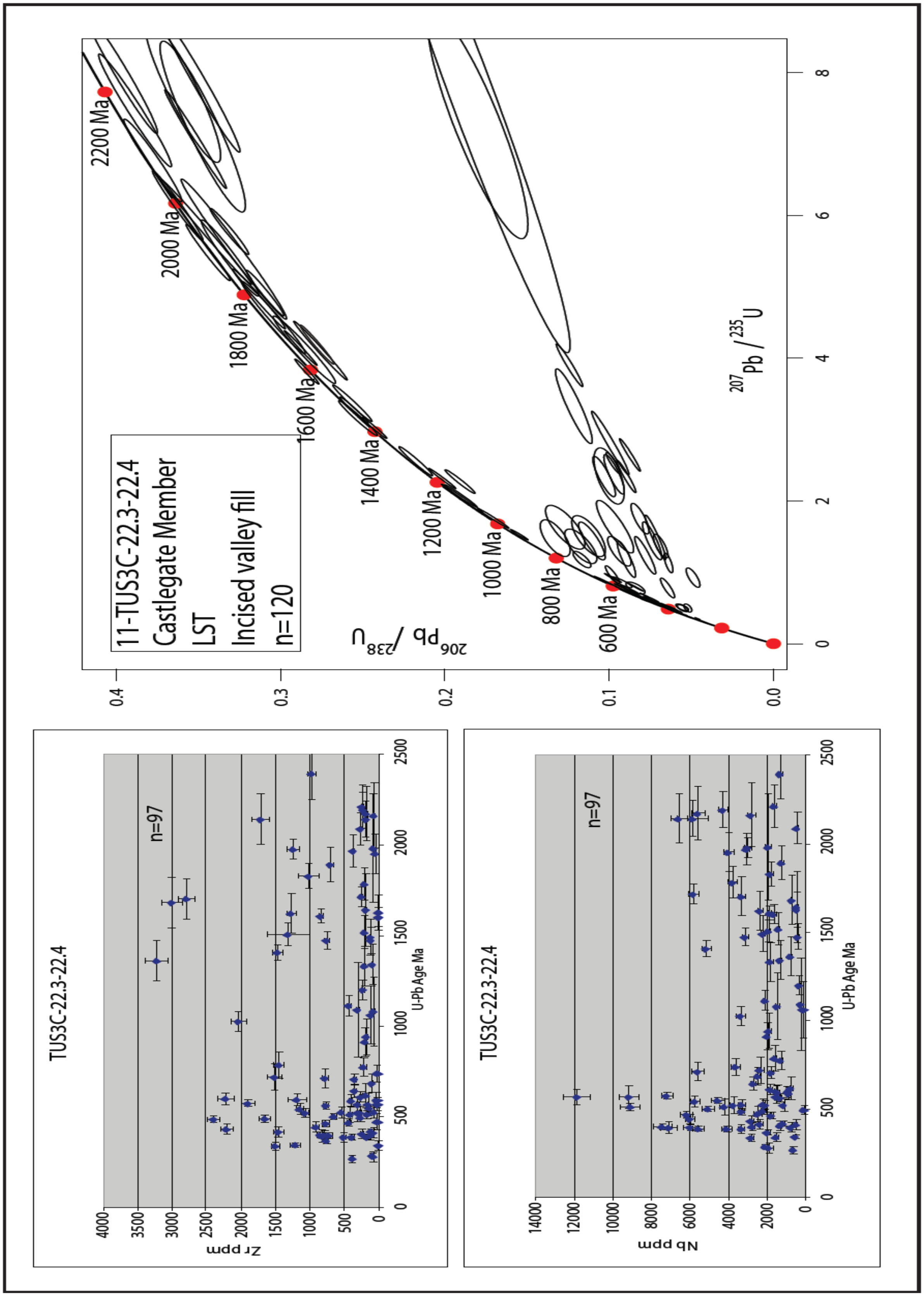
11-TUS3C-22.3-22.4
Castlegate Member
LST
Incised valley fill
n=120
$^{206}Pb/^{238}U$
$^{207}Pb/^{235}U$
2200 Ma
2000 Ma
1800 Ma
1600 Ma
1400 Ma
1200 Ma
1000 Ma
800 Ma
600 Ma
TUS3C-22.3-22.4
n=97
Zr ppm
U-Pb Age Ma
TUS3C-22.3-22.4
n=97
Nb ppm
U-Pb Age Ma

Figure 23.1-4) Zr-in-rutile temperature versus U-Pb age diagrams for rutile from the Book Cliffs, Utah. The zirconium content was used to calculate the crystallization temperatures of rutile grains using the equation from Watson et al. (2006). LA-ICP-MS trace element data can be found in Appendix G.

23.1)

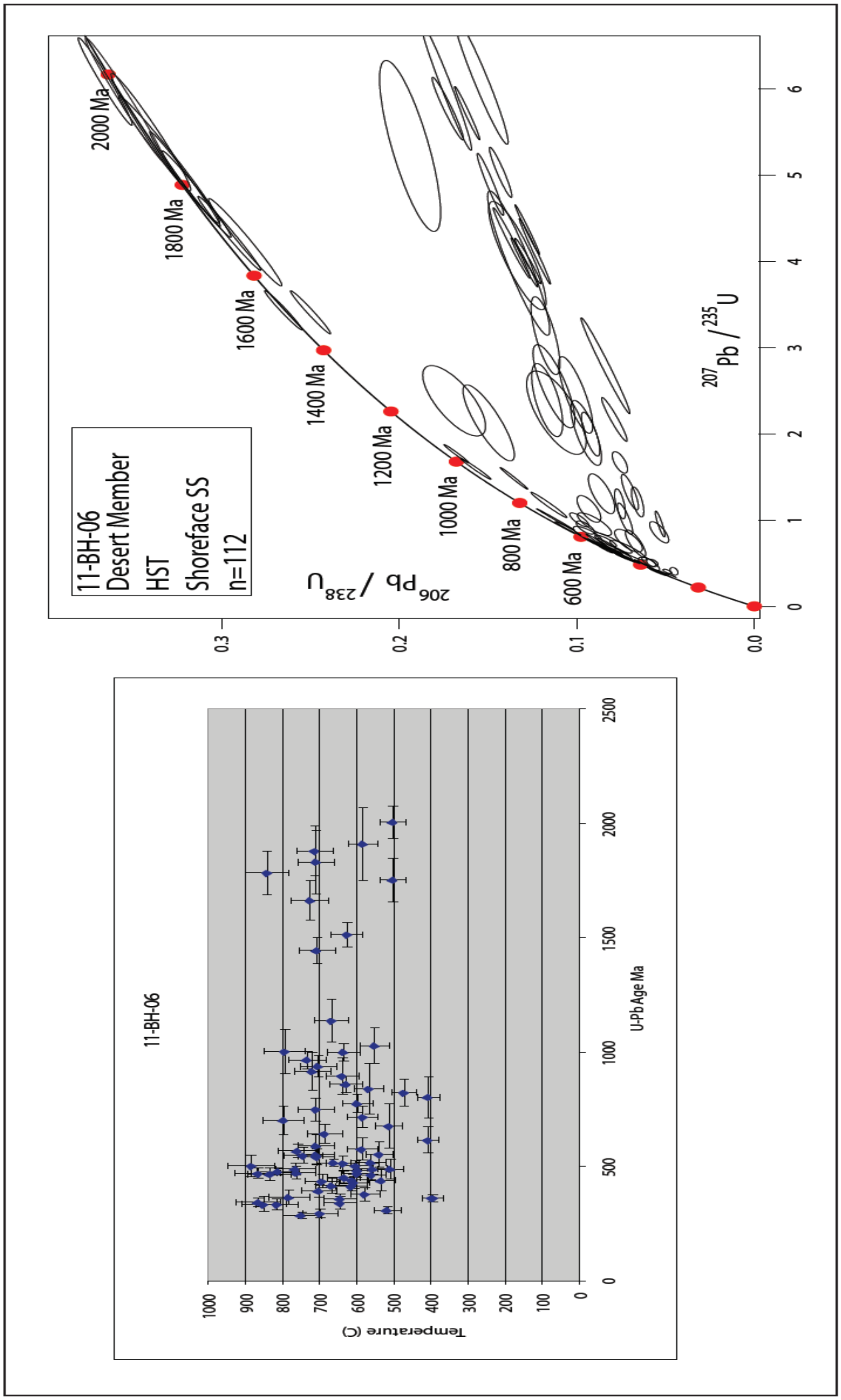
11-BH-06
Desert Member
HST
Shoreface SS
n=112
2000 Ma
1800 Ma
1600 Ma
1400 Ma
1200 Ma
1000 Ma
800 Ma
600 Ma
$^{206}Pb / ^{238}U$
$^{207}Pb / ^{235}U$
11-BH-06
Temperature (C)
U-Pb Age Ma

23.2)

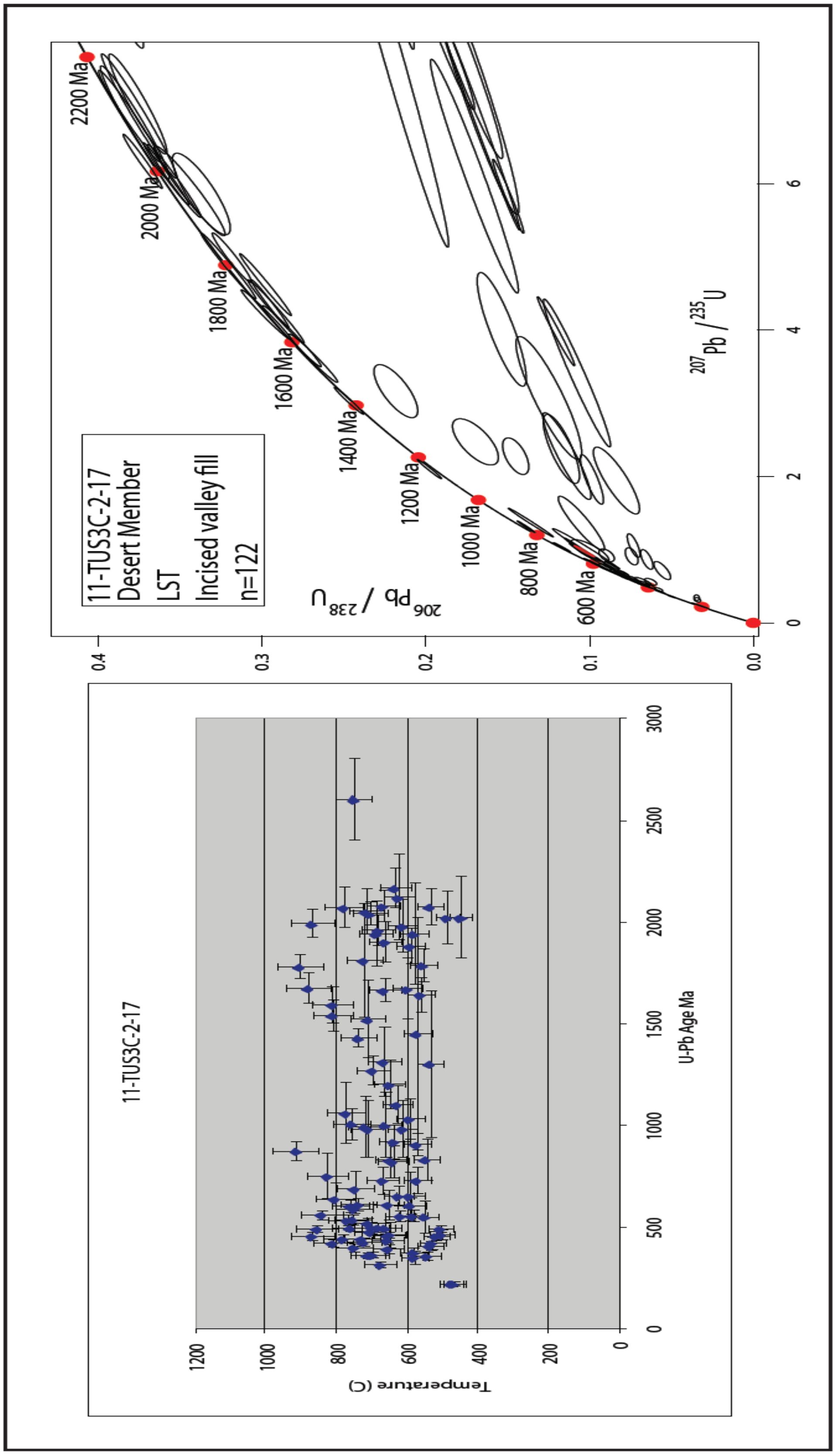
11-TUS3C-2-17
Desert Member
LST
Incised valley fill
n=122
2200 Ma
2000 Ma
1800 Ma
1600 Ma
1400 Ma
1200 Ma
1000 Ma
800 Ma
600 Ma
$^{206}Pb\ /\ ^{238}U$
$^{207}Pb\ /\ ^{235}U$
0.0
0.1
0.2
0.3
0.4
0
2
4
6
11-TUS3C-2-17
Temperature (C)
U-Pb Age Ma
0
200
400
600
800
1000
1200
0
500
1000
1500
2000
2500
3000

23.3)

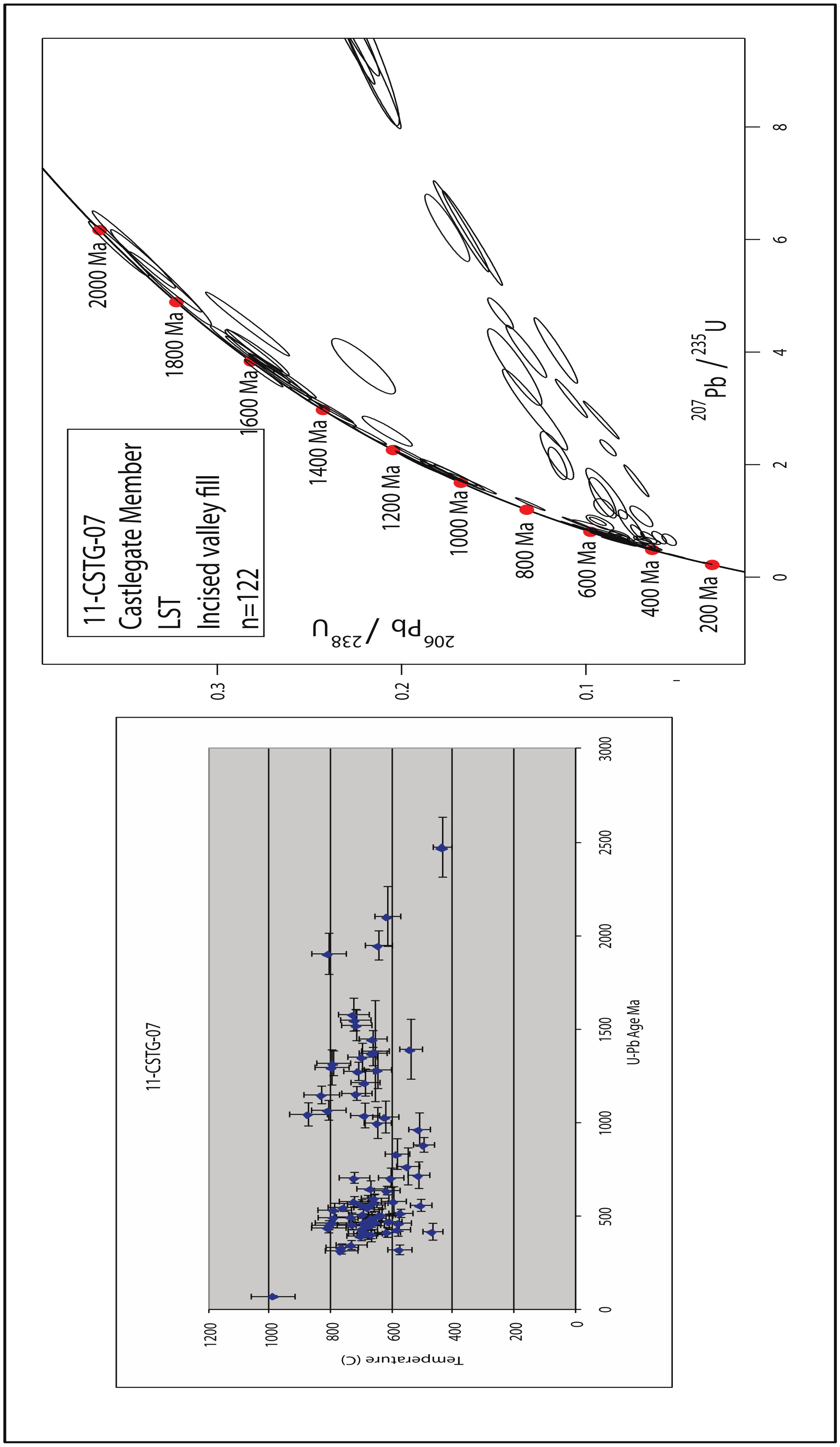

11-CSTG-07
Castlegate Member
LST
Incised valley fill
n=122
200 Ma
400 Ma
600 Ma
800 Ma
1000 Ma
1200 Ma
1400 Ma
1600 Ma
1800 Ma
2000 Ma
$^{206}Pb / ^{238}U$
$^{207}Pb / ^{235}U$
11-CSTG-07
Temperature (C)
U-Pb Age Ma

23.4)

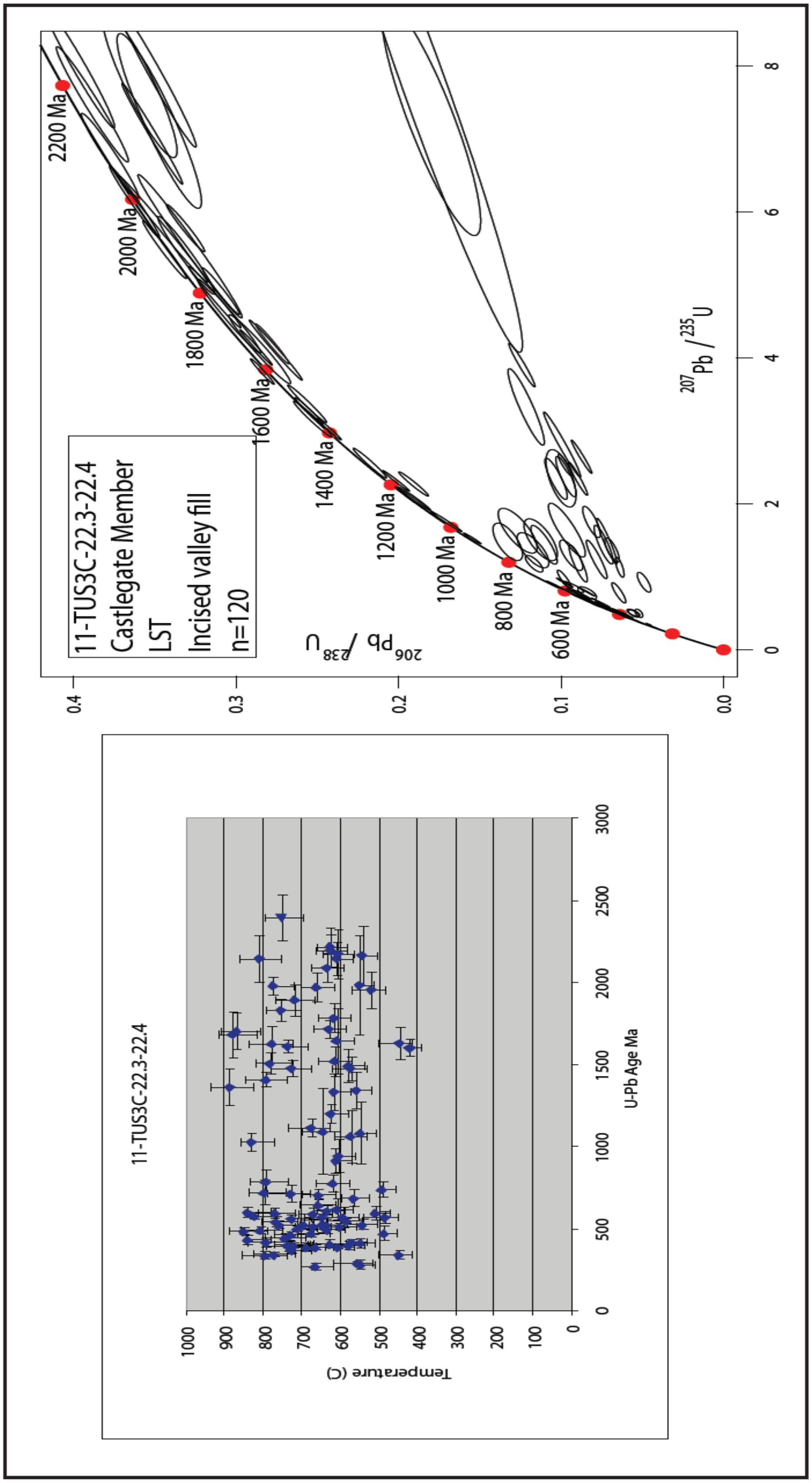
11-TUS3C-22.3-22.4
Castlegate Member
LST
Incised valley fill
n=120
2200 Ma
2000 Ma
1800 Ma
1600 Ma
1400 Ma
1200 Ma
1000 Ma
800 Ma
600 Ma
^{206}Pb / ^{238}U
^{207}Pb / ^{235}U
11-TUS3C-22.3-22.4
Temperature (C)
U-Pb Age Ma

Tables

Table 1.) Table showing the separation efficiency of SiC and pure quartz sand using heavy liquid separation methods. Heavy liquids used include Bromoform (s.g. 2.85 g/cm^3) and Methylene Iodide (s.g. 3.3 g/cm^3).

Mineral Separation of SiC from Pure Quartz Sand: Heavy Liquid Separation using Bromoform and Methylene Iodide								
	Pre-Seperation Mass (g)			Post-Seperation Mass (g)				
Test Sample	Pure Quartz Sand	Silcon Carbide	Total	Pure Quartz Sand	Silcon Carbide	Total	Silcon Carbide Lost	Total Material Lost
1	5.04	1.009	6.049	5.266	0.767	6.033	0.242	0.016
2	10.012	1.001	11.013	10.207	0.781	10.99	0.22	0.025
3	15.002	1.006	16.008	15.203	0.715	15.92	0.291	0.09
4	20.060	1.004	21.064	20.218	0.807	21.025	0.197	0.039
5	30.224	5.048	35.272	30.255	4.815	35.070	0.233	0.202
6	39.804	5.120	44.924	39.807	5.059	44.866	0.061	0.059
7	49.798	5.079	54.877	49.939	4.937	54.877	0.142	0.001

Table 2.) Description of samples from the Greater Green River Basin, Wyoming. Sandstone classification and cement composition of each sample was determined from QEMSCAN® analyses. Grain size determination was performed using a modified Wentworth grain size chart from Ingram (1953).

Description of sandstones from the Greater Green River Basin, WY						
Sample	Formation	Latitude	Longitude	Sand Grain Size	Sandstone Classification	Cement Composition
GR-09-05	Fox Hills Fm.	41.788545	-107.394683	very fine upper	Litharenite	Silica
GR-09-19	Dad Mbr. Of Lewis shale	41.851918	-107.394104	fine lower	Litharenite	Dolomite
GR-09-14	Almond Fm.	41.782577	-107.355309	very fine upper	Litharenite	Dolomite
GR-09-09	Pine Ridge sandstone	41.777649	-107.337799	very fine lower	Sublitharenite	Silica

Table 3.) Description of samples from the Book Cliffs, Utah. Sandstone classification and cement composition of each sample was determined from QEMSCAN® analyses. Grain size determination was performed using a modified Wentworth grain size chart from Ingram (1953).

Description of sandstones from the Book Cliffs, UT						
Sample	Formation	Latitude	Longitude	Sand Grain Size	Sandstone Classification	Cement Composition
11-CSTG-07	Castlegate sandstone	39.084638	-110.051250	very fine upper-fine lower	Sublitharenite	Silica
11-TUS3C-22.3-22.4	Castlegate sandstone	39.099960	-110.029793	fine lower	Sublitharenite	Dolomite
11-TUS3C-2-17	Desert Mbr. Blackhawk	39.096796	-110.080862	very fine upper	Sublitharenite	Dolomite
11-BH-06	Desert Mbr. Blackhawk	39.090501	-110.867986	very fine lower	Sublitharenite	Silica
11-AB-LST	Aberdeen Mbr. Blackhawk	39.024385	-109.708786	very fine lower	Sublitharenite	Silica
11-SPC-01	Spring Canyon Mbr. Blackhawk	39.090367	-110.053139	medium upper	Sublitharenite	Calcite
11-SPC-05	Spring Canyon Mbr. Blackhawk Fm.	39.717375	-110.876759	fine upper	Sublitharenite	Calcite
11-PTH-09	Panther Tongue Star Point Fm.	39.71186	-110.867986	very fine upper	Litharenite	Calcite
10-PTH-01	Panther Tongue Star Point Fm.	39.711941	-110.870290	fine upper-medium lower	Litharenite	Calcite

Appendix A: Cathodoluminescence Images of Zircon Grains

Prior to U-Pb and trace element analyses, grain mounts containing relevant zircon grains were imaged at the University of Kansas Microscopy and Analytical Imaging Laboratory. A LEO 1550 Field Emission Scanning Electron Microscope was used to collect grey-scale cathodoluminescence images to reveal the internal complexities in zircon grains. Imaged zircons in nearly all samples contained inherited cores, sector-zones, and oscillatory zones. During spot placement for laser ablation-inductively coupled plasma-mass spectrometry analyses, these images were consulted to target specific areas on zircon grains. Commonly, targeted zircons were ~50-120 μm. In the analyses of grains that were less than ~60 μm the internal complexities in the grains could not be differentiated. Grains that were large enough for the internal complexities in the grains to be differentiated, the inherited cores of the grains were targeted for analyses.

Appendix A: CL Images of Zircon

Zircon from the Greater Green River Basin, Wyoming

GR-09-05

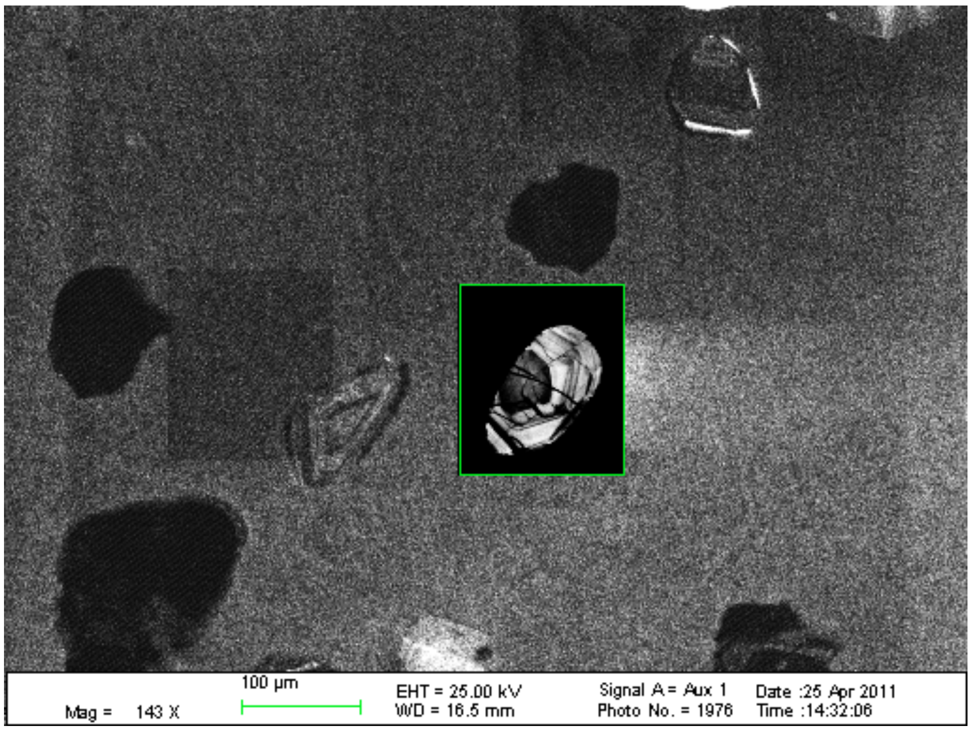

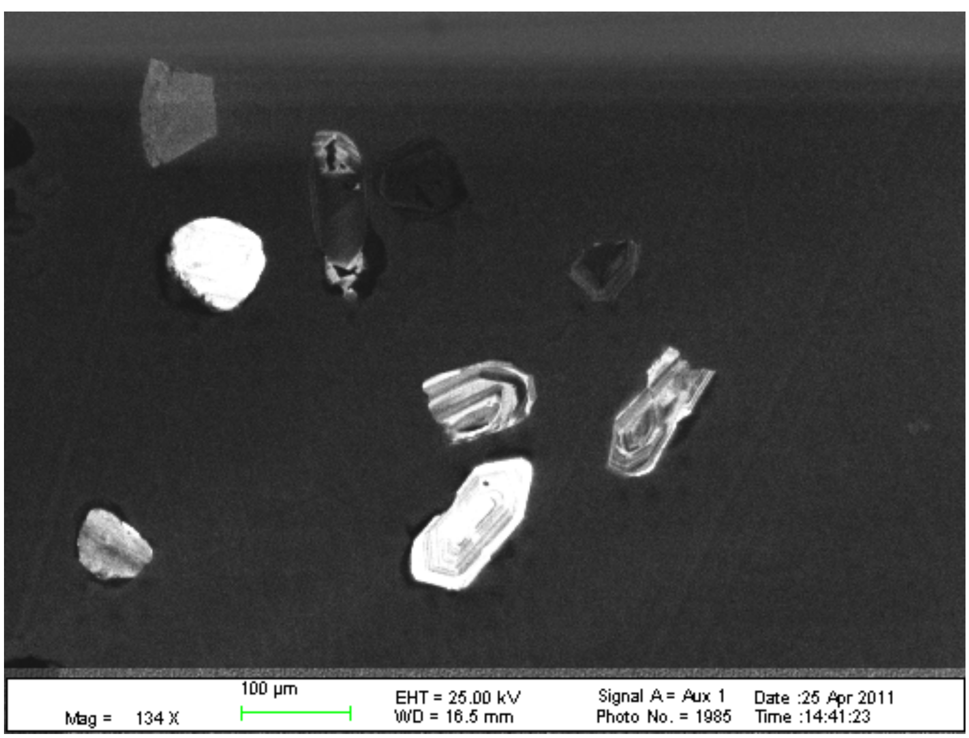

GR-09-05 continued

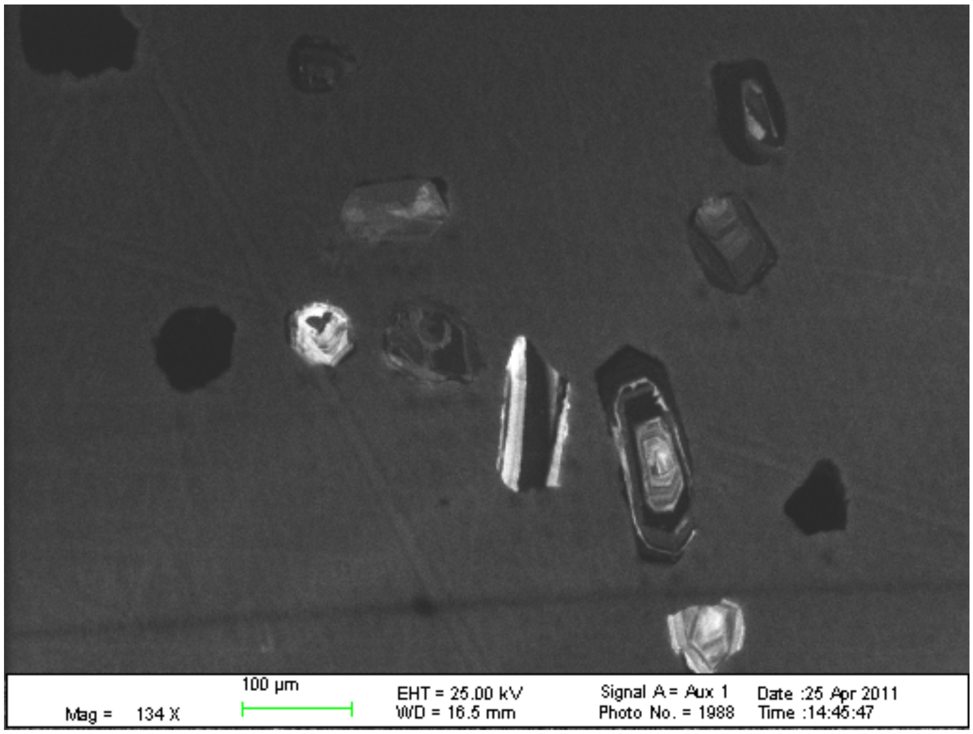

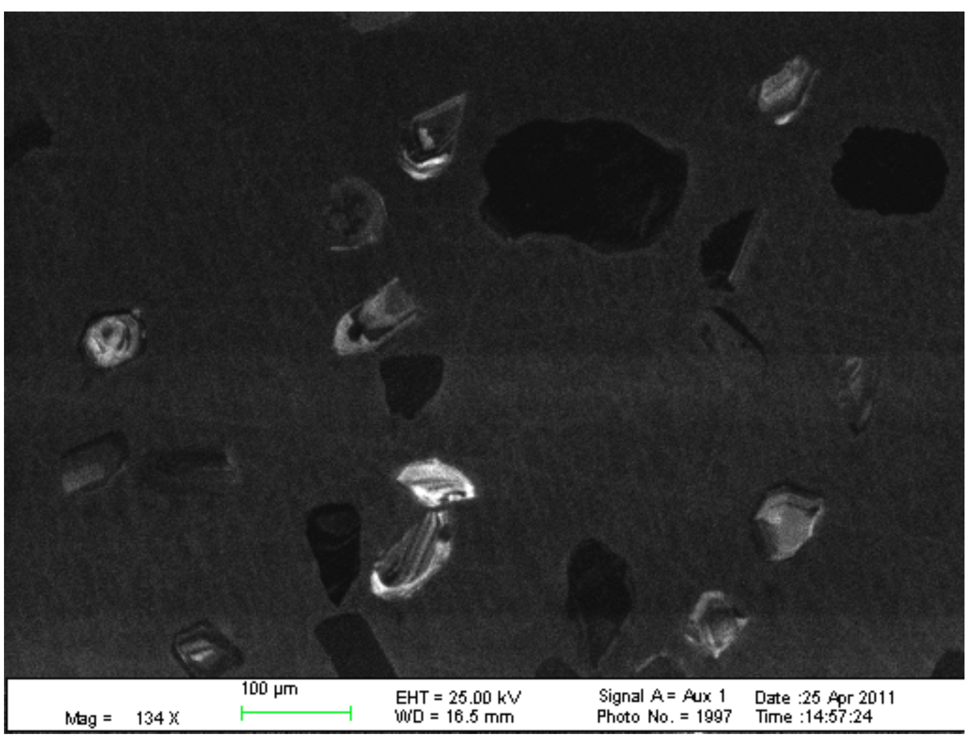

GR-09-09

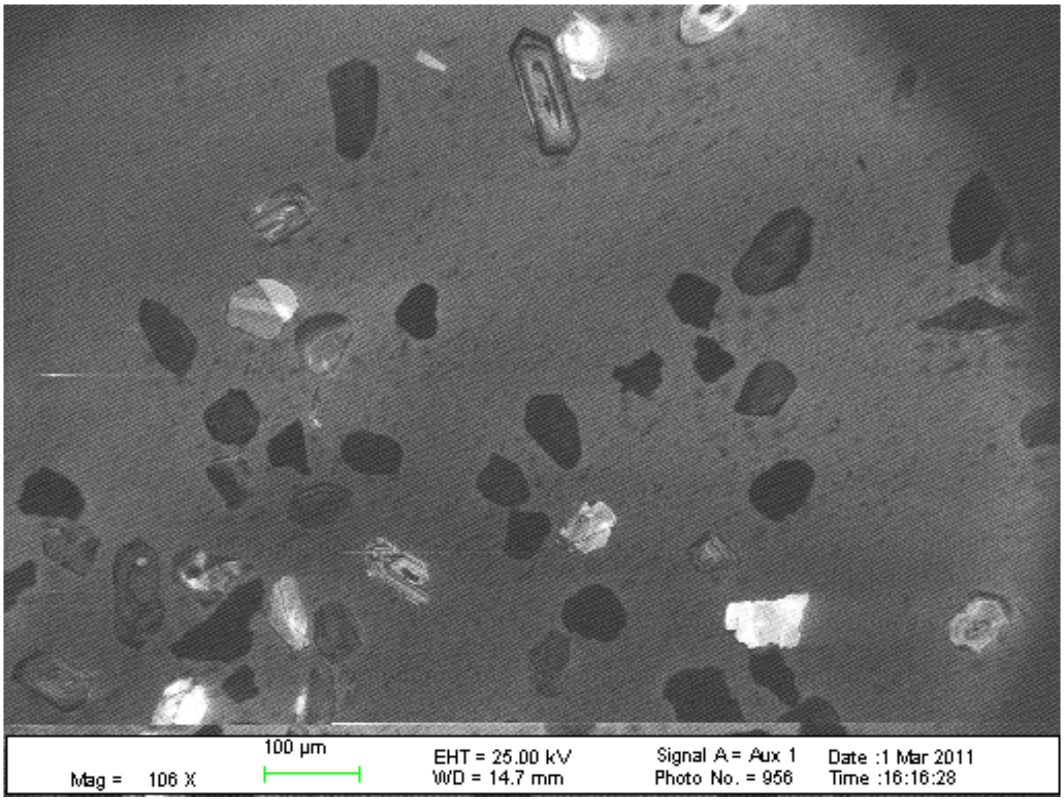
100 µm
Mag = 106 X
EHT = 25.00 kV
WD = 14.7 mm
Signal A = Aux 1
Photo No. = 956
Date :1 Mar 2011
Time :16:16:28

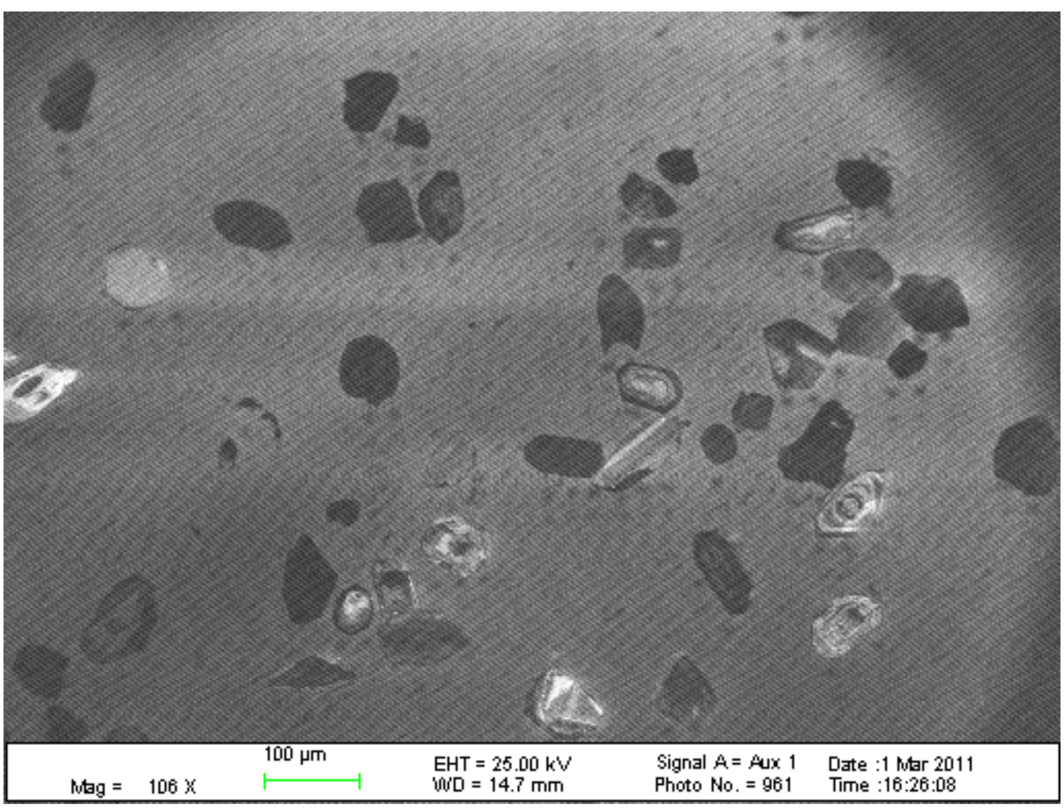
100 µm
Mag = 106 X
EHT = 25.00 kV
WD = 14.7 mm
Signal A = Aux 1
Photo No. = 961
Date :1 Mar 2011
Time :16:26:08

GR-09-14

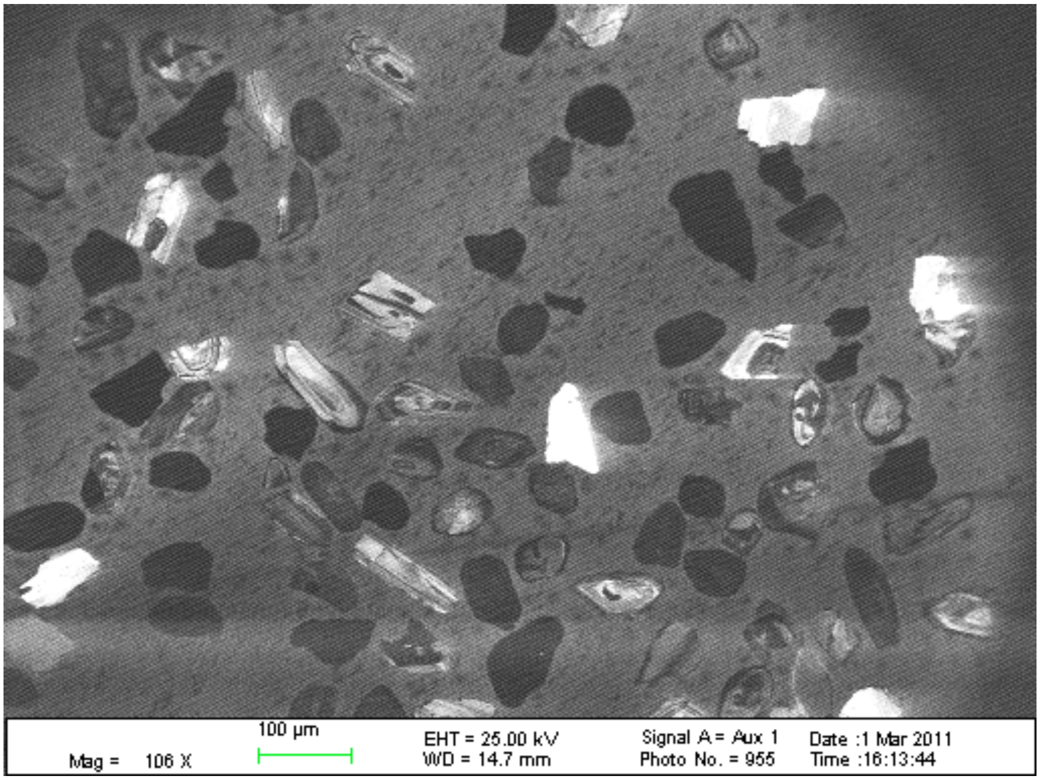

100 µm
Mag = 106 X
EHT = 25.00 kV
WD = 14.7 mm
Signal A = Aux 1
Photo No. = 955
Date :1 Mar 2011
Time :16:13:44

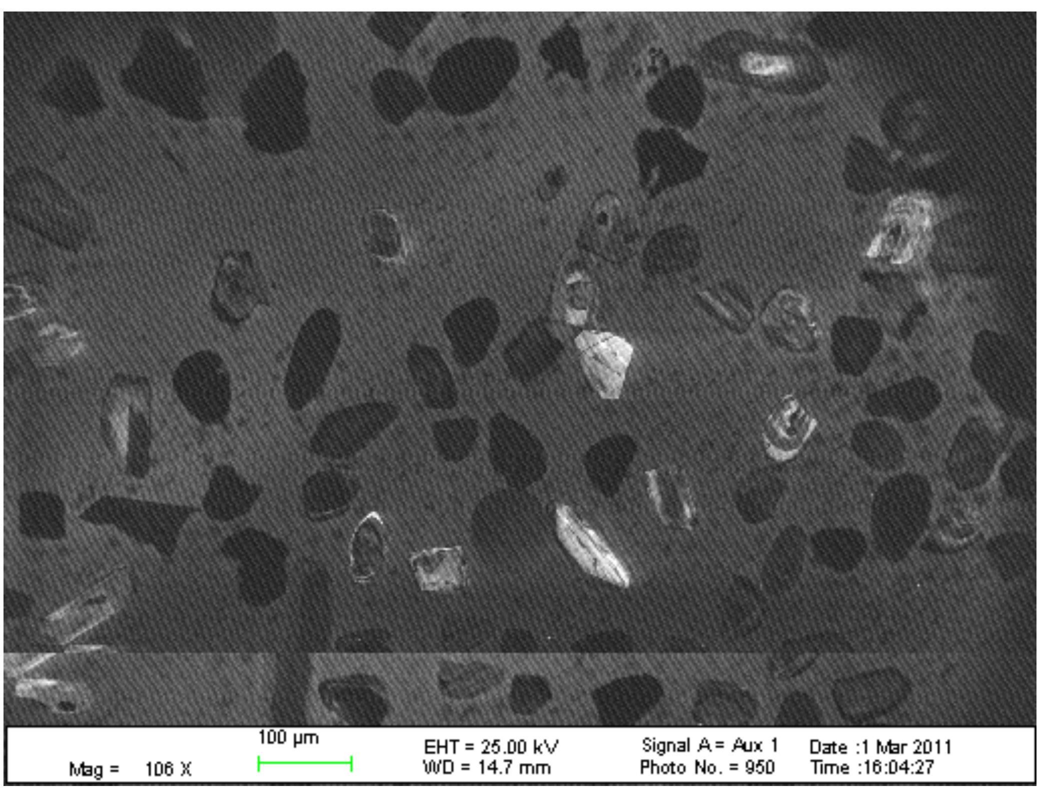

100 µm
Mag = 106 X
EHT = 25.00 kV
WD = 14.7 mm
Signal A = Aux 1
Photo No. = 950
Date :1 Mar 2011
Time :16:04:27

GR-09-19

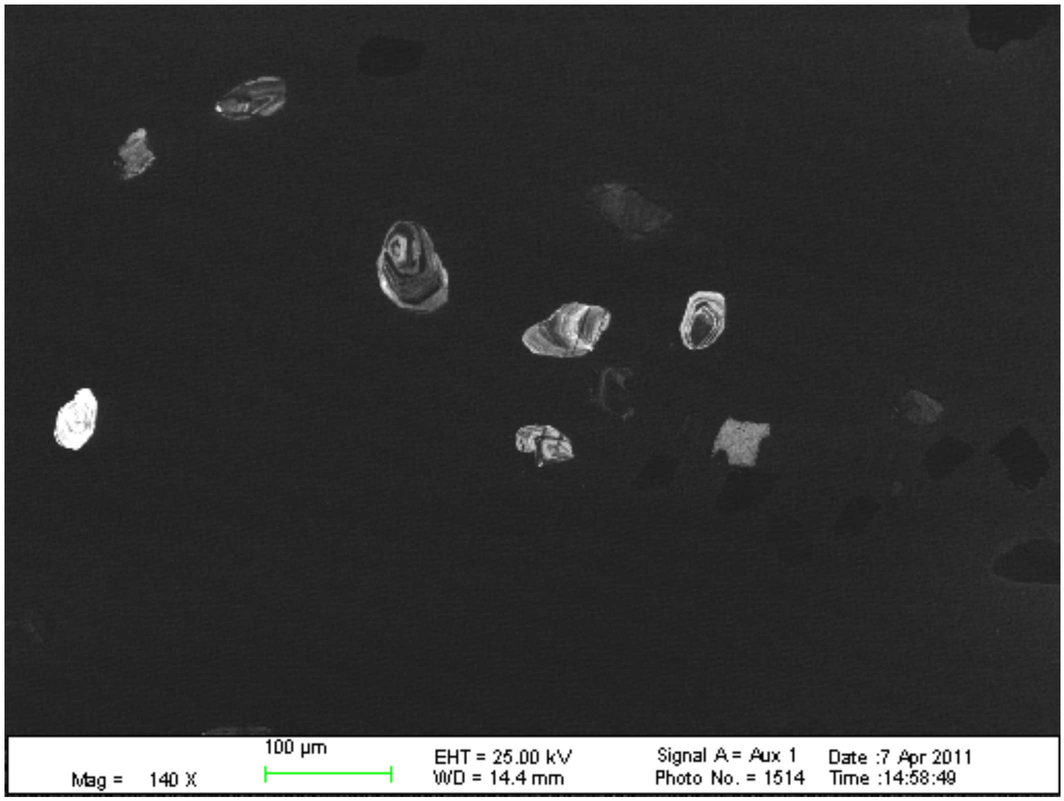
100 µm
Mag = 140 X
EHT = 25.00 kV
WD = 14.4 mm
Signal A = Aux 1
Photo No. = 1514
Date :7 Apr 2011
Time :14:58:49

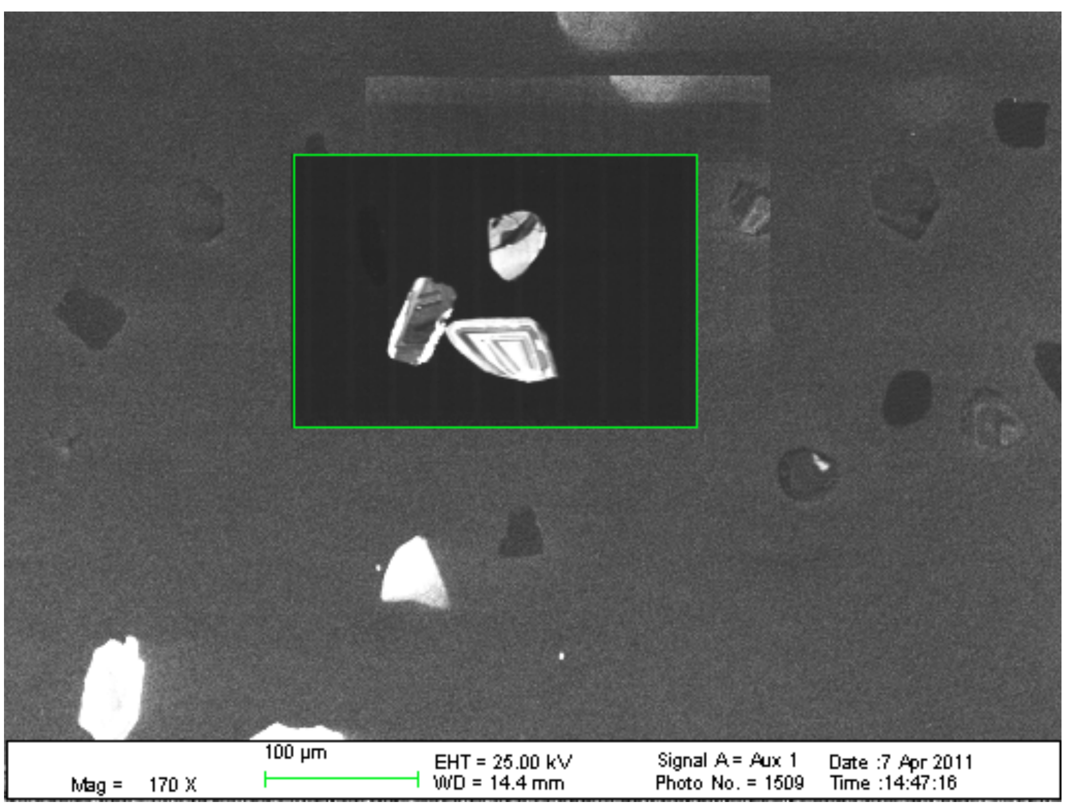
100 µm
Mag = 170 X
EHT = 25.00 kV
WD = 14.4 mm
Signal A = Aux 1
Photo No. = 1509
Date :7 Apr 2011
Time :14:47:16

GR-09-19 continued

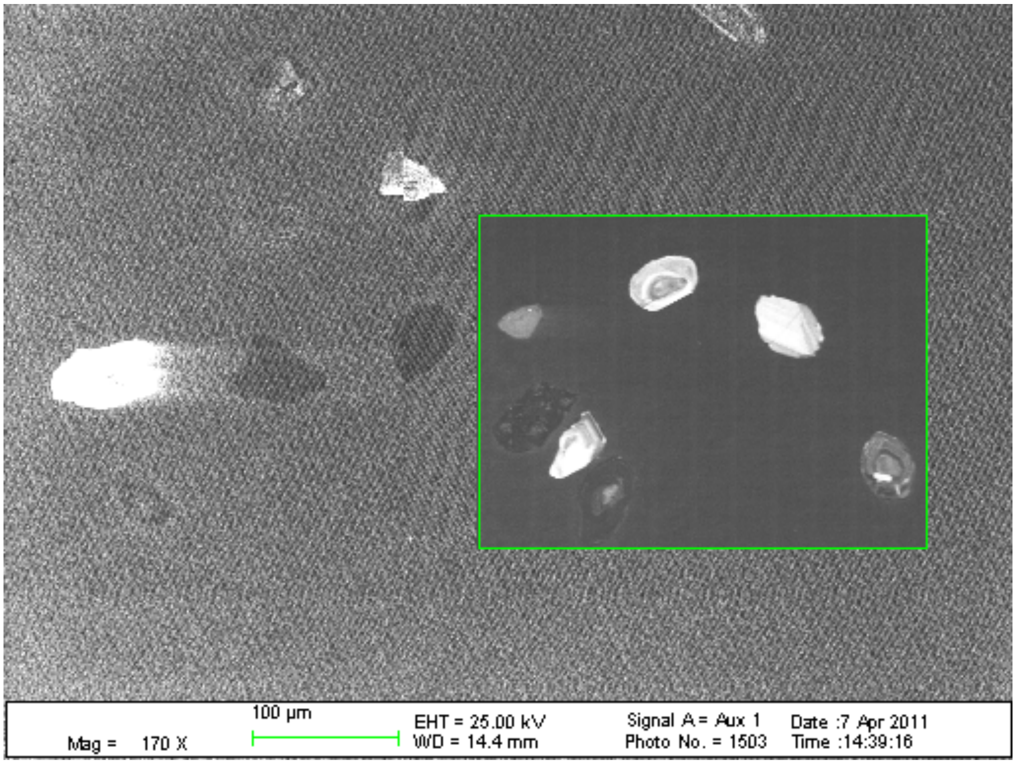

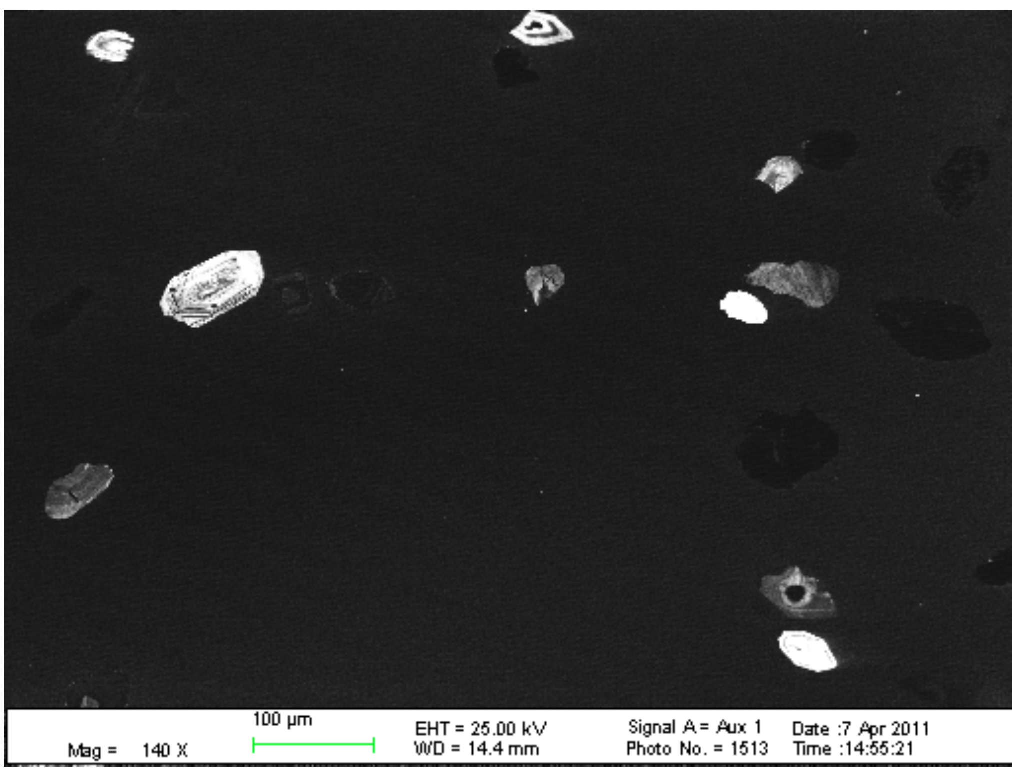

Zircon from the Book Cliffs, Utah

11-CSTG-07

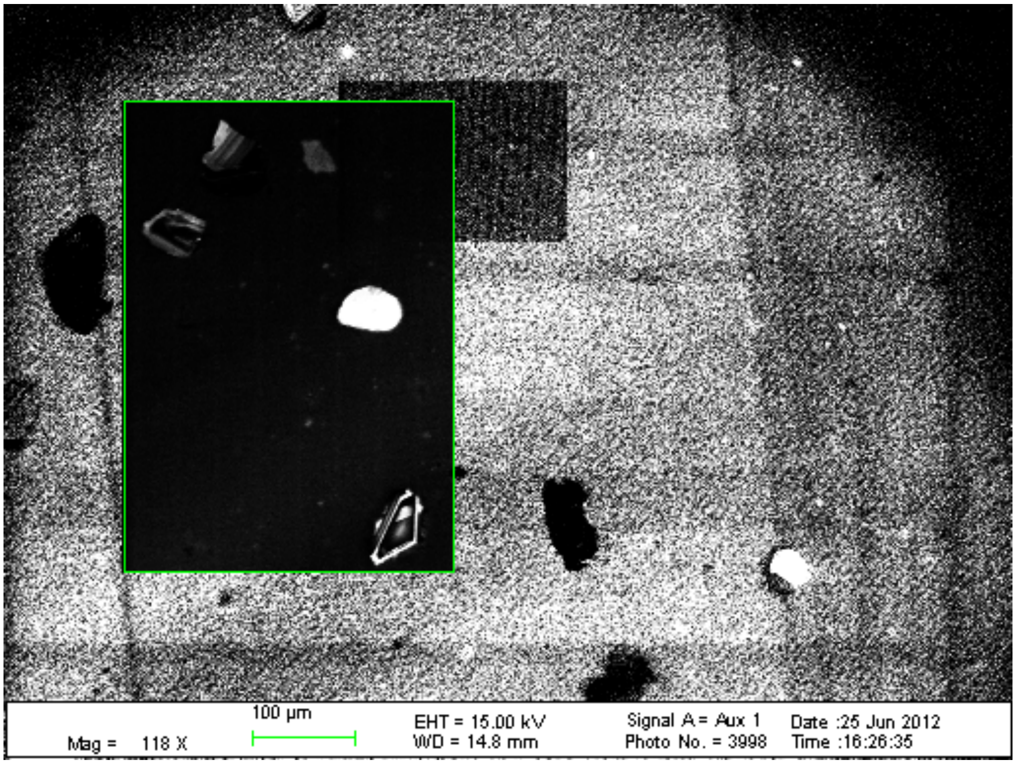

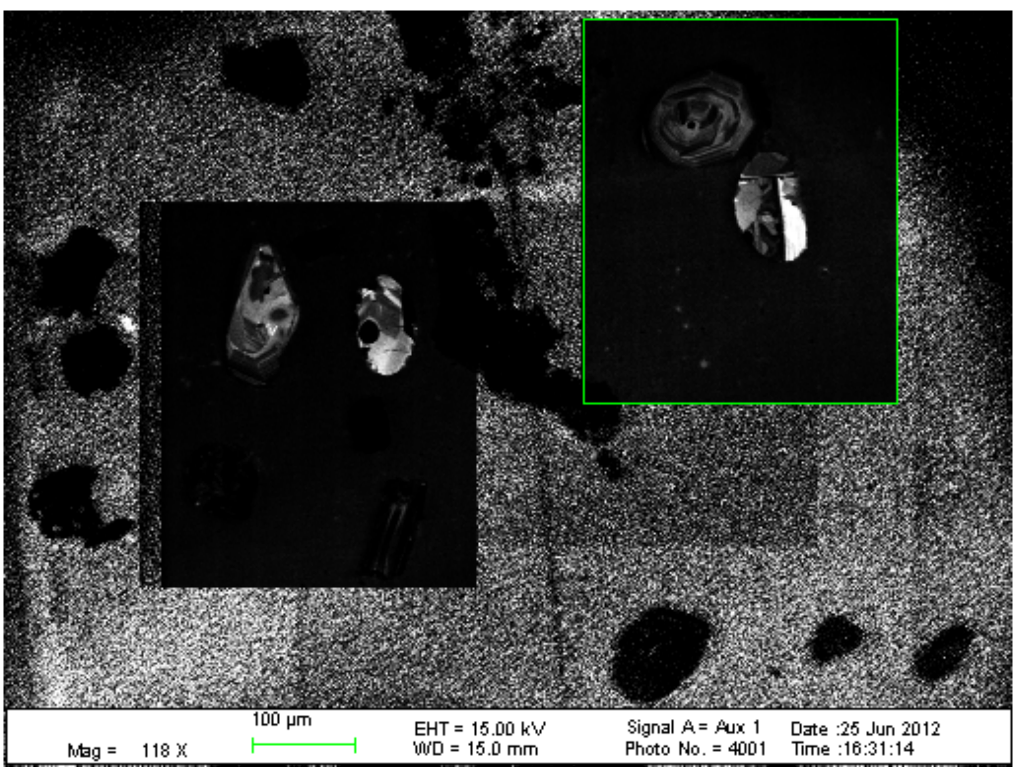

11-CSTG-07 continued

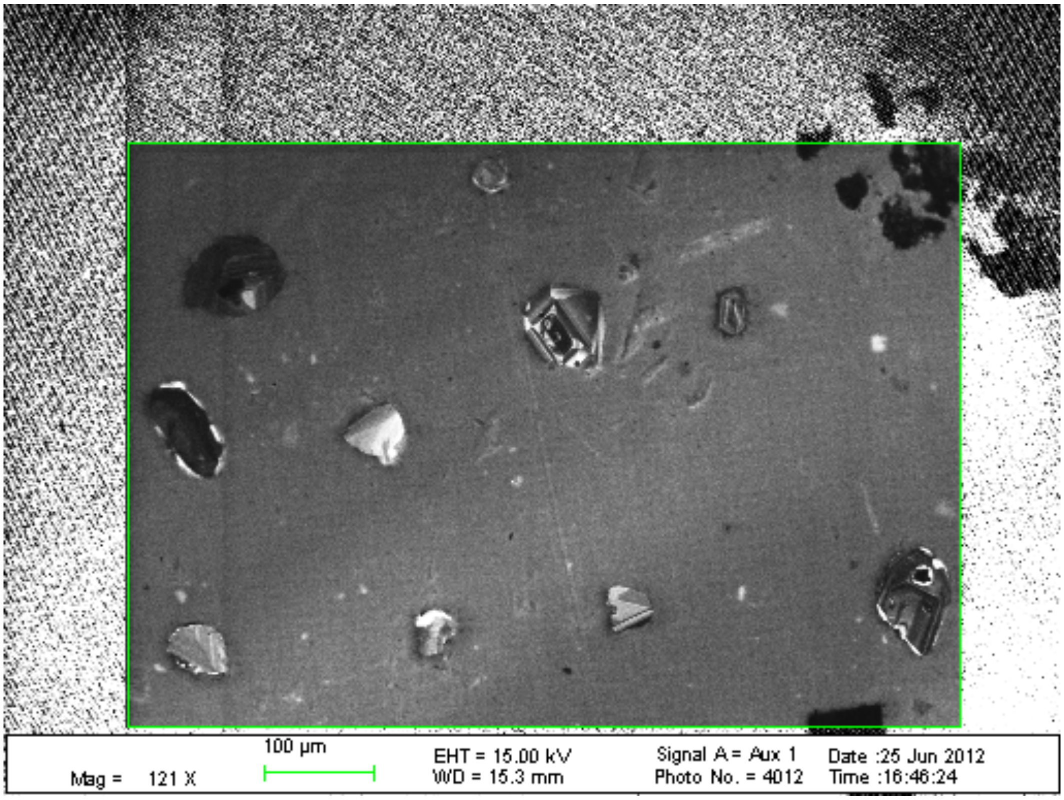

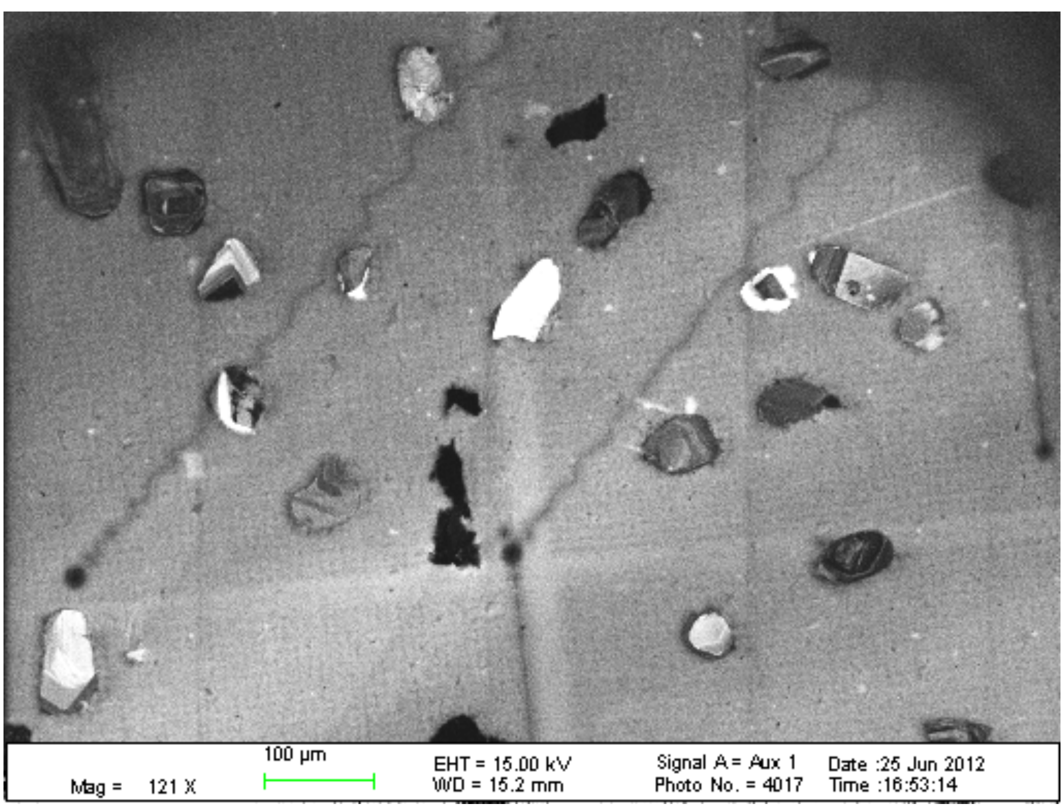

11-TUS3C-22.3-22.4

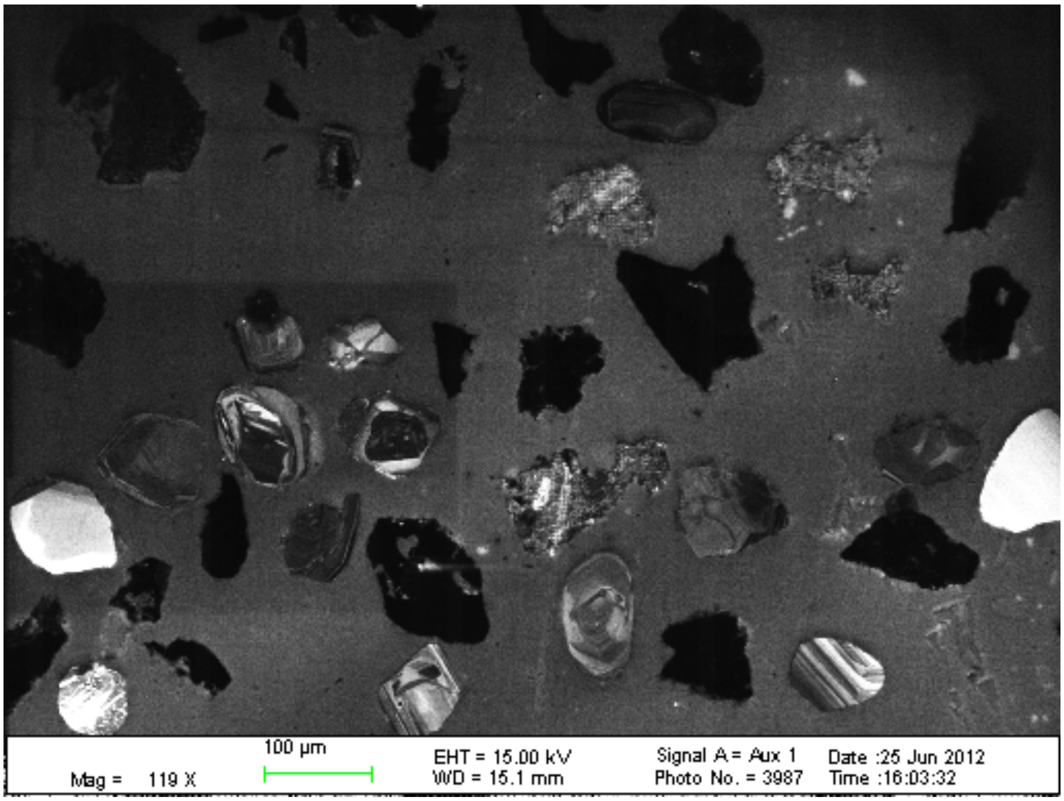

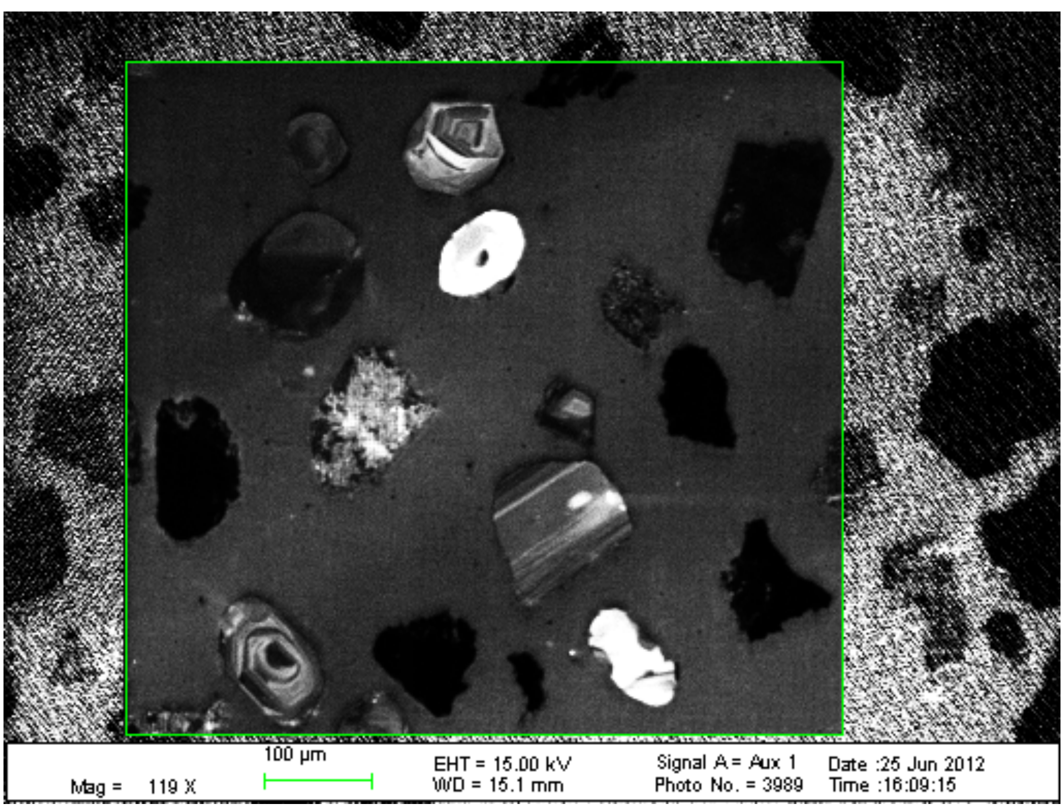

11-TUS3C-22.3-22.4 continued

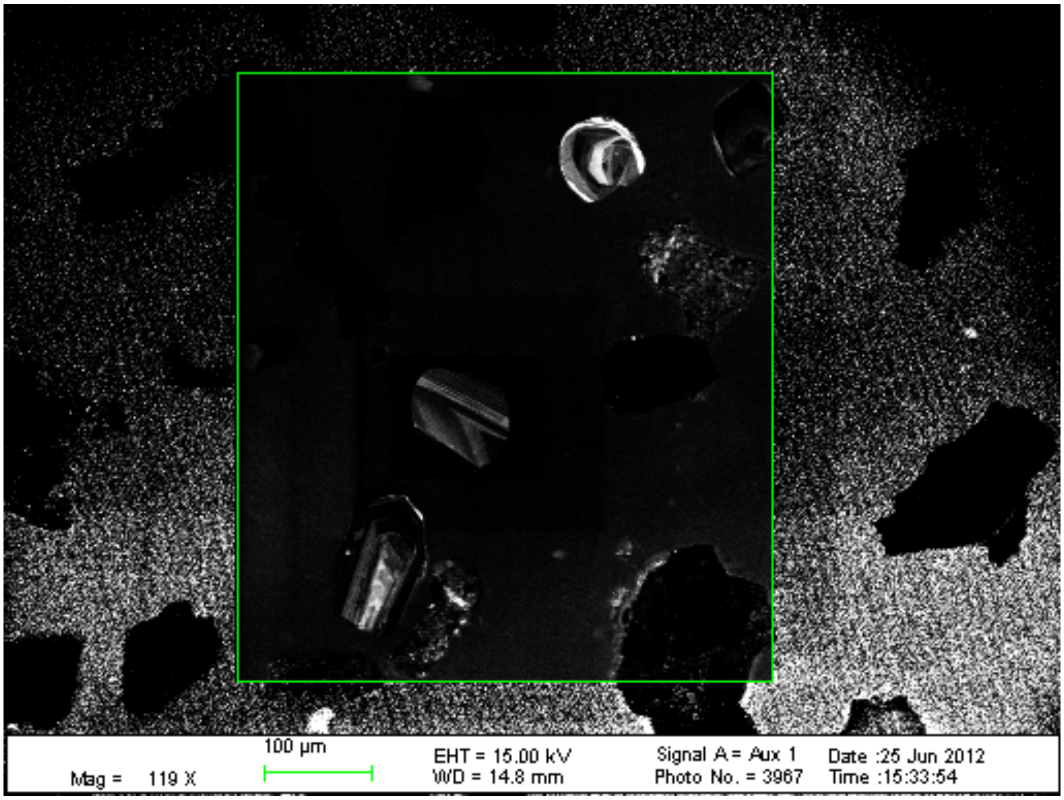

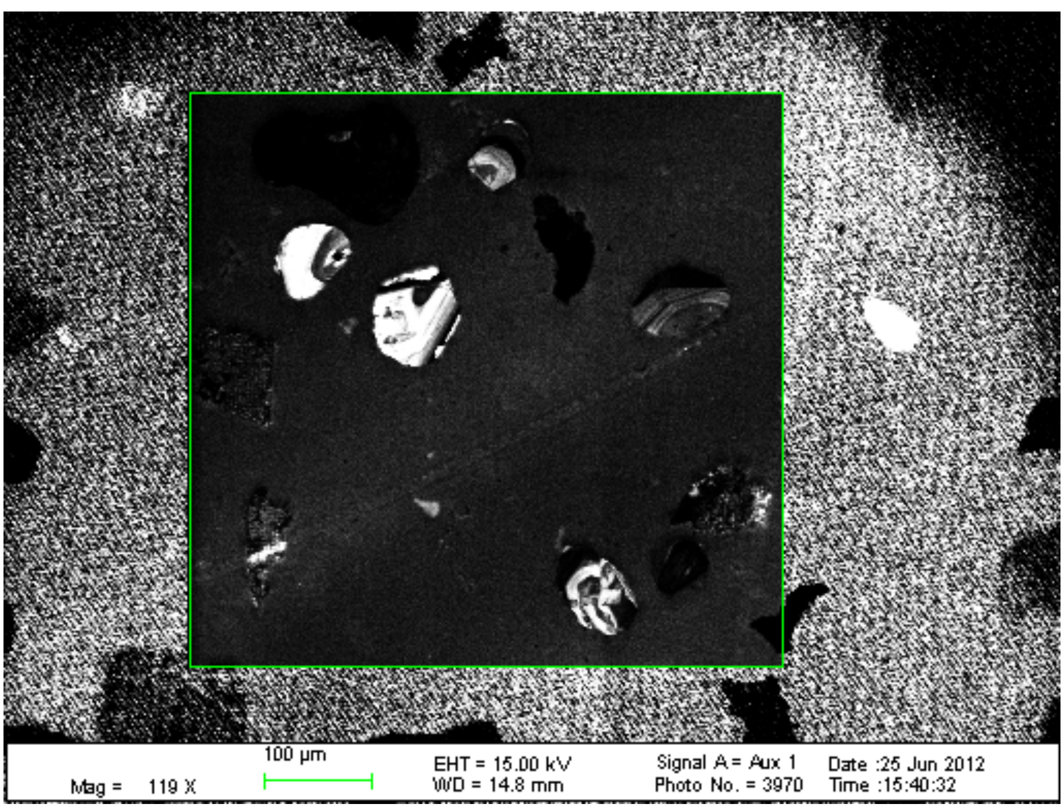

11-TUS3C-2-17

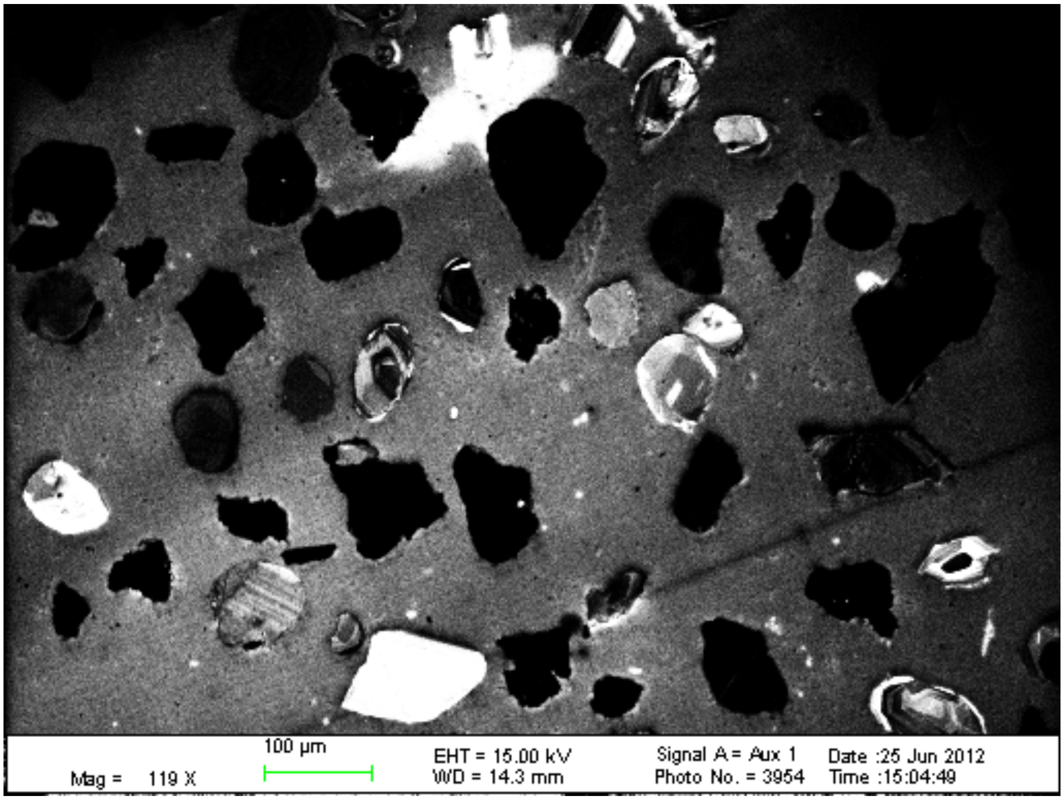
100 µm
Mag = 119 X
EHT = 15.00 kV
WD = 14.3 mm
Signal A = Aux 1
Photo No. = 3954
Date :25 Jun 2012
Time :15:04:49

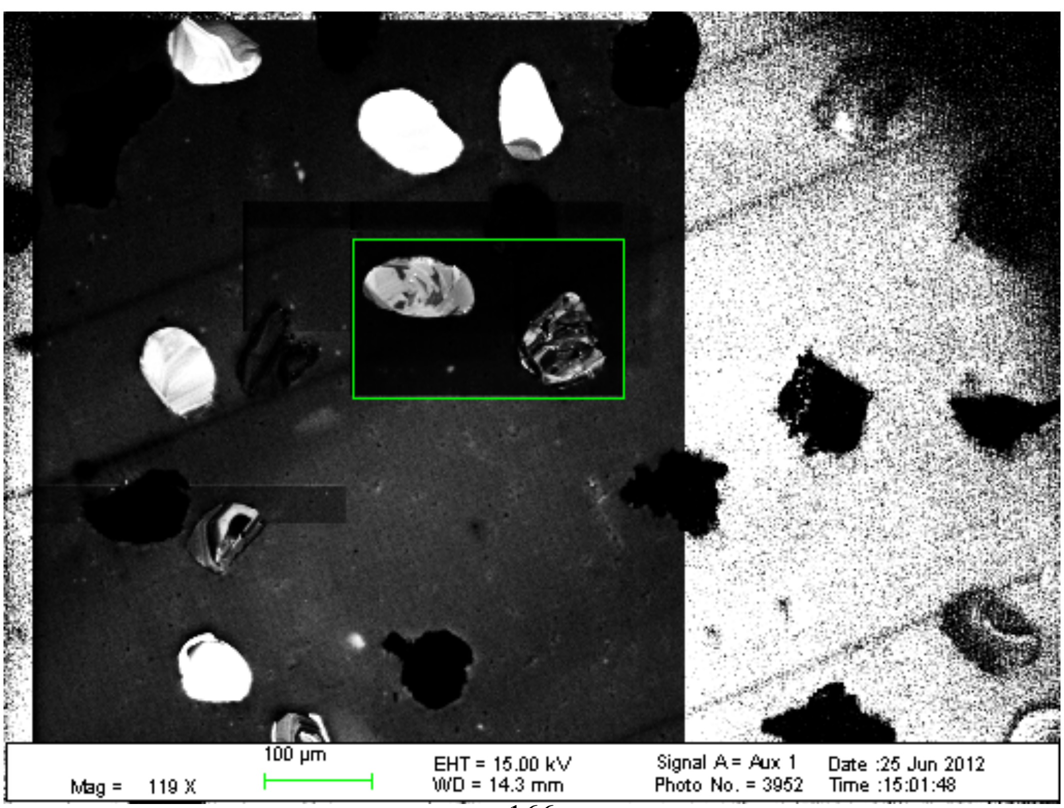
100 µm
Mag = 119 X
EHT = 15.00 kV
WD = 14.3 mm
Signal A = Aux 1
Photo No. = 3952
Date :25 Jun 2012
Time :15:01:48

11-AB-LST

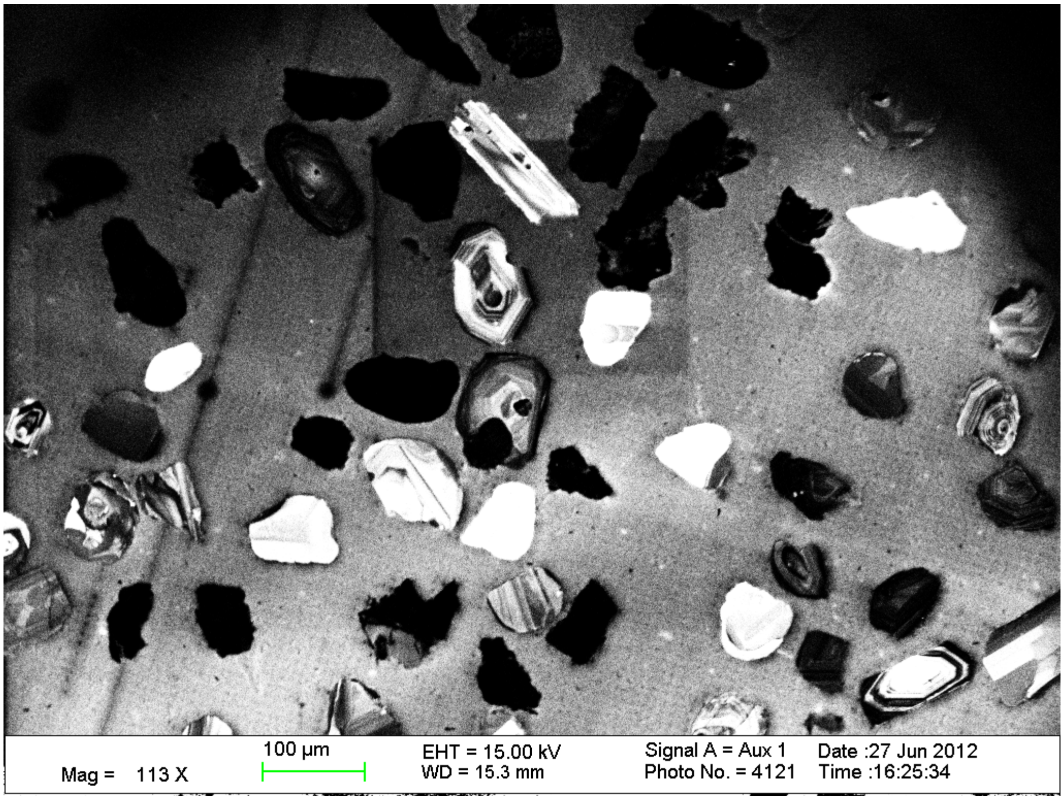
Mag = 113 X
100 µm
EHT = 15.00 kV
WD = 15.3 mm
Signal A = Aux 1
Photo No. = 4121
Date :27 Jun 2012
Time :16:25:34

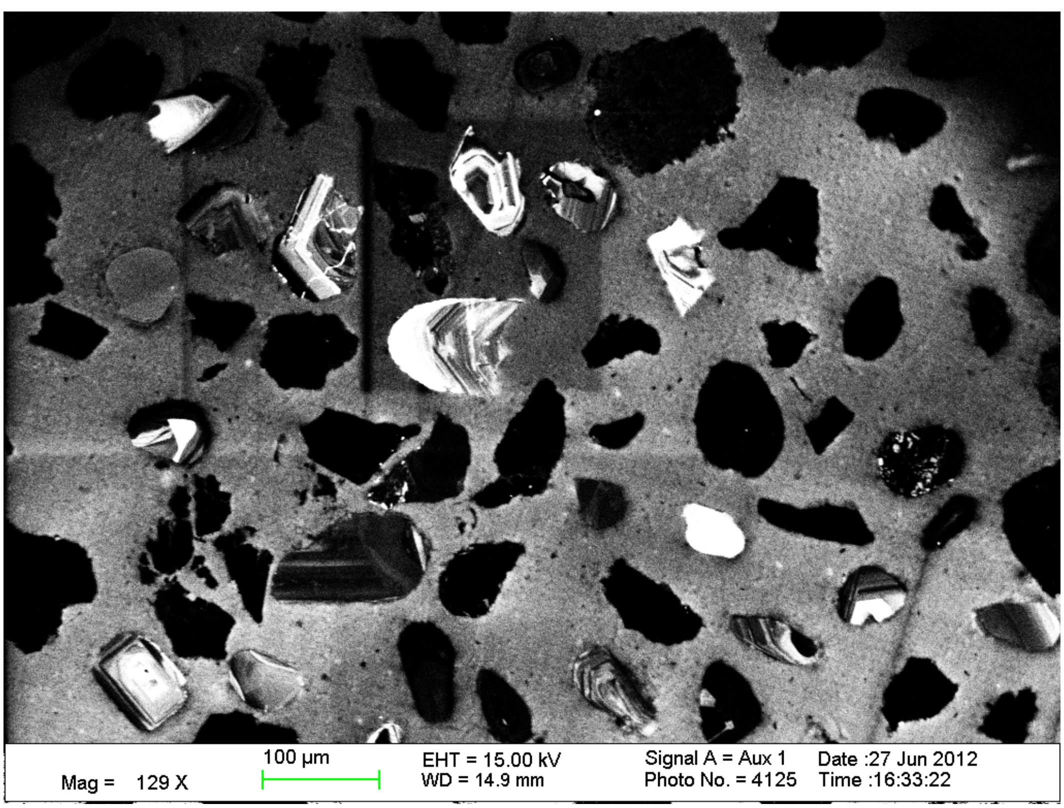
Mag = 129 X
100 µm
EHT = 15.00 kV
WD = 14.9 mm
Signal A = Aux 1
Photo No. = 4125
Date :27 Jun 2012
Time :16:33:22

11-AB-LST

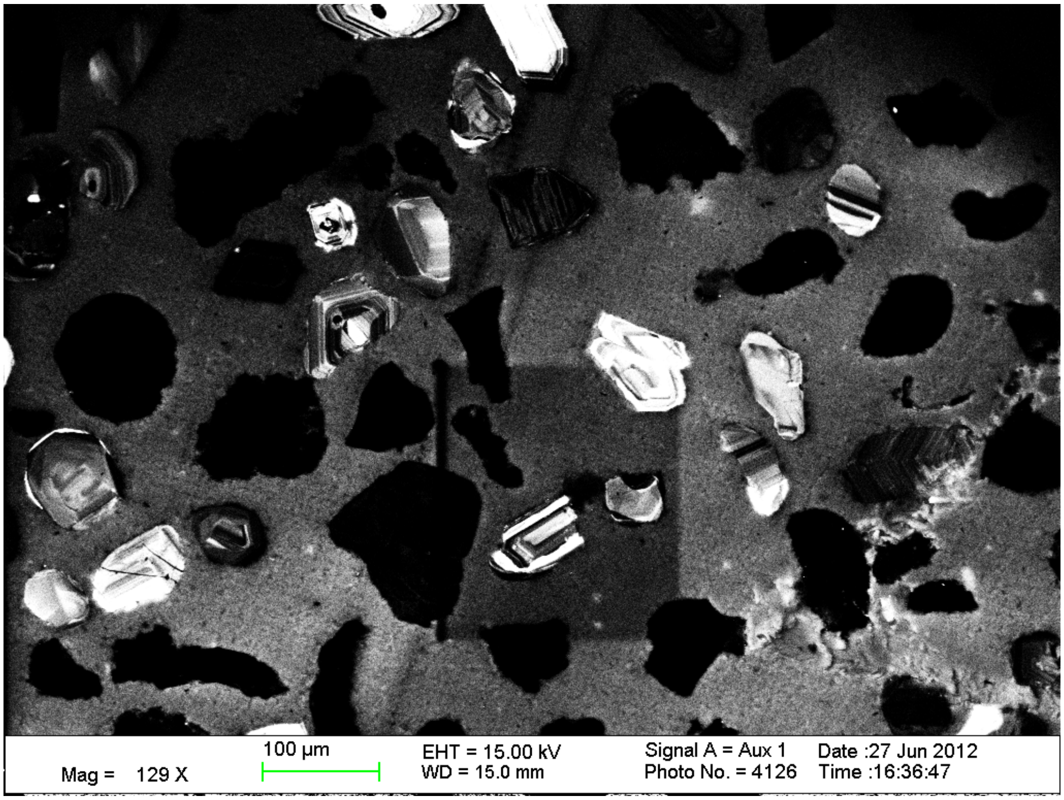
100 µm
Mag = 129 X
EHT = 15.00 kV
WD = 15.0 mm
Signal A = Aux 1
Photo No. = 4126
Date :27 Jun 2012
Time :16:36:47

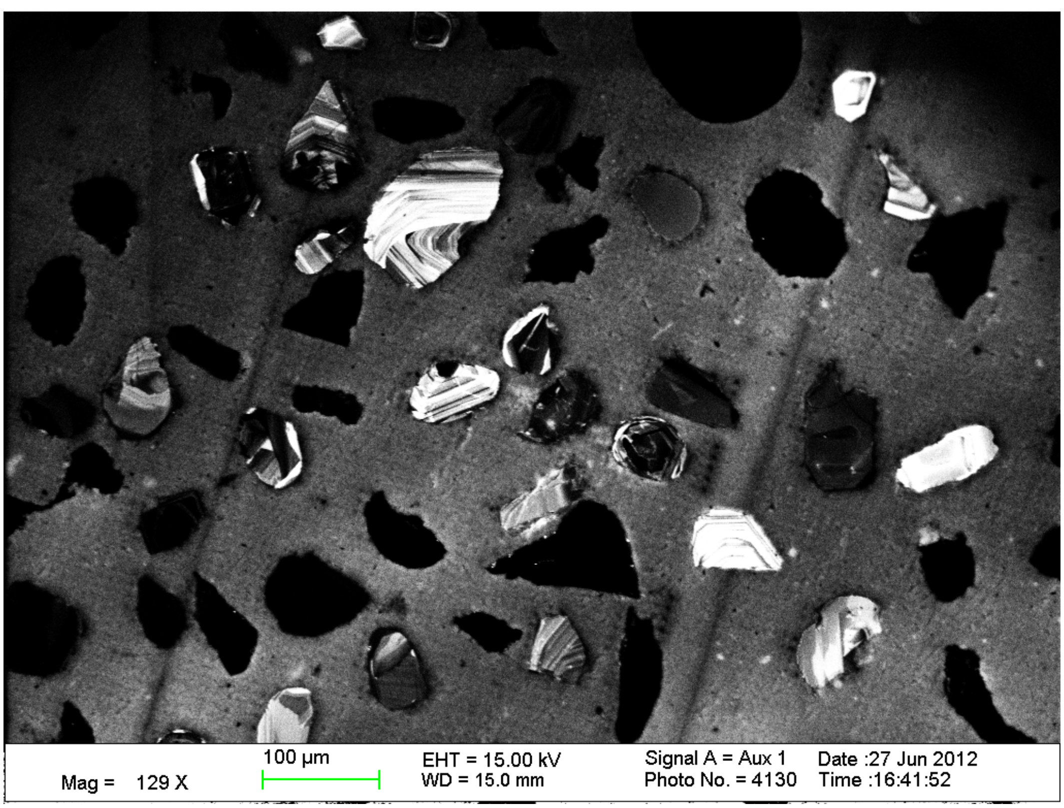
100 µm
Mag = 129 X
EHT = 15.00 kV
WD = 15.0 mm
Signal A = Aux 1
Photo No. = 4130
Date :27 Jun 2012
Time :16:41:52

11-BH-06

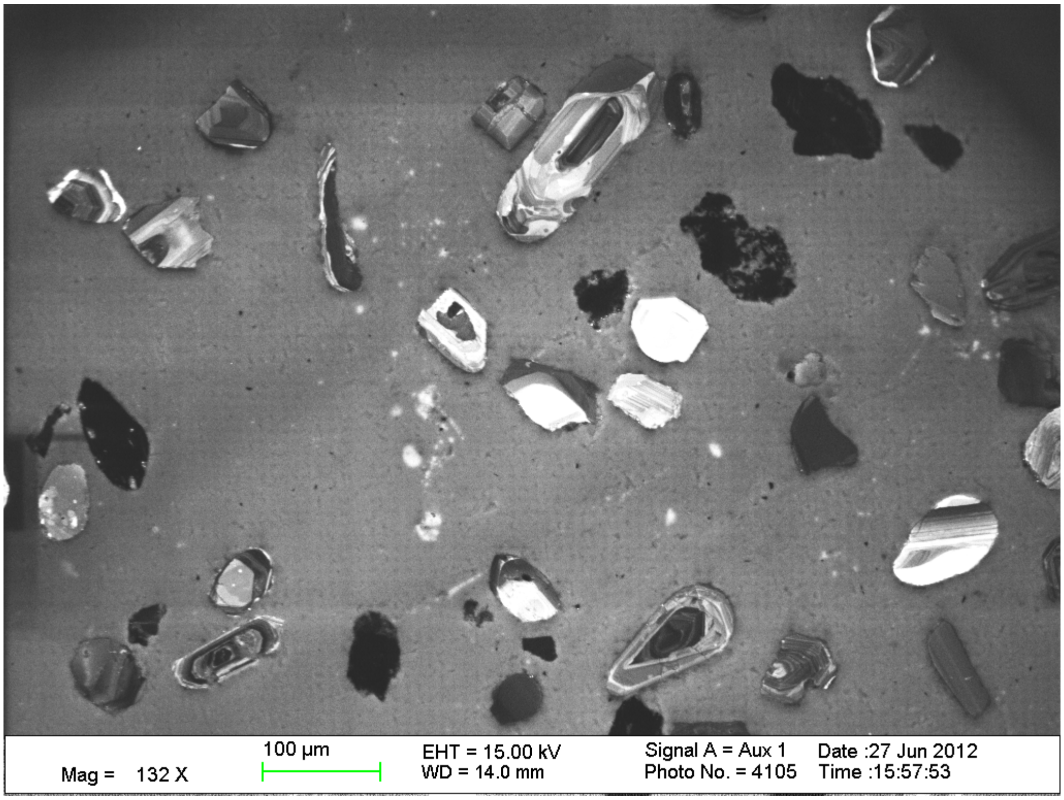
Mag = 132 X
100 µm
EHT = 15.00 kV
WD = 14.0 mm
Signal A = Aux 1
Photo No. = 4105
Date :27 Jun 2012
Time :15:57:53

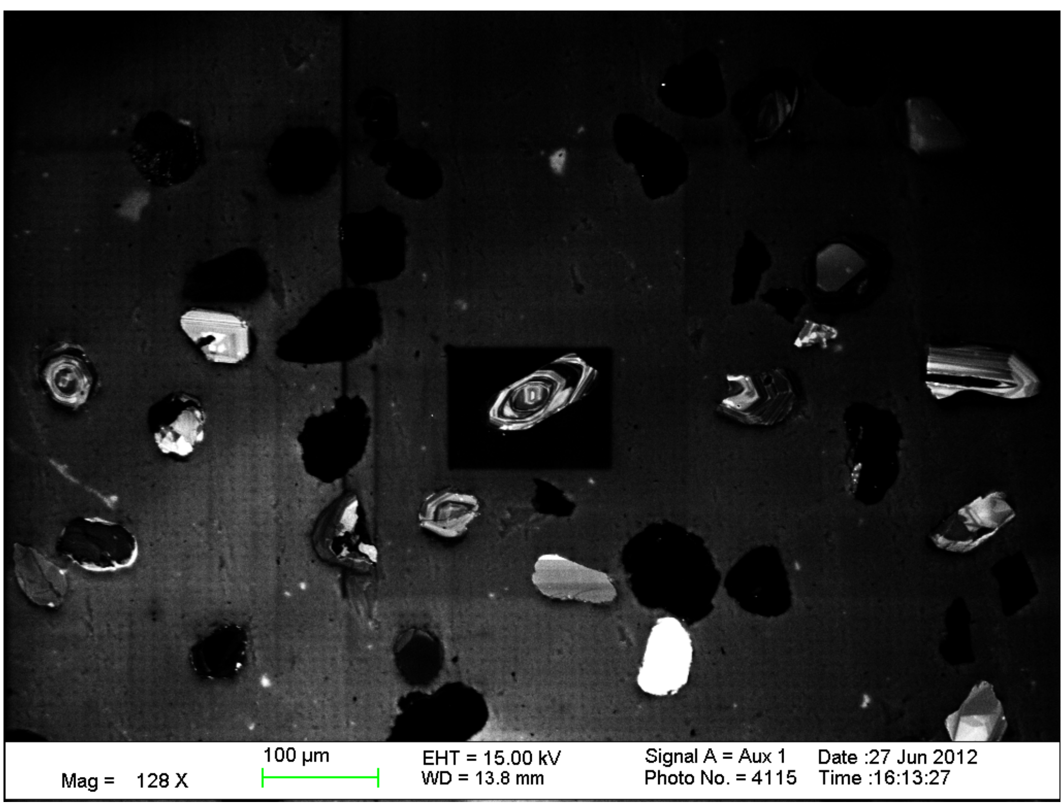
Mag = 128 X
100 µm
EHT = 15.00 kV
WD = 13.8 mm
Signal A = Aux 1
Photo No. = 4115
Date :27 Jun 2012
Time :16:13:27

11-SPC-05

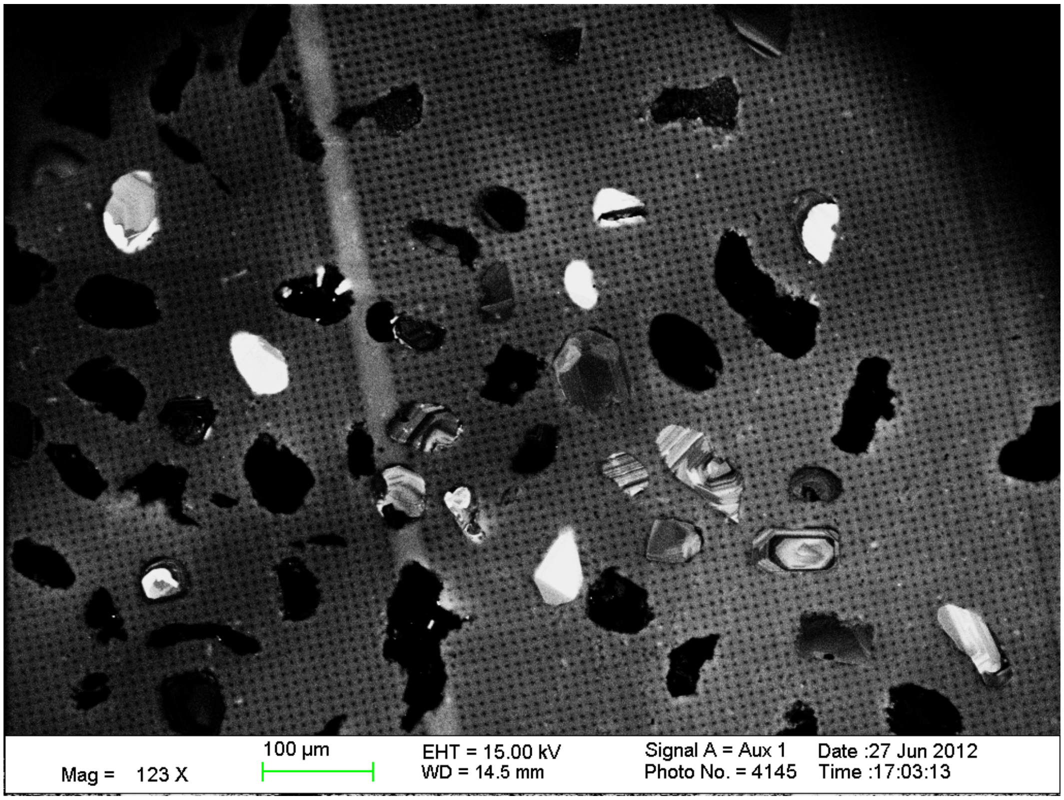
100 µm
Mag = 123 X
EHT = 15.00 kV
WD = 14.5 mm
Signal A = Aux 1
Photo No. = 4145
Date :27 Jun 2012
Time :17:03:13

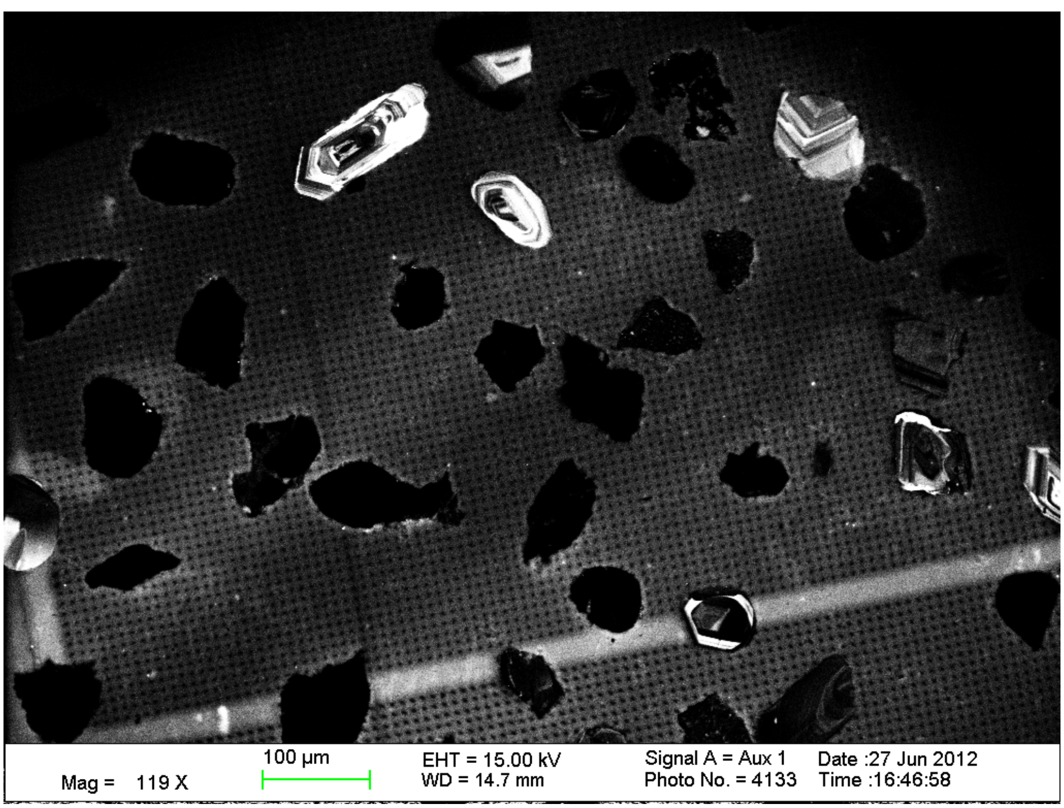
100 µm
Mag = 119 X
EHT = 15.00 kV
WD = 14.7 mm
Signal A = Aux 1
Photo No. = 4133
Date :27 Jun 2012
Time :16:46:58

11-CTSG-01

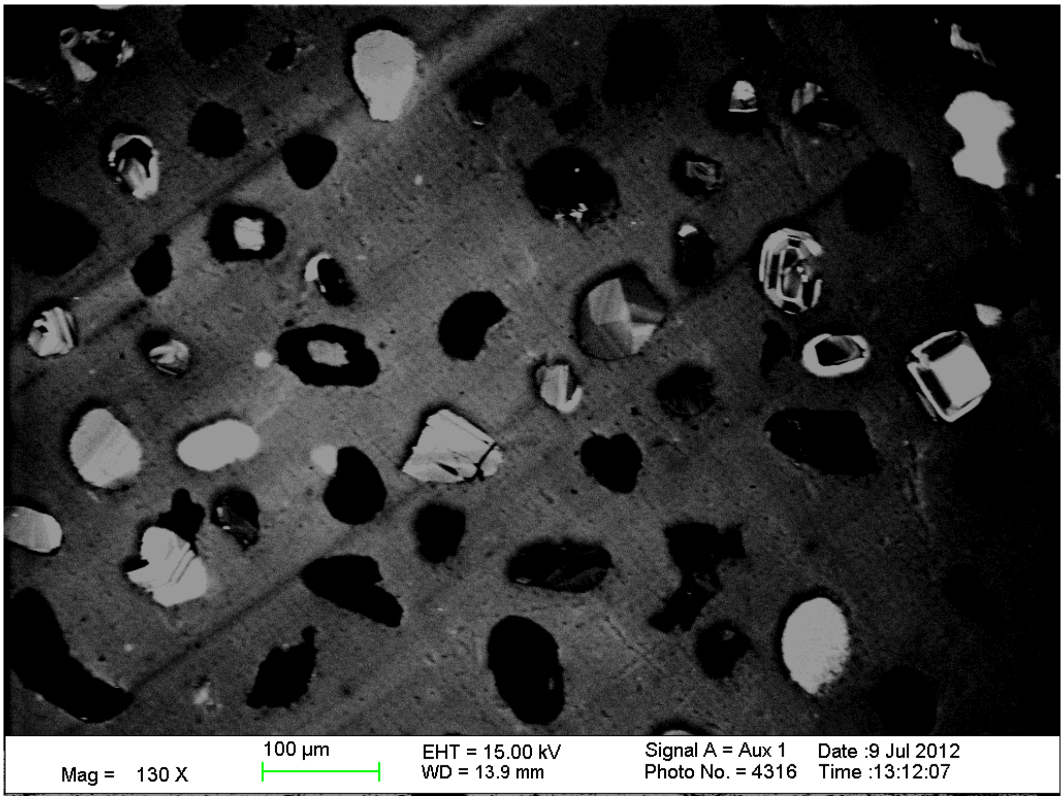
Mag = 130 X
100 µm
EHT = 15.00 kV
WD = 13.9 mm
Signal A = Aux 1
Photo No. = 4316
Date :9 Jul 2012
Time :13:12:07

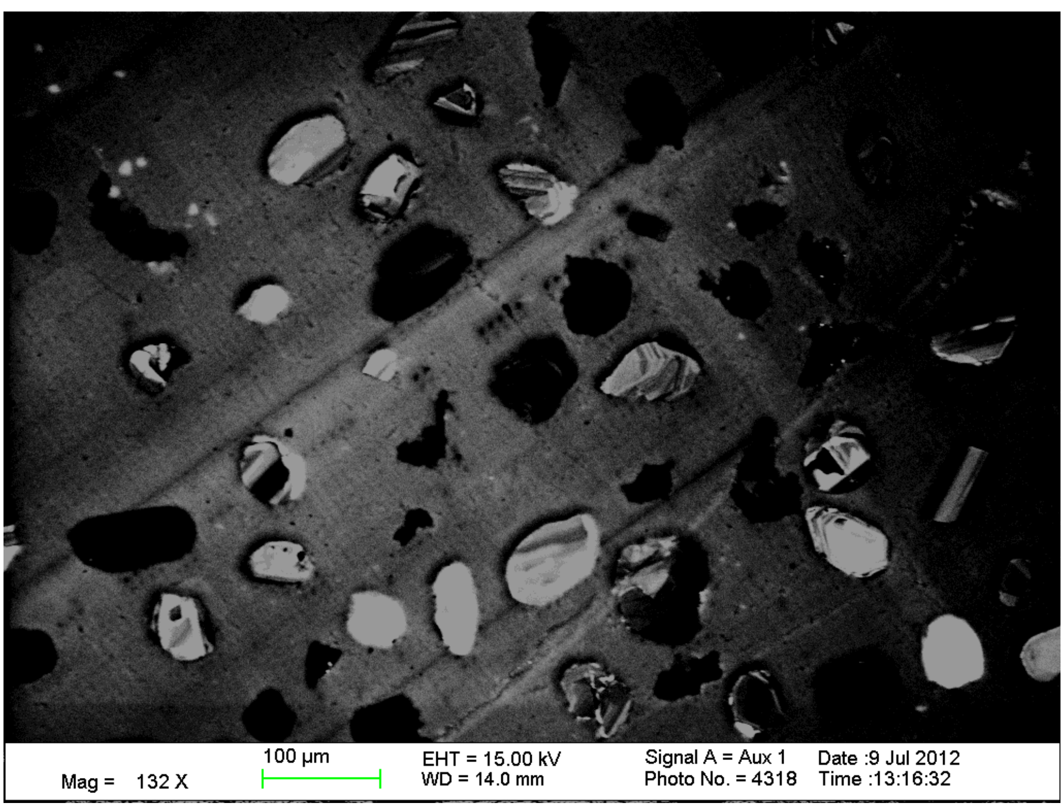
Mag = 132 X
100 µm
EHT = 15.00 kV
WD = 14.0 mm
Signal A = Aux 1
Photo No. = 4318
Date :9 Jul 2012
Time :13:16:32

11-BH-09

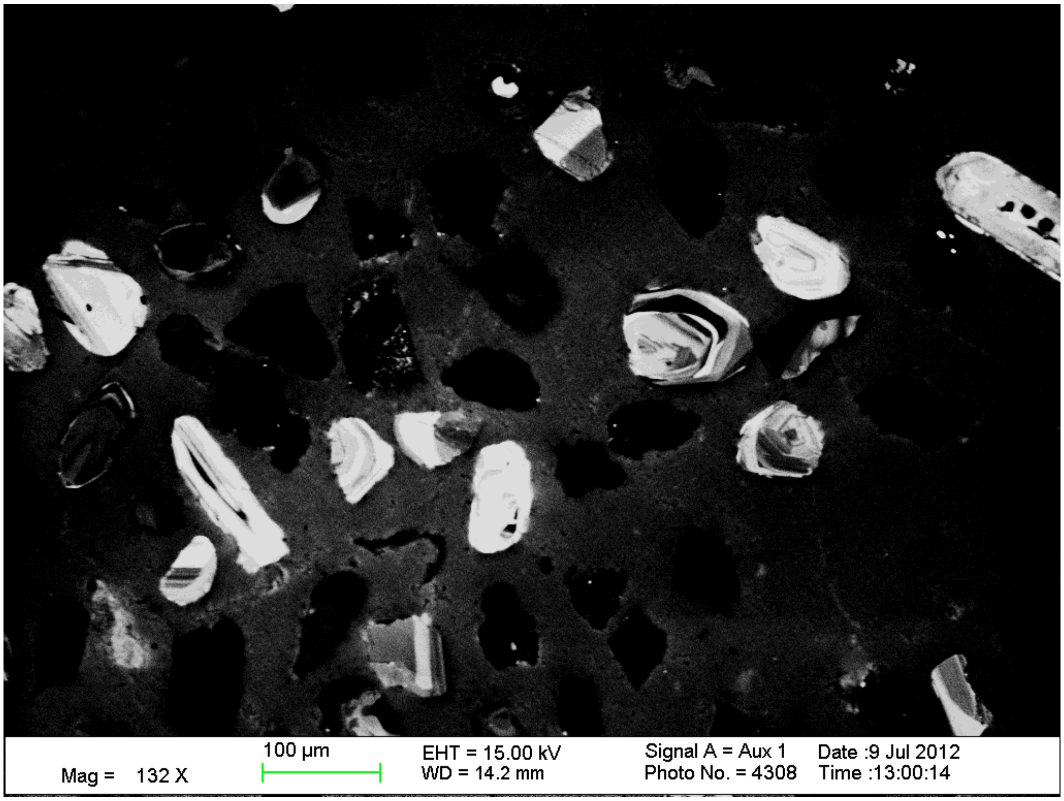
100 µm
Mag = 132 X
EHT = 15.00 kV
WD = 14.2 mm
Signal A = Aux 1
Photo No. = 4308
Date :9 Jul 2012
Time :13:00:14

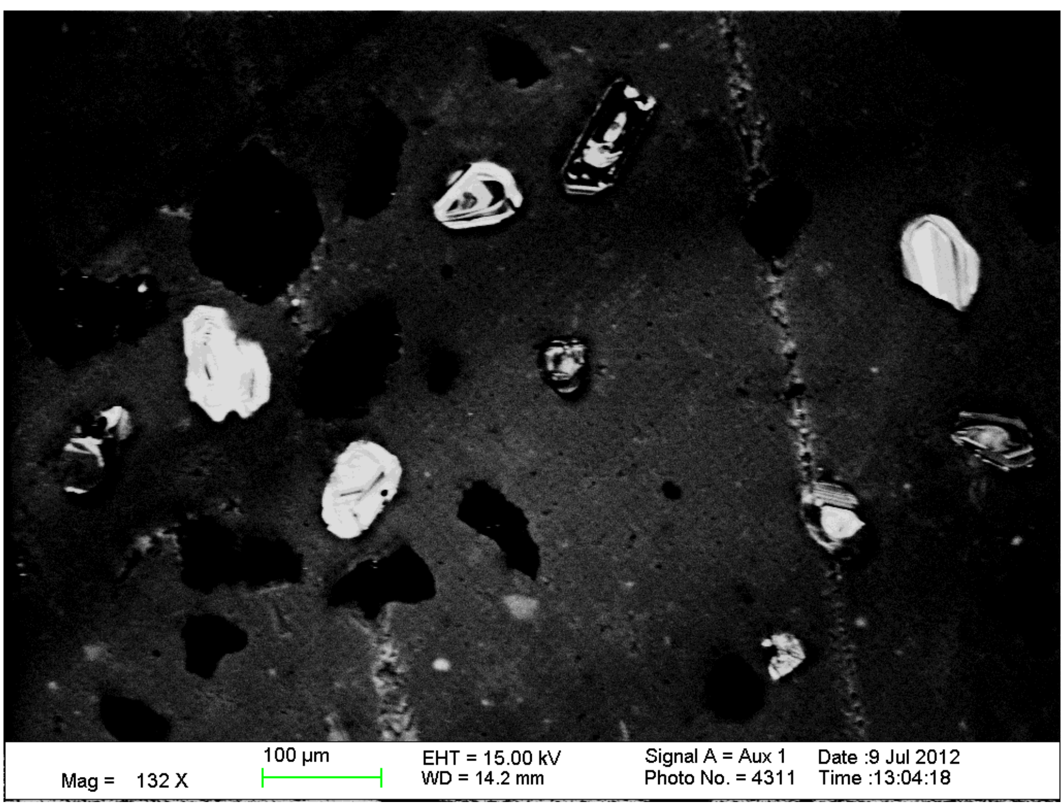
100 µm
Mag = 132 X
EHT = 15.00 kV
WD = 14.2 mm
Signal A = Aux 1
Photo No. = 4311
Date :9 Jul 2012
Time :13:04:18

Appendix B: Qualitative Evaluation of Minerals by Scanning Electron Microscope Images

Thin section billets and grain mounts were sent to the Colorado School of Mines (CSM) Advanced Mineralogy Research Center for quantitative mineral analysis. An automated scanning electron microscope (SEM) called the Qualitative Evaluation of Minerals by Scanning Electron Microscope or QEMSCAN® provides mineralogical and textural data. The SEM contains a unique electron-beam system with four Bruker energy-dispersive x-ray spectrometers (EDS) for rapid measurement of the EDS spectrum. Measurements of the EDS spectrum and the collection of the backscatter electron signal provides rapid mineral identification producing a false colored map.

Samples from the Greater Green River Basin, Wyoming, grain mounts were made containing minerals that were heavier than >2.8 g/cm^3 and non magnetic at .7 A on the Frantz Magnetic separator. The light minerals (<2.8 g/cm^3) separated from the Greater Green River samples were also mounted in epoxy and sent to the QEMSCAN® laboratory at CSM to measure the separation efficiency. After further honing of the mineral separation method, samples from the Book Cliffs, Utah heavy minerals, >3.3 g/cm^3, were mounted in epoxy to be analyzed. Thin sections from the Greater Green River Basin, WY and the Book Cliffs, UT were made and were analyzed by the QEMSCAN® in the same manner.

Examples of the images produced during QEMSCAN® analyses

Mineralogy scan of GR-09-05 grain mount containing minerals <2.84 g/cm^3

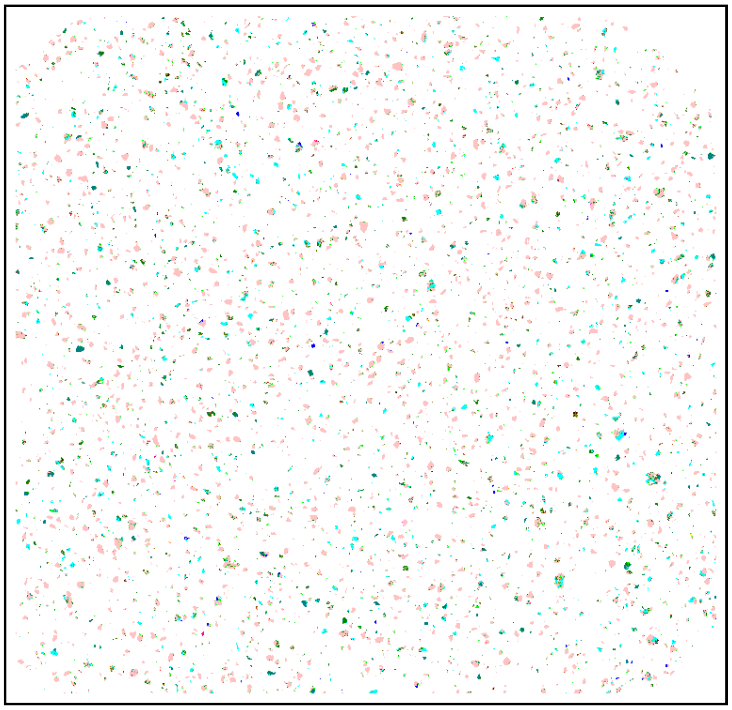

Backscatter electron scan of GR-09-05 grain mount containing minerals <2.84 g/cm^3

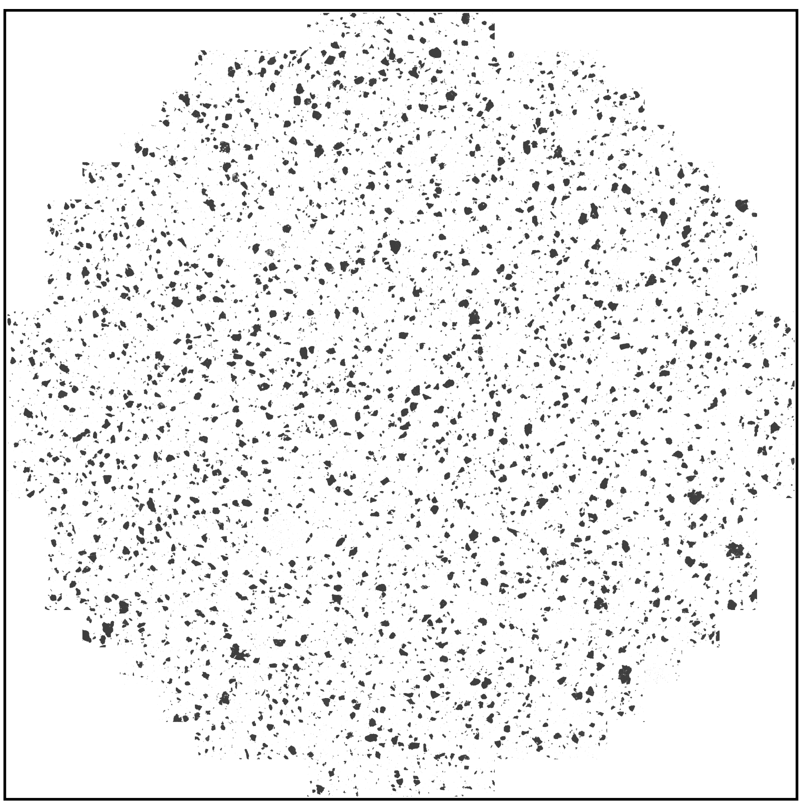

Mineralogy scan of GR-09-05 grain mount containing minerals >2.84 g/cm^3

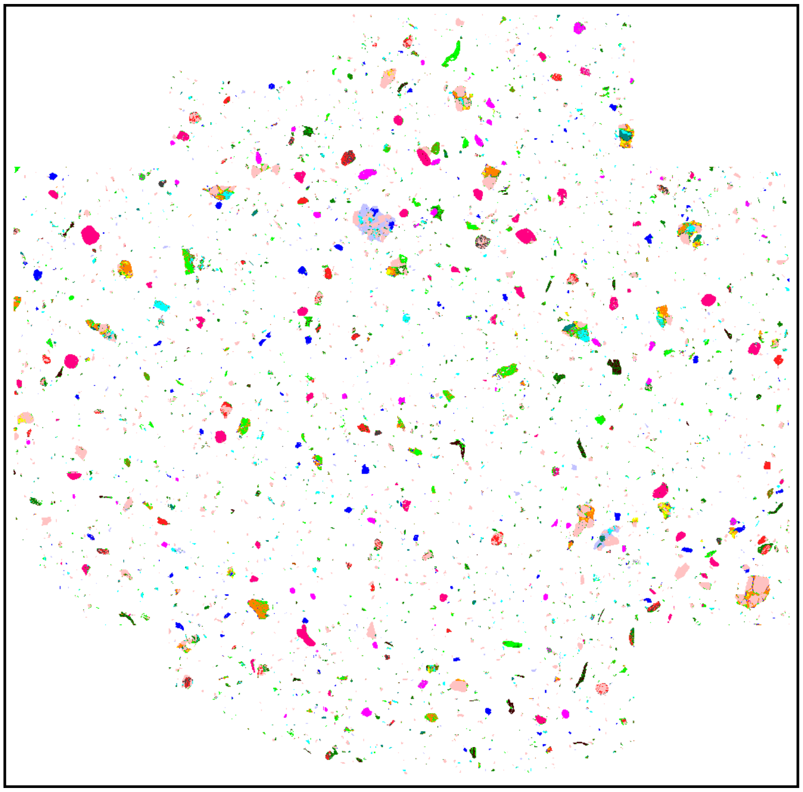

Backscatter electron scan of GR-09-05 grain mount containing minerals >2.84 g/cm^3

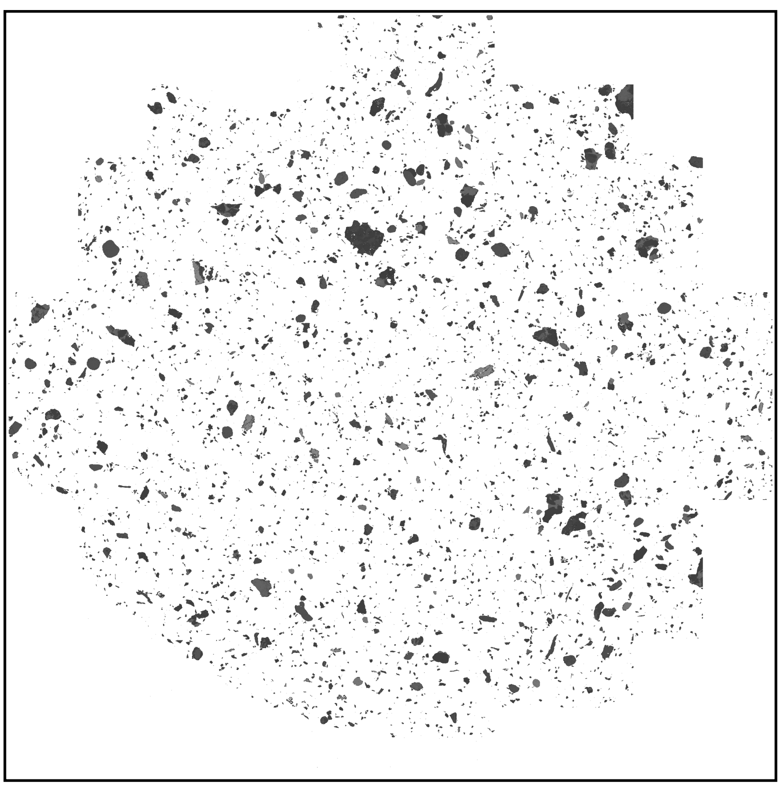

Mineralogy scan of GR-09-05 thin-section

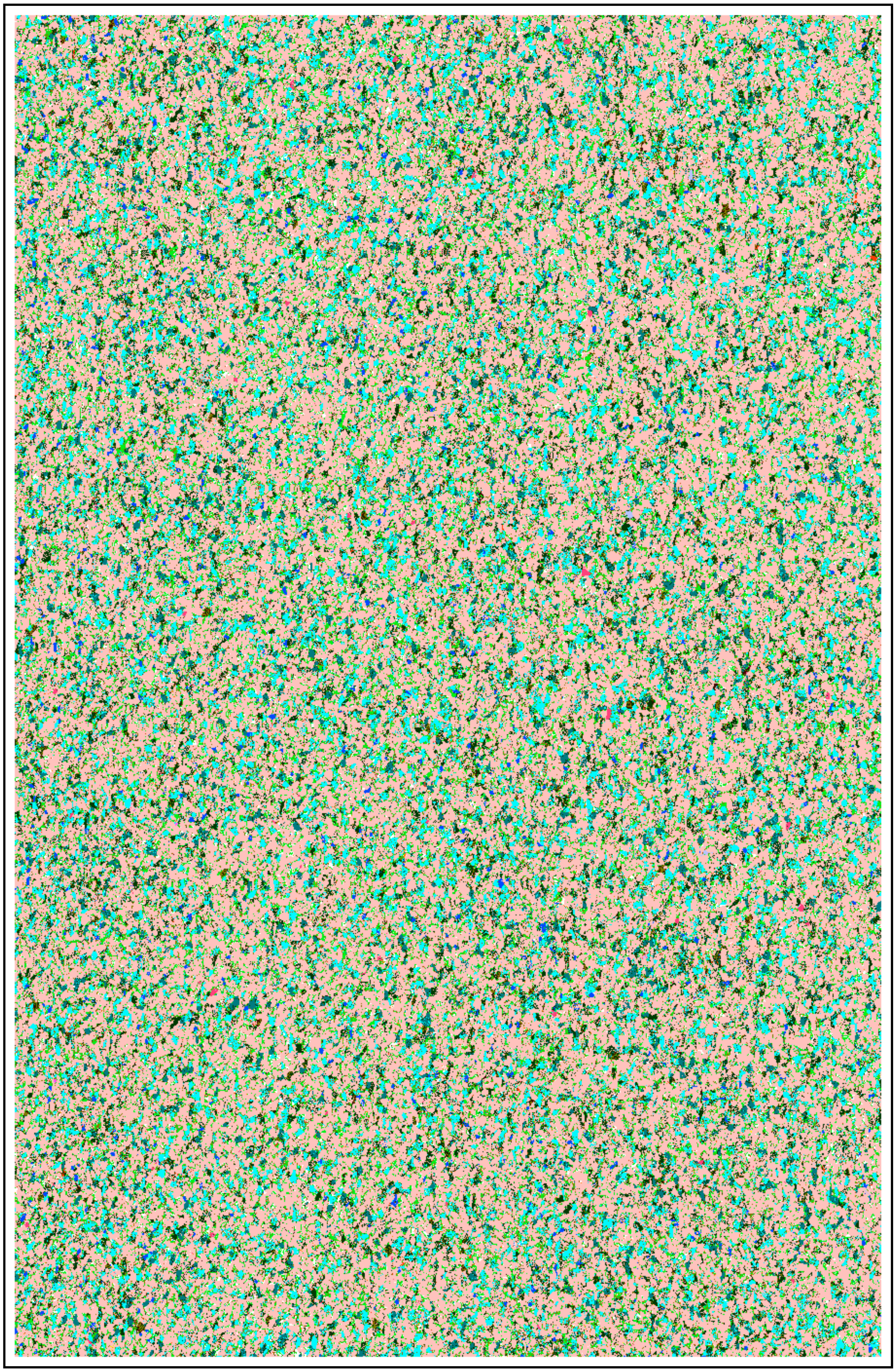

Legend for the QEMSCAN® false color mineral maps.

Graph showing the volume percent of minerals for the Bromoform heavy minerals (>2.84 g/cm^3) in sample GR-09-05.

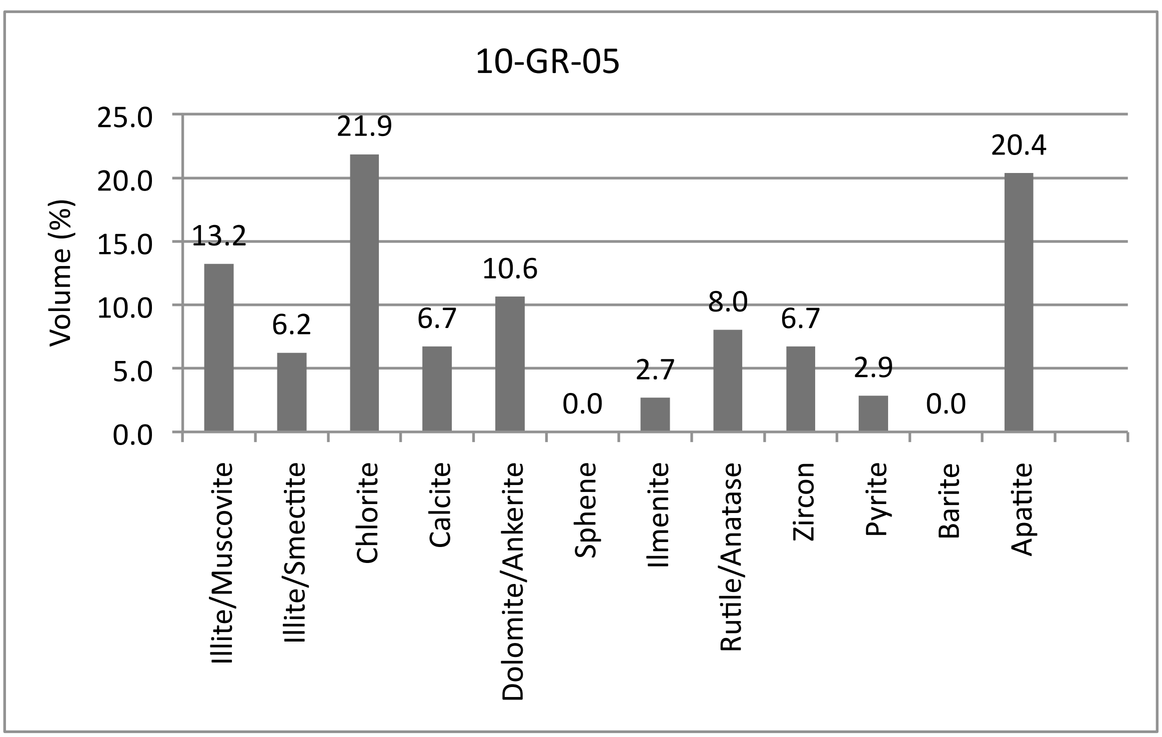

Table A-1: Zircon LA-ICP-MS U-Pb Isotopic Data and Ages Sample GR-09-19: Dad Member, Lewis Shale. Frantz Setting NA

Grain #.	U[a] [ppm]	Th[a] [cps]	Th/U	Corrected isotopic ratios							Ages (Ma)[f]						
				$^{207}Pb^{b}/^{235}U$	±2s[d]	$^{206}Pb^{b}/^{238}U$	±2s[d]	Rho[c]	$^{207}Pb^{e}/^{206}Pb$	±2s[d]	$^{207}Pb/^{235}U$	±2s	$^{206}Pb/^{238}U$	±2s	$^{207}Pb/^{206}Pb$	±2s	Disc. %[g]
1	348	214	0.61	0.101	0.006	0.017	0.001	0.99	0.044	0.001	103	5	107	6	39	17	-4
2	503	526	1.05	3.720	0.220	0.276	0.013	0.93	0.097	0.004	1591	77	1573	73	1619	85	1
3	100	47	0.47	2.240	0.170	0.192	0.013	0.96	0.086	0.006	1148	79	1120	77	1226	88	2
4	171	62	0.36	1.274	0.089	0.112	0.009	1.00	0.085	0.003	675	52	668	51	713	65	1
5	180	123	0.69	0.910	0.069	0.105	0.007	0.97	0.062	0.002	638	43	649	43	700	52	-2
6	227	91	0.40	0.118	0.006	0.012	0.000	0.99	0.072	0.003	72	3	74	3	3.4	2.1	-2
7	62	97	1.55	5.320	0.280	0.346	0.025	0.97	0.115	0.004	2060	150	1970	150	2170	150	4
8	99	70	0.70	4.050	0.330	0.280	0.023	0.95	0.104	0.006	1590	120	1570	130	1590	110	1
9	2420	583	0.24	2.140	0.170	0.201	0.011	0.88	0.079	0.006	1122	57	1173	61	1093	82	-5
10	77	54	0.70	0.083	0.006	0.012	0.001	0.99	0.052	0.004	75	6	77	6	64	57	-2
11	145	163	1.13	0.252	0.020	0.017	0.001	1.00	0.105	0.006	95	4	99	4	1.516	0.06	-4
12	794	28	0.03	3.780	0.130	0.267	0.010	0.96	0.103	0.002	1539	46	1512	55	1615	52	2
13	154	127	0.83	1.637	0.060	0.162	0.007	0.96	0.073	0.002	977	41	970	40	1004	47	1
14	442	110	0.25	4.650	0.200	0.314	0.013	0.95	0.108	0.003	1777	53	1762	69	1815	46	1
15	714	170	0.24	2.370	0.150	0.171	0.011	0.97	0.102	0.003	1016	69	988	62	1068	83	3
16	2920	297	0.10	1.095	0.061	0.091	0.005	0.99	0.089	0.002	548	30	539	29	567	31	2
17	2210	1003	0.45	1.323	0.082	0.079	0.005	1.00	0.120	0.003	457	30	451	29	491	31	1
18	257	113	0.44	4.440	0.220	0.297	0.014	0.94	0.110	0.003	1719	74	1670	78	1751	77	3
19	1068	396	0.37	0.097	0.005	0.013	0.001	0.98	0.053	0.001	85	5	85	5	154	47	-1
20	893	627	0.70	0.097	0.005	0.015	0.001	0.97	0.047	0.002	95	5	95	5	91	33	-1
21	335	144	0.43	0.102	0.007	0.015	0.001	0.98	0.050	0.002	92	6	93	6	92	34	-1
22	233	92	0.40	5.050	0.220	0.316	0.017	0.96	0.117	0.003	1738	74	1744	91	1766	65	0
23	310	144	0.46	3.200	0.180	0.259	0.013	0.94	0.089	0.003	1466	64	1486	71	1489	68	-1
24	353	176	0.50	3.220	0.180	0.243	0.015	0.93	0.096	0.005	1470	100	1399	88	1590	120	5
25	36	84	2.36	22.100	1.100	0.645	0.029	0.94	0.242	0.008	3287	90	3310	140	3304	66	-1
26	950	243	0.26	4.170	0.200	0.301	0.015	0.93	0.101	0.003	1690	58	1718	78	1678	59	-2
27	1051	628	0.60	1.780	0.150	0.097	0.008	1.00	0.132	0.006	555	48	545	47	597	48	2
28	180	58	0.32	8.130	0.700	0.344	0.026	0.98	0.170	0.004	1960	140	1850	140	2050	150	6
29	378	547	1.45	3.040	0.160	0.246	0.013	0.94	0.091	0.003	1415	90	1423	75	1530	110	-1
30	93	47	0.50	0.171	0.006	0.012	0.000	1.00	0.104	0.004	70	2	72	3	2.02	0.46	-3
31	171	81	0.48	12.260	0.600	0.487	0.024	0.97	0.180	0.004	2520	88	2520	120	2543	70	0
32	430	216	0.50	0.071	0.004	0.011	0.001	0.99	0.048	0.002	67	4	68	4	59	26	-2
33	67	76	1.13	4.980	0.520	0.297	0.019	0.97	0.121	0.011	1650	110	1650	110	1730	120	0
34	1643	84	0.05	0.824	0.037	0.047	0.002	1.00	0.124	0.004	272	14	269	14	296	14	1
35	207	77	0.37	2.960	0.100	0.238	0.009	0.97	0.088	0.001	1396	38	1377	47	1437	27	1
36	331	18	0.05	2.750	0.250	0.204	0.018	0.96	0.100	0.004	1220	110	1170	100	1320	130	4
37	448	266	0.59	0.543	0.018	0.068	0.002	0.96	0.059	0.001	423	13	419	13	500	26	1
38	351	212	0.60	2.440	0.180	0.173	0.013	0.97	0.106	0.003	1008	72	996	72	1037	72	1
39	29	12	0.40	1.788	0.066	0.176	0.007	0.97	0.073	0.001	1056	37	1046	39	1057	38	1
40	1	0	0.16	102.100	7.400	0.928	0.070	0.98	0.785	0.015	3350	200	2200	240	4240	100	34
41	516	572	1.11	0.601	0.022	0.061	0.003	0.95	0.072	0.002	351	19	373	15	160	53	-6
42	102	59	0.57	4.040	0.110	0.268	0.006	0.94	0.110	0.002	1569	35	1515	33	1653	45	3
43	184	135	0.74	3.100	0.130	0.231	0.011	0.94	0.095	0.004	1381	69	1342	68	1496	84	3
44	293	9	0.03	0.809	0.030	0.098	0.003	0.92	0.060	0.001	587	18	602	20	552	37	-3
45	74	39	0.52	4.200	0.200	0.287	0.014	0.95	0.104	0.003	1625	63	1613	77	1688	54	1
46	588	281	0.48	0.339	0.031	0.030	0.002	0.99	0.077	0.003	178	13	185	14	109	28	-4
47	49	48	0.97	14.170	0.680	0.527	0.024	0.93	0.198	0.006	2765	78	2710	120	2810	62	2
48	146	87	0.60	13.160	0.460	0.499	0.020	0.95	0.187	0.004	2708	50	2604	97	2752	34	4
49	483	525	1.09	1.575	0.099	0.119	0.007	0.99	0.096	0.003	701	45	694	41	767	61	1
50	75	52	0.69	3.009	0.092	0.255	0.007	0.94	0.086	0.001	1488	41	1477	42	1509	46	1

Table A-1: Zircon LA-ICP-MS U-Pb Isotopic Data and Ages Sample GR-09-19: Dad Member, Lewis Shale. Frantz Setting NA

				Corrected isotopic ratios							Ages (Ma)[f]						
Grain #.	U[a] [ppm]	Th[a] [cps]	Th/U	$^{207}Pb^{b}/^{235}U$	±2s[d]	$^{206}Pb^{b}/^{238}U$	±2s[d]	Rho[c]	$^{207}Pb^{e}/^{206}Pb$	±2s[d]	$^{207}Pb/^{235}U$	±2s	$^{206}Pb/^{238}U$	±2s	$^{207}Pb/^{206}Pb$	±2s	Disc. %[g]
51	964	38	0.04	4.290	0.150	0.306	0.014	0.90	0.103	0.003	1705	32	1722	70	1603	47	-1
52	273	272	1.00	0.099	0.004	0.012	0.001	0.97	0.058	0.003	74	4	74	4	86	58	0
53	416	713	1.72	9.970	0.300	0.476	0.012	0.96	0.150	0.003	2720	100	2625	83	2770	120	3
54	89	22	0.25	5.170	0.170	0.340	0.011	0.92	0.109	0.002	1882	34	1898	52	1843	28	-1
55	47	19	0.39	3.058	0.086	0.238	0.007	0.95	0.093	0.002	1413	30	1379	39	1471	28	2
56	250	123	0.49	0.070	0.004	0.011	0.001	0.99	0.047	0.002	68	4	68	4	41	21	-1
57	287	151	0.53	0.091	0.004	0.011	0.001	0.98	0.058	0.002	70	3	71	3	19	13	-1
58	2619	6630	2.53	1.521	0.056	0.131	0.005	0.99	0.084	0.002	780	31	778	31	788	33	0
59	628	149	0.24	3.420	0.180	0.227	0.013	0.97	0.109	0.003	1336	79	1286	73	1413	88	4
60	670	120	0.18	2.930	0.110	0.190	0.008	0.97	0.111	0.002	1102	50	1077	46	1113	50	2
61	418	114	0.27	4.490	0.160	0.320	0.014	0.94	0.105	0.002	1784	43	1795	71	1788	39	-1
62	558	416	0.75	5.070	0.210	0.308	0.015	0.96	0.117	0.004	1741	94	1720	90	1790	100	1
63	332	646	1.95	4.070	0.180	0.285	0.013	0.99	0.106	0.002	1596	69	1601	73	1632	70	0
64	550	292	0.53	0.100	0.004	0.015	0.000	0.96	0.048	0.001	95	3	96	3	81	23	-2
65	90	75	0.83	3.232	0.080	0.259	0.006	0.93	0.092	0.002	1535	39	1493	35	1600	53	3

[a]U, Th, and Pb concentrations and Th/U ratios are calculated relative to GJ-1 zircon standard

[b]U-Pb fractionation correction and corrected for background interference based on GJ-1 zircon standard and Pb/U ratios are corrected according to Anderson (2002)

[c]Rho is the error correlation defined as the quotient of the propagated errors of the $^{206}Pb/^{238}U$ and the $^{207}/^{235}U$ ratio

[d]Quadratic addition of inter-run errors (2 SD) and daily reproducibility of GJ-1 (2 SD)

[e]Corrected for mass-bias by normalising to GJ-1 zircon standard (~.6 per atomic mass unit)

[f]U-Pb ages are calculated relative to GJ-1 zircon standard and corrected based on Anderson model (2002)

[g]Discordance %: for $^{206}Pb/^{238}U$ ages <1Ga calculated as $((1-(^{206}Pb/^{238}U)/(^{207}Pb/^{235}U))*100)$, for $^{206}Pb/^{238}U$ ages >1Ga calculated as $((1-(^{206}Pb/^{238}U)/(^{207}Pb/^{206}Pb))*100)$

Table A-2: Zircon LA-ICP-MS U-Pb Isotopic Data and Ages Sample GR-09-19: Dad Member, Lewis Shale. Frantz Setting .7 A at 10°

				Corrected isotopic ratios							Ages (Ma)[f]						
Grain #.	U[a] [cps]	Th[a] [cps]	Th/U	$^{207}Pb^{b}/^{235}U$	±2s[d]	$^{206}Pb^{b}/^{238}U$	±2s[d]	Rho[c]	$^{207}Pb^{e}/^{206}Pb$	±2s[d]	$^{207}Pb/^{235}U$	±2s	$^{206}Pb/^{238}U$	±2s	$^{207}Pb/^{206}Pb$	±2s	Disc. %[g]
1	8972735	2185913	0.24	0.108	0.001	0.0190	0.0003	0.75	0.050	0.013	94	3	91	2	171	43	3
2	4762089	776977	0.16	4.480	0.002	0.3317	0.0056	0.83	0.103	0.010	1542	19	1447	26	1674	26	6
3	2303997	532326	0.23	1.833	0.067	0.2976	0.0054	0.88	0.110	0.007	1504	19	1310	25	1790	20	13
4	1366167	285748	0.21	5.666	0.002	0.4199	0.0055	0.84	0.109	0.007	1779	16	1775	25	1783	20	0
5	2106699	259257	0.12	5.091	0.003	0.3945	0.0067	0.87	0.105	0.008	1707	19	1708	30	1706	22	0
6	5905617	2455819	0.42	0.675	0.002	0.1083	0.0019	0.43	0.069	0.032	596	21	519	10	903	89	13
7	773578	155528	0.20	4.911	0.003	0.3988	0.0068	0.86	0.106	0.008	1692	18	1657	28	1736	22	2
8	2000453	1054865	0.53	3.225	0.004	0.3239	0.0055	0.68	0.092	0.015	1440	22	1417	24	1474	38	2
9	2351073	455784	0.19	5.123	0.006	0.3228	0.0129	0.93	0.115	0.013	1551	36	1321	49	1879	31	15
10	1246146	173744	0.14	5.383	0.004	0.3888	0.0074	0.81	0.116	0.011	1743	22	1626	30	1886	27	7
11	5314129	2119486	0.40	5.173	0.002	0.4055	0.0077	0.84	0.108	0.010	1702	21	1659	31	1755	24	3
12	1426880	139714	0.10	2.342	0.002	0.2484	0.0035	0.85	0.077	0.008	1109	14	1101	17	1125	22	1
13	1284952	152332	0.12	2.489	0.002	0.2357	0.0050	0.88	0.080	0.010	1106	18	1067	23	1182	26	3
14	1343078	137392	0.10	5.258	0.004	0.3803	0.0080	0.85	0.125	0.011	1802	23	1616	33	2023	25	10
15	2212150	372959	0.17	4.912	0.003	0.4003	0.0072	0.87	0.105	0.008	1703	19	1692	30	1716	20	1
16	571794	251292	0.44	4.919	0.005	0.3534	0.0060	0.53	0.099	0.023	1560	29	1531	26	1599	57	2
17	1737363	674382	0.39	3.387	0.002	0.3146	0.0082	0.84	0.088	0.013	1376	24	1368	33	1390	33	1
18	355036	104633	0.29	2.836	0.004	0.3008	0.0054	0.74	0.079	0.014	1269	20	1321	24	1181	36	-4
19	2941253	967369	0.33	2.702	0.004	0.2090	0.0063	0.91	0.111	0.010	1254	25	954	28	1814	24	24
20	1988250	635934	0.32	0.118	0.002	0.0207	0.0005	0.62	0.050	0.022	102	4	99	2	180	69	3
21	676388	188706	0.28	2.945	0.004	0.2903	0.0064	0.85	0.087	0.011	1315	20	1282	27	1368	29	2
22	3378394	604880	0.18	5.368	0.002	0.4300	0.0086	0.88	0.106	0.009	1761	21	1794	35	1723	22	-2
23	810304	320603	0.40	2.749	0.004	0.2484	0.0057	0.83	0.092	0.013	1240	21	1115	25	1464	33	10
24	11113503	3303473	0.30	1.675	0.003	0.1084	0.0023	0.79	0.151	0.014	1001	18	499	11	2362	31	50
25	3415334	651428	0.19	4.886	0.005	0.2784	0.0075	0.82	0.169	0.014	1820	29	1256	32	2544	32	31
26	2057141	2058803	1.00	3.149	0.003	0.2828	0.0051	0.86	0.089	0.008	1332	17	1290	22	1400	21	3
27	4226286	2694212	0.64	3.112	0.002	0.2502	0.0053	0.85	0.103	0.011	1339	20	1133	23	1686	26	15
28	5271467	649718	0.12	0.118	0.002	0.0161	0.0004	0.72	0.063	0.017	102	3	77	2	718	47	24
29	4553089	384152	0.08	5.320	0.002	0.4090	0.0082	0.88	0.110	0.009	1777	20	1752	32	1807	22	1
30	728877	213256	0.29	15.043	0.009	0.6300	0.0139	0.85	0.197	0.011	2699	26	2561	49	2804	23	5
31	989417	373441	0.38	2.716	0.003	0.2677	0.0048	0.79	0.080	0.011	1198	17	1198	21	1199	30	0
32	812110	180994	0.22	4.437	0.004	0.3642	0.0095	0.87	0.106	0.012	1629	26	1551	37	1731	30	5
34	1270871	283244	0.22	6.484	0.004	0.4391	0.0083	0.80	0.129	0.011	1980	22	1878	33	2089	27	5
35	813504	225117	0.28	4.562	0.003	0.3791	0.0053	0.76	0.101	0.010	1630	17	1621	23	1642	24	1
36	5244400	434375	0.08	0.625	0.001	0.0939	0.0015	0.77	0.058	0.011	457	8	445	7	520	31	3
37	1085903	371187	0.34	9.798	0.010	0.4521	0.0190	0.88	0.193	0.018	2395	45	1976	72	2773	38	17
38	796261	337341	0.42	14.823	0.007	0.6486	0.0110	0.82	0.184	0.009	2664	21	2625	39	2694	20	1
39	557206	128120	0.23	2.728	0.003	0.2469	0.0044	0.70	0.080	0.015	1166	19	1149	20	1199	38	1
40	1801535	514047	0.29	4.814	0.003	0.4232	0.0102	0.81	0.106	0.014	1757	26	1771	39	1740	33	-1
41	364938	78515	0.22	2.134	0.006	0.2585	0.0065	0.79	0.078	0.015	1169	23	1174	28	1159	40	0
42	8782311	3163562	0.36	0.115	0.001	0.0192	0.0004	0.75	0.049	0.016	97	3	94	2	173	50	3
43	500269	154419	0.31	15.395	0.010	0.6689	0.0154	0.86	0.193	0.012	2706	27	2626	52	2767	25	3
44	622526	606935	0.97	0.179	0.003	0.0158	0.0004	0.35	0.063	0.052	99	7	76	2	704	152	24
45	12699300	3552795	0.28	5.670	0.019	0.4223	0.0146	0.81	0.113	0.205	1838	18	1831	27	1845	24	0
46	1973592	699358	0.35	1.954	0.003	0.1609	0.0068	0.98	0.103	0.010	1046	28	766	30	1690	21	27
47	3259393	258820	0.08	0.143	0.006	0.0215	0.0066	0.48	0.049	0.008	111	5	109	2	149	94	2
48	1411553	271952	0.19	6.180	0.002	0.4275	0.0004	0.80	0.108	0.030	1798	21	1828	32	1764	28	-2
49	241724	65358	0.27	3.845	0.005	0.3631	0.0081	0.79	0.092	0.012	1553	23	1608	31	1480	35	-4
50	442047	116806	0.26	1.057	0.004	0.1429	0.0076	0.83	0.063	0.014	686	12	682	13	698	30	1
51	4501595	2033246	0.45	0.772	0.001	0.1047	0.0027	0.61	0.061	0.011	532	13	504	9	651	52	5

Table A-2: Zircon LA-ICP-MS U-Pb Isotopic Data and Ages Sample GR-09-19: Dad Member, Lewis Shale. Frantz Setting .7 A at 10°

Grain #.	U[a] [cps]	Th[a] [cps]	Th/U	Corrected isotopic ratios $^{207}Pb^{b}/^{235}U$	±2s[d]	$^{206}Pb^{b}/^{238}U$	±2s[d]	Rho[c]	$^{207}Pb^{e}/^{206}Pb$	±2s[d]	Ages (Ma)[f] $^{207}Pb/^{235}U$	±2s	$^{206}Pb/^{238}U$	±2s	$^{207}Pb/^{206}Pb$	±2s	Disc. %[g]
52	816136	400297	0.49	2.798	0.002	0.2806	0.0019	0.79	0.080	0.018	1229	17	1242	22	1207	28	-1
53	729678	506963	0.69	4.285	0.003	0.3545	0.0051	0.83	0.101	0.011	1609	20	1580	28	1646	24	2
54	867054	827963	0.95	4.493	0.003	0.3660	0.0067	0.87	0.104	0.010	1651	19	1617	29	1695	22	2
55	2744338	1517368	0.55	0.089	0.003	0.0147	0.0070	0.30	0.058	0.009	87	10	71	3	542	271	18
56	1518404	749441	0.49	5.401	0.010	0.4217	0.0005	0.81	0.110	0.088	1801	18	1805	27	1797	24	0
57	1594994	537159	0.34	3.723	0.003	0.3244	0.0067	0.83	0.104	0.010	1552	19	1442	26	1706	26	7
58	4072471	1166302	0.29	4.571	0.002	0.3767	0.0062	0.83	0.104	0.011	1674	19	1650	28	1704	24	1
59	2221634	475295	0.21	3.050	0.003	0.3020	0.0068	0.77	0.085	0.010	1340	17	1356	21	1316	27	-1
60	2538707	781428	0.31	4.814	0.002	0.3708	0.0048	0.88	0.105	0.011	1668	22	1623	33	1725	22	3
61	1874324	355870	0.19	11.675	0.003	0.5888	0.0082	0.84	0.169	0.009	2517	24	2468	43	2556	22	2
62	939588	262352	0.28	4.865	0.005	0.4260	0.0118	0.80	0.104	0.010	1768	17	1820	25	1708	22	-3
63	1073714	182035	0.17	0.115	0.003	0.0151	0.0064	0.36	0.052	0.009	87	6	80	2	299	148	9
64	716523	291224	0.41	0.129	0.003	0.0214	0.0003	0.61	0.049	0.048	109	3	107	2	149	57	2
65	2757602	1293966	0.47	4.642	0.002	0.3560	0.0004	0.83	0.104	0.019	1628	20	1573	28	1700	26	3
67	3158512	216362	0.07	0.117	0.002	0.0191	0.0068	0.72	0.049	0.011	99	2	96	2	158	40	2
68	7035009	1852800	0.26	4.924	0.001	0.4070	0.0003	0.87	0.113	0.013	1813	20	1780	31	1851	22	2
69	3489100	152771	0.04	0.123	0.002	0.0190	0.0077	0.56	0.050	0.009	98	2	95	1	194	50	4
70	7686897	2586026	0.34	5.625	0.001	0.4202	0.0002	0.77	0.112	0.016	1843	19	1849	27	1835	26	0
71	989497	264709	0.27	6.026	0.004	0.2554	0.0067	0.82	0.177	0.011	1781	29	1151	30	2628	32	35
72	5946237	1891881	0.32	0.110	0.004	0.0181	0.0069	0.68	0.049	0.015	92	3	91	2	137	48	2
73	5056239	1214255	0.24	3.483	0.001	0.2433	0.0003	0.89	0.113	0.016	1419	30	1144	36	1861	33	19
74	1634981	652269	0.40	0.130	0.005	0.0149	0.0080	0.44	0.059	0.014	92	4	74	2	565	101	19
75	1439320	782381	0.54	3.583	0.002	0.3289	0.0003	0.80	0.092	0.035	1462	16	1458	21	1469	23	0
76	378602	79211	0.21	1.931	0.004	0.1974	0.0049	0.88	0.087	0.009	1065	17	928	20	1358	25	13
77	1586311	389448	0.25	2.814	0.003	0.2763	0.0043	0.76	0.081	0.010	1254	15	1263	18	1237	26	-1
78	1610053	658351	0.41	4.311	0.002	0.3526	0.0041	0.85	0.105	0.010	1647	28	1591	41	1719	34	3
79	1482467	530430	0.36	17.266	0.005	0.6951	0.0099	0.86	0.216	0.014	2875	21	2762	43	2956	20	4
80	1389904	749317	0.54	5.283	0.005	0.3947	0.0125	0.81	0.107	0.009	1744	18	1736	26	1754	22	0
81	884312	226704	0.26	9.677	0.003	0.4622	0.0063	0.85	0.175	0.009	2309	18	1986	29	2608	18	14
82	1777397	24530	0.01	2.159	0.005	0.2138	0.0074	0.76	0.076	0.009	1036	16	1011	18	1090	34	2
83	685716	309950	0.45	0.865	0.003	0.0891	0.0038	0.68	0.075	0.013	555	12	437	8	1075	41	21
84	3851348	2095857	0.54	15.193	0.001	0.6493	0.0016	0.81	0.188	0.016	2702	25	2659	46	2735	27	2
85	371734	150453	0.40	4.863	0.011	0.3785	0.0130	0.82	0.106	0.013	1714	18	1697	27	1734	22	1
86	2243438	568483	0.25	0.887	0.002	0.1141	0.0064	0.83	0.065	0.009	591	10	545	10	773	28	8
87	1975632	463139	0.23	3.448	0.002	0.3198	0.0021	0.83	0.091	0.010	1446	19	1440	26	1454	25	0
88	1299282	301150	0.23	4.971	0.003	0.3672	0.0061	0.79	0.104	0.010	1658	20	1616	27	1713	26	3
89	635022	312694	0.49	4.455	0.003	0.3727	0.0066	0.77	0.102	0.011	1664	22	1667	30	1661	30	0
90	359175	143958	0.40	13.571	0.005	0.6314	0.0071	0.88	0.183	0.013	2659	24	2625	48	2685	20	1
91	1046380	289937	0.28	4.919	0.005	0.3989	0.0133	0.81	0.108	0.009	1771	18	1773	26	1768	24	0
92	768665	277180	0.36	4.405	0.004	0.3691	0.0060	0.81	0.101	0.010	1635	17	1620	24	1655	22	1
93	992110	592536	0.60	3.524	0.003	0.2977	0.0055	0.81	0.090	0.009	1382	20	1355	26	1425	29	2
94	878558	253655	0.29	0.155	0.003	0.0153	0.0060	0.45	0.075	0.012	122	6	78	2	1088	95	36
95	2230247	731373	0.33	2.377	0.003	0.2313	0.0003	0.86	0.084	0.036	1162	20	1085	24	1311	29	7
96	1558653	271154	0.17	3.409	0.003	0.3145	0.0053	0.77	0.094	0.012	1490	17	1471	22	1518	27	1
97	4566428	2647542	0.58	12.914	0.001	0.5228	0.0047	0.48	0.202	0.011	2589	21	2265	36	2853	18	12
98	983910	163019	0.17	3.213	0.007	0.3023	0.0094	0.86	0.088	0.009	1390	17	1393	21	1386	27	0
99	1809849	512067	0.28	1.863	0.002	0.2203	0.0045	0.77	0.073	0.011	1047	17	1052	19	1035	31	-1
100	548385	108159	0.20	0.838	0.003	0.1093	0.0040	0.80	0.059	0.012	535	12	528	12	564	40	1
101	543535	215739	0.40	13.642	0.002	0.6424	0.0024	0.79	0.177	0.014	2648	18	2661	35	2638	18	0
102	737392	149376	0.20	4.817	0.009	0.3818	0.0090	0.84	0.104	0.009	1710	19	1709	27	1713	28	0

Table A-2: Zircon LA-ICP-MS U-Pb Isotopic Data and Ages Sample GR-09-19: Dad Member, Lewis Shale. Frantz Setting .7 A at 10°

				Corrected isotopic ratios							Ages (Ma)[f]						
Grain #.	U[a] [cps]	Th[a] [cps]	Th/U	$^{207}Pb^{b}/^{235}U$	±2s[d]	$^{206}Pb^{b}/^{238}U$	±2s[d]	Rho[c]	$^{207}Pb^{e}/^{206}Pb$	±2s[d]	$^{207}Pb/^{235}U$	±2s	$^{206}Pb/^{238}U$	±2s	$^{207}Pb/^{206}Pb$	±2s	Disc. %[g]
103	553414	89137	0.16	5.425	0.005	0.3985	0.0061	0.78	0.106	0.012	1745	19	1741	29	1750	24	0
104	652375	140046	0.21	3.655	0.004	0.3057	0.0068	0.83	0.101	0.010	1487	19	1375	26	1649	22	7
105	2281807	491589	0.22	4.215	0.003	0.3604	0.0058	0.88	0.100	0.010	1626	24	1622	36	1632	28	0
106	359211	259625	0.72	0.082	0.005	0.0149	0.0086	0.86	0.047	0.012	75	3	76	2	63	63	-1
107	2653864	702608	0.26	14.713	0.002	0.6806	0.0003	0.59	0.187	0.024	2747	20	2777	39	2725	22	-1
108	625101	11534	0.02	4.902	0.007	0.3801	0.0102	0.81	0.105	0.010	1702	18	1679	27	1731	24	1
109	761162	146316	0.19	0.116	0.004	0.0178	0.0061	0.82	0.050	0.010	95	4	90	2	212	74	5
110	1785026	577307	0.32	0.112	0.002	0.0189	0.0004	0.59	0.048	0.025	96	3	96	2	113	70	1
111	1782211	342469	0.19	0.151	0.002	0.0148	0.0003	0.54	0.071	0.023	115	8	78	3	967	117	32
112	498014	354156	0.71	4.340	0.006	0.3815	0.0006	0.59	0.101	0.044	1685	17	1708	27	1655	21	-1
113	1644036	286417	0.17	4.475	0.003	0.3202	0.0061	0.86	0.118	0.009	1673	25	1475	34	1932	27	12
114	1185963	118787	0.10	3.168	0.004	0.3105	0.0077	0.87	0.089	0.012	1419	16	1424	22	1412	23	0
115	950937	248381	0.26	0.121	0.004	0.0149	0.0047	0.81	0.056	0.010	90	5	76	2	483	117	16
116	957345	327621	0.34	5.197	0.003	0.3131	0.0003	0.44	0.135	0.041	1758	19	1429	22	2175	28	19
117	2976702	965345	0.32	0.120	0.003	0.0149	0.0047	0.74	0.052	0.013	81	5	74	2	294	146	9
118	505362	209950	0.42	12.634	0.003	0.5909	0.0005	0.48	0.176	0.049	2579	29	2524	57	2622	27	2
119	641037	186533	0.29	0.119	0.008	0.0181	0.0148	0.87	0.070	0.012	137	8	95	5	941	48	31
120	1656075	486356	0.29	3.806	0.006	0.3113	0.0010	0.92	0.099	0.018	1532	19	1471	26	1616	26	4
121	825309	733369	0.89	7.572	0.004	0.4736	0.0056	0.83	0.149	0.010	2225	25	2099	40	2343	26	6
122	2192987	396427	0.18	4.472	0.004	0.3893	0.0095	0.81	0.105	0.011	1749	19	1763	29	1733	22	-1
123	738252	289514	0.39	6.546	0.004	0.3427	0.0062	0.86	0.161	0.009	1999	23	1565	31	2482	24	22
124	1397185	813010	0.58	4.977	0.004	0.3569	0.0069	0.85	0.103	0.010	1663	21	1648	31	1682	24	1
125	1437387	820817	0.57	3.480	0.003	0.3150	0.0064	0.84	0.094	0.010	1495	17	1478	24	1520	19	1
126	1481902	332054	0.22	0.090	0.003	0.0160	0.0047	0.86	0.048	0.007	84	3	82	2	132	70	2
127	1864062	669968	0.36	3.503	0.002	0.3181	0.0004	0.63	0.098	0.023	1520	18	1462	26	1601	23	4
128	3129995	435699	0.14	4.305	0.002	0.3012	0.0054	0.87	0.134	0.009	1717	26	1374	32	2164	30	20
129	4725397	280541	0.06	4.525	0.003	0.3839	0.0072	0.84	0.104	0.014	1700	18	1696	25	1705	24	0
130	3735701	863109	0.23	0.101	0.002	0.0183	0.0054	0.81	0.049	0.010	95	2	93	2	147	38	2
131	9615147	1748004	0.18	0.115	0.001	0.0140	0.0003	0.77	0.063	0.013	98	5	74	2	728	89	24
132	1427291	879530	0.62	5.191	0.003	0.3775	0.0003	0.55	0.110	0.033	1758	25	1708	38	1818	27	3
133	1149320	475648	0.41	5.387	0.004	0.3925	0.0083	0.86	0.110	0.011	1817	19	1821	30	1814	22	0
134	1067847	133320	0.12	2.257	0.004	0.2400	0.0063	0.86	0.078	0.009	1142	19	1129	21	1166	36	1
135	422619	149676	0.35	2.024	0.004	0.2134	0.0041	0.56	0.074	0.015	1031	14	1025	16	1044	29	1
136	2089210	298142	0.14	4.292	0.002	0.3276	0.0028	0.74	0.107	0.010	1628	19	1520	27	1771	22	7
137	2887838	1080365	0.37	4.238	0.003	0.3654	0.0056	0.77	0.101	0.009	1633	19	1620	27	1649	24	1
138	961761	618677	0.64	0.264	0.004	0.0166	0.0058	0.87	0.106	0.010	182	11	85	2	1746	116	53
139	2548198	1656024	0.65	2.265	0.006	0.2414	0.0003	0.83	0.080	0.049	1185	17	1165	20	1222	28	2
140	3762748	650990	0.17	0.074	0.002	0.0133	0.0039	0.31	0.055	0.011	80	4	69	2	429	94	14

[a]U, Th, and Pb concentrations and Th/U ratios are calculated relative to GJ-1 zircon standard

[b]U-Pb fractionation correction and corrected for background interference based on GJ-1 zircon standard and Pb/U ratios are corrected according to Anderson (2002)

[c]Rho is the error correlation defined as the quotient of the propagated errors of the $^{206}Pb/^{238}U$ and the $^{207}/^{235}U$ ratio

[d]Quadratic addition of inter-run errors (2 SD) and daily reproducibility of GJ-1 (2 SD)

[e]Corrected for mass-bias by normalising to GJ-1 zircon standard (~.6 per atomic mass unit)

[f]U-Pb ages are calculated relative to GJ-1 zircon standard and corrected based on Anderson model (2002)

[g]Discordance %: for $^{206}Pb/^{238}U$ ages <1Ga calculated as $((1-(^{206}Pb/^{238}U)/(^{207}Pb/^{235}U))*100)$, for $^{206}Pb/^{238}U$ ages >1Ga calculated as $((1-(^{206}Pb/^{238}U)/(^{207}Pb/^{206}Pb))*100)$

Table A-3: Zircon LA-ICP-MS U-Pb Isotopic Data and Ages Sample GR-09-19: Dad Member, Lewis Shale. Frantz Setting 1.8 A at 5°

				Corrected isotopic ratios							Ages (Ma)[f]						
Grain #.	U[a] [cps]	Th[a] [cps]	Th/U	$^{207}Pb^{b}/^{235}U$	±2s[d]	$^{206}Pb^{b}/^{238}U$	±2s[d]	Rho[c]	$^{207}Pb^{e}/^{206}Pb$	±2s[d]	$^{207}Pb/^{235}U$	±2s	$^{206}Pb/^{238}U$	±2s	$^{207}Pb/^{206}Pb$	±2s	Disc. %[g]
1	8147988	1196672	0.15	3.898	0.002	0.237	0.006	0.87	0.115	0.017	1730	27	1617	40	1869	27	7
2	23636062	1731709	0.07	0.098	0.001	0.013	0.000	0.85	0.048	0.016	101	3	101	2	102	33	0
3	6168688	1712301	0.28	0.076	0.001	0.010	0.000	0.77	0.047	0.027	76	3	77	2	48	48	-1
4	6694718	653982	0.10	3.370	0.002	0.236	0.005	0.87	0.096	0.017	1604	25	1658	38	1534	29	-3
5	7569253	641144	0.08	4.453	0.002	0.277	0.006	0.90	0.105	0.016	1811	26	1907	45	1703	24	-5
6	11737917	2142827	0.18	0.274	0.003	0.029	0.000	0.42	0.083	0.059	340	15	223	5	1244	97	34
7	2530888	473215	0.19	12.235	0.004	0.410	0.009	0.90	0.185	0.015	2677	28	2668	57	2684	20	0
8	16529752	2704010	0.16	1.996	0.002	0.148	0.004	0.94	0.092	0.015	1320	25	1244	35	1444	23	6
9	3380595	998698	0.30	2.598	0.002	0.189	0.005	0.78	0.088	0.027	1350	27	1333	34	1377	43	1
10	8271677	1264013	0.15	0.101	0.001	0.012	0.000	0.71	0.051	0.030	101	3	96	2	231	56	5
11	4113058	567018	0.14	3.825	0.002	0.235	0.005	0.89	0.103	0.016	1663	22	1657	35	1672	24	0
12	6246359	642960	0.10	4.637	0.002	0.275	0.006	0.90	0.109	0.015	1856	25	1941	44	1762	22	-5
13	17518945	324981	0.02	0.452	0.001	0.051	0.001	0.87	0.056	0.015	414	8	409	8	443	27	1
14	5062661	1352868	0.27	3.981	0.002	0.226	0.005	0.93	0.108	0.014	1662	23	1593	37	1751	20	4
15	10698413	3498361	0.33	0.114	0.002	0.012	0.000	0.74	0.058	0.030	117	4	99	3	507	54	16
16	1427657	477716	0.33	9.544	0.004	0.372	0.008	0.89	0.163	0.015	2456	26	2433	51	2475	20	1
17	2093881	697073	0.33	3.899	0.002	0.242	0.005	0.89	0.101	0.015	1659	23	1677	37	1637	23	-1
18	6388492	1953269	0.31	1.794	0.002	0.154	0.003	0.88	0.078	0.015	1131	17	1134	23	1126	24	0
19	17037386	1159052	0.07	0.518	0.002	0.055	0.001	0.90	0.061	0.017	466	11	435	11	626	31	7
20	21226665	1227870	0.06	1.043	0.004	0.052	0.001	0.68	0.116	0.037	731	21	415	11	1877	55	43
21	3344190	2297227	0.69	0.110	0.002	0.010	0.000	0.58	0.061	0.043	99	4	78	2	634	77	21
22	20294090	3458049	0.17	0.092	0.001	0.011	0.000	0.75	0.049	0.022	92	3	90	2	129	43	2
23	6729948	661514	0.10	0.082	0.023	0.010	0.000	0.21	0.079	0.229	127	23	79	3	1147	417	38
24	4236889	670415	0.16	3.316	0.002	0.212	0.004	0.88	0.104	0.015	1576	21	1500	31	1680	22	5
25	3443210	528267	0.15	2.631	0.002	0.194	0.004	0.88	0.090	0.016	1389	20	1376	29	1409	25	1
26	8203724	1302784	0.16	1.904	0.001	0.161	0.002	0.79	0.079	0.019	1158	17	1157	20	1159	30	0
27	5746361	834975	0.15	5.037	0.003	0.281	0.008	0.91	0.117	0.019	1919	30	1940	52	1897	27	-1
28	4761976	872300	0.18	0.053	0.007	0.010	0.000	0.49	0.061	0.072	103	7	82	3	610	131	20
29	4677925	575459	0.12	4.119	0.002	0.250	0.007	0.90	0.108	0.016	1787	26	1822	45	1746	24	-2
30	13346664	1495980	0.11	2.862	0.003	0.177	0.006	0.94	0.107	0.016	1504	29	1345	41	1735	24	11
31	4993696	1704287	0.34	1.665	0.002	0.142	0.003	0.82	0.076	0.020	1055	19	1046	22	1075	33	1
32	16899022	3320326	0.20	0.086	0.001	0.011	0.000	0.85	0.051	0.021	92	3	88	3	202	40	5
33	19489293	5180077	0.27	4.012	0.002	0.262	0.005	0.85	0.097	0.019	1700	23	1827	37	1548	29	-7
34	11447457	976362	0.09	0.011	0.024	0.005	0.000	0.88	0.055	0.054	50	4	43	3	381	100	13
35	2766006	594921	0.22	4.006	0.003	0.231	0.007	0.85	0.104	0.026	1714	34	1746	52	1675	39	-2
36	3608514	1021183	0.28	0.487	0.002	0.052	0.001	0.84	0.059	0.020	433	11	409	10	563	35	6
37	1552687	286476	0.18	4.153	0.003	0.234	0.005	0.88	0.110	0.015	1733	22	1693	34	1781	22	2
38	9265942	2029698	0.22	0.469	0.001	0.050	0.001	0.83	0.056	0.016	402	8	396	8	435	29	1
39	19472449	539741	0.03	1.547	0.005	0.077	0.003	0.93	0.129	0.019	1039	29	618	24	2078	27	41
40	12139403	1655279	0.14	3.502	0.002	0.261	0.005	0.79	0.096	0.021	1686	23	1803	35	1543	32	-7
41	4835838	2558400	0.53	3.516	0.004	0.205	0.010	0.89	0.110	0.033	1589	46	1442	65	1791	48	9
42	1467691	403376	0.27	1.811	0.002	0.149	0.003	0.84	0.076	0.016	1125	17	1141	22	1093	26	-1
43	1704020	202419	0.12	0.822	0.002	0.089	0.003	0.81	0.060	0.032	667	21	691	22	588	55	-4
44	4553331	815830	0.18	4.169	0.002	0.255	0.006	0.86	0.105	0.019	1762	24	1815	38	1700	28	-3
45	3006535	916149	0.30	1.233	0.005	0.151	0.005	0.83	0.087	0.030	1257	31	1203	39	1349	47	4
46	1797857	389620	0.22	2.800	0.004	0.195	0.004	0.86	0.101	0.019	1484	22	1389	30	1621	28	6
47	5046640	443821	0.09	3.331	0.002	0.197	0.004	0.88	0.102	0.015	1543	19	1467	28	1648	22	5
48	1360479	278152	0.20	3.886	0.002	0.243	0.005	0.81	0.102	0.019	1706	22	1751	32	1652	28	-3
49	7955018	851674	0.11	4.517	0.003	0.264	0.008	0.82	0.106	0.028	1807	33	1889	51	1714	41	-5
50	4098315	756677	0.18	0.085	0.002	0.009	0.000	0.81	0.053	0.032	81	3	74	3	308	58	9

Table A-3: Zircon LA-ICP-MS U-Pb Isotopic Data and Ages Sample GR-09-19: Dad Member, Lewis Shale. Frantz Setting 1.8 A at 5°

				Corrected isotopic ratios							Ages (Ma)[f]						
Grain #	U[a] [cps]	Th[a] [cps]	Th/U	$^{207}Pb^{b}/^{235}U$	±2s[d]	$^{206}Pb^{b}/^{238}U$	±2s[d]	Rho[c]	$^{207}Pb^{e}/^{206}Pb$	±2s[d]	$^{207}Pb/^{235}U$	±2s	$^{206}Pb/^{238}U$	±2s	$^{207}Pb/^{206}Pb$	±2s	Disc. %[g]
51	1795764	468636	0.26	0.553	0.003	0.025	0.001	0.29	0.078	0.145	313	33	214	7	1130	246	31
52	10288200	2323496	0.23	0.355	0.001	0.029	0.001	0.49	0.062	0.050	280	11	237	5	657	86	15
53	3921205	546617	0.14	3.112	0.002	0.205	0.006	0.86	0.096	0.023	1495	28	1471	40	1530	34	2
54	61290227	913731	0.01	0.157	0.002	0.012	0.000	0.55	0.105	0.041	202	7	98	2	1704	60	52
55	7731403	915541	0.12	2.576	0.003	0.207	0.006	0.79	0.091	0.031	1489	31	1529	42	1433	47	-3
56	2537725	926701	0.37	0.072	0.039	0.009	0.000	0.28	0.120	0.148	179	20	75	3	1948	223	58
57	7450532	1571346	0.21	0.189	0.001	0.021	0.001	0.84	0.053	0.029	185	7	174	6	332	53	6
58	7368143	1562524	0.21	0.916	0.002	0.058	0.001	0.55	0.075	0.050	563	21	447	11	1064	81	21
59	7793065	982440	0.13	4.188	0.002	0.258	0.007	0.81	0.103	0.028	1737	31	1794	47	1669	41	-3
60	1804137	355423	0.20	0.624	0.002	0.061	0.002	0.79	0.060	0.033	517	17	501	16	586	58	3
61	4211678	766742	0.18	3.266	0.002	0.223	0.005	0.86	0.094	0.018	1566	23	1625	35	1488	27	-4
62	4279943	576824	0.13	5.403	0.003	0.277	0.006	0.86	0.122	0.019	1976	26	1976	43	1976	27	0
63	10716092	1154055	0.11	1.907	0.002	0.152	0.004	0.90	0.079	0.017	1166	21	1164	29	1168	26	0
64	9087383	1480579	0.16	8.452	0.003	0.384	0.007	0.77	0.150	0.020	2460	24	2615	43	2335	28	-6
65	3638342	1344541	0.37	0.087	0.001	0.009	0.000	0.62	0.054	0.040	81	3	72	2	351	72	11
66	1990596	712001	0.36	3.600	0.003	0.226	0.006	0.88	0.100	0.019	1641	28	1669	44	1605	28	-2
67	158174	251495	1.59	14.261	0.070	0.272	0.015	0.92	0.410	0.031	3091	63	1964	99	3936	37	36
68	63942863	1.2E+07	0.18	0.061	0.005	0.012	0.000	0.36	0.080	0.094	163	12	102	3	1182	152	38
69	4089126	636652	0.16	0.064	0.002	0.008	0.000	0.72	0.049	0.035	69	3	68	2	116	65	2
70	2585982	570474	0.22	0.645	0.001	0.073	0.002	0.88	0.059	0.021	570	15	572	16	564	35	0
71	7721843	1802595	0.23	0.105	0.001	0.012	0.000	0.81	0.048	0.028	102	4	103	3	70	53	-1
72	2841894	796694	0.28	4.360	0.003	0.252	0.006	0.93	0.111	0.015	1819	26	1831	45	1807	22	-1
73	6044573	1852911	0.31	16.974	0.006	0.482	0.012	0.82	0.233	0.026	3047	33	3022	68	3064	32	1
74	13495172	329613	0.02	9.367	0.006	0.414	0.017	0.89	0.153	0.027	2505	45	2676	93	2369	36	-7
75	16737418	4473293	0.27	0.097	0.001	0.011	0.000	0.86	0.050	0.023	97	3	93	3	197	42	4
76	7171595	1591235	0.22	0.069	0.002	0.009	0.000	0.66	0.049	0.035	74	3	71	2	155	64	3
77	3278681	640972	0.20	4.481	0.003	0.262	0.006	0.90	0.113	0.018	1876	26	1910	45	1838	26	-2
78	3910921	578917	0.15	3.772	0.003	0.217	0.005	0.84	0.109	0.023	1672	27	1599	38	1764	33	4
79	2488364	625177	0.25	9.054	0.004	0.355	0.009	0.87	0.159	0.021	2441	29	2449	55	2434	27	0
80	5633037	773877	0.14	0.071	0.001	0.009	0.000	0.70	0.051	0.034	77	3	72	2	238	61	7
81	6646373	1024642	0.15	3.927	0.002	0.231	0.005	0.90	0.107	0.014	1710	24	1695	39	1729	22	1
82	2043022	503386	0.25	0.068	0.002	0.008	0.000	0.61	0.048	0.048	70	3	70	2	89	89	1
83	11258796	1708488	0.15	9.570	0.003	0.397	0.009	0.87	0.149	0.018	2465	29	2637	59	2326	26	-7
84	4628244	443415	0.10	4.286	0.002	0.228	0.006	0.91	0.109	0.017	1740	27	1717	44	1768	26	1
85	2200732	798164	0.36	0.079	0.002	0.009	0.000	0.66	0.053	0.043	87	4	79	2	315	77	9
86	1140420	510160	0.45	0.092	0.003	0.009	0.000	0.47	0.056	0.071	88	5	75	2	438	127	14
87	7730074	2584043	0.33	0.086	0.002	0.009	0.000	0.69	0.061	0.039	92	4	73	2	631	66	21
88	2900954	411715	0.14	3.039	0.002	0.198	0.005	0.87	0.095	0.021	1509	26	1503	38	1519	31	0
89	6018927	1554925	0.26	0.513	0.001	0.055	0.001	0.81	0.057	0.023	454	11	448	11	485	40	1
90	4029162	527867	0.13	3.473	0.003	0.202	0.005	0.86	0.109	0.023	1615	29	1503	40	1764	33	7
91	7106493	1313910	0.18	3.863	0.002	0.229	0.005	0.87	0.105	0.018	1708	25	1705	39	1711	28	0
92	3217170	401886	0.12	1.915	0.002	0.146	0.003	0.87	0.079	0.018	1132	21	1121	27	1153	30	1
93	3526236	652748	0.19	2.916	0.002	0.196	0.004	0.90	0.091	0.016	1455	23	1461	34	1445	25	0
94	19156269	3762878	0.20	0.088	0.001	0.012	0.000	0.74	0.050	0.031	102	3	98	3	185	57	4
95	3275085	793324	0.24	0.083	0.002	0.010	0.000	0.56	0.053	0.050	90	4	82	2	307	89	9
96	7464558	1668521	0.22	0.106	0.008	0.019	0.001	0.41	0.061	0.097	192	14	158	5	626	168	17
97	10219450	1456466	0.14	0.083	0.001	0.009	0.000	0.70	0.052	0.031	80	3	74	2	262	56	7
98	3489288	712447	0.20	3.607	0.003	0.205	0.005	0.91	0.105	0.017	1601	26	1528	40	1699	26	5
99	2233136	296725	0.13	4.099	0.002	0.232	0.006	0.89	0.107	0.022	1722	29	1716	47	1730	32	0
100	15212219	6926656	0.46	0.073	0.001	0.009	0.000	0.82	0.048	0.026	79	3	78	2	92	48	1

Table A-3: Zircon LA-ICP-MS U-Pb Isotopic Data and Ages Sample GR-09-19: Dad Member, Lewis Shale. Frantz Setting 1.8 A at 5°

				Corrected isotopic ratios							Ages (Ma)[f]						
Grain #.	U[a] [cps]	Th[a] [cps]	Th/U	$^{207}Pb^{b}/^{235}U$	±2s[d]	$^{206}Pb^{b}/^{238}U$	±2s[d]	Rho[c]	$^{207}Pb^{e}/^{206}Pb$	±2s[d]	$^{207}Pb/^{235}U$	±2s	$^{206}Pb/^{238}U$	±2s	$^{207}Pb/^{206}Pb$	±2s	Disc. %[g]
101	15168706	2613229	0.17	0.092	0.002	0.011	0.000	0.78	0.052	0.033	102	4	94	3	276	58	7
102	5347945	628017	0.12	4.527	0.003	0.268	0.007	0.76	0.107	0.035	1854	36	1965	53	1732	50	-6
103	896795	108783	0.12	1.571	0.004	0.116	0.004	0.67	0.075	0.062	975	40	945	37	1044	98	3
104	5976695	630366	0.11	5.714	0.003	0.225	0.005	0.88	0.149	0.018	2000	29	1703	44	2322	26	15
105	3603400	474926	0.13	3.421	0.002	0.207	0.006	0.86	0.100	0.022	1601	30	1585	45	1623	34	1
106	7453236	1072258	0.14	4.031	0.003	0.236	0.006	0.84	0.103	0.026	1733	32	1787	50	1668	39	-3
107	1469960	558503	0.38	0.068	0.003	0.008	0.000	0.59	0.048	0.065	71	4	70	3	95	95	1
108	20678492	3703358	0.18	4.279	0.002	0.301	0.005	0.83	0.092	0.021	1844	26	2214	47	1450	33	-20
109	3698637	580809	0.16	5.056	0.002	0.291	0.004	0.88	0.106	0.013	1912	22	2096	40	1717	20	-10
110	4315958	677534	0.16	0.063	0.002	0.009	0.000	0.68	0.048	0.045	75	3	74	2	90	83	1
111	1329210	708269	0.53	0.111	0.003	0.009	0.000	0.46	0.059	0.083	95	7	77	3	563	144	19
112	7232344	812504	0.11	3.825	0.002	0.242	0.007	0.85	0.100	0.028	1712	34	1787	53	1621	42	-4
113	6481632	1777325	0.27	3.116	0.003	0.169	0.005	0.90	0.109	0.022	1488	33	1293	44	1778	33	13
114	16416739	5708236	0.35	0.826	0.002	0.059	0.001	0.88	0.088	0.021	660	17	469	14	1382	33	29
115	3114686	389228	0.12	4.169	0.002	0.237	0.008	0.90	0.108	0.023	1758	35	1766	57	1749	33	0
116	2946318	847180	0.29	4.080	0.003	0.225	0.009	0.86	0.107	0.034	1684	43	1644	64	1734	49	2
117	12784765	1279458	0.10	1.602	0.001	0.147	0.004	0.82	0.072	0.028	1078	27	1132	34	972	46	-5
118	1663576	477842	0.29	5.940	0.004	0.298	0.008	0.86	0.127	0.024	2097	33	2150	59	2045	34	-3
119	13933168	1182155	0.08	2.466	0.002	0.143	0.003	0.79	0.106	0.029	1380	30	1169	33	1724	43	15
120	1793488	312979	0.17	2.191	0.002	0.173	0.005	0.89	0.083	0.020	1316	28	1349	40	1263	32	-2
121	3910025	571511	0.15	0.520	0.001	0.059	0.001	0.82	0.058	0.024	497	13	491	13	524	42	1
122	2103053	1240780	0.59	5.505	0.003	0.274	0.008	0.89	0.123	0.021	2015	34	2034	60	1995	31	-1

[a]U, Th, and Pb concentrations and Th/U ratios are calculated relative to GJ-1 zircon standard

[b]U-Pb fractionation correction and corrected for background interference based on GJ-1 zircon standard and Pb/U ratios are corrected according to Anderson (2002)

[c]Rho is the error correlation defined as the quotient of the propagated errors of the $^{206}Pb/^{238}U$ and the $^{207}/^{235}U$ ratio

[d]Quadratic addition of inter-run errors (2 SD) and daily reproducibility of GJ-1 (2 SD)

[e]Corrected for mass-bias by normalising to GJ-1 zircon standard (~.6 per atomic mass unit)

[f]U-Pb ages are calculated relative to GJ-1 zircon standard and corrected based on Anderson model (2002)

[g]Discordance %: for $^{206}Pb/^{238}U$ ages <1Ga calculated as $((1-(^{206}Pb/^{238}U)/(^{207}Pb/^{235}U))*100)$, for $^{206}Pb/^{238}U$ ages >1Ga calculated as $((1-(^{206}Pb/^{238}U)/(^{207}Pb/^{206}Pb))*100)$

Table A-4: Zircon LA-ICP-MS U-Pb Isotopic Data and Ages — Sample GR-09-14: Fox Hills Sandstone, Greater Green River Basin, W~~Y~~

Grain #.	U[a] [cps]	Th[a] [cps]	Th/U	Corrected isotopic ratios							Ages (Ma)[f]						
				$^{207}Pb^{b}/^{235}U$	±2s[d]	$^{206}Pb^{b}/^{238}U$	±2s[d]	Rho[c]	$^{207}Pb^{e}/^{206}Pb$	±2s[d]	$^{207}Pb/^{235}U$	±2s	$^{206}Pb/^{238}U$	±2s	$^{207}Pb/^{206}Pb$	±2s	Disc. %[g]
1	2427871	1246630	0.51	2.622	0.002	0.2726	0.0052	0.91	0.084	0.007	1358	17	1409	27	1280	18	-4
2	1278071	430671	0.34	4.511	0.003	0.3815	0.0076	0.88	0.104	0.010	1814	21	1921	37	1694	20	-6
3	1040593	464296	0.45	4.450	0.003	0.3630	0.0051	0.84	0.109	0.009	1798	16	1815	25	1780	18	-1
4	1905854	300698	0.16	3.080	0.002	0.2929	0.0035	0.82	0.093	0.007	1498	13	1508	19	1485	17	-1
5	6325382	1580292	0.25	0.092	0.002	0.0147	0.0005	0.68	0.049	0.030	88	4	85	3	162	82	3
6	2566989	1057857	0.41	0.096	0.002	0.0170	0.0003	0.57	0.049	0.022	101	3	98	2	167	60	3
7	3944238	506690	0.13	0.070	0.006	0.0143	0.0004	0.51	0.054	0.047	90	5	80	3	373	124	12
8	2922400	169559	0.06	4.291	0.002	0.3450	0.0052	0.81	0.105	0.012	1725	18	1733	26	1714	24	-1
9	2814123	455368	0.16	0.090	0.002	0.0180	0.0003	0.45	0.047	0.035	102	4	103	2	60	60	-2
10	2943179	398862	0.14	4.369	0.001	0.3538	0.0046	0.79	0.107	0.010	1710	16	1682	22	1744	20	2
11	2391081	344428	0.14	4.163	0.002	0.3362	0.0034	0.8	0.105	0.008	1717	13	1715	18	1720	17	0
12	3371066	810974	0.24	3.994	0.002	0.3518	0.0049	0.8	0.105	0.011	1724	17	1726	24	1721	22	0
13	2779465	420526	0.15	3.766	0.003	0.3187	0.0048	0.89	0.105	0.007	1660	16	1621	24	1709	17	2
14	11177545	3868784	0.35	0.085	0.002	0.0159	0.0002	0.54	0.050	0.020	93	2	90	1	172	52	3
15	11888357	4279312	0.36	0.170	0.001	0.0145	0.0003	0.3	0.068	0.056	119	7	84	2	874	136	29
16	1783960	578598	0.32	2.651	0.002	0.2731	0.0030	0.81	0.087	0.008	1398	12	1420	17	1366	17	-2
17	1339202	376527	0.28	2.694	0.002	0.2617	0.0026	0.8	0.088	0.008	1367	11	1356	15	1385	17	1
18	8068053	1917848	0.24	3.157	0.001	0.2592	0.0023	0.73	0.101	0.009	1475	12	1364	14	1639	19	8
19	943534	336287	0.36	0.095	0.003	0.0128	0.0003	0.36	0.053	0.055	83	5	75	2	342	144	10
20	1394673	254606	0.18	4.473	0.003	0.3578	0.0039	0.81	0.110	0.009	1793	14	1791	20	1796	18	0
21	2755394	816479	0.30	3.890	0.003	0.3557	0.0046	0.78	0.106	0.010	1754	15	1779	22	1723	20	-1
22	10371944	4462884	0.43	0.972	0.003	0.0924	0.0026	0.94	0.093	0.010	740	16	519	15	1483	21	30
23	1113479	472469	0.42	3.488	0.003	0.3107	0.0068	0.92	0.102	0.009	1622	21	1592	33	1662	19	2
24	2389205	769785	0.32	3.047	0.004	0.2709	0.0035	0.7	0.091	0.670	21236	1570	1856	396			91
25	424708	191344	0.45	0.079	0.002	0.0163	0.0002	0.44	0.049	0.013	1417	15	1394	18	1452	27	2
26	4491482	2120602	0.47	1.205	0.002	0.1068	0.0018	0.9	0.101	0.027	95	3	93	1	143	72	2
27	11492085	2656682	0.23	4.392	0.001	0.3484	0.0038	0.86	0.110	0.008	860	12	588	10	1649	17	32
28	3832573	911350	0.24	0.370	0.001	0.0613	0.0009	0.85	0.053	0.007	1761	12	1728	18	1802	15	2
29	3889087	217005	0.06	4.835	0.002	0.3644	0.0036	0.75	0.116	0.011	341	6	343	5	330	27	0
30	2372073	580159	0.24	1.492	0.002	0.1791	0.0020	0.81	0.072	0.006	1851	11	1813	17	1895	13	2
31	1130331	410407	0.36	2.989	0.004	0.2815	0.0034	0.48	0.101	0.010	965	10	953	11	991	23	1
32	773302	369784	0.48	0.106	0.006	0.0154	0.0005	0.75	0.066	0.009	1531	13	1447	17	1648	19	5
33	662550	482439	0.73	2.637	0.003	0.2607	0.0029	0.81	0.090	0.048	124	7	92	3	800	118	26
34	1063246	521496	0.49	4.266	0.002	0.3181	0.0051	0.48	0.109	0.010	1382	12	1349	15	1433	21	2
35	3120738	943726	0.30	0.074	0.002	0.0128	0.0002	0.85	0.047	0.012	1687	17	1610	24	1783	24	5
36	1634463	596918	0.37	3.606	0.003	0.3012	0.0063	0.64	0.101	0.026	73	2	74	1	69	69	0
37	1372710	619663	0.45	0.088	0.002	0.0160	0.0003	0.79	0.052	0.012	1591	21	1550	30	1645	24	3
38	5311390	3720503	0.70	4.112	0.002	0.3456	0.0035	0.79	0.106	0.022	99	3	92	2	279	58	7
39	3094445	2338712	0.76	3.923	0.004	0.3149	0.0085	0.51	0.105	0.008	1729	12	1733	17	1723	17	0
40	1195233	520612	0.44	0.082	0.002	0.0138	0.0003	0.79	0.048	0.019	1625	28	1562	38	1707	39	4
41	1092790	364030	0.33	2.933	0.002	0.2816	0.0028	0.79	0.091	0.035	80	4	79	2	103	95	1
42	1175042	200130	0.17	0.357	0.001	0.0614	0.0009	0.83	0.052	0.007	1444	11	1445	14	1443	15	0
43	3666808	193299	0.05	3.417	0.003	0.3035	0.0033	0.86	0.097	0.015	335	7	342	5	286	39	-2
44	1432443	735483	0.51	0.093	0.001	0.0161	0.0002	0.85	0.048	0.006	1557	11	1550	17	1566	13	0
45	4947093	1223531	0.25	4.503	0.003	0.3600	0.0050	0.75	0.108	0.018	93	2	93	1	93	48	0
46	964085	243846	0.25	2.573	0.003	0.2697	0.0027	0.82	0.088	0.009	1770	15	1771	23	1769	18	0
47	1682006	1172896	0.70	4.097	0.002	0.3526	0.0032	0.57	0.103	0.007	1390	11	1389	14	1391	15	0
48	4895172	2380836	0.49	3.955	0.002	0.3363	0.0037	0.97	0.105	0.005	1732	10	1772	16	1685	11	-2
49	2705414	743969	0.27	3.651	0.003	0.2698	0.0043	0.79	0.115	0.006	1702	12	1692	18	1715	13	1
50	2241480	534787	0.24	3.746	0.003	0.3240	0.0036	0.67	0.105	0.010	1591	16	1386	21	1874	20	13

Table A-4: Zircon LA-ICP-MS U-Pb Isotopic Data and Ages   Sample GR-09-14: Fox Hills Sandstone, Greater Green River Basin, WY

Grain #	U[a] [cps]	Th[a] [cps]	Th/U	Corrected isotopic ratios: $^{207}Pb^{b}/^{235}U$	±2s[d]	$^{206}Pb^{b}/^{238}U$	±2s[d]	Rho[c]	$^{207}Pb^{c}/^{206}Pb$	±2s[d]	Ages (Ma)[f]: $^{207}Pb/^{235}U$	±2s	$^{206}Pb/^{238}U$	±2s	$^{207}Pb/^{206}Pb$	±2s	Disc. %[g]
51	1355353	292783	0.22	0.378	0.001	0.0593	0.0008	0.87	0.053	0.009	1674	13	1639	17	1718	19	2
52	3828719	205927	0.05	6.046	0.004	0.4370	0.0057	0.58	0.129	0.012	335	6	335	5	339	32	0
53	669417	249992	0.37	0.528	0.002	0.0789	0.0009	0.45	0.062	0.008	2102	15	2118	25	2086	16	-1
54	2453631	1073081	0.44	3.913	0.003	0.3164	0.0095	0.67	0.106	0.015	480	8	438	5	688	37	9
55	1663003	920906	0.55	2.780	0.002	0.2760	0.0028	0.79	0.089	0.008	1661	26	1600	43	1739	17	4
56	2059601	977361	0.47	4.535	0.003	0.3627	0.0040	0.79	0.108	0.007	1411	11	1420	14	1397	15	-1
57	1230426	511534	0.42	4.098	0.003	0.3461	0.0045	0.86	0.105	0.012	1779	15	1791	19	1765	26	-1
58	1655630	265661	0.16	0.086	0.001	0.0162	0.0002	0.53	0.048	0.007	1728	13	1743	21	1710	15	-1
59	4393543	1061767	0.24	1.758	0.001	0.1984	0.0024	0.85	0.071	0.017	92	2	91	1	93	46	0
60	1887434	245665	0.13	0.525	0.002	0.0832	0.0009	0.88	0.058	0.023	1016	19	1048	13	949	54	-3
61	1471173	529200	0.36	4.318	0.002	0.3726	0.0037	0.5	0.107	0.012	469	7	457	5	527	31	3
62	4817677	644691	0.13	4.333	0.002	0.3378	0.0034	0.95	0.107	0.007	1797	12	1838	18	1749	15	-2
63	2162320	2498209	1.16	3.993	0.002	0.3229	0.0036	0.45	0.104	0.007	1716	12	1692	16	1745	15	1
64	3541498	542835	0.15	4.261	0.003	0.3751	0.0064	0.57	0.112	0.006	1682	12	1663	18	1705	13	1
65	3809314	2129225	0.56	3.098	0.003	0.2866	0.0029	0.26	0.092	0.026	1854	29	1868	29	1837	54	-1
66	930295	277064	0.30	4.322	0.002	0.3385	0.0047	0.87	0.107	0.006	1402	10	1354	14	1476	13	3
67	2920145	519034	0.18	0.098	0.002	0.0169	0.0003	0.82	0.050	0.006	1730	14	1711	23	1752	13	1
68	1592585	841452	0.53	4.177	0.002	0.3521	0.0070	0.86	0.109	0.025	101	3	97	2	182	67	3
69	4515735	833507	0.18	0.359	0.001	0.0600	0.0008	0.82	0.053	0.007	1769	19	1762	33	1777	15	0
70	3491433	182379	0.05	0.070	0.002	0.0131	0.0002	0.87	0.055	0.012	332	5	334	5	318	30	-1
71	2855294	986860	0.35	0.098	0.002	0.0170	0.0003	0.69	0.047	0.035	87	4	76	2	412	90	13
72	2385792	860656	0.36	0.065	0.006	0.0143	0.0002	0.87	0.061	0.022	97	3	98	2	67	61	-1
73	2021525	700020	0.35	3.934	0.003	0.3221	0.0039	0.86	0.104	0.060	104	7	82	2	640	151	21
74	1846252	539782	0.29	1.884	0.004	0.2189	0.0037	0.96	0.082	0.006	1656	12	1617	19	1705	13	2
75	658182	244665	0.37	4.450	0.002	0.3741	0.0041	0.86	0.106	0.012	1192	16	1159	19	1253	26	3
76	1962933	226935	0.12	2.595	0.002	0.2453	0.0032	0.32	0.093	0.007	1794	12	1845	19	1736	15	-3
77	3002943	760290	0.25	0.360	0.001	0.0601	0.0007	0.44	0.053	0.008	1349	13	1268	16	1482	17	6
78	3377231	176878	0.05	4.912	0.004	0.3783	0.0049	0.59	0.118	0.011	335	5	334	4	340	27	0
79	781796	303750	0.39	6.567	0.002	0.4402	0.0044	0.63	0.129	0.007	1897	14	1863	23	1935	14	2
80	3315972	501453	0.15	3.885	0.003	0.3179	0.0038	0.8	0.105	0.010	2103	14	2126	20	2081	20	-1
81	1440718	293141	0.20	4.559	0.003	0.3640	0.0040	0.87	0.112	0.007	1664	12	1627	19	1712	15	2
82	1034426	1308749	1.27	11.238	0.006	0.5071	0.0106	0.71	0.204	0.007	1829	12	1825	19	1834	15	0
83	2685414	1288447	0.48	4.582	0.001	0.3734	0.0041	0.57	0.105	0.006	2657	22	2399	44	2859	11	10
84	5613360	477408	0.09	0.133	0.002	0.0177	0.0002	0.8	0.053	0.007	1786	12	1854	19	1709	15	-4
85	3908488	1822658	0.47	0.370	0.001	0.0606	0.0008	0.55	0.054	0.040	111	5	101	2	341	105	9
86	3613196	199424	0.06	0.106	0.002	0.0161	0.0002	0.82	0.055	0.011	345	5	342	5	362	27	1
87	3838050	1555958	0.41	0.100	0.001	0.0171	0.0003	0.98	0.050	0.028	104	3	91	1	397	71	12
88	2234790	905917	0.41	0.092	0.001	0.0158	0.0003	0.81	0.048	0.021	100	3	97	2	182	57	3
89	4025855	3790106	0.94	2.709	0.003	0.2715	0.0027	0.59	0.089	0.019	91	2	90	2	123	50	1
90	941660	749186	0.80	8.919	0.006	0.4390	0.0057	0.89	0.187	0.008	1404	12	1398	15	1413	17	0
91	1348684	473891	0.35	0.151	0.001	0.0224	0.0004	0.87	0.057	0.006	2447	15	2130	25	2722	12	13
92	6020627	1903919	0.32	0.763	0.001	0.0984	0.0012	0.79	0.062	0.015	152	3	129	2	513	38	15
93	1338295	1787278	1.34	4.092	0.003	0.3494	0.0035	0.81	0.105	0.017	562	10	537	7	665	41	4
94	1423670	348219	0.24	0.101	0.001	0.0176	0.0002	0.81	0.050	0.008	1740	13	1757	19	1719	17	-1
95	6944700	1847106	0.27	8.097	0.003	0.4662	0.0061	0.9	0.157	0.016	103	2	100	1	175	43	3
96	2547085	882785	0.35	0.920	0.004	0.0847	0.0041	0.92	0.098	0.009	2333	16	2233	27	2422	17	4
97	5069625	4721320	0.93	0.361	0.001	0.0602	0.0007	0.94	0.054	0.008	712	25	466	22	1595	17	35
98	3507397	189741	0.05	2.658	0.002	0.2657	0.0029	0.91	0.089	0.010	341	5	337	4	367	25	1
99	685740	537908	0.78	0.090	0.001	0.0168	0.0002	0.97	0.049	0.008	1378	12	1362	16	1403	17	1
100	5233240	1362736	0.26	2.966	0.002	0.2654	0.0042	0.78	0.102	0.016	97	2	95	1	140	43	2

Table A-4: Zircon LA-ICP-MS U-Pb Isotopic Data and Ages Sample GR-09-14: Fox Hills Sandstone, Greater Green River Basin, WY

Grain #.	U[a] [cps]	Th[a] [cps]	Th/U	Corrected isotopic ratios							Ages (Ma)[f]						
				$^{207}Pb^{b}/^{235}U$	±2s[d]	$^{206}Pb^{b}/^{238}U$	±2s[d]	Rho[c]	$^{207}Pb^{e}/^{206}Pb$	±2s[d]	$^{207}Pb/^{235}U$	±2s	$^{206}Pb/^{238}U$	±2s	$^{207}Pb/^{206}Pb$	±2s	Disc. %[g]
101	8273574	3002957	0.36	3.730	0.002	0.3190	0.0038	0.82	0.105	0.008	1489	15	1365	21	1669	17	8
102	2888821	1185182	0.41	4.447	0.002	0.3744	0.0034	0.92	0.106	0.006	1659	13	1614	20	1717	15	3
103	2396937	582177	0.24	4.193	0.002	0.3448	0.0038	0.74	0.109	0.007	1792	12	1838	18	1740	17	-3
104	1783863	387451	0.22	0.809	0.001	0.1160	0.0013	0.74	0.061	0.007	1742	13	1707	20	1785	17	2
105	2472064	1860086	0.75	2.710	0.003	0.2220	0.0038	0.92	0.107	0.008	638	8	637	8	641	20	0
106	1987243	1353140	0.68	3.089	0.003	0.2594	0.0054	0.83	0.106	0.007	1399	15	1176	19	1757	17	16
107	1527137	549135	0.36	2.456	0.004	0.1822	0.0055	0.68	0.115	0.008	1495	19	1335	27	1729	17	11
108	1814598	1294500	0.71	2.888	0.003	0.2419	0.0046	0.29	0.109	0.011	1297	25	976	28	1876	22	25
109	4447161	2300841	0.52	0.368	0.001	0.0608	0.0008	0.82	0.053	0.007	1458	17	1248	23	1778	17	14
110	3291625	173667	0.05	0.401	0.003	0.0348	0.0011	0.45	0.103	0.011	339	6	338	5	348	27	0
111	26916972	10587808	0.39	2.383	0.002	0.2457	0.0029	0.65	0.095	0.009	367	11	195	6	1679	19	47
112	1576397	635615	0.40	1.951	0.002	0.1989	0.0034	0.7	0.084	0.011	1367	14	1270	16	1522	23	7
113	972192	328111	0.34	7.488	0.004	0.4139	0.0087	0.81	0.162	0.012	1135	15	1058	18	1286	26	7
114	3602325	14703025	4.08	3.452	0.003	0.3343	0.0040	0.84	0.103	0.008	2265	22	2037	39	2478	15	10
115	1119504	380163	0.34	0.090	0.001	0.0169	0.0002	0.89	0.048	0.012	1680	16	1679	21	1682	24	0
116	7648844	2047854	0.27	0.363	0.001	0.0600	0.0008	0.67	0.053	0.012	95	2	95	1	102	31	0
117	3305422	177126	0.05	3.857	0.006	0.3694	0.0085	0.92	0.104	0.012	337	6	338	5	331	30	0
118	539741	187806	0.35	1.713	0.002	0.1964	0.0035	0.78	0.075	0.010	1745	22	1777	37	1708	20	-2
119	1842160	475385	0.26	0.093	0.001	0.0166	0.0002	0.63	0.048	0.012	1048	16	1043	19	1060	26	1
120	4105627	1510925	0.37	0.372	0.001	0.0602	0.0008	0.57	0.053	0.017	96	2	95	2	113	46	1
121	3465562	184773	0.05	1.778	0.003	0.1667	0.0025	0.97	0.072	0.011	338	6	338	5	339	27	0
122	1741796	419056	0.24	4.439	0.003	0.3397	0.0041	0.11257	0.113	0.051	902	36	872	14	977	121	3
123	1483878	294473	0.20	0.128	0.002	0.0170	0.0003	0.0559	0.056	0.007	1766	14	1699	21	1846	16	4
124	1792651	854665	0.48	0.089	0.001	0.0159	0.0002	0.04976	0.050	0.034	113	5	97	2	454	87	14
125	3120318	1749703	0.56	0.090	0.001	0.0166	0.0002	0.04893	0.049	0.018	94	2	90	2	189	47	4
126	7884631	1824213	0.23	15.023	0.004	0.6761	0.0128	0.18029	0.180	0.014	96	2	94	2	150	38	2
127	1355344	413181	0.30	3.993	0.003	0.3420	0.0044	0.10643	0.106	0.014	2817	25	3043	51	2660	27	-8
128	1913611	374475	0.20	3.825	0.002	0.3338	0.0043	0.10198	0.102	0.008	1727	16	1714	24	1744	18	1
129	4667233	2285418	0.49	3.467	0.005	0.3206	0.0064	0.1215	0.122	0.006	1676	15	1685	24	1665	15	-1
130	3759100	304152	0.08	3.011	0.002	0.2085	0.0042	0.12623	0.126	0.022	1728	28	1525	30	1983	45	12
131	8175906	6476078	0.79	3.891	0.003	0.3326	0.0037	0.1024	0.102	0.008	1357	18	961	20	2051	18	29
132	801170	482429	0.60	1.475	0.004	0.1884	0.0028	0.07667	0.077	0.009	1656	15	1643	20	1673	21	1
133	328968	212688	0.65	0.111	0.002	0.0180	0.0003	0.05339	0.053	0.019	1020	18	975	15	1118	43	4
134	2232174	528413	0.24	3.269	0.004	0.2748	0.0071	0.10623	0.106	0.022	112	3	101	2	351	58	10
135	3602795	1564541	0.43	0.264	0.004	0.0166	0.0058	0.87	0.106	0.006	1541	23	1400	35	1741	15	9
136	2548198	1656024	0.65	2.265	0.006	0.2414	0.0003	0.83	0.080	0.049	1185	17	1165	20	1222	28	2
140	3762748	650990	0.17	0.074	0.002	0.0133	0.0039	0.31	0.055	0.011	80	4	69	2	429	94	14

[a]U, Th, and Pb concentrations and Th/U ratios are calculated relative to GJ-1 zircon standard

[b]U-Pb fractionation correction and corrected for background interference based on GJ-1 zircon standard and Pb/U ratios are corrected according to Anderson (2002)

[c]Rho is the error correlation defined as the quotient of the propagated errors of the $^{206}Pb/^{238}U$ and the $^{207}/^{235}U$ ratio

[d]Quadratic addition of inter-run errors (2 SD) and daily reproducibility of GJ-1 (2 SD)

[e]Corrected for mass-bias by normalising to GJ-1 zircon standard (~.6 per atomic mass unit)

[f]U-Pb ages are calculated relative to GJ-1 zircon standard and corrected based on Anderson model (2002)

[g]Discordance %: for $^{206}Pb/^{238}U$ ages <1Ga calculated as ((1-($^{206}Pb/^{238}U$)/($^{207}Pb/^{235}U$))*100), for $^{206}Pb/^{238}U$ ages >1Ga calculated as ((1-($^{206}Pb/^{238}U$)/($^{207}Pb/^{206}Pb$))*100)

Table A-5: Zircon LA-ICP-MS U-Pb Isotopic Data and Ages Sample GR-09-05:Pine Ridge Sandstone, Greater Green River Basin, WY

				Corrected isotopic ratios							Ages (Ma)[f]						
Grain #.	U[a] [cps]	Th[a] [cps]	Th/U	$^{207}Pb^{b}/^{235}U$	±2s[d]	$^{206}Pb^{b}/^{238}U$	±2s[d]	Rho[c]	$^{207}Pb^{e}/^{206}Pb$	±2s[d]	$^{207}Pb/^{235}U$	±2s	$^{206}Pb/^{238}U$	±2s	$^{207}Pb/^{206}Pb$	±2s	Disc. %[g]
1	5096397	2033020	0.40	0.174	0.001	0.0216	0.0002	0.46	0.061	0.019	129	3	103	1	633	55	20
2	870348	405571	0.47	7.043	0.003	0.4822	0.0048	0.80	0.124	0.007	2002	13	1986	21	2019	16	1
3	474098	145602	0.31	2.357	0.003	0.2460	0.0027	0.72	0.076	0.009	1084	12	1083	13	1087	24	0
4	1384861	373970	0.27	0.114	0.002	0.0206	0.0003	0.48	0.049	0.020	100	3	98	2	135	65	2
5	404928	486207	1.20	8.681	0.006	0.5330	0.0053	0.75	0.140	0.007	2201	15	2168	22	2231	18	1
6	297508	143272	0.48	6.124	0.007	0.4573	0.0046	0.80	0.117	0.007	1904	13	1898	20	1910	16	0
7	9187590	1621244	0.18	0.113	0.006	0.0199	0.0002	0.15	0.056	0.063	111	9	96	1	457	198	14
8	1227995	523459	0.43	4.846	0.002	0.4195	0.0046	0.81	0.103	0.006	1713	13	1734	20	1686	17	-1
9	3263582	888666	0.27	0.116	0.001	0.0206	0.0002	0.59	0.049	0.014	102	2	99	1	165	43	3
10	590251	375730	0.64	5.987	0.004	0.4279	0.0043	0.80	0.112	0.006	1810	13	1792	19	1831	16	1
11	2447863	1101974	0.45	4.871	0.002	0.3925	0.0035	0.85	0.105	0.005	1690	11	1673	16	1711	13	1
12	21908237	3070519	0.14	1.994	0.007	0.0610	0.0025	0.84	0.202	0.020	969	31	359	14	2845	43	63
13	1524518	390701	0.26	4.837	0.003	0.3875	0.0039	0.86	0.104	0.005	1681	12	1663	18	1703	15	1
14	2669995	440063	0.16	3.100	0.002	0.3013	0.0024	0.77	0.088	0.005	1343	10	1316	12	1385	15	2
15	1817110	728521	0.40	4.849	0.002	0.3893	0.0043	0.87	0.104	0.005	1676	12	1662	19	1695	15	1
16	1588935	943303	0.59	6.200	0.002	0.4322	0.0039	0.77	0.118	0.005	1880	11	1839	16	1926	14	2
17	1777266	536843	0.30	4.939	0.002	0.3986	0.0032	0.82	0.106	0.005	1702	9	1683	13	1726	13	1
18	1698752	911398	0.54	4.963	0.002	0.4010	0.0036	0.83	0.106	0.005	1718	10	1707	15	1731	13	1
19	2495025	1074651	0.43	0.130	0.004	0.0200	0.0003	0.35	0.061	0.035	122	6	97	2	644	102	21
20	4990169	1046703	0.21	5.570	0.002	0.4430	0.0044	0.65	0.121	0.010	1906	15	1851	18	1966	23	3
21	6678876	1024640	0.15	0.096	0.002	0.0173	0.0003	0.63	0.051	0.016	90	2	84	1	259	49	7
22	2243357	568967	0.25	4.880	0.002	0.3975	0.0036	0.77	0.105	0.005	1693	11	1675	15	1715	15	1
23	3160839	1148012	0.36	0.115	0.001	0.0192	0.0002	0.54	0.049	0.015	94	2	92	1	143	48	2
24	5587091	1095310	0.20	0.099	0.001	0.0180	0.0002	0.62	0.048	0.012	87	2	87	1	89	38	0
25	1335598	364882	0.27	4.055	0.003	0.3642	0.0044	0.76	0.105	0.008	1652	14	1607	19	1710	20	3
26	205538	103890	0.51	22.360	0.011	0.8133	0.0089	0.71	0.215	0.009	2977	17	3024	29	2945	20	-2
27	741612	188348	0.25	4.589	0.003	0.3969	0.0040	0.79	0.103	0.007	1689	12	1697	16	1680	17	0
28	9237548	1317002	0.14	2.155	0.001	0.2461	0.0020	0.50	0.083	0.012	1159	13	1099	9	1275	32	5
29	2121717	601273	0.28	4.739	0.003	0.4026	0.0036	0.71	0.107	0.008	1720	12	1692	15	1753	18	2
30	2416107	301374	0.12	0.597	0.002	0.0792	0.0011	0.75	0.066	0.010	440	7	371	5	816	27	16
31	1917052	788403	0.41	4.174	0.003	0.3465	0.0042	0.81	0.107	0.007	1599	13	1491	17	1745	17	7
32	405896	235105	0.58	7.577	0.005	0.4955	0.0045	0.67	0.129	0.008	2077	13	2068	18	2087	20	0
34	1070402	474440	0.44	5.042	0.003	0.4065	0.0037	0.71	0.111	0.008	1708	12	1620	14	1818	18	5
35	2317169	381310	0.16	4.125	0.002	0.2892	0.0032	0.92	0.117	0.005	1527	10	1260	14	1918	11	17
36	2653845	320138	0.12	4.733	0.002	0.3948	0.0036	0.83	0.104	0.005	1688	10	1681	15	1696	13	0
37	6512230	968818	0.15	0.126	0.001	0.0214	0.0002	0.46	0.053	0.016	114	3	104	1	339	48	9
38	1464899	1316687	0.90	3.492	0.002	0.3297	0.0030	0.83	0.091	0.005	1438	9	1433	13	1445	13	0
39	2254461	802425	0.36	0.212	0.001	0.0330	0.0004	0.50	0.053	0.017	171	4	160	2	326	51	6
40	6939195	5503140	0.79	3.551	0.003	0.2013	0.0034	0.81	0.153	0.010	1447	16	901	14	2378	22	38
41	6186281	1499610	0.24	0.101	0.001	0.0186	0.0002	0.50	0.053	0.018	101	3	91	1	348	55	10
42	4269365	1608138	0.38	0.574	0.001	0.0865	0.0009	0.79	0.056	0.006	412	5	407	4	437	18	1
43	1183055	400631	0.34	2.405	0.002	0.2529	0.0023	0.77	0.078	0.007	1142	9	1137	10	1153	18	0
44	1502285	302154	0.20	4.450	0.002	0.3689	0.0044	0.87	0.103	0.006	1642	12	1609	19	1684	15	2
45	4731973	1293686	0.27	2.362	0.002	0.1660	0.0027	0.84	0.113	0.008	1110	13	770	12	1855	18	31
46	2167011	353669	0.16	4.847	0.002	0.3990	0.0036	0.83	0.107	0.005	1732	10	1719	15	1748	11	1
47	1458548	370816	0.25	3.648	0.002	0.3303	0.0036	0.86	0.093	0.006	1465	11	1452	16	1484	15	1
48	159771	99821	0.62	2.001	0.006	0.2386	0.0031	0.58	0.077	0.015	1084	16	1070	14	1112	41	1
49	3792367	1147567	0.30	0.126	0.001	0.0188	0.0003	0.58	0.055	0.016	105	3	92	1	413	48	12
50	1025146	396921	0.39	4.006	0.004	0.3061	0.0101	0.92	0.111	0.011	1548	29	1361	41	1813	26	12
51	1044741	685197	0.66	2.110	0.002	0.2427	0.0022	0.77	0.077	0.007	1105	9	1096	10	1122	18	1

Table A-5: Zircon LA-ICP-MS U-Pb Isotopic Data and Ages Sample GR-09-05:Pine Ridge Sandstone, Greater Green River Basin, WY

				Corrected isotopic ratios							Ages (Ma)[f]						
Grain #	U[a] [cps]	Th[a] [cps]	Th/U	$^{207}Pb^{b}/^{235}U$	±2s[d]	$^{206}Pb^{b}/^{238}U$	±2s[d]	Rho[c]	$^{207}Pb^{e}/^{206}Pb$	±2s[d]	$^{207}Pb/^{235}U$	±2s	$^{206}Pb/^{238}U$	±2s	$^{207}Pb/^{206}Pb$	±2s	Disc. %[g]
52	1015916	303282	0.30	4.665	0.003	0.3781	0.0042	0.80	0.105	0.007	1683	12	1648	18	1725	17	2
53	5753190	2300199	0.40	0.099	0.001	0.0172	0.0002	0.71	0.048	0.011	86	2	85	1	103	36	1
54	451290	190025	0.42	13.710	0.008	0.6783	0.0061	0.77	0.190	0.006	2732	12	2709	22	2749	13	1
55	2291298	301812	0.13	4.665	0.002	0.3993	0.0036	0.83	0.105	0.005	1712	10	1712	15	1711	13	0
56	2356476	367102	0.16	4.862	0.002	0.4046	0.0036	0.83	0.107	0.005	1746	10	1747	15	1745	13	0
57	18076512	2101732	0.12	1.246	0.004	0.0578	0.0010	0.63	0.216	0.016	856	16	280	5	2954	34	67
58	3145399	863328	0.27	3.923	0.002	0.3126	0.0038	0.87	0.105	0.006	1522	12	1382	16	1722	15	9
59	1714050	457373	0.27	5.281	0.002	0.4185	0.0046	0.80	0.109	0.007	1738	13	1703	18	1781	17	2
60	2972372	910920	0.31	0.106	0.001	0.0189	0.0003	0.53	0.048	0.019	93	3	93	2	116	60	1
61	1397598	462942	0.33	4.521	0.002	0.3744	0.0045	0.81	0.099	0.008	1625	13	1631	19	1617	19	0
62	3118674	459092	0.15	3.416	0.001	0.3261	0.0029	0.77	0.089	0.006	1417	10	1418	13	1416	15	0
63	4431030	570557	0.13	0.106	0.001	0.0197	0.0002	0.59	0.049	0.014	99	2	96	1	172	43	3
64	3440550	291127	0.08	5.233	0.002	0.4011	0.0048	0.87	0.109	0.006	1763	13	1750	20	1778	15	1
65	4409573	1202927	0.27	5.041	0.002	0.4267	0.0043	0.79	0.106	0.006	1772	12	1810	17	1728	15	-2
67	937802	498303	0.53	5.559	0.003	0.4267	0.0047	0.75	0.107	0.008	1798	14	1839	19	1750	20	-2
68	4637404	1143646	0.25	5.383	0.001	0.3663	0.0029	0.69	0.120	0.008	1762	11	1602	13	1957	18	9
69	8027045	3238904	0.40	0.083	0.002	0.0199	0.0002	0.32	0.055	0.029	110	4	97	1	405	87	12
70	3542622	906766	0.26	0.952	0.007	0.0756	0.0029	0.97	0.103	0.008	625	18	376	14	1675	19	40
71	2213144	705231	0.32	0.119	0.001	0.0188	0.0003	0.52	0.052	0.020	100	3	93	2	270	61	7
72	935043	139036	0.15	4.979	0.003	0.3884	0.0039	0.79	0.104	0.006	1689	12	1686	16	1694	15	0
73	1069270	432258	0.40	9.035	0.007	0.5462	0.0109	0.74	0.151	0.014	2322	25	2282	39	2357	31	2
74	2858536	1806630	0.63	5.494	0.002	0.4146	0.0054	0.82	0.120	0.008	1861	15	1773	22	1961	18	5
75	2209089	372146	0.17	5.081	0.002	0.4174	0.0038	0.77	0.109	0.006	1791	11	1788	16	1794	15	0
76	4865931	1148134	0.24	4.335	0.002	0.3539	0.0046	0.87	0.108	0.005	1642	13	1548	19	1765	13	6
77	1671242	520222	0.31	0.563	0.001	0.0866	0.0010	0.67	0.054	0.011	414	6	418	5	391	32	-1
78	1683114	698850	0.42	3.387	0.002	0.3117	0.0034	0.86	0.092	0.006	1422	11	1393	15	1466	15	2
79	999402	245708	0.25	3.596	0.002	0.3185	0.0038	0.87	0.091	0.006	1426	12	1416	17	1443	15	1
80	763722	193634	0.25	5.045	0.003	0.4076	0.0049	0.81	0.105	0.007	1740	13	1755	20	1722	17	-1
81	1121587	560311	0.50	13.069	0.006	0.6210	0.0081	0.87	0.190	0.006	2638	15	2505	29	2742	13	5
82	1409258	386701	0.27	12.159	0.003	0.6209	0.0106	0.89	0.159	0.007	2484	18	2534	36	2444	15	-2
83	1021292	401524	0.39	6.752	0.003	0.4803	0.0048	0.79	0.123	0.006	2020	12	2035	19	2004	14	-1
84	479927	337795	0.70	10.074	0.005	0.5664	0.0068	0.87	0.149	0.006	2352	14	2363	26	2343	14	0
85	520186	364526	0.70	0.875	0.003	0.1270	0.0015	0.52	0.064	0.016	630	12	601	8	738	45	5
86	158489	64279	0.41	0.942	0.007	0.1388	0.0028	0.54	0.065	0.024	693	19	662	13	792	67	4
87	4781064	2456547	0.51	0.118	0.002	0.0205	0.0002	0.33	0.057	0.029	119	4	102	1	485	84	15
88	3539776	1460355	0.41	11.656	0.003	0.6096	0.0085	0.79	0.159	0.009	2464	18	2482	31	2449	19	-1
89	2364782	435554	0.18	0.101	0.003	0.0196	0.0003	0.40	0.057	0.029	113	4	97	2	479	84	15
90	1967267	699800	0.36	0.106	0.001	0.0168	0.0003	0.57	0.050	0.018	85	2	82	1	188	54	4
91	4118385	2312034	0.56	4.311	0.002	0.3597	0.0040	0.92	0.104	0.005	1643	11	1593	17	1707	11	3
92	1677007	285679	0.17	1.740	0.002	0.2028	0.0024	0.81	0.074	0.007	970	10	933	11	1054	18	4
93	3484928	1046632	0.30	0.147	0.002	0.0184	0.0004	0.43	0.057	0.033	110	5	93	2	503	95	16
94	2904958	414931	0.14	0.100	0.001	0.0181	0.0003	0.58	0.047	0.016	89	2	90	1	72	51	-1
95	1533337	907514	0.59	5.415	0.003	0.4081	0.0045	0.86	0.119	0.006	1846	12	1761	19	1943	14	5
96	2208616	499084	0.23	0.088	0.002	0.0173	0.0002	0.39	0.047	0.027	84	3	85	1	50	50	-1
97	1996631	633438	0.32	0.078	0.006	0.0192	0.0003	0.23	0.056	0.048	110	7	96	1	438	144	13
98	1860555	634430	0.34	0.162	0.002	0.0197	0.0002	0.32	0.057	0.029	117	4	99	1	503	86	15
99	1747668	253476	0.15	4.414	0.003	0.3577	0.0036	0.85	0.106	0.005	1652	11	1585	16	1739	13	4
100	915910	695061	0.76	3.100	0.002	0.3058	0.0037	0.81	0.088	0.008	1372	12	1361	16	1390	19	1
101	579778	209289	0.36	0.145	0.002	0.0201	0.0004	0.37	0.051	0.043	104	6	98	2	229	132	5
102	1858604	713425	0.38	2.709	0.002	0.2844	0.0031	0.80	0.085	0.007	1289	11	1277	14	1309	18	1

Table A-5: Zircon LA-ICP-MS U-Pb Isotopic Data and Ages   Sample GR-09-05:Pine Ridge Sandstone, Greater Green River Basin, WY

Grain #	U[a] [cps]	Th[a] [cps]	Th/U	Corrected isotopic ratios $^{207}Pb^{b}/^{235}U$	$\pm 2s^{d}$	$^{206}Pb^{b}/^{238}U$	$\pm 2s^{d}$	Rho[c]	$^{207}Pb^{e}/^{206}Pb$	$\pm 2s^{d}$	Ages (Ma)[f] $^{207}Pb/^{235}U$	±2s	$^{206}Pb/^{238}U$	±2s	$^{207}Pb/^{206}Pb$	±2s	Disc. %[g]
103	2396221	1167321	0.49	4.600	0.005	0.4176	0.0058	0.34	0.104	0.032	1730	37	1758	23	1696	78	-2
104	9363883	2480628	0.26	0.110	0.001	0.0180	0.0002	0.58	0.049	0.012	93	2	90	1	165	38	3
105	235915	192319	0.82	5.770	0.007	0.4204	0.0046	0.75	0.112	0.009	1825	14	1819	19	1832	20	0
106	579846	152725	0.26	5.842	0.004	0.4177	0.0046	0.75	0.112	0.008	1831	14	1821	19	1842	18	1
107	506383	157943	0.31	4.382	0.004	0.3935	0.0043	0.67	0.100	0.010	1678	15	1721	18	1623	24	-3
108	838622	213746	0.25	4.987	0.003	0.4005	0.0036	0.71	0.105	0.008	1732	12	1738	15	1724	18	0
109	14518112	3056120	0.21	0.746	0.003	0.0729	0.0012	0.67	0.097	0.016	565	12	350	6	1562	38	38
110	988522	1075922	1.09	10.930	0.004	0.5354	0.0064	0.72	0.166	0.009	2389	17	2233	25	2526	20	7
111	6857614	1498485	0.22	0.118	0.001	0.0200	0.0002	0.67	0.049	0.011	100	2	98	1	144	33	2
112	4455324	1683397	0.38	0.127	0.001	0.0202	0.0002	0.68	0.052	0.011	110	2	101	1	297	32	8
113	1555449	1181612	0.76	5.933	0.008	0.3417	0.0120	0.97	0.151	0.007	1906	31	1516	48	2362	15	20
114	2904076	730860	0.25	0.099	0.002	0.0184	0.0003	0.58	0.048	0.019	92	3	92	2	105	60	1
115	3088790	1153699	0.37	4.769	0.002	0.3979	0.0044	0.80	0.106	0.006	1735	13	1730	18	1742	17	0
116	2357789	821136	0.35	0.101	0.001	0.0177	0.0002	0.47	0.050	0.022	90	3	87	1	183	67	4
117	2442999	824250	0.34	0.110	0.001	0.0184	0.0002	0.58	0.049	0.016	94	2	91	1	172	47	3
118	1809854	740997	0.41	0.188	0.001	0.0325	0.0004	0.50	0.053	0.017	172	4	162	2	319	51	6
119	1192056	319824	0.27	1.439	0.004	0.1412	0.0025	0.86	0.092	0.009	906	13	692	13	1473	23	24
120	917098	389910	0.43	0.131	0.002	0.0178	0.0003	0.42	0.054	0.030	101	4	89	2	393	90	12
121	4149109	687110	0.17	4.772	0.002	0.3975	0.0040	0.73	0.112	0.008	1779	13	1735	17	1832	18	3
122	11589239	702030	0.06	0.099	0.005	0.0188	0.0002	0.20	0.065	0.053	126	8	94	1	775	150	25
123	2415084	769047	0.32	0.179	0.001	0.0334	0.0005	0.65	0.049	0.013	163	4	164	2	153	40	0
124	2951877	894511	0.30	0.181	0.001	0.0314	0.0004	0.62	0.049	0.013	156	3	156	2	146	38	0
125	424510	308470	0.73	3.670	0.004	0.3278	0.0039	0.81	0.092	0.008	1476	13	1473	17	1480	19	0
126	533494	150363	0.28	4.854	0.003	0.3937	0.0043	0.76	0.105	0.009	1727	14	1737	20	1715	20	-1
127	2888406	923404	0.32	0.103	0.001	0.0178	0.0002	0.62	0.049	0.015	91	2	90	1	129	45	2
128	774622	222302	0.29	4.638	0.003	0.3924	0.0039	0.80	0.105	0.006	1729	13	1734	18	1723	17	0
129	2726897	669370	0.25	2.688	0.002	0.2529	0.0030	0.87	0.092	0.005	1273	11	1162	14	1465	15	9
130	3594030	524233	0.15	0.205	0.005	0.0209	0.0004	0.42	0.093	0.032	199	8	108	2	1483	80	46
131	373315	225946	0.61	6.884	0.006	0.4694	0.0061	0.82	0.129	0.008	2047	15	2012	24	2083	18	2
132	777288	161819	0.21	0.101	0.002	0.0170	0.0004	0.55	0.051	0.027	92	4	86	2	255	80	7
133	779255	319550	0.41	0.134	0.002	0.0196	0.0004	0.40	0.050	0.034	104	5	99	2	215	103	5
134	2365045	575428	0.24	0.106	0.001	0.0191	0.0002	0.48	0.048	0.020	96	3	96	1	95	60	0
135	276813	113464	0.41	0.304	0.003	0.0209	0.0005	0.29	0.088	0.064	181	14	103	3	1382	164	43
136	493239	374779	0.76	4.759	0.004	0.4102	0.0041	0.75	0.104	0.009	1752	13	1793	19	1705	20	-2
137	2066560	346755	0.17	4.616	0.002	0.3943	0.0035	0.79	0.104	0.005	1725	12	1745	17	1701	15	-1
138	1161484	519475	0.45	2.658	0.006	0.2074	0.0056	0.97	0.110	0.007	1276	21	983	26	1811	17	23
139	2656996	596676	0.22	4.529	0.002	0.3814	0.0042	0.81	0.105	0.006	1700	13	1693	19	1710	17	0
140	1001792	399081	0.40	5.125	0.003	0.4198	0.0038	0.79	0.109	0.006	1821	12	1846	18	1793	17	-1
141	3049894	427276	0.14	0.107	0.004	0.0192	0.0003	0.40	0.058	0.035	116	5	96	2	552	99	17
142	6829870	771069	0.11	0.103	0.001	0.0193	0.0002	0.63	0.048	0.012	99	2	98	1	111	36	1
143	2010643	687970	0.34	4.528	0.002	0.3586	0.0039	0.81	0.105	0.007	1663	13	1619	19	1720	17	3
144	612008	264933	0.43	6.836	0.005	0.4852	0.0058	0.81	0.124	0.007	2050	14	2084	23	2017	16	-2
145	6920164	1916728	0.28	3.341	0.002	0.2862	0.0031	0.87	0.101	0.006	1456	12	1325	16	1652	15	9
146	1134702	194686	0.17	1.830	0.002	0.2154	0.0024	0.81	0.073	0.006	1019	10	1017	12	1024	18	0
147	854488	463091	0.54	3.532	0.002	0.3233	0.0039	0.78	0.091	0.009	1458	14	1464	18	1449	21	0
148	13572741	1024828	0.08	3.585	0.005	0.2108	0.0048	0.46	0.190	0.036	1710	44	997	22	2744	78	42
149	1440945	545918	0.38	3.655	0.003	0.3439	0.0069	0.88	0.092	0.008	1504	19	1533	29	1462	21	-2
150	3636268	948072	0.26	0.113	0.003	0.0186	0.0002	0.19	0.050	0.053	96	6	93	1	190	164	4
151	2549970	503400	0.20	0.109	0.001	0.0195	0.0002	0.57	0.048	0.015	98	2	98	1	91	46	0
152	15437481	3651371	0.24	0.112	0.001	0.0193	0.0002	0.75	0.050	0.008	102	2	97	1	212	26	5

Table A-5: Zircon LA-ICP-MS U-Pb Isotopic Data and Ages Sample GR-09-05:Pine Ridge Sandstone, Greater Green River Basin, WY

				Corrected isotopic ratios							Ages (Ma)[f]						
Grain #.	U[a] [cps]	Th[a] [cps]	Th/U	$^{207}Pb^{b}/^{235}U$	±2s[d]	$^{206}Pb^{b}/^{238}U$	±2s[d]	Rho[c]	$^{207}Pb^{e}/^{206}Pb$	±2s[d]	$^{207}Pb/^{235}U$	±2s	$^{206}Pb/^{238}U$	±2s	$^{207}Pb/^{206}Pb$	±2s	Disc. %[g]
153	1448488	687542	0.47	5.115	0.002	0.4045	0.0044	0.81	0.108	0.006	1785	14	1793	20	1775	17	0
154	3143953	844027	0.27	0.110	0.001	0.0195	0.0003	0.58	0.048	0.017	98	2	99	2	90	51	0
155	5437861	1517213	0.28	0.143	0.001	0.0173	0.0003	0.36	0.054	0.035	97	4	87	2	368	102	11
156	1089369	694971	0.64	0.857	0.002	0.1199	0.0016	0.68	0.060	0.013	590	10	583	8	618	35	1
157	1845519	612602	0.33	0.101	0.002	0.0177	0.0003	0.50	0.049	0.024	92	3	89	2	176	72	3
158	2607272	581659	0.22	0.098	0.001	0.0177	0.0002	0.56	0.047	0.017	89	2	90	1	74	51	-1
159	1535267	425976	0.28	4.664	0.002	0.3877	0.0039	0.86	0.103	0.006	1695	12	1704	18	1684	15	-1
160	761144	169006	0.22	1.894	0.003	0.2212	0.0027	0.74	0.073	0.009	1035	12	1039	13	1028	27	0

[a]U, Th, and Pb concentrations and Th/U ratios are calculated relative to GJ-1 zircon standard

[b]U-Pb fractionation correction and corrected for background interference based on GJ-1 zircon standard and Pb/U ratios are corrected according to Anderson (2002)

[c]Rho is the error correlation defined as the quotient of the propagated errors of the $^{206}Pb/^{238}U$ and the $^{207}/^{235}U$ ratio

[d]Quadratic addition of inter-run errors (2 SD) and daily reproducibility of GJ-1 (2 SD)

[e]Corrected for mass-bias by normalising to GJ-1 zircon standard (~.6 per atomic mass unit)

[f]U-Pb ages are calculated relative to GJ-1 zircon standard and corrected based on Anderson model (2002)

[g]Discordance %: for $^{206}Pb/^{238}U$ ages <1Ga calculated as ((1-($^{206}Pb/^{238}U$)/($^{207}Pb/^{235}U$))*100), for $^{206}Pb/^{238}U$ ages >1Ga calculated as ((1-($^{206}Pb/^{238}U$)/($^{207}Pb/^{206}Pb$))*100)

Table A-6: Zircon LA-ICP-MS U-Pb Isotopic Data and Ages Sample GR-09-09:Almond Formation, Greater Green River Basin, WY

Grain #.	U[a] [cps]	Th[a] [cps]	Th/U	Corrected isotopic ratios $^{207}Pb^{b}/^{235}U$	±2s[d]	$^{206}Pb^{b}/^{238}U$	±2s[d]	Rho[c]	$^{207}Pb^{e}/^{206}Pb$	±2s[d]	Ages (Ma)[f] $^{207}Pb/^{235}U$	±2s	$^{206}Pb/^{238}U$	±2s	$^{207}Pb/^{206}Pb$	±2s	Disc. %[g]
1	13566477	3180274	0.23	3.601	0.002	0.2253	0.0070	0.80	0.11356	0.024	1499	33	1265	38	1849	46	16
2	9462546	3789787	0.40	0.530	0.001	0.0749	0.0007	0.72	0.05766	0.010	456	7	446	6	507	27	2
3	5771852	811490	0.14	1.817	0.001	0.1873	0.0017	0.81	0.07517	0.009	1055	11	1051	13	1064	20	0
4	3765726	1300474	0.35	0.374	0.320	0.1976	0.0061	0.27	0.16786	0.110	1698	105	1109	34	2529	209	35
5	5370376	660266	0.12	4.176	0.002	0.3257	0.0023	0.80	0.1052	0.008	1729	13	1745	18	1710	17	-1
6	4707231	1783805	0.38	4.083	0.002	0.3102	0.0022	0.79	0.10704	0.009	1707	12	1679	16	1742	17	2
7	10254037	1636472	0.16	4.626	0.002	0.2996	0.0051	0.76	0.11368	0.015	1738	21	1645	28	1851	29	5
8	50469027	6523898	0.13	1.239	0.006	0.0725	0.0022	0.82	0.13446	0.021	833	22	430	13	2149	39	48
9	6345862	1591901	0.25	2.973	0.003	0.2376	0.0043	0.91	0.10182	0.008	1443	17	1308	24	1650	17	9
10	7299410	1355273	0.19	0.163	0.002	0.0169	0.0002	0.25	0.05663	0.052	120	6	104	1	468	124	14
11	4028710	1418747	0.35	3.868	0.002	0.3065	0.0031	0.72	0.10655	0.012	1699	15	1671	19	1733	22	2
12	17254623	389770	0.02	11.066	0.002	0.4792	0.0043	0.80	0.17792	0.009	2556	14	2469	25	2626	15	3
13	15197154	915863	0.06	1.465	0.001	0.1637	0.0020	0.67	0.07808	0.015	1000	13	937	12	1140	32	6
14	4434469	1048799	0.24	1.880	0.001	0.1916	0.0019	0.76	0.07649	0.011	1105	12	1108	13	1099	22	0
15	9375157	2382263	0.25	0.099	0.001	0.0146	0.0002	0.64	0.04979	0.018	94	2	91	1	175	45	3
16	14528474	2840559	0.20	0.116	0.014	0.0149	0.0003	0.18	0.07573	0.118	143	17	93	2	1079	266	35
17	6108864	1146948	0.19	17.249	0.008	0.5051	0.0167	0.61	0.21287	0.043	2740	55	2502	71	2921	73	9
18	5408620	1039813	0.19	0.088	0.002	0.0130	0.0002	0.48	0.05246	0.028	89	3	82	1	296	68	8
19	7080922	1312914	0.19	4.764	0.002	0.3365	0.0034	0.80	0.11226	0.008	1831	13	1833	19	1829	16	0
20	13192924	9232837	0.70	1.455	0.001	0.1535	0.0015	0.71	0.07432	0.012	941	11	899	10	1042	24	5
21	5570783	1094870	0.20	0.429	0.002	0.0486	0.0005	0.31	0.0585	0.039	327	12	297	4	540	90	9
22	3828435	985731	0.26	3.407	0.002	0.2652	0.0027	0.75	0.10202	0.011	1569	13	1508	16	1654	21	4
23	8596053	1462830	0.17	4.216	0.003	0.3039	0.0036	0.82	0.1105	0.009	1737	14	1685	21	1800	16	3
24	41794173	12521597	0.30	0.674	0.003	0.0439	0.0009	0.85	0.09981	0.013	488	10	284	6	1613	24	42
25	12862294	1293700	0.10	2.758	0.002	0.2078	0.0025	0.82	0.10489	0.009	1409	13	1222	16	1705	17	13
26	6232428	2011068	0.32	1.124	0.001	0.1321	0.0013	0.80	0.06767	0.009	805	8	789	9	850	19	2
27	22345887	4833852	0.22	0.518	0.001	0.0612	0.0009	0.79	0.06472	0.011	441	7	383	6	757	23	13
28	30532144	29329315	0.96	1.481	0.010	0.0578	0.0038	0.98	0.18722	0.014	895	40	345	22	2711	23	61
29	5382904	5730194	1.06	0.439	0.001	0.0602	0.0007	0.81	0.05549	0.010	385	5	379	5	423	23	2
30	1569159	629568	0.40	3.994	0.003	0.2934	0.0026	0.69	0.10197	0.012	1658	13	1663	16	1653	22	0
31	12560632	4601777	0.37	0.094	0.001	0.0156	0.0002	0.54	0.04876	0.020	100	2	99	1	127	48	1
32	14704089	184422	0.01	0.445	0.001	0.0627	0.0006	0.79	0.05522	0.009	399	5	396	4	412	20	1
34	22180354	5006205	0.23	0.101	0.001	0.0146	0.0001	0.52	0.0493	0.018	96	2	94	1	153	43	2
35	2235206	597623	0.27	6.909	0.004	0.3956	0.0040	0.71	0.13545	0.012	2154	15	2144	22	2163	21	0
36	6726171	2832596	0.42	0.131	0.001	0.0149	0.0002	0.32	0.05645	0.039	112	4	96	1	461	89	14
37	865182	928299	1.07	1.554	0.003	0.1604	0.0024	0.64	0.07338	0.019	976	16	958	14	1017	39	2
38	4144009	792184	0.19	1.746	0.002	0.1739	0.0014	0.77	0.07587	0.009	1055	9	1041	10	1084	18	1
39	5153057	1420864	0.28	3.325	0.003	0.2231	0.0036	0.94	0.11332	0.007	1531	14	1314	20	1846	13	14
40	16559168	5921773	0.36	0.606	0.001	0.0737	0.0007	0.58	0.06656	0.016	525	8	460	5	816	34	12
41	4062753	1654070	0.41	4.056	0.002	0.2947	0.0027	0.71	0.10283	0.010	1685	12	1699	15	1669	19	-1
42	8517457	3087907	0.36	4.171	0.002	0.2885	0.0026	0.77	0.10769	0.009	1702	11	1661	15	1754	17	2
43	2679569	659673	0.25	2.272	0.002	0.2150	0.0017	0.60	0.08332	0.012	1279	11	1285	11	1269	24	0
44	5050011	849466	0.17	2.147	0.001	0.2101	0.0019	0.77	0.07702	0.009	1202	9	1252	11	1114	18	-4
45	5566656	1506734	0.27	4.201	0.002	0.3000	0.0021	0.82	0.10809	0.007	1732	9	1709	14	1761	13	1
46	12243833	1783745	0.15	3.865	0.002	0.2509	0.0023	0.67	0.111	0.011	1616	12	1473	13	1809	20	9
47	10454448	6231413	0.60	2.327	0.002	0.2100	0.0025	0.76	0.0896	0.011	1306	13	1244	15	1410	21	5
48	4636764	1379234	0.30	0.594	0.001	0.0751	0.0009	0.72	0.06283	0.013	519	7	480	6	694	28	8
49	16936552	391582	0.02	0.490	0.001	0.0649	0.0006	0.62	0.05564	0.012	417	6	414	4	430	27	1
50	40043664	8068895	0.20	1.372	0.003	0.0827	0.0016	0.71	0.12446	0.020	909	17	524	10	2015	34	42
51	8105600	1367107	0.17	1.970	0.002	0.1518	0.0014	0.53	0.09067	0.014	1105	12	946	9	1433	27	14

Table A-6: Zircon LA-ICP-MS U-Pb Isotopic Data and Ages Sample GR-09-09:Almond Formation, Greater Green River Basin, WY

				Corrected isotopic ratios							Ages (Ma)[f]						
Grain #.	U[a] [cps]	Th[a] [cps]	Th/U	$^{207}Pb^{b}/^{235}U$	±2s[d]	$^{206}Pb^{b}/^{238}U$	±2s[d]	Rho[c]	$^{207}Pb^{e}/^{206}Pb$	±2s[d]	$^{207}Pb/^{235}U$	±2s	$^{206}Pb/^{238}U$	±2s	$^{207}Pb/^{206}Pb$	±2s	Disc. %[g]
52	3572297	1091468	0.31	0.677	0.002	0.0792	0.0015	0.59	0.06368	0.013	553	10	513	10	723	28	7
53	9748287	1215710	0.12	4.031	0.002	0.2509	0.0020	0.83	0.12349	0.008	1721	11	1500	13	2001	14	13
54	23462801	18764735	0.80	5.429	0.004	0.2372	0.0064	0.77	0.17588	0.014	1940	27	1378	35	2608	24	29
55	13389264	3015211	0.23	3.432	0.002	0.2420	0.0036	0.90	0.107	0.008	1545	14	1405	20	1742	15	9
56	928635	292559	0.32	11.026	0.006	0.4379	0.0057	0.89	0.18377	0.010	2563	16	2416	28	2681	17	6
57	2401773	1012780	0.42	3.036	0.003	0.2414	0.0027	0.82	0.09687	0.019	1484	17	1433	17	1558	34	3
58	5903235	1821078	0.31	3.618	0.002	0.2724	0.0025	0.59	0.10301	0.009	1636	11	1607	16	1672	17	2
59	3814898	1193828	0.31	3.847	0.002	0.2791	0.0028	0.79	0.10314	0.010	1656	13	1641	17	1675	19	1
60	4703252	1453109	0.31	2.393	0.004	0.1797	0.0038	0.75	0.10789	0.010	1358	18	1119	23	1758	19	18
61	41458897	3940116	0.10	0.999	0.002	0.0472	0.0007	0.92	0.14488	0.018	699	12	313	5	2280	30	55
62	10172890	2321888	0.23	2.780	0.003	0.1418	0.0031	0.65	0.12098	0.024	1191	23	812	18	1964	42	32
63	2253427	1004926	0.45	0.811	0.002	0.0933	0.0012	0.70	0.06074	0.018	602	10	597	8	622	37	1
64	3415251	1638358	0.48	3.875	0.002	0.2819	0.0031	0.64	0.10489	0.010	1685	13	1668	19	1706	19	1
65	16095163	7379262	0.46	0.521	0.001	0.0680	0.0005	0.81	0.05704	0.016	453	6	446	4	485	34	1
67	7787736	1373259	0.18	0.899	0.001	0.1035	0.0008	0.53	0.06267	0.011	672	7	666	6	690	22	1
68	54429740	13928690	0.26	3.326	0.002	0.2253	0.0025	0.71	0.11053	0.012	1555	14	1380	16	1802	20	11
69	8064228	2023759	0.25	0.088	0.001	0.0138	0.0002	0.76	0.04829	0.022	94	2	93	2	105	50	1
70	50787589	16755410	0.33	1.237	0.002	0.0713	0.0013	0.63	0.12869	0.008	851	12	462	9	2074	16	46
71	48671757	5998220	0.12	2.850	0.007	0.1184	0.0044	0.90	0.15184	0.049	1326	45	782	28	2361	81	41
72	10776145	4000513	0.37	0.689	0.001	0.0855	0.0009	0.63	0.06318	0.015	590	9	560	7	707	30	5
73	6496556	1532471	0.24	4.684	0.002	0.3119	0.0022	0.68	0.1129	0.007	1840	11	1839	16	1840	15	0
74	2975369	789903	0.27	2.418	0.002	0.2120	0.0023	0.77	0.08725	0.011	1332	12	1315	16	1359	19	1
75	14339127	2087401	0.15	2.855	0.002	0.1999	0.0022	0.81	0.10428	0.008	1412	12	1233	15	1695	17	13
76	3818983	1515957	0.40	4.815	0.002	0.3331	0.0027	0.81	0.10533	0.006	1839	11	1952	19	1714	13	-6
77	1284060	232915	0.18	3.841	0.005	0.2916	0.0105	0.85	0.10434	0.020	1822	36	1934	62	1696	35	-6
78	5376675	1532942	0.29	7.839	0.005	0.3181	0.0045	0.88	0.18364	0.011	2300	17	1897	26	2680	17	18
79	1666665	377866	0.23	1.907	0.003	0.1848	0.0020	0.84	0.07888	0.012	1160	12	1159	14	1162	22	0
80	5996999	692784	0.12	1.879	0.002	0.1840	0.0020	0.76	0.0801	0.011	1169	12	1156	15	1193	20	1
81	11007816	3246707	0.29	0.092	0.002	0.0128	0.0003	0.82	0.04981	0.023	92	3	89	2	178	50	4
82	15175964	384671	0.03	0.462	0.001	0.0489	0.0008	0.73	0.05898	0.024	357	9	327	6	559	49	8
83	100206599	15361114	0.15	0.576	0.003	0.0191	0.0002	0.66	0.19861	0.018	449	8	130	2	2809	28	71
84	9103527	4278435	0.47	0.483	0.002	0.0617	0.0006	0.64	0.06373	0.026	469	10	419	5	726	52	11
85	6742762	983693	0.15	0.102	0.001	0.0145	0.0002	0.44	0.05173	0.020	109	3	102	1	266	44	6
86	70537688	55493997	0.79	0.494	0.002	0.0233	0.0002	0.58	0.16032	0.011	446	6	159	2	2454	17	64
87	6226969	1817996	0.29	3.991	0.002	0.2932	0.0023	0.75	0.10365	0.006	1735	11	1778	17	1684	13	-2
88	8325293	963597	0.12	1.421	0.003	0.0938	0.0025	0.85	0.10047	0.016	873	19	607	16	1627	30	31
89	14128680	1292724	0.09	4.172	0.002	0.2862	0.0026	0.87	0.10731	0.010	1745	13	1742	20	1748	19	0
90	3178170	2244110	0.71	4.780	0.003	0.3024	0.0030	0.81	0.11679	0.012	1869	16	1840	21	1902	22	2
91	36792452	9091444	0.25	1.409	0.005	0.0946	0.0014	0.72	0.1895	0.058	1322	42	630	10	2733	90	52
92	2439382	491296	0.20	2.089	0.003	0.1852	0.0017	0.30	0.07909	0.013	1183	13	1191	14	1168	26	-1
93	3485093	906570	0.26	2.007	0.002	0.1697	0.0020	0.72	0.07597	0.011	1102	13	1108	15	1088	22	-1
94	12172168	3767478	0.31	0.099	0.001	0.0135	0.0002	0.79	0.04937	0.021	97	2	95	2	158	45	2
95	11503853	4197106	0.36	0.527	0.090	0.0184	0.0019	0.68	0.22155	0.232	493	96	131	13	2987	390	73
96	10820039	1629725	0.15	0.579	0.002	0.0462	0.0007	0.43	0.08535	0.022	488	10	330	6	1317	39	32
97	7670640	1724479	0.22	11.637	0.003	0.4446	0.0040	0.65	0.18809	0.009	2652	15	2562	28	2720	15	3
98	3723839	1525142	0.41	3.817	0.002	0.2441	0.0039	0.81	0.10806	0.012	1613	18	1502	26	1761	22	7
99	1747668	253476	0.15	4.414	0.003	0.3577	0.0036	0.86	0.106	0.005	1652	11	1585	16	1739	13	4
100	915910	695061	0.76	3.100	0.002	0.3058	0.0037	0.81	0.088	0.008	1372	12	1361	16	1390	19	1

[a]U, Th, and Pb concentrations and Th/U ratios are calculated relative to GJ-1 zircon standard

[b]U-Pb fractionation correction and corrected for background interference based on GJ-1 zircon standard and Pb/U ratios are corrected according to Anderson (2002)

Table A-6: Zircon LA-ICP-MS U-Pb Isotopic Data and Ages   Sample GR-09-09:Almond Formation, Greater Green River Basin, WY

				Corrected isotopic ratios							Ages (Ma)[f]						
Grain #.	U[a] [cps]	Th[a] [cps]	Th/U	$^{207}Pb^{b}/^{235}U$	±2s[d]	$^{206}Pb^{b}/^{238}U$	±2s[d]	Rho[c]	$^{207}Pb^{e}/^{206}Pb$	±2s[d]	$^{207}Pb/^{235}U$	±2s	$^{206}Pb/^{238}U$	±2s	$^{207}Pb/^{206}Pb$	±2s	Disc. %[g]

[c]Rho is the error correlation defined as the quotient of the propagated errors of the $^{206}Pb/^{238}U$ and the $^{207/235}U$ ratio

[d]Quadratic addition of inter-run errors (2 SD) and daily reproducibility of GJ-1 (2 SD)

[e]Corrected for mass-bias by normalising to GJ-1 zircon standard (~.6 per atomic mass unit)

[f]U-Pb ages are calculated relative to GJ-1 zircon standard and corrected based on Anderson model (2002)

[g]Discordance %: for $^{206}Pb/^{238}U$ ages <1Ga calculated as ((1-($^{206}Pb/^{238}U$)/($^{207}Pb/^{235}U$))*100), for $^{206}Pb/^{238}U$ ages >1Ga calculated as ((1-($^{206}Pb/^{238}U$)/($^{207}Pb/^{206}Pb$))*100)

Table B-1: Rutile LA-ICP-MS U-Pb Isotopic Data and Ages   Sample: GR-09-19: Dad Member, Greater Green River Basin, WY

				Corrected isotopic ratios							Ages (Ma)[f]						
Grain #.	U[a] [ppm]	Th[a] [ppm]	U/Th	$^{207}Pb^{b}/^{235}U$	±2s[d]	$^{206}Pb^{b}/^{238}U$	±2s[d]	Rho[c]	$^{207}Pb^{e}/^{206}Pb$	±2s[d]	$^{207}Pb/^{235}U$	±2s	$^{206}Pb/^{238}U$	±2s	$^{207}Pb/^{206}Pb$	±2s	Disc. %[g]
1	266	278	0.96	2.89	0.27	0.208	0.013	0.90	0.101	0.004	1390	61	1212	71	1628	75	13
2	29	0	125.44	3.33	0.25	0.260	0.010	0.98	0.094	0.002	1492	52	1489	53	1507	43	0
3	12	0	181.23	5.01	0.85	0.316	0.029	0.99	0.115	0.008	1760	130	1760	140	1870	130	0
4	6	0	18.03	6.28	0.96	0.352	0.029	0.97	0.125	0.009	1930	140	1920	140	2000	120	1
5	9	131	0.07	43.70	5.20	0.569	0.056	0.96	0.554	0.023	3840	120	2900	220	4397	59	24
6	56	b.d.	na	1.54	0.17	0.131	0.011	0.73	0.084	0.004	946	76	793	62	1282	83	16
7	18	b.d.	na	5.71	0.70	0.322	0.016	0.87	0.123	0.007	1895	91	1797	77	1977	93	5
8	7	84	0.08	36.60	6.90	0.550	0.075	0.97	0.476	0.035	3600	190	2840	330	4150	110	21
9	72	b.d.	na	0.43	0.03	0.057	0.004	0.99	0.054	0.001	360	23	358	22	372	30	1
10	27	1	20.31	5.23	0.32	0.332	0.011	0.97	0.114	0.003	1859	51	1847	52	1864	51	1
11	0	7	0.07	84.00	84.00	0.980	0.980	0.92	0.720	0.720	4500.0	4500	4400	4400	4800	4800	2
12	15	13	1.16	7.10	1.20	0.367	0.027	0.95	0.130	0.010	2020	130	2000	130	2010	110	1
13	3	b.d.	na	72.00	28.00	0.760	0.210	0.99	0.636	0.064	4290	400	3520	720	4570	150	18
14	2	15	0.11	61.00	11.00	0.788	0.099	0.99	0.531	0.037	4100	210	3650	360	4290	110	11
15	0	b.d.	na	1.38	0.29	0.093	0.015	0.73	0.113	0.016	810	110	570	87	1660	260	30
16	14	93	0.15	9.14	0.82	0.217	0.012	0.99	0.302	0.010	2330	80	1261	65	3476	52	46
17	31	241	0.13	7.21	0.66	0.314	0.013	0.92	0.166	0.009	2147	77	1754	63	2548	84	18
18	22	107	0.21	13.80	3.20	0.272	0.055	0.97	0.392	0.032	2780	260	1600	290	3860	120	42
19	21	7	2.86	0.13	0.01	0.016	0.001	0.33	0.062	0.008	127	12	104.6	6.1	530	200	18
20	5	2	3.58	0.86	0.12	0.087	0.006	0.85	0.069	0.003	617	57	539	36	871	77	13
21	10	73	0.14	11.30	1.50	0.325	0.021	0.88	0.252	0.024	2520	140	1810	100	3100	170	28
22	31	47	0.66	2.92	0.19	0.096	0.005	0.98	0.220	0.004	1375	49	592	30	2978	27	57
23	8	294	0.03	11.70	2.20	0.407	0.040	0.97	0.189	0.019	2410	180	2170	180	2660	170	10
24	53	b.d.	na	2.27	0.18	0.170	0.009	0.99	0.095	0.003	1186	56	1010	47	1522	57	15
25	4	b.d.	na	20.40	4.50	0.566	0.062	0.98	0.239	0.029	2950	220	2860	250	3020	190	3
26	3	57	0.05	18.00	6.70	0.278	0.074	0.99	0.407	0.057	2610	380	1490	350	3820	210	43
27	40	262	0.15	2.04	0.26	0.136	0.008	0.65	0.104	0.010	1094	78	820	42	1610	150	25
28	61	5	12.08	0.62	0.03	0.074	0.003	1.00	0.061	0.000	490	16	458	15	640	17	7
29	70	b.d.	na	0.09	0.01	0.013	0.001	1.00	0.048	0.000	84.2	5.8	83.4	5.7	104.4	7.4	1
30	7	15	0.46	0.68	0.38	0.019	0.012	1.00	0.236	0.010	450	270	150	78	3086	68	67
31	23	18	1.22	3.26	0.45	0.220	0.012	0.97	0.100	0.005	1427	87	1279	66	1607	81	10
32	1	19	0.05	100.00	100.00	0.950	0.950	0.67	0.780	0.780	4700	4700	4300	4300	4900	4900	9
34	23	b.d.	na	4.27	0.54	0.292	0.021	0.99	0.104	0.005	1650	100	1640	100	1682	88	1
35	51	119	0.43	13.30	1.00	0.319	0.016	0.95	0.306	0.007	2692	70	1779	77	3498	35	34
36	71	b.d.	na	4.16	0.44	0.293	0.019	0.99	0.106	0.005	1668	93	1648	95	1732	82	1
37	43	231	0.19	0.13	0.03	0.016	0.001	0.98	0.055	0.006	117	20	102	7.3	152	11	13
38	7	74	0.09	4.29	0.57	0.113	0.012	0.98	0.278	0.009	1680	120	698	71	3358	51	58
39	5	71	0.07	12.10	1.30	0.303	0.022	0.96	0.293	0.010	2590	100	1700	110	3433	58	34
40	65	3600	0.02	34.00	26.00	0.450	0.270	0.99	0.436	0.093	3000	830	2000	1000	3980	310	33
41	57	462	0.12	10.50	1.50	0.436	0.029	0.97	0.170	0.013	2460	130	2340	120	2510	120	5
42	10	b.d.	na	8.40	1.10	0.421	0.025	0.99	0.142	0.011	2240	120	2250	110	2210	130	0
43	2	6	0.40	150.00	150.00	1.400	1.300	1.00	0.796	0.042	5000	1100	5300	3500	4915	76	-6
44	36	b.d.	na	0.10	0.01	0.014	0.001	0.98	0.048	0.000	92.4	4.6	92	4.9	101.4	5.3	0
45	10	58	0.17	11.30	2.60	0.390	0.050	0.96	0.197	0.025	2460	220	2100	230	2740	220	15
46	65	6	11.87	0.14	0.03	0.015	0.001	0.86	0.065	0.009	130	22	98.4	6.8	560	230	24
47	1	b.d.	na	0.54	0.06	0.067	0.006	0.99	0.059	0.001	439	36	418	35	553	38	5
48	14	94	0.14	4.40	0.39	0.254	0.013	0.91	0.123	0.005	1709	75	1457	67	1979	73	15
49	10	11	0.87	31.70	5.70	0.528	0.059	0.96	0.400	0.032	3540	180	2730	240	3910	140	23
50	13	92	0.14	5.05	0.87	0.217	0.017	0.87	0.174	0.023	1750	150	1259	90	2410	220	28
51	16	75	0.21	6.05	0.81	0.312	0.023	0.98	0.139	0.009	1970	120	1740	110	2190	120	12
52	61	266	0.23	5.98	0.66	0.320	0.019	0.97	0.131	0.007	1924	95	1781	92	2084	93	7

Table B-1: Rutile LA-ICP-MS U-Pb Isotopic Data and Ages Sample: GR-09-19: Dad Member, Greater Green River Basin, WY

Grain #.	U[a] [ppm]	Th[a] [ppm]	U/Th	Corrected isotopic ratios: $^{207}Pb^{b}/^{235}U$	±2s[d]	$^{206}Pb^{b}/^{238}U$	±2s[d]	Rho[c]	$^{207}Pb^{e}/^{206}Pb$	±2s[d]	Ages (Ma)[f]: $^{207}Pb/^{235}U$	±2s	$^{206}Pb/^{238}U$	±2s	$^{207}Pb/^{206}Pb$	±2s	Disc. %[g]
53	12	b.d.	na	0.58	0.04	0.074	0.005	0.99	0.058	0.001	462	26	461	28	536	51	0
54	2	b.d.	na	8.13	0.92	0.392	0.024	0.99	0.145	0.008	2220	100	2140	110	2315	89	4
55	46	3	17.21	0.56	0.04	0.072	0.005	1.00	0.056	0.001	451	29	448	28	450	29	1
56	5	4	1.10	0.90	0.19	0.085	0.007	0.88	0.072	0.009	614	82	526	44	870	170	14
57	1	1	2.14	13.20	6.00	0.268	0.060	0.99	0.222	0.066	1880	400	1460	280	2280	460	22
58	11	19	0.58	62.00	14.00	0.800	0.130	0.99	0.557	0.036	4050	250	3650	460	4370	100	10
59	46	19	2.37	5.96	0.60	0.344	0.017	0.98	0.123	0.006	1936	79	1903	79	1978	80	2
60	2	3	0.72	6.49	0.87	0.178	0.017	0.93	0.270	0.011	2030	110	1065	96	3307	67	48
61	38	11	3.31	0.42	0.13	0.027	0.004	0.98	0.094	0.016	318	84	168	28	1140	330	47
62	40	1	45.34	0.16	0.04	0.018	0.002	0.87	0.066	0.010	147	31	114	11	590	250	22
63	11	119	0.09	68.00	11.00	0.726	0.090	0.99	0.668	0.028	4240	160	3440	330	4651	61	19
64	3	4	0.88	3.92	0.52	0.243	0.024	0.92	0.114	0.008	1570	120	1390	130	1820	120	11
65	71	b.d.	na	0.09	0.01	0.014	0.001	0.99	0.049	0.002	87.2	5.3	86.9	5.3	122	45	0
67	b.d.	1	na	39.00	15.00	0.640	0.200	0.96	0.535	0.090	3830	430	3120	740	4300	240	19
68	20	b.d.	na	0.10	0.01	0.015	0.001	1.00	0.048	0.000	97	5.2	95.8	5.1	120.7	7.6	1
69	16	31	0.50	b.d.	na	1.100	1.500	0.95	7.500	4.000	5920	800	5390	930	6740	790	9
70	2	b.d.	na	5.32	0.51	0.331	0.020	0.98	0.119	0.005	1865	84	1834	95	1915	74	2
71	24	7	3.33	11.10	2.00	0.441	0.031	0.97	0.168	0.014	2420	130	2340	140	2500	130	3
72	252	381	0.66	0.91	0.07	0.098	0.006	0.99	0.067	0.001	648	36	600	33	829	40	7
73	1	5	0.12	87.00	20.00	0.920	0.150	0.97	0.659	0.054	4460	250	4140	520	4630	120	7
74	14	6	2.49	4.30	0.70	0.180	0.014	0.90	0.166	0.020	1620	150	1061	76	2350	220	35
75	10	6	1.65	1.52	0.28	0.089	0.008	0.70	0.121	0.017	870	110	547	47	1720	260	37
76	22	32	0.69	7.69	0.78	0.194	0.015	0.97	0.280	0.011	2160	100	1138	80	3347	67	47
77	1	b.d.	na	0.09	0.02	0.013	0.003	0.96	0.059	0.006	92	15	80	16	540	200	13
78	25	550	0.05	134.00	98.00	1.270	0.860	0.99	0.764	0.026	4760	800	4900	2400	4855	49	-3
79	13	b.d.	na	6.03	0.40	0.361	0.013	0.99	0.120	0.004	1962	57	1983	59	1945	60	-1
80	20	b.d.	na	330.00	430.00	0.510	0.460	0.91	2.600	3.300	2960	830	2910	880	3050	820	2
81	64	60	1.07	0.10	0.01	0.016	0.001	1.00	0.048	0.000	100.7	7.5	100.2	7.4	114.2	8.9	0
82	b.d.	2	na	66.00	19.00	0.850	0.160	0.99	0.486	0.066	3910	320	3770	510	4090	230	4
83	52	2	30.71	0.10	0.00	0.015	0.000	1.00	0.049	0.000	99.5	3	98.6	3	123.8	4.4	1
84	130	26	5.01	0.09	0.01	0.014	0.001	0.99	0.049	0.001	91.2	4.9	90.8	4.7	120	37	0
85	120	1	91.60	0.11	0.01	0.017	0.001	1.00	0.049	0.000	110.1	5.7	110.3	5.9	132	11	0
86	27	540	0.05	16.10	2.40	0.276	0.030	0.97	0.415	0.025	2920	140	1580	140	3981	86	46
87	9	3	2.75	2.10	0.19	0.186	0.010	0.98	0.081	0.003	1131	59	1098	56	1203	62	3
88	22	48	0.47	7.46	0.59	0.400	0.015	0.98	0.137	0.005	2167	67	2166	71	2176	58	0
89	16	2	8.57	9.51	0.64	0.453	0.016	0.99	0.147	0.006	2368	62	2405	69	2294	70	-2
90	4	1	4.01	0.49	0.05	0.060	0.005	0.95	0.059	0.001	407	35	374	32	568	45	8
91	24	1	42.63	0.56	0.05	0.072	0.005	1.00	0.057	0.001	446	31	445	30	482	45	0
92	5	b.d.	na	0.57	0.05	0.071	0.005	0.99	0.058	0.001	452	33	439	31	522	45	3
93	4	1	4.88	0.57	0.06	0.068	0.006	0.98	0.059	0.001	452	40	423	35	558	47	6
94	1	7	0.16	110.00	120.00	0.900	1.000	0.98	0.791	0.015	5242	22	3700	4100	4905	27	29
95	b.d.	1	na	45.40	6.40	0.559	0.072	0.83	0.560	0.110	3880	150	2850	300	4470	210	27
96	22	b.d.	na	1.16	0.06	0.127	0.005	0.99	0.066	0.001	778	27	769	27	808	32	1
97	19	74	0.25	30.90	4.90	0.415	0.053	0.97	0.526	0.024	3410	160	2200	240	4302	67	35
98	4	b.d.	na	0.64	0.03	0.080	0.003	0.98	0.056	0.001	499	18	498	19	468	35	0
99	6	b.d.	na	0.64	0.03	0.081	0.003	0.99	0.058	0.001	506	17	502	18	530	22	1
100	22	898	0.02	4.53	0.44	0.290	0.016	0.99	0.111	0.005	1736	88	1651	85	1836	87	5
101	4	b.d.	na	7.40	0.73	0.394	0.018	0.96	0.135	0.007	2156	84	2135	81	2136	91	1
102	1	4	0.28	3.23	0.46	0.238	0.022	0.98	0.096	0.006	1440	120	1400	120	1510	120	3
103	4	31	0.12	15.50	3.10	0.483	0.040	0.98	0.213	0.020	2700	150	2510	170	2860	130	7
104	20	24	0.84	6.60	1.10	0.357	0.029	0.96	0.127	0.009	1930	120	1950	130	2040	120	-1

Table B-1: Rutile LA-ICP-MS U-Pb Isotopic Data and Ages Sample: GR-09-19: Dad Member, Greater Green River Basin, WY

				Corrected isotopic ratios							Ages (Ma)[f]						
Grain #.	U[a] [ppm]	Th[a] [ppm]	U/Th	$^{207}Pb^{b}/^{235}U$	±2s[d]	$^{206}Pb^{b}/^{238}U$	±2s[d]	Rho[c]	$^{207}Pb^{e}/^{206}Pb$	±2s[d]	$^{207}Pb/^{235}U$	±2s	$^{206}Pb/^{238}U$	±2s	$^{207}Pb/^{206}Pb$	±2s	Disc. %[g]
105	3	1	2.09	1.60	1.40	0.037	0.018	0.98	0.159	0.042	640	340	230	110	2250	530	64
106	8	2	3.99	6.19	0.96	0.352	0.029	0.99	0.126	0.009	1980	130	1950	140	2030	120	2
107	7	1	8.63	0.66	0.07	0.080	0.006	1.00	0.059	0.002	510	40	497	38	525	43	3
108	7	b.d.	na	5.58	0.70	0.340	0.024	0.99	0.116	0.006	1890	110	1880	120	1906	98	1
109	36	b.d.	na	0.10	0.01	0.015	0.001	1.00	0.048	0.000	94.9	7.2	94.4	7.1	106.5	9	1
110	40	64	0.63	3.07	0.22	0.231	0.010	0.99	0.095	0.003	1417	56	1346	56	1529	51	5
111	5	17	0.28	12.00	1.60	0.465	0.034	0.98	0.186	0.014	2580	140	2440	150	2700	130	5

[a]U and Th concentrations and Th/U ratios calculated relative to the R10 rutile standard using 287±76 ppm for U and 8.4±2.6 ppm for Th (Jackson, 2004)

[b]Corrected for U-Pb fractionation and background and normalised to R10 rutile standard ID-TIMS values (Jackson, 2004) and Pb/U ratios are corrected according to Anderson (2002)

[c]Error correlation defined as the quotient of the propagated errors of the $^{206}Pb/^{238}U$ and the $^{207}/^{235}U$ ratio

[d]The propagated error of quadratic addition of internal errors (2 SD) and within run reproducibility of R10 (2 SD)

[e]Corrected for mass-bias by normalising to R10 rutile standard (~.6 per atomic mass unit)

[f]U-Pb ages are calculated relative to R10 rutile standard and corrected for common Pb using Anderson (2002)

[g]Discordance %: for $^{206}Pb/^{238}U$ ages <1Ga calculated as $((1-(^{206}Pb/^{238}U)/(^{207}Pb/^{235}U))*100)$, for $^{206}Pb/^{238}U$ ages >1Ga calculated as $((1-(^{206}Pb/^{238}U)/(^{207}Pb/^{206}Pb))*100)$

b.d.= below detection limit

na = not applicable

Table B-2: Rutile LA-ICP-MS U-Pb Isotopic Data and Ages Sample: GR-09-09: Pine Ridge Sandstone, Greater Green River Basin, WY

				Corrected isotopic ratios							Ages (Ma)[f]						
Grain #.	U[a] [ppm]	Th[a] [ppm]	U/Th	$^{207}Pb^{b}/^{235}U$	±2s[d]	$^{206}Pb^{b}/^{238}U$	±2s[d]	Rho[c]	$^{207}Pb^{e}/^{206}Pb$	±2s[d]	$^{207}Pb/^{235}U$	±2s	$^{206}Pb/^{238}U$	±2s	$^{207}Pb/^{206}Pb$	±2s	Disc. %[g]
1	15	b.d.	na	30.00	17.00	0.660	0.250	0.98	0.390	0.120	3460	650	3130	920	3740	480	10
2	2	b.d.	na	37.00	20.00	0.540	0.260	0.98	0.510	0.150	3400	1000	2600	1100	4100	590	24
3	3	57	0.05	9.80	2.20	0.289	0.032	0.93	0.229	0.031	2250	210	1620	160	2880	250	28
4	11	915	0.01	26.50	4.90	0.492	0.057	0.96	0.377	0.031	3260	180	2540	240	3850	120	22
5	12	b.d.	na	9.70	1.10	0.240	0.019	0.95	0.302	0.011	2430	110	1380	100	3468	54	43
6	20	b.d.	na	14.30	1.10	0.283	0.017	0.96	0.362	0.010	2758	76	1614	81	3773	40	41
7	27	b.d.	na	65.00	13.00	0.720	0.110	0.98	0.653	0.044	4170	220	3410	390	4610	100	18
8	8	4	1.86	14.20	2.10	0.270	0.033	0.97	0.382	0.020	2750	160	1520	170	3833	84	45
9	86	0	1190.28	5.34	0.48	0.333	0.017	0.98	0.115	0.004	1848	75	1846	83	1866	63	0
10	81	325	0.25	0.36	0.03	0.046	0.003	0.75	0.057	0.001	312	18	290	16	485	23	7
11	8	3	2.71	9.90	1.20	0.241	0.020	0.95	0.299	0.012	2400	110	1380	100	3452	65	43
12	7	1	7.18	0.28	0.04	0.023	0.002	0.45	0.089	0.012	246	32	148	10	1170	270	40
13	21	2	11.45	1.11	0.09	0.049	0.004	0.95	0.167	0.004	747	45	308	21	2524	43	59
14	2	b.d.	na	45.20	5.60	0.670	0.055	0.98	0.495	0.031	3820	130	3280	210	4213	90	14
15	11	62	0.18	2.57	0.34	0.137	0.009	0.42	0.138	0.017	1240	100	832	55	2020	230	33
16	67	0	820.99	0.36	0.13	0.025	0.004	0.98	0.082	0.016	273	84	159	27	1010	360	42
17	20	4	4.99	0.49	0.08	0.029	0.003	0.81	0.117	0.013	387	56	185	17	1720	270	52
18	11	7	1.63	5.26	0.53	0.280	0.015	0.86	0.136	0.009	1826	91	1589	79	2130	110	13
19	45	375	0.12	18.10	2.40	0.415	0.026	0.94	0.303	0.026	2920	150	2230	120	3400	160	24
20	3	45	0.07	17.80	2.40	0.433	0.027	0.91	0.294	0.025	2930	140	2330	130	3370	140	20
21	27	3920	0.01	4.82	0.52	0.143	0.011	0.95	0.245	0.007	1768	84	860	65	3152	50	51
22	8	1340	0.01	7.20	1.10	0.298	0.021	0.84	0.156	0.014	2040	130	1680	100	2350	140	18
23	2	2	1.15	0.37	0.08	0.025	0.003	0.90	0.116	0.014	302	54	160	21	1650	290	47
24	3	b.d.	na	94.00	19.00	1.050	0.170	0.98	0.631	0.036	4540	230	4570	540	4572	85	-1
25	3	b.d.	na	260.00	160.00	2.300	1.300	1.00	0.810	0.046	5590	650	7500	2600	4938	82	-34
26	6	103	0.06	8.50	1.80	0.200	0.029	0.96	0.280	0.019	2120	190	1160	150	3330	110	45
27	2	17	0.12	52.00	12.00	0.660	0.130	0.98	0.615	0.040	4080	260	3180	490	4530	93	22
28	5	78	0.07	13.00	1.70	0.265	0.025	0.96	0.343	0.012	2610	120	1500	130	3666	53	43
29	1	7	0.13	61.00	56.00	0.650	0.400	0.99	0.510	0.120	3890	910	3100	1500	4250	340	20
30	8	154	0.05	9.10	1.50	0.273	0.026	0.89	0.244	0.025	2380	160	1570	140	3110	180	34
31	13	12	1.09	23.90	7.30	0.341	0.063	0.99	0.422	0.043	2940	250	1830	280	3980	140	38
32	51	9	5.78	0.39	0.03	0.051	0.003	0.98	0.055	0.001	329	20	322	18	408	42	2
34	8	1250	0.01	9.70	1.40	0.326	0.022	0.85	0.212	0.022	2370	140	1810	110	2850	180	24
35	18	b.d.	na	54.00	12.00	0.800	0.110	1.00	0.485	0.043	3960	210	3680	360	4160	130	7
36	5	b.d.	na	61.00	10.00	0.782	0.091	0.97	0.557	0.030	4090	160	3650	330	4397	75	11
37	13	34	0.39	6.30	1.00	0.287	0.021	0.88	0.146	0.013	1950	140	1620	110	2240	130	17
38	7	17	0.42	27.90	5.80	0.493	0.058	0.99	0.388	0.035	3310	210	2550	240	3920	130	23
39	22	6	3.79	1.21	0.08	0.052	0.003	0.89	0.167	0.003	798	34	329	16	2522	27	59
40	8	20	0.41	4.26	0.82	0.126	0.018	0.98	0.247	0.015	1640	160	760	100	3170	100	54
41	64	b.d.	na	0.11	0.01	0.015	0.001	0.59	0.049	0.000	103	6	99	5	154	9	4
42	30	b.d.	na	6.50	1.20	0.289	0.025	0.92	0.144	0.012	1940	150	1620	120	2240	150	16
43	20	b.d.	na	0.60	0.11	0.038	0.003	0.78	0.111	0.014	464	67	241	19	1570	280	48
44	9	17	0.54	4.04	0.54	0.119	0.013	0.98	0.247	0.009	1590	100	719	74	3156	55	55
45	20	b.d.	na	0.15	0.02	0.016	0.001	0.78	0.068	0.009	135	20	104	5	650	240	23
46	13	15	0.87	35.10	9.50	0.471	0.076	0.99	0.486	0.030	3400	180	2420	310	4176	90	29
47	178	30	5.93	0.86	0.09	0.083	0.005	0.30	0.070	0.004	627	48	515	28	862	45	18
48	59	28	2.11	0.62	0.08	0.064	0.004	0.53	0.071	0.009	494	52	400	22	850	170	19
49	48	27	1.77	0.59	0.04	0.073	0.004	0.99	0.058	0.001	470	27	456	26	528	34	3
50	3	b.d.	na	5.37	0.82	0.167	0.018	0.87	0.247	0.012	1830	140	990	100	3144	80	46

Table B-2: Rutile LA-ICP-MS U-Pb Isotopic Data and Ages Sample: GR-09-09: Pine Ridge Sandstone, Greater Green River Basin, WY

				Corrected isotopic ratios							Ages (Ma)[f]						
Grain #.	U[a] [ppm]	Th[a] [ppm]	U/Th	$^{207}Pb^{b}/^{235}U$	±2s[d]	$^{206}Pb^{b}/^{238}U$	±2s[d]	Rho[c]	$^{207}Pb^{e}/^{206}Pb$	±2s[d]	$^{207}Pb/^{235}U$	±2s	$^{206}Pb/^{238}U$	±2s	$^{207}Pb/^{206}Pb$	±2s	Disc. %[g]
51	1	1	1.32	3.00	1.30	0.102	0.024	0.98	0.160	0.031	1100	250	610	140	2140	390	45
52	36	b.d.	na	1.95	0.16	0.179	0.009	0.99	0.080	0.002	1096	51	1057	50	1178	53	4
53	2	b.d.	na	430.00	640.00	1.260	0.530	0.83	1.800	2.000	5300	1200	5100	1500	5400	1100	4
54	19	b.d.	na	4.60	0.45	0.275	0.016	0.98	0.121	0.006	1735	83	1560	79	1959	81	10
55	6	b.d.	na	0.70	0.18	0.070	0.005	0.91	0.063	0.005	481	45	435	32	680	110	10
56	9	b.d.	na	0.51	0.05	0.060	0.003	0.58	0.058	0.001	415	34	373	19	536	51	10
57	61	24	2.55	5.73	0.71	0.158	0.016	0.97	0.280	0.010	1970	110	941	87	3360	54	52
58	17	b.d.	na	5.72	0.40	0.358	0.016	0.99	0.118	0.004	1949	67	1969	74	1923	63	-1
59	1	1	1.54	4.50	1.30	0.228	0.030	0.95	0.113	0.012	1490	180	1300	150	1750	170	13
60	8	b.d.	na	12.40	2.00	0.386	0.031	0.91	0.222	0.022	2550	140	2090	140	2940	150	18
61	12	b.d.	na	14.50	4.40	0.357	0.052	0.99	0.249	0.041	2450	270	1930	240	3080	300	21
62	0	2	0.10	84.00	20.00	0.890	0.170	0.99	0.685	0.051	4550	290	4050	570	4728	91	11
63	143	30	4.72	10.30	1.90	0.340	0.032	0.91	0.210	0.025	2350	180	1870	150	2770	190	20
64	1	1	0.44	14.70	2.60	0.280	0.037	0.97	0.360	0.022	2660	180	1570	180	3723	92	41
65	53	74	0.71	14.90	5.60	0.257	0.059	0.99	0.323	0.047	2330	300	1410	280	3550	200	39
67	42	10	4.10	4.39	0.39	0.305	0.016	0.99	0.107	0.004	1712	74	1712	80	1753	71	0
68	14	7	1.92	77.00	24.00	0.800	0.210	0.99	0.671	0.053	4310	350	3610	790	4650	120	16
69	3	b.d.	na	0.40	0.05	0.046	0.004	0.61	0.057	0.001	348	42	289	22	481	42	17
70	1	1	1.62	1.30	0.15	0.126	0.010	0.93	0.073	0.003	828	63	760	59	975	70	8
71	17	32	0.53	17.10	3.80	0.540	0.053	0.97	0.202	0.019	2730	170	2700	190	2770	150	1
72	9	44	0.20	33.70	6.20	0.470	0.065	0.99	0.527	0.035	3490	190	2430	270	4300	100	30
73	5	23	0.23	33.70	4.60	0.571	0.051	0.94	0.427	0.029	3580	140	2990	200	3990	100	16
74	26	2	12.32	2.89	0.19	0.236	0.010	0.98	0.088	0.003	1366	50	1363	49	1397	64	0
75	130	20	6.47	0.91	0.18	0.063	0.004	0.82	0.104	0.016	632	93	395	25	1410	280	38
76	5	b.d.	na	2.00	0.42	0.152	0.017	0.95	0.085	0.007	1040	130	905	92	1240	140	13
77	24	14	1.77	4.09	0.37	0.280	0.015	0.99	0.105	0.004	1648	75	1599	75	1689	72	3
78	17	70	0.25	6.21	0.52	0.164	0.011	0.97	0.272	0.007	1994	70	977	58	3321	40	51
79	17	45	0.38	2.01	0.20	0.069	0.006	0.96	0.207	0.004	1109	62	426	35	2881	34	62
80	7	9	0.73	12.70	2.00	0.358	0.021	0.94	0.247	0.026	2620	140	1970	100	3180	170	25
81	30	b.d.	na	0.56	0.04	0.073	0.004	0.98	0.057	0.001	450	23	452	22	472	32	0
82	24	9	2.53	3.58	0.73	0.108	0.017	0.98	0.234	0.015	1440	150	653	95	3050	100	55
83	39	45	0.86	50.00	7.00	0.561	0.067	0.93	0.626	0.022	3950	130	2830	280	4574	47	28
84	45	b.d.	na	0.50	0.02	0.066	0.002	0.98	0.056	0.001	410	14	409	14	452	22	0
85	14	b.d.	na	0.97	0.06	0.111	0.005	0.99	0.065	0.002	687	28	679	28	755	56	1
86	22	b.d.	na	6.59	0.40	0.381	0.012	0.98	0.125	0.004	2044	53	2076	55	2021	50	-2
87	3	8	0.38	4.16	0.66	0.197	0.014	0.81	0.156	0.020	1620	130	1155	73	2300	210	29
88	35	22	1.60	0.51	0.05	0.063	0.006	0.99	0.059	0.001	423	37	399	35	550	46	6
89	4	b.d.	na	0.50	0.05	0.064	0.006	0.99	0.057	0.001	403	35	397	35	479	46	1
90	19	45	0.41	103.00	19.00	1.120	0.150	0.98	0.632	0.038	4620	200	4770	460	4567	93	-3
91	13	27	0.47	125.00	29.00	1.130	0.230	0.98	0.762	0.061	4950	330	4790	760	4850	120	3
92	5	b.d.	na	0.55	0.05	0.069	0.005	1.00	0.058	0.001	442	30	430	30	514	32	3
93	2	9	0.23	88.00	19.00	0.950	0.170	0.99	0.651	0.040	4490	240	4190	580	4610	93	7
94	65	74	0.88	4.13	0.62	0.171	0.013	0.71	0.177	0.020	1610	120	1028	70	2460	220	36
95	15	b.d.	na	0.63	0.03	0.079	0.003	0.99	0.057	0.001	497	16	492	15	510	20	1
96	12	59	0.20	37.00	6.80	0.522	0.071	0.98	0.526	0.036	3650	230	2640	310	4300	100	28
97	5	1	7.32	1.64	0.19	0.157	0.012	0.99	0.074	0.003	962	69	936	68	1035	74	3
98	78	486	0.16	1.30	0.22	0.083	0.006	0.60	0.113	0.016	806	90	511	36	1620	250	37
99	17	b.d.	na	0.49	0.07	0.047	0.003	0.43	0.085	0.013	395	45	293	21	1060	260	26
100	186	b.d.	na	1.05	0.18	0.059	0.004	0.69	0.119	0.016	689	89	368	26	1790	300	47

Table B-2: Rutile LA-ICP-MS U-Pb Isotopic Data and Ages Sample: GR-09-09: Pine Ridge Sandstone, Greater Green River Basin, WY

				Corrected isotopic ratios							Ages (Ma)[f]						
Grain #.	U[a] [ppm]	Th[a] [ppm]	U/Th	$^{207}Pb^{b}/^{235}U$	±2s[d]	$^{206}Pb^{b}/^{238}U$	±2s[d]	Rho[c]	$^{207}Pb^{e}/^{206}Pb$	±2s[d]	$^{207}Pb/^{235}U$	±2s	$^{206}Pb/^{238}U$	±2s	$^{207}Pb/^{206}Pb$	±2s	Disc. %[g]
101	19	4	5.11	0.57	0.04	0.072	0.005	0.99	0.058	0.002	451	28	446	28	526	62	1

[a]U and Th concentrations and Th/U ratios calculated relative to the R10 rutile standard using 287±76 ppm for U and 8.4±2.6 ppm for Th (Jackson, 2004)
[b]Corrected for U-Pb fractionation and background and normalised to R10 rutile standard ID-TIMS values (Jackson, 2004) and Pb/U ratios are corrected according to Anderson (2002)
[c]Error correlation defined as the quotient of the propagated errors of the $^{206}Pb/^{238}U$ and the $^{207}/^{235}U$ ratio
[d]The propagated error of quadratic addition of internal errors (2 SD) and within run reproducibility of R10 (2 SD)
[e]Corrected for mass-bias by normalising to R10 rutile standard (~.6 per atomic mass unit)
[f]U-Pb ages are calculated relative to R10 rutile standard and corrected for common Pb using Anderson (2002)
[g]Discordance %: for $^{206}Pb/^{238}U$ ages <1Ga calculated as $((1-(^{206}Pb/^{238}U)/(^{207}Pb/^{235}U))*100)$, for $^{206}Pb/^{238}U$ ages >1Ga calculated as $((1-(^{206}Pb/^{238}U)/(^{207}Pb/^{206}Pb))*100)$
b.d.= below detection limit
na = not applicable

Table B-3: Rutile LA-ICP-MS U-Pb Isotopic Data and Ages   Sample: GR-09-14: Almond Formation , Greater Green River Basin, WY

				Corrected isotopic ratios							Ages (Ma)[f]						
Grain #.	U[a] [ppm]	Th[a] [ppm]	U/Th	$^{207}Pb^{b}/^{235}U$	±2s[d]	$^{206}Pb^{b}/^{238}U$	±2s[d]	Rho[c]	$^{207}Pb^{e}/^{206}Pb$	±2s[d]	$^{207}Pb/^{235}U$	±2s	$^{206}Pb/^{238}U$	±2s	$^{207}Pb/^{206}Pb$	±2s	Disc. %[g]
1	53	21	2.49	5.26	0.53	0.332	0.019	0.98	0.115	0.005	1828	85	1840	90	1869	76	-1
2	10	b.d.	na	1.00	0.08	0.108	0.006	0.97	0.066	0.001	709	35	662	32	804	43	7
3	4	b.d.	na	2.74	0.61	0.187	0.027	0.98	0.094	0.009	1230	170	1090	150	1450	190	11
4	27	1	40.15	0.61	0.06	0.071	0.005	0.77	0.060	0.001	487	40	441	32	582	47	9
5	25	34	0.72	6.04	0.74	0.296	0.019	0.98	0.141	0.008	1930	100	1666	94	2228	98	14
6	8	b.d.	na	5.01	0.69	0.312	0.024	0.99	0.114	0.007	1760	110	1740	120	1820	110	1
7	5	3	1.67	6.18	0.80	0.313	0.024	0.98	0.137	0.008	1940	120	1740	120	2160	110	10
8	9	8	1.17	86.00	14.00	0.960	0.120	0.98	0.632	0.025	4480	160	4320	370	4573	58	4
9	23	b.d.	na	5.42	0.56	0.338	0.021	0.99	0.116	0.005	1875	89	1885	96	1871	84	-1
10	2	9	0.26	7.10	1.70	0.162	0.025	0.99	0.290	0.023	1950	190	950	130	3390	120	51
11	12	b.d.	na	0.59	0.05	0.073	0.005	0.99	0.058	0.001	466	29	454	27	523	35	3
12	26	4	6.63	0.09	0.00	0.014	0.001	1.00	0.048	0.000	89.4	3.6	88.1	3.7	108.8	4.5	1
13	66	328	0.20	4.98	0.38	0.156	0.009	0.99	0.230	0.005	1797	63	934	50	3047	33	48
14	18	b.d.	na	0.11	0.01	0.014	0.001	0.58	0.055	0.006	105	12	91.8	9	320	160	13
15	2	b.d.	na	0.91	0.24	0.045	0.007	0.93	0.155	0.018	620	110	281	45	2280	270	55
16	28	991	0.03	1.76	0.21	0.077	0.006	0.86	0.180	0.006	1030	74	478	34	2642	55	54
17	30	34	0.89	0.11	0.01	0.015	0.001	1.00	0.049	0.000	101.6	6	98.8	5.3	130.6	9.1	3
18	49	107	0.46	0.25	0.02	0.033	0.003	0.66	0.053	0.001	224	19	211	16	333	30	6
19	34	1	28.10	0.38	0.13	0.025	0.004	0.99	0.081	0.016	285	86	159	26	940	330	44
20	5	6	0.89	1.56	0.38	0.066	0.013	0.97	0.165	0.010	860	140	407	78	2504	99	53
21	7	b.d.	na	0.61	0.19	0.031	0.007	0.97	0.139	0.017	429	98	196	40	2010	300	54
22	2	12	0.18	7.20	1.60	0.319	0.031	0.94	0.148	0.018	1980	170	1770	150	2210	180	11
23	4	b.d.	na	0.70	0.08	0.080	0.005	0.62	0.061	0.002	516	37	494	31	630	59	4
24	19	b.d.	na	4.66	0.42	0.306	0.016	0.99	0.112	0.005	1763	81	1732	81	1828	73	2
25	22	16	1.35	2.79	0.20	0.223	0.011	0.99	0.091	0.003	1348	56	1295	56	1434	53	4
26	87	b.d.	na	0.09	0.00	0.014	0.001	1.00	0.048	0.000	90.2	3.4	89.8	3.4	100.3	4.9	0
27	67	b.d.	na	0.69	0.07	0.086	0.007	0.99	0.061	0.002	527	41	528	40	643	73	0
28	75	b.d.	na	6.10	1.20	0.361	0.038	0.98	0.117	0.010	1960	170	1990	180	1920	150	-2
29	3	6	0.54	7.00	1.30	0.309	0.023	0.96	0.146	0.010	1990	120	1730	110	2260	110	13
30	8	1	5.28	10.00	11.00	0.098	0.077	0.87	0.129	0.082	480	280	370	170	700	380	23
31	8	b.d.	na	7.20	1.00	0.374	0.028	0.96	0.139	0.013	2060	130	2030	130	2140	140	1
32	7	2	2.90	0.11	0.01	0.015	0.001	0.52	0.049	0.000	102.7	9.6	93.2	7.5	148	17	9
34	8	236	0.03	30.00	16.00	0.370	0.150	0.99	0.411	0.087	2780	650	2000	690	3740	380	28
35	21	b.d.	na	4.81	0.68	0.313	0.025	0.99	0.111	0.007	1780	130	1770	130	1800	120	1
36	16	b.d.	na	7.40	1.50	0.379	0.039	0.97	0.130	0.012	2030	160	2050	180	2020	150	-1
37	14	99	0.14	8.70	1.40	0.385	0.030	0.97	0.154	0.012	2210	140	2080	140	2330	130	6
38	2	b.d.	na	0.54	0.09	0.052	0.006	0.62	0.077	0.011	425	56	323	37	960	230	24
39	18	37	0.49	0.67	0.12	0.050	0.003	0.78	0.097	0.014	495	72	311	18	1290	280	37
40	16	b.d.	na	4.81	0.63	0.308	0.023	0.98	0.121	0.009	1730	110	1720	110	1910	130	1
41	39	57	0.68	2.70	0.22	0.218	0.011	1.00	0.091	0.003	1325	58	1266	56	1430	59	4
42	3	b.d.	na	5.38	0.52	0.324	0.017	0.98	0.118	0.005	1849	80	1806	82	1905	80	2
43	10	b.d.	na	5.60	0.54	0.333	0.017	0.99	0.120	0.006	1898	84	1847	81	1951	89	3
44	18	b.d.	na	4.97	0.44	0.320	0.016	0.99	0.110	0.004	1788	73	1784	78	1793	60	0
45	114	b.d.	na	3.99	0.24	0.286	0.011	0.98	0.100	0.002	1629	50	1622	53	1626	45	0
46	15	8	2.03	6.76	0.71	0.361	0.019	0.99	0.133	0.007	2040	92	1996	96	2110	92	2
47	17	b.d.	na	4.71	0.56	0.304	0.021	0.99	0.110	0.006	1724	97	1700	100	1783	98	1
48	18	4	4.49	4.86	0.44	0.312	0.015	0.98	0.116	0.006	1770	74	1745	74	1865	85	1
49	3	b.d.	na	0.93	0.09	0.098	0.006	0.96	0.068	0.002	658	46	602	35	857	67	9
50	19	b.d.	na	0.13	0.02	0.015	0.001	0.69	0.067	0.009	124	19	92.5	6.9	710	250	25

Table B-3: Rutile LA-ICP-MS U-Pb Isotopic Data and Ages Sample: GR-09-14: Almond Formation , Greater Green River Basin, WY

				Corrected isotopic ratios							Ages (Ma)[f]						
Grain #.	U[a] [ppm]	Th[a] [ppm]	U/Th	$^{207}Pb^{b}/^{235}U$	±2s[d]	$^{206}Pb^{b}/^{238}U$	±2s[d]	Rho[c]	$^{207}Pb^{e}/^{206}Pb$	±2s[d]	$^{207}Pb/^{235}U$	±2s	$^{206}Pb/^{238}U$	±2s	$^{207}Pb/^{206}Pb$	±2s	Disc. %[g]
51	18	b.d.	na	0.55	0.03	0.071	0.003	1.00	0.056	0.000	444	19	440	19	462	18	1
52	48	2180	0.02	2.50	0.19	0.206	0.009	1.00	0.087	0.002	1260	47	1208	46	1349	47	4
53	19	b.d.	na	5.05	0.41	0.325	0.014	0.99	0.116	0.004	1830	68	1813	70	1885	70	1
54	49	b.d.	na	4.56	0.47	0.314	0.019	0.99	0.109	0.005	1747	88	1752	93	1770	75	0
55	34	b.d.	na	4.45	0.41	0.307	0.016	0.98	0.108	0.004	1723	76	1722	81	1746	70	0
56	8	b.d.	na	0.75	0.08	0.086	0.006	0.98	0.062	0.001	559	41	529	36	655	42	5
57	45	8	5.70	6.00	0.58	0.351	0.017	0.98	0.124	0.006	1943	80	1935	82	1996	83	0
58	1	b.d.	na	37.30	8.70	0.507	0.093	0.98	0.545	0.040	3740	230	2730	380	4360	110	27
59	43	b.d.	na	5.48	0.75	0.330	0.025	0.99	0.117	0.007	1870	120	1850	130	1900	110	1
60	30	5	5.63	5.97	0.83	0.347	0.025	0.98	0.123	0.008	1910	110	1910	120	1950	110	0
61	31	1860	0.02	5.73	0.95	0.333	0.030	0.99	0.122	0.008	1920	140	1860	140	1950	120	3
62	5	6	0.80	1.61	0.10	0.155	0.007	0.99	0.075	0.001	970	36	930	36	1062	36	4
63	75	6	11.84	0.10	0.01	0.014	0.001	1.00	0.048	0.000	92.8	5.5	92.2	5.4	106.9	6.1	1
64	3	1	2.76	1.01	0.09	0.105	0.007	0.75	0.068	0.002	708	42	643	38	872	52	9
65	10	b.d.	na	4.88	0.77	0.307	0.026	0.98	0.111	0.007	1720	130	1710	130	1770	120	1
67	7	2	3.42	0.47	0.07	0.051	0.008	0.93	0.066	0.007	377	49	321	49	700	160	15
68	8	b.d.	na	0.28	0.06	0.019	0.002	0.93	0.097	0.014	237	46	122	12	1330	310	49
69	9	b.d.	na	5.09	0.53	0.325	0.017	0.99	0.114	0.005	1815	79	1807	83	1854	79	0
70	0	2	0.26	19.30	5.60	0.415	0.062	0.94	0.307	0.043	2870	270	2190	280	3400	240	24
71	67	b.d.	na	4.39	0.53	0.295	0.021	0.99	0.110	0.006	1680	100	1680	110	1770	100	0
72	17	b.d.	na	4.16	0.53	0.287	0.022	0.98	0.106	0.006	1620	100	1620	110	1700	110	0
73	44	1	51.83	5.27	0.58	0.331	0.021	0.98	0.111	0.005	1821	96	1830	100	1790	83	0
74	b.d.	b.d.	na	5.80	1.90	0.166	0.037	0.94	0.231	0.029	1680	240	960	200	2950	240	43
75	27	b.d.	na	4.96	0.82	0.316	0.029	0.99	0.111	0.007	1750	140	1760	140	1800	110	-1
76	7	b.d.	na	0.47	0.02	0.059	0.002	0.99	0.056	0.001	386	17	369	14	464	25	4
77	27	b.d.	na	8.90	1.40	0.417	0.033	0.97	0.148	0.011	2240	140	2230	150	2260	120	0
78	28	b.d.	na	8.70	1.40	0.408	0.034	0.98	0.149	0.011	2210	140	2190	160	2300	130	1
79	26	b.d.	na	0.56	0.04	0.072	0.004	1.00	0.057	0.001	450	25	445	25	475	29	1
80	10	14	0.76	1.95	0.45	0.079	0.011	0.95	0.168	0.019	1000	140	487	62	2370	270	51
81	36	b.d.	na	0.50	0.04	0.066	0.005	1.00	0.056	0.001	416	31	409	30	452	33	2
82	15	b.d.	na	5.27	0.49	0.327	0.016	0.98	0.116	0.004	1836	77	1820	79	1886	69	1
83	6	b.d.	na	0.54	0.16	0.026	0.005	0.98	0.128	0.015	380	83	165	29	1890	280	57
84	94	b.d.	na	4.91	0.81	0.308	0.030	0.99	0.108	0.007	1710	140	1710	150	1720	120	0
85	7	b.d.	na	0.41	0.05	0.053	0.006	0.98	0.055	0.001	339	36	332	35	389	35	2
86	8	b.d.	na	0.51	0.05	0.065	0.006	1.00	0.057	0.001	417	35	406	33	483	41	3
87	7	3	2.31	2.10	0.29	0.090	0.006	0.86	0.161	0.016	1100	100	555	33	2340	230	50
88	21	b.d.	na	0.50	0.03	0.066	0.004	0.99	0.056	0.002	412	22	409	22	450	49	1
89	77	b.d.	na	0.11	0.01	0.017	0.001	1.00	0.049	0.000	108.3	8.4	107.4	8.3	126.7	8.9	1
90	1	b.d.	na	2.91	0.81	0.084	0.016	0.98	0.230	0.011	1290	160	516	90	3042	69	60
91	13	b.d.	na	0.23	0.07	0.021	0.002	0.93	0.077	0.015	202	53	133	14	800	330	34
92	15	b.d.	na	6.02	0.63	0.359	0.022	0.99	0.120	0.006	1954	96	1970	100	1937	82	-1
93	113	b.d.	na	4.74	0.49	0.310	0.018	0.98	0.110	0.005	1754	89	1734	90	1779	84	1
94	10	1	10.93	0.25	0.05	0.020	0.002	0.79	0.087	0.012	219	37	129.1	9.4	1110	280	41
95	4	4	1.13	31.90	7.70	0.488	0.078	0.98	0.450	0.042	3410	240	2560	350	4040	140	25
96	25	b.d.	na	5.33	0.36	0.339	0.013	0.98	0.115	0.003	1879	56	1878	62	1876	44	0
97	4	b.d.	na	0.88	0.13	0.092	0.008	0.96	0.065	0.002	606	54	566	45	755	70	7
98	8	16	0.49	6.70	1.20	0.284	0.025	0.83	0.159	0.019	1970	150	1600	120	2430	200	19
99	20	17	1.17	1.75	0.25	0.062	0.007	0.98	0.200	0.008	1014	95	384	44	2824	62	62
100	201	b.d.	na	0.11	0.00	0.016	0.001	1.00	0.048	0.000	104.1	3.7	103.7	3.7	110.7	5.2	0

Table B-3: Rutile LA-ICP-MS U-Pb Isotopic Data and Ages Sample: GR-09-14: Almond Formation , Greater Green River Basin, WY

				Corrected isotopic ratios							Ages (Ma)[f]						
Grain #.	U[a] [ppm]	Th[a] [ppm]	U/Th	$^{207}Pb^{b}/^{235}U$	±2s[d]	$^{206}Pb^{b}/^{238}U$	±2s[d]	Rho[c]	$^{207}Pb^{e}/^{206}Pb$	±2s[d]	$^{207}Pb/^{235}U$	±2s	$^{206}Pb/^{238}U$	±2s	$^{207}Pb/^{206}Pb$	±2s	Disc. %[g]
101	33	550	0.06	9.80	2.70	0.215	0.035	0.98	0.292	0.023	2140	160	1190	150	3440	110	44
102	33	6	5.32	5.31	0.52	0.327	0.018	0.97	0.117	0.006	1836	82	1817	85	1882	87	1
103	5	1	3.78	0.63	0.05	0.076	0.005	1.00	0.059	0.001	489	30	472	29	567	35	3
104	11	2	6.50	0.15	0.01	0.022	0.001	1.00	0.050	0.000	142	8.8	141.1	8.8	176	13	1
105	21	256	0.08	25.50	8.80	0.359	0.089	0.98	0.476	0.057	3150	350	1940	420	4130	180	38
106	163	b.d.	na	0.08	0.01	0.012	0.001	1.00	0.049	0.001	80.3	5.9	79.7	5.9	101	35	1
107	30	b.d.	na	0.11	0.00	0.016	0.001	1.00	0.048	0.000	101.8	4.3	101.2	4.3	113.8	5.2	1
108	4	b.d.	na	0.82	0.07	0.094	0.006	0.98	0.063	0.001	601	35	576	34	716	44	4
109	87	30	2.87	0.12	0.01	0.018	0.001	1.00	0.049	0.000	116.9	7.2	116.2	7.1	132	8.8	1
110	148	b.d.	na	0.08	0.00	0.013	0.001	1.00	0.048	0.000	82	3.3	81.4	3.3	101.9	3.9	1
111	5	b.d.	na	6.00	1.30	0.317	0.023	0.91	0.121	0.008	1840	110	1760	110	1930	110	4
112	22	b.d.	na	7.30	1.30	0.381	0.033	0.98	0.132	0.010	2060	140	2060	150	2070	120	0
113	9	28	0.32	0.73	0.05	0.082	0.005	0.75	0.065	0.001	555	29	507	27	762	31	9

[a]U and Th concentrations and Th/U ratios calculated relative to the R10 rutile standard using 287±76 ppm for U and 8.4±2.6 ppm for Th (Jackson, 2004)

[b]Corrected for U-Pb fractionation and background and normalised to R10 rutile standard ID-TIMS values (Jackson, 2004) and Pb/U ratios are corrected according to Anderson (2002)

[c]Error correlation defined as the quotient of the propagated errors of the $^{206}Pb/^{238}U$ and the $^{207}/^{235}U$ ratio

[d]The propagated error of quadratic addition of internal errors (2 SD) and within run reproducibility of R10 (2 SD)

[e]Corrected for mass-bias by normalising to R10 rutile standard (~.6 per atomic mass unit)

[f]U-Pb ages are calculated relative to R10 rutile standard and corrected for common Pb using Anderson (2002)

[g]Discordance %: for $^{206}Pb/^{238}U$ ages <1Ga calculated as $((1-(^{206}Pb/^{238}U)/(^{207}Pb/^{235}U))*100)$. for $^{206}Pb/^{238}U$ ages >1Ga calculated as $((1-(^{206}Pb/^{238}U)/(^{207}Pb/^{206}Pb))*100)$

b.d.= below detection limit

na = not applicable

Table B-4: Rutile LA-ICP-MS U-Pb Isotopic Data and Ages Sample: GR-09-05: Fox Hills Sandstone, Greater Green River Basin, WY

				Corrected isotopic ratios							Ages (Ma)[f]						
Grain #.	U[a] [ppm]	Th[a] [ppm]	U/Th	$^{207}Pb^{b}/^{235}U$	±2s[d]	$^{206}Pb^{b}/^{238}U$	±2s[d]	Rho[c]	$^{207}Pb^{e}/^{206}Pb$	±2s[d]	$^{207}Pb/^{235}U$	±2s	$^{206}Pb/^{238}U$	±2s	$^{207}Pb/^{206}Pb$	±2s	Disc. %[g]
1	26	b.d.	na	0.15	0.03	0.016	0.001	0.85	0.063	0.010	136	28	102.4	6.9	520	260	25
2	36	b.d.	na	0.09	0.01	0.014	0.001	0.53	0.049	0.000	87.9	4.7	86.8	4.7	123.7	7.3	1
3	19	43	0.45	37.80	2.70	0.624	0.028	0.96	0.450	0.010	3686	75	3110	110	4081	32	16
4	1	b.d.	na	4.18	0.80	0.157	0.015	0.84	0.185	0.024	1550	160	932	85	2460	270	40
5	41	19	2.16	0.81	0.52	0.056	0.014	0.98	0.058	0.005	390	120	346	84	460	140	11
6	20	8	2.45	2.94	0.17	0.213	0.008	0.99	0.099	0.002	1381	44	1245	41	1606	41	10
7	82	b.d.	na	4.36	0.55	0.301	0.023	0.99	0.101	0.005	1680	110	1690	110	1665	96	-1
8	17	b.d.	na	0.08	0.01	0.013	0.001	1.00	0.048	0.000	80.9	5.7	80.6	5.7	91.7	6.5	0
9	10	b.d.	na	5.58	0.42	0.346	0.014	0.98	0.122	0.004	1913	64	1911	69	1979	57	0
10	3	b.d.	na	0.50	0.04	0.064	0.004	1.00	0.056	0.001	410	26	402	25	459	25	2
11	0	b.d.	na	21.70	8.40	0.357	0.077	0.98	0.357	0.068	2710	380	1890	340	3470	340	30
12	6	b.d.	na	0.11	0.01	0.014	0.001	0.68	0.050	0.002	100.1	9.7	90.8	5.9	135	10	9
13	5	29	0.17	31.80	8.50	0.512	0.070	0.99	0.381	0.053	3200	260	2600	280	3700	240	19
14	23	94	0.24	0.38	0.02	0.050	0.003	1.00	0.055	0.001	326	17	313	16	417	22	4
15	14	b.d.	na	0.44	0.07	0.024	0.003	0.98	0.140	0.005	360	49	150	16	2217	63	58
16	6	17	0.32	9.10	1.20	0.194	0.019	0.98	0.330	0.013	2290	130	1140	110	3609	61	50
17	3	2	1.96	0.70	0.14	0.080	0.012	0.98	0.062	0.003	523	80	493	72	648	93	6
18	4	12	0.33	88.00	16.00	0.860	0.140	0.99	0.752	0.028	4610	170	4230	470	4829	54	8
19	5	1	3.89	34.00	12.00	0.440	0.130	0.99	0.485	0.058	3190	420	2200	550	4180	180	31
20	8	b.d.	na	0.10	0.01	0.014	0.001	0.79	0.050	0.003	98	10	86.5	7.5	147	12	12
21	53	40	1.35	0.08	0.01	0.012	0.001	1.00	0.048	0.000	79	4.7	78.9	4.7	83	4.7	0
22	143	b.d.	na	3.59	0.18	0.122	0.005	0.99	0.214	0.002	1551	39	742	29	2935	18	52
23	2	b.d.	na	5.20	1.40	0.218	0.024	0.88	0.139	0.024	1620	210	1280	130	2040	270	21
24	5	5	0.95	14.40	2.90	0.272	0.036	0.99	0.368	0.030	2700	210	1540	180	3740	130	43
25	1	b.d.	na	4.33	0.62	0.262	0.021	0.96	0.116	0.008	1630	110	1490	110	1850	110	9
26	2	2	1.16	7.00	2.00	0.339	0.042	0.57	0.138	0.016	2010	200	1870	200	2150	180	7
27	14	b.d.	na	0.10	0.01	0.015	0.001	1.00	0.049	0.000	94.5	4.8	92.9	4.6	131.1	8.9	2
28	5	b.d.	na	0.18	0.03	0.020	0.001	0.85	0.061	0.007	152	21	125.6	8	450	180	17
29	18	294	0.06	8.45	0.90	0.340	0.018	0.86	0.172	0.011	2230	100	1883	84	2560	110	16
30	16	b.d.	na	4.66	0.26	0.312	0.010	0.99	0.108	0.003	1749	46	1750	50	1772	46	0
31	14	b.d.	na	5.73	0.41	0.338	0.013	0.98	0.122	0.005	1916	60	1874	63	1983	67	2
32	18	b.d.	na	0.08	0.01	0.012	0.001	0.74	0.048	0.000	79.9	8	78.7	6.3	108	12	2
34	103	b.d.	na	0.08	0.00	0.013	0.000	0.98	0.049	0.002	82.1	3.1	81.2	2.7	130	65	1
35	2	2	1.12	0.85	0.17	0.091	0.017	0.96	0.064	0.003	602	92	550	100	740	110	9
36	17	b.d.	na	4.67	0.24	0.310	0.010	0.98	0.110	0.002	1774	43	1737	47	1812	35	2
37	22	b.d.	na	0.09	0.01	0.013	0.001	0.61	0.048	0.000	89	11	82.2	6.5	115	18	8
38	107	b.d.	na	3.79	0.31	0.281	0.013	0.99	0.103	0.004	1601	65	1593	68	1700	76	0
39	3	b.d.	na	0.49	0.04	0.061	0.003	0.97	0.057	0.001	401	24	384	20	491	30	4
40	117	21	5.57	0.25	0.06	0.020	0.002	0.92	0.088	0.014	219	48	125	12	1080	330	43
41	41	b.d.	na	0.08	0.00	0.012	0.001	1.00	0.048	0.000	77.4	4.5	77.1	4.5	88.1	5	0
42	12	1	8.80	2.78	0.23	0.198	0.011	0.99	0.102	0.003	1338	58	1165	57	1649	57	13
43	2	b.d.	na	1.30	0.22	0.124	0.014	0.97	0.073	0.004	812	87	749	79	989	91	8
44	36	5	6.95	0.74	0.07	0.088	0.007	1.00	0.061	0.001	556	39	542	38	618	37	3
45	24	b.d.	na	0.08	0.01	0.013	0.001	1.00	0.048	0.000	81.6	6.5	80.9	6.4	101	8.2	1
46	5	b.d.	na	1.56	0.10	0.158	0.007	0.99	0.074	0.003	954	39	944	39	1029	63	1
47	8	10	0.81	3.92	0.73	0.159	0.013	0.79	0.183	0.025	1580	160	946	69	2490	270	40
48	2	b.d.	na	0.75	0.34	0.033	0.009	0.97	0.123	0.017	391	98	208	52	1820	320	47
49	14	b.d.	na	0.07	0.00	0.011	0.001	1.00	0.048	0.000	70.8	4.4	70.6	4.4	79.3	3.6	0
50	22	17	1.26	0.80	0.03	0.088	0.003	0.99	0.067	0.001	598	17	544	15	830	21	9

Table B-4: Rutile LA-ICP-MS U-Pb Isotopic Data and Ages   Sample: GR-09-05: Fox Hills Sandstone, Greater Green River Basin, WY

				Corrected isotopic ratios							Ages (Ma)[f]						
Grain #.	U[a] [ppm]	Th[a] [ppm]	U/Th	$^{207}Pb^{b}/^{235}U$	±2s[d]	$^{206}Pb^{b}/^{238}U$	±2s[d]	Rho[c]	$^{207}Pb^{e}/^{206}Pb$	±2s[d]	$^{207}Pb/^{235}U$	±2s	$^{206}Pb/^{238}U$	±2s	$^{207}Pb/^{206}Pb$	±2s	Disc. %[g]
51	32	b.d.	na	0.08	0.01	0.011	0.001	1.00	0.048	0.000	73.4	6	73.1	6	80	6	0
52	4	b.d.	na	5.70	1.30	0.148	0.023	0.98	0.259	0.023	1760	220	880	130	3190	170	50
53	4	b.d.	na	4.91	0.55	0.288	0.013	0.98	0.122	0.008	1782	88	1627	66	1960	110	9
54	145	1	107.11	0.08	0.01	0.012	0.001	1.00	0.051	0.003	77.3	5.6	75.9	5.3	168	85	2
55	95	2	53.26	0.09	0.00	0.013	0.000	1.00	0.048	0.000	86.7	3.1	85.6	3	115.4	5.2	1
56	41	13	3.12	0.08	0.01	0.012	0.001	1.00	0.048	0.000	79	4.9	78.3	4.9	99.6	5.4	1
57	60	b.d.	na	0.08	0.01	0.012	0.001	1.00	0.048	0.000	76.4	5.2	76.1	5.2	84.8	6.1	0
58	24	176	0.13	0.29	0.02	0.040	0.003	1.00	0.053	0.000	258	17	252	16	315	19	2
59	15	2	8.35	0.08	0.01	0.012	0.001	1.00	0.048	0.000	79.3	5.7	79	5.7	87.1	5.9	0
60	5	36	0.14	10.70	2.00	0.275	0.030	0.98	0.292	0.017	2520	160	1560	150	3413	88	38
61	15	b.d.	na	0.09	0.01	0.014	0.001	1.00	0.048	0.000	87.5	6.1	86.8	6	102.9	7	1
62	3	1	3.82	4.92	0.53	0.309	0.019	0.99	0.116	0.006	1795	91	1732	94	1876	88	4
63	6	7	0.89	2.34	0.29	0.206	0.017	0.98	0.087	0.005	1208	89	1234	99	1330	110	-2
64	28	b.d.	na	0.09	0.00	0.014	0.001	1.00	0.048	0.000	90.9	4.2	89.6	4	116.8	5.7	1
65	4	b.d.	na	0.20	0.01	0.029	0.002	1.00	0.050	0.000	182.2	9.2	182	9.4	205.6	9.8	0
67	30	2	19.24	0.15	0.03	0.015	0.001	0.70	0.073	0.010	137	24	95.9	9	800	260	30
68	27	2	17.88	4.96	0.53	0.318	0.020	0.99	0.114	0.006	1795	93	1773	97	1830	100	1
69	15	61	0.24	3.05	0.24	0.211	0.011	0.99	0.104	0.003	1412	61	1233	56	1695	56	13
70	8	13	0.63	5.64	0.93	0.328	0.031	0.98	0.120	0.010	1840	150	1810	150	1930	160	2
71	34	6	5.52	0.28	0.08	0.019	0.003	0.90	0.107	0.015	246	58	119	20	1430	310	52
72	54	14	3.80	4.70	0.45	0.312	0.017	0.98	0.109	0.004	1755	77	1747	84	1781	65	0
73	30	17	1.78	4.24	0.24	0.295	0.009	0.97	0.105	0.003	1688	43	1667	43	1724	46	1
74	10	267	0.04	4.65	0.47	0.132	0.011	0.93	0.261	0.006	1754	81	797	65	3246	37	55
75	111	80	1.38	0.16	0.03	0.015	0.002	0.76	0.074	0.010	143	25	98	11	820	270	31
76	29	1409	0.02	0.68	0.12	0.064	0.005	0.31	0.070	0.009	514	68	398	30	775	60	23
77	29	1470	0.02	4.56	0.53	0.273	0.019	0.99	0.120	0.006	1740	100	1549	96	1961	97	11
78	4	b.d.	na	2.53	0.23	0.216	0.012	0.99	0.085	0.003	1270	65	1274	68	1317	67	0
79	4	b.d.	na	1.74	0.14	0.164	0.010	0.97	0.077	0.002	1023	53	977	55	1116	51	4
80	18	b.d.	na	0.11	0.01	0.016	0.002	1.00	0.048	0.000	101.7	9.9	101	9.9	117	10	1
81	5	1	4.07	0.25	0.04	0.034	0.005	0.99	0.052	0.001	223	29	216	29	281	32	3
82	5	b.d.	na	0.11	0.01	0.016	0.002	0.99	0.050	0.001	108	9	100.8	9.6	175	31	7
83	43	b.d.	na	0.10	0.00	0.015	0.001	1.00	0.048	0.000	94.7	4.4	94.6	4.4	98.5	4.6	0
84	6	8	0.69	5.58	0.47	0.335	0.015	0.98	0.122	0.005	1931	65	1880	67	1984	70	3
85	6	4	1.47	0.27	0.06	0.021	0.002	0.82	0.097	0.016	263	56	132	12	1340	380	50
86	26	3	8.65	0.16	0.03	0.017	0.001	0.80	0.069	0.011	149	25	108.7	5.6	690	270	27
87	11	b.d.	na	0.66	0.03	0.081	0.003	0.99	0.059	0.001	514	19	500	18	577	26	3
88	11	7	1.51	6.28	0.89	0.355	0.028	0.98	0.125	0.008	1980	130	1950	140	2010	130	2
89	56	3	21.49	0.13	0.01	0.019	0.002	1.00	0.049	0.000	122.1	9.6	121.7	9.6	129	10	0
90	5	89	0.06	27.20	6.40	0.390	0.086	0.97	0.529	0.029	3470	240	2200	350	4316	80	37
91	1	1	1.15	3.96	0.93	0.226	0.028	0.91	0.108	0.012	1520	190	1300	150	1740	220	14
92	8	1	7.51	5.61	0.87	0.338	0.030	0.99	0.117	0.008	1860	140	1860	150	1880	130	0
93	4	5	0.81	6.90	1.30	0.369	0.034	0.98	0.137	0.013	2080	160	2040	170	2170	160	2
94	4	b.d.	na	6.90	1.20	0.368	0.036	0.98	0.129	0.010	1990	160	1990	170	2010	140	0
95	15	b.d.	na	0.63	0.03	0.079	0.003	0.99	0.057	0.001	497	16	492	15	510	20	1
96	21	460	0.05	0.27	0.02	0.036	0.002	1.00	0.053	0.000	241	13	230	12	342	17	5
97	21	b.d.	na	0.09	0.01	0.014	0.001	0.69	0.048	0.000	88.8	6.8	87.3	6.4	109.1	7.4	2
98	21	10	2.04	0.09	0.01	0.014	0.001	1.00	0.048	0.000	90.2	4.7	89.3	4.6	115.5	9.4	1
99	3	11	0.29	0.27	0.02	0.037	0.002	1.00	0.052	0.000	239	15	234	14	287	16	2
100	4	5	0.91	1.18	0.20	0.125	0.016	0.98	0.070	0.004	810	100	751	92	890	110	7

Table B-4: Rutile LA-ICP-MS U-Pb Isotopic Data and Ages   Sample: GR-09-05: Fox Hills Sandstone, Greater Green River Basin, WY

Grain #.	U[a] [ppm]	Th[a] [ppm]	U/Th	Corrected isotopic ratios: $^{207}Pb^{b}/^{235}U$	±2s[d]	$^{206}Pb^{b}/^{238}U$	±2s[d]	Rho[c]	$^{207}Pb^{e}/^{206}Pb$	±2s[d]	Ages (Ma)[f]: $^{207}Pb/^{235}U$	±2s	$^{206}Pb/^{238}U$	±2s	$^{207}Pb/^{206}Pb$	±2s	Disc. %[g]
101	19	4	5.11	0.57	0.04	0.072	0.005	0.99	0.058	0.002	451	28	446	28	526	62	1
102	7	b.d.	na	0.57	0.06	0.073	0.006	1.00	0.058	0.001	458	36	454	35	488	42	1
103	18	19	0.98	5.63	0.96	0.332	0.034	0.98	0.118	0.010	1850	160	1830	160	1870	150	1
104	6	31	0.18	0.35	0.08	0.035	0.007	0.92	0.066	0.008	282	57	218	43	720	220	23
105	11	b.d.	na	0.09	0.01	0.014	0.001	0.94	0.050	0.002	90.4	6.3	87.9	5.9	155	58	3
106	1	b.d.	na	0.96	0.11	0.105	0.009	0.97	0.065	0.002	674	56	643	54	782	59	5
107	91	b.d.	na	6.80	1.20	0.378	0.037	0.98	0.124	0.010	2050	160	2080	180	2010	150	-1
108	17	b.d.	na	4.92	0.42	0.325	0.015	0.98	0.110	0.003	1800	68	1811	72	1783	51	-1
109	3	14800	0.00	3.84	0.44	0.253	0.017	0.98	0.107	0.005	1572	90	1445	85	1730	85	8
110	11	530	0.02	3.03	0.80	0.122	0.012	0.96	0.164	0.028	1320	210	737	71	2240	360	44
111	28	b.d.	na	0.10	0.01	0.015	0.001	1.00	0.048	0.000	94.4	4.6	93.3	4.5	121.2	6.7	1
112	1	b.d.	na	84.00	32.00	0.860	0.260	1.00	0.634	0.092	4320	470	3780	930	4600	210	13
113	1	b.d.	na	3.26	0.44	0.240	0.018	0.96	0.095	0.005	1403	80	1356	80	1476	77	3

[a]U and Th concentrations and Th/U ratios calculated relative to the R10 rutile standard using 287±76 ppm for U and 8.4±2.6 ppm for Th (Jackson, 2004)
[b]Corrected for U-Pb fractionation and background and normalised to R10 rutile standard ID-TIMS values (Jackson, 2004) and Pb/U ratios are corrected according to Anderson (2002)
[c]Error correlation defined as the quotient of the propagated errors of the $^{206}Pb/^{238}U$ and the $^{207}/^{235}U$ ratio
[d]The propagated error of quadratic addition of internal errors (2 SD) and within run reproducibility of R10 (2 SD)
[e]Corrected for mass-bias by normalising to R10 rutile standard (~.6 per atomic mass unit)
[f]U-Pb ages are calculated relative to R10 rutile standard and corrected for common Pb using Anderson (2002)
[g]Discordance %: for $^{206}Pb/^{238}U$ ages <1Ga calculated as $((1-(^{206}Pb/^{238}U)/(^{207}Pb/^{235}U))*100)$, for $^{206}Pb/^{238}U$ ages >1Ga calculated as $((1-(^{206}Pb/^{238}U)/(^{207}Pb/^{206}Pb))*100)$
b.d.= below detection limit
na = not applicable

Table C-1: Zircon LA-ICP-MS U-Pb Isotopic Data and Ages Sample 10-PTH-01: Panther Tongue, Book Cliffs, UT, TST

				Corrected isotopic ratios							Ages (Ma)[f]						
Grain #.	U[a] [ppm]	Th[a] [ppm]	U/Th	$^{207}Pb^{b}/^{235}U$	±2s[d]	$^{206}Pb^{b}/^{238}U$	±2s[d]	Rho[c]	$^{207}Pb^{e}/^{206}Pb$	±2s[d]	$^{207}Pb/^{235}U$	±2s	$^{206}Pb/^{238}U$	±2s	$^{207}Pb/^{206}Pb$	±2s	Disc. %[g]
1	105	72	1.73	0.03	0.03	0.066	0.003	0.97	0.053	0.001	394	18	411	17	394	18	-4
2	534	96	5.74	0.07	0.06	0.128	0.007	0.87	0.060	0.002	732	33	776	38	732	33	-6
3	156	45	3.52	0.10	0.11	0.189	0.008	0.93	0.073	0.002	1073	36	1111	43	1073	36	-4
4	394	129	2.99	0.09	0.09	0.194	0.006	0.94	0.080	0.001	1161	26	1142	31	1161	26	2
5	161	118	1.35	0.22	0.17	0.208	0.012	0.94	0.083	0.004	1227	65	1213	64	1227	65	1
6	150	69	2.11	0.16	0.16	0.209	0.009	0.92	0.080	0.003	1202	49	1220	47	1202	49	-1
7	58	34	1.70	0.33	0.35	0.287	0.016	0.95	0.097	0.005	1589	74	1621	81	1589	74	-2
8	99	105	1.00	0.06	0.06	0.109	0.005	0.96	0.061	0.002	651	30	663	28	651	30	-2
9	77	25	3.13	0.03	0.04	0.087	0.003	0.95	0.059	0.001	540	19	539	18	540	19	0
10	322	91	3.60	0.31	0.23	0.236	0.017	0.98	0.093	0.004	1386	83	1360	88	1386	83	2
11	434	169	2.61	0.29	0.24	0.277	0.012	0.88	0.102	0.004	1599	62	1598	66	1599	62	0
12	76	77	0.97	1.20	0.79	0.468	0.032	0.95	0.164	0.007	2470	100	2460	140	2470	100	0
13	447	249	1.84	0.04	0.04	0.068	0.004	0.96	0.052	0.001	409	27	421	26	409	27	-3
14	227	101	2.10	0.04	0.03	0.064	0.004	0.97	0.052	0.002	383	29	399	27	383	29	-4
15	534	296	1.84	0.14	0.13	0.201	0.008	0.94	0.082	0.002	1198	44	1177	45	1198	44	2
16	110	104	1.08	0.03	0.03	0.068	0.003	0.96	0.054	0.002	409	21	424	19	409	21	-4
17	728	218	3.34	0.09	0.09	0.175	0.007	0.91	0.073	0.002	1022	33	1038	36	1022	33	-2
18	118	86	1.40	0.11	0.11	0.179	0.007	0.94	0.078	0.003	1075	40	1062	39	1075	40	1
19	261	40	6.81	0.45	0.35	0.319	0.018	0.89	0.109	0.005	1774	79	1775	90	1774	79	0
20	85	43	1.96	0.24	0.19	0.273	0.013	0.93	0.093	0.003	1509	55	1558	67	1509	55	-3
21	41	36	1.19	0.31	0.30	0.276	0.014	0.96	0.097	0.004	1551	71	1564	69	1551	71	-1
22	158	44	3.70	0.29	0.20	0.242	0.015	0.93	0.088	0.004	1398	73	1390	79	1398	73	1
23	15	5	2.75	0.25	0.17	0.208	0.015	0.90	0.077	0.004	1190	77	1214	78	1190	77	-2
24	145	75	1.87	0.06	0.05	0.076	0.006	0.96	0.054	0.002	455	39	470	37	455	39	-3
25	193	295	0.67	0.49	0.39	0.283	0.019	0.95	0.102	0.007	1570	110	1591	96	1570	110	-1
26	758	450	1.89	0.06	0.05	0.067	0.006	1.00	0.058	0.001	435	37	422	35	435	37	3
27	80	76	1.07	0.05	0.05	0.107	0.004	0.96	0.063	0.001	655	25	656	23	655	25	0
28	142	115	1.26	0.36	0.21	0.273	0.017	0.93	0.102	0.005	1595	81	1548	84	1595	81	3
29	63	72	0.91	0.12	0.10	0.166	0.006	0.91	0.069	0.003	949	46	988	35	949	46	-4
30	58	34	1.83	0.13	0.11	0.173	0.008	0.93	0.072	0.003	1009	51	1024	46	1009	51	-1
31	209	90	2.36	0.09	0.10	0.164	0.007	0.96	0.071	0.002	965	36	975	40	965	36	-1
32	83	28	2.91	0.25	0.20	0.280	0.015	0.88	0.096	0.004	1551	57	1595	75	1551	57	-3
34	45	17	2.78	0.13	0.13	0.198	0.008	0.92	0.077	0.002	1146	42	1162	44	1146	42	-1
35	150	120	1.26	0.27	0.27	0.300	0.012	0.97	0.102	0.003	1681	53	1683	60	1681	53	0
36	572	230	2.52	0.00	0.02	0.015	0.001	0.98	0.047	0.001	94.6	3.9	97.2	4.2	94.6	3.9	-3
37	260	107	2.69	0.26	0.26	0.304	0.013	0.91	0.104	0.003	1710	50	1718	66	1710	50	0
38	20	13	1.58	0.20	0.20	0.265	0.010	0.91	0.098	0.003	1533	44	1514	52	1533	44	1
39	21	8	2.66	0.20	0.20	0.228	0.010	0.88	0.092	0.004	1351	52	1323	54	1351	52	2
40	234	76	3.11	0.22	0.23	0.266	0.012	0.93	0.098	0.003	1532	51	1521	61	1532	51	1
41	176	31	5.95	0.15	0.08	0.154	0.011	0.95	0.072	0.002	947	61	922	62	947	61	3
42	74	41	1.81	0.31	0.31	0.323	0.013	0.93	0.114	0.003	1816	50	1813	64	1816	50	0
43	129	69	1.97	0.33	0.33	0.255	0.017	0.96	0.093	0.004	1459	80	1451	86	1459	80	1
44	73	27	2.80	0.30	0.19	0.239	0.015	0.90	0.089	0.005	1368	77	1375	78	1368	77	-1
45	95	41	2.34	0.19	0.15	0.204	0.011	0.90	0.084	0.004	1197	59	1194	59	1197	59	0
46	67	45	1.52	0.11	0.12	0.168	0.008	0.95	0.074	0.002	993	43	1003	42	993	43	-1
47	152	208	0.76	0.05	0.05	0.087	0.004	0.97	0.057	0.002	518	27	536	24	518	27	-3
48	116	51	2.42	1.00	0.94	0.506	0.027	0.90	0.174	0.007	2624	77	2610	120	2624	77	1
49	865	806	1.16	0.27	0.27	0.254	0.012	0.94	0.097	0.004	1469	63	1453	61	1469	63	1
50	134	66	2.02	0.31	0.31	0.316	0.014	0.90	0.111	0.003	1798	56	1775	69	1798	56	1

Table C-1: Zircon LA-ICP-MS U-Pb Isotopic Data and Ages Sample 10-PTH-01: Panther Tongue, Book Cliffs, UT, TST

Grain #.	U[a] [ppm]	Th[a] [ppm]	U/Th	Corrected isotopic ratios: $^{207}Pb^{b}/^{235}U$	±2s[d]	$^{206}Pb^{b}/^{238}U$	±2s[d]	Rho[c]	$^{207}Pb^{e}/^{206}Pb$	±2s[d]	Ages (Ma)[f]: $^{207}Pb/^{235}U$	±2s	$^{206}Pb/^{238}U$	±2s	$^{207}Pb/^{206}Pb$	±2s	Disc. %[g]
51	519	564	0.93	0.30	0.30	0.243	0.012	0.96	0.093	0.005	1418	76	1394	63	1418	76	2
52	228	8	57.70	0.09	0.09	0.160	0.008	0.92	0.068	0.002	923	37	951	42	923	37	-3
53	121	57	2.08	0.10	0.10	0.161	0.007	0.95	0.071	0.002	945	39	960	37	945	39	-2
54	24	6	3.83	0.12	0.10	0.181	0.008	0.92	0.080	0.003	1099	44	1070	43	1099	44	3
55	46	24	1.96	0.25	0.25	0.283	0.012	0.93	0.095	0.003	1569	52	1604	62	1569	52	-2
56	144	228	0.82	0.89	0.86	0.464	0.023	0.90	0.169	0.008	2516	76	2470	100	2516	76	2
57	123	63	1.97	0.32	0.28	0.291	0.016	0.92	0.102	0.004	1643	67	1639	80	1643	67	0
58	206	42	5.16	0.36	0.29	0.313	0.018	0.89	0.102	0.004	1720	66	1764	92	1720	66	-3
59	541	103	5.15	0.21	0.17	0.212	0.015	0.92	0.082	0.004	1229	69	1232	82	1229	69	0
60	107	43	2.47	0.03	0.03	0.068	0.003	0.98	0.056	0.001	421	18	427	17	421	18	-1
61	62	27	2.38	0.23	0.20	0.241	0.012	0.91	0.087	0.003	1388	57	1387	63	1388	57	0
62	89	59	1.54	0.23	0.24	0.241	0.012	0.93	0.094	0.003	1435	57	1390	60	1435	57	3
63	487	72	6.58	0.15	0.13	0.177	0.010	0.89	0.072	0.003	1025	52	1054	56	1025	52	-3
64	49	87	0.56	0.58	0.38	0.293	0.017	0.96	0.105	0.008	1680	110	1663	89	1680	110	1
65	80	22	3.66	0.10	0.11	0.179	0.008	0.92	0.073	0.002	1042	39	1060	42	1042	39	-2
67	81	53	1.52	0.36	0.33	0.298	0.015	0.94	0.107	0.004	1683	71	1670	76	1683	71	1
68	127	56	2.25	0.07	0.07	0.129	0.006	0.97	0.067	0.001	789	32	778	32	789	32	1
69	52	42	1.43	0.37	0.37	0.322	0.016	0.93	0.114	0.004	1829	64	1788	77	1829	64	2
70	168	42	4.08	0.36	0.29	0.272	0.016	0.86	0.101	0.005	1583	77	1545	79	1583	77	2
71	39	20	1.95	0.06	0.05	0.071	0.006	0.94	0.052	0.002	424	37	443	36	424	37	-4
72	183	110	1.64	0.14	0.14	0.161	0.009	0.97	0.075	0.002	990	52	956	49	990	52	3
73	258	71	3.61	0.37	0.37	0.311	0.017	0.90	0.102	0.004	1710	68	1744	85	1710	68	-2
74	61	55	1.45	0.30	0.27	0.290	0.014	0.90	0.099	0.004	1621	59	1636	69	1621	59	-1
75	111	66	1.68	1.50	1.10	0.501	0.051	0.96	0.167	0.005	2580	110	2630	230	2580	110	-2
76	178	74	2.33	0.29	0.30	0.273	0.014	0.91	0.096	0.004	1533	63	1546	71	1533	63	-1
77	93	52	1.80	0.53	0.33	0.299	0.022	0.91	0.103	0.007	1680	110	1670	110	1680	110	1
78	202	249	0.85	0.03	0.04	0.067	0.003	0.98	0.052	0.001	398	22	415	18	398	22	-4
79	96	46	2.01	0.28	0.29	0.283	0.014	0.93	0.099	0.003	1593	60	1606	71	1593	60	-1
80	66	77	0.88	0.12	0.12	0.164	0.007	0.94	0.072	0.003	963	46	982	38	963	46	-2
81	252	80	3.26	0.21	0.21	0.256	0.012	0.93	0.090	0.002	1444	52	1460	61	1444	52	-1
82	107	63	1.69	0.26	0.26	0.244	0.013	0.92	0.093	0.004	1435	65	1400	66	1435	65	2
83	16	7	2.52	0.11	0.12	0.182	0.008	0.88	0.075	0.003	1053	41	1081	41	1053	41	-3
84	42	20	2.19	0.17	0.13	0.183	0.011	0.92	0.071	0.003	1043	60	1077	59	1043	60	-3
85	151	52	2.97	0.96	0.97	0.476	0.029	0.90	0.162	0.007	2532	82	2510	120	2532	82	1
86	491	298	1.66	0.01	0.02	0.015	0.001	0.99	0.047	0.000	95.4	5.8	97.7	6.1	95.4	5.8	-2
87	50	43	1.17	0.33	0.34	0.253	0.014	0.95	0.092	0.004	1477	77	1462	77	1477	77	1
88	155	48	3.53	0.24	0.24	0.242	0.013	0.91	0.092	0.003	1408	63	1391	69	1408	63	1
89	259	198	1.40	0.07	0.06	0.095	0.006	0.98	0.059	0.002	587	40	586	34	587	40	0
90	32	13	2.60	0.03	0.04	0.070	0.003	0.96	0.053	0.001	416	20	434	20	416	20	-4
91	365	21	17.00	0.03	0.04	0.067	0.004	0.97	0.054	0.001	410	22	419	23	410	22	-2
92	63	22	2.88	0.12	0.12	0.179	0.009	0.91	0.070	0.002	1019	45	1057	46	1019	45	-4
93	344	147	2.38	0.17	0.17	0.200	0.011	0.94	0.077	0.003	1140	54	1171	57	1140	54	-3
94	148	86	1.76	0.13	0.12	0.161	0.010	0.95	0.070	0.003	939	51	956	55	939	51	-2
95	16	11	1.49	0.90	0.91	0.505	0.028	0.88	0.163	0.007	2537	77	2640	120	2537	77	-4
96	47	24	2.08	0.23	0.23	0.230	0.013	0.92	0.081	0.003	1279	65	1325	69	1279	65	-4
97	14	19	0.75	1.10	1.10	0.508	0.028	0.91	0.172	0.009	2577	90	2630	120	2577	90	-2
98	152	62	2.59	0.14	0.14	0.179	0.009	0.93	0.074	0.003	1039	52	1055	48	1039	52	-2
99	258	143	1.81	0.38	0.38	0.299	0.017	0.90	0.106	0.005	1660	75	1674	84	1660	75	-1
100	144	51	3.01	0.18	0.18	0.202	0.011	0.91	0.077	0.003	1154	58	1177	59	1154	58	-2

Table C-1: Zircon LA-ICP-MS U-Pb Isotopic Data and Ages Sample 10-PTH-01: Panther Tongue, Book Cliffs, UT, TST

				Corrected isotopic ratios							Ages (Ma)[f]						
Grain #.	U[a] [ppm]	Th[a] [ppm]	U/Th	$^{207}Pb^{b}/^{235}U$	±2s[d]	$^{206}Pb^{b}/^{238}U$	±2s[d]	Rho[c]	$^{207}Pb^{e}/^{206}Pb$	±2s[d]	$^{207}Pb/^{235}U$	±2s	$^{206}Pb/^{238}U$	±2s	$^{207}Pb/^{206}Pb$	±2s	Disc. %[g]
101	244	91	2.71	0.28	0.28	0.248	0.014	0.90	0.087	0.004	1376	71	1427	73	1376	71	-4
102	456	198	2.45	0.00	0.02	0.015	0.001	0.99	0.047	0.000	93.1	4.5	96.3	4.8	93.1	4.5	-3
103	273	185	1.49	0.05	0.03	0.059	0.006	0.98	0.051	0.002	350	36	367	35	350	36	-5
104	102	35	2.88	0.41	0.43	0.330	0.019	0.89	0.106	0.005	1781	77	1833	92	1781	77	-3
105	114	34	3.45	0.12	0.12	0.166	0.008	0.90	0.071	0.003	977	47	985	44	977	47	-1
106	51	31	1.57	0.39	0.30	0.250	0.018	0.92	0.086	0.005	1377	94	1427	90	1377	94	-4

[a]U and Th concentrations and Th/U ratios calculated relative to the GJ-1 zircon standard using 287±76 ppm for U and 8.4±2.6 ppm for Th (Jackson, 2004)
[b]Corrected for U-Pb fractionation and background and normalised to GJ-1 zircon standard ID-TIMS values (Jackson, 2004) and Pb/U ratios are corrected according to Anderson (2002)
[c]Error correlation defined as the quotient of the propagated errors of the $^{206}Pb/^{238}U$ and the $^{207}/^{235}U$ ratio
[d]The propagated error of quadratic addition of internal errors (2 SD) and within run reproducibility of GJ-1 (2 SD)
[e]Corrected for mass-bias by normalising to GJ-1 zircon standard (~.6 per atomic mass unit)
[f]U-Pb ages are calculated relative to GJ-1 zircon standard and corrected for common Pb using Anderson (2002)
[g]Discordance calculated as (1-(206Pb/238U age/207Pb/206Pb age))*100

Table C-2: Zircon LA-ICP-MS U-Pb Isotopic Data and Ages Sample 11-PTH-09: Panther Tongue, Book Cliffs, UT, LST

Grain #.	U[a] [ppm]	Th[a] [ppm]	Th/U	Corrected isotopic ratios $^{207}Pb^{b}/^{235}U$	±2s[d]	$^{206}Pb^{b}/^{238}U$	±2s[d]	Rho[c]	$^{207}Pb^{c}/^{206}Pb$	±2s[d]	Ages (Ma)[f] $^{207}Pb/^{235}U$	±2s	$^{206}Pb/^{238}U$	±2s	$^{207}Pb/^{206}Pb$	±2s	Disc %[g]
1	89	44	1.97	2.71	0.09	0.230	0.005	0.73	0.086	0.001	1331	24	1331	26	1329	31	5
2	201	59	3.46	4.05	0.23	0.291	0.014	0.76	0.100	0.002	1642	45	1643	69	1617	42	7
3	171	48	3.82	5.50	0.15	0.336	0.010	0.84	0.118	0.002	1902	25	1866	47	1929	34	8
4	61	29	2.05	0.79	0.03	0.098	0.003	0.62	0.060	0.001	595	17	604	16	604	31	5
5	86	20	4.27	2.03	0.06	0.190	0.005	0.71	0.079	0.001	1124	18	1119	25	1166	22	5
6	142	41	3.53	1.62	0.05	0.163	0.005	0.69	0.073	0.001	977	19	971	26	999	28	5
7	98	162	0.61	3.17	0.23	0.253	0.008	0.66	0.092	0.003	1443	55	1449	43	1482	78	6
8	277	155	1.82	0.76	0.03	0.094	0.003	0.66	0.059	0.001	575	19	580	19	572	33	4
9	190	59	3.19	14.79	0.33	0.539	0.012	0.76	0.201	0.003	2800	22	2774	50	2827	22	8
10	105	24	4.50	4.47	0.13	0.304	0.009	0.75	0.107	0.002	1728	26	1715	43	1755	27	6
11	63	43	1.53	3.96	0.25	0.282	0.012	0.77	0.106	0.004	1627	51	1601	58	1718	66	8
12	424	154	2.80	0.09	0.00	0.013	0.001	0.70	0.048	0.001	86.4	3.7	86.4	3.6	74	35	5
13	57	15	3.74	2.23	0.10	0.199	0.007	0.78	0.081	0.002	1194	31	1168	40	1223	39	5
14	163	93	1.76	3.94	0.17	0.282	0.010	0.77	0.102	0.002	1624	35	1609	48	1668	31	7
15	76	25	2.99	4.54	0.19	0.297	0.010	0.80	0.110	0.002	1737	36	1684	50	1788	33	7
16	986	397	2.45	0.10	0.00	0.015	0.000	0.67	0.048	0.000	93.1	2.6	94.6	2.6	81	20	4
17	427	226	1.91	3.10	0.18	0.240	0.009	0.00	0.094	0.002	1417	44	1382	48	1497	41	34
18	56	25	2.36	3.76	0.14	0.276	0.007	0.74	0.099	0.002	1577	29	1574	35	1607	31	6
19	489	121	4.04	3.01	0.13	0.238	0.009	0.79	0.092	0.002	1409	32	1371	45	1469	30	7
20	116	54	2.16	1.98	0.06	0.188	0.005	0.71	0.078	0.001	1104	20	1111	26	1159	29	5
21	180	38	4.70	0.53	0.02	0.070	0.002	0.56	0.055	0.001	428	12	435	13	424	28	4
22	62	22	2.86	3.08	0.13	0.241	0.008	0.83	0.092	0.002	1429	31	1391	42	1456	36	7
23	343	84	4.01	1.90	0.07	0.180	0.006	0.77	0.076	0.001	1077	26	1064	33	1096	33	6
24	48	21	2.30	5.88	0.26	0.346	0.013	0.82	0.124	0.003	1957	40	1909	60	2002	40	10
25	60	32	1.89	1.65	0.07	0.165	0.005	0.67	0.074	0.002	984	27	984	28	1021	42	6
26	249	162	1.53	3.69	0.19	0.274	0.010	0.85	0.098	0.002	1560	43	1563	52	1580	43	8
27	148	54	2.77	0.53	0.02	0.070	0.003	0.60	0.054	0.001	433	15	434	15	361	57	4
28	140	30	5.26	0.55	0.02	0.072	0.002	0.49	0.056	0.001	443	10	445	12	447	25	5
29	82	64	1.30	6.30	0.28	0.356	0.010	0.81	0.128	0.002	2019	40	1966	49	2076	34	8
30	118	37	3.36	1.90	0.06	0.181	0.005	0.72	0.077	0.001	1080	20	1070	25	1116	26	5
31	39	8	4.90	1.81	0.07	0.174	0.005	0.64	0.077	0.001	1052	23	1037	28	1104	33	6
32	213	60	3.55	3.01	0.08	0.240	0.006	0.77	0.092	0.001	1414	21	1383	31	1455	21	6
34	212	79	2.69	0.36	0.01	0.051	0.001	0.50	0.052	0.001	315.1	7.4	318.8	7	266	33	4
35	52	40	1.29	3.89	0.19	0.282	0.009	0.81	0.101	0.002	1608	38	1601	45	1653	41	7
36	237	102	2.34	4.32	0.17	0.295	0.009	0.82	0.107	0.001	1696	32	1665	46	1755	23	6
37	607	195	3.12	1.69	0.12	0.164	0.008	0.00	0.073	0.001	994	44	979	42	1008	47	18
38	97	26	3.75	1.73	0.06	0.173	0.004	0.70	0.073	0.001	1020	21	1024	24	1003	27	5
39	71	34	2.03	3.04	0.11	0.246	0.006	0.73	0.090	0.001	1413	28	1417	32	1423	27	5
40	199	42	5.94	0.55	0.02	0.072	0.002	0.52	0.055	0.001	439	13	448	13	427	31	5
41	145	131	1.09	1.79	0.09	0.175	0.005	0.71	0.074	0.002	1035	31	1041	29	1045	42	5
42	87	34	2.55	2.44	0.09	0.214	0.006	0.77	0.083	0.001	1252	26	1253	33	1255	27	5
43	167	74	2.32	0.43	0.02	0.058	0.002	0.57	0.053	0.001	359	13	364	12	308	38	4
44	69	46	1.54	1.58	0.07	0.159	0.004	0.72	0.072	0.001	963	25	954	24	989	40	5
45	20	10	2.01	2.14	0.08	0.195	0.005	0.75	0.080	0.001	1159	26	1151	26	1199	36	6
46	190	60	3.15	4.81	0.19	0.313	0.010	0.80	0.112	0.002	1782	33	1749	51	1829	29	8
47	46	40	1.14	4.75	0.26	0.318	0.011	0.80	0.108	0.003	1772	46	1777	52	1790	46	7
48	241	136	1.77	1.63	0.08	0.163	0.006	0.75	0.074	0.001	980	32	969	33	1019	40	6
49	987	241	4.01	1.66	0.09	0.161	0.006	0.57	0.076	0.002	996	32	970	30	1082	53	7
50	302	110	2.73	1.76	0.07	0.170	0.006	0.76	0.073	0.001	1022	26	1012	31	1018	32	5
51	331	6	129.00	0.35	0.02	0.048	0.003	0.33	0.054	0.001	307	16	302	16	380	42	5

Table C-2: Zircon LA-ICP-MS U-Pb Isotopic Data and Ages Sample 11-PTH-09: Panther Tongue, Book Cliffs, UT, LST

				Corrected isotopic ratios							Ages (Ma)[f]						
Grain #.	U[a] [ppm]	Th[a] [ppm]	Th/U	$^{207}Pb^{b}/^{235}U$	±2s[d]	$^{206}Pb^{b}/^{238}U$	±2s[d]	Rho[c]	$^{207}Pb^{c}/^{206}Pb$	±2s[d]	$^{207}Pb/^{235}U$	±2s	$^{206}Pb/^{238}U$	±2s	$^{207}Pb/^{206}Pb$	±2s	Disc %[g]
52	164	141	1.21	4.63	0.24	0.309	0.011	0.81	0.110	0.003	1758	44	1731	54	1789	46	8
53	350	116	4.40	1.61	0.11	0.161	0.009	0.78	0.074	0.002	974	41	966	49	1034	48	7
54	55	23	2.37	3.15	0.16	0.245	0.009	0.86	0.095	0.003	1438	40	1411	47	1522	50	8
55	372	201	1.81	0.78	0.03	0.098	0.003	0.60	0.058	0.001	587	19	600	18	513	54	4
56	162	80	2.40	1.63	0.07	0.163	0.006	0.81	0.072	0.002	976	28	974	30	981	44	6
57	134	48	2.79	1.39	0.05	0.147	0.005	0.68	0.070	0.001	887	22	884	26	922	29	5
58	446	194	2.30	0.10	0.00	0.016	0.000	0.66	0.047	0.000	99.7	2.5	101	2.6	53	19	5
59	401	389	1.04	0.85	0.13	0.100	0.011	0.00	0.060	0.003	606	66	610	61	560	100	25
60	233	94	2.43	0.53	0.02	0.068	0.003	0.59	0.057	0.001	429	16	426	15	494	34	3
61	190	213	0.85	4.54	0.25	0.309	0.010	0.76	0.107	0.003	1743	45	1731	47	1750	52	6
62	35	23	1.52	1.89	0.08	0.185	0.005	0.76	0.075	0.002	1074	27	1091	28	1055	46	6
63	41	19	2.15	2.01	0.07	0.186	0.004	0.69	0.080	0.001	1113	23	1097	23	1189	35	5
64	82	18	4.55	4.54	0.11	0.307	0.007	0.78	0.107	0.002	1733	20	1722	33	1738	28	6
65	58	35	1.78	0.71	0.03	0.088	0.003	0.57	0.059	0.001	543	16	546	15	547	41	6
67	57	32	1.76	11.21	0.35	0.486	0.013	0.81	0.168	0.002	2541	31	2556	56	2537	25	8
68	106	41	2.56	3.07	0.11	0.246	0.007	0.77	0.091	0.002	1438	28	1415	34	1447	40	6
69	62	3	20.10	1.72	0.07	0.176	0.007	0.82	0.071	0.003	1011	27	1042	38	987	72	7
70	127	69	1.85	0.10	0.00	0.016	0.001	0.56	0.046	0.000	100.2	3.5	103.8	3.8	19.3	9.9	8
71	115	39	2.93	1.93	0.06	0.185	0.005	0.72	0.076	0.001	1088	21	1090	25	1082	28	5
72	46	32	1.45	3.83	0.17	0.284	0.009	0.80	0.098	0.002	1606	37	1607	47	1586	37	6
73	130	119	1.12	3.86	0.16	0.282	0.008	0.77	0.100	0.002	1600	34	1599	41	1619	36	7
74	99	59	1.87	0.48	0.02	0.064	0.002	0.47	0.053	0.001	395	15	402	13	303	52	6
75	37	20	1.81	1.76	0.09	0.177	0.007	0.80	0.073	0.002	1031	33	1046	36	1005	45	6
76	21	8	2.77	2.11	0.08	0.197	0.006	0.77	0.079	0.002	1152	26	1163	34	1165	41	6
77	192	105	1.81	3.19	0.08	0.249	0.006	0.76	0.094	0.001	1460	20	1431	31	1506	28	6
78	171	63	2.79	2.96	0.11	0.241	0.008	0.79	0.090	0.001	1403	26	1391	40	1415	26	7
79	360	65	5.43	1.76	0.05	0.174	0.005	0.73	0.072	0.001	1027	20	1038	26	989	25	5
80	549	492	1.12	0.09	0.00	0.013	0.000	0.68	0.047	0.000	83.4	2.5	85.6	2.7	48	20	4
81	41	25	1.60	0.69	0.03	0.087	0.002	0.57	0.058	0.001	527	16	538	14	515	40	6
82	37	8	5.00	1.55	0.06	0.160	0.005	0.65	0.070	0.002	948	24	957	28	942	49	6
83	40	34	1.16	17.74	0.46	0.587	0.014	0.84	0.222	0.003	2971	26	2971	57	2988	21	9
84	275	213	1.32	0.31	0.01	0.044	0.001	0.30	0.051	0.001	275.2	8	277.9	7.9	212	39	4
85	16	6	2.65	1.53	0.06	0.160	0.004	0.76	0.069	0.001	937	23	961	23	908	40	6
86	185	55	3.38	3.84	0.09	0.273	0.006	0.74	0.101	0.001	1599	20	1558	33	1644	24	6
87	97	68	1.62	1.84	0.08	0.179	0.005	0.76	0.075	0.002	1065	27	1065	29	1072	37	5
88	171	121	1.40	4.94	0.20	0.325	0.010	0.83	0.111	0.002	1821	33	1808	47	1811	28	7
89	137	45	3.09	1.61	0.06	0.161	0.005	0.75	0.073	0.001	978	22	959	27	1013	27	5
90	207	70	2.94	2.68	0.09	0.227	0.007	0.71	0.085	0.002	1316	26	1318	37	1319	35	5
91	166	55	2.96	2.24	0.08	0.201	0.006	0.72	0.081	0.001	1192	25	1187	33	1210	35	5
92	23	18	1.30	5.15	0.22	0.335	0.010	0.80	0.111	0.002	1848	36	1860	47	1825	30	7
93	47	15	3.21	3.89	0.14	0.282	0.009	0.74	0.100	0.002	1617	28	1605	43	1626	34	6
94	122	77	1.61	4.01	0.19	0.289	0.010	0.80	0.101	0.002	1635	41	1632	50	1642	35	6
95	234	103	2.25	1.90	0.10	0.180	0.007	0.79	0.078	0.002	1088	31	1071	37	1146	42	6
96	58	37	1.55	1.55	0.12	0.160	0.006	0.65	0.073	0.002	946	48	957	33	1008	58	4
97	450	131	3.58	0.54	0.03	0.070	0.003	0.49	0.055	0.001	435	17	436	18	434	36	4
98	43	16	2.70	3.36	0.15	0.261	0.009	0.75	0.093	0.002	1497	36	1494	46	1489	32	5
99	56	29	1.98	4.38	0.14	0.298	0.007	0.79	0.107	0.002	1707	27	1679	33	1735	33	6
100	129	55	2.32	3.20	0.20	0.249	0.011	0.83	0.092	0.003	1460	46	1432	56	1454	56	9
101	187	45	4.19	4.41	0.23	0.307	0.013	0.78	0.104	0.002	1730	42	1722	62	1696	36	7
102	245	97	2.53	0.29	0.01	0.041	0.001	0.51	0.051	0.001	257.8	6.6	257.2	6.4	235	27	4

Table C-2: Zircon LA-ICP-MS U-Pb Isotopic Data and Ages Sample 11-PTH-09: Panther Tongue, Book Cliffs, UT, LST

				Corrected isotopic ratios							Ages (Ma)[f]						
Grain #.	U[a] [ppm]	Th[a] [ppm]	Th/U	$^{207}Pb^{b}/^{235}U$	±2s[d]	$^{206}Pb^{b}/^{238}U$	±2s[d]	Rho[c]	$^{207}Pb^{e}/^{206}Pb$	±2s[d]	$^{207}Pb/^{235}U$	±2s	$^{206}Pb/^{238}U$	±2s	$^{207}Pb/^{206}Pb$	±2s	Disc %[g]
103	173	54	3.34	2.27	0.09	0.202	0.006	0.75	0.081	0.002	1202	28	1184	34	1221	36	5
104	37	31	1.20	2.80	0.15	0.229	0.008	0.80	0.088	0.002	1339	40	1328	42	1380	47	7
105	130	68	1.88	4.77	0.19	0.317	0.010	0.79	0.108	0.002	1777	34	1776	46	1765	34	7
106	559	16	35.50	4.28	0.17	0.295	0.010	0.81	0.105	0.002	1698	32	1663	51	1705	43	8
107	235	130	1.70	0.55	0.02	0.071	0.002	0.54	0.056	0.001	443	11	444	11	465	28	4
108	87	176	0.51	0.32	0.01	0.047	0.002	0.36	0.049	0.001	281	10	295	10	149	38	5
109	493	202	2.36	0.10	0.00	0.015	0.000	0.67	0.048	0.000	94.7	2.3	95.7	2.4	82	20	4
110	23	42	0.54	1.60	0.16	0.162	0.010	0.53	0.074	0.004	980	64	966	54	1022	97	7
111	221	30	7.37	4.42	0.15	0.305	0.010	0.81	0.104	0.002	1710	29	1716	48	1692	31	7
112	1019	12	87.50	0.79	0.09	0.093	0.007	0.23	0.061	0.002	587	50	575	43	619	81	12

[a]U and Th concentrations and Th/U ratios calculated relative to the GJ-1 zircon standard using 287±76 ppm for U and 8.4±2.6 ppm for Th (Jackson, 2004)

[b]Corrected for U-Pb fractionation and background and normalised to GJ-1 zircon standard ID-TIMS values (Jackson, 2004) and Pb/U ratios are corrected according to Anderson (2002)

[c]Error correlation defined as the quotient of the propagated errors of the $^{206}Pb/^{238}U$ and the $^{207}/^{235}U$ ratio

[d]The propagated error of quadratic addition of internal errors (2 SD) and within run reproducibility of GJ-1 (2 SD)

[e]Corrected for mass-bias by normalising to GJ-1 zircon standard (~.6 per atomic mass unit)

[f]U-Pb ages are calculated relative to GJ-1 zircon standard and corrected for common Pb using Anderson (2002)

[g]Discordance %: for $^{206}Pb/^{238}U$ ages <1Ga calculated as $((1-(^{206}Pb/^{238}U)/(^{207}Pb/^{235}U))*100)$, for $^{206}Pb/^{238}U$ ages >1Ga calculated as $((1-(^{206}Pb/^{238}U)/(^{207}Pb/^{206}Pb))*100)$

Table C-3: Zircon LA-ICP-MS U-Pb Isotopic Data and Ages Sample 10-SPC-01: Spring Canyon Member, Book Cliffs, UT, HST

				Corrected isotopic ratios							Ages (Ma)[f]						
Grain #.	U[a] [ppm]	Th[a] [ppm]	U/Th	$^{207}Pb^{b}/^{235}U$	±2s[d]	$^{206}Pb^{b}/^{238}U$	±2s[d]	Rho[c]	$^{207}Pb^{e}/^{206}Pb$	±2s[d]	$^{207}Pb/^{235}U$	±2s	$^{206}Pb/^{238}U$	±2s	$^{207}Pb/^{206}Pb$	±2s	Disc. %[g]
1	172	37	4.68	4.65	0.20	0.317	0.014	0.76	0.103	0.003	1756	37	1775	70	1702	56	6
2	39	31	1.18	2.69	0.23	0.232	0.011	0.69	0.081	0.004	1300	64	1347	56	1273	88	8
3	461	233	2.03	0.10	0.00	0.016	0.001	0.60	0.047	0.001	98.2	3.8	100.1	4.3	66	29	4
4	506	131	3.79	2.16	0.12	0.204	0.009	0.79	0.076	0.002	1159	38	1195	48	1081	49	7
5	363	100	3.66	3.31	0.18	0.261	0.010	0.81	0.090	0.002	1465	42	1492	51	1419	47	9
6	108	59	1.84	2.03	0.13	0.193	0.008	0.78	0.076	0.002	1105	41	1132	45	1069	53	8
7	138	97	1.40	5.08	0.37	0.330	0.016	0.84	0.110	0.003	1811	61	1827	75	1778	55	10
8	59	22	2.68	3.43	0.40	0.246	0.017	0.47	0.098	0.005	1512	95	1444	89	1580	110	21
9	60	37	1.69	2.80	0.19	0.222	0.010	0.61	0.093	0.003	1360	50	1295	53	1475	57	10
10	373	201	1.83	1.92	0.15	0.185	0.010	0.80	0.072	0.003	1070	53	1091	52	968	69	8
11	94	66	1.46	0.44	0.02	0.061	0.002	0.34	0.053	0.001	370	16	380	14	321	53	8
12	263	102	2.52	5.07	0.33	0.328	0.014	0.85	0.112	0.004	1819	57	1820	70	1815	57	9
13	47	12	3.89	2.12	0.13	0.199	0.009	0.83	0.077	0.002	1146	45	1176	52	1103	63	9
14	261	108	2.43	0.54	0.03	0.072	0.003	0.52	0.054	0.001	432	20	446	19	370	50	7
15	519	35	15.00	4.70	0.39	0.321	0.018	0.80	0.106	0.004	1776	61	1790	87	1741	63	6
16	171	65	2.72	4.33	0.23	0.298	0.011	0.80	0.106	0.003	1686	44	1682	54	1728	52	10
17	176	58	3.07	2.46	0.18	0.207	0.010	0.35	0.087	0.003	1250	56	1212	52	1355	73	17
18	691	211	3.52	4.33	0.44	0.276	0.016	0.04	0.111	0.006	1647	90	1571	83	1762	96	32
19	139	191	0.72	4.40	0.40	0.298	0.015	0.82	0.109	0.005	1698	80	1672	75	1783	90	10
20	107	62	1.75	1.89	0.11	0.178	0.006	0.78	0.077	0.002	1068	38	1055	34	1136	50	6
21	924	207	4.94	0.11	0.01	0.018	0.002	0.51	0.047	0.000	112	11	113	11	48	24	13
22	74	23	3.17	3.31	0.19	0.266	0.011	0.84	0.091	0.003	1481	44	1519	56	1424	55	8
23	92	54	1.71	1.63	0.13	0.162	0.009	0.79	0.073	0.002	966	51	967	50	995	58	7
24	277	30	9.95	1.00	0.06	0.113	0.006	0.28	0.064	0.001	695	33	690	33	722	37	11
25	65	28	2.30	0.45	0.02	0.062	0.003	0.40	0.052	0.001	372	16	384	15	285	56	9
26	241	157	1.47	1.67	0.10	0.163	0.007	0.36	0.074	0.002	982	37	971	38	1019	44	11
27	155	53	3.04	2.16	0.12	0.200	0.008	0.76	0.077	0.002	1162	38	1173	44	1125	41	6
28	14	10	1.45	1.77	0.12	0.177	0.008	0.79	0.071	0.002	1016	46	1045	45	976	64	9
29	289	107	2.64	0.09	0.00	0.015	0.001	0.66	0.047	0.000	91.9	3.9	94.6	4	47	19	8
30	431	30	14.50	5.32	0.41	0.322	0.016	0.60	0.119	0.005	1833	70	1786	79	1910	78	14
31	317	170	2.03	5.21	0.36	0.334	0.016	0.85	0.113	0.004	1827	60	1854	76	1820	56	10
32	47	48	0.96	15.60	1.20	0.565	0.027	0.87	0.198	0.007	2841	73	2890	110	2804	55	14
34	81	35	2.33	3.61	0.23	0.271	0.013	0.86	0.096	0.003	1549	54	1539	63	1532	56	9
35	411	262	1.81	0.73	0.05	0.091	0.005	0.50	0.058	0.002	548	30	562	28	493	66	11
36	149	38	3.93	3.30	0.22	0.261	0.016	0.86	0.091	0.003	1473	56	1490	82	1458	63	10
37	87	38	2.27	5.62	0.37	0.339	0.015	0.83	0.120	0.004	1900	56	1880	72	1944	57	10
38	112	101	1.12	4.54	0.36	0.307	0.015	0.85	0.104	0.004	1702	63	1714	73	1705	67	11
39	304	473	0.73	2.49	0.24	0.212	0.015	0.00	0.087	0.003	1275	80	1234	81	1345	75	34
40	269	8	34.15	0.79	0.01	0.096	0.002	0.61	0.061	0.001	592.1	7.4	589.8	9.7	629	19	3
41	97	27	3.64	12.10	0.88	0.505	0.026	0.88	0.176	0.007	2603	75	2630	120	2615	62	16
42	37	37	1.02	5.79	0.45	0.352	0.017	0.83	0.117	0.005	1923	70	1935	79	1899	77	10
43	347	109	3.19	2.35	0.19	0.214	0.014	0.80	0.081	0.003	1216	61	1243	72	1210	71	9
44	63	19	3.24	1.74	0.10	0.172	0.007	0.64	0.074	0.002	1013	37	1017	38	1022	51	8
45	520	699	0.75	0.79	0.06	0.095	0.005	0.30	0.060	0.002	586	33	582	29	660	47	10
46	285	91	3.22	1.79	0.19	0.171	0.013	0.63	0.075	0.003	1008	68	1011	73	1027	77	15
47	1145	560	2.07	1.35	0.10	0.140	0.008	0.46	0.070	0.002	846	45	841	44	914	57	10
48	25	5	4.64	2.93	0.18	0.240	0.010	0.81	0.088	0.003	1382	45	1385	53	1384	61	9
49	326	116	2.79	2.96	0.18	0.235	0.010	0.85	0.091	0.003	1383	48	1357	51	1427	61	10
50	17	11	1.43	0.82	0.08	0.101	0.008	0.36	0.059	0.002	608	48	621	45	572	94	8

Table C-3: Zircon LA-ICP-MS U-Pb Isotopic Data and Ages Sample 10-SPC-01: Spring Canyon Member, Book Cliffs, UT, HST

Grain #.	U[a] [ppm]	Th[a] [ppm]	U/Th	Corrected isotopic ratios $^{207}Pb^{b}/^{235}U$	±2s[d]	$^{206}Pb^{b}/^{238}U$	±2s[d]	Rho[c]	$^{207}Pb^{e}/^{206}Pb$	±2s[d]	Ages (Ma)[f] $^{207}Pb/^{235}U$	±2s	$^{206}Pb/^{238}U$	±2s	$^{207}Pb/^{206}Pb$	±2s	Disc. %[g]
51	223	117	2.00	1.83	0.12	0.178	0.008	0.72	0.076	0.002	1055	42	1051	44	1068	58	10
52	465	52	8.74	0.49	0.03	0.065	0.004	0.43	0.055	0.001	402	23	405	25	403	54	8
53	320	279	1.23	0.27	0.01	0.040	0.001	0.32	0.049	0.001	242.8	8.4	252.7	8	142	37	8
54	237	117	2.03	0.83	0.14	0.103	0.012	0.67	0.059	0.004	602	76	628	70	510	170	9
55	66	0	27.00	5.76	0.31	0.353	0.013	0.84	0.114	0.003	1943	46	1948	64	1865	55	10
56	73	39	1.84	1.66	0.11	0.159	0.007	0.66	0.075	0.002	976	43	951	41	1047	59	27
57	28	20	1.41	14.60	0.60	0.532	0.016	0.86	0.199	0.004	2779	41	2740	68	2814	32	10
58	26	1	25.80	15.93	0.59	0.561	0.016	0.84	0.202	0.005	2861	36	2869	69	2843	41	10
59	423	151	2.87	0.11	0.01	0.016	0.001	0.60	0.048	0.001	102.3	4.9	101.7	4.7	98	52	6
60	575	57	10.61	0.77	0.03	0.098	0.003	0.58	0.058	0.001	579	16	600	19	527	40	5
61	651	358	1.83	0.43	0.02	0.058	0.002	0.31	0.054	0.001	360	13	366	12	348	48	5
62	301	123	2.44	0.54	0.02	0.070	0.002	0.49	0.056	0.001	435	13	433	14	467	31	5
63	207	122	1.72	2.74	0.18	0.224	0.011	0.79	0.089	0.002	1329	49	1297	58	1414	49	7
64	49	38	1.32	3.26	0.18	0.259	0.009	0.83	0.091	0.003	1468	42	1480	44	1446	49	8
65	170	194	0.89	0.42	0.02	0.060	0.002	0.17	0.053	0.002	356	13	372.1	9.5	304	63	7
67	162	17	9.75	1.70	0.06	0.168	0.005	0.75	0.073	0.001	1008	22	997	25	1034	37	6
68	167	21	8.16	5.25	0.25	0.336	0.013	0.87	0.111	0.003	1854	41	1861	62	1824	45	9
69	71	51	1.47	4.78	0.27	0.312	0.010	0.79	0.110	0.003	1786	47	1744	51	1809	50	7
70	281	125	2.18	0.77	0.04	0.095	0.004	0.64	0.058	0.001	578	23	588	22	508	49	7
71	141	71	1.95	1.53	0.10	0.157	0.007	0.80	0.071	0.002	929	40	940	38	935	67	8
72	480	274	1.80	2.95	0.22	0.234	0.012	0.74	0.089	0.003	1374	57	1354	61	1427	60	14
73	30	32	0.91	4.02	0.30	0.285	0.012	0.81	0.101	0.004	1616	60	1614	59	1635	66	8
74	88	47	1.88	0.50	0.03	0.068	0.003	0.43	0.053	0.001	415	22	425	20	327	47	7
75	294	92	3.16	0.98	0.06	0.111	0.005	0.03	0.064	0.001	691	29	675	26	728	38	17
76	307	36	8.50	1.54	0.10	0.156	0.007	0.74	0.072	0.002	949	37	932	39	995	60	5
77	67	43	1.54	1.50	0.09	0.156	0.006	0.81	0.069	0.002	934	36	931	33	919	56	8
78	100	16	6.58	3.94	0.20	0.281	0.011	0.82	0.101	0.003	1634	43	1598	52	1633	52	9
79	664	17	39.80	2.18	0.20	0.191	0.010	0.01	0.082	0.003	1163	64	1123	51	1243	80	30
80	110	42	2.88	3.36	0.17	0.259	0.009	0.81	0.094	0.003	1491	43	1480	48	1487	50	8
81	82	34	2.44	5.66	0.31	0.344	0.013	0.83	0.120	0.004	1921	47	1898	61	1947	56	10
82	32	19	1.68	2.37	0.13	0.207	0.007	0.82	0.083	0.002	1219	38	1209	38	1235	57	8
83	162	85	1.89	5.34	0.39	0.329	0.015	0.82	0.116	0.005	1874	61	1825	74	1877	73	9
84	176	48	3.74	2.47	0.20	0.214	0.013	0.88	0.084	0.003	1265	61	1244	66	1286	79	12
85	42	19	2.27	1.79	0.08	0.176	0.005	0.79	0.074	0.002	1047	28	1043	29	1049	43	7
86	144	76	1.88	7.49	0.49	0.397	0.017	0.83	0.134	0.005	2167	60	2160	76	2145	67	11
87	80	33	2.77	1.99	0.07	0.188	0.005	0.76	0.077	0.001	1117	24	1108	28	1135	30	6
88	81	32	2.60	6.62	0.29	0.368	0.012	0.79	0.130	0.003	2054	40	2016	57	2102	37	7
89	30	7	3.99	4.61	0.13	0.319	0.008	0.77	0.105	0.002	1746	24	1784	40	1706	29	6
90	151	63	2.46	0.44	0.02	0.060	0.002	0.51	0.053	0.001	375	13	376	12	330	42	4
91	220	134	1.69	0.39	0.02	0.055	0.002	0.13	0.053	0.002	331	15	348	13	284	67	9
92	312	144	2.10	2.00	0.15	0.179	0.009	0.68	0.080	0.002	1097	51	1059	51	1197	57	10
93	103	18	5.83	6.84	0.27	0.385	0.012	0.83	0.128	0.003	2087	37	2098	57	2072	40	9
94	570	16	35.20	0.82	0.06	0.097	0.005	0.38	0.061	0.001	601	33	598	32	634	41	3
95	84	62	1.35	4.13	0.17	0.288	0.009	0.76	0.105	0.002	1664	35	1645	43	1708	31	6
96	188	39	4.92	6.85	0.39	0.376	0.016	0.85	0.128	0.004	2073	52	2067	73	2067	58	10
97	96	20	4.58	0.26	0.02	0.037	0.002	0.15	0.052	0.002	234	12	236	10	256	69	11
98	177	53	3.37	3.23	0.12	0.257	0.009	0.83	0.091	0.002	1465	28	1470	44	1445	34	8
99	179	69	2.59	0.80	0.08	0.095	0.007	0.57	0.060	0.002	585	43	585	40	621	69	14
100	126	56	2.41	4.45	0.14	0.304	0.008	0.78	0.107	0.002	1720	26	1708	40	1750	24	7

Table C-3: Zircon LA-ICP-MS U-Pb Isotopic Data and Ages   Sample 10-SPC-01: Spring Canyon Member, Book Cliffs, UT, HST

				Corrected isotopic ratios							Ages (Ma)[f]						
Grain #.	U[a] [ppm]	Th[a] [ppm]	U/Th	$^{207}Pb^{b}/^{235}U$	±2s[d]	$^{206}Pb^{b}/^{238}U$	±2s[d]	Rho[c]	$^{207}Pb^{e}/^{206}Pb$	±2s[d]	$^{207}Pb/^{235}U$	±2s	$^{206}Pb/^{238}U$	±2s	$^{207}Pb/^{206}Pb$	±2s	Disc. %[g]
101	101	106	0.92	0.86	0.04	0.101	0.003	0.43	0.061	0.001	625	19	619	19	622	27	4
102	602	215	2.76	2.07	0.11	0.192	0.009	0.78	0.081	0.002	1133	38	1129	48	1214	43	7
103	350	126	2.74	0.97	0.04	0.114	0.004	0.68	0.062	0.001	688	22	693	25	682	31	4
104	104	13	8.03	5.60	0.23	0.338	0.014	0.83	0.119	0.003	1917	36	1870	65	1939	40	8
105	490	246	1.92	0.85	0.04	0.100	0.004	0.00	0.062	0.001	621	23	611	23	658	23	36
106	92	40	2.20	2.87	0.12	0.232	0.008	0.78	0.091	0.002	1379	32	1340	40	1439	34	7
107	120	34	3.31	0.47	0.04	0.063	0.005	0.03	0.054	0.001	395	29	394	28	382	44	22
108	19	2	8.13	1.61	0.07	0.169	0.005	0.64	0.070	0.002	972	25	1008	30	926	50	6
109	71	25	3.48	1.77	0.06	0.174	0.005	0.64	0.075	0.001	1035	23	1030	27	1055	35	6
110	110	29	3.65	2.99	0.10	0.244	0.007	0.74	0.089	0.001	1414	25	1402	37	1391	32	6
111	66	31	2.19	0.85	0.07	0.101	0.006	0.57	0.060	0.002	617	39	618	35	588	68	29
112	125	38	3.35	1.68	0.07	0.168	0.006	0.57	0.073	0.001	996	28	1000	33	1011	32	5
113	136	76	1.94	4.39	0.15	0.298	0.009	0.76	0.106	0.001	1704	28	1687	41	1732	25	6
114	50	21	2.36	2.83	0.10	0.233	0.006	0.76	0.088	0.001	1363	25	1348	30	1373	28	5
115	141	81	1.74	3.04	0.13	0.237	0.008	0.59	0.094	0.003	1429	33	1369	44	1503	61	6
116	208	56	3.66	4.46	0.25	0.306	0.014	0.81	0.106	0.003	1712	48	1719	71	1717	48	8
117	182	30	6.18	2.74	0.09	0.233	0.008	0.73	0.084	0.002	1341	24	1346	41	1275	37	6
118	37	18	2.01	0.14	0.02	0.018	0.001	0.27	0.053	0.004	134	13	118	4.7	129	91	83
119	182	360	0.51	1.59	0.07	0.160	0.005	0.28	0.073	0.001	968	26	960	27	998	32	5
120	246	111	2.28	4.30	0.24	0.296	0.016	0.84	0.109	0.003	1707	52	1670	78	1785	41	7
121	521	236	2.24	0.22	0.02	0.032	0.002	0.33	0.049	0.001	197	14	202	14	130	43	10
122	32	37	0.87	0.35	0.02	0.052	0.002	0.41	0.051	0.001	305	13	326	11	200	62	9
123	64	42	1.56	0.77	0.03	0.093	0.003	0.29	0.060	0.001	580	16	575	16	607	26	5
124	37	11	3.18	2.45	0.09	0.219	0.007	0.76	0.081	0.001	1250	28	1273	35	1233	32	7
125	111	55	2.05	2.89	0.23	0.229	0.010	0.47	0.092	0.004	1376	58	1326	52	1479	84	7
126	177	51	3.56	1.97	0.07	0.185	0.005	0.75	0.077	0.001	1108	23	1097	27	1119	30	6
127	397	128	3.04	0.09	0.00	0.015	0.001	0.64	0.047	0.000	91.9	3.1	93.4	3.2	52	23	8
128	44	11	3.92	4.35	0.17	0.307	0.009	0.78	0.103	0.002	1697	34	1731	43	1674	39	6
129	79	33	2.38	1.83	0.09	0.177	0.006	0.81	0.075	0.002	1051	32	1050	33	1066	44	7

[a]U and Th concentrations and Th/U ratios calculated relative to the GJ-1 zircon standard using 287±76 ppm for U and 8.4±2.6 ppm for Th (Jackson, 2004)
[b]Corrected for U-Pb fractionation and background and normalised to GJ-1 zircon standard ID-TIMS values (Jackson, 2004) and Pb/U ratios are corrected according to Anderson (2002)
[c]Error correlation defined as the quotient of the propagated errors of the $^{206}Pb/^{238}U$ and the $^{207}/^{235}U$ ratio
[d]The propagated error of quadratic addition of internal errors (2 SD) and within run reproducibility of GJ-1 (2 SD)
[e]Corrected for mass-bias by normalising to GJ-1 zircon standard (~.6 per atomic mass unit)
[f]U-Pb ages are calculated relative to GJ-1 zircon standard and corrected for common Pb using Anderson (2002)
[g]Discordance %: for $^{206}Pb/^{238}U$ ages <1Ga calculated as ((1-($^{206}Pb/^{238}U$)/($^{207}Pb/^{235}U$))*100), for $^{206}Pb/^{238}U$ ages >1Ga calculated as ((1-($^{206}Pb/^{238}U$)/($^{207}Pb/^{206}Pb$))*100)

Table C-4: Zircon LA-ICP-MS U-Pb Isotopic Data and Ages   Sample 11-SPC-05: Spring Canyon Member, Book Cliffs, UT, HST

				Corrected isotopic ratios							Ages (Ma)[f]						
Grain #.	U[a] [ppm]	Th[a] [ppm]	U/Th	$^{207}Pb^{b}/^{235}U$	±2s[d]	$^{206}Pb^{b}/^{238}U$	±2s[d]	Rho[c]	$^{207}Pb^{e}/^{206}Pb$	±2s[d]	$^{207}Pb/^{235}U$	±2s	$^{206}Pb/^{238}U$	±2s	$^{207}Pb/^{206}Pb$	±2s	Disc. %[g]
1	226	50	4.39	3.40	0.07	0.261	0.005	0.85	0.095	0.001	1503	16	1491	26	1520	17	1
2	1498	579	2.78	1.49	0.08	0.153	0.006	0.99	0.070	0.001	926	34	915	33	937	34	1
3	137	30	4.78	5.76	0.13	0.345	0.008	0.84	0.121	0.001	1937	19	1908	38	1968	20	1
4	444	30	14.01	4.80	0.17	0.314	0.012	0.89	0.111	0.002	1781	30	1756	60	1815	31	1
5	117	45	2.59	2.00	0.04	0.190	0.004	0.80	0.077	0.001	1118	14	1121	20	1124	23	0
6	158	75	2.11	3.39	0.09	0.265	0.006	0.57	0.094	0.002	1500	21	1513	28	1514	32	-1
7	217	68	3.21	4.47	0.12	0.305	0.008	0.87	0.106	0.001	1722	23	1711	39	1733	21	1
8	142	59	2.35	2.10	0.06	0.194	0.005	0.90	0.080	0.001	1156	19	1139	26	1200	24	1
9	98	113	0.87	1.80	0.08	0.176	0.005	0.94	0.077	0.002	1046	30	1043	27	1134	40	0
10	110	34	3.25	3.44	0.12	0.261	0.009	0.83	0.093	0.001	1509	28	1502	46	1492	27	0
11	195	124	1.61	3.44	0.14	0.263	0.007	0.91	0.094	0.002	1514	31	1510	34	1513	39	0
12	544	143	3.80	3.02	0.15	0.239	0.011	0.88	0.090	0.003	1407	38	1381	55	1425	54	2
13	73	38	1.96	3.69	0.12	0.278	0.007	0.89	0.096	0.001	1571	25	1579	34	1543	27	-1
14	62	39	1.62	0.10	0.00	0.015	0.001	0.99	0.047	0.000	94.4	3.3	95.7	3.2	41	18	-1
15	94	46	2.07	0.69	0.03	0.087	0.003	0.91	0.059	0.001	534	15	537	15	556	28	-1
16	221	35	6.34	1.92	0.07	0.183	0.005	0.87	0.075	0.001	1086	23	1085	29	1068	34	0
17	247	72	3.50	5.21	0.14	0.332	0.008	0.89	0.114	0.001	1848	23	1850	36	1852	22	0
18	144	86	1.65	4.81	0.26	0.319	0.011	0.93	0.110	0.002	1775	44	1783	52	1795	37	0
19	385	131	2.95	4.06	0.14	0.289	0.008	0.93	0.102	0.001	1635	29	1634	40	1656	26	0
20	59	25	2.45	0.81	0.04	0.099	0.004	0.94	0.060	0.001	601	20	610	20	596	40	-1
21	379	134	2.78	1.94	0.18	0.175	0.010	0.98	0.080	0.003	1086	64	1048	56	1188	79	3
22	287	165	1.74	2.98	0.18	0.235	0.009	0.92	0.094	0.002	1417	43	1357	46	1496	47	4
23	2620	888	3.07	0.59	0.04	0.074	0.004	1.00	0.057	0.001	465	25	459	25	496	24	1
24	114	60	1.89	9.53	0.26	0.443	0.011	0.89	0.158	0.002	2385	26	2364	50	2435	22	1
25	366	20	18.74	4.57	0.14	0.313	0.010	0.88	0.107	0.002	1740	27	1754	50	1744	30	-1
26	188	122	1.62	3.23	0.14	0.252	0.008	0.92	0.094	0.002	1461	33	1453	38	1506	37	1
27	1167	377	3.28	1.43	0.11	0.149	0.008	0.97	0.070	0.002	898	46	895	44	933	50	0
28	168	67	2.56	4.58	0.22	0.309	0.012	0.94	0.108	0.002	1743	38	1738	59	1761	33	0
29	214	224	0.96	0.83	0.03	0.101	0.003	0.95	0.061	0.001	615	19	618	17	635	28	0
30	165	76	2.25	4.57	0.21	0.311	0.013	0.94	0.106	0.002	1737	39	1743	62	1733	27	0
31	495	183	2.74	4.55	0.27	0.308	0.013	0.92	0.106	0.003	1743	46	1728	66	1724	42	1
32	64	20	3.26	1.65	0.09	0.165	0.007	0.84	0.075	0.002	985	36	982	38	1068	60	0
34	41	20	1.96	0.83	0.03	0.101	0.002	0.91	0.061	0.001	612	14	619	14	622	30	-1
35	62	54	1.18	3.06	0.14	0.238	0.007	0.89	0.093	0.002	1423	35	1372	36	1499	43	4
36	281	212	1.39	3.33	0.25	0.259	0.014	0.95	0.097	0.004	1502	60	1481	71	1568	66	1
37	343	160	2.15	3.27	0.17	0.242	0.008	0.92	0.099	0.003	1476	43	1394	44	1590	53	6
38	174	101	1.80	0.37	0.03	0.052	0.003	0.96	0.053	0.002	315	18	325	17	296	66	-3
39	312	134	2.38	2.05	0.09	0.194	0.007	0.94	0.077	0.001	1134	31	1139	39	1126	35	0
40	293	59	4.88	5.45	0.17	0.342	0.009	0.87	0.114	0.002	1891	27	1894	45	1859	27	0
41	170	26	6.39	0.49	0.02	0.065	0.002	0.94	0.055	0.001	406	13	406	14	416	27	0
42	53	62	0.82	1.65	0.10	0.166	0.006	0.93	0.072	0.002	984	36	988	35	987	51	0
43	158	135	1.28	1.81	0.11	0.179	0.007	0.94	0.074	0.002	1056	40	1058	39	1054	52	0
44	65	28	2.32	12.10	0.43	0.498	0.017	0.88	0.176	0.003	2611	34	2598	72	2614	30	0
45	201	128	1.66	3.20	0.17	0.254	0.009	0.94	0.091	0.002	1477	40	1460	46	1467	41	1
46	459	250	1.89	1.09	0.06	0.120	0.005	0.98	0.065	0.001	747	30	731	28	771	40	2
47	111	51	2.27	4.77	0.19	0.310	0.010	0.91	0.111	0.002	1771	34	1736	49	1812	34	2
48	53	30	1.78	2.10	0.09	0.192	0.006	0.91	0.080	0.002	1141	28	1130	30	1191	36	1
49	173	154	1.09	13.89	0.75	0.528	0.020	0.93	0.191	0.005	2737	54	2727	84	2755	42	0
50	210	109	1.95	3.42	0.12	0.264	0.006	0.93	0.095	0.001	1511	28	1508	32	1525	27	0

Table C-4: Zircon LA-ICP-MS U-Pb Isotopic Data and Ages   Sample 11-SPC-05: Spring Canyon Member, Book Cliffs, UT, HST

				Corrected isotopic ratios							Ages (Ma)[f]						
Grain #.	U[a] [ppm]	Th[a] [ppm]	U/Th	$^{207}Pb^{b}/^{235}U$	±2s[d]	$^{206}Pb^{b}/^{238}U$	±2s[d]	Rho[c]	$^{207}Pb^{e}/^{206}Pb$	±2s[d]	$^{207}Pb/^{235}U$	±2s	$^{206}Pb/^{238}U$	±2s	$^{207}Pb/^{206}Pb$	±2s	Disc. %[g]
51	301	88	3.45	4.73	0.17	0.319	0.009	0.88	0.107	0.002	1767	30	1781	45	1747	33	-1
52	92	36	2.64	2.19	0.07	0.200	0.004	0.91	0.080	0.001	1180	22	1176	23	1183	27	0
53	199	191	1.05	4.19	0.21	0.293	0.010	0.93	0.105	0.002	1670	39	1659	48	1713	46	1
54	479	549	0.87	3.24	0.21	0.252	0.011	0.92	0.094	0.003	1447	50	1446	54	1499	57	0
55	256	144	1.85	3.35	0.12	0.259	0.007	0.95	0.095	0.001	1494	29	1483	37	1526	28	1
56	565	122	4.58	4.49	0.16	0.314	0.010	0.90	0.105	0.002	1736	31	1761	50	1718	30	-1
57	89	63	1.39	0.47	0.03	0.065	0.003	0.93	0.053	0.002	387	20	404	18	318	74	-4
58	117	66	1.75	2.05	0.07	0.189	0.005	0.92	0.078	0.001	1130	24	1117	25	1152	31	1
59	250	82	3.10	5.36	0.16	0.334	0.009	0.90	0.117	0.002	1876	26	1857	45	1912	24	1
60	152	36	4.19	1.70	0.07	0.169	0.006	0.93	0.073	0.001	1003	26	1005	32	1015	34	0
61	61	57	1.10	1.88	0.11	0.180	0.006	0.94	0.078	0.002	1087	33	1064	33	1157	53	2
62	493	213	2.43	0.10	0.00	0.015	0.000	0.92	0.048	0.000	98.4	2.2	99	2	100	22	-1
63	112	68	1.64	2.89	0.15	0.240	0.008	0.96	0.089	0.002	1378	41	1381	44	1404	44	0
64	56	28	1.93	4.91	0.30	0.318	0.014	0.95	0.111	0.003	1802	56	1785	73	1828	44	1
65	142	74	1.92	0.58	0.03	0.076	0.003	0.95	0.056	0.001	468	18	471	15	439	57	-1
67	46	30	1.48	4.64	0.22	0.315	0.010	0.94	0.106	0.002	1752	40	1770	50	1732	38	-1
68	774	401	2.53	0.70	0.06	0.087	0.006	0.99	0.057	0.001	520	37	534	37	452	58	-3
69	27	20	1.34	1.83	0.08	0.179	0.004	0.89	0.076	0.002	1062	28	1063	24	1105	50	0
70	30	25	1.21	3.41	0.25	0.268	0.012	0.94	0.092	0.004	1492	58	1523	59	1489	74	-2
71	78	13	6.40	5.00	0.21	0.329	0.012	0.81	0.110	0.002	1810	36	1830	57	1794	38	-1
72	117	48	2.45	3.39	0.15	0.262	0.007	0.88	0.096	0.002	1513	35	1496	37	1539	42	1
73	209	137	1.49	5.08	0.27	0.328	0.012	0.91	0.111	0.003	1830	47	1832	58	1831	50	0
74	1460	337	5.40	1.42	0.13	0.145	0.009	0.98	0.071	0.002	883	49	872	49	953	62	1
75	803	412	1.91	0.17	0.01	0.026	0.001	0.96	0.049	0.001	162.1	7.9	165.5	8.2	129	41	-2
76	174	217	0.81	2.29	0.22	0.204	0.013	1.00	0.082	0.003	1217	70	1196	71	1240	62	2
77	129	76	1.94	4.19	0.16	0.294	0.008	0.89	0.104	0.002	1672	32	1664	41	1688	41	0
78	252	92	2.71	1.87	0.09	0.181	0.007	0.95	0.075	0.001	1069	33	1068	36	1059	38	0
79	37	50	0.75	1.86	0.09	0.179	0.005	0.94	0.078	0.002	1080	32	1062	28	1170	51	2
80	37	17	2.13	1.78	0.10	0.177	0.007	0.91	0.073	0.002	1030	34	1050	35	1011	53	-2
81	113	50	2.24	3.39	0.15	0.260	0.008	0.89	0.095	0.002	1500	35	1491	39	1519	45	1
82	113	48	2.37	2.60	0.14	0.224	0.008	0.96	0.084	0.002	1305	40	1301	44	1286	39	0
83	323	108	3.08	4.21	0.25	0.295	0.013	0.95	0.105	0.003	1659	50	1658	62	1691	53	0
84	145	36	4.14	3.99	0.28	0.282	0.017	0.97	0.101	0.002	1653	50	1621	82	1649	40	2
85	89	57	1.58	4.16	0.21	0.295	0.011	0.93	0.102	0.002	1664	40	1661	55	1667	42	0
86	195	47	4.24	4.67	0.17	0.324	0.010	0.89	0.105	0.002	1762	30	1809	48	1706	34	-3
87	29	12	2.57	1.76	0.09	0.174	0.006	0.90	0.074	0.002	1030	31	1031	33	1047	43	0
88	294	148	2.02	3.41	0.21	0.250	0.011	0.91	0.102	0.003	1518	44	1437	55	1668	57	5
89	564	89	6.77	0.31	0.02	0.045	0.002	0.98	0.051	0.001	272	15	282	13	230	38	-4
90	108	70	1.60	3.45	0.19	0.259	0.011	0.93	0.096	0.003	1523	46	1488	55	1564	48	2
91	32	17	2.09	1.93	0.12	0.185	0.008	0.92	0.075	0.002	1073	42	1088	44	1056	48	-1
92	194	54	3.70	4.60	0.17	0.309	0.009	0.84	0.107	0.002	1745	31	1735	43	1746	40	1
93	462	373	1.49	0.50	0.02	0.067	0.002	0.96	0.054	0.001	409	16	418	14	384	43	-2
94	158	75	2.16	4.75	0.44	0.313	0.020	0.93	0.109	0.005	1756	80	1750	100	1756	76	0
95	197	67	2.99	3.22	0.14	0.259	0.009	0.90	0.090	0.002	1461	35	1483	44	1419	39	-2
96	720	174	4.10	2.01	0.22	0.181	0.013	0.99	0.078	0.003	1100	73	1071	68	1136	78	3
97	139	59	2.38	0.18	0.01	0.027	0.001	0.95	0.048	0.001	164	5.7	169.6	6.1	94	29	-3
98	1322	124	11.60	0.80	0.06	0.097	0.006	0.98	0.061	0.001	588	32	593	33	624	37	-1
99	88	40	2.20	0.60	0.03	0.078	0.003	0.94	0.055	0.001	477	19	488	19	386	48	-2
100	196	51	3.96	4.84	0.20	0.320	0.010	0.88	0.110	0.002	1801	36	1791	47	1785	40	1

Table C-4: Zircon LA-ICP-MS U-Pb Isotopic Data and Ages Sample 11-SPC-05: Spring Canyon Member, Book Cliffs, UT, HST

				Corrected isotopic ratios							Ages (Ma)[f]						
Grain #.	U[a] [ppm]	Th[a] [ppm]	U/Th	$^{207}Pb^{b}/^{235}U$	±2s[d]	$^{206}Pb^{b}/^{238}U$	±2s[d]	Rho[c]	$^{207}Pb^{e}/^{206}Pb$	±2s[d]	$^{207}Pb/^{235}U$	±2s	$^{206}Pb/^{238}U$	±2s	$^{207}Pb/^{206}Pb$	±2s	Disc. %[g]
101	124	50	2.60	4.42	0.21	0.302	0.011	0.93	0.108	0.002	1743	42	1702	52	1761	41	2
102	242	207	1.28	4.49	0.32	0.305	0.013	0.95	0.107	0.003	1715	54	1712	63	1741	52	0
103	21	11	1.92	1.92	0.09	0.184	0.005	0.86	0.077	0.002	1090	28	1088	28	1106	61	0
104	893	117	7.79	1.97	0.13	0.183	0.007	0.97	0.078	0.002	1094	40	1079	38	1138	48	1
105	339	439	0.85	3.06	0.22	0.241	0.009	0.94	0.092	0.003	1416	54	1389	49	1463	68	2
106	53	14	4.03	4.18	0.19	0.301	0.010	0.89	0.101	0.002	1675	36	1690	51	1637	41	-1
107	164	51	3.47	5.02	0.27	0.328	0.013	0.87	0.112	0.003	1823	48	1822	63	1821	54	0
108	106	28	3.88	1.69	0.08	0.168	0.007	0.91	0.073	0.002	1010	28	997	37	1005	48	1
109	12	7	1.56	1.93	0.13	0.188	0.008	0.90	0.075	0.003	1079	43	1109	42	1089	73	-3
110	73	41	1.70	3.42	0.21	0.265	0.012	0.95	0.095	0.002	1530	48	1512	59	1553	46	1
111	505	180	2.80	1.98	0.26	0.183	0.017	0.96	0.080	0.004	1108	96	1077	93	1160	100	3
112	124	35	3.58	4.77	0.19	0.319	0.009	0.85	0.107	0.002	1794	33	1788	47	1750	42	0
113	17	17	1.00	3.38	0.24	0.263	0.010	0.91	0.094	0.004	1489	54	1501	52	1506	76	-1
114	40	29	1.39	1.91	0.10	0.181	0.006	0.92	0.076	0.002	1081	32	1070	30	1077	48	1
115	423	129	3.33	3.17	0.14	0.246	0.008	0.88	0.094	0.002	1445	32	1421	40	1504	43	2
116	143	85	1.79	0.09	0.00	0.015	0.000	1.00	0.046	0.000	90.8	2.2	93.9	2.3	3.7	2.5	-3
117	151	111	1.38	4.15	0.24	0.293	0.011	0.95	0.103	0.003	1654	47	1651	54	1684	49	0
118	212	153	1.41	0.43	0.02	0.060	0.003	0.94	0.053	0.001	361	16	373	15	293	49	-3
119	83	36	2.18	4.14	0.18	0.290	0.009	0.88	0.103	0.002	1657	35	1647	47	1671	40	1
120	269	82	3.35	2.96	0.12	0.242	0.008	0.92	0.089	0.002	1404	32	1392	41	1393	34	1
121	205	125	1.63	0.10	0.00	0.016	0.000	0.97	0.047	0.001	97.7	3	99.6	3	57	22	-2
122	148	34	4.30	4.30	0.24	0.300	0.014	0.88	0.106	0.003	1683	46	1686	69	1737	38	0
123	441	302	1.48	3.04	0.20	0.239	0.011	0.95	0.093	0.003	1407	54	1380	57	1469	59	2
124	154	219	0.71	0.35	0.01	0.051	0.002	0.91	0.049	0.001	305	11	319	11	144	41	-5
125	50	21	2.61	4.46	0.13	0.306	0.007	0.87	0.107	0.002	1716	25	1716	36	1751	27	0

[a]U and Th concentrations and Th/U ratios calculated relative to the GJ-1 zircon standard using 287±76 ppm for U and 8.4±2.6 ppm for Th (Jackson, 2004)
[b]Corrected for U-Pb fractionation and background and normalised to GJ-1 zircon standard ID-TIMS values (Jackson, 2004) and Pb/U ratios are corrected according to Anderson (2002)
[c]Error correlation defined as the quotient of the propagated errors of the $^{206}Pb/^{238}U$ and the $^{207}/^{235}U$ ratio
[d]The propagated error of quadratic addition of internal errors (2 SD) and within run reproducibility of GJ-1 (2 SD)
[e]Corrected for mass-bias by normalising to GJ-1 zircon standard (~.6 per atomic mass unit)
[f]U-Pb ages are calculated relative to GJ-1 zircon standard and corrected for common Pb using Anderson (2002)
[g]Discordance calculated as (1-(206Pb/238U age/207Pb/206Pb age))*100

Table C-5: Zircon LA-ICP-MS U-Pb Isotopic Data and Ages Sample 11-AB-LST: Aberdeen Member, Book Cliffs, UT, LST

				Corrected isotopic ratios							Ages (Ma)[f]						
Grain #.	U[a] [ppm]	Th[a] [ppm]	U/Th	$^{207}Pb^{b}/^{235}U$	±2s[d]	$^{206}Pb^{b}/^{238}U$	±2s[d]	Rho[c]	$^{207}Pb^{e}/^{206}Pb$	±2s[d]	$^{207}Pb/^{235}U$	±2s	$^{206}Pb/^{238}U$	±2s	$^{207}Pb/^{206}Pb$	±2s	Disc. %[g]
1	180	57	3.04	3.04	0.15	0.250	0.010	0.92	0.087	0.002	1426	38	1441	50	1372	43	-1
2	81	41	2.00	2.18	0.17	0.196	0.010	0.95	0.079	0.002	1164	54	1158	53	1178	55	1
3	205	46	4.21	5.61	0.29	0.350	0.013	0.88	0.116	0.003	1913	43	1934	64	1883	44	-1
4	217	76	2.72	1.54	0.09	0.156	0.006	0.95	0.072	0.002	936	35	934	36	995	43	0
5	296	154	1.95	0.38	0.02	0.055	0.002	0.96	0.051	0.001	326	15	343	14	208	46	-5
6	194	48	3.87	4.42	0.26	0.303	0.013	0.89	0.104	0.003	1693	49	1697	64	1699	51	0
7	183	92	2.00	3.34	0.23	0.258	0.012	0.95	0.094	0.003	1484	55	1469	64	1497	52	1
8	104	47	2.16	4.12	0.21	0.293	0.011	0.95	0.102	0.002	1643	42	1652	54	1653	36	-1
9	57	24	2.36	0.49	0.03	0.066	0.003	0.97	0.054	0.001	402	17	411	16	362	48	-2
10	231	72	3.28	2.13	0.11	0.194	0.007	0.93	0.081	0.002	1155	38	1141	40	1222	49	1
11	790	240	3.27	0.15	0.01	0.023	0.001	0.99	0.047	0.001	142	6.8	146.3	7	68	24	-3
12	114	54	2.16	2.29	0.15	0.201	0.009	0.95	0.085	0.003	1195	46	1182	48	1298	56	1
13	60	64	0.94	2.12	0.16	0.194	0.008	0.96	0.080	0.003	1133	53	1141	41	1198	80	-1
14	362	218	1.65	4.16	0.33	0.279	0.014	0.97	0.108	0.004	1651	69	1576	72	1757	66	5
15	118	37	3.09	1.45	0.09	0.153	0.008	0.95	0.068	0.002	904	39	916	42	874	44	-1
16	294	135	2.14	4.41	0.29	0.290	0.013	0.93	0.107	0.003	1703	54	1651	63	1746	47	3
17	181	107	1.61	1.49	0.18	0.148	0.013	0.96	0.072	0.004	906	75	888	73	984	91	2
18	397	125	3.16	4.34	0.33	0.297	0.016	0.93	0.103	0.004	1671	64	1690	82	1684	62	-1
19	156	115	1.44	1.45	0.09	0.150	0.006	0.96	0.072	0.002	913	36	900	35	976	43	1
20	51	59	0.84	4.33	0.38	0.301	0.015	0.94	0.103	0.005	1652	76	1692	74	1721	82	-2
21	88	41	2.08	5.27	0.50	0.308	0.015	0.96	0.121	0.006	1805	80	1722	72	1930	91	5
22	83	49	1.70	3.37	0.20	0.259	0.011	0.93	0.096	0.003	1491	49	1483	55	1542	50	1
23	55	47	1.35	1.91	0.12	0.178	0.007	0.95	0.079	0.002	1069	42	1072	41	1149	58	0
24	65	38	1.74	0.58	0.05	0.075	0.005	0.97	0.057	0.002	463	32	467	30	473	77	-1
25	69	39	1.72	2.55	0.18	0.217	0.011	0.95	0.086	0.003	1254	53	1261	56	1320	60	-1
26	203	92	2.22	4.42	0.42	0.306	0.020	0.89	0.107	0.005	1702	86	1710	100	1722	84	0
27	152	42	3.69	3.94	0.23	0.275	0.010	0.92	0.103	0.003	1610	47	1567	51	1687	53	3
28	183	89	1.98	0.42	0.04	0.057	0.004	0.94	0.051	0.001	351	25	357	25	249	61	-2
29	74	86	0.88	1.78	0.12	0.173	0.006	0.95	0.077	0.002	1043	43	1029	36	1115	53	1
30	369	267	1.37	0.49	0.03	0.067	0.004	0.98	0.053	0.001	403	23	416	21	328	57	-3
31	149	73	2.00	2.97	0.28	0.232	0.015	0.96	0.092	0.003	1387	68	1356	81	1485	63	2
32	163	100	1.59	4.93	0.56	0.309	0.021	0.97	0.117	0.007	1778	99	1740	100	1880	100	2
34	114	4	43.40	1.76	0.15	0.169	0.010	0.91	0.075	0.003	1008	53	1008	54	1047	74	0
35	223	109	2.03	3.54	0.27	0.272	0.014	0.92	0.094	0.003	1523	65	1543	72	1507	68	-1
36	64	31	2.04	1.94	0.14	0.182	0.009	0.94	0.078	0.002	1082	48	1077	51	1132	61	0
37	199	65	2.98	0.79	0.06	0.097	0.006	0.96	0.060	0.002	580	32	593	33	617	64	-2
38	64	17	4.36	2.42	0.13	0.215	0.008	0.90	0.081	0.002	1237	37	1252	41	1226	43	-1
39	301	74	4.24	2.67	0.16	0.225	0.011	0.92	0.087	0.002	1323	45	1311	59	1341	50	1
40	348	192	1.84	1.57	0.10	0.164	0.007	0.96	0.072	0.002	965	40	978	39	980	55	-1
41	298	25	12.08	1.95	0.13	0.186	0.009	0.93	0.077	0.002	1096	44	1098	51	1092	56	0
42	230	141	1.59	2.41	0.21	0.206	0.012	0.98	0.088	0.003	1236	64	1202	63	1360	71	3
43	68	50	1.38	2.71	0.15	0.228	0.008	0.95	0.087	0.002	1322	40	1325	42	1348	48	0
44	84	46	1.80	10.14	0.69	0.463	0.026	0.96	0.158	0.004	2448	62	2470	110	2427	38	-1
45	258	87	2.93	4.91	0.20	0.329	0.011	0.91	0.110	0.002	1806	35	1830	54	1792	36	-1
46	23	31	0.73	1.71	0.10	0.170	0.006	0.95	0.074	0.002	1011	36	1010	34	1018	45	0
47	210	73	2.89	5.28	0.31	0.334	0.013	0.90	0.114	0.003	1879	47	1859	64	1852	47	1
48	72	2	41.30	11.63	0.71	0.494	0.024	0.83	0.167	0.006	2600	54	2580	100	2537	57	1
49	164	79	2.10	4.22	0.26	0.299	0.013	0.92	0.102	0.003	1666	47	1681	64	1651	46	-1
50	748	137	5.30	4.21	0.38	0.274	0.014	0.96	0.111	0.005	1642	79	1554	71	1771	89	5

Table C-5: Zircon LA-ICP-MS U-Pb Isotopic Data and Ages Sample 11-AB-LST: Aberdeen Member, Book Cliffs, UT, LST

				Corrected isotopic ratios							Ages (Ma)[f]						
Grain #.	U[a] [ppm]	Th[a] [ppm]	U/Th	$^{207}Pb^{b}/^{235}U$	±2s[d]	$^{206}Pb^{b}/^{238}U$	±2s[d]	Rho[c]	$^{207}Pb^{e}/^{206}Pb$	±2s[d]	$^{207}Pb/^{235}U$	±2s	$^{206}Pb/^{238}U$	±2s	$^{207}Pb/^{206}Pb$	±2s	Disc. %[g]
51	123	34	3.68	1.79	0.10	0.177	0.007	0.93	0.073	0.001	1041	35	1053	41	1022	40	-1
52	349	89	3.94	0.73	0.05	0.091	0.005	0.97	0.060	0.002	552	29	564	27	565	67	-2
53	141	33	4.24	2.78	0.13	0.237	0.009	0.90	0.085	0.002	1343	37	1367	47	1319	43	-2
54	47	29	1.60	11.96	0.53	0.495	0.018	0.89	0.175	0.004	2591	43	2581	77	2599	36	0
55	31	35	0.86	1.75	0.12	0.172	0.007	0.95	0.073	0.003	1003	44	1021	37	1026	68	-2
56	91	20	4.55	4.66	0.29	0.318	0.015	0.86	0.105	0.003	1751	51	1769	75	1684	59	-1
57	112	79	1.45	5.12	0.37	0.330	0.015	0.94	0.112	0.003	1833	57	1831	72	1823	54	0
58	352	229	1.48	1.82	0.15	0.176	0.008	0.94	0.073	0.003	1021	52	1039	46	1029	71	-2
59	238	113	2.10	2.22	0.23	0.201	0.015	0.97	0.078	0.003	1172	71	1177	78	1141	79	0
60	598	312	1.96	3.67	0.22	0.275	0.011	0.94	0.096	0.003	1576	46	1559	56	1551	49	1
61	449	68	6.49	1.33	0.09	0.142	0.010	0.96	0.068	0.001	854	39	853	53	876	40	0
62	356	3	129.00	0.47	0.02	0.063	0.003	0.96	0.054	0.001	388	16	396	18	355	33	-2
63	635	228	2.91	0.09	0.00	0.014	0.000	0.98	0.047	0.000	89.3	3	92.1	3.1	55	21	-3
64	60	42	1.43	3.96	0.23	0.276	0.010	0.94	0.106	0.003	1626	46	1566	50	1725	45	4
65	215	181	1.17	0.50	0.04	0.067	0.004	0.98	0.054	0.002	403	24	419	23	349	65	-4
67	207	87	2.35	1.57	0.09	0.158	0.007	0.96	0.073	0.002	954	34	943	37	1013	42	1
68	57	29	1.94	3.34	0.20	0.261	0.011	0.93	0.092	0.002	1485	47	1494	53	1475	46	-1
69	106	40	2.63	3.98	0.28	0.280	0.013	0.93	0.103	0.004	1631	60	1588	66	1674	63	3
70	164	77	2.17	0.09	0.00	0.015	0.001	0.99	0.047	0.000	90.5	3.6	93.2	3.7	44	21	-3
71	44	15	2.91	1.82	0.11	0.182	0.008	0.92	0.074	0.002	1053	40	1074	45	1058	53	-2
72	130	91	1.42	2.13	0.21	0.192	0.012	0.94	0.079	0.003	1131	67	1129	65	1163	81	0
73	72	36	2.00	1.77	0.14	0.173	0.009	0.96	0.072	0.002	1019	50	1026	48	998	59	-1
74	186	12	16.40	1.60	0.12	0.163	0.010	0.82	0.070	0.003	968	46	970	58	936	84	0
75	179	78	2.32	2.98	0.22	0.238	0.013	0.94	0.086	0.003	1373	58	1370	66	1338	62	0
76	272	167	1.65	0.42	0.02	0.058	0.003	0.98	0.052	0.001	352	18	365	16	286	52	-4
77	210	98	2.21	3.22	0.24	0.250	0.013	0.94	0.094	0.003	1451	60	1437	67	1483	65	1
78	52	15	3.34	2.76	0.14	0.229	0.009	0.93	0.088	0.002	1340	38	1343	46	1378	45	0
79	31	9	3.64	2.05	0.12	0.191	0.008	0.92	0.077	0.002	1117	41	1121	43	1137	48	0
80	102	33	3.09	1.81	0.08	0.173	0.005	0.89	0.077	0.002	1046	27	1029	28	1124	42	2
81	72	86	0.81	0.76	0.05	0.095	0.004	0.98	0.059	0.002	570	28	582	25	539	69	-2
82	485	4	136.00	2.77	0.20	0.228	0.011	0.90	0.089	0.003	1332	55	1317	58	1370	66	1
83	718	184	9.00	1.97	0.22	0.179	0.014	0.96	0.079	0.003	1065	72	1057	74	1146	77	1
84	99	84	1.16	4.76	0.39	0.305	0.015	0.94	0.111	0.005	1746	73	1715	73	1805	76	2
85	159	80	1.90	2.60	0.18	0.220	0.010	0.95	0.085	0.003	1275	51	1278	54	1316	56	0
86	68	15	4.36	1.91	0.10	0.183	0.007	0.90	0.076	0.002	1087	33	1083	35	1081	48	0
87	71	45	1.58	3.90	0.24	0.278	0.011	0.94	0.102	0.003	1599	51	1581	56	1646	50	1
88	179	58	3.11	1.72	0.13	0.169	0.009	0.97	0.074	0.002	1007	48	1004	51	1028	46	0
89	144	69	2.17	3.81	0.28	0.282	0.015	0.94	0.094	0.003	1555	63	1601	74	1532	60	-3
90	231	56	4.17	3.32	0.25	0.252	0.013	0.92	0.095	0.003	1460	59	1450	67	1506	64	1
91	77	19	4.03	1.66	0.09	0.163	0.006	0.95	0.074	0.002	985	32	973	32	1046	42	1
92	261	95	2.58	2.08	0.17	0.189	0.011	0.94	0.080	0.003	1108	54	1111	57	1160	66	0
93	28	28	1.09	1.54	0.10	0.159	0.006	0.96	0.071	0.002	928	41	950	35	951	58	-2
94	321	70	4.61	4.80	0.38	0.324	0.019	0.90	0.111	0.004	1791	72	1800	93	1802	65	-1
95	392	251	1.62	1.64	0.14	0.161	0.009	0.95	0.073	0.003	967	54	958	48	1040	68	1
96	241	112	2.11	0.74	0.05	0.093	0.005	0.98	0.058	0.001	557	31	572	29	493	55	-3
97	568	253	2.21	3.15	0.19	0.249	0.010	0.93	0.092	0.002	1441	50	1425	54	1466	50	1
98	104	81	1.31	2.88	0.27	0.240	0.015	0.96	0.089	0.004	1362	75	1378	76	1407	83	-1
99	595	269	2.27	0.11	0.01	0.016	0.001	0.98	0.047	0.001	103.6	5.9	104.9	6	63	40	-1
100	48	11	4.39	4.35	0.41	0.303	0.021	0.91	0.104	0.005	1698	84	1690	110	1684	83	0

Table C-5: Zircon LA-ICP-MS U-Pb Isotopic Data and Ages   Sample 11-AB-LST: Aberdeen Member, Book Cliffs, UT, LST

				Corrected isotopic ratios							Ages (Ma)[f]						
Grain #.	U[a] [ppm]	Th[a] [ppm]	U/Th	$^{207}Pb^{b}/^{235}U$	±2s[d]	$^{206}Pb^{b}/^{238}U$	±2s[d]	Rho[c]	$^{207}Pb^{e}/^{206}Pb$	±2s[d]	$^{207}Pb/^{235}U$	±2s	$^{206}Pb/^{238}U$	±2s	$^{207}Pb/^{206}Pb$	±2s	Disc. %[g]
101	126	38	3.35	2.81	0.22	0.235	0.014	0.92	0.085	0.003	1359	58	1374	78	1314	61	-1
102	106	40	2.59	2.12	0.17	0.194	0.011	0.91	0.078	0.003	1153	55	1148	61	1164	70	0
103	80	10	7.63	10.47	0.78	0.459	0.026	0.89	0.170	0.005	2513	63	2420	120	2548	52	4
104	85	61	1.35	0.33	0.02	0.048	0.002	0.95	0.050	0.001	290	12	300	13	185	41	-3
105	171	46	3.62	2.63	0.19	0.229	0.011	0.91	0.081	0.003	1293	53	1323	58	1214	60	-2
106	106	56	1.92	3.32	0.20	0.261	0.010	0.94	0.094	0.003	1483	48	1490	51	1504	51	0
107	97	43	2.23	4.31	0.37	0.297	0.017	0.93	0.103	0.004	1656	72	1665	86	1686	76	-1
108	314	91	3.42	4.19	0.28	0.289	0.014	0.92	0.104	0.003	1657	57	1634	68	1676	56	1
109	346	48	7.53	1.74	0.18	0.173	0.013	0.90	0.069	0.003	1003	66	1024	73	930	82	-2
110	24	5	5.04	1.63	0.15	0.171	0.012	0.91	0.067	0.003	959	60	1011	68	881	89	-5
111	256	85	2.94	3.33	0.33	0.260	0.018	0.93	0.093	0.004	1444	75	1478	92	1465	87	-2
112	634	134	4.65	0.47	0.05	0.065	0.006	0.97	0.052	0.002	383	34	405	38	286	76	-6
113	420	91	4.67	1.82	0.13	0.176	0.010	0.91	0.074	0.002	1046	46	1045	53	1035	53	0
114	339	141	2.43	4.49	0.59	0.299	0.027	0.96	0.104	0.005	1680	110	1670	130	1703	89	1
115	295	72	3.91	1.67	0.11	0.168	0.009	0.93	0.072	0.002	975	42	998	48	972	50	-2
116	83	14	5.84	2.00	0.16	0.184	0.010	0.91	0.077	0.003	1093	54	1085	53	1116	69	1
117	174	161	1.14	0.80	0.05	0.097	0.005	0.97	0.060	0.001	589	29	598	28	608	46	-2
118	445	201	2.31	2.93	0.20	0.244	0.012	0.93	0.085	0.003	1382	53	1413	64	1303	57	-2
119	427	216	1.99	2.28	0.19	0.197	0.010	0.95	0.084	0.003	1210	59	1167	55	1346	89	4
120	390	210	1.75	1.62	0.18	0.160	0.013	0.98	0.073	0.003	964	72	953	71	1008	79	1
121	84	50	1.67	8.39	0.60	0.431	0.023	0.92	0.139	0.005	2239	66	2290	100	2229	58	-2
122	396	91	9.20	2.98	0.37	0.243	0.018	0.93	0.091	0.006	1350	84	1393	94	1400	120	-3
123	218	158	1.40	2.29	0.20	0.207	0.012	0.94	0.079	0.004	1170	61	1216	62	1188	85	-4
124	362	100	3.61	2.30	0.21	0.214	0.016	0.95	0.077	0.002	1200	65	1243	83	1124	60	-4
125	147	92	1.58	0.47	0.03	0.065	0.003	0.96	0.054	0.001	391	18	405	16	365	62	-4
126	171	71	2.48	4.89	0.34	0.318	0.015	0.94	0.114	0.004	1789	61	1767	75	1851	57	1
127	147	57	2.67	2.80	0.21	0.236	0.013	0.91	0.084	0.003	1339	55	1367	66	1281	61	-2
128	102	56	1.83	5.01	0.49	0.321	0.019	0.87	0.106	0.005	1793	82	1784	91	1721	85	1
129	141	98	1.41	1.91	0.16	0.180	0.010	0.97	0.080	0.003	1066	57	1061	54	1197	71	0
130	81	62	1.30	5.09	0.35	0.329	0.015	0.95	0.114	0.003	1856	58	1822	73	1867	50	2
131	43	22	2.02	4.31	0.38	0.302	0.017	0.88	0.099	0.005	1675	74	1723	87	1639	93	-3

[a]U and Th concentrations and Th/U ratios calculated relative to the GJ-1 zircon standard using 287±76 ppm for U and 8.4±2.6 ppm for Th (Jackson, 2004)

[b]Corrected for U-Pb fractionation and background and normalised to GJ-1 zircon standard ID-TIMS values (Jackson, 2004) and Pb/U ratios are corrected according to Anderson (2002)

[c]Error correlation defined as the quotient of the propagated errors of the $^{206}Pb/^{238}U$ and the $^{207/235}U$ ratio

[d]The propagated error of quadratic addition of internal errors (2 SD) and within run reproducibility of GJ-1 (2 SD)

[e]Corrected for mass-bias by normalising to GJ-1 zircon standard (~.6 per atomic mass unit)

[f]U-Pb ages are calculated relative to GJ-1 zircon standard and corrected for common Pb using Anderson (2002)

[g]Discordance calculated as (1-(206Pb/238U age/207Pb/206Pb age))*100

Table C-6: Zircon LA-ICP-MS U-Pb Isotopic Data and Ages   Sample 11-BH-06: Desert Member, Book Cliffs, UT, HST

				Corrected isotopic ratios							Ages (Ma)[f]						
Grain #.	U[a] [ppm]	Th[a] [ppm]	U/Th	$^{207}Pb^{b}/^{235}U$	±2s[d]	$^{206}Pb^{b}/^{238}U$	±2s[d]	Rho[c]	$^{207}Pb^{e}/^{206}Pb$	±2s[d]	$^{207}Pb/^{235}U$	±2s	$^{206}Pb/^{238}U$	±2s	$^{207}Pb/^{206}Pb$	±2s	Disc %[g]
1	422	371	1.18	0.78	0.05	0.096	0.005	0.28	0.060	0.001	594	25	588	28	609	36	1
2	311	276	1.08	0.52	0.03	0.069	0.003	0.37	0.054	0.001	419	21	428	19	370	60	-2
3	418	80	5.40	1.19	0.06	0.133	0.006	0.72	0.064	0.001	786	30	801	34	734	41	-2
4	51	51	1.00	1.85	0.12	0.177	0.007	0.61	0.076	0.002	1058	40	1056	36	1100	64	0
5	250	80	3.20	1.33	0.09	0.139	0.007	0.00	0.068	0.001	847	38	836	38	870	40	1
6	147	79	1.84	4.35	0.24	0.303	0.011	0.79	0.105	0.002	1712	45	1710	57	1716	38	0
7	240	222	1.28	4.30	0.26	0.311	0.013	0.82	0.101	0.002	1706	52	1739	62	1655	47	-2
8	206	97	2.03	2.75	0.18	0.230	0.011	0.81	0.087	0.002	1330	50	1331	57	1349	46	0
9	65	24	2.68	2.08	0.10	0.195	0.008	0.78	0.078	0.001	1140	34	1145	42	1133	36	0
10	270	95	3.01	3.09	0.15	0.248	0.010	0.75	0.091	0.001	1422	38	1430	50	1444	30	-1
11	13	13	1.04	4.47	0.32	0.307	0.013	0.81	0.108	0.003	1742	63	1718	63	1777	60	1
12	340	141	2.45	2.18	0.10	0.200	0.007	0.72	0.082	0.001	1183	30	1173	38	1241	28	1
13	154	51	2.95	0.49	0.03	0.066	0.004	0.47	0.055	0.001	406	23	412	26	426	47	-1
14	217	18	12.07	1.58	0.08	0.160	0.006	0.57	0.071	0.002	954	33	956	35	961	48	0
15	72	37	1.96	2.02	0.14	0.184	0.008	0.81	0.080	0.003	1118	48	1084	45	1192	62	3
16	109	31	3.48	2.94	0.20	0.238	0.013	0.71	0.087	0.002	1385	52	1389	60	1364	45	0
17	62	31	2.07	3.30	0.25	0.253	0.012	0.80	0.097	0.003	1514	57	1450	64	1549	59	4
18	7	2	3.57	2.17	0.14	0.201	0.009	0.78	0.078	0.002	1159	43	1176	50	1130	59	-1
19	365	139	2.88	0.52	0.04	0.068	0.004	0.35	0.055	0.002	422	27	427	26	405	61	-1
20	112	64	1.70	4.96	0.33	0.326	0.015	0.81	0.108	0.003	1786	57	1815	72	1750	60	-2
21	155	53	2.83	2.05	0.14	0.196	0.010	0.82	0.075	0.003	1120	47	1151	52	1061	65	-3
22	58	22	2.66	4.22	0.37	0.291	0.017	0.90	0.103	0.004	1675	73	1637	84	1683	64	2
23	88	26	3.33	3.09	0.24	0.250	0.013	0.70	0.092	0.003	1444	58	1433	67	1469	64	1
24	21	6	3.53	2.02	0.18	0.182	0.011	0.59	0.080	0.003	1100	62	1080	62	1196	73	2
25	85	50	1.72	15.70	1.30	0.567	0.035	0.87	0.203	0.007	2860	80	2870	140	2840	58	0
26	188	29	7.23	1.73	0.16	0.168	0.011	0.66	0.074	0.003	1000	60	995	59	1005	70	1
27	114	84	1.29	4.08	0.38	0.294	0.017	0.81	0.096	0.004	1617	75	1650	86	1552	83	-2
28	832	44	19.00	4.35	0.36	0.301	0.017	0.90	0.103	0.004	1692	68	1694	87	1652	78	0
29	209	130	1.70	0.48	0.05	0.065	0.005	0.46	0.053	0.002	393	30	407	28	330	81	-4
30	195	92	2.14	3.15	0.31	0.254	0.018	0.80	0.091	0.004	1439	78	1469	93	1421	91	-2
31	112	64	1.76	0.73	0.05	0.091	0.005	0.57	0.057	0.002	548	28	562	27	495	66	-3
32	55	51	1.17	4.21	0.35	0.297	0.016	0.85	0.107	0.006	1681	73	1670	77	1713	93	1
34	43	20	2.30	2.68	0.17	0.220	0.008	0.55	0.088	0.004	1321	47	1282	41	1372	74	3
35	155	50	3.03	1.91	0.16	0.187	0.011	0.83	0.072	0.002	1060	54	1102	60	967	70	-4
36	57	32	1.83	3.01	0.36	0.242	0.019	0.72	0.089	0.004	1388	92	1391	98	1445	72	0
37	169	132	1.39	3.09	0.43	0.246	0.024	0.89	0.091	0.006	1390	110	1410	120	1410	120	-1
38	197	94	2.21	1.83	0.17	0.178	0.011	0.73	0.071	0.003	1022	61	1051	60	953	84	-3
39	89	43	2.17	4.10	0.35	0.284	0.015	0.87	0.106	0.005	1663	72	1612	72	1705	88	3
40	149	55	2.84	3.15	0.30	0.251	0.016	0.80	0.089	0.004	1413	74	1434	83	1389	78	-1
41	119	115	1.01	2.86	0.28	0.239	0.013	0.86	0.086	0.005	1321	74	1374	70	1320	110	-4
42	82	45	1.88	0.50	0.05	0.070	0.005	0.41	0.054	0.001	410	32	432	32	326	58	-5
43	27	33	0.85	2.99	0.35	0.236	0.016	0.61	0.089	0.005	1383	94	1364	83	1460	100	1
44	153	89	1.84	1.98	0.16	0.185	0.010	0.60	0.076	0.003	1090	55	1092	51	1109	78	0
45	32	34	0.97	3.65	0.39	0.277	0.017	0.73	0.094	0.005	1533	85	1579	90	1492	99	-3
46	42	39	1.18	4.54	0.39	0.297	0.015	0.86	0.109	0.005	1725	71	1668	73	1755	83	3
47	53	29	1.85	3.15	0.30	0.242	0.016	0.90	0.094	0.004	1421	77	1402	85	1483	86	1
48	42	13	3.38	2.21	0.18	0.199	0.012	0.73	0.079	0.003	1157	59	1172	63	1149	76	-1
49	171	36	4.91	3.86	0.32	0.300	0.018	0.84	0.092	0.004	1595	72	1690	91	1443	82	-6
50	374	109	3.39	4.10	0.36	0.298	0.018	0.89	0.097	0.004	1623	76	1671	90	1518	82	-3
51	129	67	1.96	4.42	0.66	0.311	0.033	0.85	0.100	0.006	1690	130	1750	170	1610	120	-4
52	163	44	3.93	4.03	0.38	0.294	0.019	0.89	0.096	0.004	1603	72	1648	95	1524	66	-3
53	662	319	2.07	12.10	1.60	0.466	0.040	0.89	0.199	0.011	2660	110	2450	180	2799	97	8

Table C-6: Zircon LA-ICP-MS U-Pb Isotopic Data and Ages Sample 11-BH-06: Desert Member, Book Cliffs, UT, HST

				Corrected isotopic ratios							Ages (Ma)[f]						
Grain #.	U[a] [ppm]	Th[a] [ppm]	U/Th	$^{207}Pb^{b}/^{235}U$	±2s[d]	$^{206}Pb^{b}/^{238}U$	±2s[d]	Rho[c]	$^{207}Pb^{c}/^{206}Pb$	±2s[d]	$^{207}Pb/^{235}U$	±2s	$^{206}Pb/^{238}U$	±2s	$^{207}Pb/^{206}Pb$	±2s	Disc %[g]
54	11	8	1.36	4.42	0.36	0.300	0.015	0.88	0.104	0.004	1696	68	1695	78	1686	75	0
55	40	20	2.08	1.97	0.15	0.187	0.010	0.69	0.078	0.003	1083	51	1100	52	1134	77	-2
56	9	2	4.40	2.01	0.16	0.190	0.010	0.61	0.077	0.003	1101	52	1115	56	1091	65	-1
57	96	49	2.02	2.84	0.23	0.226	0.011	0.70	0.090	0.004	1361	62	1325	61	1427	82	3
58	94	59	1.60	4.06	0.35	0.288	0.016	0.84	0.100	0.004	1622	69	1624	79	1607	68	0
59	175	59	2.90	1.76	0.13	0.181	0.010	0.79	0.070	0.003	1011	49	1069	55	920	81	-6
60	380	338	1.13	0.50	0.04	0.068	0.004	0.40	0.053	0.001	405	24	420	22	316	60	-4
61	65	44	1.50	2.74	0.25	0.233	0.013	0.85	0.083	0.004	1307	72	1345	69	1309	96	-3
62	80	48	1.71	4.31	0.33	0.299	0.016	0.86	0.103	0.003	1683	67	1677	80	1672	58	0
63	63	27	2.34	0.47	0.03	0.065	0.003	0.49	0.052	0.001	391	20	408	19	290	47	-4
64	927	266	3.64	0.29	0.03	0.042	0.003	0.32	0.050	0.001	255	20	263	18	198	48	-3
65	107	50	2.16	1.59	0.13	0.165	0.009	0.69	0.071	0.003	956	53	979	51	942	82	-2
67	183	57	3.22	4.87	0.30	0.334	0.015	0.84	0.105	0.003	1789	53	1848	73	1699	57	-3
68	245	86	2.84	4.36	0.43	0.310	0.021	0.86	0.102	0.005	1689	85	1740	110	1632	84	-3
69	186	129	1.47	4.25	0.38	0.296	0.017	0.85	0.103	0.005	1658	74	1660	85	1657	88	0
70	494	93	5.12	0.90	0.06	0.111	0.006	0.68	0.058	0.001	642	31	677	34	502	51	-5
71	72	33	2.11	1.87	0.16	0.181	0.010	0.82	0.073	0.003	1042	55	1067	52	1014	87	-2
72	86	95	0.96	0.58	0.03	0.076	0.003	0.37	0.055	0.002	466	21	469	16	426	80	-1
73	181	209	0.87	1.70	0.15	0.166	0.007	0.55	0.079	0.004	1031	55	986	41	1149	81	4
74	26	6	4.20	1.73	0.17	0.176	0.012	0.84	0.070	0.003	1013	66	1040	66	912	87	-3
75	132	54	2.39	4.49	0.39	0.315	0.017	0.87	0.101	0.004	1707	74	1756	84	1616	77	-3
76	169	91	1.93	2.16	0.22	0.197	0.013	0.82	0.082	0.005	1156	74	1154	69	1240	110	0
77	444	73	6.13	4.35	0.31	0.310	0.017	0.84	0.103	0.003	1681	60	1728	85	1667	54	-3
78	195	170	1.48	2.70	0.24	0.227	0.013	0.83	0.084	0.004	1300	70	1312	69	1326	83	-1
79	56	41	1.40	12.30	1.10	0.496	0.026	0.90	0.180	0.009	2619	81	2610	110	2615	83	0
80	603	97	6.50	0.93	0.10	0.106	0.009	0.12	0.063	0.002	656	52	649	52	695	67	1
81	327	63	5.26	0.51	0.03	0.069	0.003	0.28	0.054	0.001	416	19	428	19	363	48	-3
82	469	143	3.35	2.15	0.23	0.193	0.015	0.58	0.083	0.005	1145	75	1133	82	1230	110	1
83	662	242	2.78	0.98	0.07	0.111	0.006	0.32	0.064	0.002	686	34	675	33	743	52	2
84	43	24	1.85	0.63	0.08	0.080	0.007	0.52	0.054	0.002	489	48	493	44	340	100	-1
85	59	36	1.68	0.89	0.07	0.108	0.006	0.62	0.060	0.002	640	35	662	34	575	70	-3
86	96	97	0.87	4.21	0.40	0.293	0.015	0.89	0.104	0.005	1664	80	1650	77	1653	89	1
87	363	124	3.00	3.05	0.27	0.249	0.015	0.79	0.087	0.004	1412	68	1436	77	1338	88	-2
88	73	20	3.93	3.96	0.27	0.291	0.014	0.86	0.095	0.004	1601	57	1638	69	1523	72	-2
89	42	23	1.96	3.26	0.41	0.245	0.020	0.56	0.091	0.005	1420	99	1400	100	1420	100	1
90	263	183	1.46	6.16	0.50	0.362	0.018	0.83	0.125	0.006	1994	74	1983	86	2004	79	1
91	205	59	3.50	2.96	0.22	0.237	0.013	0.79	0.090	0.003	1373	60	1363	66	1416	62	1
92	310	176	1.83	0.11	0.01	0.017	0.001	0.52	0.047	0.001	107.2	6.2	108.9	6.4	41	29	-2
93	199	80	2.83	4.33	0.31	0.307	0.016	0.86	0.102	0.003	1675	59	1717	79	1671	60	-3
94	186	182	1.05	2.16	0.08	0.196	0.005	0.31	0.081	0.001	1160	24	1150	26	1208	30	1
95	287	141	2.19	0.48	0.03	0.066	0.003	0.54	0.052	0.001	394	20	411	20	278	49	-4
96	45	21	2.22	2.69	0.18	0.230	0.011	0.81	0.083	0.003	1318	51	1336	57	1283	60	-1

[a]U and Th concentrations and Th/U ratios calculated relative to the GJ-1 zircon standard using 287±76 ppm for U and 8.4±2.6 ppm for Th (Jackson, 2004)

[b]Corrected for U-Pb fractionation and background and normalised to GJ-1 zircon standard ID-TIMS values (Jackson, 2004) and Pb/U ratios are corrected according to Anderson (2002)

[c]Error correlation defined as the quotient of the propagated errors of the $^{206}Pb/^{238}U$ and the $^{207}/^{235}U$ ratio

[d]The propagated error of quadratic addition of internal errors (2 SD) and within run reproducibility of GJ-1 (2 SD)

[e]Corrected for mass-bias by normalising to GJ-1 zircon standard (~.6 per atomic mass unit)

[f]U-Pb ages are calculated relative to GJ-1 zircon standard and corrected for common Pb using Anderson (2002)

[g]Discordance calculated as (1-(206Pb/238U age/207Pb/206Pb age))*100

Table C-7: Zircon LA-ICP-MS U-Pb Isotopic Data and Ages Sample 11-CSTG-07: Castlegate Member, Book Cliffs, UT, LST

				Corrected isotopic ratios							Ages (Ma)[f]						
Grain #.	U[a] [ppm]	Th[a] [ppm]	Th/U	$^{207}Pb^{b}/^{235}U$	±2s[d]	$^{206}Pb^{b}/^{238}U$	±2s[d]	Rho[c]	$^{207}Pb^{e}/^{206}Pb$	±2s[d]	$^{207}Pb/^{235}U$	±2s	$^{206}Pb/^{238}U$	±2s	$^{207}Pb/^{206}Pb$	±2s	Disc. %[g]
1	63	27	2.40	2.74	0.11	0.231	0.007	0.70	0.086	0.001	1336	30	1344	37	1328	31	5
2	30	39	0.76	1.55	0.07	0.158	0.005	0.56	0.073	0.002	942	29	947	26	1009	46	6
3	141	67	2.10	0.28	0.01	0.040	0.001	0.47	0.050	0.001	251	7.6	252.6	7.7	213	34	4
4	68	29	2.39	3.63	0.12	0.276	0.007	0.76	0.096	0.002	1556	24	1567	36	1553	30	5
5	41	30	1.35	5.55	0.19	0.344	0.009	0.74	0.118	0.002	1917	29	1911	40	1918	30	5
6	36	15	2.46	1.92	0.05	0.184	0.005	0.73	0.076	0.001	1090	19	1089	25	1096	32	5
7	272	106	2.54	0.10	0.00	0.015	0.000	0.76	0.048	0.001	94.2	2.2	95.7	2.1	96	26	7
8	127	98	1.35	1.70	0.05	0.170	0.004	0.67	0.074	0.001	1008	21	1012	23	1031	28	4
9	39	9	4.23	3.14	0.08	0.248	0.006	0.76	0.093	0.001	1438	19	1425	29	1476	25	5
10	89	58	1.59	2.04	0.04	0.189	0.004	0.66	0.079	0.001	1126	14	1115	19	1159	23	4
11	31	43	0.72	3.25	0.13	0.251	0.006	0.69	0.094	0.002	1470	28	1440	31	1496	33	5
12	104	30	3.69	2.72	0.10	0.220	0.007	0.73	0.089	0.002	1328	28	1279	38	1408	32	5
13	91	33	2.81	2.84	0.09	0.231	0.006	0.71	0.092	0.001	1370	25	1339	33	1458	20	5
14	104	22	5.07	2.56	0.05	0.217	0.004	0.70	0.086	0.001	1289	14	1266	22	1327	23	4
15	37	11	3.52	2.18	0.06	0.200	0.004	0.72	0.079	0.001	1174	17	1177	23	1166	20	5
16	115	61	2.26	2.09	0.06	0.194	0.004	0.72	0.078	0.001	1142	20	1144	23	1143	27	5
17	67	42	1.54	4.22	0.18	0.299	0.009	0.64	0.103	0.002	1674	34	1686	45	1668	29	4
18	40	30	1.34	6.67	0.18	0.370	0.008	0.78	0.129	0.002	2065	24	2034	38	2078	22	6
19	86	60	1.46	3.65	0.19	0.263	0.010	0.71	0.104	0.002	1559	44	1513	49	1691	42	6
20	76	18	4.09	1.90	0.05	0.177	0.004	0.70	0.078	0.001	1081	18	1051	21	1140	23	4
21	137	44	3.23	1.83	0.05	0.175	0.003	0.71	0.076	0.001	1054	17	1039	18	1095	23	4
22	109	57	1.83	1.74	0.05	0.172	0.003	0.67	0.075	0.001	1022	17	1023	18	1062	26	4
23	61	54	1.14	14.05	0.32	0.519	0.010	0.80	0.197	0.002	2748	21	2702	42	2798	16	7
24	126	34	4.49	4.24	0.09	0.299	0.006	0.73	0.104	0.001	1688	18	1688	31	1699	18	5
25	89	38	2.38	2.21	0.06	0.201	0.005	0.70	0.080	0.001	1188	19	1181	24	1190	23	5
26	96	56	2.66	0.97	0.03	0.114	0.002	0.65	0.062	0.001	689	13	696	12	684	26	4
27	107	101	1.07	2.18	0.07	0.199	0.004	0.66	0.079	0.001	1175	23	1168	21	1180	27	4
28	80	46	1.75	0.57	0.01	0.074	0.001	0.52	0.056	0.001	458	8	462	7.8	456	26	4
29	355	367	0.98	0.45	0.01	0.062	0.002	0.39	0.053	0.001	378	9	387	12	298	46	3
30	32	10	3.39	2.11	0.05	0.197	0.004	0.71	0.078	0.001	1148	16	1158	19	1132	31	5
31	78	25	2.84	4.82	0.16	0.326	0.009	0.78	0.104	0.002	1792	28	1824	44	1695	30	6
32	117	73	1.60	0.93	0.03	0.111	0.003	0.60	0.062	0.001	663	14	677	14	669	32	4
34	73	28	2.67	3.46	0.08	0.267	0.005	0.74	0.093	0.001	1524	17	1527	28	1499	21	5
35	118	52	2.28	5.27	0.15	0.336	0.009	0.73	0.115	0.002	1869	27	1866	44	1873	27	5
36	77	21	3.51	2.40	0.06	0.217	0.004	0.73	0.080	0.001	1238	18	1267	21	1181	24	5
37	400	135	3.18	0.50	0.01	0.066	0.001	0.63	0.055	0.001	407.5	7.5	412	7.5	409	22	3
38	109	128	0.88	4.08	0.21	0.290	0.007	0.72	0.101	0.003	1652	43	1640	37	1656	55	5
39	155	99	1.61	1.21	0.04	0.134	0.003	0.66	0.066	0.001	804	16	810	18	799	22	4
40	26	47	0.58	6.21	0.38	0.360	0.012	0.82	0.126	0.005	2035	54	1976	56	2046	65	8
41	13	6	2.13	2.18	0.10	0.201	0.006	0.74	0.081	0.002	1176	32	1181	34	1212	47	6
42	159	63	3.11	0.81	0.02	0.100	0.002	0.67	0.059	0.001	604	13	616	12	579	32	4
43	22	24	1.05	0.77	0.02	0.094	0.002	0.50	0.060	0.001	579	13	576	11	604	36	6
44	92	20	4.80	1.82	0.04	0.178	0.004	0.65	0.074	0.001	1055	15	1057	20	1033	20	4
45	111	34	3.32	3.52	0.13	0.269	0.009	0.72	0.095	0.001	1534	27	1532	44	1517	20	4
46	94	13	7.13	1.26	0.03	0.135	0.002	0.69	0.068	0.001	829	12	818	13	873	25	4
47	66	53	1.27	14.47	0.37	0.565	0.012	0.83	0.186	0.002	2782	24	2888	52	2705	17	8
48	121	48	2.48	3.44	0.08	0.270	0.005	0.74	0.091	0.001	1510	17	1540	27	1447	18	5
49	53	37	1.48	0.83	0.03	0.101	0.003	0.57	0.060	0.001	612	19	618	17	602	30	5
50	46	30	1.57	16.56	0.33	0.585	0.011	0.79	0.204	0.002	2905	19	2969	44	2856	15	7
51	153	35	5.28	2.93	0.10	0.246	0.007	0.72	0.086	0.001	1386	26	1422	33	1321	30	5

Table C-7: Zircon LA-ICP-MS U-Pb Isotopic Data and Ages   Sample 11-CSTG-07: Castlegate Member, Book Cliffs, UT, LST

				Corrected isotopic ratios							Ages (Ma)[f]						
Grain #.	U[a] [ppm]	Th[a] [ppm]	Th/U	$^{207}Pb^{b}/^{235}U$	±2s[d]	$^{206}Pb^{b}/^{238}U$	±2s[d]	Rho[c]	$^{207}Pb^{e}/^{206}Pb$	±2s[d]	$^{207}Pb/^{235}U$	±2s	$^{206}Pb/^{238}U$	±2s	$^{207}Pb/^{206}Pb$	±2s	Disc. %[g]
52	41	25	1.68	2.10	0.06	0.196	0.004	0.75	0.078	0.001	1149	20	1154	22	1163	32	6
53	99	29	3.45	1.96	0.06	0.188	0.005	0.71	0.075	0.001	1097	19	1112	26	1062	25	4
54	67	20	3.49	2.73	0.14	0.236	0.010	0.65	0.084	0.002	1333	38	1365	51	1299	40	4
55	23	7	3.41	4.21	0.14	0.304	0.009	0.77	0.100	0.002	1673	28	1706	42	1630	39	7
56	202	70	2.56	0.98	0.04	0.115	0.004	0.71	0.062	0.001	694	19	704	20	678	38	5
57	126	70	2.10	1.95	0.06	0.188	0.005	0.73	0.075	0.001	1100	20	1111	24	1064	25	5
58	113	45	2.53	2.07	0.07	0.198	0.006	0.72	0.076	0.001	1141	23	1161	31	1086	27	5
59	99	26	4.02	4.91	0.12	0.327	0.009	0.79	0.109	0.002	1803	20	1822	44	1777	27	6
60	296	95	3.18	0.54	0.02	0.071	0.002	0.61	0.055	0.001	439	10	444	11	425	21	3
61	67	31	2.21	4.22	0.10	0.298	0.006	0.75	0.101	0.001	1678	20	1685	32	1643	21	5
62	41	12	3.68	2.05	0.07	0.198	0.005	0.71	0.074	0.002	1129	23	1163	29	1030	44	5
63	131	71	2.36	2.09	0.06	0.195	0.005	0.67	0.077	0.001	1139	22	1148	27	1110	29	4
64	20	33	0.59	15.86	0.61	0.592	0.014	0.83	0.192	0.004	2865	36	3006	55	2756	34	9
65	153	38	4.01	4.78	0.13	0.331	0.009	0.77	0.105	0.001	1784	24	1838	43	1709	21	5
67	164	43	3.89	5.27	0.11	0.347	0.007	0.78	0.109	0.001	1862	18	1921	34	1782	22	6
68	88	37	2.43	3.50	0.11	0.275	0.007	0.80	0.092	0.002	1528	25	1562	34	1459	31	6
69	91	24	3.87	3.54	0.08	0.279	0.005	0.71	0.091	0.001	1532	17	1590	23	1438	18	5
70	120	86	1.40	0.55	0.02	0.074	0.002	0.48	0.055	0.001	446	13	458	11	394	44	5
71	71	15	4.80	6.13	0.18	0.389	0.010	0.85	0.114	0.002	1992	26	2116	47	1856	28	8
72	178	123	1.50	0.76	0.02	0.095	0.002	0.64	0.058	0.001	571	13	583	13	523	28	3
73	44	51	0.87	16.96	0.70	0.608	0.018	0.87	0.201	0.004	2946	41	3059	71	2828	34	9
74	85	49	1.74	3.90	0.12	0.298	0.007	0.79	0.093	0.001	1607	25	1683	35	1487	29	6
75	32	26	1.21	4.81	0.23	0.330	0.010	0.78	0.105	0.003	1786	40	1841	48	1720	51	6
76	57	34	1.82	8.17	0.25	0.446	0.012	0.88	0.132	0.002	2249	30	2393	48	2125	24	9
77	28	19	1.50	15.58	0.54	0.588	0.016	0.87	0.188	0.004	2854	35	2976	66	2728	30	9
78	76	46	1.69	3.52	0.14	0.273	0.009	0.68	0.092	0.002	1535	32	1555	45	1473	36	5
79	73	32	2.28	2.45	0.06	0.224	0.004	0.76	0.080	0.001	1256	19	1302	23	1181	30	6
80	128	62	2.20	0.43	0.01	0.058	0.001	0.55	0.053	0.001	359.6	8.3	365.9	8.2	316	32	4
81	42	15	2.71	2.77	0.08	0.238	0.005	0.71	0.084	0.002	1346	22	1373	28	1300	37	6
82	28	15	1.87	2.26	0.09	0.203	0.005	0.83	0.081	0.002	1197	30	1190	25	1235	53	9
83	310	95	3.29	2.29	0.08	0.207	0.006	0.71	0.080	0.001	1211	23	1209	34	1203	33	5
84	131	39	3.37	3.44	0.08	0.269	0.006	0.77	0.092	0.001	1514	19	1535	30	1475	29	7
85	192	47	4.04	5.24	0.15	0.350	0.010	0.77	0.107	0.002	1866	24	1932	48	1756	24	7
86	77	28	2.82	2.09	0.05	0.197	0.004	0.71	0.076	0.001	1149	16	1161	21	1087	29	4
87	40	18	2.36	5.06	0.15	0.352	0.009	0.81	0.105	0.002	1824	26	1940	42	1718	35	7
88	177	137	1.36	4.12	0.20	0.302	0.010	0.73	0.098	0.002	1648	42	1699	51	1581	42	5
89	386	14	29.40	2.39	0.09	0.213	0.008	0.71	0.080	0.002	1242	27	1252	46	1202	50	5
90	127	65	1.97	3.68	0.12	0.292	0.008	0.80	0.092	0.002	1569	28	1651	40	1458	31	7
91	170	80	2.13	3.59	0.11	0.272	0.009	0.64	0.094	0.003	1546	23	1550	46	1495	55	4
92	49	20	2.58	2.06	0.07	0.203	0.006	0.78	0.072	0.001	1133	23	1190	32	996	33	6
93	49	18	2.72	3.33	0.13	0.264	0.009	0.76	0.092	0.002	1492	29	1509	46	1470	39	5

[a]U and Th concentrations and Th/U ratios calculated relative to the GJ-1 zircon standard using 287±76 ppm for U and 8.4±2.6 ppm for Th (Jackson, 2004)

[b]Corrected for U-Pb fractionation and background and normalised to GJ-1 zircon standard ID-TIMS values (Jackson, 2004) and Pb/U ratios are corrected according to Anderson (2002)

[c]Error correlation defined as the quotient of the propagated errors of the $^{206}Pb/^{238}U$ and the $^{207}/^{235}U$ ratio

[d]The propagated error of quadratic addition of internal errors (2 SD) and within run reproducibility of GJ-1 (2 SD)

[e]Corrected for mass-bias by normalising to GJ-1 zircon standard (~.6 per atomic mass unit)

[f]U-Pb ages are calculated relative to GJ-1 zircon standard and corrected for common Pb using Anderson (2002)

[g]Discordance %: for $^{206}Pb/^{238}U$ ages <1Ga calculated as $((1-(^{206}Pb/^{238}U)/(^{207}Pb/^{235}U))*100)$, for $^{206}Pb/^{238}U$ ages >1Ga calculated as $((1-(^{206}Pb/^{238}U)/(^{207}Pb/^{206}Pb))*100)$

Table C-8: Zircon LA-ICP-MS U-Pb Isotopic Data and Ages Sample 11-TUS3C-2-17: Desert Member, Book Cliffs, UT, LST

				Corrected isotopic ratios							Ages (Ma)[f]						
Grain #.	U[a] [ppm]	Th[a] [ppm]	U/Th	$^{207}Pb^{b}/^{235}U$	±2s[d]	$^{206}Pb^{b}/^{238}U$	±2s[d]	Rho[c]	$^{207}Pb^{e}/^{206}Pb$	±2s[d]	$^{207}Pb/^{235}U$	±2s	$^{206}Pb/^{238}U$	±2s	$^{207}Pb/^{206}Pb$	±2s	Disc. %[g]
1	124	85	1.49	4.07	0.15	0.288	0.008	0.83	0.102	0.002	1648	30	1637	37	1662	31	1
2	160	46	3.45	3.04	0.10	0.242	0.007	0.94	0.091	0.001	1417	25	1394	36	1447	23	2
3	263	154	1.69	8.68	0.48	0.427	0.020	0.94	0.149	0.003	2292	50	2285	91	2331	29	0
4	90	43	2.14	2.97	0.15	0.238	0.009	0.91	0.092	0.002	1392	38	1376	45	1465	42	1
5	262	100	2.55	2.02	0.06	0.189	0.004	0.91	0.078	0.001	1119	19	1115	23	1143	24	0
6	66	35	1.86	3.22	0.10	0.254	0.006	0.89	0.091	0.001	1457	24	1463	29	1448	27	0
7	267	24	11.80	1.43	0.05	0.149	0.007	0.82	0.069	0.002	899	21	897	37	890	46	0
8	208	13	16.60	11.23	0.31	0.466	0.015	0.68	0.175	0.004	2540	25	2464	65	2600	40	3
9	340	154	2.25	0.27	0.01	0.038	0.001	0.92	0.050	0.001	240.9	7.2	242.7	6.6	197	36	-1
10	67	12	5.60	4.05	0.10	0.284	0.006	0.83	0.103	0.001	1642	20	1609	32	1667	25	2
11	153	27	7.50	2.15	0.07	0.196	0.006	0.88	0.079	0.001	1164	24	1154	31	1168	31	1
12	113	42	2.66	3.03	0.08	0.244	0.007	0.91	0.091	0.001	1416	21	1406	34	1447	20	1
13	208	72	3.01	1.82	0.05	0.176	0.004	0.92	0.075	0.001	1050	19	1046	23	1059	22	0
14	45	33	1.39	11.26	0.55	0.461	0.020	0.94	0.178	0.003	2532	46	2450	87	2629	32	3
15	332	128	2.55	2.06	0.15	0.183	0.008	0.95	0.081	0.003	1129	52	1085	45	1218	80	4
16	671	78	8.37	1.66	0.04	0.166	0.004	0.88	0.073	0.001	998	15	990	20	1006	24	1
17	888	218	4.08	0.31	0.01	0.044	0.002	0.91	0.051	0.001	273.1	9.7	278.2	9	252	43	-2
18	167	86	2.05	13.37	0.41	0.521	0.015	0.91	0.186	0.002	2699	31	2696	63	2709	22	0
19	358	83	4.23	1.87	0.05	0.182	0.004	0.92	0.075	0.001	1078	17	1075	21	1076	21	0
20	11	11	1.04	1.79	0.07	0.177	0.005	0.87	0.073	0.002	1038	26	1051	26	1013	46	-1
21	1073	345	3.17	0.46	0.03	0.061	0.003	0.95	0.057	0.002	385	21	381	18	543	61	1
22	270	123	2.22	0.71	0.03	0.087	0.003	0.94	0.059	0.001	543	17	535	17	583	37	1
23	75	35	2.05	9.06	0.25	0.428	0.011	0.89	0.153	0.002	2339	25	2294	48	2380	23	2
24	56	37	1.51	3.27	0.13	0.255	0.007	0.91	0.094	0.002	1472	30	1464	35	1505	31	1
25	543	262	2.02	4.03	0.16	0.277	0.008	0.92	0.104	0.002	1640	32	1574	38	1712	32	4
26	127	50	2.53	2.51	0.06	0.220	0.005	0.87	0.083	0.001	1275	18	1279	24	1273	27	0
27	87	21	4.22	4.61	0.13	0.315	0.008	0.87	0.106	0.002	1745	23	1762	39	1735	27	-1
28	76	32	2.36	3.13	0.10	0.252	0.006	0.91	0.089	0.001	1439	24	1446	31	1404	21	0
29	319	80	4.00	5.16	0.17	0.326	0.010	0.86	0.116	0.002	1843	29	1814	47	1888	31	2
30	79	25	3.09	3.22	0.12	0.252	0.007	0.91	0.093	0.001	1460	30	1449	37	1481	28	1
31	72	15	4.76	2.33	0.06	0.207	0.005	0.88	0.081	0.001	1226	20	1222	27	1222	24	0
32	59	90	0.66	13.80	0.68	0.507	0.017	0.93	0.197	0.004	2730	46	2665	74	2793	33	2
34	173	38	4.46	5.23	0.14	0.333	0.008	0.87	0.112	0.001	1856	24	1852	39	1841	22	0
35	70	32	2.15	1.83	0.06	0.176	0.005	0.91	0.075	0.001	1052	22	1050	25	1064	26	0
36	102	58	1.76	3.07	0.11	0.243	0.007	0.91	0.093	0.002	1419	29	1401	35	1480	31	1
37	160	44	3.51	4.15	0.13	0.288	0.007	0.90	0.105	0.001	1669	27	1634	36	1717	25	2
38	65	54	1.23	4.11	0.19	0.284	0.008	0.91	0.106	0.002	1664	37	1610	41	1735	41	3
39	46	19	2.36	3.19	0.10	0.252	0.006	0.84	0.093	0.002	1450	24	1446	31	1482	29	0
40	416	294	1.42	15.25	0.75	0.541	0.023	0.94	0.205	0.004	2829	47	2790	98	2865	28	1
41	259	76	3.42	4.50	0.15	0.301	0.007	0.84	0.110	0.002	1724	27	1699	35	1781	34	1
42	50	39	1.29	3.99	0.17	0.283	0.008	0.89	0.103	0.003	1630	37	1610	37	1675	45	1
43	68	37	1.88	1.75	0.06	0.167	0.005	0.90	0.076	0.001	1026	24	996	25	1084	36	3
44	393	51	7.69	2.95	0.11	0.236	0.007	0.86	0.089	0.002	1392	30	1365	36	1401	34	2
45	180	66	2.68	0.10	0.00	0.015	0.001	0.99	0.047	0.000	95.6	3.8	98.7	4	34	22	-3
46	525	10	50.80	4.39	0.19	0.307	0.013	0.89	0.101	0.002	1707	38	1720	62	1652	35	-1
47	226	134	1.72	0.46	0.02	0.062	0.002	0.94	0.054	0.001	388	12	387	10	372	44	0
48	210	107	1.94	0.22	0.01	0.033	0.001	0.94	0.050	0.001	204.1	6.2	207.2	6	181	34	-2
49	132	50	2.65	1.97	0.07	0.183	0.005	0.87	0.078	0.002	1109	23	1084	25	1147	37	2
50	432	159	2.75	4.26	0.16	0.292	0.009	0.92	0.106	0.001	1679	32	1651	45	1724	22	2

Table C-8: Zircon LA-ICP-MS U-Pb Isotopic Data and Ages Sample 11-TUS3C-2-17: Desert Member, Book Cliffs, UT, LST

Grain #.	U[a] [ppm]	Th[a] [ppm]	U/Th	Corrected isotopic ratios							Ages (Ma)[f]						
				$^{207}Pb^{b}/^{235}U$	±2s[d]	$^{206}Pb^{b}/^{238}U$	±2s[d]	Rho[c]	$^{207}Pb^{e}/^{206}Pb$	±2s[d]	$^{207}Pb/^{235}U$	±2s	$^{206}Pb/^{238}U$	±2s	$^{207}Pb/^{206}Pb$	±2s	Disc. %[g]
51	142	101	1.42	4.56	0.14	0.300	0.007	0.90	0.110	0.002	1746	26	1693	34	1796	28	3
52	807	325	2.61	1.55	0.13	0.152	0.009	0.98	0.072	0.002	916	51	906	50	962	58	1
53	38	21	1.83	2.43	0.08	0.210	0.005	0.90	0.084	0.001	1251	24	1226	27	1301	30	2
54	203	59	3.42	4.68	0.14	0.302	0.009	0.90	0.113	0.002	1758	25	1703	41	1839	25	3
55	26	10	2.51	1.67	0.06	0.167	0.004	0.84	0.073	0.002	997	24	993	22	1002	42	0
56	131	53	2.49	10.95	0.36	0.466	0.014	0.88	0.171	0.003	2509	31	2460	61	2558	24	2
57	73	25	2.80	1.62	0.04	0.164	0.003	0.87	0.073	0.001	974	17	977	19	993	29	0
58	1832	214	8.39	0.11	0.00	0.016	0.001	0.91	0.048	0.001	105.2	3.9	105.9	4	94	30	-1
59	53	25	2.17	1.43	0.07	0.149	0.005	0.95	0.070	0.001	898	27	899	28	934	34	0
60	512	368	1.38	2.30	0.14	0.197	0.006	0.94	0.084	0.003	1210	40	1157	34	1307	60	4
61	74	16	4.31	1.62	0.07	0.157	0.005	0.94	0.075	0.001	976	27	947	26	1048	36	3
62	97	47	2.13	4.03	0.14	0.285	0.007	0.91	0.103	0.002	1637	29	1615	37	1685	30	1
63	81	107	0.78	0.29	0.01	0.044	0.001	0.93	0.047	0.001	257.2	8	277.2	8.1	60	25	-8
64	85	40	2.11	1.71	0.05	0.164	0.004	0.92	0.074	0.001	1009	20	981	21	1050	25	3
65	116	18	6.52	4.39	0.12	0.302	0.007	0.84	0.106	0.002	1710	23	1698	34	1733	27	1
67	92	29	3.17	3.56	0.09	0.268	0.005	0.83	0.096	0.001	1544	20	1533	28	1547	23	1
68	249	59	4.28	4.30	0.10	0.293	0.007	0.85	0.106	0.001	1691	19	1663	32	1734	21	2
69	170	67	2.47	1.92	0.06	0.183	0.004	0.88	0.078	0.001	1091	20	1089	23	1136	29	0
70	285	52	5.34	1.55	0.04	0.157	0.003	0.86	0.071	0.001	949	15	939	16	964	20	1
71	426	63	6.50	4.76	0.21	0.311	0.012	0.83	0.112	0.004	1786	31	1746	59	1827	59	2
72	268	31	8.60	1.44	0.05	0.149	0.005	0.93	0.069	0.001	909	19	894	26	907	25	2
73	32	30	1.06	1.47	0.06	0.152	0.004	0.92	0.071	0.001	919	23	914	22	955	39	1
74	232	148	1.52	2.11	0.08	0.192	0.006	0.93	0.081	0.001	1162	25	1134	30	1227	28	2
75	98	45	2.09	1.78	0.07	0.174	0.005	0.94	0.074	0.001	1036	28	1034	28	1038	26	0
76	100	63	1.57	5.20	0.18	0.333	0.009	0.92	0.114	0.002	1851	30	1854	42	1851	26	0
77	259	312	0.85	1.46	0.07	0.148	0.005	0.95	0.070	0.001	907	28	892	27	927	37	2
78	124	32	4.22	4.56	0.13	0.319	0.008	0.85	0.105	0.001	1746	23	1782	38	1713	25	-2
79	80	21	3.99	1.41	0.05	0.149	0.004	0.92	0.068	0.001	890	20	899	24	882	31	-1
80	106	40	2.63	3.81	0.17	0.274	0.009	0.94	0.102	0.002	1605	34	1561	46	1673	28	3
81	155	73	2.12	1.96	0.10	0.181	0.006	0.94	0.079	0.001	1099	32	1069	33	1165	34	3
82	228	55	4.22	2.14	0.06	0.194	0.005	0.89	0.079	0.001	1160	20	1140	29	1159	29	2
83	187	56	3.27	4.61	0.13	0.309	0.008	0.92	0.108	0.001	1752	24	1734	39	1762	19	1
84	88	52	1.70	5.34	0.18	0.333	0.009	0.92	0.117	0.002	1872	29	1853	43	1900	24	1
85	274	221	1.41	1.51	0.07	0.157	0.005	0.94	0.070	0.001	939	28	936	27	944	39	0
86	6	6	1.04	11.62	0.62	0.487	0.018	0.90	0.170	0.004	2562	49	2556	75	2556	43	0
87	56	22	2.48	5.48	0.17	0.341	0.009	0.91	0.117	0.001	1889	26	1888	43	1912	20	0
88	135	47	2.76	0.53	0.02	0.070	0.002	0.93	0.055	0.001	428	13	433	14	393	30	-1
89	20	18	1.10	1.91	0.09	0.185	0.005	0.92	0.075	0.002	1079	31	1094	27	1083	49	-1
90	176	98	1.83	4.49	0.22	0.306	0.010	0.96	0.108	0.002	1726	41	1718	51	1757	31	0
91	114	54	2.13	3.08	0.15	0.241	0.009	0.93	0.091	0.002	1432	37	1396	46	1444	34	3
92	97	96	1.03	3.06	0.12	0.247	0.006	0.94	0.091	0.002	1429	30	1431	31	1439	37	0
93	295	70	4.16	13.28	0.43	0.525	0.018	0.83	0.186	0.003	2696	31	2715	78	2702	26	-1
94	247	123	2.17	4.58	0.14	0.307	0.008	0.94	0.108	0.001	1744	25	1724	38	1769	16	1
95	670	755	0.88	0.51	0.05	0.068	0.005	0.98	0.053	0.002	412	34	426	31	298	79	-3
96	251	129	1.92	0.10	0.00	0.015	0.000	0.96	0.047	0.000	92.4	2.1	94.5	2	50	15	-2
97	69	44	1.76	4.17	0.16	0.293	0.009	0.88	0.103	0.002	1661	30	1656	42	1668	31	0
98	80	22	3.69	2.16	0.06	0.196	0.005	0.86	0.079	0.001	1168	18	1160	24	1187	25	1
99	38	31	1.27	1.85	0.09	0.181	0.005	0.93	0.074	0.002	1062	31	1069	28	1068	48	-1
100	49	48	0.98	1.86	0.06	0.182	0.004	0.79	0.075	0.002	1069	22	1077	22	1071	39	-1

Table C-8: Zircon LA-ICP-MS U-Pb Isotopic Data and Ages Sample 11-TUS3C-2-17: Desert Member, Book Cliffs, UT, LST

				Corrected isotopic ratios							Ages (Ma)[f]						
Grain #.	U[a] [ppm]	Th[a] [ppm]	U/Th	$^{207}Pb^{b}/^{235}U$	±2s[d]	$^{206}Pb^{b}/^{238}U$	±2s[d]	Rho[c]	$^{207}Pb^{e}/^{206}Pb$	±2s[d]	$^{207}Pb/^{235}U$	±2s	$^{206}Pb/^{238}U$	±2s	$^{207}Pb/^{206}Pb$	±2s	Disc. %[g]
101	345	154	2.22	3.47	0.10	0.263	0.006	0.92	0.097	0.001	1516	23	1504	33	1557	21	1
102	160	33	4.85	3.13	0.11	0.250	0.008	0.87	0.091	0.001	1436	27	1434	42	1455	30	0
103	132	17	7.53	1.56	0.05	0.159	0.004	0.89	0.072	0.001	951	18	952	23	972	24	0
104	82	56	1.42	0.53	0.02	0.070	0.002	0.93	0.054	0.001	429	14	439	13	380	44	-2
105	97	40	2.37	2.94	0.08	0.237	0.005	0.86	0.090	0.001	1390	21	1374	26	1425	26	1
106	193	69	2.90	6.43	0.16	0.375	0.009	0.83	0.124	0.001	2042	22	2054	41	2016	20	-1
107	90	27	3.48	2.17	0.07	0.198	0.005	0.89	0.079	0.001	1172	22	1166	28	1183	26	1
108	74	16	4.61	4.31	0.12	0.301	0.009	0.85	0.104	0.001	1694	24	1694	43	1696	24	0
109	1122	627	1.79	0.52	0.04	0.068	0.004	0.99	0.055	0.001	417	27	422	26	394	53	-1
110	103	94	1.09	11.41	0.44	0.483	0.013	0.93	0.170	0.002	2549	37	2537	59	2555	24	0
111	316	87	3.89	4.38	0.27	0.295	0.015	0.96	0.107	0.003	1697	55	1662	75	1756	43	2
112	77	55	1.40	1.43	0.05	0.151	0.004	0.92	0.069	0.001	896	21	906	22	908	36	-1
113	1060	122	11.70	1.46	0.09	0.147	0.005	0.96	0.072	0.002	910	35	884	28	981	55	3
114	433	140	3.17	0.38	0.01	0.053	0.001	0.95	0.052	0.001	328	10	335.7	8.4	278	40	-2
115	53	20	2.72	2.57	0.12	0.219	0.007	0.87	0.086	0.002	1296	34	1275	39	1331	37	2
116	135	20	8.02	5.25	0.12	0.331	0.008	0.86	0.116	0.002	1860	19	1841	38	1890	23	1
117	63	35	1.85	11.31	0.26	0.487	0.010	0.89	0.167	0.002	2550	22	2568	46	2523	16	-1
118	327	155	2.16	4.24	0.17	0.284	0.009	0.90	0.108	0.002	1682	33	1619	44	1758	31	4
119	49	18	2.86	1.90	0.06	0.182	0.004	0.89	0.076	0.001	1085	21	1075	23	1104	32	1
120	292	122	2.39	1.81	0.07	0.177	0.007	0.93	0.074	0.001	1046	26	1049	37	1051	26	0
121	355	419	0.86	3.07	0.23	0.240	0.010	0.94	0.093	0.004	1413	59	1383	54	1461	77	2
122	327	50	6.51	1.67	0.05	0.165	0.004	0.89	0.073	0.001	996	17	981	22	1029	23	2
123	68	32	2.20	1.96	0.07	0.185	0.005	0.83	0.077	0.001	1101	23	1093	25	1112	37	1
124	177	130	1.34	4.79	0.14	0.317	0.008	0.90	0.111	0.002	1782	26	1770	38	1819	30	1
125	65	15	4.32	4.15	0.10	0.293	0.007	0.75	0.105	0.002	1661	20	1655	37	1707	34	0
126	54	59	0.93	3.20	0.29	0.249	0.012	0.90	0.092	0.005	1436	74	1433	62	1440	110	0
127	959	813	1.20	0.08	0.00	0.013	0.000	0.94	0.047	0.001	81.8	2.6	83	2.5	63	38	-1
128	73	26	2.77	1.89	0.05	0.183	0.004	0.83	0.075	0.001	1081	18	1082	21	1071	31	0

[a]U and Th concentrations and Th/U ratios calculated relative to the GJ-1 zircon standard using 287±76 ppm for U and 8.4±2.6 ppm for Th (Jackson, 2004)

[b]Corrected for U-Pb fractionation and background and normalised to GJ-1 zircon standard ID-TIMS values (Jackson, 2004) and Pb/U ratios are corrected according to Anderson (2002)

[c]Error correlation defined as the quotient of the propagated errors of the $^{206}Pb/^{238}U$ and the $^{207/235}U$ ratio

[d]The propagated error of quadratic addition of internal errors (2 SD) and within run reproducibility of GJ-1 (2 SD)

[e]Corrected for mass-bias by normalising to GJ-1 zircon standard (~.6 per atomic mass unit)

[f]U-Pb ages are calculated relative to GJ-1 zircon standard and corrected for common Pb using Anderson (2002)

[g]Discordance calculated as (1-(206Pb/238U age/207Pb/206Pb age))*100

Table C-9: Zircon LA-ICP-MS U-Pb Isotopic Data and Ages Sample 11-TUS3C-22.3-22.4: Castlegate Member, Book Cliffs, UT, LST

				Corrected isotopic ratios							Ages (Ma)[f]						
Grain #	U[a] [ppm]	Th[a] [ppm]	U/Th	$^{207}Pb^{b}/^{235}U$	±2s[d]	$^{206}Pb^{b}/^{238}U$	±2s[d]	Rho[c]	$^{207}Pb^{c}/^{206}Pb$	±2s[d]	$^{207}Pb/^{235}U$	±2s	$^{206}Pb/^{238}U$	±2s	$^{207}Pb/^{206}Pb$	±2s	Disc %[g]
1	90	145	0.62	12.90	0.45	0.507	0.012	0.79	0.186	0.003	2677	36	2647	51	2709	26	1
2	185	90	2.14	4.08	0.14	0.291	0.009	0.78	0.102	0.002	1656	26	1644	43	1654	28	1
3	151	77	1.95	1.92	0.06	0.180	0.005	0.62	0.077	0.001	1086	21	1066	26	1122	28	2
4	654	538	1.24	3.11	0.24	0.225	0.010	0.59	0.098	0.004	1422	58	1304	51	1575	74	8
5	204	106	1.89	2.26	0.09	0.192	0.005	0.70	0.087	0.002	1205	29	1132	29	1345	39	6
6	60	24	3.09	1.97	0.06	0.188	0.005	0.70	0.077	0.001	1106	21	1110	27	1125	29	0
7	259	109	2.52	0.23	0.01	0.034	0.001	0.55	0.049	0.001	213.3	5.2	213.6	4.7	156	28	0
8	212	0	10.00	0.46	0.01	0.063	0.001	0.40	0.055	0.000	385.6	6.5	390.9	6.8	415	18	-1
9	86	70	1.24	2.29	0.16	0.209	0.006	0.94	0.080	0.004	1200	48	1225	30	1192	87	-2
10	164	71	2.30	2.49	0.07	0.213	0.005	0.74	0.086	0.001	1269	20	1243	28	1333	21	2
11	16	5	3.49	1.35	0.06	0.143	0.004	0.70	0.070	0.002	861	25	860	20	915	50	0
12	101	44	2.35	1.86	0.05	0.181	0.004	0.69	0.075	0.001	1066	18	1073	22	1058	22	-1
13	99	20	4.98	1.26	0.04	0.132	0.003	0.73	0.070	0.001	831	20	798	19	925	32	4
14	68	37	1.83	3.70	0.12	0.271	0.006	0.74	0.100	0.001	1571	25	1547	33	1627	23	2
15	53	19	2.80	1.19	0.05	0.128	0.004	0.72	0.069	0.001	798	25	773	22	901	39	3
16	202	16	12.70	1.68	0.07	0.166	0.006	0.67	0.074	0.001	1001	26	989	31	1034	33	1
17	127	27	4.74	3.21	0.12	0.261	0.009	0.75	0.091	0.002	1474	31	1491	48	1437	34	-1
18	92	28	3.24	2.01	0.06	0.188	0.004	0.69	0.077	0.001	1116	19	1108	23	1129	25	1
19	37	19	1.97	1.22	0.06	0.132	0.004	0.79	0.067	0.002	804	25	799	20	862	49	1
20	48	39	1.18	3.81	0.15	0.265	0.006	0.91	0.104	0.002	1593	29	1514	29	1702	39	5
21	355	124	2.77	3.69	0.12	0.258	0.006	0.65	0.104	0.002	1574	26	1476	31	1703	36	6
22	123	53	2.30	3.28	0.12	0.235	0.006	0.93	0.101	0.002	1470	28	1360	32	1636	33	7
23	98	40	2.41	1.96	0.05	0.185	0.004	0.72	0.076	0.001	1098	16	1095	21	1101	23	0
24	67	24	2.81	2.95	0.07	0.235	0.005	0.73	0.092	0.001	1397	18	1365	25	1458	24	2
25	80	21	3.70	1.87	0.05	0.179	0.005	0.74	0.077	0.001	1069	18	1057	25	1124	24	1
26	81	35	2.09	12.65	0.35	0.503	0.012	0.76	0.182	0.002	2646	26	2625	50	2668	18	1
27	179	54	3.20	2.25	0.06	0.200	0.005	0.68	0.082	0.001	1197	17	1175	26	1237	23	2
28	7	6	1.20	1.34	0.08	0.145	0.005	0.54	0.069	0.002	857	33	875	29	904	57	-2
29	359	166	2.11	10.11	0.25	0.418	0.009	0.90	0.173	0.002	2439	23	2261	42	2589	21	7
30	121	56	2.18	6.38	0.12	0.361	0.006	0.74	0.128	0.001	2032	17	1986	29	2072	16	2
31	55	27	1.97	1.36	0.05	0.141	0.003	0.69	0.071	0.002	864	24	851	19	945	45	2
32	28	22	1.29	1.93	0.10	0.182	0.005	0.82	0.077	0.003	1082	36	1075	27	1139	68	1
34	28	23	1.19	4.43	0.22	0.305	0.008	0.85	0.106	0.003	1719	42	1716	42	1712	52	0
35	18	7	2.35	1.60	0.06	0.158	0.004	0.64	0.075	0.002	976	26	943	24	1059	39	3
36	57	17	3.32	2.03	0.05	0.190	0.004	0.66	0.077	0.001	1127	17	1118	23	1119	25	1
37	271	101	2.68	0.08	0.00	0.012	0.000	0.75	0.047	0.000	78.2	1.7	79.1	1.6	58	22	-1
38	215	69	3.14	1.92	0.04	0.183	0.004	0.66	0.076	0.001	1088	15	1084	19	1103	18	0
39	89	53	1.66	4.88	0.11	0.325	0.006	0.72	0.110	0.001	1795	19	1813	29	1791	19	-1
40	31	36	0.85	2.93	0.19	0.239	0.008	0.82	0.092	0.003	1411	49	1381	39	1473	72	2
41	27	16	1.55	1.93	0.12	0.180	0.007	0.83	0.077	0.002	1091	43	1069	38	1156	57	2
42	84	37	2.21	3.99	0.11	0.288	0.006	0.68	0.101	0.001	1629	22	1632	32	1646	15	0
43	220	68	3.19	4.41	0.12	0.298	0.007	0.71	0.107	0.001	1714	22	1686	35	1753	25	2
44	72	29	2.47	3.42	0.10	0.246	0.005	0.83	0.101	0.002	1504	23	1414	26	1648	29	6
45	70	25	2.68	2.06	0.04	0.191	0.004	0.68	0.078	0.001	1136	14	1126	22	1140	21	1
46	107	105	1.06	1.87	0.06	0.180	0.004	0.64	0.076	0.001	1075	21	1064	21	1116	35	1
47	181	68	2.70	3.13	0.08	0.248	0.005	0.68	0.090	0.001	1436	18	1427	26	1431	19	1
48	40	22	1.79	1.57	0.07	0.157	0.005	0.62	0.073	0.002	957	30	941	30	994	51	2
49	193	101	1.95	4.81	0.11	0.316	0.006	0.74	0.111	0.001	1792	19	1769	30	1818	15	1
50	47	17	2.66	2.01	0.09	0.183	0.005	0.88	0.080	0.002	1111	29	1081	26	1197	45	3
51	173	74	2.30	6.62	0.15	0.371	0.008	0.76	0.130	0.002	2063	19	2037	35	2099	22	1
52	162	47	3.38	1.91	0.07	0.181	0.006	0.68	0.078	0.001	1082	26	1071	32	1145	28	1
53	198	126	1.53	1.59	0.05	0.159	0.004	0.64	0.071	0.001	965	19	952	24	968	22	1

Table C-9: Zircon LA-ICP-MS U-Pb Isotopic Data and Ages Sample 11-TUS3C-22.3-22.4: Castlegate Member, Book Cliffs, UT, LST

				Corrected isotopic ratios							Ages (Ma)[f]						
Grain #	U[a] [ppm]	Th[a] [ppm]	U/Th	$^{207}Pb^{b}/^{235}U$	±2s[d]	$^{206}Pb^{b}/^{238}U$	±2s[d]	Rho[c]	$^{207}Pb^{e}/^{206}Pb$	±2s[d]	$^{207}Pb/^{235}U$	±2s	$^{206}Pb/^{238}U$	±2s	$^{207}Pb/^{206}Pb$	±2s	Disc %[g]
54	636	8	160.00	4.26	0.14	0.294	0.010	0.66	0.106	0.003	1674	31	1656	48	1722	45	1
55	29	12	2.44	1.44	0.05	0.149	0.004	0.80	0.071	0.002	900	23	895	21	941	45	1
56	156	141	1.10	12.10	0.47	0.478	0.018	0.80	0.182	0.004	2609	36	2515	77	2674	35	4
57	46	10	4.52	3.31	0.13	0.243	0.007	0.71	0.098	0.002	1484	31	1402	36	1591	36	6
58	69	34	2.07	2.29	0.08	0.198	0.005	0.84	0.085	0.001	1210	24	1166	25	1305	33	4
59	52	39	1.34	6.38	0.21	0.371	0.009	0.80	0.125	0.002	2028	29	2039	44	2022	26	-1
60	46	34	1.39	4.48	0.19	0.291	0.007	0.98	0.112	0.003	1723	37	1643	34	1808	55	5
61	128	56	2.27	4.29	0.11	0.295	0.006	0.77	0.106	0.001	1687	21	1663	31	1727	20	1
62	30	11	2.70	2.96	0.12	0.227	0.006	0.82	0.096	0.002	1393	31	1316	34	1545	42	6
63	270	124	2.18	1.85	0.08	0.179	0.006	0.76	0.076	0.001	1055	29	1058	31	1087	34	0
64	63	32	1.97	2.42	0.08	0.209	0.005	0.73	0.084	0.001	1251	23	1227	25	1294	27	2
65	1842	381	5.08	0.56	0.04	0.072	0.004	0.00	0.056	0.001	451	26	448	26	464	26	1
67	129	308	0.43	0.76	0.03	0.094	0.002	0.35	0.058	0.001	576	16	581	13	611	29	-1
68	44	18	2.48	1.65	0.06	0.165	0.004	0.79	0.074	0.001	990	23	984	24	1036	38	1
69	44	26	1.89	2.05	0.06	0.192	0.004	0.68	0.077	0.001	1128	21	1134	23	1130	26	-1
70	68	12	5.53	4.39	0.23	0.301	0.012	0.65	0.105	0.002	1702	46	1695	61	1707	44	0
71	364	52	7.53	4.51	0.09	0.301	0.007	0.75	0.110	0.001	1730	17	1696	32	1792	23	2
72	151	38	3.99	1.89	0.08	0.183	0.007	0.61	0.075	0.001	1077	27	1080	37	1057	27	0
73	129	47	2.80	4.20	0.10	0.292	0.006	0.78	0.104	0.001	1672	19	1657	29	1702	22	1
74	204	80	2.62	1.84	0.05	0.177	0.004	0.70	0.076	0.001	1057	16	1051	21	1093	24	1
75	103	46	2.23	6.86	0.18	0.385	0.008	0.73	0.130	0.002	2090	23	2097	38	2093	20	0
76	60	35	1.73	2.60	0.07	0.220	0.005	0.67	0.088	0.001	1304	20	1288	28	1375	24	1
77	70	11	6.53	4.74	0.11	0.322	0.007	0.75	0.107	0.002	1770	19	1800	31	1753	29	-2
78	54	68	0.81	5.11	0.19	0.328	0.008	0.76	0.113	0.002	1833	30	1827	37	1848	35	0
79	27	13	2.20	1.44	0.06	0.149	0.004	0.81	0.072	0.002	906	23	892	22	979	41	2
80	56	23	2.63	14.47	0.42	0.522	0.013	0.82	0.203	0.002	2782	26	2709	55	2850	18	3
81	152	34	4.48	1.89	0.04	0.182	0.004	0.71	0.076	0.001	1077	15	1075	21	1089	21	0
82	1190	205	5.82	1.25	0.07	0.133	0.005	0.06	0.068	0.002	814	31	802	28	842	43	1
83	103	46	2.35	4.46	0.12	0.309	0.007	0.77	0.104	0.001	1722	22	1736	36	1704	24	-1
84	53	29	1.81	2.01	0.11	0.184	0.005	0.80	0.080	0.002	1127	36	1086	28	1185	60	4
85	117	59	1.97	1.92	0.06	0.186	0.004	0.65	0.074	0.001	1090	20	1101	21	1041	40	-1
86	22	30	0.74	4.45	0.27	0.302	0.008	0.88	0.109	0.004	1728	51	1700	39	1750	72	2
87	24	6	3.86	4.25	0.13	0.294	0.007	0.76	0.106	0.002	1682	26	1659	35	1729	31	1
88	94	32	2.89	4.22	0.18	0.299	0.009	0.72	0.101	0.001	1671	35	1687	47	1655	29	-1
89	92	83	1.11	2.54	0.12	0.216	0.006	0.74	0.085	0.002	1279	33	1261	31	1321	47	1
90	238	81	2.76	4.26	0.14	0.288	0.008	0.76	0.108	0.002	1684	26	1633	42	1770	27	3
91	71	64	1.11	0.26	0.01	0.038	0.001	0.39	0.048	0.001	234.7	7.5	242.1	7.6	103	35	-3
92	45	31	1.53	2.85	0.13	0.223	0.006	0.84	0.093	0.002	1359	34	1295	32	1500	42	5
93	44	91	0.50	13.48	0.53	0.511	0.011	0.82	0.193	0.005	2716	38	2659	49	2763	42	2
94	52	18	3.01	4.35	0.13	0.301	0.007	0.74	0.105	0.001	1699	24	1692	36	1703	25	0
95	100	39	2.75	2.83	0.09	0.235	0.005	0.74	0.086	0.001	1361	23	1362	28	1340	27	0

[a]U and Th concentrations and Th/U ratios calculated relative to the GJ-1 zircon standard using 287±76 ppm for U and 8.4±2.6 ppm for Th (Jackson, 2004)

[b]Corrected for U-Pb fractionation and background and normalised to GJ-1 zircon standard ID-TIMS values (Jackson, 2004) and Pb/U ratios are corrected according to Anderson (2002)

[c]Error correlation defined as the quotient of the propagated errors of the $^{206}Pb/^{238}U$ and the $^{207/235}U$ ratio

[d]The propagated error of quadratic addition of internal errors (2 SD) and within run reproducibility of GJ-1 (2 SD)

[e]Corrected for mass-bias by normalising to GJ-1 zircon standard (~.6 per atomic mass unit)

[f]U-Pb ages are calculated relative to GJ-1 zircon standard and corrected for common Pb using Anderson (2002)

[g]Discordance calculated as (1-(206Pb/238U age/207Pb/206Pb age))*100

Table D-1: Rutile LA-ICP-MS U-Pb Isotopic Data and Ages — Sample 11-TUS3C-22.3-22.4: Castlegate Member, Book Cliffs, UT, LST

Sample	Grain #.	U[a] [ppm]	Th[a] [ppm]	U/Th	Corrected isotopic ratios: $^{207}Pb^{b}/^{235}U$	±2s[d]	$^{206}Pb^{b}/^{238}U$	±2s[d]	Rho[c]	$^{207}Pb^{e}/^{206}Pb$	±2s[d]	Ages (Ma)[f]: $^{207}Pb/^{235}U$	±2s	$^{206}Pb/^{238}U$	±2s	$^{207}Pb/^{206}Pb$	±2s	Disc. %[g]
TUS3C22.3_22.4Rt_1	1	58	b.d.	na	3.30	0.20	0.257	0.010	0.98	0.093	0.002	1468	47	1472	49	1472	43	0
TUS3C22.3_22.4Rt_2	2	6	1	8.19	7.52	0.79	0.358	0.019	0.92	0.148	0.009	2134	94	1966	89	2293	98	8
TUS3C22.3_22.4Rt_3	3	12	b.d.	na	0.43	0.03	0.054	0.003	0.91	0.058	0.001	362	22	337	21	504	48	7
TUS3C22.3_22.4Rt_4	4	9	b.d.	na	1.76	0.35	0.130	0.013	0.76	0.099	0.016	980	120	785	73	1590	270	20
TUS3C22.3_22.4Rt_5	5	13	2	5.98	1.26	0.12	0.128	0.009	0.99	0.071	0.002	821	54	773	51	953	57	6
TUS3C22.3_22.4Rt_6	6	5	b.d.	na	10.90	1.50	0.453	0.031	0.98	0.171	0.012	2440	130	2390	140	2520	120	2
TUS3C22.3_22.4Rt_7	7	4	b.d.	na	0.47	0.02	0.062	0.002	0.98	0.056	0.001	397	16	388	14	462	40	2
TUS3C22.3_22.4Rt_8	8	0	b.d.	na	10.20	4.10	0.192	0.049	0.97	0.281	0.042	2040	370	1090	260	3450	220	47
TUS3C22.3_22.4Rt_9	9	26	2	14.51	0.35	0.02	0.046	0.002	1.00	0.055	0.000	302	12	287	11	423	16	5
TUS3C22.3_22.4Rt_10	10	3	b.d.	na	3.06	0.44	0.117	0.009	0.82	0.187	0.018	1350	120	712	52	2710	180	47
TUS3C22.3_22.4Rt_11	11	15	b.d.	na	4.66	0.31	0.305	0.011	0.99	0.110	0.004	1743	54	1713	55	1784	56	2
TUS3C22.3_22.4Rt_12	12	21	b.d.	na	0.70	0.13	0.063	0.004	0.69	0.077	0.011	511	66	396	27	980	210	23
TUS3C22.3_22.4Rt_13	13	15	106	0.14	0.98	0.19	0.065	0.004	0.79	0.112	0.017	666	95	405	26	1520	290	39
TUS3C22.3_22.4Rt_14	14	96	1	165.34	4.90	0.45	0.317	0.018	0.99	0.109	0.004	1782	83	1781	89	1775	74	0
TUS3C22.3_22.4Rt_15	15	5	13	0.39	0.33	0.02	0.045	0.002	1.00	0.053	0.000	289	12	286	12	325	17	1
TUS3C22.3_22.4Rt_16	16	26	2	13.10	0.62	0.03	0.079	0.003	0.99	0.059	0.001	490	19	489	20	540	44	0
TUS3C22.3_22.4Rt_17	17	104	1124	0.09	4.90	0.33	0.310	0.012	0.98	0.113	0.003	1785	57	1736	61	1845	52	3
TUS3C22.3_22.4Rt_18	18	6	b.d.	na	5.71	0.63	0.342	0.020	0.98	0.118	0.006	1890	89	1889	95	1892	85	0
TUS3C22.3_22.4Rt_19	19	104	5	20.55	5.49	0.42	0.323	0.014	0.98	0.124	0.004	1914	65	1827	68	2012	59	5
TUS3C22.3_22.4Rt_20	20	3	b.d.	na	0.94	0.09	0.096	0.006	0.73	0.068	0.002	660	46	587	36	853	59	11
TUS3C22.3_22.4Rt_21	21	10	6	1.62	0.61	0.04	0.075	0.004	0.99	0.059	0.001	479	23	467	20	555	29	3
TUS3C22.3_22.4Rt_22	22	18	5	3.67	8.60	1.00	0.411	0.025	0.98	0.146	0.009	2240	110	2210	120	2260	100	1
TUS3C22.3_22.4Rt_23	23	14	150	0.09	4.43	0.52	0.288	0.020	0.99	0.109	0.005	1699	99	1625	98	1750	90	4
TUS3C22.3_22.4Rt_24	24	35	b.d.	na	6.96	0.65	0.383	0.019	0.98	0.126	0.006	2071	80	2086	88	2024	80	-1
TUS3C22.3_22.4Rt_25	25	18	2	8.28	0.90	0.07	0.105	0.006	0.99	0.062	0.001	642	35	643	36	659	37	0
TUS3C22.3_22.4Rt_26	26	12	b.d.	na	0.41	0.02	0.055	0.002	1.00	0.054	0.000	349	13	343	12	378	19	2
TUS3C22.3_22.4Rt_27	27	1	7	0.10	7.30	1.50	0.180	0.030	0.87	0.288	0.019	2060	180	1060	160	3420	110	49
TUS3C22.3_22.4Rt_28	28	9	7	1.23	0.61	0.03	0.074	0.003	1.00	0.059	0.001	481	19	462	19	576	22	4
TUS3C22.3_22.4Rt_29	29	65	211	0.31	2.47	0.16	0.097	0.005	0.93	0.184	0.003	1267	50	594	31	2686	23	53
TUS3C22.3_22.4Rt_30	30	363	313	1.16	0.37	0.02	0.050	0.002	0.99	0.055	0.002	316	13	315	13	428	63	0
TUS3C22.3_22.4Rt_31	31	5	b.d.	na	2.21	0.18	0.189	0.010	0.99	0.084	0.003	1166	57	1112	56	1278	59	5
TUS3C22.3_22.4Rt_32	32	3	17	0.20	2.46	0.25	0.092	0.006	0.96	0.195	0.007	1263	71	568	37	2782	58	55
TUS3C22.3_22.4Rt_33	34	5	b.d.	na	4.25	0.59	0.267	0.018	0.96	0.112	0.009	1620	110	1516	91	1770	130	6
TUS3C22.3_22.4Rt_34	35	3	1	3.20	0.49	0.05	0.054	0.004	0.69	0.059	0.001	406	37	340	26	562	45	16
TUS3C22.3_22.4Rt_35	36	6	10	0.56	2.41	0.28	0.083	0.008	0.98	0.216	0.006	1256	80	511	45	2944	49	59
TUS3C22.3_22.4Rt_36	37	9	b.d.	na	1.47	0.28	0.119	0.013	0.83	0.090	0.015	880	110	719	74	1300	230	18
TUS3C22.3_22.4Rt_37	38	7	1	6.75	0.76	0.03	0.089	0.003	0.99	0.062	0.001	570	18	547	17	663	21	4
TUS3C22.3_22.4Rt_38	39	23	b.d.	na	0.66	0.02	0.081	0.002	0.97	0.060	0.001	512	14	503	14	593	41	2
TUS3C22.3_22.4Rt_39	40	18	1	14.37	0.67	0.04	0.078	0.003	0.99	0.062	0.001	519	21	485	19	669	29	7
TUS3C22.3_22.4Rt_40	41	3	b.d.	na	0.76	0.09	0.085	0.006	0.72	0.063	0.002	562	50	522	35	686	67	7
TUS3C22.3_22.4Rt_41	42	5	b.d.	na	0.47	0.03	0.062	0.003	0.99	0.055	0.001	389	17	386	17	403	26	1
TUS3C22.3_22.4Rt_42	43	7	2	3.53	1.51	0.35	0.084	0.008	0.92	0.126	0.020	840	130	520	47	1740	310	38
TUS3C22.3_22.4Rt_43	44	34	0	######	1.76	0.14	0.173	0.010	0.99	0.074	0.002	1023	53	1025	54	1032	51	0
TUS3C22.3_22.4Rt_44	45	315	19	16.24	3.51	0.27	0.264	0.012	0.98	0.098	0.003	1522	62	1505	63	1596	62	1
TUS3C22.3_22.4Rt_45	46	20	200	0.10	10.10	1.20	0.238	0.021	0.98	0.309	0.009	2420	110	1360	110	3508	45	44
TUS3C22.3_22.4Rt_46	47	18	b.d.	na	14.40	1.70	0.295	0.029	0.93	0.372	0.013	2790	110	1680	140	3792	55	40
TUS3C22.3_22.4Rt_47	48	6	b.d.	na	0.68	0.04	0.083	0.004	0.98	0.061	0.001	523	21	511	21	607	38	2
TUS3C22.3_22.4Rt_48	49	7	b.d.	na	82.00	23.00	0.830	0.180	0.98	0.646	0.071	4300	340	3780	630	4580	160	12
TUS3C22.3_22.4Rt_49	50	5	b.d.	na	0.73	0.06	0.087	0.005	0.99	0.061	0.001	562	34	542	31	617	37	4

Table D-1: Rutile LA-ICP-MS U-Pb Isotopic Data and Ages — Sample 11-TUS3C-22.3-22.4: Castlegate Member, Book Cliffs, UT, LST

Sample	Grain #.	U[a] [ppm]	Th[a] [ppm]	U/Th	Corrected isotopic ratios $^{207}Pb^{b}/^{235}U$	±2s[d]	$^{206}Pb^{b}/^{238}U$	±2s[d]	Rho[c]	$^{207}Pb^{e}/^{206}Pb$	±2s[d]	Ages (Ma)[f] $^{207}Pb/^{235}U$	±2s	$^{206}Pb/^{238}U$	±2s	$^{207}Pb/^{206}Pb$	±2s	Disc. %[g]
TUS3C22.3_22.4Rt_50	51	17	3	6.90	7.86	0.87	0.406	0.022	0.98	0.142	0.008	2230	100	2190	100	2280	96	2
TUS3C22.3_22.4Rt_51	52	7	15	0.48	2.89	0.41	0.101	0.011	0.98	0.208	0.011	1320	100	616	66	2893	76	53
TUS3C22.3_22.4Rt_52	53	55	b.d.	na	0.56	0.04	0.071	0.005	1.00	0.057	0.001	450	28	443	27	479	30	2
TUS3C22.3_22.4Rt_53	54	8	b.d.	na	0.50	0.05	0.063	0.005	0.87	0.058	0.002	412	38	393	33	524	67	5
TUS3C22.3_22.4Rt_54	55	24	b.d.	na	1.57	0.35	0.112	0.009	0.87	0.102	0.016	910	120	684	51	1510	240	25
TUS3C22.3_22.4Rt_55	56	22	b.d.	na	3.30	0.31	0.257	0.014	0.98	0.097	0.004	1475	73	1472	73	1550	74	0
TUS3C22.3_22.4Rt_56	57	72	16	4.38	0.80	0.06	0.085	0.005	1.00	0.069	0.001	599	37	524	31	893	42	13
TUS3C22.3_22.4Rt_57	58	15	1	23.71	7.20	1.20	0.347	0.026	0.92	0.138	0.011	2070	110	1950	110	2170	110	6
TUS3C22.3_22.4Rt_58	59	12	6	2.02	11.00	1.90	0.393	0.033	0.97	0.191	0.017	2450	150	2140	140	2750	140	13
TUS3C22.3_22.4Rt_59	60	5	b.d.	na	11.60	2.30	0.404	0.032	0.95	0.192	0.026	2380	190	2170	150	2610	230	9
TUS3C22.3_22.4Rt_60	61	14	b.d.	na	0.51	0.04	0.064	0.004	0.99	0.058	0.001	414	26	400	24	514	39	3
TUS3C22.3_22.4Rt_61	62	38	b.d.	na	4.20	0.55	0.289	0.022	0.97	0.102	0.005	1620	100	1620	110	1632	93	0
TUS3C22.3_22.4Rt_62	63	7	b.d.	na	0.88	0.07	0.099	0.005	0.84	0.065	0.003	633	34	609	28	726	58	4
TUS3C22.3_22.4Rt_63	64	5	b.d.	na	1.08	0.09	0.116	0.006	0.80	0.069	0.003	736	39	705	32	879	77	4
TUS3C22.3_22.4Rt_64	65	3	b.d.	na	0.63	0.04	0.080	0.004	0.99	0.058	0.001	495	24	494	24	516	25	0
TUS3C22.3_22.4Rt_65	67	50	1	79.21	4.67	0.65	0.304	0.023	0.98	0.107	0.006	1690	110	1700	110	1718	99	-1
TUS3C22.3_22.4Rt_66	68	15	b.d.	na	0.53	0.05	0.067	0.005	0.99	0.059	0.002	434	32	415	27	566	55	4
TUS3C22.3_22.4Rt_67	69	2	b.d.	na	1.21	0.17	0.092	0.007	0.71	0.102	0.015	776	73	567	43	1500	250	27
TUS3C22.3_22.4Rt_68	70	119	b.d.	na	3.03	0.16	0.244	0.009	0.99	0.090	0.002	1412	42	1405	44	1434	49	0
TUS3C22.3_22.4Rt_69	71	71	b.d.	na	0.30	0.03	0.042	0.003	0.99	0.052	0.001	267	20	267	20	292	34	0
TUS3C22.3_22.4Rt_70	72	8	1	11.88	4.72	0.77	0.153	0.014	0.91	0.224	0.020	1730	150	911	77	2960	180	47
TUS3C22.3_22.4Rt_71	73	409	65	6.31	2.16	0.20	0.195	0.012	0.99	0.081	0.003	1147	61	1146	64	1203	64	0
TUS3C22.3_22.4Rt_72	74	9	b.d.	na	0.48	0.02	0.063	0.002	0.99	0.056	0.001	399	15	395	15	452	42	1
TUS3C22.3_22.4Rt_73	75	3	8	0.39	15.50	3.20	0.284	0.047	0.98	0.379	0.031	2720	240	1610	250	3820	120	41
TUS3C22.3_22.4Rt_74	76	1	2	0.41	25.40	6.50	0.379	0.070	0.98	0.423	0.041	2970	240	1980	300	3940	150	33
TUS3C22.3_22.4Rt_75	77	4	1	5.48	2.29	0.31	0.096	0.007	0.85	0.174	0.015	1173	98	591	42	2680	140	50
TUS3C22.3_22.4Rt_76	78	38	b.d.	na	0.77	0.03	0.093	0.003	1.00	0.060	0.001	580	19	574	18	609	23	1
TUS3C22.3_22.4Rt_77	79	23	b.d.	na	1.60	0.36	0.076	0.007	0.95	0.134	0.021	860	140	471	44	1820	330	45
TUS3C22.3_22.4Rt_78	80	5	b.d.	na	4.29	0.29	0.282	0.010	0.98	0.109	0.004	1676	55	1600	53	1773	57	5
TUS3C22.3_22.4Rt_79	81	37	b.d.	na	8.50	1.10	0.259	0.020	0.82	0.243	0.020	2230	120	1490	100	3100	150	33
TUS3C22.3_22.4Rt_80	82	146	2	78.49	0.65	0.03	0.081	0.003	0.99	0.058	0.001	506	16	500	16	543	34	1
TUS3C22.3_22.4Rt_81	83	20	54	0.38	0.93	0.12	0.044	0.005	0.88	0.156	0.004	641	61	279	28	2425	52	56
TUS3C22.3_22.4Rt_82	84	6	1	8.44	10.80	1.40	0.232	0.021	0.98	0.334	0.015	2470	120	1340	110	3627	68	46
TUS3C22.3_22.4Rt_83	85	6	1	4.73	7.70	2.10	0.189	0.036	0.98	0.282	0.026	1940	270	1080	190	3320	150	44
TUS3C22.3_22.4Rt_84	86	10	b.d.	na	1.28	0.14	0.067	0.003	0.68	0.139	0.012	825	68	418	15	2070	220	49
TUS3C22.3_22.4Rt_85	87	23	b.d.	na	0.69	0.04	0.085	0.004	0.99	0.060	0.001	529	25	522	24	600	42	1
TUS3C22.3_22.4Rt_86	88	88	4	21.90	1.55	0.08	0.156	0.006	0.98	0.074	0.002	944	32	933	31	1026	48	1
TUS3C22.3_22.4Rt_87	89	89	b.d.	na	3.82	0.18	0.283	0.008	0.98	0.096	0.002	1589	38	1606	39	1550	41	-1
TUS3C22.3_22.4Rt_88	90	12	b.d.	na	0.92	0.07	0.098	0.005	0.99	0.068	0.001	656	35	599	32	857	41	9
TUS3C22.3_22.4Rt_89	91	14	4	3.29	3.92	0.32	0.122	0.008	0.97	0.231	0.005	1607	66	737	47	3065	32	54
TUS3C22.3_22.4Rt_90	92	12	b.d.	na	0.49	0.03	0.064	0.003	1.00	0.056	0.000	406	17	400	17	444	17	1
TUS3C22.3_22.4Rt_91	93	11	1	11.37	9.05	0.97	0.396	0.022	0.99	0.161	0.008	2295	94	2140	100	2439	83	7
TUS3C22.3_22.4Rt_92	94	7	1	4.85	0.78	0.04	0.091	0.004	0.99	0.062	0.001	584	20	562	21	669	21	4
TUS3C22.3_22.4Rt_93	95	18	b.d.	na	0.44	0.02	0.059	0.002	1.00	0.054	0.000	369	15	367	15	381	16	1
TUS3C22.3_22.4Rt_94	96	2	3	0.91	2.97	0.81	0.156	0.019	0.87	0.123	0.021	1250	180	940	100	1830	280	25
TUS3C22.3_22.4Rt_95	97	34	124	0.27	9.80	1.10	0.232	0.021	0.98	0.303	0.009	2360	110	1330	110	3478	45	44
TUS3C22.3_22.4Rt_96	98	84	b.d.	na	0.54	0.04	0.069	0.005	0.99	0.057	0.001	432	27	431	28	480	43	0
TUS3C22.3_22.4Rt_97	99	34	b.d.	na	14.60	2.30	0.403	0.039	0.91	0.254	0.023	2720	160	2160	180	3250	140	21
TUS3C22.3_22.4Rt_98	100	2	b.d.	na	14.10	2.50	0.288	0.038	0.97	0.364	0.022	2680	180	1640	200	3736	88	39

Table D-1: Rutile LA-ICP-MS U-Pb Isotopic Data and Ages   Sample 11-TUS3C-22.3-22.4: Castlegate Member, Book Cliffs, UT, LST

					Corrected isotopic ratios							Ages (Ma)[f]						
Sample	Grain #.	U[a] [ppm]	Th[a] [ppm]	U/Th	$^{207}Pb^{b}/^{235}U$	±2s[d]	$^{206}Pb^{b}/^{238}U$	±2s[d]	Rho[c]	$^{207}Pb^{e}/^{206}Pb$	±2s[d]	$^{207}Pb/^{235}U$	±2s	$^{206}Pb/^{238}U$	±2s	$^{207}Pb/^{206}Pb$	±2s	Disc. %[g]
TUS3C22.3_22.4Rt_99	101	18	b.d.	na	2.34	0.17	0.205	0.010	0.99	0.084	0.003	1220	55	1198	55	1281	58	2
TUS3C22.3_22.4Rt_100	102	3	b.d.	na	1.35	0.26	0.092	0.011	0.82	0.119	0.019	810	100	567	63	1640	280	30
TUS3C22.3_22.4Rt_101	103	8	b.d.	na	0.94	0.15	0.085	0.005	0.76	0.079	0.010	646	68	523	30	1040	180	19
TUS3C22.3_22.4Rt_102	104	10	b.d.	na	0.48	0.04	0.062	0.004	1.00	0.055	0.001	393	27	386	26	427	29	2
TUS3C22.3_22.4Rt_103	105	46	b.d.	na	5.88	0.35	0.357	0.011	0.99	0.118	0.003	1955	53	1975	55	1916	46	-1
TUS3C22.3_22.4Rt_104	106	8	b.d.	na	1.30	0.18	0.066	0.005	0.63	0.139	0.016	809	82	410	29	2010	260	49
TUS3C22.3_22.4Rt_105	107	3	b.d.	na	2.34	0.21	0.097	0.005	0.64	0.192	0.006	1238	65	594	31	2749	63	52
TUS3C22.3_22.4Rt_106	108	6	5	1.23	1.99	0.22	0.088	0.006	0.76	0.180	0.005	1103	76	546	34	2645	43	50
TUS3C22.3_22.4Rt_107	109	1	b.d.	na	5.80	1.50	0.167	0.020	0.96	0.210	0.031	1710	210	990	110	2660	300	42
TUS3C22.3_22.4Rt_108	110	3	b.d.	na	9.20	1.80	0.404	0.034	0.94	0.145	0.011	2190	140	2170	150	2220	130	1
TUS3C22.3_22.4Rt_109	111	7	b.d.	na	0.66	0.05	0.082	0.005	1.00	0.060	0.001	510	29	505	28	569	44	1
TUS3C22.3_22.4Rt_110	112	21	b.d.	na	5.38	0.42	0.345	0.017	0.98	0.116	0.005	1895	74	1906	82	1894	70	-1
TUS3C22.3_22.4Rt_111	113	46	b.d.	na	0.73	0.03	0.090	0.003	0.99	0.059	0.000	559	17	552	17	573	18	1
TUS3C22.3_22.4Rt_112	114	10	b.d.	na	1.77	0.27	0.090	0.007	0.54	0.144	0.019	1030	110	553	43	2080	290	46
TUS3C22.3_22.4Rt_113	115	52	1	52.42	0.80	0.04	0.095	0.004	1.00	0.061	0.001	594	23	585	22	635	27	2
TUS3C22.3_22.4Rt_114	116	4	5	0.67	89.00	18.00	0.900	0.150	0.99	0.692	0.028	4520	220	4260	560	4719	56	6
TUS3C22.3_22.4Rt_115	117	3	b.d.	na	0.63	0.08	0.079	0.008	1.00	0.059	0.002	500	51	489	49	558	56	2
TUS3C22.3_22.4Rt_116	118	4	b.d.	na	0.54	0.06	0.071	0.007	0.99	0.058	0.003	456	45	438	40	505	89	4
TUS3C22.3_22.4Rt_117	119	22	b.d.	na	0.61	0.02	0.078	0.003	0.98	0.056	0.001	480	14	484	15	458	25	-1
TUS3C22.3_22.4Rt_118	120	26	b.d.	na	0.62	0.03	0.079	0.003	0.96	0.057	0.001	493	19	487	17	487	24	1
TUS3C22.3_22.4Rt_119	121	10	b.d.	na	0.50	0.04	0.055	0.003	0.53	0.062	0.001	407	28	342	17	675	32	16
TUS3C22.3_22.4Rt_119	122	20	b.d.	na	2.09	0.21	0.191	0.013	0.99	0.076	0.002	1120	69	1123	69	1074	54	0

[a]U and Th concentrations and Th/U ratios calculated relative to the R10 rutile standard using 287±76 ppm for U and 8.4±2.6 ppm for Th (Jackson, 2004)
[b]Corrected for U-Pb fractionation and background and normalised to R10 rutile standard ID-TIMS values (Jackson, 2004) and Pb/U ratios are corrected according to Anderson (2002)
[c]Error correlation defined as the quotient of the propagated errors of the $^{206}Pb/^{238}U$ and the $^{207}/^{235}U$ ratio
[d]The propagated error of quadratic addition of internal errors (2 SD) and within run reproducibility of R10 (2 SD)
[e]Corrected for mass-bias by normalising to R10 rutile standard (~.6 per atomic mass unit)
[f]U-Pb ages are calculated relative to R10 rutile standard and corrected for common Pb using Anderson (2002)
[g]Discordance %: for $^{206}Pb/^{238}U$ ages <1Ga calculated as $((1-(^{206}Pb/^{238}U)/(^{207}Pb/^{235}U))*100)$, for $^{206}Pb/^{238}U$ ages >1Ga calculated as $((1-(^{206}Pb/^{238}U)/(^{207}Pb/^{206}Pb))*100)$
b.d.= below detection limit
na = not applicable

Table D-2: Rutile LA-ICP-MS U-Pb Isotopic Data and Ages Sample 11-CSTG-07: Castelgate Member, Book Cliffs, UT, LST

					Corrected isotopic ratios							Ages (Ma)[f]						
Sample	Grain #.	U[a] [ppm]	Th[a] [ppm]	U/Th	$^{207}Pb^{b}/^{235}U$	±2s[d]	$^{206}Pb^{b}/^{238}U$	±2s[d]	Rho[c]	$^{207}Pb^{e}/^{206}Pb$	±2s[d]	$^{207}Pb/^{235}U$	±2s	$^{206}Pb/^{238}U$	±2s	$^{207}Pb/^{206}Pb$	±2s	Disc. %[g]
CSTG07Rt_1	1	9	4	2.54	0.81	0.04	0.097	0.004	0.99	0.061	0.001	599	22	594	22	628	33	1
CSTG07Rt_2	2	10	b.d.	na	0.49	0.03	0.065	0.004	0.98	0.055	0.001	403	21	404	21	416	31	0
CSTG07Rt_3	3	24	b.d.	na	0.56	0.04	0.072	0.004	0.99	0.056	0.001	449	24	450	24	470	29	0
CSTG07Rt_4	4	28	b.d.	na	0.36	0.02	0.050	0.003	1.00	0.053	0.001	317	18	313	17	335	25	1
CSTG07Rt_5	5	89	b.d.	na	0.63	0.08	0.082	0.009	0.99	0.057	0.002	493	51	508	55	500	58	-3
CSTG07Rt_6	6	2	4	0.46	0.97	0.13	0.092	0.008	0.77	0.069	0.003	662	62	568	44	876	72	14
CSTG07Rt_7	7	1	20	0.05	2.98	0.72	0.128	0.018	0.96	0.154	0.019	1230	160	764	99	2140	240	38
CSTG07Rt_8	8	4	326	0.01	9.49	0.73	0.227	0.013	0.99	0.299	0.007	2365	71	1315	66	3457	34	44
CSTG07Rt_9	9	1	b.d.	na	0.62	0.07	0.075	0.007	0.98	0.059	0.001	480	44	461	44	566	49	4
CSTG07Rt_10	10	128	1922	0.07	0.70	0.04	0.086	0.004	0.98	0.061	0.001	535	25	530	25	644	41	1
CSTG07Rt_11	11	2730	5500	0.50	0.03	0.01	0.003	0.001	0.66	0.088	0.024	29	13	18.7	9.2	1170	660	36
CSTG07Rt_12	12	17	1	22.03	0.54	0.04	0.070	0.004	0.99	0.057	0.001	435	27	435	26	469	38	0
CSTG07Rt_13	13	38	120	0.32	5.83	0.49	0.353	0.016	0.98	0.120	0.004	1941	72	1945	78	1956	65	0
CSTG07Rt_14	14	332	1630	0.20	1.66	0.19	0.162	0.013	0.99	0.075	0.004	976	75	961	72	1071	98	2
CSTG07Rt_15	15	10	b.d.	na	1.91	0.15	0.180	0.010	0.99	0.075	0.002	1067	53	1064	53	1052	49	0
CSTG07Rt_16	16	73	12	6.12	2.92	0.24	0.238	0.013	0.98	0.095	0.004	1382	66	1369	67	1505	84	1
CSTG07Rt_17	17	11	6	1.90	0.69	0.07	0.079	0.005	0.81	0.063	0.002	520	40	490	32	668	70	6
CSTG07Rt_18	18	6	1	4.31	1.48	0.45	0.089	0.011	0.90	0.101	0.019	760	150	544	65	1240	300	28
CSTG07Rt_19	19	6	74	0.08	0.70	0.10	0.066	0.004	0.76	0.081	0.010	521	56	411	26	1130	210	21
CSTG07Rt_20	20	14	b.d.	na	3.52	0.34	0.264	0.016	0.99	0.096	0.004	1518	78	1518	82	1532	71	0
CSTG07Rt_21	21	9	17	0.51	0.80	0.13	0.072	0.004	0.83	0.080	0.011	558	57	447	23	1000	200	20
CSTG07Rt_22	22	6	4	1.52	0.50	0.05	0.065	0.005	1.00	0.056	0.001	406	31	405	31	444	36	0
CSTG07Rt_23	23	23	278	0.08	3.75	0.49	0.221	0.017	0.85	0.113	0.008	1520	100	1293	94	1830	130	15
CSTG07Rt_24	24	6	58	0.11	9.20	1.20	0.219	0.019	0.97	0.296	0.015	2320	120	1280	100	3424	76	45
CSTG07Rt_25	25	38	4	10.22	0.88	0.04	0.104	0.004	0.99	0.063	0.001	639	23	635	23	701	37	1
CSTG07Rt_26	26	4	80	0.05	13.30	6.30	0.251	0.061	0.99	0.277	0.037	2210	270	1380	270	3450	200	38
CSTG07Rt_27	27	70	20	3.57	2.12	0.12	0.196	0.007	0.98	0.077	0.002	1147	38	1154	37	1106	37	-1
CSTG07Rt_28	28	44	b.d.	na	0.57	0.05	0.073	0.005	0.99	0.056	0.001	453	29	453	28	448	27	0
CSTG07Rt_29	29	4	67	0.06	0.65	0.06	0.079	0.005	0.99	0.059	0.001	499	34	487	32	543	39	2
CSTG07Rt_30	30	6	820	0.01	0.66	0.10	0.055	0.004	0.60	0.091	0.011	495	58	344	24	1210	220	31
CSTG07Rt_31	31	279	44900	0.01	1.75	0.08	0.169	0.005	0.99	0.074	0.001	1022	31	1008	30	1037	30	1
CSTG07Rt_32	32	468	83000	0.01	1.77	0.23	0.169	0.014	0.99	0.075	0.004	1020	82	1022	69	1060	100	0
CSTG07Rt_33	33	2	b.d.	na	0.97	0.10	0.105	0.008	0.99	0.065	0.002	675	48	644	43	749	56	5
CSTG07Rt_34	34	17	b.d.	na	32.70	3.10	0.473	0.038	0.98	0.514	0.018	3550	100	2470	160	4279	49	30
CSTG07Rt_36	35	1	b.d.	na	0.65	0.07	0.067	0.007	0.72	0.081	0.010	499	45	415	45	1030	190	17
CSTG07Rt_37	36	3	b.d.	na	0.69	0.04	0.083	0.004	0.98	0.060	0.001	531	24	513	22	603	40	3
CSTG07Rt_38	37	2	b.d.	na	6.03	0.84	0.162	0.016	0.99	0.262	0.010	1950	120	961	89	3252	57	51
CSTG07Rt_40	38	15	b.d.	na	0.47	0.04	0.063	0.004	1.00	0.055	0.001	390	25	392	25	406	26	-1
CSTG07Rt_41	39	27	b.d.	na	5.82	0.69	0.345	0.023	0.98	0.118	0.006	1880	100	1900	110	1890	89	-1
CSTG07Rt_42	40	12	b.d.	na	0.59	0.05	0.075	0.005	1.00	0.058	0.001	469	30	462	29	509	38	1
CSTG07Rt_43	41	86	b.d.	na	0.58	0.03	0.075	0.003	0.98	0.056	0.001	464	18	467	18	433	23	-1
CSTG07Rt_44	42	29	b.d.	na	3.19	0.19	0.252	0.009	0.98	0.092	0.002	1448	43	1445	45	1462	38	0
CSTG07Rt_45	43	7	b.d.	na	0.59	0.03	0.075	0.003	0.99	0.058	0.001	469	16	466	15	526	40	1
CSTG07Rt_46	44	12	b.d.	na	10.92	0.82	0.234	0.014	0.97	0.336	0.008	2494	70	1348	74	3652	35	46
CSTG07Rt_47	45	4	b.d.	na	0.57	0.05	0.069	0.004	0.71	0.059	0.001	450	29	427	26	555	40	5
CSTG07Rt_48	46	21	b.d.	na	1.82	0.17	0.175	0.011	0.99	0.077	0.003	1046	62	1042	62	1092	67	0
CSTG07Rt_49	47	56	b.d.	na	22.60	3.00	0.392	0.036	0.97	0.410	0.017	3130	120	2100	160	3929	60	33
CSTG07Rt_50	48	112	b.d.	na	4.69	0.27	0.146	0.007	0.90	0.226	0.004	1759	51	879	39	3024	25	50
CSTG07Rt_51	49	22	b.d.	na	0.39	0.03	0.053	0.003	0.99	0.054	0.001	334	19	331	19	363	32	1

Table D-2: Rutile LA-ICP-MS U-Pb Isotopic Data and Ages Sample 11-CSTG-07: Castelgate Member, Book Cliffs, UT, LST

					Corrected isotopic ratios							Ages (Ma)[f]						
Sample	Grain #.	U[a] [ppm]	Th[a] [ppm]	U/Th	$^{207}Pb^{b}/^{235}U$	±2s[d]	$^{206}Pb^{b}/^{238}U$	±2s[d]	Rho[c]	$^{207}Pb^{e}/^{206}Pb$	±2s[d]	$^{207}Pb/^{235}U$	±2s	$^{206}Pb/^{238}U$	±2s	$^{207}Pb/^{206}Pb$	±2s	Disc. %[g]
CSTG07Rt_52	50	7	b.d.	na	0.75	0.08	0.082	0.005	0.84	0.063	0.002	543	40	505	32	677	60	7
CSTG07Rt_53	51	8	b.d.	na	0.76	0.04	0.090	0.004	1.00	0.061	0.001	576	23	558	22	647	24	3
CSTG07Rt_55	52	11	b.d.	na	0.65	0.07	0.069	0.004	0.61	0.063	0.001	501	38	426	24	715	44	15
CSTG07Rt_56	53	8	b.d.	na	0.67	0.06	0.081	0.006	1.00	0.060	0.001	524	37	499	34	596	37	5
CSTG07Rt_57	54	14	b.d.	na	0.68	0.04	0.080	0.004	0.98	0.061	0.001	522	25	494	21	633	27	5
CSTG07Rt_58	55	1	b.d.	na	3.73	0.68	0.139	0.015	0.92	0.183	0.019	1450	140	830	82	2540	220	43
CSTG07Rt_59	56	3	b.d.	na	0.58	0.09	0.068	0.006	0.62	0.060	0.003	458	53	426	35	590	96	7
CSTG07Rt_60	57	1	b.d.	na	0.87	0.14	0.094	0.013	0.95	0.067	0.003	640	80	577	78	827	89	10
CSTG07Rt_61	58	3	b.d.	na	2.59	0.27	0.208	0.014	0.93	0.087	0.003	1263	74	1212	72	1343	73	4
CSTG07Rt_62	59	36	b.d.	na	0.18	0.02	0.011	0.001	0.97	0.121	0.002	163	15	68.1	5.3	1969	31	58
CSTG07Rt_63	60	0	b.d.	na	10.80	1.90	0.244	0.032	0.98	0.310	0.016	2420	170	1390	160	3508	79	43
CSTG07Rt_64	61	13	b.d.	na	2.52	0.16	0.217	0.009	0.98	0.083	0.002	1264	45	1272	49	1257	40	-1
CSTG07Rt_65	62	7	b.d.	na	1.71	0.28	0.073	0.007	0.97	0.167	0.017	990	120	450	40	2440	230	55
CSTG07Rt_66	63	10	b.d.	na	0.49	0.03	0.064	0.004	0.99	0.056	0.001	408	23	400	22	441	25	2
CSTG07Rt_67	64	41	b.d.	na	1.23	0.16	0.090	0.005	0.47	0.104	0.012	797	69	556	32	1500	200	30
CSTG07Rt_68	65	15	b.d.	na	2.02	0.29	0.115	0.005	0.71	0.130	0.015	1109	99	703	29	1880	210	37
CSTG07Rt_69	66	1	b.d.	na	0.38	0.04	0.051	0.004	1.00	0.054	0.001	320	26	318	26	349	31	1
CSTG07Rt_71	67	3	b.d.	na	0.93	0.26	0.076	0.007	0.84	0.085	0.016	610	110	469	40	1050	280	23
CSTG07Rt_72	68	8	b.d.	na	0.71	0.07	0.086	0.006	1.00	0.060	0.001	535	39	530	37	591	50	1
CSTG07Rt_73	69	7	b.d.	na	4.03	0.58	0.116	0.012	0.96	0.224	0.010	1550	120	717	71	3021	73	54
CSTG07Rt_74	70	21	b.d.	na	0.57	0.04	0.074	0.004	0.99	0.056	0.001	459	25	462	25	459	26	-1
CSTG07Rt_75	71	10	b.d.	na	0.78	0.05	0.091	0.004	1.00	0.062	0.001	583	27	560	26	685	28	4
CSTG07Rt_76	72	27	b.d.	na	2.18	0.15	0.195	0.009	0.99	0.082	0.003	1161	47	1146	47	1225	58	1
CSTG07Rt_77	73	63	b.d.	na	0.72	0.04	0.088	0.004	0.97	0.060	0.001	547	20	545	21	597	38	0
CSTG07Rt_78	74	83	b.d.	na	0.99	0.07	0.094	0.005	0.74	0.074	0.002	691	36	576	27	1034	39	17
CSTG07Rt_79	75	8	b.d.	na	2.16	0.43	0.116	0.009	0.85	0.124	0.018	1060	130	703	52	1780	240	34
CSTG07Rt_80	76	7	b.d.	na	6.24	0.81	0.168	0.015	0.98	0.267	0.012	2040	110	996	83	3296	63	51
CSTG07Rt_81	77	31	b.d.	na	3.72	0.26	0.272	0.011	0.98	0.101	0.003	1564	55	1546	57	1642	61	1
CSTG07Rt_82	78	54	b.d.	na	3.99	0.41	0.278	0.017	0.96	0.102	0.005	1586	85	1575	88	1650	87	1
CSTG07Rt_83	79	19	9900	0.00	6.21	0.60	0.175	0.012	0.92	0.259	0.010	1960	86	1036	66	3247	66	47
CSTG07Rt_84	80	10	1	15.93	0.49	0.06	0.064	0.006	0.99	0.055	0.001	406	41	400	39	396	42	1
CSTG07Rt_85	81	68	7	10.49	1.86	0.24	0.174	0.015	0.99	0.076	0.003	1033	85	1028	85	1076	78	0
CSTG07Rt_86	82	12	6070	0.00	1.30	0.11	0.130	0.008	0.99	0.073	0.002	843	50	800	45	986	55	5
CSTG07Rt_87	83	9	8	1.13	0.71	0.03	0.088	0.003	0.98	0.059	0.001	542	20	546	20	553	32	-1
CSTG07Rt_88	84	7	8	0.83	0.94	0.06	0.109	0.005	1.00	0.063	0.001	670	29	664	29	693	26	1
CSTG07Rt_89	85	27	1	30.57	0.72	0.08	0.090	0.008	0.99	0.058	0.001	555	49	553	47	535	48	0
CSTG07Rt_90	86	44	8010	0.01	0.25	0.02	0.034	0.002	1.00	0.053	0.001	224	16	215	15	313	24	4
CSTG07Rt_91	87	3	1840	0.00	17.30	3.90	0.278	0.050	0.96	0.407	0.026	2760	240	1540	250	3920	97	44
CSTG07Rt_92	88	6	635	0.01	0.70	0.11	0.060	0.004	0.78	0.089	0.012	527	63	377	24	1200	230	28
CSTG07Rt_93	89	33	b.d.	na	0.68	0.07	0.084	0.007	0.99	0.059	0.002	515	39	519	40	572	66	-1
CSTG07Rt_94	90	14	2	7.24	3.57	0.39	0.264	0.017	0.99	0.098	0.004	1527	88	1515	91	1550	84	1
CSTG07Rt_95	91	25	b.d.	na	0.65	0.07	0.081	0.007	1.00	0.058	0.001	498	40	498	40	507	50	0
CSTG07Rt_96	92	5	41	0.13	5.25	0.54	0.328	0.020	0.99	0.115	0.005	1837	86	1825	95	1870	82	1
CSTG07Rt_97	93	26	11	2.36	0.82	0.06	0.097	0.005	0.99	0.063	0.002	604	31	596	31	703	59	1
CSTG07Rt_98	94	5	b.d.	na	0.70	0.06	0.086	0.006	0.99	0.059	0.001	542	33	535	32	577	40	1
CSTG07Rt_99	95	10	27	0.39	0.87	0.08	0.101	0.007	0.99	0.062	0.002	626	41	617	39	667	54	1
CSTG07Rt_100	96	184	b.d.	na	3.63	0.25	0.275	0.010	0.98	0.093	0.003	1546	50	1562	52	1492	50	-1
CSTG07Rt_101	97	21	3450	0.01	2.79	0.34	0.092	0.010	0.99	0.220	0.005	1314	90	562	57	2975	38	57
CSTG07Rt_102	98	3	103	0.03	4.50	0.57	0.284	0.023	0.99	0.112	0.006	1700	110	1600	110	1830	100	6

Table D-2: Rutile LA-ICP-MS U-Pb Isotopic Data and Ages   Sample 11-CSTG-07: Castelgate Member, Book Cliffs, UT, LST

					Corrected isotopic ratios							Ages (Ma)[f]						
Sample	**Grain #.**	**U[a] [ppm]**	**Th[a] [ppm]**	**U/Th**	**$^{207}Pb^{b}/^{235}U$**	**±2s[d]**	**$^{206}Pb^{b}/^{238}U$**	**±2s[d]**	**Rho[c]**	**$^{207}Pb^{e}/^{206}Pb$**	**±2s[d]**	**$^{207}Pb/^{235}U$**	**±2s**	**$^{206}Pb/^{238}U$**	**±2s**	**$^{207}Pb/^{206}Pb$**	**±2s**	**Disc. %[g]**
CSTG07Rt_103	99	18	b.d.	na	4.05	0.41	0.286	0.017	0.98	0.098	0.004	1603	82	1616	86	1562	75	-1
CSTG07Rt_104	100	4	5	0.75	0.51	0.03	0.062	0.003	0.86	0.059	0.001	415	22	388	20	571	34	7
CSTG07Rt_105	101	36	2300	0.02	1.08	0.18	0.070	0.006	0.80	0.121	0.014	716	84	435	37	1740	240	39
CSTG07Rt_106	102	b.d.	b.d.	na	0.78	0.09	0.089	0.009	0.94	0.062	0.002	584	52	549	51	677	52	6
CSTG07Rt_107	103	49	4680	0.01	0.74	0.07	0.083	0.005	0.79	0.064	0.002	555	37	514	30	733	50	7
CSTG07Rt_108	104	23	48	0.47	4.03	0.38	0.280	0.015	0.99	0.105	0.005	1614	77	1595	79	1692	81	1
CSTG07Rt_109	105	2	1	2.91	1.41	0.36	0.091	0.007	0.80	0.104	0.017	810	120	559	43	1440	270	31
CSTG07Rt_110	106	8	456	0.02	2.30	0.14	0.088	0.004	0.87	0.192	0.004	1208	43	543	26	2759	34	55
CSTG07Rt_111	107	9	1	6.87	2.00	0.16	0.189	0.010	0.99	0.077	0.002	1099	53	1113	56	1112	49	-1
CSTG07Rt_112	108	279	7	39.30	2.99	0.24	0.239	0.013	0.99	0.089	0.003	1379	63	1376	67	1387	60	0
CSTG07Rt_113	109	30	b.d.	na	3.80	0.48	0.275	0.021	0.99	0.096	0.004	1543	99	1550	100	1541	85	0
CSTG07Rt_114	110	45	4800	0.01	4.01	0.46	0.132	0.011	0.95	0.225	0.007	1606	97	808	65	3009	49	50
CSTG07Rt_115	111	16	613	0.03	9.60	1.60	0.222	0.021	0.94	0.294	0.015	2320	130	1280	110	3436	84	45
CSTG07Rt_116	112	149	2	99.40	0.64	0.04	0.082	0.004	0.99	0.057	0.001	506	26	508	26	490	30	0
CSTG07Rt_117	113	28	b.d.	na	0.54	0.03	0.070	0.003	0.98	0.056	0.001	438	19	437	18	451	28	0
CSTG07Rt_118	114	6	b.d.	na	0.51	0.05	0.066	0.005	0.99	0.056	0.001	414	31	412	30	440	41	0
CSTG07Rt_119	115	39	b.d.	na	5.33	0.85	0.330	0.027	0.98	0.112	0.007	1810	130	1830	130	1790	110	-1
CSTG07Rt_120	116	39	354	0.11	34.20	2.80	0.572	0.032	0.98	0.432	0.015	3615	94	2900	130	4012	51	20
CSTG07Rt_121	117	4	b.d.	na	0.69	0.06	0.081	0.005	0.94	0.061	0.002	528	34	501	30	621	54	5
CSTG07Rt_122	118	157	3100	0.05	3.18	0.34	0.108	0.009	0.98	0.212	0.005	1427	75	658	50	2938	46	54

[a]U and Th concentrations and Th/U ratios calculated relative to the R10 rutile standard using 287±76 ppm for U and 8.4±2.6 ppm for Th (Jackson, 2004)

[b]Corrected for U-Pb fractionation and background and normalised to R10 rutile standard ID-TIMS values (Jackson, 2004) and Pb/U ratios are corrected according to Anderson (2002)

[c]Error correlation defined as the quotient of the propagated errors of the $^{206}Pb/^{238}U$ and the $^{207/235}U$ ratio

[d]The propagated error of quadratic addition of internal errors (2 SD) and within run reproducibility of R10 (2 SD)

[e]Corrected for mass-bias by normalising to R10 rutile standard (~.6 per atomic mass unit)

[f]U-Pb ages are calculated relative to R10 rutile standard and corrected for common Pb using Anderson (2002)

[g]Discordance %: for $^{206}Pb/^{238}U$ ages <1Ga calculated as $((1-(^{206}Pb/^{238}U)/(^{207}Pb/^{235}U))*100)$, for $^{206}Pb/^{238}U$ ages >1Ga calculated as $((1-(^{206}Pb/^{238}U)/(^{207}Pb/^{206}Pb))*100)$

b.d.= below detection limit

na = not applicable

Table D-3: Rutile LA-ICP-MS U-Pb Isotopic Data and Ages Sample 11-TUS3C-2-17: Desert Member, Book Cliffs, UT, LST

					Corrected isotopic ratios							Ages (Ma)[f]						
Sample	Grain #.	U[a] [ppm]	Th[a] [ppm]	U/Th	$^{207}Pb^{b}/^{235}U$	±2s[d]	$^{206}Pb^{b}/^{238}U$	±2s[d]	Rho[c]	$^{207}Pb^{e}/^{206}Pb$	±2s[d]	$^{207}Pb/^{235}U$	±2s	$^{206}Pb/^{238}U$	±2s	$^{207}Pb/^{206}Pb$	±2s	Disc. %[g]
TUS3C2_17Rt_1	1	12	62.1	0.19	6.92	0.85	0.375	0.023	0.982	0.136	0.008	2080	110	2050	110	2156	99	1
TUS3C2_17Rt_2	2	1	9.54	0.14	4.01	0.78	0.154	0.015	0.856	0.190	0.024	1560	170	917	83	2550	270	41
TUS3C2_17Rt_3	3	7	65	0.10	7.90	1.60	0.181	0.028	0.968	0.316	0.023	2170	200	1060	150	3560	110	51
TUS3C2_17Rt_4	4	206	652	0.32	1.37	0.20	0.136	0.014	0.995	0.072	0.003	864	84	820	78	1004	97	5
TUS3C2_17Rt_5	5	24	142.3	0.17	2.38	0.47	0.117	0.011	0.786	0.150	0.023	1230	160	727	68	2140	300	41
TUS3C2_17Rt_6	6	5	91	0.06	2.47	0.32	0.170	0.014	0.673	0.099	0.009	1239	91	1004	77	1640	170	19
TUS3C2_17Rt_7	7	22	871	0.03	0.91	0.12	0.074	0.004	0.478	0.089	0.011	634	58	461	23	1230	200	27
TUS3C2_17Rt_8	8	8	0.78	10.14	0.45	0.04	0.059	0.004	0.999	0.055	0.001	383	28	372	26	414	29	3
TUS3C2_17Rt_9	9	14	82.8	0.17	0.90	0.06	0.098	0.005	0.992	0.066	0.001	647	33	602	30	804	33	7
TUS3C2_17Rt_10	10	16	720	0.02	6.04	0.50	0.354	0.016	0.983	0.126	0.005	1962	68	1958	75	2030	69	0
TUS3C2_17Rt_11	11	1	25.6	0.05	7.50	1.90	0.173	0.030	0.962	0.260	0.016	1900	200	1000	160	3226	92	47
TUS3C2_17Rt_12	12	7	15.9	0.42	1.96	0.34	0.099	0.007	0.844	0.138	0.017	1020	110	604	41	1940	250	41
TUS3C2_17Rt_13	13	2	2.2	0.70	0.87	0.13	0.065	0.004	0.655	0.098	0.014	603	68	406	23	1360	250	33
TUS3C2_17Rt_14	14	28	297	0.10	26.20	6.70	0.362	0.055	0.983	0.461	0.040	3230	220	1940	250	4100	130	40
TUS3C2_17Rt_15	15	11	4.41	2.52	0.77	0.05	0.091	0.004	0.708	0.061	0.001	572	26	558	22	651	33	2
TUS3C2_17Rt_16	16	5	20	0.24	3.17	0.36	0.218	0.013	0.740	0.098	0.004	1419	87	1268	71	1549	84	11
TUS3C2_17Rt_17	17	0	3.08	0.10	71.00	18.00	0.730	0.120	0.990	0.634	0.040	4200	220	3440	420	4564	95	18
TUS3C2_17Rt_18	18	1	2.05	0.29	7.40	1.60	0.228	0.033	0.877	0.236	0.028	2100	210	1310	170	3110	180	38
TUS3C2_17Rt_19	19	2140	1490	1.44	0.23	0.04	0.032	0.005	0.997	0.051	0.001	206	33	204	32	224	34	1
TUS3C2_17Rt_20	20	19	39.8	0.47	6.84	0.77	0.378	0.021	0.969	0.131	0.007	2080	100	2070	100	2127	98	0
TUS3C2_17Rt_21	21	34	5.19	6.45	6.13	0.43	0.359	0.014	0.989	0.124	0.004	1991	61	1991	70	2001	57	0
TUS3C2_17Rt_22	22	47	2.78	16.83	0.36	0.02	0.050	0.002	0.974	0.054	0.001	310	14	314	14	354	33	-1
TUS3C2_17Rt_23	23	2	39.6	0.04	6.20	1.50	0.138	0.019	0.978	0.299	0.024	1830	160	830	100	3400	110	55
TUS3C2_17Rt_24	24	5	186	0.03	23.70	3.90	0.350	0.037	0.712	0.435	0.018	3150	140	1940	160	4015	62	38
TUS3C2_17Rt_25	25	310	1720	0.18	2.28	0.25	0.145	0.008	0.543	0.121	0.013	1183	80	872	45	1830	170	26
TUS3C2_17Rt_26	26	6	67	0.10	3.07	0.84	0.125	0.020	0.875	0.183	0.031	1380	230	750	110	2600	360	46
TUS3C2_17Rt_27	27	0	2.82	0.13	1.32	0.23	0.074	0.010	0.627	0.144	0.017	830	100	460	62	2100	260	45
TUS3C2_17Rt_28	28	9	0.027	####	0.83	0.06	0.099	0.005	0.990	0.061	0.001	611	31	609	31	648	39	0
TUS3C2_17Rt_29	29	2	11.81	0.21	21.20	5.60	0.329	0.058	0.976	0.403	0.040	2850	260	1810	280	3870	150	36
TUS3C2_17Rt_30	30	1	4.01	0.23	7.20	1.50	0.167	0.026	0.973	0.296	0.012	2000	170	980	140	3437	64	51
TUS3C2_17Rt_31	31	13	81.5	0.16	3.98	0.47	0.120	0.011	0.985	0.245	0.007	1627	97	729	65	3153	45	55
TUS3C2_17Rt_32	32	4	22.96	0.18	0.31	0.03	0.034	0.002	0.376	0.071	0.008	278	25	217	12	770	190	22
TUS3C2_17Rt_33	33	4	43.3	0.10	0.34	0.04	0.035	0.002	0.197	0.077	0.010	299	29	219	9.9	880	210	27
TUS3C2_17Rt_34	34	3	32	0.09	28.00	21.00	0.350	0.200	0.964	0.330	0.120	2120	630	1450	570	3130	570	32
TUS3C2_17Rt_35	35	9	23.6	0.37	0.74	0.04	0.087	0.004	0.986	0.061	0.001	558	26	534	24	651	28	4
TUS3C2_17Rt_36	36	15	1.58	9.37	0.54	0.03	0.067	0.003	0.995	0.057	0.001	437	22	423	20	506	27	3
TUS3C2_17Rt_37	37	1	64	0.01	19.00	10.00	0.244	0.082	0.993	0.373	0.065	2390	420	1300	360	3620	250	46
TUS3C2_17Rt_38	38	14	0.159	87.61	4.87	0.45	0.320	0.017	0.990	0.107	0.003	1780	80	1785	81	1753	62	0
TUS3C2_17Rt_39	39	1	16.35	0.05	22.50	3.50	0.377	0.044	0.958	0.410	0.023	3110	160	2020	200	3942	84	35
TUS3C2_17Rt_40	40	0	2.51	0.09	99.00	50.00	0.950	0.440	0.998	0.707	0.080	4800	540	4600	1700	4800	110	4
TUS3C2_17Rt_41	41	17	0.118	####	4.25	0.43	0.291	0.017	0.988	0.105	0.004	1642	81	1641	85	1682	75	0
TUS3C2_17Rt_42	42	62	246	0.25	0.68	0.03	0.079	0.003	0.988	0.063	0.001	528	17	491	16	691	19	7
TUS3C2_17Rt_43	43	2	23.6	0.08	40.00	12.00	0.530	0.130	0.960	0.524	0.050	3640	330	2780	530	4260	140	24
TUS3C2_17Rt_44	44	3	37.8	0.08	7.80	2.60	0.221	0.034	0.984	0.212	0.023	1900	160	1200	120	2890	240	37
TUS3C2_17Rt_45	45	0	1.26	0.30	3.00	1.20	0.090	0.013	0.961	0.181	0.026	1070	160	548	78	2440	300	49
TUS3C2_17Rt_46	46	2	2.4	0.65	0.43	0.03	0.057	0.003	0.996	0.055	0.001	361	21	357	21	419	37	1
TUS3C2_17Rt_47	47	0	29.4	0.02	7.94	0.93	0.188	0.017	0.974	0.309	0.010	2250	110	1100	93	3508	47	51
TUS3C2_17Rt_48	48	14	10.1	1.42	0.60	0.04	0.073	0.003	0.857	0.059	0.002	465	23	454	20	530	41	2
TUS3C2_17Rt_49	49	6	31.3	0.20	5.83	0.51	0.150	0.010	0.980	0.277	0.007	1940	71	905	55	3342	37	53

Table D-3: Rutile LA-ICP-MS U-Pb Isotopic Data and Ages Sample 11-TUS3C-2-17: Desert Member, Book Cliffs, UT, LST

					Corrected isotopic ratios							Ages (Ma)[f]						
Sample	Grain #.	U[a] [ppm]	Th[a] [ppm]	U/Th	$^{207}Pb^{b}/^{235}U$	±2s[d]	$^{206}Pb^{b}/^{238}U$	±2s[d]	Rho[c]	$^{207}Pb^{e}/^{206}Pb$	±2s[d]	$^{207}Pb/^{235}U$	±2s	$^{206}Pb/^{238}U$	±2s	$^{207}Pb/^{206}Pb$	±2s	Disc. %[g]
TUS3C2_17Rt_50	50	3	3.4	0.98	0.68	0.05	0.080	0.004	0.801	0.061	0.001	519	27	495	23	622	41	5
TUS3C2_17Rt_51	51	15	10.4	1.45	0.52	0.03	0.067	0.003	0.998	0.056	0.000	424	17	419	17	451	17	1
TUS3C2_17Rt_52	52	12	15.8	0.78	1.36	0.37	0.105	0.014	0.921	0.073	0.008	760	120	637	80	850	150	16
TUS3C2_17Rt_53	53	9	1.63	5.82	0.56	0.03	0.071	0.003	0.995	0.057	0.001	455	21	440	20	497	24	3
TUS3C2_17Rt_54	54	6	428	0.01	17.70	2.90	0.300	0.032	0.967	0.393	0.017	2860	130	1670	150	3875	66	42
TUS3C2_17Rt_55	55	26	1410	0.02	12.50	2.60	0.274	0.039	0.983	0.304	0.021	2430	200	1520	190	3450	110	37
TUS3C2_17Rt_56	56	26	0.39	66.67	0.53	0.04	0.069	0.004	0.996	0.057	0.001	430	25	428	24	478	35	0
TUS3C2_17Rt_57	57	65	47.5	1.37	0.60	0.03	0.076	0.003	0.995	0.057	0.000	477	16	474	16	491	17	1
TUS3C2_17Rt_58	58	6	0.14	44.21	3.92	0.42	0.282	0.018	0.985	0.099	0.004	1603	87	1592	89	1613	82	1
TUS3C2_17Rt_59	59	6	0.116	53.45	3.62	0.33	0.269	0.015	0.982	0.100	0.004	1531	73	1539	77	1608	72	-1
TUS3C2_17Rt_60	60	5	58.1	0.08	4.70	1.10	0.171	0.018	0.907	0.184	0.028	1610	200	1030	100	2400	290	36
TUS3C2_17Rt_61	61	10	0.036	####	0.54	0.02	0.070	0.002	0.981	0.057	0.001	434	13	433	12	491	29	0
TUS3C2_17Rt_62	62	2	103	0.02	0.57	0.05	0.067	0.005	0.845	0.060	0.001	448	34	419	31	579	44	6
TUS3C2_17Rt_63	63	5	b.d.	na	0.46	0.03	0.058	0.002	0.677	0.057	0.001	379	18	362	14	501	28	4
TUS3C2_17Rt_64	64	17	b.d.	na	0.43	0.02	0.057	0.003	0.998	0.054	0.001	361	15	359	15	388	25	1
TUS3C2_17Rt_65	65	16	b.d.	na	107.00	25.00	0.980	0.170	0.976	0.739	0.048	4770	300	4350	590	4802	95	9
TUS3C2_17Rt_66	66	5	19.2	0.28	11.70	3.90	0.245	0.038	0.982	0.253	0.030	2150	230	1380	180	3290	210	36
TUS3C2_17Rt_67	67	8	11.3	0.74	0.56	0.05	0.063	0.004	0.626	0.061	0.001	446	30	392	22	645	44	12
TUS3C2_17Rt_68	68	38	2.19	17.26	0.79	0.04	0.096	0.004	0.994	0.060	0.001	594	22	587	21	603	22	1
TUS3C2_17Rt_69	69	33	4.12	8.11	4.21	0.34	0.297	0.015	0.987	0.103	0.003	1686	73	1673	74	1671	57	1
TUS3C2_17Rt_70	70	15	1.21	12.64	1.02	0.13	0.107	0.009	0.990	0.067	0.003	691	61	651	50	821	91	6
TUS3C2_17Rt_71	71	9	4.64	2.01	0.79	0.05	0.086	0.004	0.987	0.066	0.001	586	31	532	26	801	46	9
TUS3C2_17Rt_72	72	6	8.8	0.71	6.92	0.62	0.381	0.019	0.981	0.132	0.006	2102	78	2072	88	2137	72	1
TUS3C2_17Rt_73	73	12	25.4	0.48	1.05	0.16	0.073	0.004	0.747	0.103	0.013	693	77	454	23	1490	240	34
TUS3C2_17Rt_74	74	8	54.6	0.15	22.50	2.30	0.371	0.027	0.959	0.452	0.017	3220	100	2020	130	4092	56	37
TUS3C2_17Rt_75	75	20	43.1	0.46	4.99	0.34	0.318	0.012	0.969	0.116	0.004	1798	54	1778	58	1870	63	1
TUS3C2_17Rt_76	76	10	24.5	0.39	0.60	0.02	0.074	0.002	0.980	0.059	0.001	476	14	459	13	552	19	4
TUS3C2_17Rt_77	77	0	6.5	0.02	53.00	49.00	0.560	0.460	0.995	0.620	0.200	3500	1500	2600	1900	4480	530	26
TUS3C2_17Rt_78	78	404	2270	0.18	0.54	0.04	0.070	0.005	0.987	0.056	0.001	437	29	434	30	466	37	1
TUS3C2_17Rt_79	79	5	36.7	0.15	3.91	0.87	0.138	0.016	0.938	0.197	0.028	1540	210	828	89	2600	330	46
TUS3C2_17Rt_80	80	3	4.96	0.55	3.40	1.00	0.108	0.020	0.972	0.183	0.025	1210	220	650	120	2380	290	46
TUS3C2_17Rt_81	81	17	3.7	4.54	4.36	0.33	0.295	0.012	0.986	0.108	0.004	1701	55	1664	57	1771	62	2
TUS3C2_17Rt_82	82	8	55.2	0.15	0.98	0.15	0.100	0.011	0.797	0.070	0.003	677	76	611	67	897	90	10
TUS3C2_17Rt_83	83	6	2.82	2.28	0.66	0.03	0.080	0.003	0.994	0.060	0.001	514	19	494	18	604	21	4
TUS3C2_17Rt_84	84	2	25.5	0.09	6.90	1.60	0.168	0.026	0.994	0.253	0.026	1800	220	980	140	3220	150	46
TUS3C2_17Rt_85	85	6	24.2	0.24	9.60	1.00	0.401	0.021	0.875	0.175	0.013	2370	100	2165	96	2560	120	9
TUS3C2_17Rt_86	86	6	13.7	0.43	21.40	4.50	0.524	0.053	0.990	0.258	0.031	2880	210	2600	200	3050	200	10
TUS3C2_17Rt_87	87	1	4.38	0.13	52.00	12.00	0.595	0.093	0.992	0.582	0.039	3890	220	2950	360	4470	100	24
TUS3C2_17Rt_88	88	59	4.06	14.41	0.73	0.05	0.090	0.005	0.995	0.060	0.001	564	29	553	28	601	33	2
TUS3C2_17Rt_89	89	8	1.1	6.91	1.01	0.28	0.102	0.020	0.989	0.069	0.006	690	140	630	120	890	170	9
TUS3C2_17Rt_90	90	20	0.331	61.63	0.56	0.06	0.071	0.006	0.985	0.057	0.001	447	37	440	37	501	48	2
TUS3C2_17Rt_91	91	7	5.9	1.13	5.90	0.61	0.344	0.022	0.962	0.128	0.009	1946	97	1900	100	2070	120	2
TUS3C2_17Rt_92	92	5	3.58	1.37	0.92	0.09	0.090	0.005	0.515	0.068	0.002	667	48	552	28	865	54	17
TUS3C2_17Rt_93	93	13	2.3	5.74	0.66	0.05	0.080	0.005	0.979	0.060	0.001	513	31	495	28	596	47	4
TUS3C2_17Rt_94	94	7	1.9	3.76	0.50	0.03	0.064	0.003	0.784	0.057	0.001	409	22	397	21	490	30	3
TUS3C2_17Rt_95	95	5	0.029	####	1.31	0.08	0.139	0.005	0.991	0.070	0.002	851	33	837	31	903	48	2
TUS3C2_17Rt_96	96	8	272	0.03	0.71	0.12	0.056	0.005	0.733	0.100	0.013	530	72	348	31	1340	250	34
TUS3C2_17Rt_97	97	48	6.1	7.90	0.92	0.17	0.100	0.013	0.986	0.066	0.003	635	82	608	72	790	110	4
TUS3C2_17Rt_98	98	5	4.8	0.94	0.66	0.05	0.079	0.005	0.986	0.059	0.001	507	28	492	27	581	27	3

Table D-3: Rutile LA-ICP-MS U-Pb Isotopic Data and Ages Sample 11-TUS3C-2-17: Desert Member, Book Cliffs, UT, LST

					Corrected isotopic ratios							Ages (Ma)[f]						
Sample	Grain #.	U[a] [ppm]	Th[a] [ppm]	U/Th	$^{207}Pb^{b}/^{235}U$	±2s[d]	$^{206}Pb^{b}/^{238}U$	±2s[d]	Rho[c]	$^{207}Pb^{e}/^{206}Pb$	±2s[d]	$^{207}Pb/^{235}U$	±2s	$^{206}Pb/^{238}U$	±2s	$^{207}Pb/^{206}Pb$	±2s	Disc. %[g]
TUS3C2_17Rt_99	99	6	0.524	10.59	0.43	0.02	0.058	0.002	0.997	0.055	0.001	363	14	361	14	377	15	1
TUS3C2_17Rt_10	100	2	1.6	1.17	6.10	1.60	0.170	0.027	0.975	0.216	0.036	1700	280	990	150	2450	380	42
TUS3C2_17Rt_10	101	8	7.27	1.15	7.09	0.68	0.376	0.018	0.955	0.138	0.007	2076	85	2076	77	2187	85	0
TUS3C2_17Rt_10	102	44	193	0.23	2.28	0.59	0.114	0.015	0.915	0.120	0.020	1000	170	687	85	1560	290	31
TUS3C2_17Rt_10	103	4	1.6	2.43	5.86	0.56	0.337	0.018	0.846	0.123	0.005	1926	80	1879	88	1980	78	2
TUS3C2_17Rt_10	104	13	137	0.10	16.70	1.80	0.364	0.027	0.930	0.337	0.012	2880	110	1980	130	3634	54	31
TUS3C2_17Rt_10	105	14	2.96	4.83	0.71	0.04	0.084	0.004	0.991	0.061	0.001	543	25	518	24	653	28	5
TUS3C2_17Rt_10	106	24	0.007	####	3.03	0.18	0.247	0.009	0.986	0.087	0.002	1411	45	1428	44	1344	48	-1
TUS3C2_17Rt_10	107	12	7.71	1.60	6.30	0.37	0.373	0.012	0.983	0.121	0.003	2021	51	2040	56	1985	48	-1
TUS3C2_17Rt_10	108	15	0.082	####	0.62	0.03	0.079	0.003	0.979	0.058	0.001	490	17	488	16	529	31	0
TUS3C2_17Rt_10	109	4	43.8	0.08	48.30	9.90	0.637	0.091	0.982	0.568	0.034	3920	190	3140	360	4425	83	20
TUS3C2_17Rt_11	110	2	89	0.02	24.60	4.30	0.398	0.046	0.980	0.428	0.029	3190	180	2120	210	3960	100	34
TUS3C2_17Rt_11	111	6	b.d.	na	9.70	1.80	0.410	0.037	0.976	0.162	0.015	2290	160	2190	170	2430	160	4
TUS3C2_17Rt_11	112	55	b.d.	na	1.03	0.06	0.117	0.005	0.993	0.065	0.001	715	31	712	30	759	41	0
TUS3C2_17Rt_11	113	82	282	0.29	2.10	0.13	0.198	0.007	0.987	0.079	0.002	1160	39	1162	40	1158	41	0
TUS3C2_17Rt_11	114	10	10.8	0.96	0.54	0.04	0.067	0.004	0.722	0.058	0.001	431	25	418	23	508	37	3
TUS3C2_17Rt_11	115	1	47.2	0.01	22.90	3.80	0.377	0.045	0.896	0.421	0.026	3150	180	2020	210	3967	85	36
TUS3C2_17Rt_11	116	9	b.d.	na	0.98	0.08	0.103	0.006	0.988	0.069	0.002	688	40	632	36	901	48	8
TUS3C2_17Rt_11	117	20	b.d.	na	4.62	0.42	0.298	0.016	0.990	0.112	0.005	1760	76	1686	80	1820	74	4
TUS3C2_17Rt_11	118	14	21.5	0.63	0.70	0.04	0.085	0.004	0.995	0.060	0.001	533	22	528	22	595	44	1
TUS3C2_17Rt_11	119	13	0.039	####	0.67	0.03	0.083	0.003	0.988	0.060	0.001	517	18	511	18	581	41	1
TUS3C2_17Rt_12	120	8	62.1	0.13	0.76	0.04	0.088	0.003	0.991	0.063	0.001	573	20	547	20	697	25	5
TUS3C2_17Rt_12	121	74	3980	0.02	1.94	0.46	0.084	0.014	0.850	0.178	0.020	1040	140	515	83	2690	170	50

[a]U and Th concentrations and Th/U ratios calculated relative to the R10 rutile standard using 287±76 ppm for U and 8.4±2.6 ppm for Th (Jackson, 2004)
[b]Corrected for U-Pb fractionation and background and normalised to R10 rutile standard ID-TIMS values (Jackson, 2004) and Pb/U ratios are corrected according to Anderson (2002)
[c]Error correlation defined as the quotient of the propagated errors of the $^{206}Pb/^{238}U$ and the $^{207}/^{235}U$ ratio
[d]The propagated error of quadratic addition of internal errors (2 SD) and within run reproducibility of R10 (2 SD)
[e]Corrected for mass-bias by normalising to R10 rutile standard (~.6 per atomic mass unit)
[f]U-Pb ages are calculated relative to R10 rutile standard and corrected for common Pb using Anderson (2002)
[g]Discordance %: for $^{206}Pb/^{238}U$ ages <1Ga calculated as $((1-(^{206}Pb/^{238}U)/(^{207}Pb/^{235}U))*100)$, for $^{206}Pb/^{238}U$ ages >1Ga calculated as $((1-(^{206}Pb/^{238}U)/(^{207}Pb/^{206}Pb))*100)$
b.d.= below detection limit
na = not applicable

Table D-4: Rutile LA-ICP-MS U-Pb Isotopic Data and Ages Sample 11-BH-06: Desert Member, Book Cliffs, UT, HST

					Corrected isotopic ratios							Ages (Ma)[f]						
Sample	Grain #.	U[a] [ppm]	Th[a] [ppm]	U/Th	$^{207}Pb^{b}/^{235}U$	±2s[d]	$^{206}Pb^{b}/^{238}U$	±2s[d]	Rho[c]	$^{207}Pb^{e}/^{206}Pb$	±2s[d]	$^{207}Pb/^{235}U$	±2s	$^{206}Pb/^{238}U$	±2s	$^{207}Pb/^{206}Pb$	±2s	Disc. %[g]
BH06Rt_1	1	54	b.d.	na	0.41	0.03	0.049	0.003	0.71	0.060	0.001	344	18	308	15	597	25	10
BH06Rt_2	2	28	b.d.	na	1.32	0.21	0.070	0.005	0.82	0.130	0.014	811	91	436	29	1900	250	46
BH06Rt_3	3	1	b.d.	na	0.95	0.13	0.090	0.010	0.80	0.070	0.004	650	66	552	56	870	100	15
BH06Rt_4	4	4	b.d.	na	56.00	12.00	0.665	0.094	0.99	0.583	0.048	4020	220	3290	370	4420	120	18
BH06Rt_5	5	48	b.d.	na	1.19	0.17	0.076	0.003	0.57	0.113	0.014	759	78	470	18	1630	240	38
BH06Rt_6	6	43	b.d.	na	4.37	0.29	0.128	0.007	0.99	0.247	0.004	1696	55	775	39	3163	23	54
BH06Rt_7	7	119	b.d.	na	0.36	0.03	0.047	0.003	1.00	0.056	0.001	311	19	294	18	433	22	5
BH06Rt_8	8	11	b.d.	na	5.03	0.29	0.143	0.006	0.94	0.256	0.005	1807	50	859	36	3216	29	52
BH06Rt_9	9	6	b.d.	na	0.65	0.04	0.081	0.004	0.99	0.058	0.001	514	25	503	23	544	30	2
BH06Rt_10	10	7	b.d.	na	0.90	0.08	0.105	0.007	0.99	0.063	0.002	646	43	642	42	697	50	1
BH06Rt_11	11	3	b.d.	na	2.01	0.38	0.095	0.009	0.75	0.146	0.021	1030	130	590	49	2040	300	43
BH06Rt_12	12	3	b.d.	na	5.18	0.74	0.330	0.028	0.99	0.116	0.007	1860	130	1830	140	1910	120	2
BH06Rt_13	13	2	b.d.	na	10.70	1.50	0.437	0.032	0.97	0.177	0.014	2450	140	2330	150	2590	140	5
BH06Rt_14	14	15	b.d.	na	0.63	0.05	0.079	0.005	0.99	0.058	0.001	494	28	489	27	535	32	1
BH06Rt_15	15	25	b.d.	na	4.96	0.55	0.321	0.020	0.99	0.109	0.005	1778	93	1784	96	1805	75	0
BH06Rt_16	16	4	b.d.	na	0.65	0.05	0.075	0.005	0.99	0.062	0.001	501	29	466	27	665	33	7
BH06Rt_17	17	3	b.d.	na	0.73	0.16	0.067	0.006	0.80	0.068	0.008	521	79	416	34	750	180	20
BH06Rt_18	18	41	b.d.	na	0.53	0.04	0.069	0.004	0.99	0.057	0.002	432	26	429	26	498	57	1
BH06Rt_19	19	23	b.d.	na	0.41	0.03	0.055	0.003	1.00	0.054	0.001	348	21	343	20	376	21	1
BH06Rt_20	20	16	b.d.	na	0.73	0.06	0.088	0.006	1.00	0.060	0.001	557	37	543	34	607	39	3
BH06Rt_21	21	5	b.d.	na	0.61	0.03	0.077	0.003	0.99	0.058	0.001	482	17	477	16	523	35	1
BH06Rt_22	22	102	b.d.	na	0.63	0.04	0.079	0.004	0.99	0.058	0.001	498	24	490	23	527	39	2
BH06Rt_23	23	0	b.d.	na	2.13	0.44	0.150	0.014	0.84	0.089	0.007	1090	120	895	80	1350	130	18
BH06Rt_24	24	2	b.d.	na	2.25	0.48	0.111	0.017	0.69	0.167	0.026	1210	170	677	97	2350	330	44
BH06Rt_25	25	7	b.d.	na	0.65	0.12	0.071	0.010	0.90	0.062	0.003	497	70	441	62	676	93	11
BH06Rt_26	26	4	b.d.	na	0.51	0.06	0.060	0.005	0.58	0.061	0.002	418	37	378	30	640	56	10
BH06Rt_27	27	11	b.d.	na	1.77	0.11	0.168	0.007	0.99	0.076	0.002	1029	39	999	38	1093	42	3
BH06Rt_28	28	6	b.d.	na	0.61	0.04	0.076	0.005	1.00	0.058	0.001	482	27	472	27	539	25	2
BH06Rt_29	29	6	b.d.	na	0.50	0.04	0.063	0.005	1.00	0.057	0.001	408	29	394	27	486	33	3
BH06Rt_30	30	14	b.d.	na	6.09	0.51	0.366	0.015	0.98	0.119	0.005	1985	65	2005	71	1945	70	-1
BH06Rt_31	31	1	b.d.	na	3.98	0.84	0.133	0.017	0.93	0.222	0.022	1590	170	840	110	3040	170	47
BH06Rt_32	32	19	b.d.	na	4.22	0.51	0.287	0.021	0.98	0.105	0.006	1650	110	1620	100	1700	110	2
BH06Rt_33	33	12	b.d.	na	0.64	0.04	0.078	0.004	0.95	0.060	0.001	497	23	483	22	605	35	3
BH06Rt_34	34	6	b.d.	na	0.50	0.08	0.058	0.005	0.84	0.062	0.007	398	47	365	31	540	110	8
BH06Rt_35	35	8	b.d.	na	3.41	0.25	0.250	0.011	0.98	0.098	0.003	1513	60	1444	57	1598	61	5
BH06Rt_36	36	1	b.d.	na	16.70	8.60	0.270	0.087	0.98	0.284	0.047	2180	370	1430	380	3430	280	34
BH06Rt_37	37	27	b.d.	na	6.03	0.74	0.174	0.014	0.98	0.251	0.012	1960	110	1028	78	3206	83	48
BH06Rt_38	38	4	b.d.	na	2.38	0.41	0.169	0.018	0.75	0.093	0.007	1200	120	1003	97	1440	150	16
BH06Rt_39	39	6	b.d.	na	0.77	0.07	0.089	0.006	0.99	0.063	0.002	569	41	548	35	688	76	4
BH06Rt_40	40	1	b.d.	na	0.76	0.13	0.071	0.008	0.70	0.073	0.009	547	70	439	47	850	160	20
BH06Rt_41	41	4	b.d.	na	0.76	0.07	0.084	0.006	0.85	0.066	0.002	580	42	517	36	783	50	11
BH06Rt_42	42	229	b.d.	na	0.40	0.04	0.054	0.005	0.99	0.056	0.001	335	27	340	28	450	53	-1
BH06Rt_43	43	221	b.d.	na	0.86	0.12	0.054	0.005	0.72	0.129	0.016	608	63	335	33	1840	270	45
BH06Rt_44	44	26	b.d.	na	1.59	0.12	0.157	0.009	0.99	0.073	0.002	957	47	937	47	1009	54	2
BH06Rt_45	45	11	b.d.	na	5.34	0.99	0.194	0.017	0.79	0.193	0.025	1820	160	1138	93	2630	260	37
BH06Rt_46	46	87	b.d.	na	19.60	2.50	0.347	0.034	0.97	0.399	0.018	3030	130	1910	160	3919	68	37
BH06Rt_47	47	4	b.d.	na	6.10	0.74	0.154	0.015	0.96	0.283	0.010	1950	100	916	84	3369	55	53
BH06Rt_48	48	69	b.d.	na	85.00	14.00	0.840	0.110	0.96	0.731	0.033	4480	170	3930	390	4797	65	12
BH06Rt_49	49	12	b.d.	na	0.50	0.04	0.057	0.003	0.51	0.061	0.001	411	28	360	19	646	32	12

Table D-4: Rutile LA-ICP-MS U-Pb Isotopic Data and Ages — Sample 11-BH-06: Desert Member, Book Cliffs, UT, HST

					Corrected isotopic ratios							Ages (Ma)[f]						
Sample	Grain #.	U[a] [ppm]	Th[a] [ppm]	U/Th	$^{207}Pb^{b}/^{235}U$	±2s[d]	$^{206}Pb^{b}/^{238}U$	±2s[d]	Rho[c]	$^{207}Pb^{e}/^{206}Pb$	±2s[d]	$^{207}Pb/^{235}U$	±2s	$^{206}Pb/^{238}U$	±2s	$^{207}Pb/^{206}Pb$	±2s	Disc. %[g]
BH06Rt_50	50	9	b.d.	na	2.17	0.25	0.079	0.007	0.95	0.196	0.006	1134	85	488	43	2784	53	57
BH06Rt_51	51	7	b.d.	na	2.45	0.44	0.101	0.010	0.85	0.187	0.026	1200	150	616	56	2630	310	49
BH06Rt_52	52	26	b.d.	na	3.14	0.45	0.118	0.008	0.73	0.208	0.007	1430	110	716	47	2820	140	50
BH06Rt_53	53	6	b.d.	na	97	26	1.150	0.200	0.63	0.668	0.053	4650	260	4840	590	4650	120	-4
BH06Rt_54	54	39	b.d.	na	5.72	0.31	0.162	0.007	0.98	0.256	0.004	1936	45	965	39	3222	21	50
BH06Rt_55	55	89	b.d.	na	4.12	0.38	0.124	0.009	0.99	0.241	0.006	1648	80	749	50	3123	42	55
BH06Rt_56	56	3	b.d.	na	3.67	0.45	0.116	0.011	0.95	0.231	0.008	1562	94	701	63	3062	55	55
BH06Rt_57	57	3	b.d.	na	4.07	0.63	0.133	0.016	0.86	0.246	0.009	1640	130	802	91	3150	61	51
BH06Rt_58	58	12	b.d.	na	0.723	0.062	0.083	0.005	0.93	0.062	0.002	552	37	514	32	661	59	7
BH06Rt_59	59	8	b.d.	na	1.18	0.15	0.116	0.010	0.98	0.070	0.002	766	64	702	58	922	63	8
BH06Rt_60	60	16	b.d.	na	1.02	0.18	0.073	0.004	0.83	0.103	0.015	675	81	452	26	1470	250	33
BH06Rt_61	61	3	b.d.	na	4.78	0.5	0.314	0.019	0.99	0.109	0.005	1751	90	1753	95	1764	81	0
BH06Rt_62	62	376	b.d.	na	1.21	0.17	0.066	0.004	0.64	0.131	0.015	769	82	413	20	1890	260	46
BH06Rt_63	63	5	b.d.	na	0.406	0.044	0.045	0.002	0.34	0.067	0.008	348	33	285	14	720	170	18
BH06Rt_64	64	267	b.d.	na	4.21	0.41	0.137	0.010	0.99	0.225	0.004	1671	76	823	59	3013	30	51
BH06Rt_65	65	4	b.d.	na	0.433	0.023	0.058	0.003	1.00	0.054	0.000	364	16	361	16	387	16	1
BH06Rt_66	66	26	b.d.	na	0.727	0.072	0.090	0.007	1.00	0.061	0.002	556	42	551	40	623	55	1
BH06Rt_67	67	21	b.d.	na	0.67	0.03	0.083	0.003	0.98	0.059	0.001	519	18	516	17	559	35	1
BH06Rt_68	68	87	b.d.	na	2	0.25	0.092	0.005	0.77	0.148	0.014	1061	90	568	31	2150	210	46
BH06Rt_69	69	13	b.d.	na	0.586	0.041	0.075	0.004	0.99	0.058	0.001	464	26	464	24	507	33	0
BH06Rt_70	70	14	b.d.	na	0.598	0.036	0.076	0.004	1.00	0.058	0.001	477	24	470	23	527	41	1
BH06Rt_71	71	7	b.d.	na	3.43	0.23	0.265	0.010	0.98	0.094	0.003	1513	53	1514	54	1507	50	0
BH06Rt_72	72	11	b.d.	na	4.33	0.43	0.296	0.018	0.99	0.107	0.005	1691	80	1663	87	1733	77	2
BH06Rt_73	73	15	b.d.	na	5.5	0.68	0.340	0.022	0.98	0.118	0.008	1880	110	1880	110	1930	120	0
BH06Rt_74	74	13	b.d.	na	0.391	0.033	0.053	0.004	0.99	0.053	0.001	333	23	333	24	338	35	0
BH06Rt_75	75	20	b.d.	na	0.653	0.077	0.081	0.008	0.99	0.058	0.002	504	47	503	47	537	68	0
BH06Rt_76	76	1	b.d.	na	0.831	0.095	0.094	0.008	0.78	0.064	0.002	604	53	576	48	723	66	5
BH06Rt_77	77	36	b.d.	na	0.551	0.042	0.071	0.005	0.99	0.058	0.002	442	27	440	27	530	55	0
BH06Rt_78	78	4	b.d.	na	0.625	0.049	0.079	0.005	1.00	0.058	0.001	491	30	489	28	533	48	0
BH06Rt_79	79	11	b.d.	na	0.594	0.049	0.074	0.005	0.84	0.060	0.002	468	31	460	29	552	60	2
BH06Rt_80	80	21	b.d.	na	5.77	0.36	0.173	0.009	0.96	0.241	0.005	1934	53	1025	48	3132	33	47
BH06Rt_81	81	45	b.d.	na	13.9	1.7	0.291	0.029	0.88	0.376	0.016	2740	120	1680	150	3797	67	39
BH06Rt_82	82	90	b.d.	na	0.659	0.041	0.084	0.004	0.98	0.057	0.001	515	24	517	22	498	35	0
BH06Rt_83	83	125	b.d.	na	0.569	0.038	0.074	0.004	0.98	0.057	0.001	458	25	457	26	486	39	0
BH06Rt_84	84	154	b.d.	na	1.31	0.23	0.086	0.007	0.72	0.115	0.016	802	92	539	46	1640	250	33
BH06Rt_85	85	57	b.d.	na	0.388	0.028	0.051	0.003	1.00	0.055	0.001	331	20	320	19	401	24	3
BH06Rt_86	86	6	b.d.	na	0.611	0.056	0.077	0.006	0.99	0.060	0.003	480	35	484	32	596	83	-1
BH06Rt_87	87	20	b.d.	na	0.913	0.076	0.095	0.005	0.72	0.067	0.002	651	40	591	29	839	59	9
BH06Rt_88	88	26	b.d.	na	0.601	0.04	0.076	0.005	0.99	0.057	0.001	475	26	474	28	488	41	0
BH06Rt_89	89	55	b.d.	na	0.579	0.058	0.073	0.006	0.99	0.057	0.001	458	37	456	37	484	41	0
BH06Rt_90	90	2	b.d.	na	17.7	2.2	0.322	0.031	0.97	0.391	0.016	2900	110	1780	150	3844	54	39
BH06Rt_91	91	14	b.d.	na	0.664	0.061	0.081	0.006	0.99	0.059	0.001	510	37	499	36	550	38	2
BH06Rt_92	92	3	b.d.	na	17	2.5	0.310	0.031	0.98	0.386	0.020	2870	150	1720	150	3849	75	40
BH06Rt_93	93	94	b.d.	na	1.13	0.15	0.093	0.007	0.69	0.085	0.009	741	69	573	39	1220	150	23
BH06Rt_94	94	107	b.d.	na	1.48	0.13	0.135	0.008	0.99	0.079	0.002	919	49	817	44	1174	50	11
BH06Rt_95	95	53	b.d.	na	2.55	0.48	0.113	0.012	0.79	0.168	0.021	1240	140	714	69	2360	270	42
BH06Rt_96	96	9	b.d.	na	1.003	0.081	0.099	0.005	0.77	0.073	0.002	699	40	605	31	1008	53	13
BH06Rt_97	97	10	b.d.	na	0.586	0.075	0.075	0.008	1.00	0.057	0.001	463	47	464	48	477	55	0
BH06Rt_98	98	155	b.d.	na	0.95	0.15	0.053	0.003	0.77	0.125	0.016	659	85	333	17	1870	310	49

Table D-4: Rutile LA-ICP-MS U-Pb Isotopic Data and Ages — Sample 11-BH-06: Desert Member, Book Cliffs, UT, HST

					Corrected isotopic ratios							Ages (Ma)[f]						
Sample	Grain #.	U[a] [ppm]	Th[a] [ppm]	U/Th	$^{207}Pb^{b}/^{235}U$	±2s[d]	$^{206}Pb^{b}/^{238}U$	±2s[d]	Rho[c]	$^{207}Pb^{e}/^{206}Pb$	±2s[d]	$^{207}Pb/^{235}U$	±2s	$^{206}Pb/^{238}U$	±2s	$^{207}Pb/^{206}Pb$	±2s	Disc. %[g]
BH06Rt_99	99	1	b.d.	na	38.5	8.9	0.551	0.094	0.99	0.522	0.046	3750	210	2780	360	4330	120	26
BH06Rt_100	100	2	b.d.	na	49	17	0.560	0.170	0.98	0.649	0.053	3970	330	2640	720	4590	130	34
BH06Rt_101	101	50	b.d.	na	4.01	0.26	0.128	0.007	0.98	0.229	0.003	1622	53	772	42	3045	23	52
BH06Rt_102	102	9	b.d.	na	5.87	0.73	0.354	0.023	0.99	0.119	0.007	1950	100	1950	110	1945	89	0
BH06Rt_103	103	7	b.d.	na	0.55	0.055	0.070	0.006	1.00	0.057	0.001	441	36	437	36	490	44	1
BH06Rt_104	104	54	b.d.	na	10.9	0.97	0.235	0.019	0.94	0.345	0.012	2512	94	1357	98	3701	56	46
BH06Rt_105	105	0	b.d.	na	0.74	0.12	0.079	0.010	0.92	0.063	0.003	537	65	489	62	675	87	9
BH06Rt_106	106	96	b.d.	na	3.99	0.29	0.129	0.008	0.99	0.224	0.004	1622	56	784	43	3005	25	52
BH06Rt_107	107	4	b.d.	na	1.01	0.12	0.112	0.011	1.00	0.064	0.002	698	62	683	61	748	62	2
BH06Rt_108	108	14	b.d.	na	2.39	0.42	0.117	0.009	0.65	0.144	0.020	1190	130	709	50	2070	280	40
BH06Rt_109	109	41	b.d.	na	9.93	0.78	0.225	0.014	0.99	0.318	0.006	2413	72	1307	75	3559	27	46
BH06Rt_110	110	4	b.d.	na	2.79	0.56	0.084	0.014	0.98	0.227	0.013	1250	170	515	82	3028	88	59
BH06Rt_111	111	13	b.d.	na	1.67	0.13	0.076	0.004	0.64	0.173	0.003	1012	50	470	26	2586	32	54
BH06Rt_112	112	36	b.d.	na	4.89	0.36	0.149	0.007	0.97	0.237	0.006	1797	62	892	41	3091	42	50

[a]U and Th concentrations and Th/U ratios calculated relative to the R10 rutile standard using 287±76 ppm for U and 8.4±2.6 ppm for Th (Jackson, 2004)
[b]Corrected for U-Pb fractionation and background and normalised to R10 rutile standard ID-TIMS values (Jackson, 2004) and Pb/U ratios are corrected according to Anderson (2002)
[c]Error correlation defined as the quotient of the propagated errors of the $^{206}Pb/^{238}U$ and the $^{207}/^{235}U$ ratio
[d]The propagated error of quadratic addition of internal errors (2 SD) and within run reproducibility of R10 (2 SD)
[e]Corrected for mass-bias by normalising to R10 rutile standard (~.6 per atomic mass unit)
[f]U-Pb ages are calculated relative to R10 rutile standard and corrected for common Pb using Anderson (2002)
[g]Discordance %: for $^{206}Pb/^{238}U$ ages <1Ga calculated as $((1-(^{206}Pb/^{238}U)/(^{207}Pb/^{235}U))*100)$, for $^{206}Pb/^{238}U$ ages >1Ga calculated as $((1-(^{206}Pb/^{238}U)/(^{207}Pb/^{206}Pb))*100)$
b.d.= below detection limit
na = not applicable

Table E-1: Rutile Trace Element Data   Sample: 11-TUS3C-22.3-22.4, Castlegate Member, Blackhawk Formation, Book Cliffs, UT

Grain #.	Si (mass 29) ppm[a]	Si (mass 29) Std. Error ±2σ	V (mass 51) ppm[a]	V (mass 51) Std. Error ±2σ	Zr (mass 90) ppm[a]	Zr (mass 90) Std. Error ±2σ	Nb (mass 93) ppm[a]	Nb (mass 93) Std. Error ±2σ	Mo (mass 95) ppm[a]	Mo (mass 95) Std. Error ±2σ	Sn (mass 118) ppm[a]	Sn (mass 118) Std. Error ±2σ	Sn (mass 120) ppm[a]	Sn (mass 120) Std. Error ±2σ
1	1300	1729	53	757	34	3120	170	20.3	1.9	364.0	20.0	360.0	19.0	1300
2	b.d.	1522	55	378	18	3050	160	1.3	0.9	39.8	2.4	39.3	2.5	b.d.
3	1000	1953	68	1503	61	2800	130	3.0	0.9	46.9	3.0	47.5	2.8	1000
4	1400	4440	210	1454	78	1590	100	22.5	1.8	44.2	3.0	41.8	2.8	1400
5	4200	3230	550	223	44	1267	80	b.d.	b.d.	3450.0	250.0	3400.0	270.0	4200
6	1600	825	31	980	63	1304	93	0.4	0.4	67.5	4.0	63.4	4.2	1600
7	1600	355	13	187	9	5560	300	-1.3	1.4	75.4	3.8	75.2	3.9	1600
8	1300	714	32	309	17	252	15	36.7	2.7	20.1	1.6	18.9	1.2	1300
9	b.d.	364	18	92	10	2090	130	29.6	2.6	15.5	1.2	16.4	1.3	b.d.
10	b.d.	1505	60	783	47	5580	310	2.1	2.6	27.8	2.0	26.0	1.7	b.d.
11	2000	1030	40	252	12	5810	260	7.0	3.3	480.0	23.0	464.0	27.0	2000
12	1100	517	18	127	6	735	46	1.8	0.5	199.0	10.0	190.5	9.4	1100
13	24000	236	15	249	28	1319	72	12.3	2.8	25.0	2.9	25.8	2.4	24000
14	990	550	21	215	14	3780	240	55.8	4.3	358.0	23.0	352.0	24.0	990
15	1100	3720	150	1660	82	2180	130	13.6	1.2	53.8	3.4	53.9	3.3	1100
16	970	674	32	706	37	1233	79	5.6	0.9	17.5	1.2	17.4	1.1	970
17	1200	563	25	1020	150	1800	110	7.7	1.1	70.8	5.4	70.8	5.1	1200
18	920	959	39	412	20	847	43	22.6	1.6	6.8	0.5	7.6	0.5	920
19	930	268	11	125	7	4690	310	22.1	3.8	56.2	3.7	54.9	4.3	930
20	980	994	36	442	30	6170	330	10.4	3.5	127.1	8.4	127.9	9.2	980
21	710	398	18	244	16	1629	98	4.8	0.8	12.0	1.0	11.9	0.9	710
22	39000	1688	66	14	2	438	39	0.7	1.1	84.1	7.3	90.8	9.1	39000
23	1000	2014	77	271	13	422	25	8.1	1.2	109.8	6.6	112.0	7.9	1000
24	1100	6240	260	357	18	2710	150	-0.4	0.6	66.9	3.6	67.6	4.6	1100
25	980	4730	200	1218	77	504	29	9.3	1.1	11.8	1.0	11.4	1.0	980
26	4000	1008	34	117	9	107	8	2.2	2.3	67.0	4.3	67.0	4.2	4000
27	770	1574	79	777	58	1763	93	5.7	1.0	109.8	6.5	112.4	8.5	770
28	3200	819	35	1190	140	943	59	7.5	1.0	40.5	2.8	39.4	2.8	3200
29	2100	3940	160	438	24	2100	120	13.8	1.4	29.6	2.0	28.2	1.8	2100
30	1300	541	26	29	2	1519	76	0.6	0.7	47.9	3.1	47.6	2.9	1300
31	980	626	27	108	7	3100	210	28.8	3.2	25.5	2.2	25.7	2.3	980
32	1000	1145	42	210	9	1400	58	1.0	0.5	48.4	2.5	47.6	2.4	1000
34	780	437	20	14	1	1490	110	0.9	0.6	11.3	0.9	10.9	0.8	780
35	14000	2010	130	420	29	4200	240	4.3	2.3	4.5	0.5	4.3	0.6	14000
36	850	1660	66	1520	100	2340	180	17.9	2.5	25.0	2.2	24.1	2.5	850
37	980	547	23	179	11	508	29	5.2	0.9	20.8	1.4	20.5	1.4	980
38	820	2013	87	139	10	4550	340	0.4	1.8	93.6	7.3	90.9	7.4	820
39	630	1963	64	2402	93	3320	140	20.0	1.6	41.8	2.1	40.3	2.2	630
40	610	1136	39	279	14	1106	47	1.5	0.5	62.0	2.7	61.1	3.0	610
41	700	652	29	392	23	4070	270	2.2	1.8	97.7	7.4	98.9	7.3	700
42	610	594	25	316	16	3720	200	2.1	1.3	100.1	5.7	101.0	6.3	610
43	680	3440	160	2040	110	3360	220	46.2	3.7	37.3	2.8	35.2	2.7	680
44	740	864	36	1320	310	1910	100	3.4	0.8	71.0	4.4	74.2	5.0	740
45	860	1428	54	3230	170	775	45	6.0	1.2	35.5	2.3	35.5	2.2	860
46	880	1428	41	3010	150	714	26	4.5	0.9	28.3	1.4	28.4	1.6	880
47	720	1098	45	176	10	9100	530	0.6	2.5	300.0	18.0	308.0	20.0	720
48	570	84	8	388	32	2340	190	3.4	1.1	33.8	3.9	31.5	3.5	570

Table E-1: Rutile Trace Element Data Sample: 11-TUS3C-22.3-22.4, Castlegate Member, Blackhawk Formation, Book Cliffs, UT

Grain #.	Si (mass 29) ppm[a]	Si (mass 29) Std. Error ±2σ	V (mass 51) ppm[a]	V (mass 51) Std. Error ±2σ	Zr (mass 90) ppm[a]	Zr (mass 90) Std. Error ±2σ	Nb (mass 93) ppm[a]	Nb (mass 93) Std. Error ±2σ	Mo (mass 95) ppm[a]	Mo (mass 95) Std. Error ±2σ	Sn (mass 118) ppm[a]	Sn (mass 118) Std. Error ±2σ	Sn (mass 120) ppm[a]	Sn (mass 120) Std. Error ±2σ
49	620	1034	46	1144	52	5740	250	7.3	3.2	114.6	5.1	109.1	4.9	620
50	870	579	28	239	26	4280	230	3.8	1.9	120.0	7.7	118.2	7.3	870
51	820000	1350	110	194	43	745	65	33.0	55.0	38.0	17.0	38.0	19.0	820000
52	690	398	19	153	14	2060	110	2.2	0.8	132.0	13.0	130.0	11.0	690
53	880	4880	200	918	41	5990	220	6.3	3.4	124.5	6.4	116.2	5.9	880
54	620	1737	53	832	44	7090	430	0.5	2.0	89.3	6.6	90.3	7.1	620
55	11000	598	26	105	6	2470	120	7.1	1.2	101.3	6.5	103.4	6.3	11000
56	520	485	21	117	6	389	77	10.7	1.0	11.3	0.8	11.3	0.8	520
57	4100	327	11	74	5	2195	87	3.5	1.0	41.4	2.2	42.1	2.4	4100
58	1300	812	35	53	5	3990	250	1.7	1.3	115.0	8.3	115.1	7.4	1300
59	830	171	15	1720	130	6570	430	3.7	3.3	965.0	95.0	949.0	89.0	830
60	1200	2570	130	187	13	5580	350	b.d.	b.d.	138.2	9.3	133.4	8.7	1200
61	630	1123	43	792	42	2750	130	0.5	0.6	115.9	8.4	112.4	6.6	630
62	1000	1047	43	204	14	1503	91	4.7	0.9	23.8	1.9	23.4	1.8	1000
63	420	1934	75	1274	70	2360	140	2.1	0.7	301.0	20.0	307.0	18.0	420
64	650	1404	57	269	17	1820	110	1.5	0.6	106.4	9.0	104.3	8.5	650
65	1100	1435	53	357	28	1770	110	1.2	1.0	110.5	7.7	112.5	8.2	1100
67	680	862	40	267	14	67	4	2.0	0.6	5.6	0.5	5.7	0.5	680
68	630	3740	160	2790	120	3320	200	30.2	2.6	17.0	1.3	16.8	1.1	630
69	17000	687	23	143	10	993	55	5.3	8.1	41.5	9.8	44.0	10.0	17000
70	1500	3360	110	1464	74	2360	140	7.5	1.8	34.9	4.5	35.3	4.3	1500
71	2000	1089	40	313	18	11870	690	b.d.	b.d.	173.0	12.0	162.0	10.0	2000
72	620	1189	43	1473	76	5140	240	162.2	8.3	146.3	8.8	138.0	6.8	620
73	670	627	23	391	20	633	44	15.2	1.3	17.3	1.4	17.7	1.4	670
74	690	486	28	280	17	615	40	5.3	0.9	18.0	1.7	18.5	1.7	690
75	440	1473	61	204	12	1963	97	7.9	1.3	11.1	0.7	11.2	0.7	440
76	740	1709	62	732	48	5980	380	7.4	3.9	125.0	10.0	126.0	10.0	740
77	710	62	5	86	10	1940	150	0.7	0.7	1.5	0.3	1.2	0.3	710
78	1400	287	21	43	3	1445	94	8.1	1.5	5.1	0.7	4.7	0.6	1400
79	560	4150	170	1903	93	7180	310	60.7	5.4	69.3	3.7	62.4	3.7	560
80	4200	432	18	30	3	2470	200	0.6	0.8	20.1	1.5	20.3	1.8	4200
81	560	182	8	8	1	1640	110	0.7	0.6	11.1	1.8	11.3	1.7	560
82	4700	1399	52	130	7	2210	110	2.2	1.0	104.8	7.6	105.6	7.6	4700
83	690	1079	48	660	39	5050	320	20.8	3.6	535.0	36.0	562.0	40.0	690

[a]Trace element concentrations are calculated relative to R10 rutile standard and checked using T-139 rutile as a secondary standard
b.d.= Below Detection limit

Table E-2: Rutile Trace Element Data Sample: 11-BH-06, Desert Memebr, Blackhawk Formation, Book Cliffs, UT

Grain #.	Si (mass 29) ppm[a]	Si (mass 29) Std. Error ±2σ	V (mass 51) ppm[a]	V (mass 51) Std. Error ±2σ	Zr (mass 90) ppm[a]	Zr (mass 90) Std. Error ±2σ	Nb (mass 93) ppm[a]	Nb (mass 93) Std. Error ±2σ	Mo (mass 95) ppm[a]	Mo (mass 95) Std. Error ±2σ	Sn (mass 118) ppm[a]	Sn (mass 118) Std. Error ±2σ	Sn (mass 120) ppm[a]	Sn (mass 120) Std. Error ±2σ
1	28800	6300	716	35	49	4	1567	74	6	2	77	4	76	4
2	122000	13000	1167	69	535	42	2990	130	3	1	54	3	55	3
3	17000	4500	552	31	71	5	866	60	b.d.	b.d.	8	1	8	1
4	9100	4000	898	39	91	7	5200	290	9	4	101	11	98	11
5	b.d.	b.d.	1523	70	351	21	1179	70	0	0	27	2	29	2
6	1900	4100	1415	43	170	14	3940	180	1	1	106	6	108	7
7	161000	31000	114	6	168	12	3730	250	0	1	5	1	5	1
8	49200	6100	1229	41	564	31	1803	72	2	1	194	10	198	11
9	55600	7500	843	30	66	4	1488	74	23	2	33	2	34	2
10	3700	3600	1376	85	249	16	3720	250	0	2	86	8	94	9
11	5900	3100	103	9	177	9	1553	91	0	0	7	1	7	1
12	b.d.	b.d.	804	33	493	28	11430	590	2	3	174	11	175	10
13	3400	2500	748	45	640	38	2650	160	26	3	12	1	13	1
14	b.d.	b.d.	1550	60	640	38	2890	150	1	1	42	2	39	3
15	b.d.	b.d.	1592	56	1111	44	2270	110	9	1	61	4	59	4
16	b.d.	b.d.	2261	87	2220	110	1663	74	17	1	27	2	27	2
17	4900	3400	1735	63	2090	130	1800	110	32	2	17	1	17	1
18	2300	2700	2270	140	396	39	3590	410	1	3	41	5	40	4
19	500	2800	1220	56	186	13	3410	240	b.d.	b.d.	79	7	77	6
20	2800	3200	2870	110	2690	170	3110	210	15	2	36	3	34	3
21	1900	2500	1605	55	629	32	3550	170	25	2	23	2	24	2
22	b.d.	b.d.	3870	200	1744	89	2420	120	31	3	44	3	42	3
23	b.d.	b.d.	1347	56	93	5	155	6	1	0	90	5	91	4
24	4700	2400	723	31	281	15	4200	200	17	4	128	9	132	10
25	1700	3100	1778	79	47	5	2000	120	1	1	74	7	73	6
26	6500	3200	594	26	126	10	865	59	5	1	12	1	13	1
27	312000	30000	1450	67	272	17	4460	240	1	1	96	7	96	7
28	b.d.	2300	1101	46	1094	59	2510	110	7	2	14	1	14	1
29	4200	2500	637	40	588	35	429	27	6	1	108	7	103	7
30	b.d.	b.d.	846	28	39	3	273	16	0	0	177	13	171	13
31	2700	2400	2178	81	2203	87	1308	57	42	2	5	0	5	0
32	8000	2400	498	23	107	10	562	57	5	1	20	2	21	2
34	16400	6800	3770	130	166	16	516	41	2	1	107	9	102	8
35	b.d.	b.d.	1650	62	1319	74	3680	230	18	3	118	8	113	7
36	3700	1900	3600	140	619	37	2380	140	5	1	52	4	51	4
37	6900	2400	828	33	86	7	121	11	3	1	28	2	29	2
38	2600	2300	1142	42	1466	73	1656	86	7	1	61	3	64	4
39	2900	2700	1980	120	908	72	90	11	1	1	102	29	110	32
40	b.d.	b.d.	2390	130	1494	91	4040	290	34	4	44	3	44	4
41	3900	2200	957	36	65	3	4130	300	1	1	33	2	33	2
42	43300	5900	815	33	99	6	1610	100	0	0	56	4	55	4
43	1100	1700	1650	62	302	30	1135	57	9	1	48	3	48	3
44	b.d.	b.d.	38	2	112	6	1233	61	23	2	1434	85	1447	85
45	45500	7500	931	40	2390	450	1217	63	1	1	55	4	56	3
46	45800	5100	4920	390	600	58	1510	120	5	2	42	4	42	4
47	3500	1900	2960	130	401	32	2930	310	32	4	15	2	16	2

Table E-2: Rutile Trace Element Data Sample: 11-BH-06, Desert Memebr, Blackhawk Formation, Book Cliffs, UT

Grain #.	Si (mass 29) ppm[a]	Si (mass 29) Std. Error ±2σ	V (mass 51) ppm[a]	V (mass 51) Std. Error ±2σ	Zr (mass 90) ppm[a]	Zr (mass 90) Std. Error ±2σ	Nb (mass 93) ppm[a]	Nb (mass 93) Std. Error ±2σ	Mo (mass 95) ppm[a]	Mo (mass 95) Std. Error ±2σ	Sn (mass 118) ppm[a]	Sn (mass 118) Std. Error ±2σ	Sn (mass 120) ppm[a]	Sn (mass 120) Std. Error ±2σ
48	5000	2200	1251	43	136	39	5430	220	5	3	327	18	332	17
49	21500	4100	563	22	709	49	1210	51	7	1	79	5	78	5
50	37400	4600	374	18	1360	620	1760	110	b.d.	b.d.	62	6	63	6
51	166000	15000	1304	59	305	23	1061	65	4	2	111	8	107	9
52	235000	22000	530	21	43	8	936	62	1	1	50	4	52	4
53	3600	2500	22	1	6	1	2700	160	1	1	60	4	61	4
54	71100	9300	498	20	138	20	2320	150	1	1	29	2	30	2
55	37700	5300	1085	45	59	4	2300	140	1	1	70	5	70	4
56	57000	10000	159	31	820	210	1830	140	5	2	3	0	3	0
57	11400	2000	391	17	645	37	3300	170	24	2	40	2	40	2
58	63000	15000	1480	110	1510	140	770	63	10	3	95	6	94	5
59	b.d.	b.d.	1520	59	6	1	605	38	0	0	2	0	2	0
60	54000	5500	55	3	278	18	1431	84	b.d.	b.d.	1	0	1	0
61	1060	900	2355	82	269	17	7230	420	7	3	168	11	168	11
62	2000	1700	1382	58	39	2	2068	96	1	0	65	4	66	4
63	800	1300	1014	41	207	12	2000	120	12	1	14	1	13	1
64	12700	2000	5160	440	950	140	1780	250	9	3	114	14	113	14
65	26800	6300	222	11	23	2	1656	90	10	1	27	3	27	3
67	10400	5700	434	24	8570	510	4850	280	2	2	173	15	178	13
68	3900	3800	3140	180	5	2	2180	130	3	1	225	17	223	17
69	3100	1500	925	35	636	31	2070	100	2	1	178	9	175	10
70	b.d.	b.d.	1510	110	378	30	1600	150	7	1	169	19	180	22
71	1600	1500	1564	61	1056	53	3810	180	30	3	160	9	162	8
72	191000	18000	629	32	98	9	3190	220	4	1	77	6	74	6
73	b.d.	b.d.	3430	140	2710	140	2300	120	19	2	15	1	14	1
74	1700	1600	1102	52	443	24	9080	560	8	4	119	8	120	8
75	2300	1400	1079	35	689	37	118	7	7	1	10	1	10	1
76	2400	1100	2400	110	242	12	4810	260	6	3	267	18	263	18
77	b.d.	b.d.	2530	100	760	43	1864	97	3	1	72	4	71	4
78	8100	2700	1248	58	656	37	1531	84	22	2	10	1	11	1
79	1000	1700	2110	150	1770	240	1980	310	19	4	13	1	13	2
80	b.d.	b.d.	3840	140	3130	150	2373	99	34	2	49	3	50	3
81	1400	1500	2110	140	2510	230	1760	170	24	3	21	2	20	2
82	1000	1100	772	33	139	9	733	47	13	1	8	1	8	1
83	7600	2100	2220	110	199	13	415	27	0	1	10	2	10	1

[a]Trace element concentrations are calculated relative to R10 rutile standard and checked using T-139 rutile as a secondary standard

b.d.= Below detection limit

Table E-3: Rutile Trace Element Data Sample: 11-TUS3C-2-17, Desert Member, Blackhawk Formation, Book Cliffs, UT

Grain #.	Si (mass 29) ppm[a]	Si (mass 29) Std. Error ±2σ	V (mass 51) ppm[a]	V (mass 51) Std. Error ±2σ	Zr (mass 90) ppm[a]	Zr (mass 90) Std. Error ±2σ	Nb (mass 93) ppm[a]	Nb (mass 93) Std. Error ±2σ	Mo (mass 95) ppm[a]	Mo (mass 95) Std. Error ±2σ	Sn (mass 118) ppm[a]	Sn (mass 118) Std. Error ±2σ	Sn (mass 120) ppm[a]	Sn (mass 120) Std. Error ±2σ
1	2900	1400	1184	2470	110	0.3	688	60	2740	300	11	2.1	12	1
2	1160	870	1404	1057	44	0.4	282	18	1620	110	8	1.0	35	3
3	2200	1100	1270	642	35	0.4	1230	110	4470	410	1	1.3	11	1
4	2060	750	1224	1001	44	0.4	232	18	258	23	7	1.0	18	2
5	14100	2700	1111	1442	68	0.3	287	22	4770	370	7	2.9	150	12
6	4500	1400	1110	1132	71	0.3	410	120	5260	480	4	2.2	99	9
7	1900	1100	1031	2320	100	0.4	71	9	2310	300	1	0.5	175	15
8	950	490	776	3590	220	0.3	1045	80	197	23	1	0.4	11	1
9	91000	22000	1397	816	41	0.6	39	4	1790	110	4	1.2	51	4
10	1880	550	809	940	41	0.3	134	11	622	69	1	0.4	90	8
11	1900	530	788	1596	59	0.3	1091	83	1680	140	4	0.8	106	10
12	1750	560	901	2275	79	0.4	480	37	4670	370	3	2.2	94	7
13	2380	570	867	459	28	0.3	374	47	1330	190	17	2.8	20	3
14	1760	470	802	4080	170	0.4	147	10	1670	100	0	0.5	39	3
15	13200	4500	990	1352	54	0.5	66	4	2490	150	1	0.6	15	2
16	2690	640	884	3360	130	0.4	131	16	2030	140	5	1.1	56	4
17	2070	370	990	749	48	0.4	290	22	420	29	23	3.0	11	1
18	2140	570	1171	3160	110	0.4	2240	140	2330	160	12	1.1	30	2
19	1140	550	860	359	13	0.4	562	39	1078	72	36	3.3	20	2
20	1060	530	1304	370	34	0.7	105	14	1030	130	2	1.2	2	1
21	3400	1300	1460	2150	220	0.8	390	130	1440	500	1	0.7	113	20
22	1430	480	771	4530	170	0.4	1293	91	1460	110	30	2.9	18	2
23	1580	540	809	1903	89	0.4	2790	190	2210	170	40	3.7	83	7
24	1210	440	678	1637	63	0.4	447	34	1450	120	19	2.4	104	10
25	4800	1000	869	652	22	0.5	78	7	6760	480	-1	1.6	49	4
26	17400	3000	838	598	28	0.5	513	43	1980	150	11	1.3	33	4
27	9100	1700	806	352	25	0.4	3990	410	1640	180	54	6.5	6	1
28	1720	450	1060	2280	120	0.6	1960	250	1790	220	12	1.9	13	2
29	4600	1400	1384	886	34	0.9	321	94	131	13	2	1.0	16	2
30	810	420	696	3370	110	0.4	873	53	1920	120	6	0.9	83	9
31	223000	63000	881	3410	170	0.6	728	83	1510	140	17	2.0	80	8
32	10100	3300	793	1058	39	0.6	651	49	350	24	14	2.0	30	5
34	2160	440	691	646	31	0.5	117	9	1270	120	14	1.6	6	1
35	1760	450	731	498	26	0.4	24	2	2510	230	0	0.6	11	1
36	4340	600	745	545	22	0.5	20	2	1430	110	0	0.6	8	1
37	2060	330	602	2262	94	0.4	115	9	147	12	1	0.4	28	2
38	490	410	804	6320	260	0.8	1005	73	1700	130	11	1.5	37	3
39	1340	600	777	1651	81	0.7	734	82	4200	460	0	1.5	97	11
40	4340	810	698	2590	110	0.5	66	12	2890	260	0	0.6	140	11
41	1290	300	478	626	22	0.3	91	6	1850	130	2	0.6	344	28
42	1200	640	888	2220	110	0.6	15	1	143	10	0	0.6	2	0
43	25600	8500	484	727	30	0.4	93	9	92	13	1	0.7	5	1
44	1310	290	445	628	29	0.3	100	8	1950	150	1	0.5	347	28
45	44100	9000	696	209	10	0.5	40	4	2660	200	1	0.8	16	2
46	2170	380	514	40	3	0.4	476	68	1790	240	2	0.9	3	0
47	2350	470	541	31	2	0.4	327	46	1660	220	2	1.0	2	1
48	164000	18000	1028	1115	53	0.8	84	6	4040	350	0	1.0	72	7

Table E-3: Rutile Trace Element Data Sample: 11-TUS3C-2-17, Desert Member, Blackhawk Formation, Book Cliffs, UT

Grain #.	Si (mass 29) ppm[a]	Si (mass 29) Std. Error ±2σ	V (mass 51) ppm[a]	V (mass 51) Std. Error ±2σ	Zr (mass 90) ppm[a]	Zr (mass 90) Std. Error ±2σ	Nb (mass 93) ppm[a]	Nb (mass 93) Std. Error ±2σ	Mo (mass 95) ppm[a]	Mo (mass 95) Std. Error ±2σ	Sn (mass 118) ppm[a]	Sn (mass 118) Std. Error ±2σ	Sn (mass 120) ppm[a]	Sn (mass 120) Std. Error ±2σ
49	1720	390	729	823	31	0.4	75	6	2320	140	2	0.6	60	4
50	940	350	596	1227	45	0.5	247	18	4760	320	3	1.9	85	7
51	2100	480	716	2750	100	0.6	2790	170	1112	74	3	0.7	133	9
52	3840	550	600	502	66	0.5	116	10	1171	69	5	1.0	26	2
53	1860	370	628	1312	52	0.5	479	30	9170	520	9	4.2	75	6
54	1500	330	464	2035	81	0.5	1690	130	1910	160	13	1.4	38	3
55	1890	340	710	1920	140	0.5	1610	180	9000	1000	96	12.0	83	9
56	1880	730	427	2170	150	0.4	1340	110	1690	150	38	3.4	60	6
57	3530	600	513	151	9	0.5	173	16	5440	500	-1	1.2	5	1
58	5510	820	573	1958	81	0.5	651	34	3240	220	2	1.1	291	22
59	940	370	532	2012	69	0.7	596	34	2730	150	1	0.7	125	8
60	1080	280	494	1582	61	0.4	1730	120	2640	190	21	1.8	53	4
61	1080	390	484	1646	83	0.4	1700	120	2740	170	24	2.4	55	5
62	1090	250	568	1930	120	0.4	155	17	3240	390	4	2.0	111	13
63	1340	360	524	2672	96	0.5	356	18	12380	730	2	2.9	97	6
64	1770	360	407	828	27	0.4	61	4	338	18	2	1.0	58	5
65	1500	240	502	1362	55	0.5	578	41	3640	240	5	1.6	78	6
67	1540	300	499	4920	240	0.5	654	30	2230	150	0	0.4	87	6
68	5130	490	603	1479	65	0.6	451	31	3060	210	19	2.2	150	12
69	1020	270	488	1518	58	0.5	342	17	6120	280	2	2.3	90	5
70	1210	250	380	904	29	0.4	344	19	854	41	11	1.0	18	1
71	4050	540	385	733	30	0.4	970	100	10500	1300	24	4.8	58	7
72	1240	260	433	3910	140	0.6	3020	150	1880	100	21	1.8	8	1
73	1030	330	751	500	36	0.7	240	26	2240	220	3	1.6	55	6
74	1110	230	420	1723	67	0.4	1174	79	1890	140	8	1.2	91	8
75	1770	380	564	1166	48	0.5	66	5	821	75	3	0.8	79	7
76	1960	290	531	4710	200	0.5	51	4	3370	280	0	0.8	225	22
77	3470	460	404	383	17	0.5	30	4	1910	150	4	1.1	28	5
78	1270	240	482	3930	160	0.8	3640	230	1950	140	3	0.7	32	2
79	8400	1600	879	76	4	0.8	154	16	8080	550	1	2.3	645	47
80	1290	350	515	1522	65	0.5	333	24	7470	510	1	2.7	102	7
81	4600	1100	554	852	35	0.5	48	5	476	54	2	0.7	10	1
82	360000	130000	777	4310	420	1.1	318	93	3530	390	39	77.0	1650	560
83	1700	310	389	1122	48	0.5	156	9	8450	590	-1	2.0	141	12
84	1260	200	466	1572	64	0.4	387	16	660	27	1	0.4	57	3
85	1120	230	529	2910	120	0.5	1080	67	2200	150	0	0.6	10	1
86	1270	290	494	843	30	0.5	205	15	676	54	13	1.3	20	2
87	1760	370	535	2175	99	0.5	269	21	4270	260	2	1.4	76	5
88	6500	1200	601	3410	140	1.2	994	85	2270	200	14	2.1	44	5
89	141000	68000	687	697	50	0.7	248	37	115	12	-19	58.0	520	220
90	2470	640	518	234	10	0.6	136	10	4590	320	14	2.6	199	12
91	1030000	470000	693	3270	280	0.8	780	180	1030	130	-100	260.0	5000	1800
92	3370	620	624	2186	65	0.8	379	43	2920	280	133	13.0	23	3
93	1150	210	327	1049	45	0.4	224	17	3980	310	-1	1.0	92	8
94	1080	200	300	1458	60	0.4	586	43	7460	650	17	3.1	61	5
95	1050	260	518	3100	130	0.5	973	39	1248	52	21	1.6	9	1
96	1980	310	424	1426	61	0.5	129	68	974	61	3	0.7	20	2

Table E-3: Rutile Trace Element Data Sample: 11-TUS3C-2-17, Desert Member, Blackhawk Formation, Book Cliffs, UT

Grain #.	Si (mass 29) ppm[a]	Si (mass 29) Std. Error ±2σ	V (mass 51) ppm[a]	V (mass 51) Std. Error ±2σ	Zr (mass 90) ppm[a]	Zr (mass 90) Std. Error ±2σ	Nb (mass 93) ppm[a]	Nb (mass 93) Std. Error ±2σ	Mo (mass 95) ppm[a]	Mo (mass 95) Std. Error ±2σ	Sn (mass 118) ppm[a]	Sn (mass 118) Std. Error ±2σ	Sn (mass 120) ppm[a]	Sn (mass 120) Std. Error ±2σ
97	3400	830	386	2600	110	0.4	342	42	1820	180	9	1.4	366	36
98	1360	180	359	1115	37	0.4	380	27	278	21	2	0.4	17	1
99	1150	250	602	1396	53	0.5	574	33	4550	250	0	1.1	74	5
100	8100	2600	678	1055	48	0.8	703	55	717	53	22	4.1	77	13
101	1080	180	374	2389	92	0.4	404	26	3390	250	1	1.0	145	13
102	7090	710	377	1519	70	0.5	950	310	1710	120	0	0.5	826	59
103	1920	240	432	2810	250	0.4	150	14	4900	490	14	5.0	396	72
104	3320	430	445	558	63	0.5	205	51	5180	360	-1	1.2	20	2
105	4400	1400	418	1162	52	0.4	650	120	3180	280	7	1.8	147	12
106	2000	410	465	2430	110	0.6	876	75	1870	140	1	0.6	127	11
107	1630	310	443	935	39	0.5	622	54	1034	95	1	0.6	31	3
108	1880	460	496	2173	92	0.6	2480	240	4250	360	20	2.5	130	10
109	19400	5400	467	714	29	0.5	235	22	5400	410	4	2.4	210	32

[a]Trace element concentrations are calculated relative to R10 rutile standard and checked using T-139 rutile as a secondary standard

Table E-4: Rutile Trace Element Data   Sample: 11-CSTG-07, Castlegate Member, Blackhawk Formation, Book Cliffs, UT

Grain #.	Si (mass 29) ppm[a]	Si (mass 29) Std. Error ±2σ	V (mass 51) ppm[a]	V (mass 51) Std. Error ±2σ	Zr (mass 90) ppm[a]	Zr (mass 90) Std. Error ±2σ	Nb (mass 93) ppm[a]	Nb (mass 93) Std. Error ±2σ	Mo (mass 95) ppm[a]	Mo (mass 95) Std. Error ±2σ	Sn (mass 118) ppm[a]	Sn (mass 118) Std. Error ±2σ	Sn (mass 120) ppm[a]	Sn (mass 120) Std. Error ±2σ
1	1670	550	1096	43	354	21	1163	67	1.6	0.4	124.8	9.1	122.3	7.7
2	2590	470	447	18	554	29	7080	400	-1.2	0.4	65.9	4.6	65.7	4.4
3	2990	470	1727	64	1652	71	4100	210	14.1	3.2	58.3	3.9	57.1	4.0
4	2930	560	627	25	1136	64	1514	80	1.5	0.5	49.9	3.0	47.0	2.4
5	3440	820	3190	160	546	31	4810	290	7.5	2.7	261.0	13.0	275.0	18.0
6	3530	570	939	44	367	18	3120	180	1.9	1.3	79.0	5.2	75.6	5.2
7	2170	440	687	32	82	4	1887	93	1.5	0.5	52.4	3.1	51.8	3.2
8	1790	620	1951	77	1447	67	2270	110	6.9	1.5	62.9	3.5	62.1	3.6
9	3600	1400	2000	110	126	11	2400	170	1.4	1.2	48.1	3.3	50.6	4.1
10	1950	470	2800	140	1670	110	1880	110	18.4	1.9	38.5	3.1	36.4	3.1
11	2410	370	2205	84	304	15	833	50	6.4	0.8	193.0	13.0	190.0	12.0
12	2130	370	2960	110	1670	83	1347	72	10.3	1.0	11.7	0.8	11.7	0.8
13	3060	420	757	30	381	21	4240	230	42.0	3.0	247.0	15.0	257.0	15.0
14	2270	320	1895	74	1397	57	3050	130	12.5	2.1	67.6	3.3	69.6	3.8
15	1900	440	1974	74	461	24	3660	190	0.3	0.7	215.0	11.0	215.0	13.0
16	7600	2900	791	71	213	27	1640	160	1.0	0.5	43.3	4.5	40.7	4.0
17	2270	400	2160	84	692	42	1509	85	4.4	0.6	54.1	3.7	56.0	4.2
18	3240	470	1990	91	424	30	1490	110	5.0	0.8	31.0	2.0	30.9	1.9
19	2510	340	1621	53	463	32	5310	300	0.4	1.3	56.4	5.9	56.7	6.2
20	117000	25000	438	21	1520	330	1380	120	17.8	1.5	129.0	14.0	126.0	14.0
21	2410	340	2002	85	316	17	3550	180	1.8	1.3	152.0	10.0	149.9	8.8
22	2550	340	620	25	216	10	2330	110	3.0	0.9	64.4	3.3	64.7	3.5
23	2260	300	1900	88	349	19	3540	180	3.9	1.9	137.3	7.9	143.4	9.7
24	2570	360	838	36	689	26	608	29	103.6	5.0	34.3	2.2	35.1	2.0
25	1610	320	547	20	795	42	3030	130	17.4	1.4	158.6	9.9	151.7	8.1
26	2410	360	1672	75	399	17	3740	190	2.6	1.7	84.7	5.4	82.4	4.3
27	88000	19000	79	5	823	54	1550	100	1.8	0.9	5.7	0.7	5.6	0.6
28	3340	580	661	33	414	24	215	17	8.4	1.1	20.3	1.6	20.5	1.7
29	6000	870	1203	44	11	1	2470	130	0.4	0.5	30.3	2.0	29.8	2.0
30	7400	1600	1738	79	210	20	1445	76	2.7	0.7	42.8	3.0	39.8	2.8
31	2410	360	2320	100	21	2	2000	110	0.0	0.4	178.0	12.0	187.0	14.0
32	17000	2800	833	37	116	6	7410	390	0.4	2.3	109.4	6.7	107.6	5.7
34	2490	300	592	23	45	3	2470	110	1.2	0.6	47.6	2.7	47.7	2.6
35	3600	520	368	15	44	6	2120	140	1.0	0.6	194.0	22.0	196.0	23.0
36	1860	220	2026	83	583	31	5520	340	2.6	2.5	41.4	3.5	41.2	3.2
37	2400	300	1186	38	1657	69	3240	160	61.8	4.0	46.5	2.7	45.6	2.4
38	2090	250	954	35	534	25	8170	390	3.0	2.5	141.7	7.6	144.6	7.1
39	2610	340	1377	63	338	14	1760	110	9.4	1.2	213.0	14.0	210.0	14.0
40	1810	290	1554	66	381	22	3920	190	11.2	2.8	224.0	13.0	217.0	13.0
41	3640	900	2309	94	486	21	1791	79	8.8	0.8	87.0	5.4	86.2	5.2
42	2330	490	52	4	565	43	1970	100	7.5	1.0	2.1	0.4	2.3	0.4
43	2250	240	1447	63	561	35	4690	240	1.4	2.0	105.8	6.6	105.4	6.8
44	3860	550	2453	82	2900	130	2590	110	18.4	1.6	19.6	1.6	19.1	1.5
45	8370	610	4250	180	210	13	2100	110	9.8	1.3	59.8	4.0	63.0	4.2
46	3140	340	557	32	35	3	3330	210	9.0	1.9	221.0	13.0	225.0	16.0
47	2130	260	2104	91	1117	53	13160	700	6.3	3.3	59.1	3.2	57.1	3.1
48	1780	270	1375	63	268	12	2820	140	2.4	0.9	223.0	15.0	220.0	14.0

Table E-4: Rutile Trace Element Data Sample: 11-CSTG-07, Castlegate Member, Blackhawk Formation, Book Cliffs, UT

Grain #.	Si (mass 29) ppm[a]	Si (mass 29) Std. Error ±2σ	V (mass 51) ppm[a]	V (mass 51) Std. Error ±2σ	Zr (mass 90) ppm[a]	Zr (mass 90) Std. Error ±2σ	Nb (mass 93) ppm[a]	Nb (mass 93) Std. Error ±2σ	Mo (mass 95) ppm[a]	Mo (mass 95) Std. Error ±2σ	Sn (mass 118) ppm[a]	Sn (mass 118) Std. Error ±2σ	Sn (mass 120) ppm[a]	Sn (mass 120) Std. Error ±2σ
49	3660	300	144	19	14	3	2240	130	0.2	0.4	26.1	3.0	28.5	3.7
50	2030	260	554	27	413	20	1960	110	2.3	0.6	102.9	5.3	106.4	4.8
51	1810	280	590	24	108	7	2930	200	0.7	0.8	35.5	2.2	36.8	2.4
52	2070	270	139	5	265	14	5820	330	9.6	3.5	56.1	4.1	55.0	3.6
53	1990	320	1519	75	298	21	4950	320	-0.5	1.9	90.8	6.7	92.9	5.9
54	2560	310	1624	68	816	45	2640	160	50.4	3.3	49.8	3.9	48.7	3.4
55	1930	300	1141	41	137	9	1740	83	1.8	0.6	49.8	2.9	51.5	2.6
56	3070	780	1094	67	132	74	2340	260	1.0	2.9	236.0	32.0	226.0	29.0
57	2910	340	1089	42	161	7	396	19	11.6	0.9	12.7	0.8	13.4	0.9
58	1400	340	5430	210	508	31	160	9	1.8	0.5	130.4	7.5	126.6	7.1
59	5190	320	1748	88	6600	370	2580	140	0.4	0.4	51.1	3.8	52.3	4.5
60	4370	670	1720	65	71	4	2750	110	-0.1	0.4	56.6	3.2	57.1	2.6
61	1770	230	1425	67	646	28	3740	220	1.6	1.6	118.4	6.9	115.6	6.7
62	46200	8400	292	24	494	43	1730	87	6.9	1.1	17.0	2.5	17.7	2.5
63	1820	280	4680	390	413	28	739	49	8.0	0.9	542.0	36.0	552.0	38.0
64	12030	720	1196	53	41	3	4090	210	1.2	1.2	315.0	19.0	311.0	16.0
65	2550	250	3000	130	748	54	1398	72	7.7	0.8	68.5	4.0	70.4	3.8
67	3080	380	504	21	122	6	660	37	7.1	0.9	14.1	0.9	13.9	0.8
68	4500	1100	1624	78	198	11	8950	520	-2.1	0.9	155.0	12.0	162.0	13.0
69	2210	200	2008	73	1406	53	8720	370	88.4	6.8	43.0	2.3	43.8	2.4
70	3350	370	1165	47	47	4	276	15	0.6	0.4	4.3	0.6	4.5	0.6
71	1900	260	2068	63	1511	82	6370	340	43.4	4.6	50.9	3.7	50.2	3.8
72	1850	230	2690	120	572	26	4120	170	1.1	1.5	181.0	11.0	183.0	11.0
73	5100	640	4190	180	2040	100	393	24	0.4	0.4	6.7	0.5	6.7	0.5
74	1830	200	583	22	1049	48	1774	99	23.5	1.8	77.7	5.4	79.8	5.8
75	1820	190	1558	50	746	35	2561	99	6.3	1.5	43.3	2.5	42.4	2.2
76	6120	420	796	31	182	23	2260	110	0.8	0.6	85.2	3.9	87.3	3.4
77	1660	220	1992	71	318	15	650	27	3.4	0.6	92.1	5.5	91.4	5.8
78	15400	1400	1069	48	715	62	1044	51	19.4	2.8	30.4	1.7	31.2	2.0
79	1460	200	1498	76	764	36	2810	150	9.0	1.7	45.3	3.3	48.0	3.0
80	2160	210	428	14	515	28	3810	180	5.3	2.3	71.5	4.0	71.9	3.4
81	5200	1500	4900	180	404	27	1573	65	14.6	1.4	29.2	1.4	29.9	1.5
82	2050	200	269	13	229	21	2890	140	10.6	2.3	48.1	2.8	46.6	2.7
83	1670	550	1096	43	354	21	1163	67	1.6	0.4	124.8	9.1	122.3	7.7
84	2590	470	447	18	554	29	7080	400	-1.2	0.4	65.9	4.6	65.7	4.4
85	2990	470	1727	64	1652	71	4100	210	14.1	3.2	58.3	3.9	57.1	4.0
86	2930	560	627	25	1136	64	1514	80	1.5	0.5	49.9	3.0	47.0	2.4
87	3440	820	3190	160	546	31	4810	290	7.5	2.7	261.0	13.0	275.0	18.0
88	3530	570	939	44	367	18	3120	180	1.9	1.3	79.0	5.2	75.6	5.2
89	2170	440	687	32	82	4	1887	93	1.5	0.5	52.4	3.1	51.8	3.2
90	1790	620	1951	77	1447	67	2270	110	6.9	1.5	62.9	3.5	62.1	3.6
91	3600	1400	2000	110	126	11	2400	170	1.4	1.2	48.1	3.3	50.6	4.1
92	1950	470	2800	140	1670	110	1880	110	18.4	1.9	38.5	3.1	36.4	3.1
93	2410	370	2205	84	304	15	833	50	6.4	0.8	193.0	13.0	190.0	12.0
94	2130	370	2960	110	1670	83	1347	72	10.3	1.0	11.7	0.8	11.7	0.8
95	3060	420	757	30	381	21	4240	230	42.0	3.0	247.0	15.0	257.0	15.0
96	2270	320	1895	74	1397	57	3050	130	12.5	2.1	67.6	3.3	69.6	3.8

Table E-4: Rutile Trace Element Data Sample: 11-CSTG-07, Castlegate Member, Blackhawk Formation, Book Cliffs, UT

Grain #.	Si (mass 29) ppm[a]	Si (mass 29) Std. Error ±2σ	V (mass 51) ppm[a]	V (mass 51) Std. Error ±2σ	Zr (mass 90) ppm[a]	Zr (mass 90) Std. Error ±2σ	Nb (mass 93) ppm[a]	Nb (mass 93) Std. Error ±2σ	Mo (mass 95) ppm[a]	Mo (mass 95) Std. Error ±2σ	Sn (mass 118) ppm[a]	Sn (mass 118) Std. Error ±2σ	Sn (mass 120) ppm[a]	Sn (mass 120) Std. Error ±2σ
97	1900	440	1974	74	461	24	3660	190	0.3	0.7	215.0	11.0	215.0	13.0
98	7600	2900	791	71	213	27	1640	160	1.0	0.5	43.3	4.5	40.7	4.0
99	2270	400	2160	84	692	42	1509	85	4.4	0.6	54.1	3.7	56.0	4.2
100	3240	470	1990	91	424	30	1490	110	5.0	0.8	31.0	2.0	30.9	1.9
101	2510	340	1621	53	463	32	5310	300	0.4	1.3	56.4	5.9	56.7	6.2
102	117000	25000	438	21	1520	330	1380	120	17.8	1.5	129.0	14.0	126.0	14.0
103	2410	340	2002	85	316	17	3550	180	1.8	1.3	152.0	10.0	149.9	8.8
104	2550	340	620	25	216	10	2330	110	3.0	0.9	64.4	3.3	64.7	3.5
105	2260	300	1900	88	349	19	3540	180	3.9	1.9	137.3	7.9	143.4	9.7
106	2570	360	838	36	689	26	608	29	103.6	5.0	34.3	2.2	35.1	2.0
107	1610	320	547	20	795	42	3030	130	17.4	1.4	158.6	9.9	151.7	8.1
108	2410	360	1672	75	399	17	3740	190	2.6	1.7	84.7	5.4	82.4	4.3
109	88000	19000	79	5	823	54	1550	100	1.8	0.9	5.7	0.7	5.6	0.6

[a]Trace element concentrations are calculated relative to R10 rutile standard and checked using T-139 rutile as a secondary standard